



**HAL**  
open science

# Impact du surpoids et de l'hyperglycémie sur la barrière hémato-encéphalique et la plasticité cérébrale : Effets protecteurs de *P. mauritianum* et d'*A. borbonica*, deux plantes médicinales réunionnaises

Batoul Ghaddar

## ► To cite this version:

Batoul Ghaddar. Impact du surpoids et de l'hyperglycémie sur la barrière hémato-encéphalique et la plasticité cérébrale : Effets protecteurs de *P. mauritianum* et d'*A. borbonica*, deux plantes médicinales réunionnaises. Médecine humaine et pathologie. Université de la Réunion, 2022. Français. NNT : 2022LARE0013 . tel-03771420

**HAL Id: tel-03771420**

**<https://theses.hal.science/tel-03771420v1>**

Submitted on 7 Sep 2022

**HAL** is a multi-disciplinary open access archive for the deposit and dissemination of scientific research documents, whether they are published or not. The documents may come from teaching and research institutions in France or abroad, or from public or private research centers.

L'archive ouverte pluridisciplinaire **HAL**, est destinée au dépôt et à la diffusion de documents scientifiques de niveau recherche, publiés ou non, émanant des établissements d'enseignement et de recherche français ou étrangers, des laboratoires publics ou privés.



**Université de La Réunion**

**THÈSE**

Pour l'obtention du titre de Docteur en Sciences de l'Université de La Réunion

Spécialité : Biologie Médicale et Santé

Par

**Batoul GHADDAR**

**Impact du surpoids et de l'hyperglycémie sur la barrière hémato-encéphalique et la plasticité cérébrale :**

**Effets protecteurs de *P. mauritianum* et d'*A. borbonica*, deux plantes médicinales réunionnaises.**

Présentée et soutenue publiquement le 28 Juin 2022

### **Composition du jury**

<b>Pr. Giuseppe Montalbano</b>	<b>Université de Messine</b>	<b>Rapporteur</b>
<b>Pr. Aline Hamade</b>	<b>Université Libanaise</b>	<b>Rapporteuse</b>
<b>Dr. Arianna Servili</b>	<b>Ifremer</b>	<b>Examinatrice</b>
<b>Dr. Olivier Meilhac</b>	<b>Université de La Réunion (INSERM)</b>	<b>Examinateur</b>
<b>Dr. Nicolas Diotel</b>	<b>Université de La Réunion</b>	<b>Directeur de thèse</b>







## University of Reunion

### THESIS

To obtain the title of Doctor of Science from the University of La Réunion

Specialty: Medicinal Health Biology

By

**Batoul GHADDAR**

**Impact of overweight and hyperglycemia on the blood-brain barrier and brain plasticity:**

**protective effects of *P. mauritianum* and *A. borbonica*, two Reunionese medicinal plants**

Presented and publicly defended on June 28, 2022

#### Composition of the jury

<b>Pr. Giuseppe Montalbano</b>	<b>University of Messina</b>	<b>Reporter</b>
<b>Pr. Aline Hamade</b>	<b>Lebanese University</b>	<b>Reporter</b>
<b>Dr. Arianna Servili</b>	<b>Ifremer</b>	<b>Examiner</b>
<b>Dr. Olivier Meilhac</b>	<b>University of Reunion (INSERM)</b>	<b>Examiner</b>
<b>Dr. Nicolas Diotel</b>	<b>Université de Reunion</b>	<b>Thesis Director</b>



*In the name of Allah, the most merciful*

*To my family*

*And my husband Hasan*



## Acknowledgements

*This work was carried out within the Joint Research Unit 1188 Diabetes Atherothrombosis Therapies Réunion Océan Indien (DÉTROI) directed by Dr. Olivier Meilhac whom I thank for having welcomed me since my master's degree and for having allowed my training in research.*

*This work was made possible thanks to the financial support of the French Ministry of Education and Research through a doctoral contract of the University of La Reunion.*

*I would like to thank the members of the jury Pr. Giuseppe Montalbano and Pr. Aline Hamade for giving me the honor of judging this thesis as rapporteurs. I also express my sincere thanks to Olivier Meilhac and Arianna Servili for having accepted to be examiners of my thesis work.*

*I'm extremely grateful to my thesis supervisor Dr. Nicolas Diotel. I thank you for giving me the opportunity to do my master and thesis studies under your direction. I greatly appreciate your efforts, patience, advices and support during all these three years that give me great experience in science and help me to accomplish this work. Your motivation and humbleness teach me a lot.*

*I would like to express my gratitude to all the members of the DÉTROI laboratory and to all people who contributed in any way to the realization of this work. I also thank the members of the of the laboratory PIMIT and the platform CYROI.*

*I specially thank Philippe Rondeau, Jean-Loup Bascands, Bryan Veeren, Matthieu Bringart, Laura Gence and Chloé Turpin for helping me in technical issues in my experiments.*

*I would like to thank the members of my thesis committee for their encouragement and their advice.*

*I would like to express my deepest appreciation to my Lebanese family in Reunion Island, whom all its members were supportive for me and I spend non-forgettable memories with them. Dr. Chaker El Kalamouni your presence makes me feel that I am in Lebanon among my family, I thank you for your support since we come to this Island and until now.*

*Thanks should also go to all my friends here and in Lebanon. My friends in the laboratory: Sarah, Sandhya, Chloé, Julien, Eloise and Stéphane I am grateful for being next to me, helping me to engage in the lab environment when I was a new member of the lab. Danielle, I thank for your eunfuan in doing my stuff for the fish during the weekends. All my roommates, since 2019 till 2022, I thank you for the family ambiance you provided.*

*Alawiya, Daed, Ali, and Juliano thanks for your friendship throughout the 4 years and for standing nearby me when need you every time.*

*Sarah Rosanaly, I am really grateful to your friendship, support and sharing with me the happiness during the nice moments in my life, your room in Lebanon is being constructed.*

*Sandhya, I learned from your pure soul a lot. I am happy to know a person like you with all these calmness, purity, high values and positivity.*

*My endless thanks, till the end of my life, to my family and my lovely husband. My Mom and Dad the words don't save me to satisfy your thanking, all what I ask God is to keep you always happy. My sister who is my forever friend, I thank you for being a strong support for me, thank God for bringing you to my life. My Hasan, deep thanks and gratitude from the depth of my heart to your love that makes me feel you are behind me every time, even if you were in Lebanon. My success and the completion of my thesis would not have been possible without your support especially in the difficult moments. I'm extremely grateful to your patience all these three years without any complain, but with lot of courage and love. Again, the words are never enough. خيلي دوست دارم.*

***Thanks be to God, Lord of the world, whom I relied and all my success belong to him.***

## Contents

<b>Résumé</b> .....	5
<b>Abstract</b> .....	7
<b>List of scientific publications</b> .....	8
<b>List of figures</b> .....	9
<b>List of tables</b> .....	10
<b>List of abbreviations</b> .....	11
<b>General introduction</b> .....	15
<b>Introduction</b> .....	17
<b>I. Health risks of obesity and diabetes</b> .....	19
<b>A. General knowledge on the epidemics</b> .....	19
1. Obesity definition .....	19
2. Diabetes definition .....	20
3. Prevalence of obesity and diabetes .....	21
<b>B. Effects of metabolic disorders on the body physiology</b> .....	22
1. Obesity effects on the body .....	22
2. Obesity and stroke .....	26
3. Diabetes effects on the body .....	27
4. Stroke in diabetes .....	29
5. Mechanisms of insulin secretion and insulin resistance leading to type 2 diabetes .....	30
<b>C. The “Diabesity” concept: interrelation between obesity and the development of type 2 diabetes</b> .....	31
<b>II. Impact of metabolic disorders on the brain: focus to the blood-brain barrier and to neural stem cells</b> .....	33
<b>A. Blood-Brain Barrier (BBB)</b> .....	33
1. Definition .....	33
<b>B. Impact of metabolic disorders on BBB function</b> .....	36
1. Deleterious effect of obesity on the BBB .....	36
2. Deleterious effects of diabetes on the BBB .....	38
<b>C. Effects of metabolic disorders on brain volume, cognitive functions and the development of Alzheimer’s disease</b> .....	41
1. Obesity, brain volume and cognitive function .....	41
2. Diabetes, brain volumes and cognitive function .....	43
<b>D. Effect of metabolic disorders on neural stem cells and neurogenesis</b> .....	44
1. Embryonic neurogenesis .....	44
2. Adult neurogenesis .....	46



3.	Regulation of neurogenesis .....	48
4.	Effects of diabetes on the different aspects of neurogenesis .....	50
5.	Effects of obesity on the different aspects of neurogenesis.....	51
<b>III.</b>	<b>Zebrafish as an emerging model to understand the impact of obesity and diabetes on the central nervous system.....</b>	<b>52</b>
<b>A.</b>	<b>Zebrafish (<i>Danio rerio</i>) .....</b>	<b>52</b>
1.	Interesting facts for sciences .....	52
2.	Toxicity studies using zebrafish model .....	55
<b>B.</b>	<b>Zebrafish models of obesity and hyperglycemia models: similarities with humans .....</b>	<b>56</b>
1.	The use of zebrafish to mimic obesity.....	56
2.	Models of obesity in the literature.....	57
3.	The use of zebrafish to mimic hyperglycemia and diabetes.....	58
4.	Developed zebrafish diabetes models in literature .....	60
<b>C.</b>	<b>Zebrafish as a model to study brain plasticity including constitutive and regenerative mechanisms.....</b>	<b>61</b>
1.	Highly neurogenic regions conserved between zebrafish and mammals .....	61
2.	Similarities in zebrafish and mammalian neural stem cells .....	62
3.	Zebrafish have a high capacity for brain repair.....	64
4.	Conserved blood-brain barrier structure and function.....	65
<b>IV.</b>	<b>Plants as a source of new bioactive molecules.....</b>	<b>67</b>
<b>A.</b>	<b>Vegetal biodiversity and beneficial effects on health: focus on medicinal plants .....</b>	<b>67</b>
1.	Dietary natural bioactive compounds: focus on polyphenols.....	67
2.	Focus on medicinal plants .....	70
<b>B.</b>	<b>Reunion Island biodiversity.....</b>	<b>73</b>
<b>C.</b>	<b><i>Antirhea borbonica</i> (Bois d'Osto) .....</b>	<b>75</b>
<b>D.</b>	<b><i>Psiloxylon mauritianum</i> (Bois de pêche marron) .....</b>	<b>76</b>
<b>E.</b>	<b>Model of obese zebrafish to screen preventive and therapeutic effects of plant extract... 77</b>	<b>77</b>
<b>Objectives.....</b>		<b>79</b>
<b>A.</b>	<b>Thesis project.....</b>	<b>81</b>
<b>B.</b>	<b>Objectives of the thesis.....</b>	<b>82</b>
1.	Establishment of zebrafish models of obesity and prediabetes .....	82
2.	Characterization of the brain disruptions induced by the DIO models .....	82
3.	Preventive and/or therapeutic effects of aqueous extract of <i>Antirhea borbonica</i> and <i>Psiloxylon mauritianum</i> in our DIO models .....	83
<b>Results .....</b>		<b>85</b>
<b>Chapter 1: Deleterious effects of overfeeding on brain homeostasis and plasticity in adult zebrafish.....</b>		<b>87</b>

<b>Chapter 2: Phenolic profile of herbal infusion and polyphenol-rich extract from leaves of the medicinal plant <i>Antirhea borbonica</i>: toxicity assay determination in zebrafish embryos and larvae</b> .....	107
<b>Chapter 3: Impaired brain homeostasis and neurogenesis in diet-induced overweight zebrafish: a preventive role from <i>A. borbonica</i> extract</b> .....	127
<b>Chapter 4: Aqueous extract of <i>Psiloxylon mauritianum</i> prevents obesity and associated deleterious effects in zebrafish (ready to submit)</b> .....	147
<b>Chapter 5: Zebrafish: A new promise to study the impact of metabolic disorders on the brain (submitted manuscript)</b> .....	178
<b>Discussion</b> .....	209
<b>A. Metabolic diseases: is there a brain microvascular complication?</b> .....	211
1. Diabetes and obesity induce brain oxidative stress: impact on BBB function and brain homeostasis .....	211
2. Diabetes and obesity induce brain inflammation: impact on BBB function and brain homeostasis .....	215
3. Cognitive decline as a result of microvascular complications: what about NSCs?.....	218
<b>B. Why do medicinal plants, <i>A. borbonica</i> and <i>P. mauritianum</i>, show different beneficial effects? comparison of the polyphenolic composition and the mode of action of the two aqueous extracts</b> .....	221
<b>C. Advanced steps beyond: From zebrafish to preclinical models</b> .....	226
<b>Conclusion</b> .....	229
<b>ANNEX</b> .....	231
<b>Annex 1</b> .....	233
<b>Annex 2</b> .....	251
<b>References</b> .....	277



## Résumé

L'obésité est une épidémie mondiale qui entraîne de nombreux problèmes de santé et constitue un facteur de risque pour le développement du diabète de type 2. A la Réunion, ces maladies sont largement répandues dans la population. L'obésité et le diabète ont en commun plusieurs perturbations métaboliques et sont impliqués dans la perte de l'homéostasie et de la plasticité cérébrales, contribuant au développement de troubles cognitifs. Les mécanismes à l'origine de ces altérations au niveau central ne sont pas bien compris. En outre, aucune thérapie n'a encore été établie pour prévenir les perturbations du cerveau dans ces pathologies.

L'objectif de cette thèse est d'étudier l'impact de l'obésité/du diabète sur l'homéostasie et la plasticité du cerveau, puis de contrecarrer ces effets délétères à l'aide d'extraits de plantes médicinales réunionnaises. Pour ce faire, nous avons mis en place un protocole d'obésité induite par un régime alimentaire (DIO) chez le poisson zèbre (*Danio rerio*). Ce dernier apparaît comme un modèle pertinent pour mimer les perturbations métaboliques associées à l'obésité et au diabète, mais aussi pour étudier l'homéostasie et la plasticité cérébrale (ex : barrière hémato-encéphalique (BHE) et neurogenèse).

Notre modèle DIO, établi par une surnutrition de poissons adultes pendant 4 semaines, a entraîné des troubles métaboliques et une perte d'homéostasie du système nerveux central (SNC). En effet, les poissons DIO présentaient une augmentation du poids corporel, et de l'indice de masse corporelle (IMC), une hyperglycémie, une stéatose hépatique et un déséquilibre de la balance redox. Dans le SNC, nous avons observé une augmentation de la perméabilité de la BHE, une neuro-inflammation, un stress oxydatif et une diminution de la neurogenèse. De plus, un changement de comportement locomoteur a été observé chez les poissons obèses.

Dans une autre étape, nous avons étudié les possibles propriétés bénéfiques de deux plantes réunionnaises inscrites à la pharmacopée française : *Antirhea borbonica* (*A. borbonica*) et *Psiloxylon mauritianum* (*P. mauritianum*). Ces deux plantes sont traditionnellement utilisées pour leurs effets positifs sur les perturbations métaboliques : effets « anti-diabétiques » pour *A. borbonica* et « anti-cholestérolémiques » pour *P. mauritianum*. Cependant, les données scientifiques soutenant ces propriétés font cruellement défaut.

Tout d'abord, l'analyse chimique de l'extrait aqueux d'*A. borbonica* et de *P. mauritianum* a révélé une abondance en polyphénols corrélée à leurs propriétés antioxydantes. L'analyse par chromatographie en phase liquide avec spectrométrie de masse en tandem (LC-MS/MS) nous a permis de déterminer la nature des composés polyphénoliques de chaque extrait. Ensuite, nous avons réalisé des tests de toxicité selon la ligne directrice 36 de l'OCDE (Organisation de coopération et de développement économiques) (OCDE, 2013). Ceci nous a permis de définir une concentration maximale non toxique pour chaque extrait.

Le traitement avec l'extrait aqueux d'*A. borbonica* pendant les 4 semaines du protocole de surnutrition (DIO) a démontré des propriétés préventives contre les effets délétères de la suralimentation sur le SNC. En effet, *A. borbonica* a préservé la fonctionnalité de la BHE, a empêché l'augmentation du stress oxydatif cérébral et de la neuro-inflammation, mais a également normalisé la neurogenèse dans certaines régions.

De même, l'extrait aqueux de *P. mauritianum* a été testé sur des poissons adultes surnutris (DIO) et sur des larves traitées par un régime riche en graisse (HFD). Le traitement avec *P. mauritianum* a empêché l'accumulation de lipides chez les larves HFD. De plus, il a évité l'augmentation du poids corporel, de l'IMC, de la glycémie et le développement d'une stéatose hépatique chez les poissons DIO. De plus, *P. mauritianum* a montré un effet protecteur sur le SNC, probablement grâce à ses propriétés anti-obésogène de poids. Nous émettons l'hypothèse que *P. mauritianum* pourrait affecter de manière importante l'absorption et le métabolisme des lipides, probablement en modulant le microbiote intestinal.

En conclusion, au cours de cette thèse, nous avons développé un modèle de surnutrition (DIO) simple et rapide induisant des perturbations périphériques et centrales similaires à celles rencontrées chez les mammifères. Pour la première fois, nous avons étudié la toxicité d'un extrait aqueux des deux plantes médicinales *A. borbonica* et *P. mauritianum*. Nous avons confirmé leurs effets bénéfiques à des concentrations non toxiques sur différents paramètres métaboliques et sur le cerveau en utilisant un modèle de poisson zèbre présentant des caractéristiques d'obésité et de prédiabète. Ensemble, ces données mettent en valeur l'utilisation du poisson zèbre pour mimer des maladies métaboliques et pour cribler des propriétés d'intérêts d'extraits de plantes médicinales.

**Mots-clés :** barrière hémato-encéphalique, diabète, inflammation, neurogenèse, obésité, stress oxydatif, système nerveux central,



## Abstract

Obesity is a worldwide epidemic leading to many health concerns and is a risk factor for the development of type 2 diabetes. In Reunion Island, obesity and diabetes are widely spread among the population. Both diseases share several metabolic disorders and have been recently implicated in deteriorating brain health, contributing to cognitive impairments. The mechanisms behind the onset of altered brain homeostasis are not well understood. Besides, no therapy has yet been established to prevent brain disruptions.

The aim of this thesis is to study the impact of obesity/prediabetes on brain homeostasis and cerebral plasticity, and then to alleviate these deleterious effects using medicinal plants from Reunion Island. To this end, we set up a diet-induced obesity (DIO) protocol in zebrafish (*Danio rerio*). Zebrafish recently emerges as a relevant model to mimic metabolic diseases (obesity and diabetes), and to investigate brain homeostasis and plasticity (i.e., blood-brain barrier (BBB) and neurogenesis).

Our DIO model, established by overfeeding adult zebrafish for 4 weeks, resulted in metabolic disorders and loss of central nervous system (CNS) homeostasis. Indeed, DIO fish displayed increased body weight and body mass index (BMI), hyperglycemia, liver steatosis and disturbed redox balance. In the central nervous system, overfeeding led to BBB leakage, neuro-inflammation, cerebral oxidative stress and decreased neurogenesis. As well, a change in the locomotor behavior was observed in obese fish.

In a next step, we tested the potential beneficial properties of two Reunionese plants registered in the French pharmacopeia: *Antirhea borbonica* (*A. borbonica*) and *Psiloxylon mauritianum* (*P. mauritianum*). Both plants were traditionally used for their positive effects on metabolic disruptions as “anti-diabetic” effects for *A. borbonica* and “anti-lipidemic” for *P. mauritianum*. However, the scientific data supporting these properties are lacking.

First, the chemical analysis of aqueous extract of *A. borbonica* and *P. mauritianum* revealed their abundance in polyphenols, correlated to their antioxidant properties. LC-MS/MS analysis was used to determine the nature of the polyphenolic compounds in each extract. Next, we performed toxicity assays using OECD guidelines 36 (Organization for Economic Co-operation and Development) (OECD, 2013) and defined a maximum non-toxic concentration for each extract.

The overnight treatment with aqueous extract of *A. borbonica* (0.5g/L) during the DIO protocol demonstrated its preventive properties against the deleterious effects on the CNS induced by overfeeding. Indeed, *A. borbonica* preserved the BBB function, prevented the increase in cerebral oxidative stress, neuro-inflammation and normalized neurogenesis.

Similarly, the aqueous extract of *P. mauritianum* (0.25 g/L) was tested on adult DIO zebrafish and in high-fat diet (HFD) treated larvae. The treatment avoided lipid accumulation in HFD larvae. It also prevented body weight increase, BMI, hyperglycemia and liver steatosis in adult DIO zebrafish. Furthermore, brain homeostasis seems to be preserved probably through *P. mauritianum* anti-weight gain properties. We suggested that *P. mauritianum* could significantly affect lipid absorption and metabolism possibly through the modulation of gut microbiota.

In conclusion, during this thesis, we have developed a simple and rapid overfeeding (DIO) model inducing peripheral and CNS disruptions similar to those encountered in mammals. For the first time, we studied the toxicity of aqueous extract of the two medicinal plants *A. borbonica* and *P. mauritianum*. We confirmed their beneficial effects on different metabolic parameters and on the brain using zebrafish model of obesity and prediabetes. Together, these data highlight the use of zebrafish to mimic metabolic diseases and to screen the beneficial properties of medicinal plants extracts.

**Key words:** blood-brain barrier, central nervous system, diabetes, inflammation, neurogenesis, obesity, oxidative stress.

## List of scientific publications

### Publications related directly to this research study

- **Ghaddar B**, Veeren B, Rondeau P, Bringart M, Lefebvre d'Hellencourt C, Meilhac O, Bascands JL, Diotel N  
Impaired brain homeostasis and neurogenesis in diet-induced overweight zebrafish: a preventive role from *A. borbonica* extract. *Sci Rep* Sep 2;10(1):14496. (2020)
- Veeren B, **Ghaddar B**, Bringart M, Khazaal S, Gonthier MP, Meilhac O, Diotel N, Bascands JL.  
Phenolic Profile of Herbal Infusion and Polyphenol-Rich Extract from Leaves of the Medicinal Plant *Antirhea borbonica*: Toxicity Assay Determination in Zebrafish Embryos and Larvae. *Molecules* Sep 29;25(19):4482. (2020)
- **Ghaddar B**, Bringart M, Lefebvre d'Hellencourt C, Meilhac O, Diotel N.  
Deleterious Effects of Overfeeding on Brain Homeostasis and Plasticity in Adult Zebrafish. *Zebrafish* May 21;18(3):190-206. (2021)
- **Ghaddar B**, Gence L, Veeren B, Bringart M, Bascands JL, Meilhac O, Diotel N.  
Aqueous extract of *Psiloxylon mauritianum* prevents obesity and associated deleterious effects in zebrafish. *IJMC* (submitted). (2022)
- **Ghaddar B**, Diotel N.  
Zebrafish: A new promise to study the impact of metabolic 2 disorders on the brain. *IJMC* (review; submitted). (2022)

### Publications associated with this research study

- **Ghaddar B**, Lübke L, Couret D, Rastegar S, Diotel N.  
Cellular Mechanisms Participating in Brain Repair of Adult Zebrafish and Mammals after Injury. *Cells* Feb 14;10(2):391. (review). (2021)
- Cassam-Sulliman N, **Ghaddar B**, Gence L, Patche J, Rastegar S, Meilhac O, Diotel N.  
HDL biodistribution and brain receptors in zebrafish, using HDLs as vectors for targeting endothelial cells and neural progenitors. *Sci Rep* Mar 19;11(1):6439. (2021)

## List of figures

Figure 1: Body mass index illustration as an easy tool to estimate overweight and obesity. ....	19
Figure 2: Obesity and diabetes prevalence in the World, Europe and Reunion Island.....	21
Figure 3: The impact of obesity on different domains of health including the physical, mental, social and the spiritual ones. Adapted from (Djalalinia et al., 2015). ....	22
Figure 4: Common health conditions related to obesity. ....	24
Figure 5: Nonalcoholic fatty liver (NAFL) as a result of obesity. ....	25
Figure 6: Common health conditions related to diabetes. ....	28
Figure 7: Mechanisms of reactive oxygen species (ROS)-induced endothelial dysfunction in response to hyperglycemia leading to potential stroke. ....	30
Figure 8: Schematic representation of insulin secretion by the beta pancreatic cells in response to high blood glucose levels and insulin dependent glucose uptake by the tissues. ....	31
Figure 9: Development of insulin resistance in case of obesity due to the increased plasma free fatty acids and adipokines secreted from the saturated adipocytes. ....	32
Figure 10: Cellular constituents of the blood-brain barrier. ....	34
Figure 11: The close proximity between the neural stem cells and the blood vessels in the neurogenic subventricular zone in the brain of mouse. ....	35
Figure 12: Effects of obesity on the BBB and the brain.....	38
Figure 13: Blood-brain barrier permeability comparison between diabetic and control rats.....	39
Figure 14: Mechanisms suggested for the blood-brain barrier destruction in type 2 diabetes. ....	40
Figure 15: Examples of brain MRI of normal individual and individual of high body fat percentage...	41
Figure 16: Brain maps of the associations between BMI and cortical thickness. ....	42
Figure 17: Comparison of T2DM brain subjects with non-diabetic ones in term of functional connectivity and brain volume.....	43
Figure 18: Schematic representation of neurogenesis in the central nervous system of embryonic vertebrates. ....	45
Figure 19: The dentate gyrus and subventricular zone neurogenic niches of the adult mammalian brain. ....	47
Figure 20: Different regulators of adult neurogenesis. ....	48
Figure 21: Notch signaling pathway in zebrafish and mouse.....	49
Figure 22: Number of surviving neural progenitors in the WKY and GK rats.....	51
Figure 23: The advantages of using zebrafish model in science during all its developmental stages (embryo, larva and adult).....	53
Figure 24: Conservation of organ systems between zebrafish and humans and orthologue genes shared between the zebrafish, human, mouse and chicken genomes.....	54
Figure 25: Organ regeneration in the zebrafish. ....	54
Figure 26: The use of zebrafish in biomedical research articles has been rising since the early 1990s. ....	55
Figure 27: Three-dimensional Micro-computed tomography analysis in normally versus diet-included obesity models of zebrafish. ....	57
Figure 28: Adult zebrafish pancreas in comparison to human pancreas.....	59
Figure 29: Main brain subdivisions and neurogenic niches of zebrafish and mammalian brain. ....	62
Figure 30: Marker expression and morphology of distinct cell types at the ventricular zone of the telencephalon.....	63
Figure 31: Cell composition of the neurogenic niches in zebrafish, mice and humans. ....	64
Figure 32: Brain-brain barrier formation during early stages of development in the zebrafish.....	66



Figure 33: Major Food Bioactive Compounds sources and classification. ....	67
Figure 34: Classification and structure of polyphenols. ....	68
Figure 35: Beneficial effects of dietary polyphenols. ....	69
Figure 36: Neuroprotective intracellular signaling pathways conferred by polyphenols. ....	70
Figure 37: Major plants polyphenol and their beneficial health effects. ....	72
Figure 38: Medicinal plants in the Reunion Island registered in the French pharmacopeia. ....	74
Figure 39: <i>Antirhea borbonica</i> beneficial effects from traditional background and recent scientific records. ....	76
Figure 40: <i>Psiloxylon mauritianum</i> beneficial effects from traditional background and recent scientific records. ....	77
Figure 41: The molecular pathways of hyperglycemia induced oxidative stress production. ....	212
Figure 42: The blood–brain barrier (BBB) and oxidative stress. ....	213
Figure 43: pathways od neuronal degeneration as a result of hyperglycemia induced oxidative stress. ....	215
Figure 44: Model of neuro-inflammation and neurodegeneration cycle. ....	216
Figure 45: Simplified diagram of the microarchitecture of a neurogenic niche in the adult brain. ....	219
Figure 46: Pathophysiological links between T2DM and AD. ....	220
Figure 47: Obesity and diabetes contributing to microvascular complications. ....	221
Figure 48: Comparison of the polyphenolic content from the aqueous extracts of <i>A. borbonica</i> and <i>P. mauritianum</i> . ....	223
Figure 49: Gallic acid treatment improves body metabolism parameters in HFD mice. ....	225

## List of tables

Table 1: Description of the different types of diabetes. ....	20
---	----

## List of abbreviations

- AD:** Alzheimer's disease
- AGE:** advanced glycated end products
- AGE-R:** advanced glycated end products receptor
- AKT:** Alpha serine/threonine kinase
- Ascl:** Achaete-scute like
- A $\beta$ :**  $\beta$ -amyloid
- BBB:** blood-brain barrier
- BDNF:** brain derived neurotrophic factor
- BMI:** body mass index
- BMP:** bone morphogenetic Protein
- CNS:** central nervous system
- CRP:** C-reactive protein
- CSF:** cerebrospinal fluid
- DG:** dentate gyrus
- DIO:** diet-induced obesity
- fabp4:** fatty acid binding protein
- FFA:** free fatty acids
- Fgf:** Fibroblast growth factor
- GAE:** Gallic Acid Equivalent
- GLUT:** glucose transporter
- GPx:** glutathione peroxidase
- HDL:** high-density lipoproteins
- Hes:** hairy/enhancer of split
- HFD:** high-fat diet
- 4-HNE:** 4-hydroxynonenal
- IGF-IR:** insulin-like growth factor type 1 receptor
- IL-1 $\beta$ :** interleukin 1 beta
- IL-6:** interleukin 6

**IL-8:** interleukin 8

**IR:** insulin receptor

**IPGTT:** and intraperitoneal

**I $\kappa$ B:** IkappaB kinase complex

**LDL:** low-density lipoproteins

**MRI:** magnetic resonance imaging

**NAFLD:** nonalcoholic fatty liver disease

**NF $\kappa$ B:** nuclear factor kappa B

**NICD:** Notch intracellular domain

**NO:** nitric oxide

**NSC:** neural stem cells

**OB:** olfactory bulb

**OECD:** Organization for Economic Co-operation and Development

**OGTT:** oral glucose tolerance test

**PCNA:** proliferating cell nuclear antigen

**PI3K:** Phosphoinositide 3-kinase

**PKC:** protein kinase C

**Pparg:** peroxisome-proliferator activated receptor gamma

**RMS:** rostral migratory stream

**ROS:** reactive oxygen species

**SFA:** saturated fatty acids

**SGZ:** subgranular zone

**SOD:** superoxide dismutase

**Sox:** sex determining region Y-box

**STZ:** streptozotocin

**SVZ:** subventricular zone of the lateral ventricles

**T2DM:** type 2 diabetes mellitus

**TNF $\alpha$ :** tumor necrosis factor- $\alpha$

**WHO:** world health organization

**Wnt:** wiggless-related integration site





## General introduction

Obesity is a major health concern worldwide especially after the endemic values it reaches. Obesity is known to induce health complications as cardiovascular diseases, kidney diseases, liver steatosis and is a risk factor for developing type 2 diabetes mellitus (T2DM). The obese subjects are mostly considered in a prediabetic or a diabetic state due to the common metabolic disorders shared between obesity and T2DM. In addition, both obesity and diabetes are blamed for deteriorating the brain health. Dementia, cognitive impairments, development of Alzheimer's disease and stroke are all at higher risk percentages in case of obesity and diabetes. Until now, these brain complications occur under not-well understood conditions and the treatments in this domain are limited. Thus, it is crucial to further investigate the mechanisms that lead to the development of these complications in the context of metabolic diseases such as obesity and diabetes. To this end, several animal models had been established, among them the diet-induced obesity and high-fat diet-induced obesity models.

Zebrafish is an attractive model to explore brain disorders resulting from metabolic diseases. Indeed, it can be used to develop obesity and prediabetic states under diet-induced obesity or chronic glucose exposure protocols. In addition, the health outcomes induced by such experimental procedures are similar to their mammalian counterparts. Similarly, zebrafish is widely used to investigate brain homeostasis, namely blood-brain barrier and neurogenesis.

Nowadays, several lines of evidences are documenting the potential beneficial role of polyphenols, naturally occurring secondary metabolites in food and plants, in the treatment of metabolic disorders resulting from obesity and/or diabetes. In Reunion Island, medicinal plants registered in the French pharmacopeia have been shown to be rich in polyphenols. These plants are traditionally used by the local population to combat several disorders resulting among others from obesity and diabetes. In this context, *Antirhea borbonica* (*A. borbonica*) and *Psiloxylon mauritianum* (*P. mauritianum*) are two Reunionese medicinal plants with traditional “antidiabetic” and anti-lipidemic” properties. Some data from our laboratory proved antioxidant and protective properties of these plants in different experimental models. Nevertheless, further investigations are required to confirm this suggested “antidiabetic” and “anti-lipidemic” properties.

Therefore, this study aims to develop a relevant diet-induced obesity model using zebrafish. After characterizing the deleterious impact of overfeeding on the body and on the

brain, we investigated the potential beneficial effects of the aqueous extract of these two medicinal plants, *A. borbonica* and *P. mauritanum*, in combating the negative outcomes of obesity/prediabetic state at the periphery and in the central nervous system.

# Introduction





# I. Health risks of obesity and diabetes

## A. General knowledge on the epidemics

### 1. Obesity definition

Obesity, as well as overweight, is defined as abnormal or excessive fat accumulation presenting health risks according to the World Health Organization (WHO, 2016a; Blucher, 2020). It is a complex health issue resulting from a combination of factors including individual, behavioral and genetic ones. Obesity is associated with bundle of complications involving several metabolic disorders resulting from excess accumulation of body fats. The body mass index (BMI) appears as reliable and easy indicator of body fatness for most people, using simply the height and weight measurements ( $\text{kg}/\text{m}^2$ ) (Gray & Fujioka, 1991). Thus, individuals with BMI ranging between 25 and  $30 \text{ kg}/\text{m}^2$  are classified as overweight and those above  $30 \text{ kg}/\text{m}^2$  are obese (WHO, 2021) (Fig. 1).

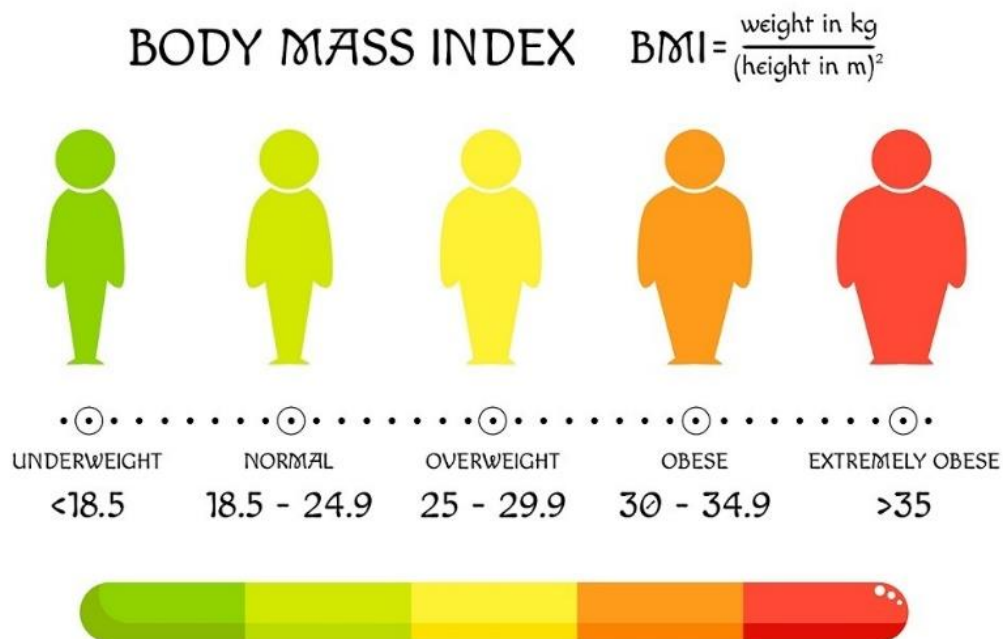


**Figure 1: Body mass index illustration as an easy tool to estimate overweight and obesity.**

The body mass index (BMI) is calculated by dividing the body weight in Kg on the square of the height in  $\text{m}^2$ . Individuals with BMI below  $18.5 \text{ Kg}/\text{m}^2$  are considered underweight, between  $18.5\text{-}24.9 \text{ Kg}/\text{m}^2$  are normal weight, between  $25\text{-}29.9 \text{ Kg}/\text{m}^2$  are overweight, between  $30\text{-}34.9 \text{ Kg}/\text{m}^2$  are obese and above  $35 \text{ Kg}/\text{m}^2$  are considered extreme obese. References: <https://www.istockphoto.com>.

## 2. Diabetes definition

Diabetes is a chronic metabolic disorder characterized by a hyperglycemic state and is defined by fasting blood glucose exceeding 126 mg/dL (7 mmol/L). There are many different types of diabetes. Type 1 diabetes corresponds to an autoimmune disease destroying the beta cells of the pancreas. It consequently leads to a lack of insulin (insulinopenia), the main glucose-lowering hormone, and so to hyperglycemia (Redondo *et al.*, 2020). This pathology accounts for approximately 10% of diabetes. In contrast, type 2 diabetes mellitus (T2DM) represents almost 90% of diabetes and is induced by insulin resistance in which the cells do not respond correctly to insulin over time (Harreiter & Roden, 2019). This will progressively lead to a possible insulinopenia aggravating the resulting hyperglycemia. In addition to type 1 and type 2 diabetes, many other diabetic states have been described: (i) gestational diabetes that develops during pregnancy in the 2<sup>nd</sup> or the 3<sup>rd</sup> trimester and it could increase the risk of developing type 2 diabetes later in the life of the child (Coustan, 2013), (ii) monogenic diabetes (neonatal or MODY -Maturity Onset Diabetes of the Young) that is due to a strong genetic risk factor developing during adolescence and does not always require insulin, the treatment depends mostly on the location of the mutation that is in any of at least 14 different genes (Shepherd *et al.*, 2016; Shields *et al.*, 2017), and (iii) other diabetic reasons are referred to pancreatic exocrine diseases and chemical/drug induced diabetes (Redondo *et al.*, 2020) (Table 1). According to WHO, the normal fasting blood glucose should be between 70 mg/dL (3.9 mmol/L) and 100 mg/dL (5.6 mmol/L). A fasting blood glucose comprised between 100 to 125 mg/dL (5.6 to 6.9 mmol/L) is considered as a pre-diabetic state. As mentioned above, in case of diabetes, the fasting blood glucose exceeds 126 mg/dL (WHO, 2016e).

**Table 1: Description of the different types of diabetes.**

*Adapted from (Redondo et al., 2020).*

Type	Description
Type 1 diabetes	Autoimmune beta cell destruction, usually leading to absolute insulin deficiency
Type 2 diabetes	Progressive loss of adequate insulin secretion, frequently with insulin resistance
Gestational diabetes	Diagnosed in the second or third trimesters, without overt diabetes prior to gestation
Monogenic diabetes	There are two subgroups: MODY, and neonatal diabetes
Disease of the exocrine pancreas	Pancreatitis, cystic fibrosis, and other disorders of the pancreas.
Chemical or drug induced	Caused by glucocorticoids, HIV/AIDS drugs, organ transplantation drugs

### 3. Prevalence of obesity and diabetes

Obesity and diabetes, that are considered by World Health Organization as global epidemics, affect at least 650 million and 422 million people worldwide, respectively (WHO, 2016d). In Europe, around 50% of the population are overweight (Marques *et al.*, 2018) and 10% are diabetic (WHO, 2016b).

In Reunion Island, a French overseas department in the Indian Ocean, the prevalence of obesity and diabetes is high among the population. Around 45% of Reunionese are overweight, of which 28% are overweight and 16% are obese (Thibault, 2019). Similarly, the prevalence of diabetes among the Reunionese population is also high, with around 10% of the population estimated to be diabetic (clés, 2019).

Obesity increases the mortality risk due to the cardiovascular complications (Whitlock *et al.*, 2009). Diabetes similarly leads to high number of annual deaths so that by 2019, 1.5 million deaths were attributed directly due to diabetes (WHO, 2016c). Due to the real threats of these two linked diseases on health, there is a serious global goal to restrict the wide and fast spread of obesity and diabetes by 2025 (WHO, 2016d) (Fig. 2).

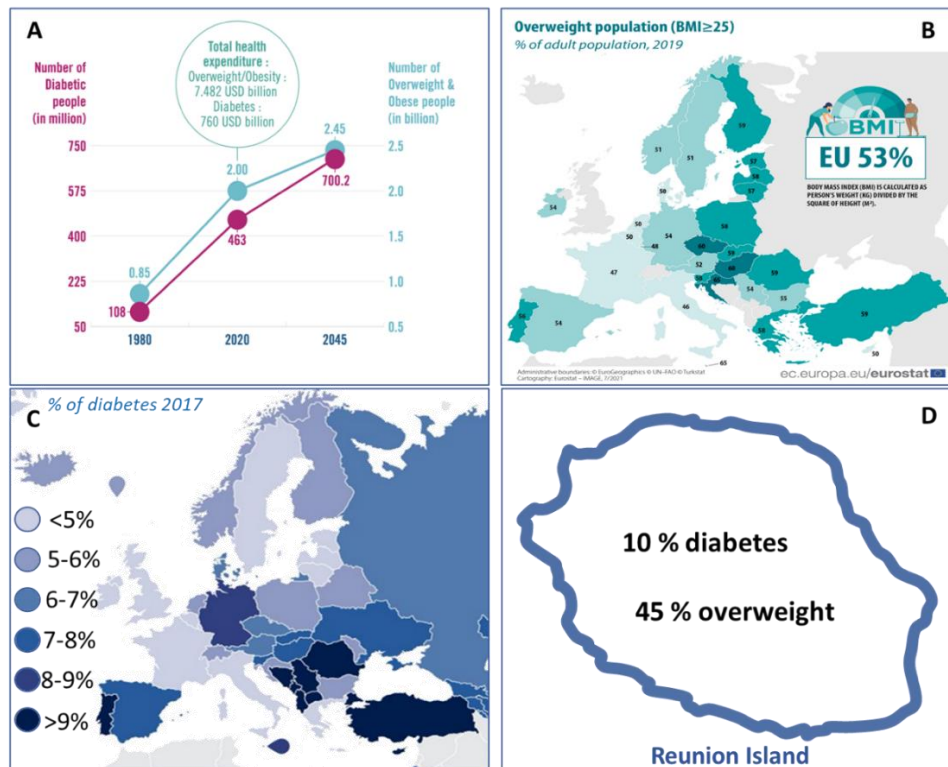


**Figure 2: Obesity and diabetes prevalence in the World, Europe and Reunion Island.**

(A) Graph showing the increase in the number of diabetic and obese people worldwide from 1980 until 2045, with the total health expenditure of both diseases. (B) European map showing the percentages of overweight individual

in the population. The highest percentages are found in Malta and Croatia (59%) and the lowest in Italy (46%) and France (47%) in 2019. (C) European map showing the percentage of diabetic individual (20-79 years) in the population. It varies from 5 to 9% among the countries in 2017. (D) The percentages of the overweight/obese and diabetic individuals among the population in the Reunion Island. References: (A) <https://www.a-mansia.com/obesity-and-diabetes-in-the-world/>; (B) Over half of adults in the EU are overweight - [ec.europa.eu/Eurostat](http://ec.europa.eu/Eurostat); (C) DiabetesAtlas <http://diabetesatlas.org>; (D) (clés, 2019; Thibault, 2019).

## B. Effects of metabolic disorders on the body physiology

### 1. Obesity effects on the body

Obesity induces many adverse effects on body and impacts health at different levels: physical, mental, social and spiritual (Djalalinia *et al.*, 2015) (Fig. 3). Beside the physical burden that will be explained more in details later, obesity leads in different domains to discrimination and social bias with a direct effect for some individuals at their self-esteem, mood disorders and even motivational disorders. Being at sometimes suffering from society rejection, ridicule and humiliation from the surrounding or the public impact their quality with outcomes on their personalities that could be more pronounced than the physical effect on health (Fig. 3) (Djalalinia *et al.*, 2015).

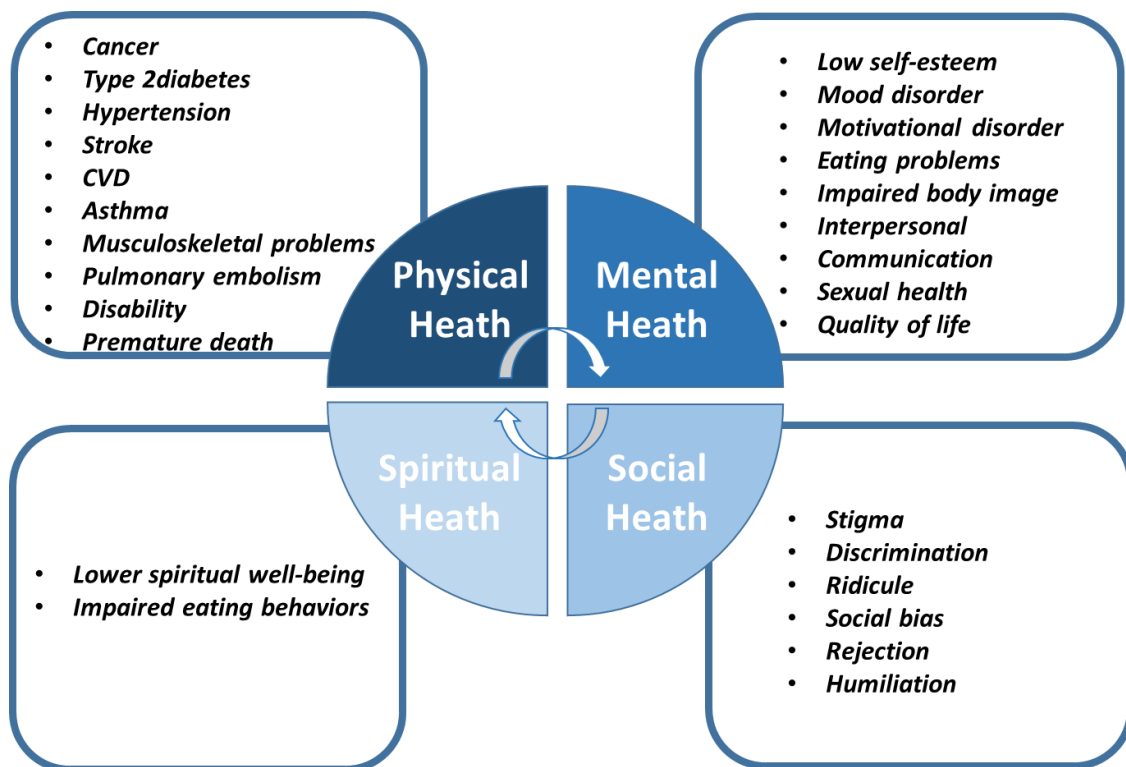


**Figure 3:** The impact of obesity on different domains of health including the physical, mental, social and the spiritual ones. Adapted from (Djalalinia *et al.*, 2015).

Concerning the effect of overweight and obesity on the physical health, the excessive adiposity in high BMI individuals alters the metabolism of some lipoproteins (Stadler & Marsche, 2020), inflammatory pathways (Saltiel & Olefsky, 2017) and even epigenetic regulations such as DNA methylation (Wahl *et al.*, 2017). It leads to many physiological disorders including hypertension, dyslipidemia, insulin resistance and hyperglycemia that could lead to severe complications affecting the physiology of key organs including the heart, the liver, the kidney and the lungs (Ramon-Arbues *et al.*, 2019). Figure 4 provides an overview of the consequences of overweight and obesity on almost all body systems and physiology. Briefly, obesity has a deleterious impact on (i) the central nervous system with an increased occurrence of strokes, dementia and depression, (ii) the respiratory system resulting in breathing complications, (iii) the digestive tract causing several types of cancers and excess fat building in the liver, (iv) the cardiovascular system with increasing risk of heart attack and atherosclerosis, (v) the urinary system favoring kidney failure, and also (vi) on the reproductive system leading sometimes to pregnancy difficulties. In addition, obesity weakens the muscles and the bones leading to disabilities, fractures and joint pains (Sethi, 2020).

Among these complications, 41% of the BMI related deaths in obese individuals are caused by the cardiovascular diseases (Collaborators *et al.*, 2017; Henning, 2018). This relation is mainly due to the high adiposity and excess in body fats because of the high-fat intake (Stefan, 2020) as explained below. Indeed, in healthy condition, the adipose tissue secretes hormones called adipokines (i.e., leptin, adiponectin) that have pleiotropic effects and notably a protective one on the myocardium. However, in case of obesity, the endocrine function of adipose tissue is disrupted with increased leptin secretion and reduced adiponectin one causing several cardiovascular problems (Fortuno *et al.*, 2003; Jung & Choi, 2014). In parallel, the adipose tissue in case of obesity secretes proinflammatory cytokines as interleukin-1 $\beta$ , interleukin-8 (IL-1 $\beta$  and IL-8) and tumor necrosis factor- $\alpha$  (TNF $\alpha$ ) that impairs the cardiac functions (Elagizi *et al.*, 2018). Alpert and his colleagues reviewed in details the impact of obesity on the heart at different levels including the cardiac morphology, cardiac performance and metabolic alterations that results finally in heart failure (Alpert *et al.*, 2014). In brief, echocardiographic analysis show that obese patients have an increased left ventricle mass and wall thickness (Alpert *et al.*, 2014). Myocardial dysfunction could occur by the accumulation of the excess of fatty acids and triglycerides in the parenchymal cardiac myocytes leading to their dysfunction and death (Alpert *et al.*, 2014). Insulin resistance, hypertriglyceridemia, hyperglycemia,

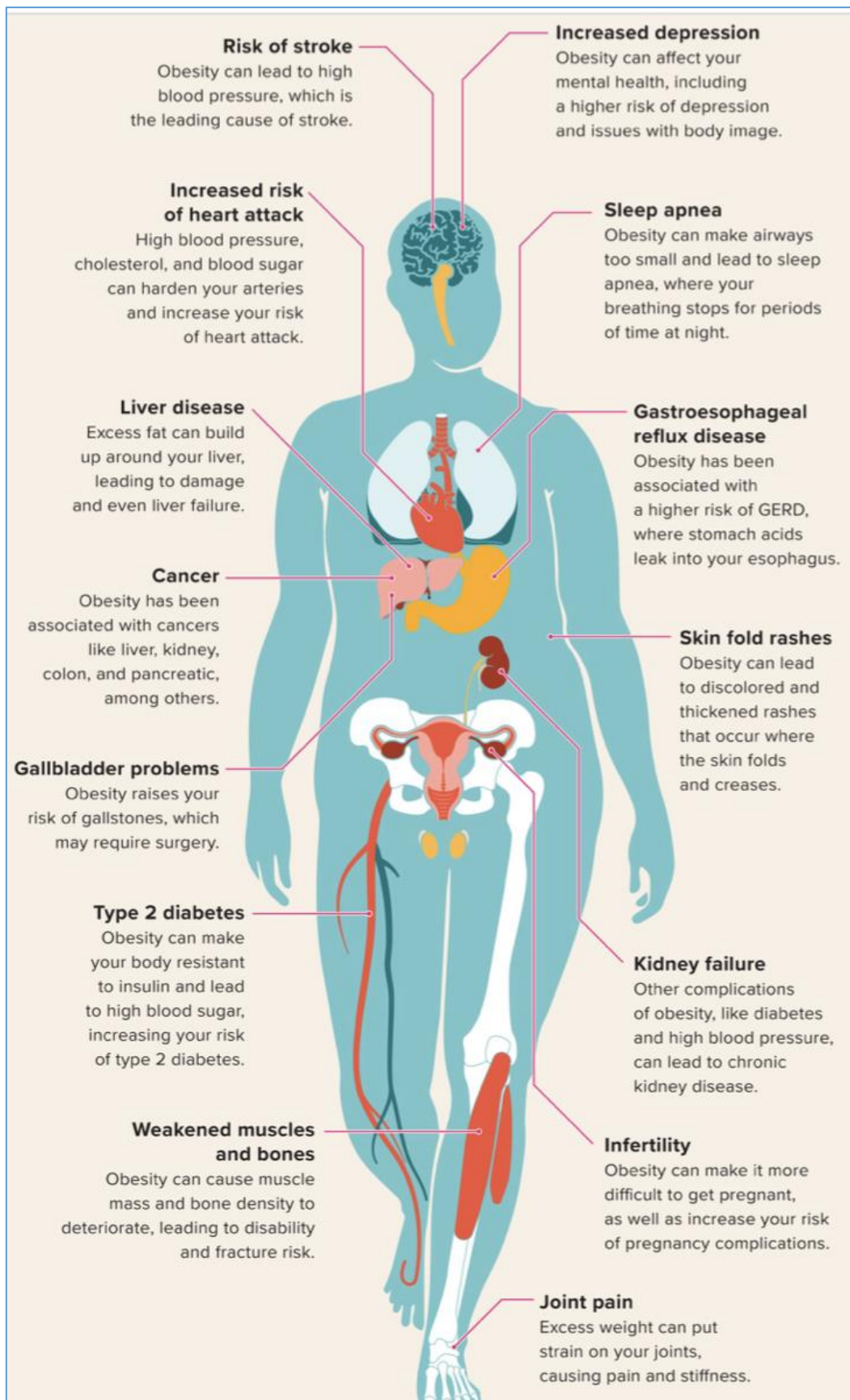


**Figure 4: Common health conditions related to obesity.**

Obesity has negative impacts on all the body systems including the central nervous system, cardiac system, digestive system, respiratory system and the reproductive system. From (Sethi, 2020).



increased low-density lipoproteins (LDL) and decreased high-density lipoproteins (HDL) levels are all factors impairing endothelium dependent vasodilation and vascular smooth muscle dysfunction with increased arterial stiffness; consequently, this situation develops to atherosclerotic vascular changes driving these cardiovascular complications (Papa *et al.*, 2013).

Obese individuals have also a great risk to develop nonalcoholic fatty liver disease (NAFLD) (Ruhl & Everhart, 2003). NAFLD is a liver abnormality condition in which the liver accumulates fatty acid and triglycerides with or without inflammation and fibrosis (Fig. 5) The high level of free fatty acids (FFA) in the blood observed in case of obesity (from the adipose tissue) is proportional to the fat mass in both men and women (Mittendorfer *et al.*, 2009), and represents the excessive uptake of FFA in the liver (Fabbrini *et al.*, 2010). In addition, cirrhosis (cryptogenic cirrhosis) and hepatocellular carcinoma are also associated with obesity (Marchesini *et al.*, 2008).

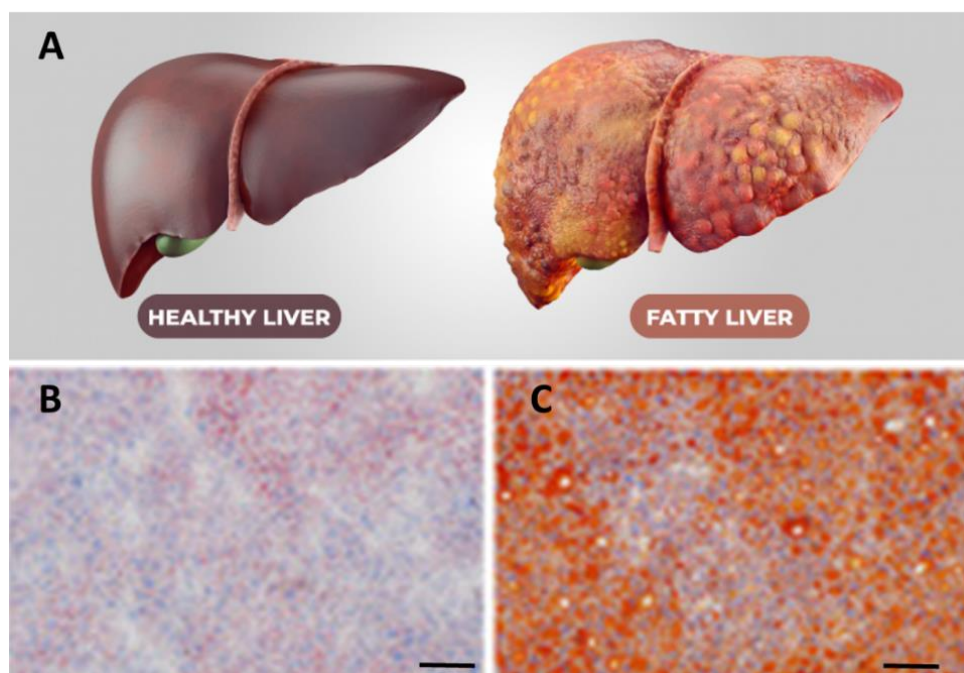


**Figure 5: Nonalcoholic fatty liver (NAFL) as a result of obesity.**

(A) Illustration of healthy human liver and non-alcoholic fatty liver (NAFL). (B) Oil Red O staining of liver sections from normal mice with normal liver and (C) high-fat diet fed mice with NAFL. Note that the red color represents the fat accumulation in the hepatic section of the NAFL. (A) From <https://hunterdongastro.com/non-alcoholic-fatty-liver-disease-nafld/>; (B) From (Li *et al.*, 2020).

Obesity has also a deleterious impact on the kidneys and their function, leading among others to Chronic kidney disease (CKD) (Nehus, 2018), a pathology characterized by a progressive loss of kidney function. Recently, chronic inflammation was associated with



obesity and it was shown that abnormal lipid metabolism can lead to kidney injury (Nehus, 2018). In addition, children with severe obesity display high prevalence of renal abnormalities (i.e., albuminuria and reduced kidney function i.e., the glomerular filtration rate GFR) associated with kidney injuries (Nehus, 2018). Furthermore, the glomerular filtration rate (GFR) of the kidneys appeared to be lower at higher BMI according to large population-based studies (Foster *et al.*, 2008). Obesity is also a risk factor for kidney malignancies and nephrolithiasis (kidney stones), corresponding to hard deposits of minerals and salts formed inside the kidneys (Curhan *et al.*, 1998; Bhaskaran *et al.*, 2014).

Other data also demonstrated an impact of obesity on lungs through unclear mechanisms. For instance, obese children and adults have greater risk for asthma disease, that is more severe, and respond less to medications compared to the non-obese asthma patients (Mittendorfer *et al.*, 2009). Obesity also affects mechanically the respiratory function due to the accumulation of fats in the abdominal and thoracic cavities that elevates the diaphragm and increases the pleural pressure (Behazin *et al.*, 2010).

## 2. Obesity and stroke

A pooled analysis on 97 cohort studies with 1.8 million participants have shown that overweight and obesity increased the risk of having stroke compared to normal individuals (excess risk 98% for overweight and 69% for obesity) (Lu *et al.*, 2014). Unfortunately, obesity not only increases the risk factor for stroke occurrence but also worsens the neurological outcomes by exacerbating the ischemic brain injury (Haley & Lawrence, 2016). For instance, it increases the hemorrhagic transformation and microvascular damage (Boillot *et al.*, 2013) as well as the risk of death after ischemic stroke by 40% (Lee *et al.*, 2018). It is probably in links with vascular abnormalities, oxidative stress and chronic inflammation (Stapleton *et al.*, 2008; Beyer *et al.*, 2013; Kozakova *et al.*, 2015). A study conducted by Lee and colleagues in 2021 was aiming to evaluate the effect of the BMI on specific cognitive outcomes 3 months after stroke. In this study the post-ischemic stroke survivors undergo comprehensive standardized neuropsychological test to investigate the effect of BMI on the domain-specific and global cognitive functions. As a result, patients with high BMI (above 25 kg/m<sup>2</sup>) despite having normal global cognitive functions, suffer from lower phonemic and semantic word fluencies (frontal dysfunction: tested by Controlled Oral Word Association Test (COWAT) examination for the verbal fluency) than those with normal BMI (21-23 Kg/m<sup>2</sup>) (Lee *et al.*, 2021).

### 3. Diabetes effects on the body

Diabetes induces many detrimental effects on the body and lead to macrovascular and microvascular complications. The macrovascular complications of type 2 diabetes are represented by cardiovascular diseases (heart attack, stroke, coronary artery disease, cardiomyopathy, arrhythmia and sudden death), cerebrovascular diseases and peripheral vascular disease (Viigimaa *et al.*, 2020). In addition, the microvascular complications of diabetes involve the diabetic nephropathy, retinopathy and neuropathy (Faselis *et al.*, 2020). As in case of obesity, diabetes also disturbs many of the metabolic body functions and damages many organs and tissues such as the brain, eyes, heart and nerves as illustrated below (Fig. 6).

Among these complications, the cardiovascular diseases are considered as the main mortality cause in diabetic individuals (Collaborators *et al.*, 2017; Henning, 2018). Insulin resistance, hyperglycemia, hypertriglyceridemia, high LDL and low HDL levels are all factors impairing endothelium dependent vasodilation and vascular smooth muscle dysfunction with increased arterial stiffness. Consequently, atherosclerotic vascular changes occur and drive cardiovascular complications (Papa *et al.*, 2013). In general, clot formation occurs after a cascade of events due to hyperglycemia that leads to oxidative stress, inflammation, insulin resistance, endothelial dysfunction and coagulation cascade activation (Stegenga *et al.*, 2006; Kaur *et al.*, 2018). In brief, chronic hyperglycemia leads to the formation of advanced glycation end products (AGE) and thus activating their receptors (AGE-R). AGE-R activation increases the superoxide production which decreases nitric oxide (NO) synthesis resulting decreased vasodilation.

In parallel to the macrovascular complications, the chronic hyperglycemic condition in diabetes impacts the microvasculature leading to nephropathy, retinopathy and neuropathy (Faselis *et al.*, 2020). Diabetic nephropathy could lead to end stage renal disease in 50 % of cases (Faselis *et al.*, 2020). Similarly, diabetic retinopathy results from vasculopathy and is the major cause of blindness worldwide (Yau *et al.*, 2012). This disease is mainly attributed to two main causes: diabetic macular edema (impaired central vision) and proliferative diabetic retinopathy that is the formation of new blood vessels in the retina, which can cause significant bleeding (Yau *et al.*, 2012). Finally, diabetic neuropathy results from peripheral nerve dysfunction (Boulton *et al.*, 2004). It affects around 50% of type 2 diabetic patients developing later to Charcot neuroarthropathy, foot ulceration and foot amputation (Hicks & Selvin, 2019).

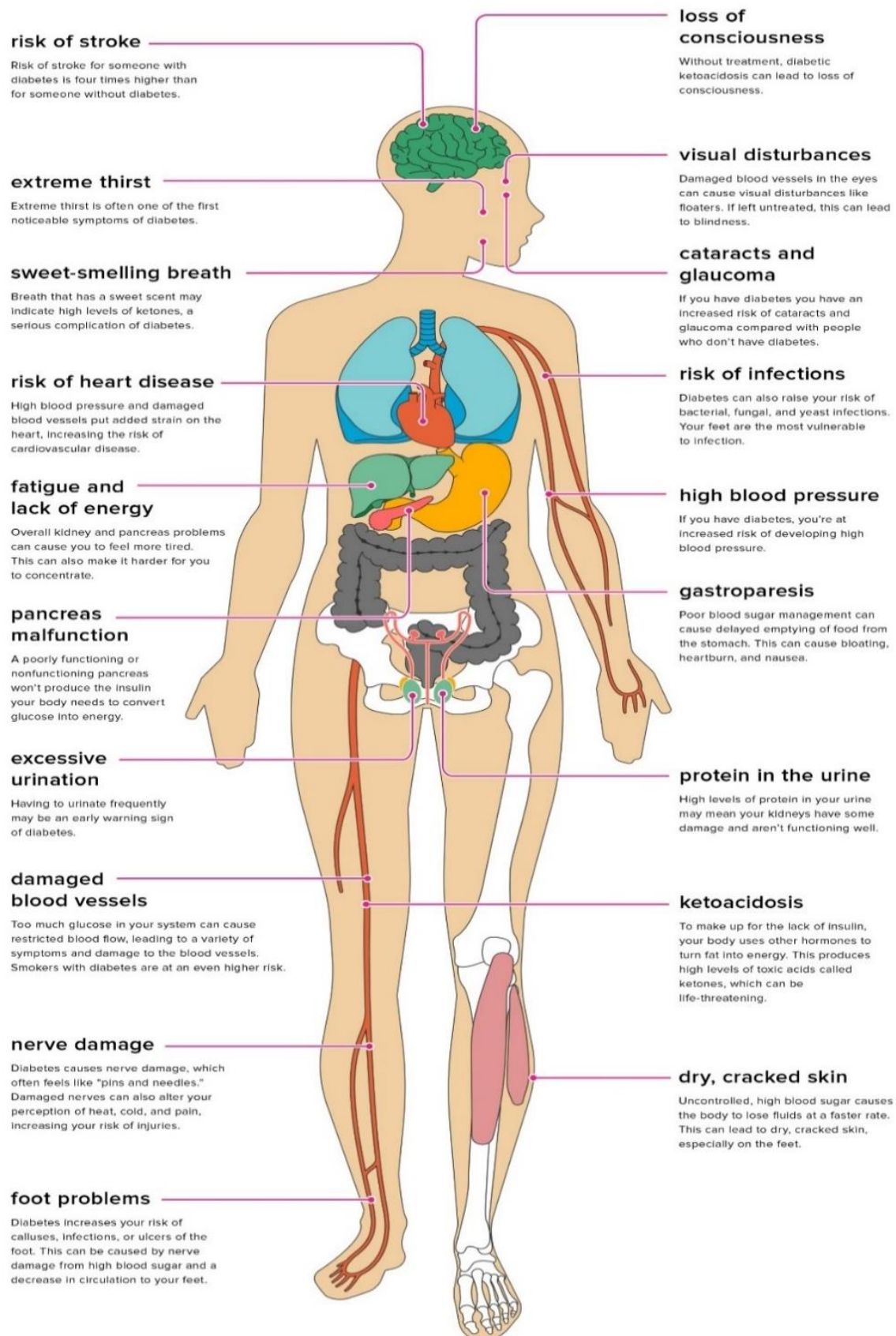


**Figure 6: Common health conditions related to diabetes.**

Diabetes has negative impacts on all the body system including the central nervous system, cardiac system, digestive system, respiratory system and the reproductive system. From <https://www.healthline.com/health/73150>.

#### 4. Stroke in diabetes

Diabetes is also a major risk factor for the initiation and deterioration of the cerebrovascular diseases. Regarding the type of the stroke, diabetic patients are more exposed to the ischemic stroke (x 1.5 to 3 times) (Folsom *et al.*, 1999; Kissela *et al.*, 2005). This type of stroke corresponds to the obstruction of a blood vessel by a blood clot and accounts for almost 80% of stroke (Lithner *et al.*, 1988). As well, the diabetic condition is an aggravating factor for stroke complications and death (Chen *et al.*, 2016). Each 1% increase in glycated hemoglobin (hemoglobin A1c, a biomarker for the presence and severity of hyperglycemia) is faced by a 1.37 times excess risk of stroke related death (UKPDS, 1998), showing the deleterious impact of diabetes on post-stroke survival. In addition, for diabetic patients who survived after stroke, the recovery was slower compared to non-diabetic ones (Jorgensen *et al.*, 1994).

The main factors explaining why diabetic individuals are more prone to have strokes, are briefly explained here (Fig. 7). First, hyperglycemia and hyperinsulinemia (due to insulin resistance) create oxidative stress due to the production of the reactive oxygen species (ROS) that damage the cells including the endothelial ones (Baynes & Thorpe, 1999; Valko *et al.*, 2004; Tangvarasittichai, 2015). The ROS also decreases the production of endothelium derived nitric oxide (NO), leading to vasoconstriction, platelet activation and increasing LDL deposition in the vascular wall (Chen *et al.*, 2018a). Hyperglycemia also increased the advanced glycosylated end products (AGEs) that are glycosylated proteins and lipoproteins. The later bind to their receptors and induce LDL deposition within the vascular wall and increase the expression of atherosclerosis promoting agent genes (adhesion molecules and inflammatory mediators) (Singh *et al.*, 2014). Furthermore, the high glucose concentration promotes its transfer through vessels wall independent of insulin; this consequently allow the activation of polyol pathway that transform glucose to sorbitol. This pathway is known to activate protein kinase C (PKC) isoforms that in turn increases the expression of atherosclerosis promoting genes, decrease vasodilation and damages the endothelial cells favoring thereby stroke occurrence (Ishii *et al.*, 1996; Oyama *et al.*, 2006) .

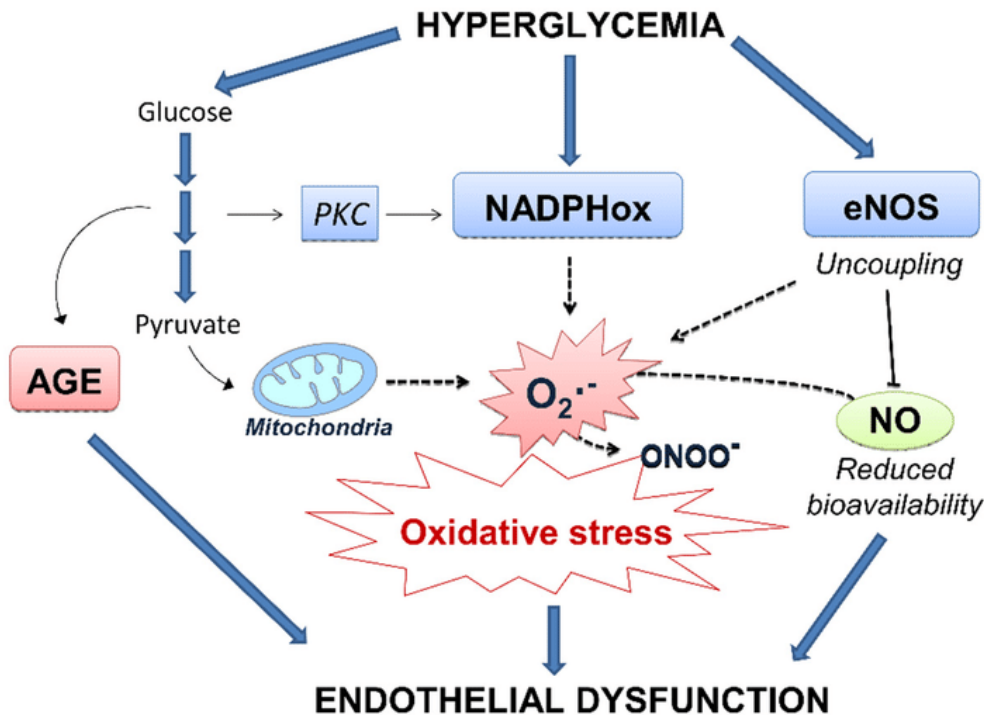


**Figure 7: Mechanisms of reactive oxygen species (ROS)-induced endothelial dysfunction in response to hyperglycemia leading to potential stroke.**

Elevated glucose levels lead to vascular damage directly via by the accumulation of AGE and indirectly due to an imbalance between ROS production and NO bioavailability in the endothelium. Resulting endothelial dysfunctions are characterized by the proinflammatory responses, recruitment of leukocytes, impaired vasodilatation and accumulation of oxidized LDL particles causing the onset of cardiovascular complications. AGE: Advanced glycation end-products; eNOS: Endothelial nitric oxide synthase; LDL: Low density lipoprotein particles; NADPHox: Nicotinamide adenine dinucleotide phosphate oxidase; NO: Nitric oxide; O<sub>2</sub><sup>•-</sup>: Superoxide anion; ONOO<sup>-</sup>: Peroxynitrite; PKC: Protein kinase C. From (Burgos-Moron *et al.*, 2019).

## 5. Mechanisms of insulin secretion and insulin resistance leading to type 2 diabetes

In normal physiological conditions, after meals, blood glucose levels increase and the pancreatic beta cells take up glucose through the glucose transporter 2 (GLUT2) (Rorsman & Braun, 2013). Glucose uptake induces intracellular changes leading to the secretion of the insulin hormone that will be transported by the blood flow to reach its target that are adipocytes, muscular cells and hepatocytes (Rorsman & Braun, 2013). The binding of insulin to its receptor leads to intracellular signaling cascades resulting in the accumulation of glucose transporter 4 (GLUT4) at the cell surface of adipocyte and muscles within 5 minutes of exposure to the hormone for insulin stimulated glucose transport and prevents the gluconeogenesis in the liver (Lebovitz, 2001; Leto & Saltiel, 2012) (Fig. 8). The mechanism by which overweight and hyperglycemia induce insulin resistance is further explained below.



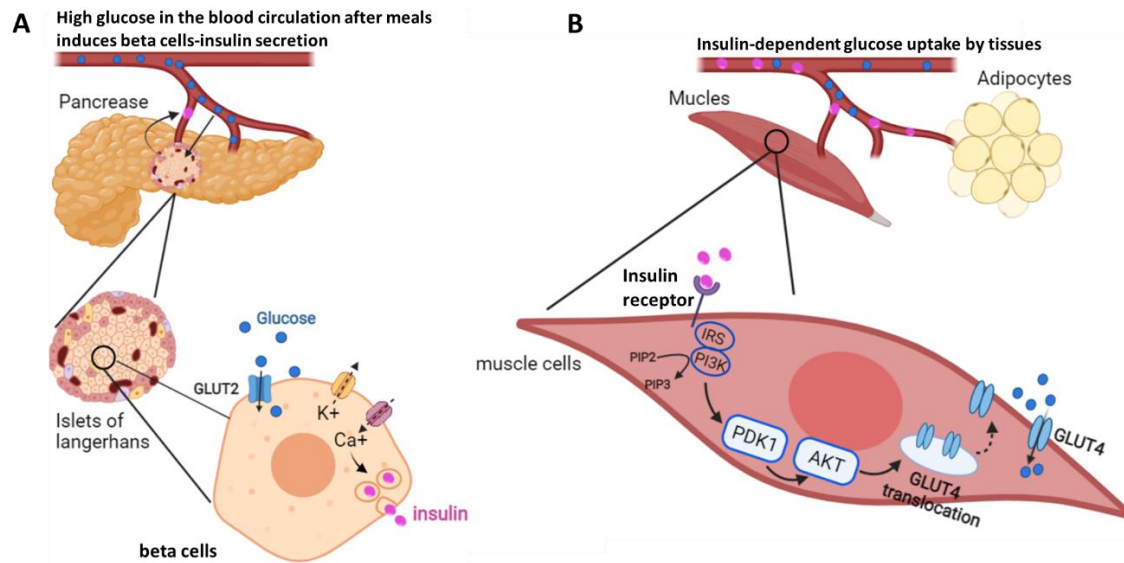


**Figure 8:** Schematic representation of insulin secretion by the beta pancreatic cells in response to high blood glucose levels and insulin dependent glucose uptake by the tissues.

(A) High blood glucose levels stimulate the beta cells of the pancreas for the glucose-stimulated insulin secretion. Briefly, glucose enters the cell through one of the glucose transporters GLUT2 and changes the ATP:ADP ratio that inactivates the ATP-sensitive potassium channel KATP. Closure of KATP in turn causes depolarization of the membrane opening voltage-gated Ca<sup>2+</sup> channels. Finally, the influx of Ca<sup>2+</sup> triggers exocytosis of insulin granules. Insulin is secreted to the blood. (B) The insulin reaches the target tissues (muscles and adipose tissue) through the blood circulation. Insulin binding to its receptor (IR) leads to conformational changes of the receptor and its auto phosphorylation, activating thereby the tyrosine kinases that stimulate the recruitment of the insulin receptor substrate (IRS). IRS binds to and activates the regulatory subunit of phosphoinositide 3-kinase (PI3-K) and phosphorylates membrane phospholipids and phosphatidylinositol 4,5-bisphosphate (PIP2) on the 3' position (PIP3). The complex activates the 3-phosphoinositide -dependent protein kinases-1 (PDK-1) resulting in activation of serine/threonine kinases (AKT). AKT is involved in the translocation of GLUT4 from cytosol to the plasma membrane, which further allows glucose uptake.

### C. The “Diabesity” concept: interrelation between obesity and the development of type 2 diabetes

Strikingly, 80% of type 2 diabetic are considered obese (Centers for Disease & Prevention, 2004; Bhupathiraju & Hu, 2016). One of the main reasons behind the development of insulin resistance and type 2 diabetes is obesity (Boles *et al.*, 2017). Any interference in insulin-insulin receptor (IR) signaling can abort the insulin mediated glucose uptake and consequently lead to insulin resistance and so to hyperglycemia (Lebovitz, 2001). In case of overweight or obesity, the high adiposity results in the increased secretion of FFAs and TNF $\alpha$ . The increased levels of FFAs in the blood block the insulin signaling through several mechanisms (fatty acid metabolite production as the acyl-CoA and interaction with the toll-like receptor-4 (TLR-4)) and thus avoid the addressing of GLUT4 to the membrane of insulin target

organs (muscles and liver). It results in insulin resistance and in the development of hyperglycemia as shown in figure 8 (Delarue & Magnan, 2007; Badawi *et al.*, 2010; Sears & Perry, 2015). In addition, inflammatory mediators such as TNF $\alpha$  and I $\kappa$ B kinase complex (I $\kappa$ B) interferes with the downstream intracellular signaling of the insulin receptor. For instance, inflammation activates I $\kappa$ B, inducing the phosphorylation and degradation of the I $\kappa$ B, an inhibitor of the nuclear factor kappa B (NF $\kappa$ B). NF $\kappa$ B consequently translocate to the nucleus and induces the expression of the inflammatory cytokines such as IL-1 $\beta$ , IL-8 and TNF $\alpha$ . These later inhibits the Phosphoinositide 3-kinase / Alpha serine/threonine kinase (PI3K/AKT) pathway from insulin signaling and decreases GLUT4 translocation to the membrane and therefore glucose uptake (Fig. 9).

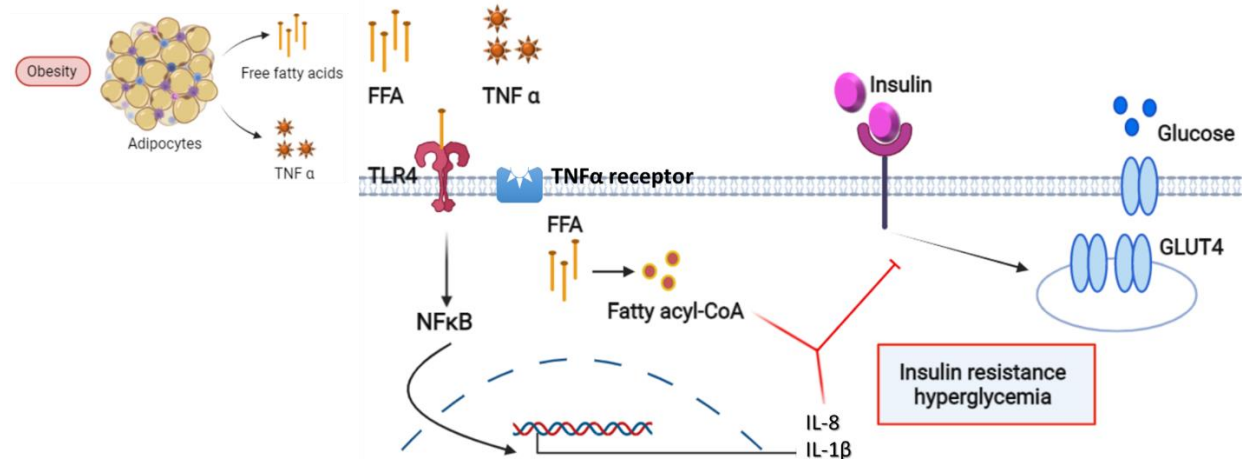


**Figure 9: Development of insulin resistance in case of obesity due to the increased plasma free fatty acids and adipokines secreted from the saturated adipocytes.**

Due to the storage saturation of fatty acids start, adipocytes release free fatty acids (FFA) and TNF $\alpha$  to the circulation. The FFAs induce insulin resistance through different mechanisms. **a.** FFA binding to the Toll Like receptor 4 (TLR4) leads to the activation of the NF $\kappa$ B that induces the transcription of the inflammatory cytokines as IL-8 and IL-1 $\beta$  that inhibit the insulin mediated GLUT4 translocation to the membrane and thereby the glucose intake. **b.** The FFA produces fatty acyl-CoA that also inhibits the activated insulin receptor from inducing the translocation of the GLUT4 to the plasma membrane. TNF $\alpha$  is internalized to the cell through TNF $\alpha$  receptor, TNF $\alpha$  activates the NF $\kappa$ B that in turns induces the transcription of the inflammatory cytokines (IL-8 and IL-1 $\beta$ ). The inflammatory cytokines have an inhibitory effect on the insulin mediated GLUT4 translocation pathway.

Considering the intrinsic links between obesity and diabetes, the “Diabesity” concept emerges to summarize these two widely spread worldwide diseases. In obese individuals, the high visceral adipose tissue strongly releases FFAs and inflammatory cytokines as TNF $\alpha$  (Sears & Perry, 2015). These products that results from adipose tissue metabolism are secreted to the blood circulation and reach different tissues as liver and muscles and induces insulin resistance (Fig. 9). The high level of FFAs as well as chronic inflammation also impact insulin clearance

(decrease) that is mainly ensured at 80% by the liver (Duckworth *et al.*, 1998). Such troubles in insulin clearance will lead to hepatic insulin resistance and later to peripheral insulin resistance that will promote the development of type 2 diabetes (Lebovitz, 2001; Sears & Perry, 2015). Therefore, obesity was considered as the onset of type 2 diabetes development due to the associated chronic inflammation and insulin resistance. However, as previously mentioned, the etiology of diabetes is not as simple and other factors could contribute to the development of type 2 diabetes. Indeed, almost 20% of type 2 diabetics are not overweight or obese suggesting other physiological and molecular mechanisms responsible of the development of type 2 diabetes in these cases (Dalton *et al.*, 2003; Vaag & Lund, 2007).

Interestingly, at the level of the central nervous system, these metabolic diseases can lead to severe complications that we will develop in the next chapter.

## **II. Impact of metabolic disorders on the brain: focus to the blood-brain barrier and to neural stem cells**

### **A. Blood-Brain Barrier (BBB)**

#### **1. Definition**

The blood-brain barrier (BBB) is a highly selective membrane separating the blood compartment from the nervous one. This barrier is composed of different cell types including endothelial cells from the cerebral microvessels (Risau & Wolburg, 1990; Begley & Brightman, 2003), pericytes surrounded by the basal lamina, and astrocytic end-feet surrounding the brain capillaries (Correale & Villa, 2009) (Fig. 10). Endothelial cells express claudin 3 and 5, zonula occludens, establishing tight junctions between endothelial cells. These peculiar junctions prevent the paracellular movements and favors the transcellular pathway through the BBB (Wolburg & Lippoldt, 2002; Hawkins & Davis, 2005). In addition, the luminal (blood facing) and abluminal (brain facing) membranes of these endothelial cells are rich in specific transport systems that facilitates the transport of the required molecules and prevents the passage of unwanted compounds (Begley & Brightman, 2003). The pericytes are important for endothelial cell survival and proliferation/angiogenesis. They play a role in vesicle trafficking, in establishment of tight junctions and regulate the blood flow (Sweeney *et al.*, 2016). Astrocytes ensure the cellular link between the BBB and the neurons of the CNS by interacting with the



endothelial cells with special transporters, receptors and channels (aquaporin-4) (Fig. 10). Besides, these astrocytic end-feet are vital for the integrity of the physical barrier of the BBB, for ionic and water homeostasis, and for the appropriate expression and polarization of transporters (transporter barrier) (Zenaro *et al.*, 2017).

The main function of the BBB is to (i) supply the crucial nutrients for the brain and exclude the harmful products from the brain creating a special sterile brain microenvironment (Abbott & Romero, 1996; Begley & Brightman, 2003), (ii) regulate the ionic transport within the brain to create optimal medium for proper neuronal signaling and functioning with the aid of specific ion transporters and channels (Abbott, 2004) and (iii) help the neurons to respond to any changes in the brain microenvironment due the close proximity between the neurons, BBB and the astrocytic connections (Zlokovic, 2008; Rhea & Banks, 2019).

So far, the BBB is an important contributor to the brain homeostasis limiting the entry of harmful molecules (i.e., inflammatory and oxidative stress factors, immunogens). Its disruption is also strongly associated with increased neuro-inflammation and unbalanced redox status in the brain.

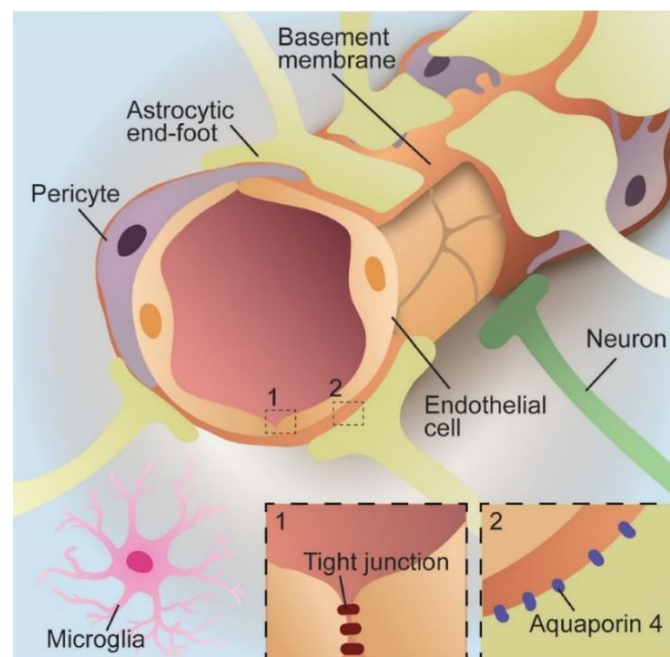


**Figure 10: Cellular constituents of the blood-brain barrier.**

The barrier is formed by endothelial cells, surrounded by basal lamina and astrocytic perivascular end-feet. Astrocytes provide the cellular link to the neurons. The figure also shows pericytes and microglial cells. **1.** Brain endothelial cell express tight junctions. **2.** The astroglial-endothelial communication occurs through the aquaporin-4 and is necessary to maintain the BBB. From (Ahn & Kim, 2021).

Very interestingly, the BBB is in a close proximity with not only neurons and astrocytes but also with neural stem cells, and it is even sometimes in direct contact with NSCs by the integrin-laminin interactions (Shen *et al.*, 2008; Tavazoie *et al.*, 2008) (Fig. 11). According to Shen and his colleagues the vascular endothelial cell of the BBB can also secrete soluble factors that have the capability to stimulate the self-renewal of the neural stem cells (NSCs) and the neuron production (Shen *et al.*, 2004). Furthermore, the angiogenesis process that allows the formation and the maintenance of the brain capillaries have been shown by several experiments to be coupled to adult neurogenesis (Palmer *et al.*, 2000; Louissaint *et al.*, 2002). Another line of evidence shows that the increase in the adult hippocampal neurogenesis was always associated with an increase in the cerebral blood volume of the dentate gyrus and increase in the density of the microvasculature (Pereira *et al.*, 2007; Van der Borght *et al.*, 2009). Therefore, all these findings emphasize that the endothelial and thereby the BBB cells are critical components of the NSC niche, and any changes in the BBB function could implicate its effects on the neurogenesis.

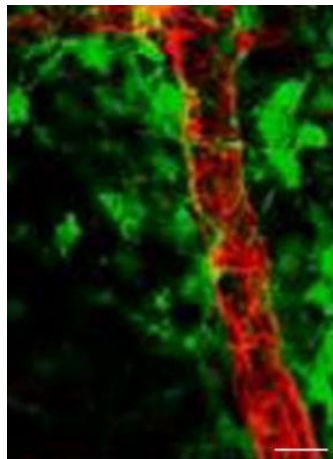


**Figure 11:** The close proximity between the neural stem cells and the blood vessels in the neurogenic subventricular zone in the brain of mouse.

Numerous GFAP-GFP<sup>+</sup> NSCs (green) are located around blood vessels (Laminin, red) and envelop them. Several GFAP-GFP<sup>+</sup> cell somas lie on the vessel walls. Note: The SVZ NSCs are a sub-population of the Type B cells expressing the astrocyte marker glial fibrillary acidic protein (GFAP). Scale bar: 50  $\mu$ m. From (Shen *et al.*, 2008).

Despite being a tightly formed barrier and a selective membrane, the BBB is subjected to several modifications that could alter its integrity (Abbott, 2005). For instance, the inflammation is a factor of weakening the BBB, by decreasing the expression of tight junctions and causing edema (Huber *et al.*, 2001). Some inflammatory mediators in the periphery (i.e., histamine and bradykinin) could increase the permeability of the cerebral endothelium, having a short-lasting effect on the brain (Abbott, 2000). Starvation or hypoxia can also modulate the

expression of the glucose transporter (GLUT1) in the BBB to ensure higher glucose delivery to the brain (Drudge *et al.*, 1975). Oxidative stress was shown also to upregulate the expression and to alter the function of P-glycoprotein (an efflux transporter responsible for the transport of several compounds across the BBB) (Nwaozuzu *et al.*, 2003; Bauer *et al.*, 2005). As well, strokes (Tran *et al.*, 1999; Lo *et al.*, 2003), trauma (Schwaninger *et al.*, 1999), infectious/inflammatory process (Gaillard *et al.*, 2003; Veldhuis *et al.*, 2003), multiple sclerosis (Minagar & Alexander, 2003), Alzheimer's disease (Berzin *et al.*, 2000; Zlokovic, 2005), brain tumors (Liebner *et al.*, 2000; Papadopoulos *et al.*, 2001) and several other factors are reported to enhance the BBB breakdown.

Obesity and diabetes are both critical factors that are known to affect the BBB integrity and function. Several experimental models prove this finding and these are more developed below.

## **B. Impact of metabolic disorders on BBB function**

### **1. Deleterious effect of obesity on the BBB**

A longitudinal study linked the midlife overweight and obesity with the lower integrity of the BBB in the late life (Gustafson *et al.*, 2007). For instance, the integrity of the BBB of elderly human (70-84 years) was examined by measuring the cerebrospinal fluid/serum albumin ratio. It was shown that overweight/obese individuals have an increase in the cerebrospinal fluid/serum albumin ratio (Gustafson *et al.*, 2007). As well, an increase in the serum levels of S100 $\beta$  (a marker of BBB disruption) was also observed in obese individual after high intensity workouts compared to the non-obese ones (Roh *et al.*, 2017). Notably, the high intake of saturated fatty acids and high-fat diet (HFD) increases plasma amyloid beta and brain amyloid beta delivery, a protein well-known to be elevated in case of Alzheimer's disease (AD) and dementia in both humans and rodent models, respectively (Hanson *et al.*, 2015; Walker *et al.*, 2017). This reinforces the idea that in HFD/obese condition, the BBB is leaky leading to impaired metabolism of beta amyloids.

Several experimental models and researches have been conducted to study the implication obesity on the BBB physiology, and its role in deteriorating the brain health. In a study, rabbits were fed for 7 months with cholesterol-enriched diet. BBB leakage was observed through the increased Immunoglobulin G (IgG) staining in the cortex of the HFD animals

(Ghribi *et al.*, 2006). In another experimental attempt, Ouyang *et al.* used proteomics to assess the protein expression levels of the brain microvessels of HFD-fed and lean mice. They show the down regulation of several proteins involved in transport, cell cycle regulation, cytoskeleton, and scaffolding adaptors of the cerebral microvessels in the high-fat diet fed mice compared to the chow fed mice (Ouyang *et al.*, 2014). Moreover, vimentin and tubulin -two important cytoskeleton proteins involved in the tight junction formation- are downregulated at the levels of BBB microvessels in obesity subjects (Ouyang *et al.*, 2014).

Several investigations discuss the role of the inflammation on BBB disruptions. HFD protocol performed in C57BL/6 mice induces systematic inflammation and BBB leakage, that were observed by the increased circulatory proinflammatory cytokines level and high presence of the immunoglobulin G in the hippocampus, respectively (Tucsek *et al.*, 2014). In these mice, BBB disruption was associated to microglial activation and the occurrence of oxidative stress in the brain (Tucsek *et al.*, 2014). Other factors to consider behind weakening the BBB integrity are saturated fatty acids (SFAs). Saturated fatty acid levels are known to be elevated in obese subjects (Zhou *et al.*, 2020). These SFAs have the ability to activate the expression of the inflammatory cytokines in the endothelial cells of BBB, decreasing therefore its integrity. SFAs interact with the TLR4 at the endothelial cell surface and activate the MyD88 protein (Milanski *et al.*, 2009), that in turns activates NF $\kappa$ B and induces endoplasmic reticulum (ER) stress. NF $\kappa$ B downstream signaling results in the upregulation of the proinflammatory cytokines as IL-1 $\beta$ , TNF $\alpha$  and IL6 (Hommelberg *et al.*, 2009; Lawrence, 2009; Jais & Bruning, 2017). These proinflammatory cytokines are known to contribute to BBB dysfunction by the transcriptional repression of the tight junction proteins (Beard *et al.*, 2014). Consequently, the decreased expression of the tight junction proteins impacts the BBB (Gustafson *et al.*, 2007) and affects greatly brain health as shown in figure 12.

Once the BBB integrity is weakened, the outcomes on the brain health and neurological functions are adverse. The exposure of rats to high saturated fat and glucose diet for 3 months shows remarkable decrease in the expression of genes involved in the tight junction establishment (Claudin 5 and 12) and increases the hippocampal BBB permeability as revealed through hippocampal sodium fluorescein extravasation assay. These impairments were associated with decreased hippocampal dependent learning and memory processes. Overall, it confirms that the high energy diet may disrupt the hippocampal function by decreasing the BBB integrity (Kanoski *et al.*, 2010).

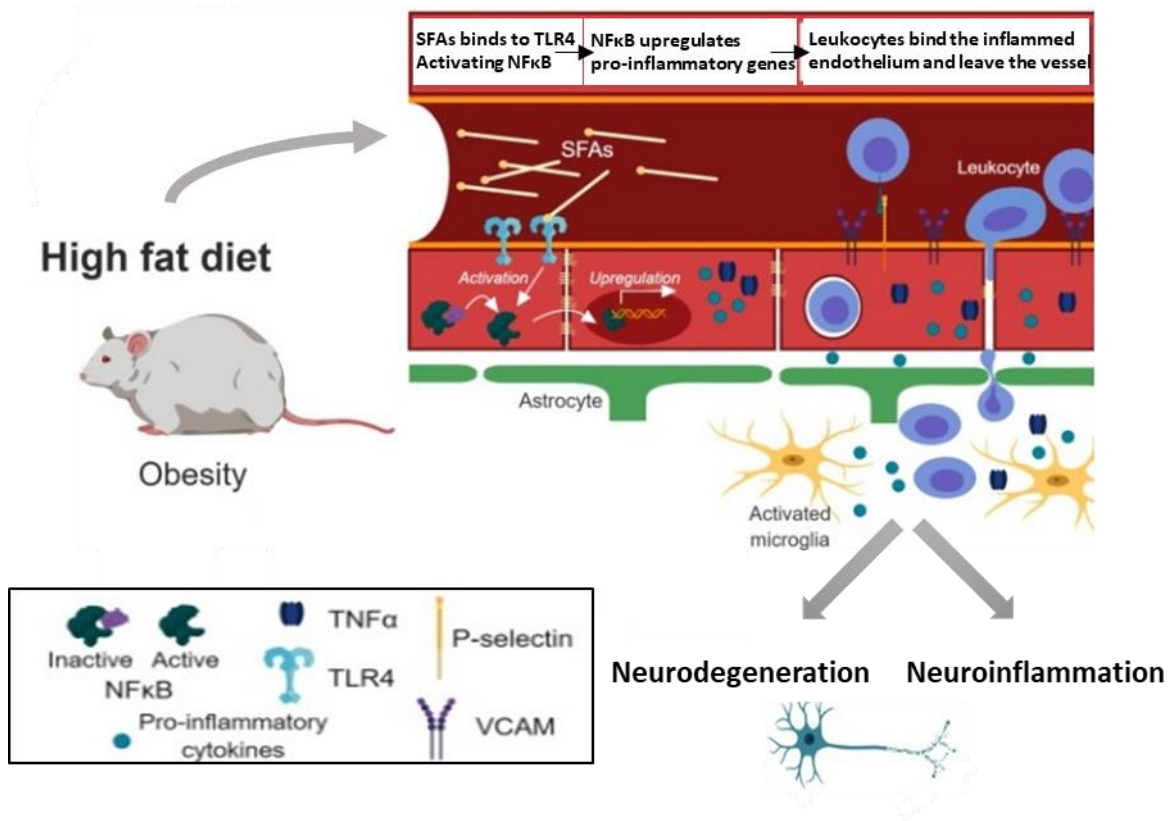


**Figure 12: Effects of obesity on the BBB and the brain.**

Increased saturated fatty acids (SFA) concentration caused by high-fat diet (HFD) or obesity enhance NFκB-mediated inflammation at the BBB via TLR4 receptor. This causes increased leukocyte extravasation, release of pro-inflammatory cytokines, and activation of microglia. From (Van Dyken & Lacoste, 2018).

## 2. Deleterious effects of diabetes on the BBB

Numerous recent findings support the causal association between T2DM and the breakdown of the BBB. However, the clinical data on human patients specifically concerning the association between T2DM and BBB leakage are so limited. In diabetic patients, the permeability of the BBB was evidenced by the (Magnetic Resonance Imaging) MRI brain imaging following intravenous gadolinium (Gd) diethylenetriamine pentaacetic acid (Gd-DTPA), a chemical substance used to enhance the quality of magnetic resonance imaging (MRI) scans. Diabetic individuals show increased signal intensity in the brain compared to the normal ones 15 minutes after Gd-DTPA injection, confirming increased BBB permeability in diabetic individuals (Starr *et al.*, 2003). In addition, the analysis of the cerebrospinal fluid (CSF) proteins in diabetic patients reveals significantly higher total CSF proteins and albumin quotient than in the nondiabetic ones (Kobessho *et al.*, 2008). In diabetic primate (rhesus monkey), contrast-enhanced MRI (DCE-MRI) revealed higher BBB permeability compared to the normal

ones. Beneath, the histological experimentations show decreased zonula occludens protein-1 and leakage of immunoglobulin G emphasizing the contribution of diabetes in impairing the BBB integrity (Xu *et al.*, 2017).

Accumulating lines of evidences on mice and rats draw the relation between diabetes and the breakdown of the BBB integrity as well as the development of cognitive impairments. For example, the structural and functional integrity of BBB was investigated using a model of STZ injected rats and murine model of a high-fat high-sugar diet mimicking obesity-induced type 2 diabetes. Immunohistochemistry analysis on cortical mouse brain sections show the decreased expression of the tight junction proteins (i.e., claudin-5 and occludens) associated to the destruction of the basal lamina and the increased expression and activity matrix metalloprotease in the diabetic brain microvessels compared to the normal ones (Hawkins *et al.*, 2007; Sheikh *et al.*, 2022). Three dimensional MRI scans in obese diabetic type 2 mice using a specific quantitative vascular biomarker documented that 84% of the brain display global capillary disruptions with the exception of prefrontal cortex, midbrain and cerebellum (Qiao *et al.*, 2020) (Fig. 13).

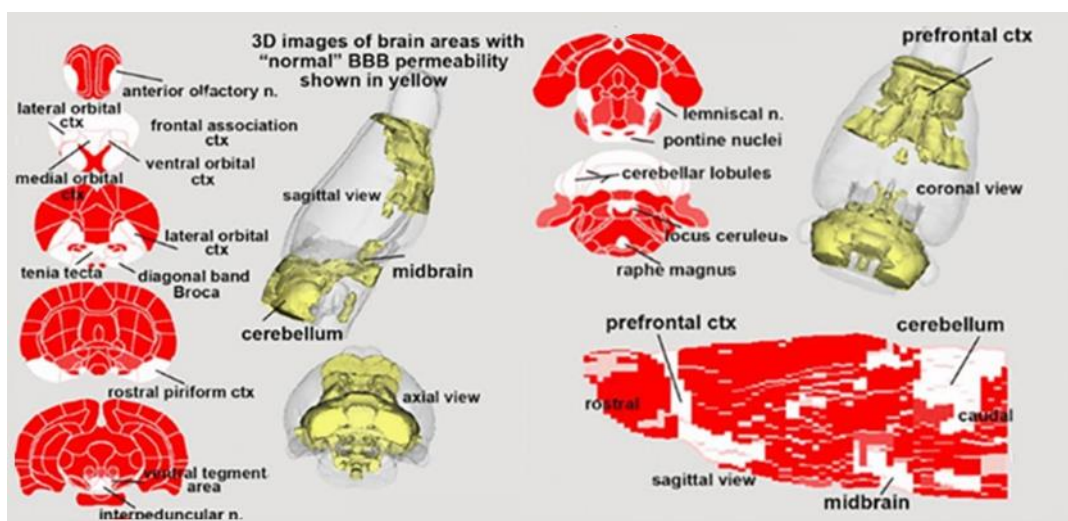


**Figure 13: Blood-brain barrier permeability comparison between diabetic and control rats.**

Quantitative ultra-short time-to-echo, contrast enhanced imaging of BBB permeability for BBZDR/Wor rats (a model of type 2 diabetes) compared to the control BBB permeability. All areas in red correspond to the significantly greater permeability of the BBB in type 2 diabetic rats compared to the control ones and the yellow area corresponds to the normal BBB permeability. From (Qiao *et al.*, 2020).

Zhao and his colleagues provide some clue to understand the mechanism behind the BBB disruption in type 2 diabetic mice. They observed increased BBB permeability, decreased protein expression of the tight junctions and increased levels of pro-inflammatory cytokines in the brain of diabetic mice. These lines of evidence document the role of the inflammation in



exacerbating the BBB leakage in type 2 diabetic mice models (Zhao *et al.*, 2019). In addition, the increased level of oxidative stress in diabetic subjects is a contributor for BBB destruction by the degradation of the BBB tight junction or by inducing the apoptosis of the endothelial cells of the BBB (Lehner *et al.*, 2011).

The figure below summarizes the mechanisms behind BBB destruction and the development of cognitive impairment and dementia (Fig. 14).

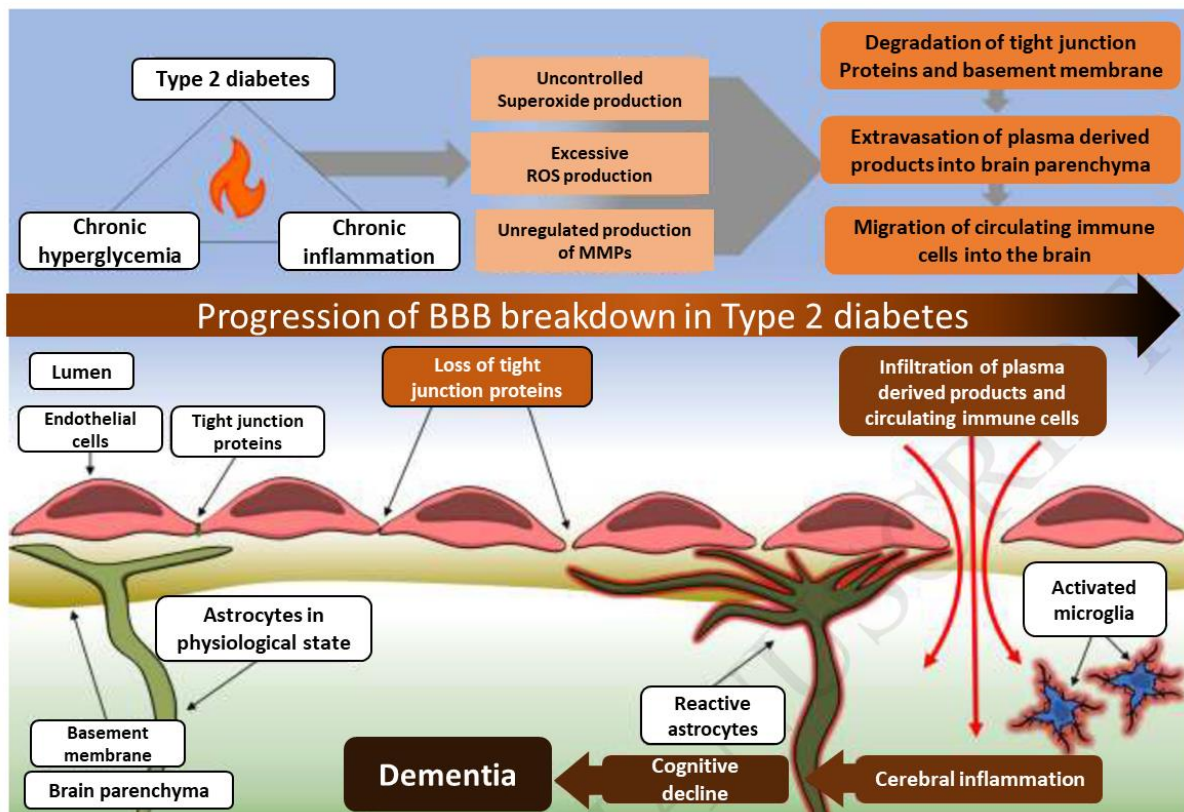


**Figure 14: Mechanisms suggested for the blood-brain barrier destruction in type 2 diabetes.**

Type 2 diabetes is associated with chronic hyperglycemia and inflammation that induces the uncontrolled production reactive oxygen species, oxidative stress and the dysregulation of regulatory metalloproteases. These events promote the loss of tight junction proteins and disturb the architecture of the BBB. These events increased the permeability of the BBB and leads to immune cells infiltration to the brain causing further cerebral inflammation. Consequently, cognitive decline and dementia become a predicted outcome for the type 2 diabetic condition. ROS: reactive oxygen species; MMPs: metalloproteases; BBB: blood-brain barrier. From (Brook *et al.*, 2019).

In diabetic insulin resistance mice model, the BBB impairment with neuro-inflammatory state precedes the occurrence of cognitive decline and neurodegeneration that appears later (Takechi *et al.*, 2017; Rom *et al.*, 2019). Therefore, as a consequence of the disrupted BBB permeability, the neuronal and cognitive functions of the brain are altered too.

## C. Effects of metabolic disorders on brain volume, cognitive functions and the development of Alzheimer's disease

### 1. Obesity, brain volume and cognitive function

Interestingly, obesity also seems to impact the size of the brain. For instance, cerebral MRI of the brains of “normal/lean” people compared to those displaying stronger body fat percentage reveals that the brain volume of the subcortical grey matter is smaller in overweight/obese people and that brain ventricles are larger (Dekkers *et al.*, 2019) (Fig. 15).

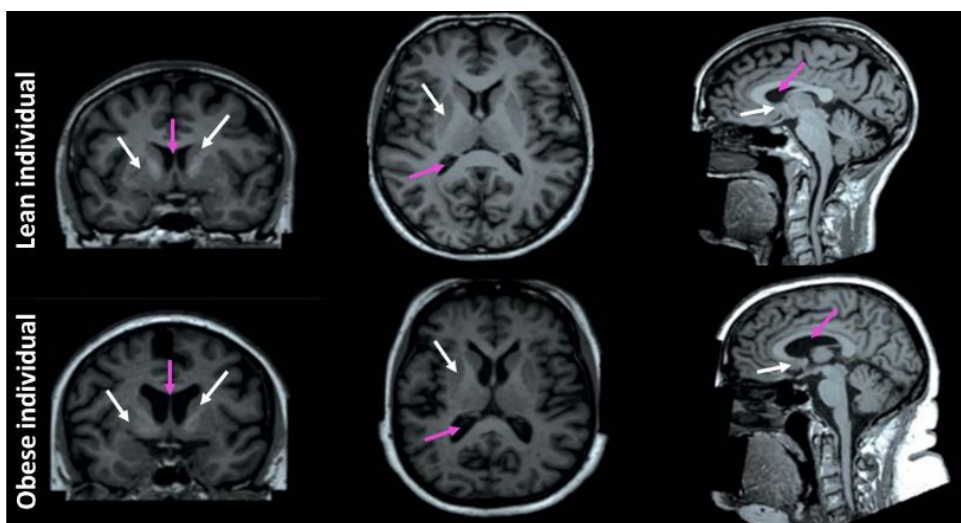


**Figure 15:** Examples of brain MRI of normal individual and individual of high body fat percentage.

Coronal (top), axial (middle) and sagittal (bottom) brain MRI views of two women participants in the UK (age: 65 years). The participant on the left has a body fat percentage of 13 % and the participant on the right has a body fat percentage of 49 %. The MRI data clearly show lower volumes of subcortical gray matter structures as noticed by the white arrows and increased ventricle dilatation as noticed by the pink arrows in the individual with higher total body fat percentage. From (Dekkers *et al.*, 2019).

Also, a negative association with BMI and the right prefrontal cortex thickness (thinner cortex) was shown, while a positive association with the left prefrontal cortex (thicker cortex) was observed (Vainik *et al.*, 2018) (Fig. 16). Interestingly, Vainik and colleagues also study the links between cognitive functions and BMI. The results show that BMI is correlated negatively with cognitive flexibility, reading abilities, working memory and verbal memory.

Furthermore, obesity increases the risk of dementia independently of type 2 diabetes (Pugazhenthil *et al.*, 2017). Indeed, a study from Xu *et al.* noticed that overweight individuals (BMI: 25-30 Kg/m<sup>2</sup>) and obese ones (BMI > 30 Kg/m<sup>2</sup>) have a 1.71 and 3.88 higher risk of dementia, respectively (Xu *et al.*, 2011). As well, higher BMI was shown to be linked to the



early onset of the AD with further advanced pathologies as (1) lower brain volumes, (2) several affected areas as the frontal, temporal, parietal, and occipital lobe regions and (3) ventricular expansion was associated with higher BMI (Ho *et al.*, 2010; Chuang *et al.*, 2016).

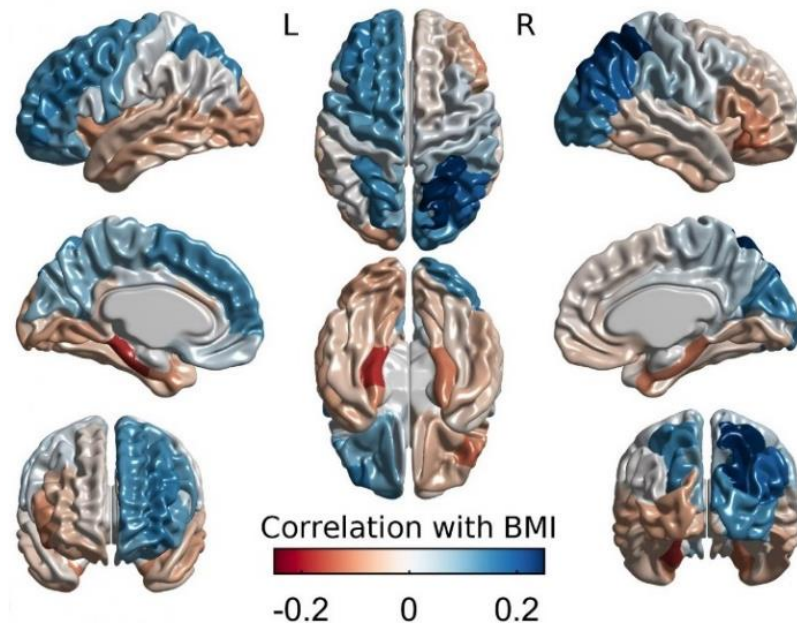


**Figure 16: Brain maps of the associations between BMI and cortical thickness.**

Parcel-based analysis identified negative associations (*red areas*) with BMI in right inferior lateral frontal cortex and bilateral entorhinal-parahippocampal cortex. Positive associations (*blue areas*) with BMI were found with the left superior frontal cortex, left inferior lateral frontal cortex, and bilateral parietal cortex parcels. BMI: body mass index; L: left; R: right. From (Vainik *et al.*, 2018).

A suggested mechanism for this observation is the low grade chronic inflammation occurring during obesity and its link with the central inflammation that deteriorates the brain tissue and cognitive functions over time (Anjum *et al.*, 2018). The links between obesity and AD disease were attributed to several mechanisms as mentioned by (Picone *et al.*, 2020): (i) a higher extracellular  $\beta$ -amyloid ( $A\beta$ ) accumulation was observed similarly in the brain of HFD mice and several mechanisms links the chronic increased plasma  $A\beta$  in obese individuals to the possibility of its accumulation in the brain, (ii) the central inflammation and oxidative stress in obesity condition plays a critical role in the pathogenesis of the AD, (iii) the increased oxidative stress in obese subjects damages the BBB integrity and consequently results in altered cerebrovascular integrity in the hippocampus that is involved in learning and memory and found to be damaged AD cases.

Together these data demonstrated that obesity has a strong impact on the brain, reducing its size and functions and increasing the risk of stroke and their subsequent complications.

## 2. Diabetes, brain volumes and cognitive function

Interestingly, the prevalence of dementia and AD (up to 80% of ADs patients are diabetic) was shown to be higher in diabetic patients (Biessels *et al.*, 2006; Kopf & Frolich, 2009). Diabetes was undoubtedly found to be strongly correlated with the incidence of AD and is considered as a main risk factor for its development (Ott *et al.*, 1999; Kroner, 2009; Akter *et al.*, 2011). In diabetic condition, both glucose intolerance and high levels of glycosylated hemoglobin were associated with dementia and lower cognitive function (Cukierman-Yaffe *et al.*, 2009; Ohara *et al.*, 2011). Several animal models studied the molecular links between diabetes and AD as increased A $\beta$  protein, tau protein phosphorylation, plaque formation and increased ROS and oxidative stress in the brain (Rasool *et al.*, 2021). A study was conducted between healthy patients and T2DM ones aiming to see the hippocampal functional connectivity using functional magnetic resonance imaging (fMRI, a MRI showing changes in regional brain activity based on increased neuronal metabolism in activated neurons) The fMRI shows lower functional connectivity in T2DM patients compared to the control ones (Zhou *et al.*, 2010) (Fig. 17A). Moreover, T2DM exerts an effect on the brain, with whole brain volume being lower volume compared to the nondiabetic healthy people, and induces mild cognitive impairments and AD disease states (Li *et al.*, 2016) (Fig. 17B).

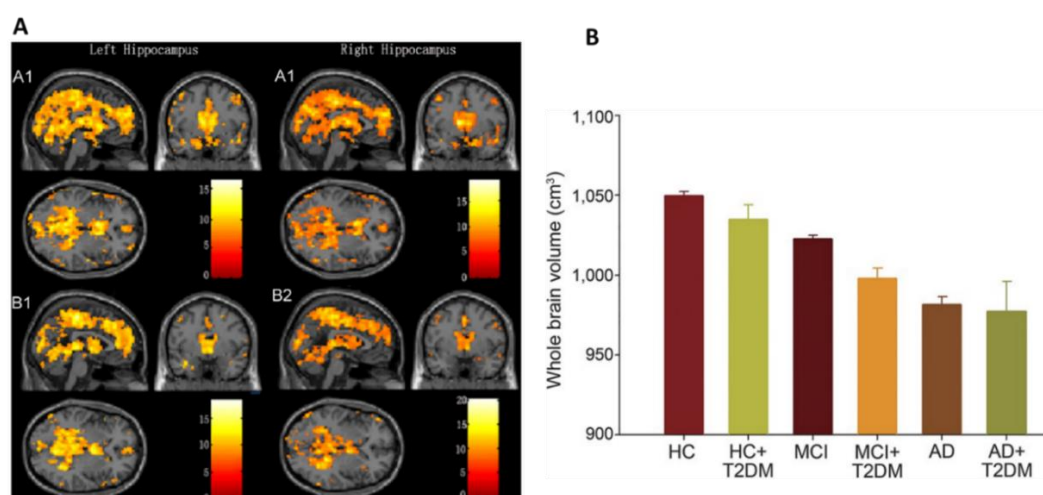


**Figure 17:** Comparison of T2DM brain subjects with non-diabetic ones in term of functional connectivity and brain volume.

(A) Functional magnetic resonance imaging showing hippocampal functional connectivity for healthy controls (A1 and A2) and T2DM patients (B1 and B2). The color index from orange to yellow reflects the functional connectivity from low functional connectivity in orange to higher in yellow. Notice the dominance of the orange color in the brain of T2DM patient compared to the dominant yellow in the healthy control brains.

(B) Graph showing whole brain volumes among 6 groups based on T2DM status. Note the decrease in the brain volume in all conditions associated with T2DM. HC: healthy controls; T2DM: type 2 diabetes mellitus; MCI: mild cognitive impairment; AD: Alzheimer disease. References: (A) (Zhou *et al.*, 2010); (B) (Li *et al.*, 2016).

## D. Effect of metabolic disorders on neural stem cells and neurogenesis

### 1. Embryonic neurogenesis

Neurogenesis is the process leading to the production of neurons from neural stem cells (NSCs). This complex and highly orchestrated process involves the proliferation of NSCs, the migration and differentiation of newborn neurons as well as their survival and functional integration (Ming & Song, 2005). It has been documented in all the vertebrate species studied so far. Neurogenesis is very high during embryogenesis and its existence was debated during adulthood. Indeed, at the beginning of the 20<sup>th</sup> century, the famous neuroanatomist Santiago Ramón y Cajal claimed “In the adult centers, the nerve paths are something fixed, ended, and immutable. Everything may die, nothing may be regenerated” (Colucci-D'Amato *et al.*, 2006). Thus, adult neurogenesis was considered as an impossible process during almost one century. However, several studies from postnatal human brains, monkeys and rodents confirm the generation of new neurons during adulthood (Altman & Das, 1965; Altman, 1969; Kaplan, 1985; Spalding *et al.*, 2013). The advanced research techniques and the developed analysis have evidenced that adult neurogenesis occurs in the brain of adult mammals, including humans, in particular regions called neurogenic niches (Eriksson *et al.*, 1998; Sanai *et al.*, 2011; Spalding *et al.*, 2013).

Neurons are generated during the embryonic development and even until the early postnatal stages (Gotz & Huttner, 2005; Ming & Song, 2011; Paridaen & Huttner, 2014). During the first stage of development, the neuro-ectoderm will give the neural plate that will then provide the neural tube (Figure 18A). The walls of the neural tube are constituted of the neuroepithelial cells, with cell body close to the ventricular surface. These cells amplified by symmetric divisions and provide also some neurons by asymmetric divisions. They consequently constitute the first NSCs of the central nervous system. (Fig. 18B). However, these cells transform rapidly into radial glial cells. Morphologically, radial glial cells also display an oval/triangle shape soma close to the ventricular surface from which two cytoplasmic process extend: one short towards the ventricle and one long extending to the periphery of the neural tube (Noctor *et al.*, 2002). Because of their morphology they were thought to be just as a scaffold supporting the neurogenesis process and directing the migration of the neurons (Rakic, 1972). However, the recent findings uncover the role of the radial glial cells as a true

neural stem cell generating directly or indirectly neurons that migrate along radial processes (Malatesta *et al.*, 2000; Hartfuss *et al.*, 2001; Sahara & O'Leary, 2009).

At the neurogenesis onset, radial glial cells divide symmetrically providing a pool of radial glial cells that will next switch from symmetric to asymmetric division. This results in the production of daughter radial glial cells and differentiating cells. These latter are either neurons or intermediate progenitors that divide further symmetrically for producing more neurons (Rakic, 2009; Lui *et al.*, 2011). Embryonic neurogenesis is critical for the correct establishment of the brain neuronal circuitry regarding the distribution of the neurons and the formation of discrete neurogenic niches (Franco & Muller, 2013). At the end of the embryogenesis, radial glia cells mostly disappear transforming into astrocytes, explaining the huge decreased in neurogenesis observed in postnatal brains. Nevertheless, a fraction of these radial glial cells set become quiescent cells and gives rise to the postnatal and adult neural stem cells (Fuentelba *et al.*, 2015; Furutachi *et al.*, 2015). The adult NSC shares common features with the embryonic radial glial cells as the expression of specific markers (Nestin, the progenitor transcription factor Sox2, and the brain lipid binding protein) (Lagace *et al.*, 2007; Ninkovic *et al.*, 2007; Giachino *et al.*, 2014).

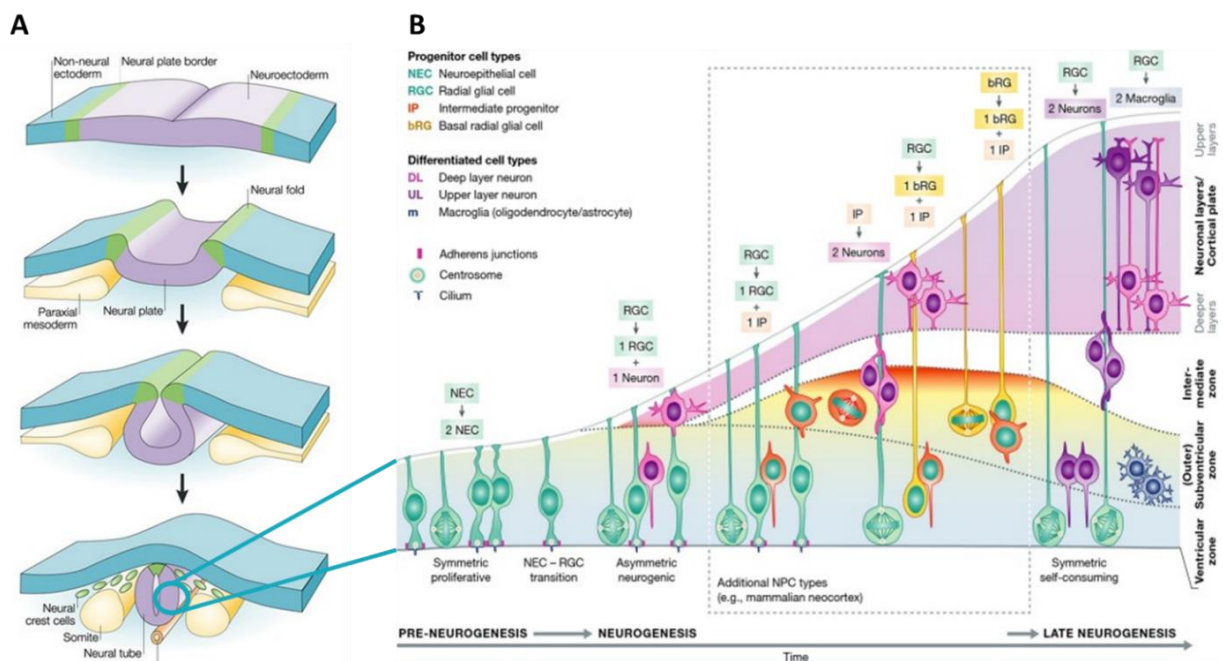


**Figure 18:** Schematic representation of neurogenesis in the central nervous system of embryonic vertebrates.

(A) Neural tube formation from the folding of the neural plate.

(B) The symmetric division of the NEC and their transition to RGC that divide symmetrically and asymmetrically to produce the variety of the neural progenitor cells that localize in their corresponding layers.

The principal types of neural progenitor cells with their progeny produced are indicated by different colors. Additional neural progenitor cells types that are typically found in mammalian neocortex are indicated in the box. NEC: neuroepithelial cells; RGC: Radial glial cell; IP: Intermediate progenitors; Brg: Basal radial glial cells; DL: Deep layer neuron; UL: upper layer neuron; m: Macroglia (oligodendrocyte/astrocyte). From (Gammill & Bronner-Fraser, 2003).

## 2. Adult neurogenesis

In the adult brain, NSCs strongly contribute to brain plasticity by generating new neurons in both normal physiological (homeostatic) and brain damage conditions (Boldrini *et al.*, 2018). Its abolition has strong effects on depressive like behaviors (Mateus-Pinheiro *et al.*, 2013) cognitive aspects (Winocur *et al.*, 2006; Hollands *et al.*, 2017; Pereira-Caixeta *et al.*, 2018), and brain repair mechanisms (Bacigaluppi *et al.*, 2009; Cuartero *et al.*, 2019). Although neurogenesis rate is low during adulthood, the persistence of neural stem cells in discrete niche still allows the maintenance of a weak but functional neurogenesis. In the brain of adult mammals, the two main neurogenic niches are (1) the subventricular zone of the lateral ventricles (SVZ) in which NSC generate neuroblasts migrating through the rostral migratory stream (RMS) to generate interneurons into the olfactory bulb (OB) and (2) the subgranular zone of the dentate gyrus (SGZ; DG) of the hippocampus that has been linked to learning, emotion and memory (Gage, 2000; Lindsey & Tropepe, 2006; Grandel & Brand, 2013) (Fig. 19A).

In the SVZ, the neurogenic niche is composed of 3 different types of cells: neural stem cells (also B cells) that generate transit amplifying cells (C cells) giving rise to neuroblasts (A cells) (Ming & Song, 2005) (Fig. 19B, D). In the DG, 3 types of cells also coexist: neural stem cells (type 1) able to self-renew and generating type 2a and 2b progenitors. These later are also able to self-renew and generate the type 3 cells that in turn gives rise to neurons (Ming & Song, 2005; Obernier & Alvarez-Buylla, 2019) (Fig. 19B, C). In addition to these two regions (SVZ and SGZ), some data evidenced the existence of new born neurons in other regions of the brain as the hypothalamus that are thought to be contributing to some physiological processes like energy balance regulation (Kokoeva *et al.*, 2005; Maggi *et al.*, 2014; Rojczyk-Golebiewska *et al.*, 2014), amygdala (Bernier *et al.*, 2002), neocortex (Gould *et al.*, 1999), medial preoptic area (MPOA) (Akbari *et al.*, 2007) and the striatum (Dayer *et al.*, 2005). Several animal models and techniques have been developed to measure the proliferation of the neural stem cells (Saravia *et al.*, 2004; Zhang *et al.*, 2008), their migration (Akter *et al.*, 2021) and the differentiation to neurons (Lazutkin *et al.*, 2019).



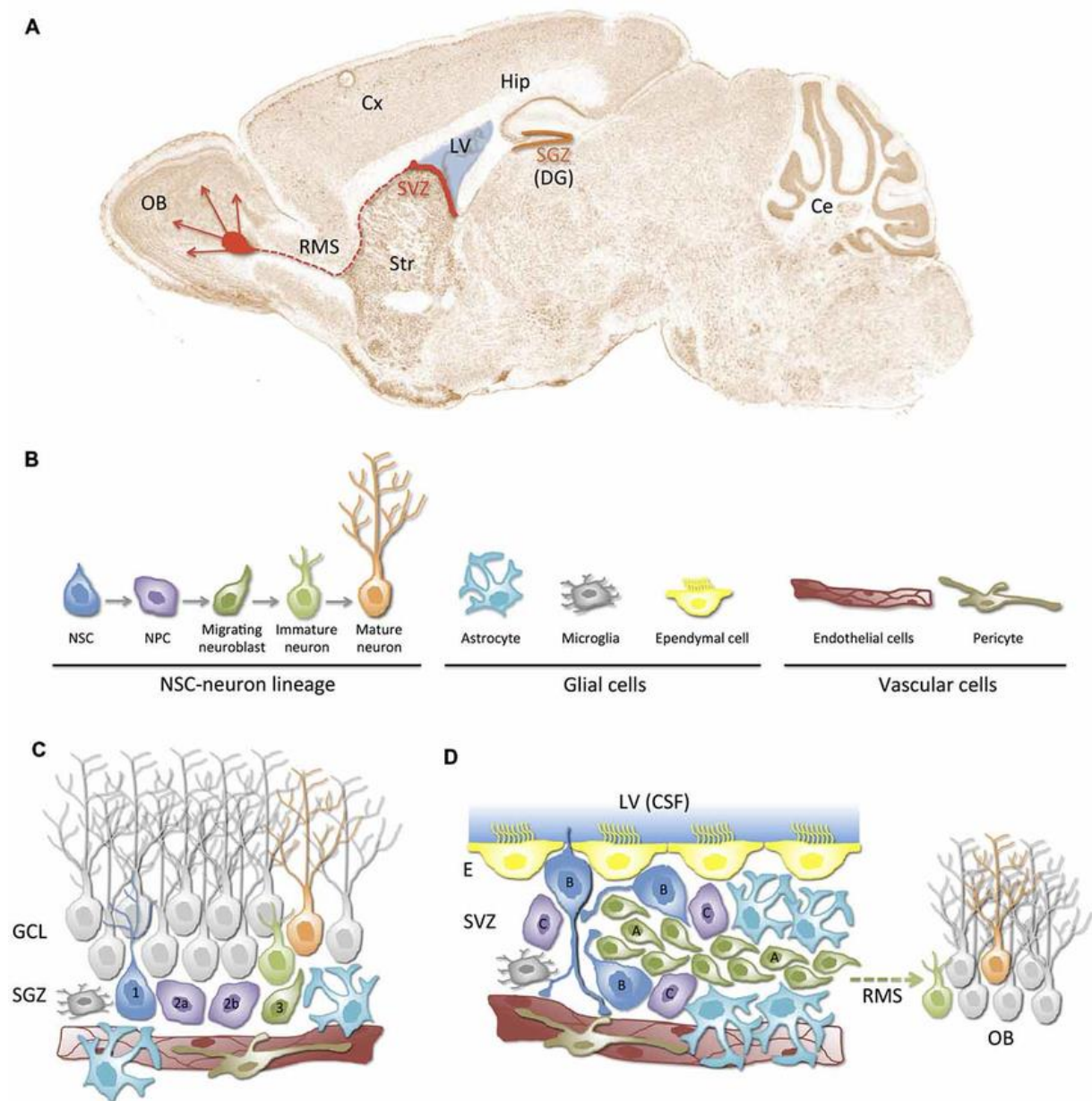


**Figure 19: The dentate gyrus and subventricular zone neurogenic niches of the adult mammalian brain.**

(A) A schematic representation of adult mouse brain neurogenic niches in a sagittal section: the subgranular zone in orange (SGZ) in dentate gyrus (DG) of the hippocampus and the subventricular zone in red (SVZ) in the lateral wall of the lateral ventricles (LV). The newborn neurons from the SVZ-derived migrate towards the olfactory bulbs (OB) along the rostral migratory stream (RMS).

(B) Neurogenic niches cellular components: Neurogenic niches are constituted of neural stem cells (NSCs), glial cells (astrocytes, microglia and ependymal cells) and vascular cells (endothelial cells and pericytes).

(C, D) SGZ and SVZ neurogenic niches illustrations: The color and shape of different cell types are shown in (B). (C) The SGZ neurogenic niche. NSCs (Radial type 1 cells) produces type 2a/b NPCs, that differentiate into type 3 neuroblasts. Neuroblasts migrate (via the guide of astrocytes) and become mature neurons that finally integrate into the granular cell layer (GCL).

(D) SVZ neurogenic niche: This niche is located underneath the ependymal lining (E) of the LV. It is composed of type B quiescent cells (NSCs), that could be activated to generate type C neural progenitor cells which rapidly proliferate to generate type A neuroblasts. Neuroblasts are capable of migrating long distances through the RMS reaching the OB where the maturation into interneurons occurs. Ce, cerebellum; Cx, cortex; Str, striatum. From (Batiz *et al.*, 2015).

### 3. Regulation of neurogenesis

Adult neurogenesis is a highly regulated process. Numerous intrinsic and extrinsic factors are involved its regulation as the epigenetics, non-coding RNA, transcription factors, metabolic and signaling pathways, hormones and immune responses (Mira & Lie, 2017; Stappert *et al.*, 2018) (Fig. 20). Among the signaling pathways involved in neurogenesis regulation are Fibroblast growth factor (Fgf), Wingless-related integration site (Wnt), sex determining region Y-box (Sox), Steroids, brain derived neurotrophic factor (BDNF), Bone Morphogenetic Protein (BMP) and Notch are important ones (Kizil *et al.*, 2012; Diotel *et al.*, 2013; Horgusluoglu *et al.*, 2017).

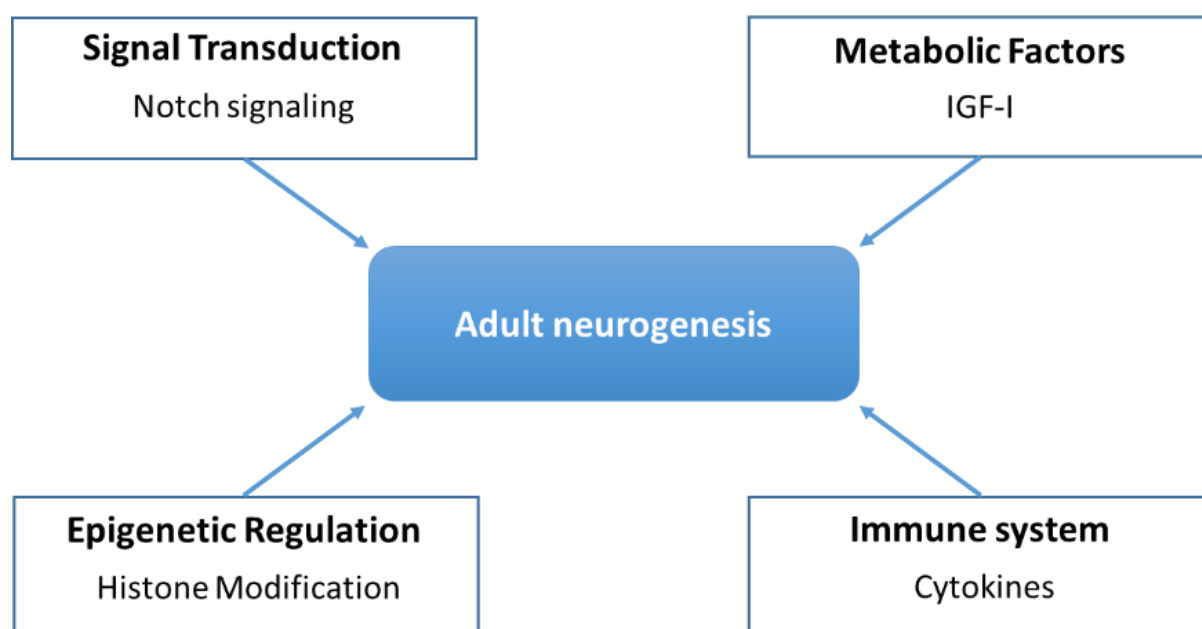


**Figure 20: Different regulators of adult neurogenesis.**

Adult neurogenesis is affected by several intrinsic factors and extrinsic factors as signal transduction pathways (Notch signaling that derives the neural stem cells quiescent), immune system (proinflammatory cytokines known to decrease neurogenesis), metabolic factors (Insulin Growth Factor 1 (IGF-I): that could induce neurogenesis) and epigenetic regulation (as histone modification that can influence the process of neurogenesis by activating or repressing gene transcription of the neural stem cells). Adapted from (Horgusluoglu *et al.*, 2017).

Notch signaling is one of the most conserved signaling pathways in animals that regulates neurogenesis in constitutive and regenerative conditions. Notch signaling occurs through cell-to-cell communication: the binding of Notch receptor to its ligands (jagged 1 and 2 and delta like proteins) leads to the cleavage of Notch intracellular domain (NICD) and to its translocation of the to the nucleus (van Tetering & Vooijs, 2011) (Fig. 21). In the nucleus NICD activates the expression of downstream genes like members of the hairy/enhancer of split

transcription factor family (*Hes* genes in mammals) (Ohtsuka *et al.*, 1999; Yeo *et al.*, 2007). These proteins form a homodimer that inhibits the transcription of bHLH proneural genes, such as *Achaete-scute like* (*Ascl*), a transcription factors inducing the neurogenic fate in the absence of Hes proteins (Fischer & Gessler, 2007; Castro *et al.*, 2011). The Hes proteins homodimers could also exert a negative feedback loop inhibiting thereby their own Notch induced expression (Lewis, 2003). Notch signaling is well conserved between taxa, from mouse and zebrafish regarding the adult neurogenesis. In both of them, Notch 1 is expressed in the activated proliferating progenitor cells and Notch 3 is expressed in both quiescent and activated NSCs (Ables *et al.*, 2010; Chapouton *et al.*, 2010; de Oliveira-Carlos *et al.*, 2013; Kawai *et al.*, 2017).

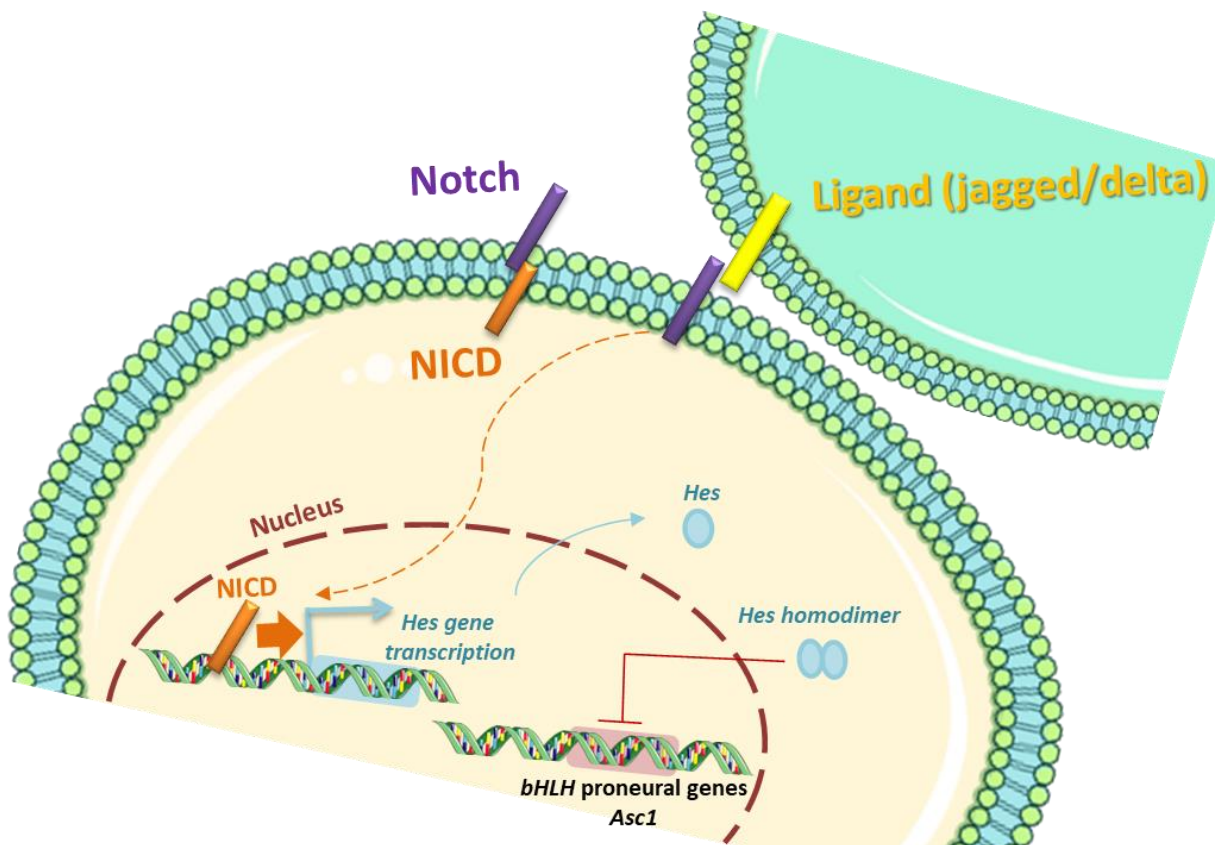


**Figure 21:** Notch signaling pathway in zebrafish and mouse.

The interaction between Notch receptor and its ligands Jagged/Delta, the NICD is cleaved and it translocates to the nucleus. In the nucleus, the NICD induces the expression of the downstream genes *Hes* in mouse. The *Hes* proteins form homodimers and bind to the promoter of bHLH proneural genes in order to inhibit neuronal fate. NICD: Notch intracellular domain; bHLH: basic helix-loop-helix; *Hes*: Hairy/enhancer of split.

Hormones are also factors affecting greatly neurogenesis and can stimulate or inhibit the genesis of new neurons. For example, androgens (testosterone and dihydrotestosterone) were shown to have a positive effect on NSC survival aspect of neurogenesis but not in NSC



proliferation. In addition, these effects appear to be region specific (Jorgensen & Wang, 2020). As well, estrogens and namely  $17\beta$ -estradiol can impact NSC proliferation, newborn cell differentiation, migration and survival with different effects according to the dose, type of estrogens, duration of exposure, and regions studied (Jorgensen & Wang, 2020). However, the stress hormones (glucocorticoids) are also important factors to consider in the endocrine regulation of neurogenesis. Several studies in rodents (mice and rats) have shown that glucocorticoid administration decreased neurogenesis (proliferation, survival and differentiation) (Murray *et al.*, 2008; Brummelte & Galea, 2010)

#### 4. Effects of diabetes on the different aspects of neurogenesis

Diabetes-related cognitive dysfunctions are usually attributed to the vascular complications (McCrimmon *et al.*, 2012). However, recent data relate these disruptions to the brain plasticity and neuronal dysfunctions (Ozawa *et al.*, 2011; Winner *et al.*, 2011). Indeed, several researches on animal models link brain dysfunctions during diabetes to neurogenesis.

For instance, mice injected with streptozotocin (STZ, a molecule leading to pancreatic  $\beta$ -cell death through the generation of oxidative stress) display impaired insulin production and high fasting blood glucose levels (Islam & Loots du, 2009), mimicking type 1 diabetes. Those mice show impaired hippocampal neurogenesis associated with memory dysfunction (Stranahan *et al.*, 2008). More specifically, these mice exhibit a reduction in SVZ and hippocampal neurogenesis, in NSC proliferation and survival correlated with a decreased expression of the brain derived neurotrophic factor (BDNF) and with increased levels glucocorticoids (Beauquis *et al.*, 2008; Guo *et al.*, 2010; Hierro-Bujalance *et al.*, 2020). This was also accompanied by neuronal loss and reduced synaptic plasticity (Kamal *et al.*, 1999).

Similarly, the obese *db/db* mice (leptin receptor-deficient mice homozygous for the diabetes spontaneous mutation in the leptin receptor *Lepr<sup>db</sup>*) widely used to study type 2 diabetes displayed also impaired hippocampal neurogenesis with decreased NSC proliferation associated with memory dysfunction (Stranahan *et al.*, 2008). In addition, a decrease in the number of neuroblasts (*Nestin<sup>+</sup>* and *Doublecortin<sup>+</sup>*) and immature neurons (*Nestin-Doublecortin<sup>+</sup>*) observed in *db/db* mice (Bonds *et al.*, 2020). Similarly, in other models of hyperglycemia (Zucker diabetic rats models), decreased hippocampal NSC proliferation is observed (Lindqvist *et al.*, 2006; Yi *et al.*, 2009; Boitard *et al.*, 2012), associated with a decreased in neuronal differentiation (Hwang *et al.*, 2008; Yi *et al.*, 2009; Bonds *et al.*, 2020).

Furthermore, T2D rats (Goto-Kakizaki) exhibit a reduced survival of the new born cells generated by neuronal progenitors from the hippocampus, although the proliferation was increased in this model (Lang *et al.*, 2009) (Fig. 22). In general, in most models, diabetes leads to a decrease of the different aspects of neurogenesis including proliferation, differentiation, cell survival and/or differentiation (Ho *et al.*, 2013).

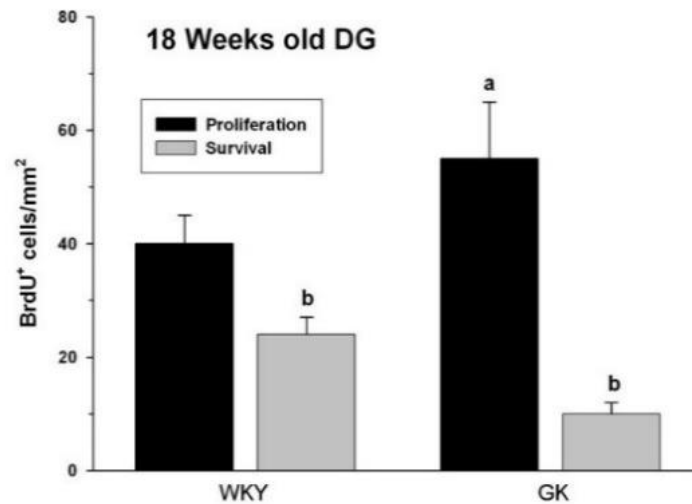


**Figure 22:** Number of surviving neural progenitors in the WKY and GK rats.

BrdU was injected twice a day for 5 days and the rats were killed on day 21 for assessing survival. Values are mean  $\pm$  SD of  $n = 6$  rats/group. In case of each rat, the number of BrdU<sup>+</sup> cells were counted using 4 brain sections. Statistics: “a” for  $p < 0.05$  compared with the respective WKY group and “b” for  $p < 0.05$  compared with the respective proliferation group (One-way ANOVA followed by Tukey-Kramer multiple comparisons test). WKY: normoglycemic Wistar-Kyoto; GK: diabetic Goto-Kakizaki; SVZ: subventricular zone; DG: dentate gyrus. From (Lang *et al.*, 2009).

## 5. Effects of obesity on the different aspects of neurogenesis

In a way similar to what was observed in diabetic models, high-fat diet protocols that result in the development of obesity result in neurogenic impairments (i.e., depletion of NSCs, impairment of NSC activity, impaired neuronal functions (Li *et al.*, 2012; Pintana *et al.*, 2019). The analysis of obese *ob/ob* mice (homozygous for the obese spontaneous mutation in gene encoding leptin, *Lep<sup>ob</sup>*) show a decreased hippocampal neurogenesis through the lower number of proliferative cells (phosphohistone H3<sup>+</sup> cells) and neuronal differentiation (doublecortin<sup>+</sup> cells) in the dentate gyrus of the hippocampus, compared to control littermates (Bracke *et al.*, 2019). In the hypothalamic neurogenic niche, a 4-month HFD induces a decreased in neural progenitor proliferation and a reduction in the survival rates of new born cells generated associated with impaired neuronal differentiation (Li *et al.*, 2012). Thus, HFD exerts a negative effect on different aspect of neurogenesis: neural progenitor proliferation, newborn cell survival

and differentiation (Li *et al.*, 2012). Strikingly, this impaired hypothalamic neurogenesis disturbs the renewal of neurons involved in the feeding behavior, favoring food intake.

Impaired neurogenesis is not only observed in normal physiological states in obesity and/or diabetic conditions, but also in regenerative ones. Indeed, obesity and/or type 2 diabetes impairs the neurological recovery after a stroke in association with decreased injury-induced neurogenesis occurring after brain damage (Pintana *et al.*, 2019). This could partly explain the lower capacity to recover from brain damage.

Therefore, all these data above and many several others support the fact that both obesity and diabetes alter the neural stem cells environment, that is the neurogenic niches; mainly by impairing neurogenesis at the level of proliferation, differentiation and survival of the neural stem cells and the neural progenitor cells leading consequently to lower brain plasticity and cognition.

### **III. Zebrafish as an emerging model to understand the impact of obesity and diabetes on the central nervous system**

#### **A. Zebrafish (*Danio rerio*)**

##### **1. Interesting facts for sciences**

The zebrafish (*Danio rerio*), belonging to *Brachydanio* genus and *Cyprinidae* family of the order Cypriniforms (McCluskey & Postlethwait, 2015), is a freshwater fish natively originating from South Asia (India, Pakistan, Bangladesh, Nepal and Bhutan) (Engeszer *et al.*, 2007; Vishwanath, 2010). It rests in a moderately flowing to non-flowing clear water (Engeszer *et al.*, 2007; Spence *et al.*, 2008; Arunachalam *et al.*, 2013), of neutral to basic pH and temperature ranging between 16.5 to 34°C (Engeszer *et al.*, 2007; Arunachalam *et al.*, 2013). Zebrafish has a laterally compressed fusiform shape and it can reach up to 1.8 cm to 5 cm maximum. Its life span ranges between 2 to 3 years and can reach 5 years in typical conditions (Gerhard *et al.*, 2002; Spence *et al.*, 2008; Arunachalam *et al.*, 2013). In 1970s and 1980s zebrafish have been first used by the American biologist George Streisinger and his colleagues at the University of Oregon.

This robust little fish can produce hundreds of offspring each week, providing a large number of embryos for a wide variety of studies. The interests to use this model lies behind

several reasons as its low cost, ease maintenance, short reproductive cycle and generation time (around 3 months) (Detrich *et al.*, 1999), its external fertilization and development, its transparency during embryogenesis that facilitates observational analysis notably for toxicity and screening assay (Chahardehi *et al.*, 2020), and the conserved genetics and physiology of adult zebrafish with mammals. Among vertebrate model organisms, zebrafish have emerged as a prominent model in the studies concerning drug development and screening (MacRae & Peterson, 2015), regenerative medicine (Doane, 1984), and has been modified to produce many transgenic lines (Zhang, 1990) (Fig. 23).

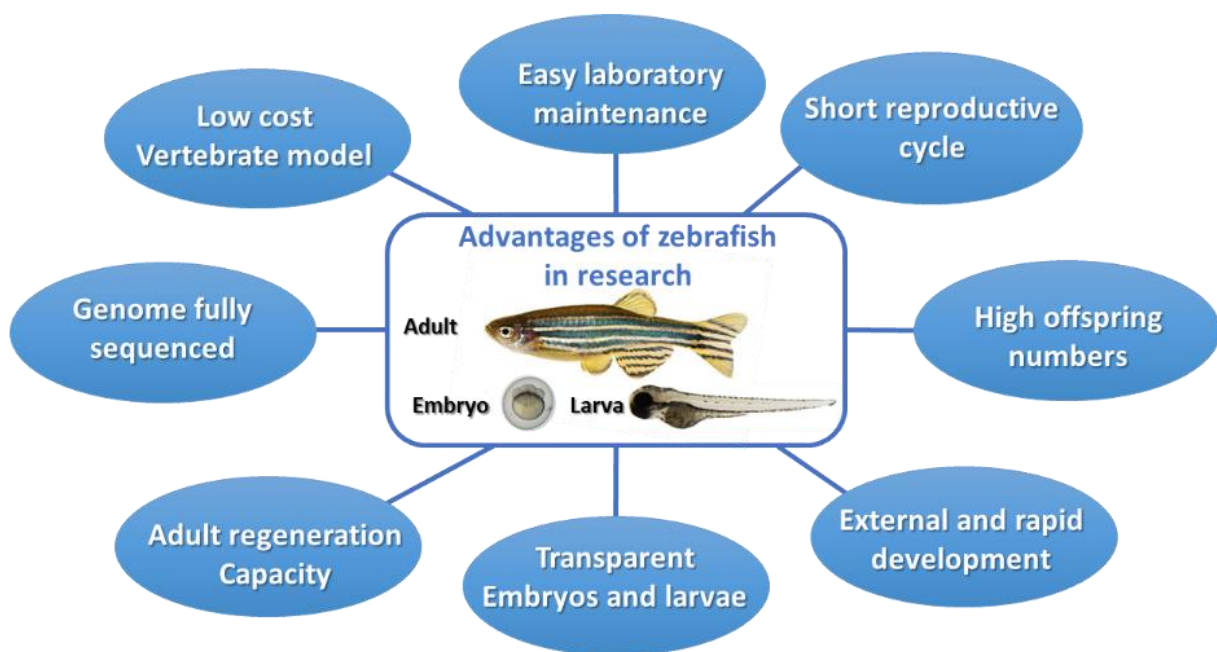


**Figure 23:** The advantages of using zebrafish model in science during all its developmental stages (embryo, larva and adult).

Interestingly, zebrafish share with mammals (rodents and humans) the main major organs and systems such as the cardiovascular system, the digestive system, and also the as the CNS (Williams & Hong, 2011) (Fig. 24A). This is notably due to the conserved genome homology and developmental processes. Indeed, zebrafish exhibit a high genomic homology with humans, 71% of human genes having at least one orthologue in zebrafish. Furthermore, in pathological conditions, this homology increases to 82% of disease related genes (genes bearing morbidity descriptions in human) in common (Howe *et al.*, 2013) (Fig. 24B).

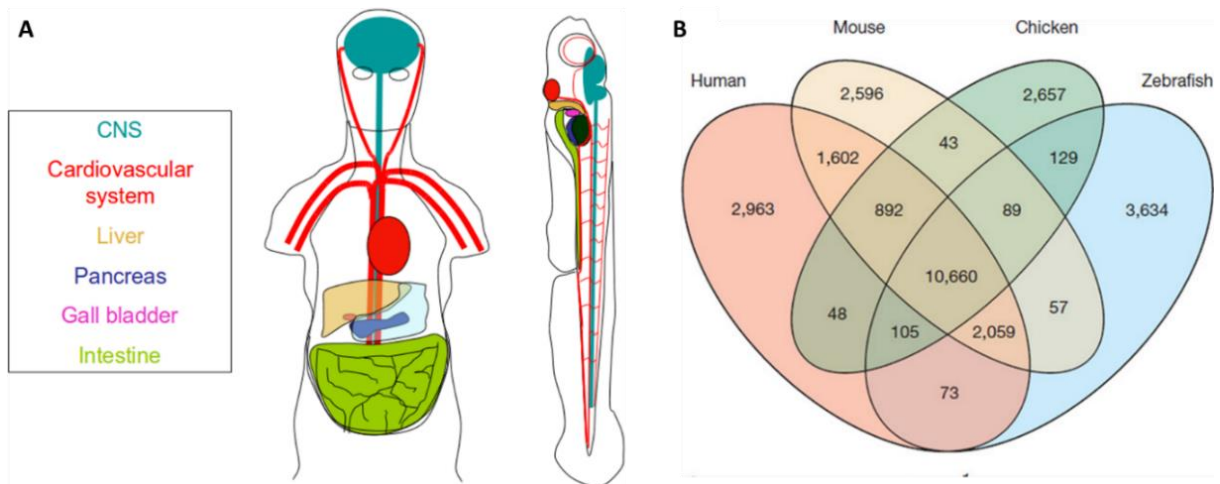


**Figure 24: Conservation of organ systems between zebrafish and humans and orthologue genes shared between the zebrafish, human, mouse and chicken genomes.**

(A) Common systems and organs shared between the zebrafish and human as the central nervous system, cardiovascular system digestive system including liver pancreas, gall bladder and intestine.

(B) Genes shared across species between human, mouse, chicken and zebrafish. From (A) (Williams & Hong, 2011); (B) (Howe *et al.*, 2013).

During decades, zebrafish have been extensively used in developmental biology to study embryonic development and notably the establishment of the central nervous system and differential regulation of gene expression (the way in which different genes are turned on and off in specific cells) (Walker & Streisinger, 1983; Streisinger *et al.*, 1986). Nowadays, zebrafish is a reliable model for studying among others angiogenesis, muscular, cardiac, hepatic and renal development and functions, metabolic diseases, neurodegenerative diseases (Schuermann *et al.*, 2014; Goessling & Sadler, 2015; Chavez *et al.*, 2016), genetics and cancer. In addition, zebrafish is also a very interesting model considering its capacity to regenerate successfully its main organs such as brain, heart, kidneys, liver, pancreas and also tail. Consequently, zebrafish play key roles in regenerative medicine research and helps to develop strategies for tissue recovery/repair in organism with poor regenerative capacity such as humans (Marques *et al.*, 2019) (Fig. 25).

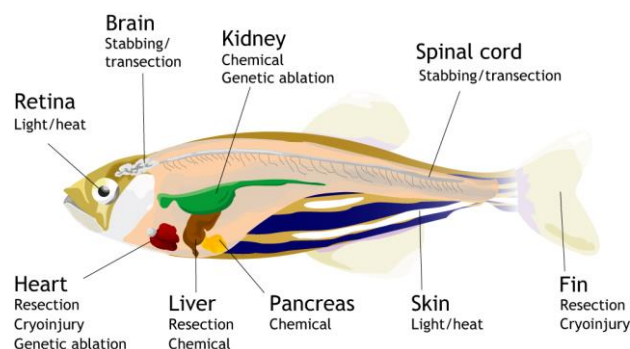


**Figure 25: Organ regeneration in the zebrafish.**

Summary of some of the organs and tissues used for regeneration studies in zebrafish. Preferred injury models are annotated for each organ. From (Marques *et al.*, 2019).

Taking in consideration all these advantages, zebrafish had been used in plenty of scientific fields. the use of zebrafish in the literature has been largely increased with time since its first uses in science (Fig. 26).

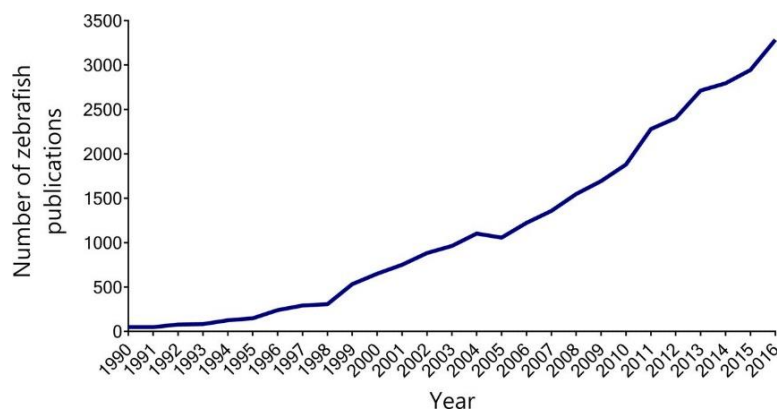


**Figure 26:** The use of zebrafish in biomedical research articles has been rising since the early 1990s. The line graph shows the number of publications indexed by PubMed under the term 'zebrafish' each year between 1990 and 2016. From (Adamson *et al.*, 2018).

## 2. Toxicity studies using zebrafish model

Zebrafish is widely used to determine the toxicity of several compounds and biodiversity extract (Zhang *et al.*, 2003; Kari *et al.*, 2007). The toxicological and pharmacological fields take advantages of the zebrafish embryos and larva to test quickly the toxicity of wide variety of chemicals (Padilla *et al.*, 2012; Truong *et al.*, 2014; Noyes *et al.*, 2015). The previously mentioned advantages of zebrafish embryo and larva as transparency and external development allow to notice any impact of the chemical treatment with non-invasive imaging (Garcia *et al.*, 2016). The high offspring produced and the fast reproduction make testing wide variety of concentrations from different molecules more feasible than other models as in rodents. An interesting feature in the zebrafish toxicity studies is the possibility to add the chemicals or extracts to the water which serves as an easy and simple administration route (Garcia *et al.*, 2016). Zebrafish express phase I (cytochromes-P450) and phase II (sulfo- and UDP-glucuronosyltransferases) drug metabolizing enzymes (Yasuda *et al.*, 2009; Huang & Wu, 2010; de Souza Anselmo *et al.*, 2018). The cytochromes P450 drug metabolizing enzymes in zebrafish are evolutionary conserved, having many orthologues with human (Goldstone *et al.*, 2010). As shown by Richter *et al.*, zebrafish larva succeeded to be an alternative of the human hepatic metabolism for toxicological testing of a newly developed drug as they were able to



produce high number of metabolites that are most actual and close to that produced by human (Richter *et al.*, 2019).

For all these advantages, Food and Drug Administration (FDA) announced the zebrafish as a model to test toxicity and safety of drugs (Garcia *et al.*, 2016). The zebrafish embryo toxicity tests are now standardized according to the Organization for Economic Cooperation and Development (OECD) test guideline 236 for acute toxicity testing of chemicals (Busquet *et al.*, 2014). According to the OECD (guideline 236), different concentrations are tested on 20 freshly fertilized zebrafish eggs until 96 hours post fertilization. Each day, five critical endpoints are checked for the acute toxicity, that are embryo coagulation, defective formation of somite, non-detached tail from the yolk sac and lack of heart beats (Busquet *et al.*, 2014). At the end of the experiment the lethal concentration in which half of the embryos are coagulated (LC<sub>50</sub>) is calculated (Busquet *et al.*, 2014).

Above all, zebrafish is widely used to understand the human disease and several zebrafish models have been established to resemble or mimic the pathophysiological states in humans. It includes neurological disorders models (Gama Sosa *et al.*, 2012), cardiovascular disease models 11967535 (Sehnert *et al.*, 2002), cancer models (Liu & Leach, 2011) and metabolic disorder models (Seth *et al.*, 2013). Considering the aim of this thesis, we will discuss some metabolic diseases models established in zebrafish.

## **B. Zebrafish models of obesity and hyperglycemia models: similarities with humans**

### **1. The use of zebrafish to mimic obesity**

Zebrafish have become a model to study metabolic diseases due to the conserved lipid metabolism, the presence of liver and pancreas, adipose tissue distribution, and the glucose homeostasis mechanisms (Zang *et al.*, 2018). The regulation of energy homeostasis and metabolism remains largely conserved with mammals with important critical organs and tissues including muscles, digestive organs (liver, pancreas, gut) and adipose tissue (i.e., visceral, intramuscular and subcutaneous) (Lieschke & Currie, 2007; Schlegel & Stainier, 2007; Song & Cone, 2007). As well, insulin regulation, glucose homeostasis and appetite regulation are

also evolutionary conserved between zebrafish and mammals including human (Elo *et al.*, 2007; Flynn *et al.*, 2009; Nishio *et al.*, 2012).

Consequently, obese zebrafish display human features of this pathology with increased body weight and body mass index resulting from lipid accumulation in the visceral adipocyte and subcutaneous ones (Fig. 27), higher levels of plasma triglyceride, dysregulated lipid metabolism pathways (i.e., PPAR gamma and leptin), nonalcoholic fatty liver (NAFLD, also called hepatic steatosis) and hyperglycemia (Flynn *et al.*, 2009; Oka *et al.*, 2010; Landgraf *et al.*, 2017). Interestingly, white adipose tissue in zebrafish displays a similar distribution than in humans and expresses same conventional adipocyte markers such as *pparg* and *fabp4* (peroxisome-proliferator activated receptor gamma and fatty acid binding protein) (Flynn *et al.*, 2009).

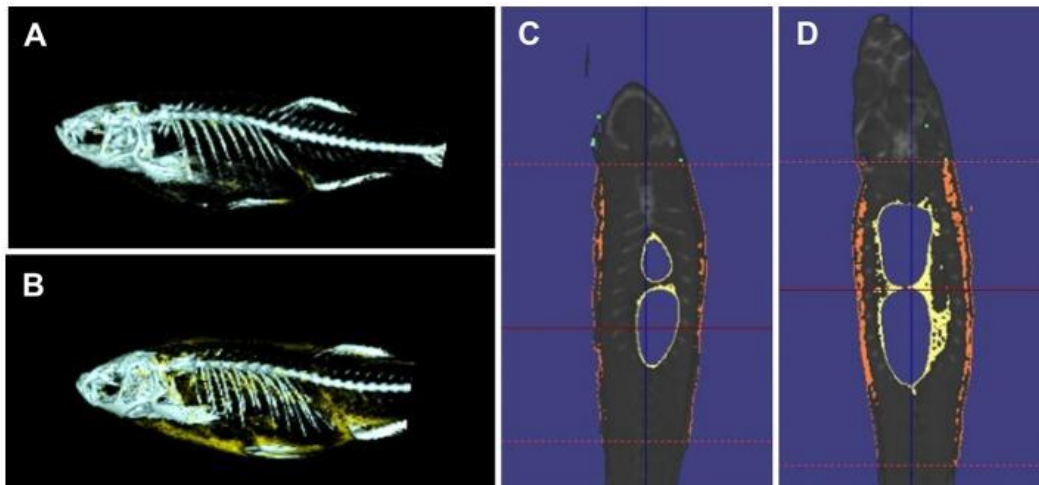


**Figure 27:** Three-dimensional Micro-computed tomography analysis in normally versus diet-induced obesity models of zebrafish.

(A) Normally fed zebrafish three-dimensional image. Gray color indicates skeleton and yellow color means adipocyte tissue.

(B) Overfed zebrafish three-dimensional image. Notice the visceral and subcutaneous yellow color.

(C) Normally fed zebrafish cross-sectional images. Yellow color indicates visceral adipose tissue and orange color indicates subcutaneous adipocyte tissue.

(D) Overfed zebrafish cross-sectional image. Notice the higher yellow and orange color in obese compared to normal fish. From (Zang *et al.*, 2018).

## 2. Models of obesity in the literature

To study obesity in zebrafish, a plenty of models have been established. It includes overfeeding models (diet-induced obesity and/or HFD protocols), transgenic models with overexpression of genes involved in obesity onset or mutant as explained below. Such models have been established in both larvae and adult zebrafish. Concerning the obesity induced



models in larvae, this could be achieved by overfeeding the larvae starting from the 7<sup>th</sup> day post fertilization. The overfed larva shows higher weight, size, BMI and triglyceride compared to the normally fed larva. In addition, the overfed larva suffers from hepatic steatosis and higher distribution of larval adipose tissue (Zheng *et al.*, 2016).

Adult zebrafish are also widely used to induce obesity. For instance, a diet-induced obesity (DIO) protocol consisting in overfeeding fish with of c for 8 weeks (60 mg corresponding to 150 calories versus 5mg corresponding to 20 calories) induced an increased gain weight and BMI as well as a hypertriglyceridemia and liver steatosis in the overfed fish compared to control ones (Oka *et al.*, 2010). Interestingly, the overfeeding of the fish with approximately the same amount of food (20 mg versus 60 mg of Artemia for CTRL and overfed groups, respectively) but for shorter period (4 or 6 weeks) leads to adverse effects. The over fed fish display higher body weight BMI, area of the adipose tissue, as well as the number, size, and density of adipocytes and altered obesity related genes (Montalbano *et al.*, 2016; Montalbano *et al.*, 2019; Montalbano *et al.*, 2021a). Besides, other protocols using high-fat feeding led to increased visceral, subcutaneous, and total body fat compared to normally fed fish, associated with cardiovascular impairments (i.e., abnormal heart morphology) (Watson & Kerr, 1985; Vargas & Vasquez, 2017; Meguro & Hasumura, 2018).

Similarly, genetic models can be used to mimic human obesity. For example, the overexpression of *akt1* (known as protein kinase B), that cross with numerous signaling pathways and play a key role in adipocyte differentiation, lipogenesis and organism development, resulted in increased body weight, BMI, adipocyte hyperplasia, abnormal fat deposition and glucose intolerance (Chu *et al.*, 2012), that constitute feature of the human pathology.

Overall, the different models of obesity developed in zebrafish share common features with obese rodents and people. This proves the relevance of using zebrafish models in research to further study and understand the obesity pathogenesis and try to find therapeutics.

### 3. The use of zebrafish to mimic hyperglycemia and diabetes

Zebrafish also recently emerged as a relevant model to study diabetes and hyperglycemia. First, the pancreatic ultrastructure (cells organization) and function are conserved in zebrafish regarding insulin secretion regulation and glucose homeostasis (Fig. 28A). Indeed, zebrafish have similar pancreatic development and cellular arrangement

compared to the mammalian pancreas, with conserved exocrine and endocrine functions (i.e., insulin producing  $\beta$ -cells), even if some difference exist as shown in the figure below (Argenton *et al.*, 1999; Biemar *et al.*, 2001; Kinkel & Prince, 2009) (Fig. 28B).

Beside the pancreatic similarity with mammals, zebrafish also exhibit conserved regulatory functions of the main organs involved in glucose homeostasis including skeletal muscles, adipocytes and liver (Maddison & Chen, 2017). Skeletal muscles are, as in mammals, the main organs for glucose disposal due to the presence of insulin sensitive glucose transporters the brown trout muscle glucose transporter (btGLUT with high sequence homology to GLUT4) (Planas *et al.*, 2000; Maddison *et al.*, 2015). In addition, Jurczyk *et al.* have shown a similar mechanism of glucoregulation in zebrafish embryos (held up by early developed zebrafish islet) that are conserved with embryonic and adult mammals (Jurczyk *et al.*, 2011) indicating that zebrafish utilizes mammalian-like mechanisms to regulate glucose abundance.

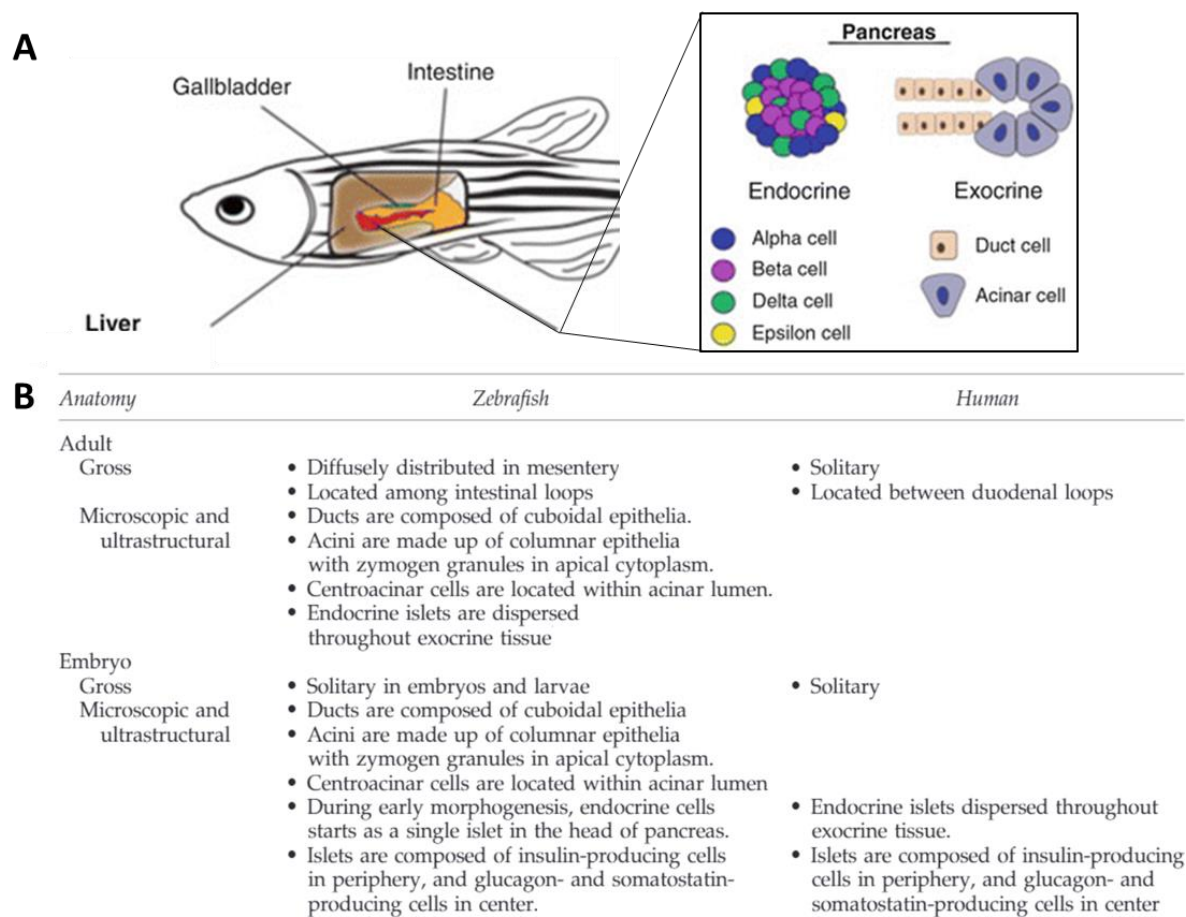


**Figure 28: Adult zebrafish pancreas in comparison to human pancreas.**

(A) Zebrafish scheme showing the main digestive organs (liver, gallbladder, intestine and pancreas) with focus on the pancreatic endocrine and exocrine cellular organization that is similar to mammalian pancreas.

**(B)** Pancreatic anatomy comparison between zebrafish and human in adult and embryonic stages. As in human, the pancreas development of the embryo and larva (2 to 7 days post fertilization) is in a solitary manner. However, during adulthood, the zebrafish pancreas is diffused through the mesentery but that of human remains a solitary organ. The pancreatic ultrastructure observed at the microscopic level is greatly similar between these species. From (A) (Yee *et al.*, 2013); (B) (Hwang & Goessling, 2016).

Above all, it is possible to measure the fasting blood glucose levels of the zebrafish and even perform the glucose tolerance test. The normal blood glucose level in zebrafish (50–75 mg/dl) being close to the normal human blood glucose level (70–110 mg/dl) (Zang *et al.*, 2015). Blood collection for measuring glycemia could be performed through several protocols (Eames *et al.*, 2010; Velasco-Santamaria *et al.*, 2011; Dorsemans *et al.*, 2017a) that requires fish euthanasia. For example, after the fish death, one of the eyes is removed with a fine pincer to allow the blood to accumulate in the ocular cavity of the eyes; then the accumulated blood is taken rapidly for glycemic measurements or other analysis (Dorsemans *et al.*, 2017a). However, repeated blood collection without sacrificing the fish has also been developed but is harder to set up (Zang *et al.*, 2013; 2015). This method is used notably in the case of intraperitoneal or oral glucose tolerance test (IPGTT and OGTT, respectively). Insulin measurements are also available in zebrafish model (Olsen *et al.*, 2012; Kimmel *et al.*, 2015).

Therefore, considering these general and overall homologies on metabolic organs and glucose homeostasis and regulation, between zebrafish and mammals (including humans) zebrafish is considered as a feasible model for better understanding diabetes and its complications.

#### 4. Developed zebrafish diabetes models in literature

For mimicking type 1, chemical ablation of the pancreas could be inducted by intraperitoneal injection of drugs such as streptozotocin (STZ) and alloxan (Intine *et al.*, 2013; Benchoula *et al.*, 2019a). These molecules lead to pancreatic  $\beta$ -cell death through the generation of oxidative stress and have been widely used in mammals and resulting in impaired insulin production and high fasting blood glucose levels (Islam & Loots du, 2009). In zebrafish, several studies have demonstrated that injection of STZ and/or alloxan results in larva and adult's hyperglycemia (Moss *et al.*, 2009; Olsen *et al.*, 2012; Nam *et al.*, 2015; Benchoula *et al.*, 2019b). For mimicking type 2 diabetes in zebrafish, different approaches have been used including among other immersion protocols within water supplemented with glucose, the diet-induced hyperglycemia and/or the genetic ones (Salehpour *et al.*, 2021). The chronic

hyperglycemia model in adults increases the blood glucose levels (around 280 mg/dl) after 14 days of glucose immersion (111mM) compared to the control fish (Capiotti *et al.*, 2014a; Capiotti *et al.*, 2014b; Dorsemans *et al.*, 2017a). Chronic hyperglycemia decreased the gene expression of proteins involved in the tight junction of the BBB in addition to decreased brain cell proliferation in the neurogenic niches (Dorsemans *et al.*, 2017b). Moreover, it leads to metabolic changes other than the increased blood glucose, as the increased levels of AGE protein levels in the eyes and decreased mRNA levels of insulin receptor in the muscles. These features were reversed when treated with “anti-diabetic” drugs (Capiotti *et al.*, 2014a). Together, these data show the deleterious impact of hyperglycemia on the CNS as in mammals.

Overfeeding was used also as an alternative model to mimic type 2 diabetes induced by obesity. The overfeeding of adult zebrafish increased the body weight, BMI, liver steatosis, and increased fasting blood glucose with higher insulin transcription levels in the liver, brain and muscles in the HFD fed fish compared to the CTRL fish (Meng *et al.*, 2017; Zang *et al.*, 2017). Similarly, the IPGTT and the OGTT tests reveal impaired glucose tolerance, a feature known in diabetic subjects with a potential increase in the insulin levels in the overfed fish compared to the normal ones. The use of “anti-diabetic” drug (metformin) ameliorates the hyperglycemic levels in the overfed group suggesting the relevance of this model to be used for type 2 diabetes investigations (Zang *et al.*, 2017).

Here is a brief overview on the genetic type 2 diabetes. The transgenic lines as the *insulin receptor a/b (insra/b)* is knock down model of liver specific insulin receptor a and b in larva (Yin *et al.*, 2015). The knock down leads to hyperglycemia and insulin resistance. Another model using adult zebrafish of skeletal muscle insulin resistance with a dominant-negative insulin-like growth factor type 1 receptor (IGF-IR). It shows blunted insulin signaling and glucose uptake (Maddison *et al.*, 2015).

### **C. Zebrafish as a model to study brain plasticity including constitutive and regenerative mechanisms.**

#### **1. Highly neurogenic regions conserved between zebrafish and mammals**

The brain of adult zebrafish, despite being morphologically different than mammals and humans, has well conserved major brain regions such as telencephalon, diencephalon, mesencephalon and rhombencephalon (Kozol *et al.*, 2016) (Fig. 29A). Very interestingly, in

contrast to mammals that display a limited neurogenesis during adulthood in mainly two regions (SVZ and DG of the hippocampus) (Fig. 29B), the brain of adult zebrafish displays a wide number of neurogenic niches spread all over the encephalon and exhibits a strong and intense neurogenesis and brain plasticity (Adolf *et al.*, 2006; Grandel *et al.*, 2006; Kaslin *et al.*, 2008; Zupanc, 2008) (Fig. 29C). This peculiar feature is due to the maintenance of neural stem cells (mainly radial glial cells) after embryonic development along the ventricular layers of the zebrafish brain, while these cells disappear greatly transforming into astrocytes in mammals. Interestingly, proliferative assays using the proliferating cell nuclear antigen (PCNA) marker and BrdU labeling experiments have shown that these cells were still actively proliferating and generating new born neurons that integrate the neural circuitry after weeks from BrdU injection. (Grandel *et al.*, 2006; Pellegrini *et al.*, 2007).

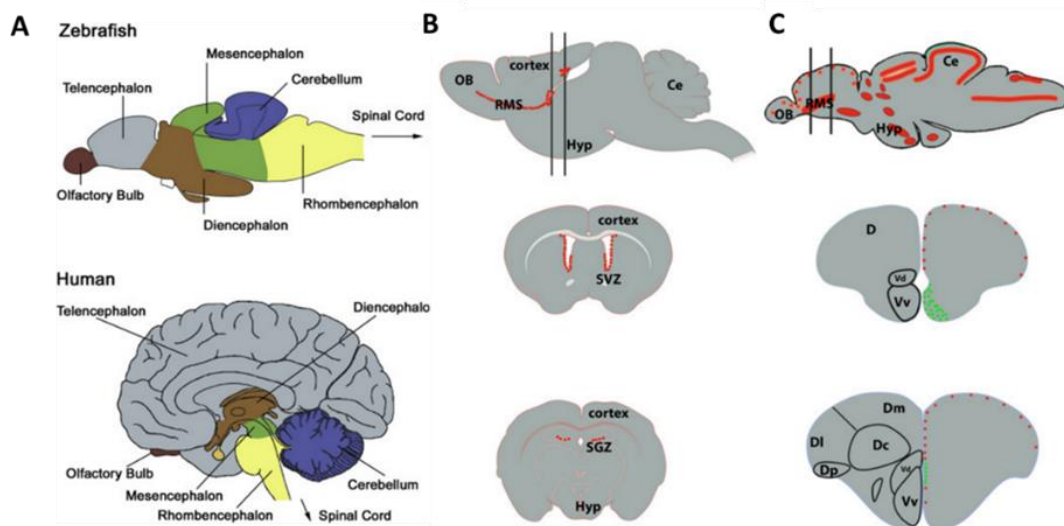


**Figure 29: Main brain subdivisions and neurogenic niches of zebrafish and mammalian brain.**

(A) Conservation of the main brain regions and their organization between human and zebrafish (similar colors corresponds to homologous region).

(B) The main proliferating regions in rodent brain represented by the red color in sagittal section (top); coronal section at the level of the subventricular zone (SVZ) proliferating region in red (middle) and the subgranular zone (SGZ) of the dentate gyrus of the hippocampus (bottom).

(C) The main proliferating regions in zebrafish brain represented by the red color in sagittal section (top); coronal section at the level of the anterior part of the telencephalon (middle) and the through the medial part of the telencephalon (bottom). Ce: cerebellum; D: telencephalic dorsal area; V: telencephalic ventral area OB: olfactory bulbs; Hyp, hypothalamus, RMS: rostral migratory stream. From (Bartel *et al.*, 2020; Diotel *et al.*, 2020).

## 2. Similarities in zebrafish and mammalian neural stem cells

In zebrafish, the neural stem cells are commonly known as radial glial cells expressing well-characterized and specific markers such as intermediate filaments (GFAP and Nestin), the calcium binding protein (S100 $\beta$ ), the estrogen-synthesizing enzyme (Aromatase-B) and the



brain lipid binding protein (BLBP) (Grandel *et al.*, 2006; März *et al.*, 2010; Than-Trong & Bally-Cuif, 2015; Jurisch-Yaksi *et al.*, 2020). Thus, most of RGC markers in zebrafish are also labeling embryonic RGCs in mammals or the neurogenic astrocytes (B-cells and Type 1 NSCs, C-cells and Type 2 the transient amplifying cells and Type 3 neuroblasts) during adulthood (Diotel *et al.*, 2020). Therefore, the brain of adult zebrafish brain is an interesting model to study neurogenesis and its regulation through stimulating and inhibiting factors. The molecular characterization of neural stem cells (März *et al.*, 2010; Lindsey *et al.*, 2012) shows different types of progenitors in the telencephalon of adult zebrafish (i.e., type 1, 2, 3a and 3b). The type 1 are quiescent radial glial cells, type 2 are proliferating radial glial cells and type 3 cells are proliferative neuroblasts (Calvo-Ochoa *et al.*, 2021). The proliferative cells from the ventricular zone corresponds to neural stem cells or progenitors. Each type of these cells has its own specific markers as shown in the figure below (März *et al.*, 2010) (Fig. 30).

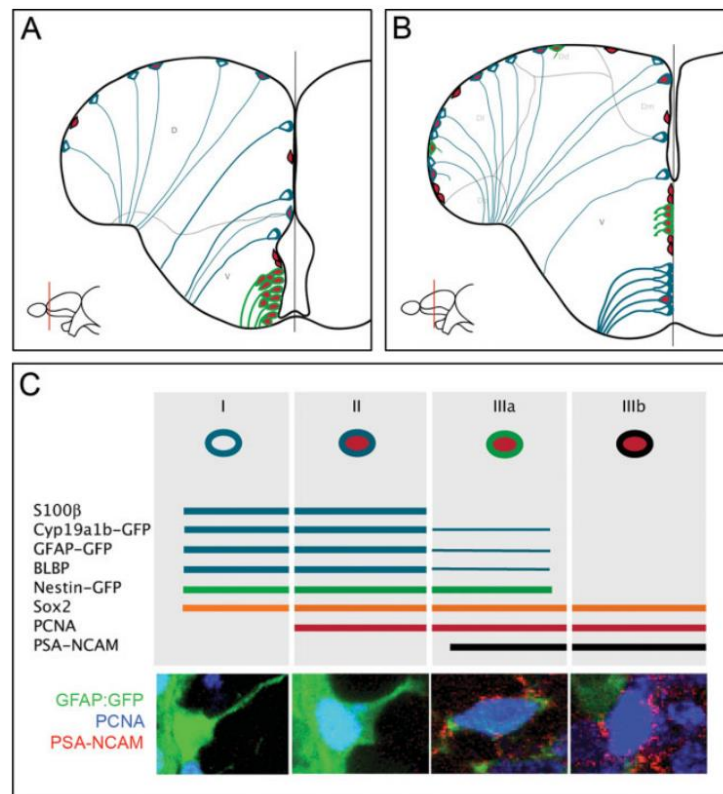


**Figure 30: Marker expression and morphology of distinct cell types at the ventricular zone of the telencephalon.**

(A) Cross section of the anterior telencephalon showing different types of neural cells with radial glia, progenitor and neuroblast markers.

(B) Cross section of the medial telencephalon showing different types of neural cells with radial glia, progenitor and neuroblast markers.

(C) The different types of neural stem cells (I, II, IIIa and IIIb) that are shown in A and B with their respective markers; at the bottom is an immunostaining representation of each cell type. From (März *et al.*, 2010).

In mammals (rodents and human) also there exist several types of neural stem cells and neural progenitors that are B-cells in the SVZ and Type 1 NSCs in the DG, C-Cells in the SVZ and Type 2 the transient amplifying cells in the DG and the A-cells in the SVZ and Type 3 neuroblasts in the DG (Ghaddar *et al.*, 2021b) (Fig. 31A,B). Therefore, zebrafish, rodents, and humans share similar features concerning the telencephalic neurogenic niches, type of NSCs and neural progenitors in addition to the type of newborn generated cells (Fig. 31C).

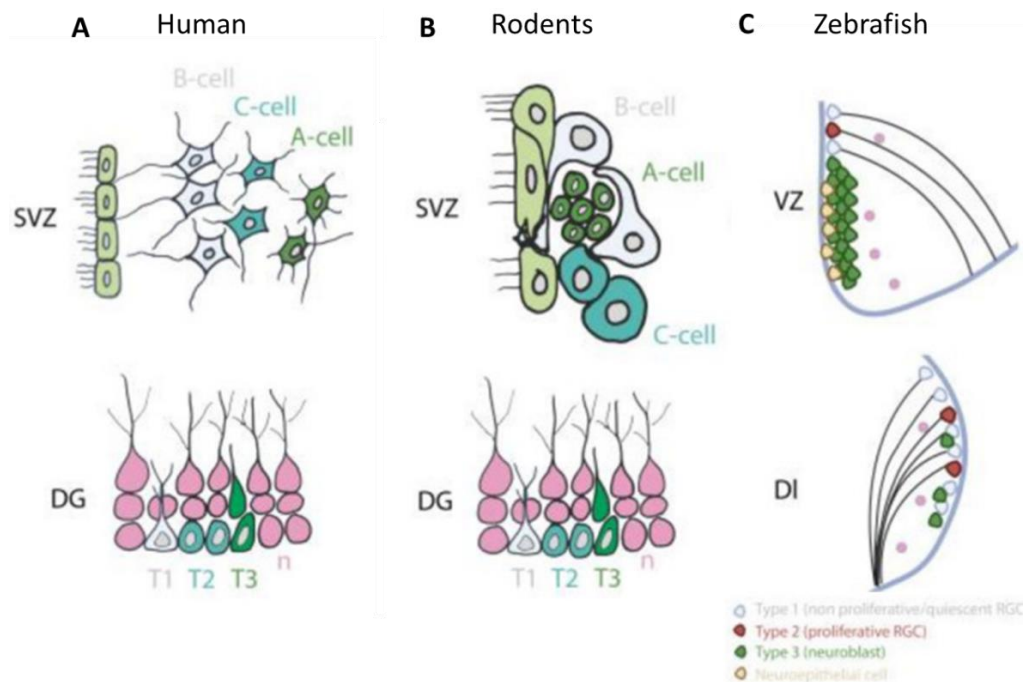


**Figure 31: Cell composition of the neurogenic niches in zebrafish, mice and humans.**

(A) The main neurogenic niches in the SVZ and the DG of the hippocampus in human

(B) The main neurogenic niches in the SVZ and the DG of the hippocampus in mouse. In mammals, the NSCs are shown in grey (B-cells and Type 1 -T1-), the transient amplifying cells in light green (C-Cells and Type -T2-) and the neuroblasts in dark green (A-cells and Type 3 -T3-).

(C) The main neurogenic niches in the subpallial ventricular zone (VZ), the dorsolateral telencephalon (DI) in zebrafish. In zebrafish, type 1 and type 2 cells are quiescent and proliferative radial glial cells (RGC), respectively (quiescent and proliferative neural stem cells (NSCs)). Type 3 cells are proliferative neuroblasts. The neuroepithelial cells are NSCs from the subpallium. Ce: cerebellum; Cx: cerebral cortex; DI: lateral zone of the dorsal telencephalic area; DG: dentate gyrus of the hippocampus; Dp: posterior zone of dorsal telencephalic area; HYP: hypothalamus; MO: medulla oblongata; OB: Olfactory bulbs; RGC: radial glial cell; RMS: rostral migratory stream; SVZ: subventricular zone VZ: ventricular zone; TEL: telencephalon; TeO: optic tectum. From (Ghaddar *et al.*, 2021b).

### 3. Zebrafish have a high capacity for brain repair

In addition to its high constitutive neurogenesis that shares similar features with mammalian neurogenesis, the brain of adult zebrafish also displays a strong regenerative capacity allowing to better understand the mechanisms sustaining brain repair mechanisms

(Grandel *et al.*, 2006; Becker & Becker, 2008; Schmidt *et al.*, 2014). Thus, brain injury can be easily performed through the insertion of a small needle via the skull or the nasal cavity that will lead to the telencephalon injury (Kroehne *et al.*, 2011; Marz *et al.*, 2011; Baumgart *et al.*, 2012). Similar process can also be done at the level of the optic tectum (Shimizu & Kawasaki, 2021). Briefly after the lesions, cell death will occur and is followed by the recruitment of microglia that proliferate (Baumgart *et al.*, 2012) become amoeboid and secrete proinflammatory cytokines (Marz *et al.*, 2011). Oligodendrocytes and OPCs are also recruited and proliferate (Marz *et al.*, 2011). Finally, neural stem cells actively divide and generate new neurons to replace the dead ones starting from 2 days post lesion peaking between days 5 and 8 post lesion (Marz *et al.*, 2011; Baumgart *et al.*, 2012). Importantly, it was shown that inflammation and microglia activation was essential to induce injury induced neurogenesis (Kizil *et al.*, 2012; Kyritsis *et al.*, 2012)

All these cellular events occurring during brain injury are common between the zebrafish and mammalian brain. However, zebrafish have the capability to repair its brain after a traumatic lesion without forming a glial scar and to totally recover its motor function that is not the case in the brain of mammals (Baumgart *et al.*, 2012; Kishimoto *et al.*, 2012; Ghaddar *et al.*, 2021b). The similarities and differences of brain repair mechanism between the zebrafish and mammals have been reviewed in a review article that we published during my doctoral internship (Ghaddar *et al.*, 2021b) (Annex 1, page 231).

#### 4. Conserved blood-brain barrier structure and function

As in mammals, the zebrafish brain is protected by a BBB that helps maintain brain homeostasis (Eliceiri *et al.*, 2011). Zebrafish also develop a BBB at 3 dpf, which is reported to be similar to happen during mammalian embryogenesis (Jeong *et al.*, 2008; Xie *et al.*, 2010) (Fig. 32). Furthermore, the BBB chemical penetration or exclusion profile has been shown to be the same between zebrafish and mammals (Fleming *et al.*, 2013). In addition, specific molecular components of a functional BBB were identified in the zebrafish brain microvasculature as zonula occludens-1 and claudin 5 that are tight junction proteins as well as “astrocyte/radial glial” markers with endothelium (Jeong *et al.*, 2008). Therefore, a high similarity exists between the zebrafish BBB and the mammalian one at cellular, structural, functional and developmental levels (Quinonez-Silvero *et al.*, 2020), making zebrafish a reliable model to study brain disorders linked to BBB breakdown as strokes, AD and Parkinson disease (Quinonez-Silvero *et al.*, 2020).



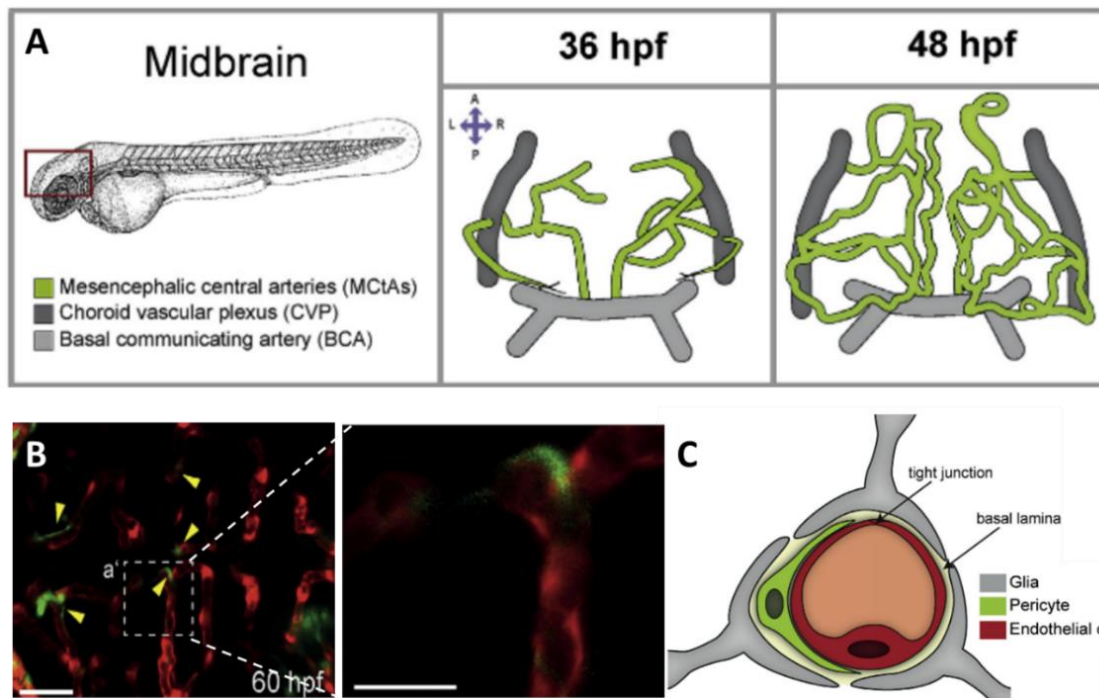


**Figure 32: Brain-brain barrier formation during early stages of development in the zebrafish.**

(A) Schematic representation of the early angiogenesis that occurs in the zebrafish larva showing the sprouting of the vessels at 36 hours post fertilization (hpf) and 48 hpf.

(B) Confocal image of immunostaining for the brain capillaries in zebrafish in double transgenic embryos with pericytes (green) and brain capillaries (red) detection. The magnified square (a) shows the pericyte (green) in contact with the brain capillary (red).

(C) Schematic representation of the neurovascular unit of the blood-brain barrier of the zebrafish embryo (60 hpf) composed of the endothelial cells wrapped by the pericytes and the glial cells sheath the brain capillaries. From (Quinonez-Silvero *et al.*, 2020).

To summarize, taking all these facts in consideration, the zebrafish have emerged as an interesting model to study the brain plasticity and brain homeostasis with a focus on different aspects that are investigated in mammals as neurogenesis, blood-brain barrier and regeneration in brain injury conditions.

Therefore, zebrafish stands as an interesting model to study metabolic disorders (as in case of obesity and diabetes) and to investigate central nervous system homeostasis. It can be an integrative model to analyze the adverse effects of the obesity and/or diabetes on the brain, with specific highlights on brain plasticity (neurogenesis), regenerative capacities and brain protection (BBB functionality). This was partly discussed in a submitted review article (Annex 2, page 249). This promising model can contribute to the better understanding of neurodegenerative processes that occur during metabolic disorders, and may help to find new synthetic or natural therapeutics.

## IV. Plants as a source of new bioactive molecules

### A. Vegetal biodiversity and beneficial effects on health: focus on medicinal plants

#### 1. Dietary natural bioactive compounds: focus on polyphenols

Accumulating lines of evidence are confirming the role of natural bioactive compounds in exerting a positive impact on body health (Biesalski *et al.*, 2009; Bernhoft, 2010). Epidemiological evidences have shown that the diet rich in such compounds lowers the risk of having cancers, neurodegenerative disease, cardiovascular disease and diabetes 31480794 (Sofi *et al.*, 2008; Mentella *et al.*, 2019). On daily bases, our bodies are consuming considerable amount of these compounds when following a healthy diet composed among others of vegetables, fruits, grains, leaves, fish (Biesalski *et al.*, 2009; Astley & Finglas, 2016. ). Among these bioactive compounds are the polyphenols, alkaloids, carotenoids, glucosinolates, terpenoids, saponins and vitamins (Camara *et al.*, 2020) (Fig. 33)

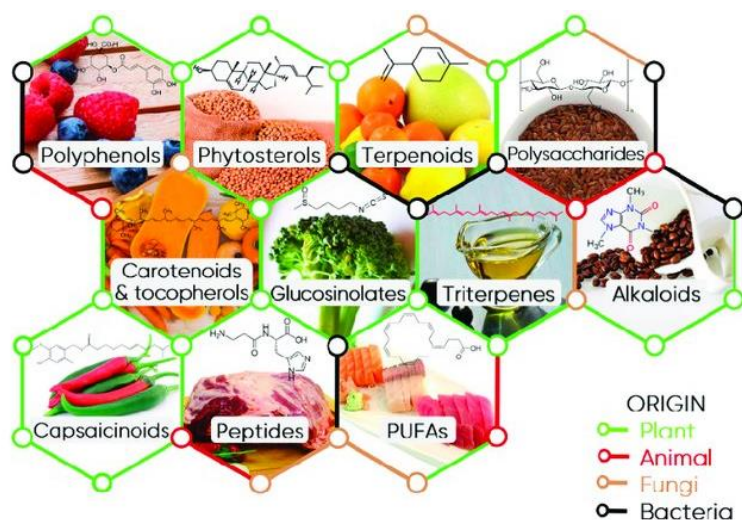


**Figure 33: Major Food Bioactive Compounds sources and classification.**

An illustrative example of a source and compound is indicated for each class: polyphenols (chlorogenic acids in blueberry and raspberry fruits), phytosterols (stigmasterol in soybean), terpenoids (limonene in citrus fruits), polysaccharides (cellulose in flax seeds), carotenoids & tocopherols ( $\beta$ -carotene/vitamin A), glucosinolates (sulforaphane in broccoli), triterpenes (squalene from olive oil), alkaloids (caffeine in coffee beans), capsaicinoids (capsaicin in peppers), bioactive peptides (carnosine in red meat), and PUFAs (polyunsaturated fatty acids, docosahexaenoic acid—DHA, in different fishes). From (Camara *et al.*, 2020).

The dietary polyphenols are among the most interesting natural bioactive molecules studied so far (Tresserra-Rimbau *et al.*, 2018). Until now, more than 8000 phenolic structures are discovered in the plant kingdom (Tsao, 2010; Cosme *et al.*, 2020). Polyphenols that are

considered as secondary metabolites are characterized by an aromatic ring with at least one hydroxyl group. They can exist as simple molecules (phenolic acids) or highly polymerized compounds (tannins) (Durazzo *et al.*, 2019). According to their chemical structure, they are classified into two main groups: flavonoids and non-flavonoids (Durazzo *et al.*, 2019) (Fig. 34).

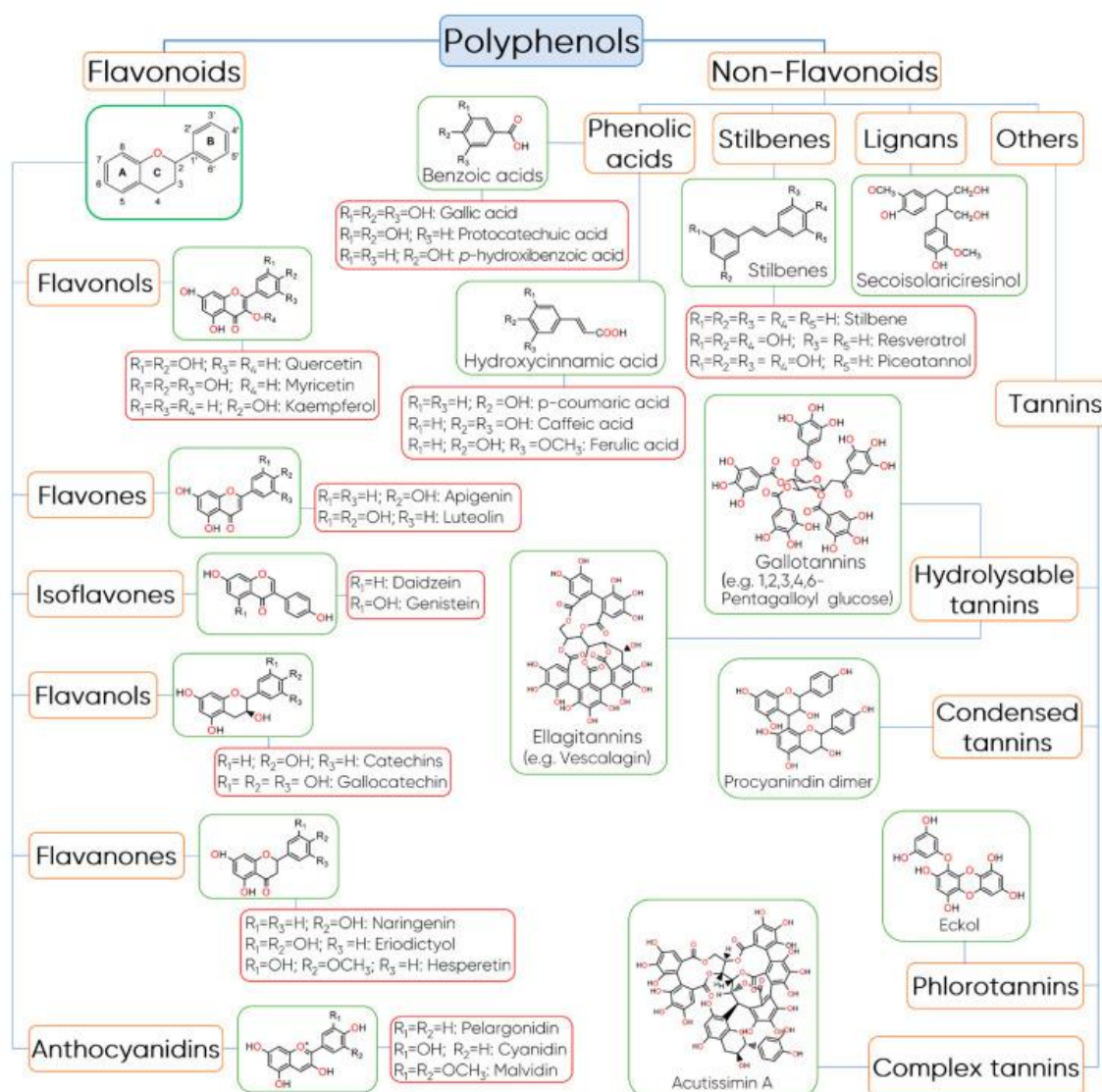


**Figure 34: Classification and structure of polyphenols.**

The polyphenols are classified into two major families: the flavonoids and the non-flavonoids. Among the non-flavonoids, phenolic acids, stilbenes, lignans and tannins are the main subfamilies. From (Camara *et al.*, 2020).

Like the natural bioactive compounds, the main dietary sources of polyphenols are fruit and beverages (fruit juice, tea, coffee, chocolate), and in less amounts in vegetable, dry legumes and cereals (Scalbert & Williamson, 2000). Approximately, the total daily intake is 1 gram (Scalbert & Williamson, 2000). As being part of the natural bioactive molecules, the natural polyphenolic families (flavonoids as an example) act on several signaling pathways and enzymes which enable them to display pleiotropic properties as anti-oxidant, anti-inflammatory

anti-oxidant, “anti-diabetic”, anticarcinogenic, neuroprotective, cardioprotective, antimicrobial, anti-adipogenic (Scalbert & Williamson, 2000; Umeno *et al.*, 2016; Wu *et al.*, 2018) (Fig. 35). For example, quercetin is a dietary polyphenol belonging to the flavonoid family and having beneficial effects against body weight increase (Leisher *et al.*, 2016). In addition, it exhibits tissue specific anti-inflammatory property that prevents the low-grade inflammatory state in the in the adipocytes (Forney *et al.*, 2018).

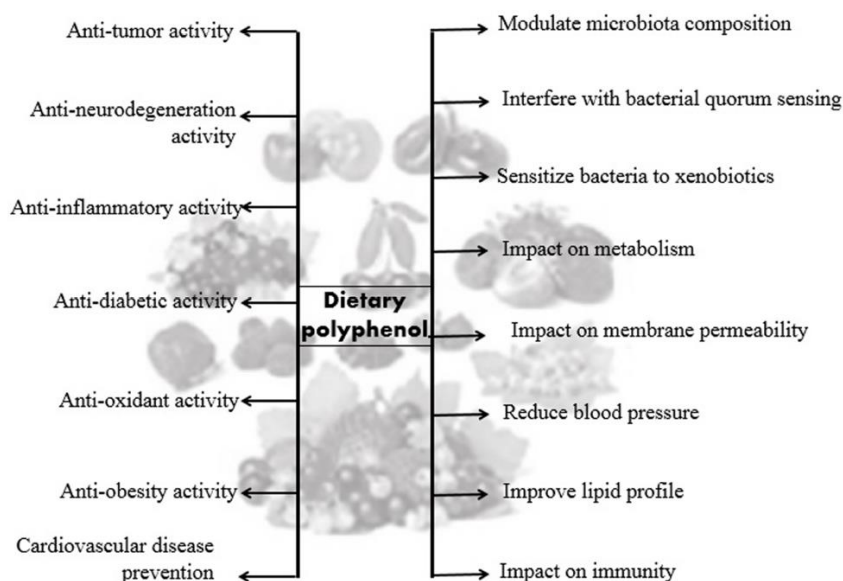


**Figure 35: Beneficial effects of dietary polyphenols.**

The dietary polyphenols harbor anti-inflammatory, anti-oxidant, anti-tumor, “anti-diabetic” and anti-obesity effects that make them beneficial against several disorders as metabolic disorders, hyperlipidemia, high blood pressure and bacterial infections. From (Ray & Mukherjee, 2021).

Anti-obesity properties have been documented in some plants rich in polyphenols (especially flavonoids), as citrus extracts such as *Citrus limon* (Nuzzo *et al.*, 2021), *Citrus sinensis* (Montalbano *et al.*, 2019), *Citrus aurantium* (Kim *et al.*, 2012). Similar properties were also observed in other quercetin rich fruits such as *Ficus opuntia* (Yeddes *et al.*, 2013) and the white grape *Vitis vinifera* (Montalbano *et al.*, 2021a), that are among the main constituents of the Mediterranean diet. These polyphenols exert beneficial effects on  $\beta$ -oxidation and increased lipolysis (Kang *et al.*, 2012), reducing lipid accumulation, decreasing pre-adipocyte differentiation, lipogenesis and inducing the adipocyte apoptosis (Seo *et al.*, 2014).

The special chemical structure of the polyphenols contributes to their beneficial bioactive properties. For example, the phenolic hydroxyl groups of the polyphenols are easily oxidized which gives them a high ability to delocalize uncoupled electrons and scavenge free



radicals (ROS and active nitrogen species) exhibiting thereby anti-oxidant activity (Kim *et al.*, 2014; Zheng *et al.*, 2021). More interestingly, the ROS and nitric oxide scavenging property of the polyphenols confers their neuroprotective characteristic by inhibiting neuronal necrosis, enhancing anti-oxidant and cell survival pathways and inhibiting the proinflammatory pathways in the neuronal cells (Zhang *et al.*, 2017) (Fig. 36). This property makes the polyphenols one of the most bioactive agents in neurodegeneration and tumor prevention (Squillaro *et al.*, 2018).

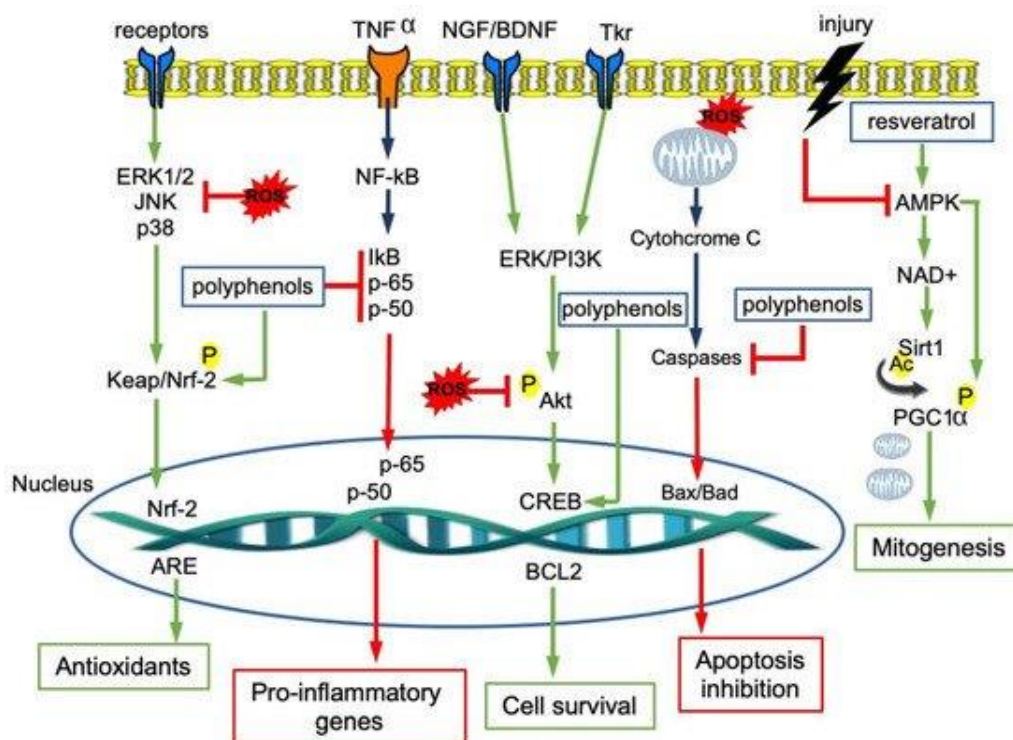


**Figure 36: Neuroprotective intracellular signaling pathways conferred by polyphenols.**

The polyphenols counteract the ROS activities in the neural cells by enhancing the anti-oxidant pathways (Nrf-2 and Keap), cell survival pathways (Akt pathway through the NGF/BDNF and Tkr receptor) and mitogenesis pathways (AMPK signaling pathway); Polyphenols inhibit however the proinflammatory gene transcription (through the TNF $\alpha$  and NF $\kappa$ B pathways) and apoptosis induction (caspases inhibition). ERK: extracellular signal-regulated kinases ; JNK: The c-Jun N-terminal kinase ; Nrf-2: nuclear factor erythroid 2-related factor 2 ; TNF $\alpha$ : tumor necrosis factor alpha; NF $\kappa$ B: nuclear factor kappa-light-chain-enhancer of activated B cells; I $\kappa$ B: IkappaB kinase; PI3K: Phosphoinositide 3-kinases; Akt: protein kinase B; CREB: cAMP response element-binding protein; BCL2: B-cell lymphoma 2; AMPK: MP-activated protein kinase; NAD $^{+}$ : nicotinamide adenine dinucleotide; Sirt1: sirtuin1; PGC1 $\alpha$ : proliferator-activated receptor gamma coactivator 1- $\alpha$ ; ROS: reactive oxygen species. From (Di Meo *et al.*, 2020).

## 2. Focus on medicinal plants

An alternative rich source of polyphenols, and other natural bioactive compounds, that has been used since long time ago by the traditional and modern health care systems are the

medicinal plants (Newman *et al.*, 2003; Newman & Cragg, 2007). The plants until the 16<sup>th</sup> century and before the discovery of the iatrochemistry were used as the only source of treatment and prevention (Petrovska, 2012). Twelve recipes for drug preparation using 250 different medicinal plants were discovered written on a Sumerian clay slab from Nagpur, aging 5000 years ago. In addition, 365 drugs originating from dried medicinal plants were described in “Pen T’Sao” book, a Chinese book written 2500 BC (Before Christ), many of which are still used until these days as *cinnamon bark*, *podophyllum*, *the great yellow gentian* and *ephedra* (Bottcher, 1965; Wiart, 2006). During the Middle Ages, the European physicians take advantage of the Arab works among them the heritage of Avicenna ‘Abu Ali ibn Sina’ (980-1037 CE (Current era)) in which over 1000 medicinal plants have been described and prescribed to treat various diseases for many centuries (Tucakov, 1964; Petrovska, 2012; Buranova, 2015).

The discovery of the isolation techniques in the 19<sup>th</sup> century serves as a turning point from using the medicinal plants to the use of the extracted alkaloids, glycosides, etheric oils, hormones and vitamins (Dervendzi, 1992). The pure form of the extracted drugs was replacing strongly the medicinal plants from which they were isolated (Petrovska, 2012). Recently, the medicinal plants are emerging again to the pharmacopeia with the decreasing efficiency of some drugs, the higher contraindications for their usage and the preference to come back to nature, the original source of all medications (Petrovska, 2012). *Opium*, *Aconitum*, *Secale cornutum*, *Punica granatum*, *Ricinus* are some examples of the old medicinal plants that have been restored back to the pharmacy for their valuable benefits in clinical studies and their active compounds. Some countries nowadays as Russia, Germany, France and the United Kingdom have separate herbal pharmacopoeias for plants with real medicinal values (Blumenthal, 1998; Petrovska, 2012)

Briefly here are some examples for some famous consumed plants and their traditional uses and benefits: Cinnamon, Peppermint and Ginger are used to promote a “good” blood circulation. Certain aromatic plants such as Aloe and Barberry are used to reduce toxins in blood. They can be used in infusion, decoction, powder and some are edible (Ahvazi *et al.*, 2012). The traditional uses of some medicinal plants is believed to cure a wide variety of diseases through various properties: wound healing, anti-inflammatory, anti-oxidant, anti-dysenteric, anti-hemorrhagic, decreasing in blood pressure, antibacterial, weight reducing (Ahvazi *et al.*, 2012).

The phytochemical screening of plants shows their richness in secondary metabolites. In addition to the polyphenols that are mostly investigated, the medicinal plants are a good source of alkaloids, cardiac glycosides, flavonoids, saponins, steroids and terpenoids (Sasidharan *et al.*, 2011). Phenols and flavonoids in the medicinal plants are the main bioactive components with high ROS scavenging and anti-oxidant properties (Mishra *et al.*, 2013; Wang *et al.*, 2016a; Wang *et al.*, 2016b; Andreu *et al.*, 2018). Anthocyanins, acid, mandelic acid and quercetin are some polyphenols conferring the anti-oxidant activity of certain medicinal plants investigated by research (*Ipomoea batatas*, *Bauhinia variegata* L., *Opuntia ficus-indica*, *Aesculus indica*, *Polygonatum verticillatum*) (Mishra *et al.*, 2013; Andreu *et al.*, 2018; Kumar Singh & Patra, 2018; Zahoor *et al.*, 2018). A different set of phenolics as gliricidin 7-*O*-hexoside, quercetin-7-*O*-rutinoside, Kaempferol, trihydroxyflavone, clindamycin and strictinin confers antibacterial properties for some medicinal plants investigated (Tsai *et al.*, 2015; Dzotam *et al.*, 2018; Geethalakshmi *et al.*, 2018). Tungmunnithum reviewed in a similar way the main phenolic compounds of specific medicinal plants with specific anticancer, cardioprotective, immune system promoting, anti-inflammatory and skin protective effects (Tungmunnithum *et al.*, 2018) (Fig. 37).

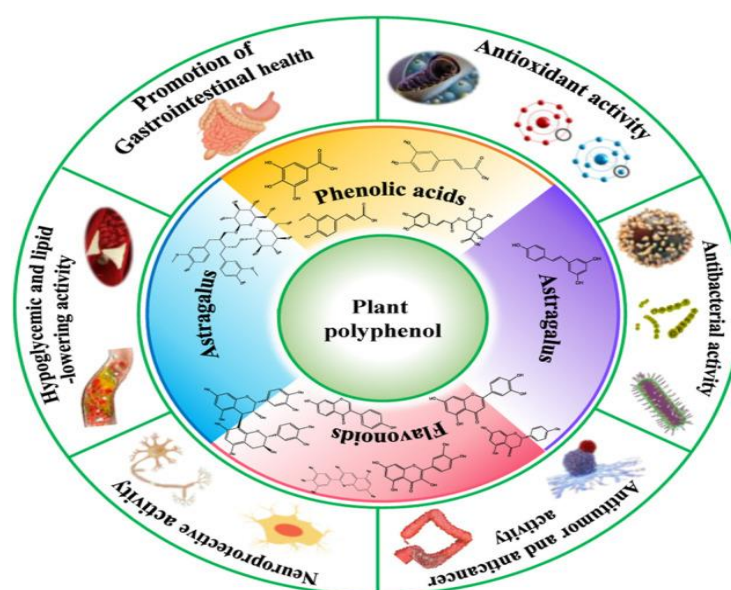


**Figure 37: Major plants polyphenol and their beneficial health effects.**

The phenolic acids, flavonoids and astragalus (known also as stilbenes) are some of the main polyphenolic families in the plants behind the neuroprotective, antitumor, antibacterial, anti-oxidant, gastro-protective, anti-hyperglycemic and anti-lipidemic effects. From (Yan *et al.*, 2021).

However, the unconscious uses of medicinal plants and the wrong thoughts that medicinal plants are fully harmless and nontoxic should be taken in consideration. Several intoxication cases are recorded after the extensive use, wrong doses and even the consumption

of some poisonous plants leading to hepatotoxicity, gastrointestinal poisoning, nephrotoxicity, respiratory toxicity and cardiac poisoning (Farzaei *et al.*, 2020). This fact uncovers the importance of the extensive research that should be done for the clear and strict prescription, preparation, and consumption of the medicinal plants all over the world

## **B. Reunion Island biodiversity**

Reunion Island is a biodiversity hotspot with a wide variety of plants used in the traditional medicine even since the 17<sup>th</sup> century (Lavergne, 1989). The geomorphology (volcanic island) and the geography of the Reunion Island provides a diversified flora since up to 30% of the plants are endemic (Strasberg *et al.*, 2005). Its flora is constituted of 550 species among them 165 are single island endemics and 140 are Mascarene endemics species. Twenty-seven of these plants have been registered in the French Pharmacopeia (Fig. 38). Several scientific records indicate beneficial effects of these plants, whereby of the 64 endemic plants from the Mascarene Islands (Reunion Island and Mauritius) have been discovered with anti-plasmodial, anti-chikungunya virus and anti-oxidant activities (Ledoux *et al.*, 2018). Some plants specific to the Reunion Island showed anti-malarial effect with *in vitro* and *in vivo* studies (Jonville *et al.*, 2008). In addition, 8 endemic medicinal plants registered in the French Pharmacopeia from Reunion Island (*Aphloia theiformis*, *Ayapana triplinervis*, *Dodonaea viscosa*, *Hubertia ambavilla*, *Hypericum lanceolatum*, *Pelargonium x graveolens*, *Psiloxylon mauritianum* and *Syzygium cumini*) were analyzed for their anti-oxidant property and phenolic content. These plants harbor diverse polyphenolic content (as quercetin, chlorogenic acid, procyanidin and mangiferin) with a potent anti-oxidative property (Checkouri *et al.*, 2020). An important proportion of the medicinal plants registered in the French Pharmacopeia are used traditionally for their believed “anti-diabetic”, anti-obesity, anti-oxidant, hypolipidemic and anti-inflammatory properties. The studies on these believed traditional effects of the plants are still limited which uncover the necessity to further investigate these effects with *in vitro* and *in vivo* models. Among the Reunionese medicinal plants registered in the French pharmacopeia *Antirhea borbonica* and the *Psiloxylon mauritianum* are interesting candidates in order to combat metabolic disorders. Their properties and use are described below.





**Figure 38: Medicinal plants in the Reunion Island registered in the French pharmacopeia.**

Until now 27 of Reunion Island plants (most of them are endemic) are registered in the French pharmacopeia for their beneficial effects on health. Adapted from Bryan Veeren thesis manuscript. Ambaville : *Hubertia ambavilla* var. *ambavilla* ; Arbre du voyageur : *Ravenala madagascariensis* Sonn ; Ayapana : *Ayapana triplinervis* ; Badamier : *Terminalia catappa* L. ; Bois de demoiselle : *Phyllanthus casticum* ; Bois de joli cœur : *Pittosporum senecia* ; Bois maigre : *Nuxia verticillata* ; Bois d'olive blanc : *Olea lancea* Lam; Bois d' olive noir : *Olea europaea africana*; Bois d'osto : *Antirhea borbonica*; Café marron : *Coffea mauritiana*; Change écorce: *Aphloia theiformis*; Faham : *Jumellea Fragans*; Fleur jaune : *Hypericum lanceolatum*; Guérit vite : *sigesbeckia orientalis*; Lingue café : *Mussaenda arcuata*; Patte poule : *Vepris lanceolata*; Tamarin : *Tamarindus indica*; Ti mangue : *Psiadia dentata*; Tombé : *Leucas aspera*; Bois jaune : *Ochrosia borbonica*; Bois de quivi : *Turreathouarsiana*; Liane d'olive : *Secamone volubilis*; Bois d'arnette : *Dodonaea viscosa*; Bois de pêche marron : *Psiloxyton mauritianum*; Jamblon : *Syzygium cumini*; Vacoa : *Pandanus utilis*.

### C. *Antirhea borbonica* (Bois d'Osto)

*Antirhea borbonica* (vernacular name: Bois d'Osto), is an endemic tree from the Mascarene Islands mainly found in the humid forests of Reunion Island. Its leaves are commonly used for its healing properties or to stop bleeding. The decoction of this plant is also traditionally used against diarrhea, dysentery and bladder problems (Giraud-Techer *et al.*, 2016). Moreover, Reunionese people also use it as an herbal tea to improve the diabetic condition and to decrease hypercholesterolemia (Smadja & Marodon, 2016). Recently, accumulating scientific data characterize the main components and beneficial properties of *A. borbonica*. Selective liquid chromatography-tandem mass spectrometry for *A. borbonica* (aqueous and acetonitrile leaves extracts) identifies 19 polyphenols with the caffeic acid and its derivatives, flavonoids and hydroxybenzoic acid being the major ones (Delveaux *et al.*, 2020; Veeren *et al.*, 2020; Veeren *et al.*, 2021).

This rich polyphenol content of *A. borbonica* explains plenty of protective effects of this plant. For example, Human albumin and erythrocytes, exposed to glycation and oxidative damage, were protected by *A. borbonica* aqueous extract by decreasing oxidative/glycation markers for glycated albumin and restoring the deformability with reduced oxidative stress in the glycation/oxidative damaged exposed erythrocytes (Delveaux *et al.*, 2020). In addition, according to recent data, the anti-inflammatory and anti-oxidant properties of the phenolic rich extract of *A. borbonica* confer an anti-inflammatory and anti-oxidant effect for the adipocytes (Marimoutou *et al.*, 2015; Le Sage *et al.*, 2017), curative anti-renal fibrosis effect in the *in vivo* renal fibrosis (unilateral ureteral obstruction) model of mice (Veeran *et al.*, 2021). Moreover, it exhibits anti-apoptotic properties on oxidized low-density lipoproteins exposed endothelial cells (Bonneville *et al.*, 2021) and a protective effect (anti-inflammatory, anti-oxidant) against hyperglycemia-mediated alterations in cerebral endothelial cells exposed to high glucose concentration and improve cerebrovascular damages a mouse stroke model (reduce cerebral infarct volume and neuro-inflammation) (Arcambal *et al.*, 2020; Taile *et al.*, 2020; Taile *et al.*, 2021). Finally, the median lethal concentration of the herbal infusion aqueous extract of *A. borbonica*, and the non-lethal concentrations was determined by Fish Embryo Acute Toxicity test according to (OECD) guidelines to be (LC<sub>50</sub>) 20.3 g/L and the 7.2 g/L respectively (Veeran *et al.*, 2020).

Taken together these data demonstrate the *A. borbonica* is rich in polyphenols namely in caffeic acid and its derivatives and flavonoids. Recent *in vitro* and *in vivo* data demonstrated

the capacity of *A. borbonica* to counteract oxidative stress, inflammation and apoptosis. Furthermore, it exerts a neuroprotective effect and anti-inflammatory effect that is supported by its main compound, the caffeic acid, according to the recent investigations (Arcambal *et al.*, 2020) (Fig. 39).

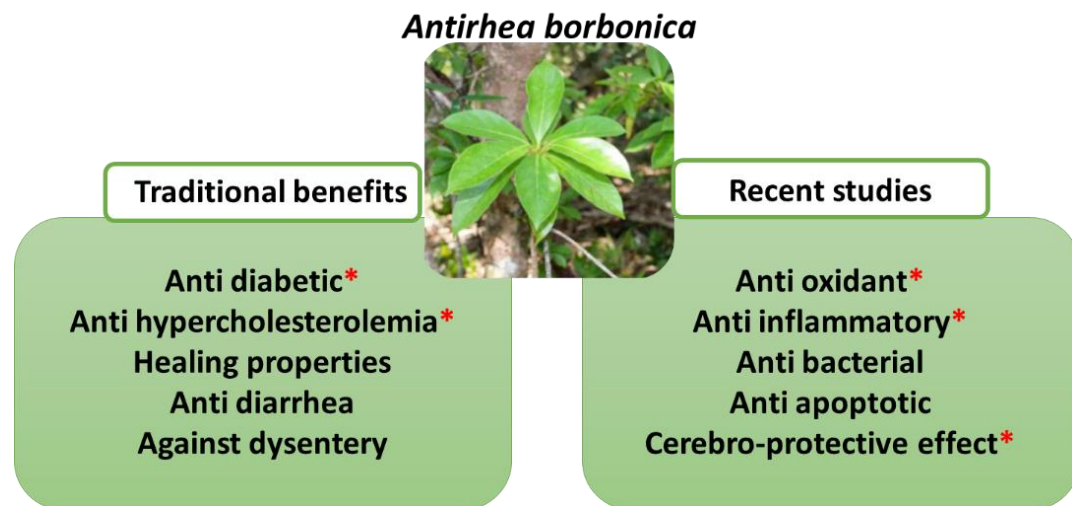


**Figure 39:** *Antirhea borbonica* beneficial effects from traditional background and recent scientific records. *Antirhea borbonica* proved anti-inflammatory, anti-oxidant, antibacterial anti-apoptotic and cerebrovascular protective effects that could explain in part the mentioned traditional benefits of this plant. Note: red stars document the interests of studying this plant against obesity and diabetes.

#### D. *Psiloxylon mauritianum* (Bois de pêche marron)

*Psiloxylon mauritianum* (vernacular name: Bois de pêche marron), is an evergreen endemic medicinal plant from the Mascarene Islands (Mauritius and Reunion Islands). This plant has shown promising uses in traditional medicine (Mahomoodally *et al.*, 2014). In Mauritius, the daily consumption of a *Psiloxylon mauritianum* leaves decoction twice a day is involved in the management of type 2 diabetes (Mootoosamy & Fawzi Mahomoodally, 2014). In addition, among the local people of Indian Ocean islands, *Psiloxylon mauritianum* wood decoction is considered an effective treatment of amenorrhea and dysentery (Gurib-Fakim & Brendler, 2004; Mahomoodally *et al.*, 2014). In Reunion Island, the leaves are reported to be traditionally used to decrease the formation of uric acid and to eliminate the excess cholesterol from the body, as an astringent agent and against diarrhea (Rivière, 2007; Mahomoodally *et al.*, 2014)

Some recent clinical data documented diuretic, antispasmodic and antiseptic properties of *P. mauritianum*. In addition, *in vitro* studies demonstrated the presence of two acids (corosolic acid and asiatic acid) with antibacterial effects mainly against *Staphylococcus aureus*



and other analyses confirm antiviral effect against early stages of dengue and zika virus infections (Clain *et al.*, 2019; Sorres *et al.*, 2020). Checkouri et al. investigated the polyphenol content of *Psiloxylon mauritianum* using infusion or decoction methods. *P. mauritianum* exhibited high polyphenol content and the main polyphenolic compounds were the quercetins (33% and 40% for the infusion and decoction respectively) and kaempferols (63% and 58% for the infusion and decoction respectively) (Checkouri *et al.*, 2020).

Taken together these data demonstrate that *P. mauritianum* is rich in polyphenols namely in quercetins and kaempferols. Recent *in vitro* data demonstrated the capacity of *P. mauritianum* to exhibit antibacterial, antiviral, anti-oxidative effects. However, the plenty of the traditional interesting benefits (antiviral, antibacterial, “anti-diabetic” and anti-cholesterol) of *P. mauritianum* and the lack *in vitro* and *in vivo* studies reveals the importance of investigating the effect of this plant in encountering the outcomes of diabetes and obesity (Fig. 40).

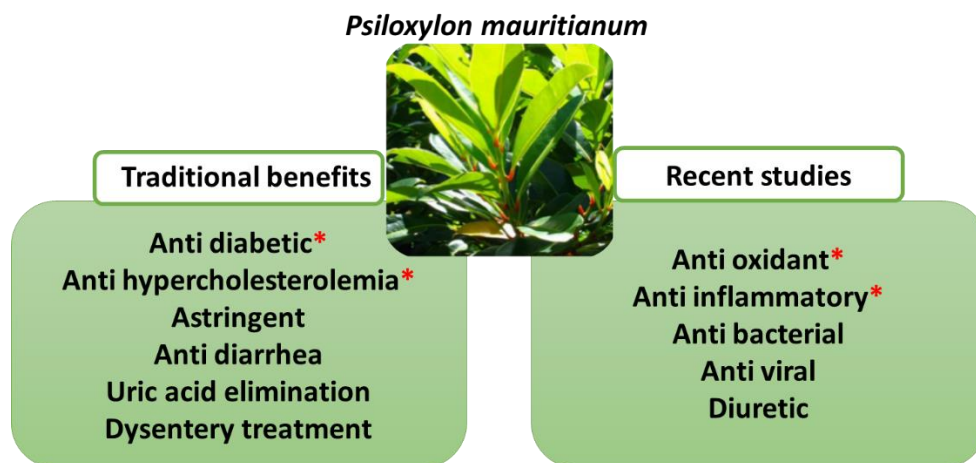


**Figure 40:** *Psiloxylon mauritianum* beneficial effects from traditional background and recent scientific records.

*Psiloxylon mauritianum* proved anti-inflammatory, anti-oxidant, antibacterial antiviral and diuretic effects that could explain in part the mentioned traditional benefits of this plant. Note: red stars document the interests of studying this plant against obesity and diabetes.

### **E. Model of obese zebrafish to screen preventive and therapeutic effects of plant extract**

Zebrafish model, in addition to its toxicity and drug screening advantages, is used as an *in vivo* reliable model to screen the beneficial properties of several dietary supplements especially in DIO models. For example, the green tea extracts tested on obesity model of zebrafish decreased the volume of visceral adipose tissue by modifying the expression of lipid

catabolism pathways (Hasumura *et al.*, 2012; Meguro *et al.*, 2015). The orange juice extracts (*Citrus sinensis*) and the white grape juice extract (*Vitis vinifera*) lowered similarly the adipose tissue on overfed obesity zebrafish model (visceral adipose tissue with orange juice extract and both visceral and subcutaneous for white grape juice extract) (Montalbano *et al.*, 2019; Montalbano *et al.*, 2021a). Besides, these juice extracts decreased the body weight and BMI as well as restoring the altered expression of some obesity related genes (leptin A, ghrelin, orexin, pro-opiomelanocortin and neuropeptide Y) (Montalbano *et al.*, 2019; Montalbano *et al.*, 2021a).

More interestingly, zebrafish serve not only as a convenient model to analyze the crude extracts of some dietary supplements, but also as a suitable model to test specific polyphenols in such plants extracts (Montalbano *et al.*, 2021b). For instance, eriocitrin, an anti-oxidative flavonoid in lemon displays lipid lowering effect on the DIO zebrafish in a way similar to that observed in rat's HFD model (Hiramitsu *et al.*, 2014). Similarly, resveratrol that is also a natural polyphenol has been shown to exert anti-obesity effect on zebrafish by meliorating diet-induced dysregulation of lipid metabolism (Ran *et al.*, 2017). Flavonoids, as kaempferols and baicalein, were also reported to have anti-adipogenic properties in zebrafish obesity models (Seo *et al.*, 2014; Torres-Villarreal *et al.*, 2019).

Taking in consideration from one side the rich polyphenolic contents of *A. borbonica* and *P. mauritianum*, their anti-oxidant, anti-inflammatory and the traditional lipid lowering properties, and from the other side the interest of using zebrafish in testing the polyphenol rich extracts of plants, it is becoming crucial to test the extracts of these two plants. To this end, the use of *in vivo* DIO model of zebrafish is a good alternative to ascertain their potential positive effects on the metabolic disorders.

# Objectives



## A. Thesis project

The prevalence of obesity and diabetes has been increasing over the years and is approaching global epidemic values. Obesity is a major risk factor for the development of type 2 diabetes, with 80% of diabetic individuals being overweight. In addition, most overweight and obese individuals are in a pre-diabetic state with a high risk of developing type 2 diabetes. As previously demonstrated, both obesity and type 2 diabetes share common health effects, some of which are lethal. Central nervous system complications emerge among the pathophysiological processes induced by obesity, prediabetes and diabetes. Early onset of dementia, decreased cognitive performance, higher risk of Alzheimer's disease and higher risk of sudden brain strokes are all problems faced by people with obesity and diabetes, without any definitive treatments. Today, scientific research is striving to better understand the causes behind brain disruptions related to obesity and type 2 diabetes. This approach is crucial to discover new preventive and therapeutic treatments and/or strategies to combat CNS disorders resulting from obesity, prediabetes and diabetes.

In Reunion Island, obesity and diabetes are two main serious health concerns due to their high prevalence among the local population (45 % of adults are overweight, with 10% of men and 20 to 30% of women considered obese) (cnr-sante, 2011). In addition, The Reunion Island is considered the first French department in terms of people with diabetes (REF and say again the prevalence). This alarming situation must be taken into account in the medium and long term within the framework of public health for stroke, but above all for vascular dementia and AD. However, these two last diseases could be worrying in few years with the ageing of the population and the proportion of obese and/or diabetic people in Reunion Island and worldwide. Reunion Island is rich in endemic medicinal plants, which opens the possibility to study the potential therapeutic and/or preventive effects of these plants in dealing with central nervous system complications.

Taking in account the high prevalence of obesity and diabetes in Reunion Island and the adverse effects of these disorders on the brain, this thesis project aims to contribute to a better understanding of the effects of obesity, as a prediabetic state, on brain homeostasis and to try to prevent or reverse these outcomes using medicinal plants from the biodiversity of Reunion Island.



## B. Objectives of the thesis

During the three years of this thesis, I had several objectives which were as follows:

- the establishment of an *in vivo* models of obesity and prediabetes using zebrafish,
- the characterization of the central perturbations of my models,
- the study of the impact of *A. borbonica* and *P. mauritianum* on these obese and prediabetic models.

### 1. Establishment of zebrafish models of obesity and prediabetes

For our first objective, we take advantage of zebrafish as a relevant model for inducing obesity and a prediabetes state. We propose that overfeeding will increase the body weight and consequently leads to obesity and prediabetes affecting thereby the central nervous system. Two diet-induced obesity models (DIO) have been developed using adult zebrafish. In the first DIO model, fish were overfed with conventional dry food for 4 weeks. This work was published in (Ghaddar *et al.*, 2021a). The second DIO model was based on overfeeding with conventional dry food and freshly hatched artemia for 4 weeks. (Ghaddar *et al.*, 2020). The models are characterized by checking the body weight increase, body mass index (BMI), fasting blood glucose, advanced glycated end products, oxidative stress and liver steatosis. Both models displayed increased body weight, BMI, glycemia and oxidative stress, while increased lipid accumulation (liver steatosis) is observed only in the second DIO model. Both models successfully mimic the development of an obese state.

### 2. Characterization of the brain disruptions induced by the DIO models

After the development of obesity and hyperglycemic models, we aimed to characterize the metabolic disorders resulting from DIO model at the central (brain) level. The second DIO model affects more severely the CNS than the first one. At the level of the brain, the investigations were focused more on the BBB integrity, neuro-inflammation, cerebral oxidative stress and glucocorticoids level. All these aspects are altered in the second DIO model, while just cerebral oxidative stress is accompanied to the first DIO model. In addition, in both models, neural stem cell proliferation in the main neurogenic niches is decreased in this obese fish and DIO fish show locomotor impairments.

### 3. Preventive and/or therapeutic effects of aqueous extract of *Antirhea borbonica* and *Psiloxylon mauritianum* in our DIO models

Reversing or preventing health concerns resulting from DIO, particularly on the brain, is one of our main interests. Thanks to the rich biodiversity of Reunion Island and the 27 medicinal plants registered in the French Pharmacopeia, we investigated the potential beneficial effects on our established and characterized DIO model of two medicinal plants: *Antirhea borbonica* and *Psiloxylon mauritianum*. These two plants were selected given their scientific literature and traditional use. In brief, *A. borbonica* is well-known to the local population for its “anti-diabetic” and anti-oxidant effects. During my thesis, the “DÉTROIT” laboratory has extended the research concerning the polyphenolic content and toxicity of *A. borbonica*, its neuroprotective properties as well as its anti-inflammatory, anti-oxidant anti- fibrosis effects (Arcambal *et al.*, 2020; Delveaux *et al.*, 2020; Taile *et al.*, 2020; Veeren *et al.*, 2020; Bonneville *et al.*, 2021; Veeren *et al.*, 2021). All these new data reinforce our idea to have selected this plant to combat the deleterious effects of obesity and prediabetes at the beginning of my research. Similarly, *P. mauritianum* was an attractive medicinal plant to investigate for my thesis project given its traditional preventive and/or curative effects on diabetes and metabolic diseases (anti-cholesterol). Recent data from the scientific research have documented the polyphenol content, antiviral and anti-oxidant properties of *P. mauritianum*. So far, the effectiveness of *P. mauritianum* against obesity and pre-diabetic disorders was not clearly demonstrated.

*A. borbonica* exerts protective effect on the brain of DIO fish without preventing obesity. However, *P. mauritianum* prevented obesity development in DIO fish treated with *P. mauritianum* and shows a protective effect at the level of the brain of these fish.



# Results



## Chapter 1: Deleterious effects of overfeeding on brain homeostasis and plasticity in adult zebrafish.

In order to answer to my first and second objectives (development of obese/prediabetic model and the impact on brain homeostasis), we aim to develop a diet-induced obesity (DIO) model using zebrafish. We assumed that DIO could be achieved by overfeeding the zebrafish with dry food (CTRL 0.034 g of food/fish/day and DIO fish >0.200 g of food/fish/day) for 4 weeks.

Indeed, model characterization after the 4<sup>th</sup> week reveals a state of overweight in the DIO zebrafish which shows increase in body weight, body size and BMI. The overfeeding protocol also induces an increase in fasting blood glucose levels compared to normally fed zebrafish, with a higher amount of advanced glycated end products (AGEs) and oxidative stress marker (4-hydroxynonenal: 4-HNE) at the periphery without any obvious lipid accumulation in the liver (liver steatosis). Despite the lack of liver steatosis in the DIO zebrafish, it can be still considered as a suitable and good model to investigate the effect of overweight on obesity, especially with the increased BMI, glycemia and oxidative stress. The lack of liver steatosis could be due to type or duration of the diet.

At the level of the central nervous system, an increase in oxidative stress was also observed (higher 4-HNE levels) in DIO fish. However, the impact of this overfeeding protocol on the BBB integrity was negligible as observed by the Evans blue injection, and the neuro-inflammatory state was almost comparable between control and DIO fish as revealed by qPCR analysis for pro-inflammatory cytokines. Finally, immunohistochemistry against the proliferative cellular nuclear antigen (PCNA) shows slight reduced cell proliferation in the neurogenic niche brain neurogenesis mainly at the telencephalic.

Interestingly, our overfeeding protocol altered also the behavior of the DIO zebrafish compared to the CTRL fish tending them to be more inactive. Moreover, DIO zebrafish show a higher gene expression of *fkbp5*, a glucocorticoid stress hormone-responsive gene. Therefore, this overfeeding protocol induces some peripheral (metabolic parameters and oxidative stress) and central nervous system (oxidative stress and decreased neurogenesis) modifications that could be explained by a state of chronic stress correlated to the central and peripheral oxidative stress. Reversing the overfeeding by normal feeding normalized the body weight, BMI and restores all the disruptions observed in the DIO model at the peripheral and central level except for the AGEs, mostly due to the half-life of AGEs (Brings *et al.*, 2017).

In this article, we introduce a simple and fast overfeeding model using zebrafish that induces peripheral and central disruptions. Further investigations of the mechanisms behind such the loss of brain homeostasis and plasticity may lead to a better understanding of the disrupted signaling pathways that cause CNS disturbances.



# Deleterious Effects of Overfeeding on Brain Homeostasis and Plasticity in Adult Zebrafish

Batoul Ghaddar,<sup>1</sup> Matthieu Bringart,<sup>1</sup> Christian Lefebvre d'Hellencourt,<sup>1</sup>  
Olivier Meilhac,<sup>1,2</sup> and Nicolas Diotel<sup>1</sup>

## Abstract

Overweight and obesity are worldwide epidemic health threats. They recently emerged as disruptors of brain homeostasis leading to a wide variety of neurologic disorders. This study aims at developing a fast and easy overfeeding model using zebrafish for investigating the impact of overweight on brain homeostasis. We established a 4-week overfeeding protocol using commercially available dry food in an *ad libitum*-like feeding. In the diet-induced obesity/overweight (DIO) fish model, weight, size, and body mass index were increased compared with controls. Also, DIO fish displayed hyperglycemia, and had higher levels of advanced glycation end products and oxidative stress (4-hydroxynonenal [4-HNE]) in a peripheral organ (tail). Although overfed fish did not display major blood–brain barrier leakage, they showed an increased cerebral oxidative stress, blunted brain cell proliferation as well as a striking decreased locomotor activity. Interestingly, switching from an overfeeding to a normal diet partially improved peripheral and central disruptions induced by overfeeding in solely 2 weeks. As a conclusion, this study provides a rapid and easy overfeeding model in zebrafish with relevant peripheral and central disruptions. This model could open the way for further investigations to better understand by which mechanisms overfeeding could disturb brain homeostasis. It also reinforces and contrasts with another zebrafish overweight model, showing that the type of the food provided could impair differently brain homeostasis.

**Keywords:** overweight, obesity, central nervous system, blood–brain barrier, *fkbp5*, oxidative stress, neurogenesis, advanced glycation end products, hyperglycemia

## Introduction

**M**ETABOLIC DISORDERS SUCH as obesity and diabetes are among the main health issues worldwide, with ~13% of the world's adult population being obese.<sup>1,2</sup> Obesity is defined as an imbalance between energy intake, storage, and expenditure leading to the hypertrophy and hyperplasia of adipose tissue and resulting in health risks.<sup>2–4</sup> An easy way to estimate overweight and obesity is the calculation of the body mass index (BMI). For people with European background, the normal BMI range is comprised between 18.5 and 25 kg/cm<sup>2</sup>. People displaying a BMI between 25.0 and 29.9 are considered as overweight, and >30 are classified as obese. However, for South Asians who are at more risk of metabolic disorders (i.e., overweight and diabetes), these ranges are different. Both overweight and obesity constitute comorbidity factors, and lead to several physiological complications such

as cardiovascular diseases (i.e., atherosclerosis, stroke), obesity-related cancers, and the development of type 2 diabetes.<sup>5,6</sup>

During the progress of overweight, peripheral homeostasis is disturbed resulting in increased chronic inflammation and oxidative stress.<sup>7–9</sup> Also, overweight/obesity is associated with liver steatosis that participates in the progress of insulin resistance and the development of type 2 diabetes.<sup>7,10,11</sup> Recently, it was shown that obesity was also associated with central nervous system dysfunctions and constituted a risk factor for developing dementia, cognitive impairments, and neurodegenerative disorders such as Alzheimer's disease.<sup>12–17</sup> These impairments are correlated with the deleterious effects of overweight on the blood–brain barrier (BBB).<sup>18,19</sup> Interestingly, some data suggest that obesity could also impair brain plasticity, including neurogenesis.<sup>20–22</sup> Indeed, in high-fat diet (HFD) and diet-induced obesity/overweight (DIO) models, cognitive impairments and hippocampal dysfunctions

<sup>1</sup>Diabète athérombose Thérapies Réunion Océan Indien (DÉTROÏ), INSERM, UMR 1188, Université de La Réunion, Saint-Denis, France.

<sup>2</sup>CHU de La Réunion, Saint-Denis, France.

have been reported, associated with blunted neurogenesis in the hippocampus, a key structure involved in memory.<sup>20,22–24</sup> Although obesity disrupts brain homeostasis and plasticity, the molecular and cellular mechanisms responsible for such deleterious effects are not well characterized and studied.

To investigate the impact of obesity on health, several mammalian models have been developed, among others genetic (ob/ob and db/db), optogenetic, chemogenetic, surgical and chemical models, as well as nutritional ones (HFD and DIO).<sup>25,26</sup> More recently, zebrafish emerged as an interesting and a valuable model for studying metabolic disorders. First, it shares a high genomic homology with humans as well as evolutionary conserved physiological processes.<sup>27,28</sup> Then, zebrafish has been successfully used as a model of obesity,<sup>29–32</sup> hyperglycemia,<sup>33–35</sup> and diabetes.<sup>36,37</sup> These different pathological models exhibit features of their respective human counterparts. Finally, zebrafish is also widely used for studying brain plasticity, including constitutive and regenerative neurogenesis.<sup>38–40</sup> In contrast to mammals, adult fish display >16 neurogenic niches through the whole brain,<sup>41,42</sup> and have a high capability for repairing their brain.<sup>43–45</sup> They also show strong similarities with the mammalian brain.<sup>38,40,45</sup> Taken together, these data make zebrafish an easy model for studying brain plasticity.

Given that zebrafish is widely used in metabolic diseases and brain plasticity studies, it has consequently emerged as a reliable model for investigating the impact of metabolic syndrome on brain homeostasis, in particular concerning the impact of hyperglycemia on neurogenesis and brain plasticity.<sup>33–35,46,47</sup> Thus, some studies performed in zebrafish have highlighted the deleterious effects of (1) hyperglycemia on memory processes and neurogenesis under homeostatic and regenerative conditions,<sup>33,47</sup> as well as of (2) HFD on cognitive function in zebrafish.<sup>48</sup>

However, there are almost no data concerning the effect of overweight on brain homeostasis, although some data document an impact on BBB, neuroinflammation, and neurogenesis.<sup>49</sup> Recently, we showed that overfeeding fish with a mix of dry food and artemia was able to induce such deleterious effects on the BBB, neuroinflammation, and neurogenesis in just 4 weeks.<sup>50</sup> Nevertheless, this overnutrition protocol involves the production of artemia that is sometimes complicated and inconsistent. In addition, it would be interesting to determine if a simpler kind of diet (only dry food) could induce such deleterious effects.

This study aims at establishing a fast and easy DIO protocol for investigating the impact of overweight on brain homeostasis (BBB functions, neuroinflammation, oxidative stress, neurogenesis). In this context, adult zebrafish were overfed for 4 weeks with dry food, and metabolic parameters were investigated, including body weight, BMI, fasting blood glucose, and liver steatosis. As well, the impact of DIO was investigated on BBB leakage, cerebral oxidative stress, and neuroinflammation, as well as on brain cell proliferation and locomotor behavior. Last but not least, the potential beneficial effects of a switch from an overfeeding to a normal diet were also investigated.

## Materials and Methods

### *Animals and ethics*

Three- to six-month-old adult wild-type zebrafish (*Danio rerio*) from the CYROI/DéTROI zebrafish facility were

maintained under standard conditions (temperature: 28.5°C; photoperiod: 14/10 h light/dark cycle; pH: 7.4; conductivity: 400  $\mu$ S). For each independent experiment, control (CTRL) and DIO fish are siblings, and have similar age resulting in no age and genetic variation. For euthanasia, zebrafish were sacrificed by immersion in ice water (2°C–4°C). All experiments were conducted in accordance with the French and European Community Guidelines for the Use of Animals in Research (authorization APAFIS\_20191105105351\_v10).

### *Diet-induced overweight/obesity*

Adult zebrafish (male and female) were divided into two groups: CTRL versus diet-induced overweight/obesity (DIO) fish. The control group was fed twice a day with dry food ( $\sim$ 0.034 g/fish/day; GEMMA 300; Planktovie), and the DIO group was fed six times a day with the same dry food in an *ad libitum*-like way ( $>$ 0.200 g/fish/day) for a 4-week period. The water was continuously renewed (Techniplast System). However, the water flow was stopped for 10 min during the feeding time (the water flow of CTRL fish was also stopped during the feeding time of DIO fish). To provide a positive control for Oil Red O staining (00625; Sigma-Aldrich), fish were fed during 1 week with egg yolks powder from chicken (E0625: 90 mg/fish/day; Sigma-Aldrich) and dry food (GEMMA 300), while control fish receive only dry food.

For determining if the deleterious effects of DIO were reversible, we performed the same overfeeding protocols with CTRL ( $\sim$ 0.034 g of food/fish/day) and DIO fish ( $>$ 0.200 g of food/fish/day; GEMMA 300; Planktovie) for 4 weeks. Then, at the end of this experimental procedure, CTRL and DIO fish were fed identically for 2 additional weeks with  $\sim$ 0.034 g of food/fish/day. These DIO fish submitted to a switch from overfeeding to normal diet were called “DIO Reversible” fish.

### *Body weight, BMI, and fasting blood glucose measurements*

Fish of each group were weighed every week. In addition, the body length of the fish was measured at the end of the experiment from the tip of the mouth to the end of the body (end of the tail). The BMI was calculated by dividing the body weight (g) with the square of the length (cm<sup>2</sup>).

For measuring the blood glucose levels, fasted fish were euthanized using ice water (2°C–4°C), and gently dried with a tissue before removing one eye. The ocular cavity filled with blood, and the glycemia (mg/dL) was measured using a glucometer (One-Touch Ultra; LifeScan), as previously described.<sup>34</sup>

### *Tissue preparation*

Fish were euthanized before being fixed in 4% PFA (paraformaldehyde) dissolved in 1  $\times$  PBS (phosphate-buffered saline). Brains and livers were dissected, cryopreserved in 1  $\times$  PBS containing 30% sucrose before embedding in optimal cutting temperature compound matrix. Then, 12  $\mu$ m-thick cryostat sections were made. For quantitative polymerase chain reaction (qPCR) or protein analyses, the brain and the tail were sampled, and immediately frozen before being stored at  $-80^\circ\text{C}$ .

### Immunohistochemistry

For immunohistochemistry (IHC), brain sections were rehydrated with 1×PBS followed by 1×PBS containing 0.2% Triton (PBS-T). Sodium citrate buffer (pH 6; 80°C for 15 min) was next used for antigen retrieval. Then, sections were washed with PBS-T, blocked with PBS-T containing 2% bovine serum albumin, and incubated overnight at room temperature with the primary antibodies: rabbit antizebrafish L-plastin (1:5000, provided by Dr. M. Redd) and/or mouse anti-PCNA (Proliferating Cell Nuclear Antigen; 1:100; clone PC10; Dako). The next day, after washing with PBS-T, an incubation with secondary antibodies was performed for 1h30 at room temperature using donkey antirabbit Alexa Fluor 488 (1:300; A21206; RRID: AB\_10049650; Life Technologies, Bethesda, MD) and goat antimouse Alexa Fluor 594 (1:300; A11005; RRID: AB\_141372; Life Technologies). DAPI counterstaining was also performed to label cell nuclei. Finally, the slides were rinsed and mounted with antifading medium (50001; IMM Ibbidi). The anti-PCNA allows the detection of proliferative cells along the neurogenic niches as previously described,<sup>51</sup> and the anti-L-plastin allows the detection of microglial cells.

### Oil Red O staining

After drying, cryostat liver sections were rehydrated and treated with 60% isopropanol. Staining with Oil Red O (00625; Sigma-Aldrich) was performed for 40 min according to standard protocol followed by nuclear Mayer's hematoxylin counterstaining.

### Investigation of BBB permeability (Evans blue dye injection)

For investigating BBB leakage, fish were anesthetized with 0.02% tricaine, injected within the intraperitoneal cavity with 1% Evans blue (diluted in 1×PBS). Fish were allowed to recover (10 min) before being sacrificed. They were then fixed in 4% PFA-PBS before being dissected. To ascertain the Evans blue staining, a fish was injected with the dye 1h30 before receiving a stab wound injury in the telencephalon as previously described.<sup>34,51</sup> The fish was next sacrificed 1h30 after brain injury and fixed.

### Protein extraction and dot blot

The lysis of brain and tail tissues was performed with Tris HCl buffer (50 mM pH7.4 EDTA 0.01 mM), before being centrifuged (10,000 rpm [9100 g], 4°C for 5 min). Supernatants were stored at -80°C until use. Using Bradford protein assay, the protein concentration was determined according to manufacturer's protocol. Ten or twenty micro-

grams of protein were spotted on a nitrocellulose membrane. The membranes were incubated with blocking buffer (5% nonfat milk in 1×PBS containing 0.02% TWEEN-20) after Ponceau S (Ponceau Red) staining. Then, the membranes were incubated for 1h30 with rabbit anti-4-hydroxynonenal (4-HNE, a marker of oxidative stress; ab46545; 1:1000; Abcam) and anti-AGE (advanced glycation end products; ab23722; 1:1000; Abcam) antibodies. After the two washing steps, a 1h30 incubation was performed with secondary antibody coupled to HRP (1:2000) (Goat antirabbit coupled with horseradish peroxidase, JII035003; Jackson's Laboratories). Finally, the results were obtained with enhanced chemiluminescence substrates and imaged with Amersham Imager 680.

### RNA extraction and reverse transcription

Freshly dissected zebrafish brains were collected in pools of 2 for each sample, and stored at -80°C before RNA extraction. Pools of two brains were grinded with TissueLyser II (Qiagen, Chatsworth, CA), and RNA extraction was performed using RNA easy Mini Kit (Qiagen). Then, reverse transcription of 2 µg of RNA was performed using random hexamer primers (100026484; Invitrogen) and MMLV reverse transcriptase (28025-021; Invitrogen).

### Gene expression analysis by qPCR

Semiquantitative PCR was performed using Biorad CFX Connect Real-Time System (BR006305) and SYBR green (Eurogentec). Each PCR cycle was conducted for 15 s at 95°C and 1 min at 60°C. Melting curve analyses and PCR efficiency were performed to confirm correct amplification. Normalization of the relative expressions of the proinflammatory cytokine genes (*il1β*, *il6*, and *tnfα*) and *fkbp5* (marker of glucocorticoid signaling) was processed against the housekeeping *ef1a* gene. The sequence of the specific primers used is provided in Table 1.

### Locomotor activity analysis

The zebrafish locomotion was monitored using the ZebraCube equipment (Viewpoint). In brief, CTRL and DIO fish were individually placed in separate tanks in an equal volume of water (750 mL in each tank, corresponding to a column height of 7 cm) inside the ZebraCube. After adaptation of the fish to their new tank, the locomotor activity was monitored during 10 min. The inactivity (<4 mm/s), small activity (4–8 mm/s), or large activity (>8 mm/s) counts, distance, and duration were analyzed.

TABLE 1. ZEBRAFISH QUANTITATIVE POLYMERASE CHAIN REACTION PRIMER SEQUENCES OF *EF1α*, *IL1β*, *IL6*, *TNFα*, AND *FKBP5* GENES

Gene	Forward primer	Reverse primer
<i>ef1α</i>	AGCAGCAGCTGAGGAGTGAT	CCGCATTTGTAGATCAGATGG
<i>il1β</i>	GCTGGAGATCCAAACGGATA	ATACGCGGTGCTGATAAACC
<i>tnfα</i>	GCGCTTTTCTGAATCCTACGT	GCCCAGTCTGTCTCCTTCT
<i>il6</i>	TCAACTTCTCCAGCGTGATG	TCTTTCCTCTTTTCCTCCTG
<i>fkbp5</i>	CAAAGGGGGAATGCTGTT	TTCTTTTCTGCCCTCTTTGC



### Microscopy

Digital pictures were obtained with a nanozoomer S60 (Hamamatsu). Pictures were adjusted for brightness and contrast in Adobe Photoshop.

### Cell counting

For analyzing brain cell proliferation, PCNA-positive cells from two to three cryostat sections (12  $\mu\text{m}$  thickness) were studied by region of interest. Quantification was performed by using ImageJ software (RRID: SCR\_003070; National Institutes of Health, Bethesda, MD) following the adjustment of several parameters (threshold, binary, and watershed). Neuroanatomical structures were identified with DAPI counterstaining. Counting was performed in blind conditions by two different persons. The number of ramified, intermediate, and amoeboid microglia was manually counted on two consecutive brain cryosections (12  $\mu\text{m}$  thickness/section) for the ventral telencephalon. This counting was performed on five to six fish per condition, and corresponds to the mean of cells per section.

### Statistical analysis

For statistical analysis, two groups were compared using statistical Student's *t*-test. For the body weight analyses during the 4-week period, multiple testing was performed by two-way analysis of variance. Error bars correspond to the standard error of the mean, and *n* values correspond to the number of animals or to the number of pooled brains. *p*-Values <0.05 were considered statistically significant (\**p*<0.05, \*\**p*<0.01, \*\*\**p*<0.001, \*\*\*\**p*<0.0001).

## Results

### Overfeeding increases body weight, length, and BMI

To characterize the efficiency of the overfeeding protocol performed in this study, the body weight was followed from weeks 1–4. In addition, at the end of the experimental procedure, the size, weight, and BMI were investigated. The CTRL and DIO fish received the same type of food; control fish being fed twice a day while DIO fish were fed six times a day for a 4-week period.

From the first week of treatment, a significant increase in body weight was observed, and was maintained until week 4 in the DIO group in both male and female (204% and 317% increase for male and female, respectively, at week 4) (Fig. 1A–E). Females appeared to display higher gain weight compared with males probably due to increased egg production (Fig. 1A–C). Indeed, at the end of the experimental protocol, the weight of DIO male was 0.474 g versus 0.753 g for DIO female (*p*<0.001; data not shown), while there was no significant change in body weight of CTRL male and female at week 4. At the end of the overfeeding protocol, the length of CTRL and DIO fish was also measured to calculate fish BMI. The total length of DIO fish was significantly higher than that of CTRL ones (123% increase and 127% increase for male and female, respectively) (Fig. 1F, G). Similarly, the BMI of DIO fish was also significantly increased compared with CTRL, suggesting that the gain in body weight is not only due to an increase in size (129% increase and 200% increase in male and female, respectively)

(Fig. 1H, I). As for the body weight, the BMI of DIO male was significantly lower than the one of DIO female ( $\sim$ 0.03 vs.  $\sim$ 0.05 for male and female, respectively; *p*<0.001; data not shown).

Consequently, the overfeeding protocol proposed in this study efficiently leads to increased body weight and BMI in both males and females. Many reports document the roles of female hormones, particularly estrogens, in brain homeostasis, including BBB physiology and neurogenesis in mammals and/or zebrafish.<sup>51–54</sup> Given that the aim of this work is to determine the potential impact of overfeeding in such processes, only males were chosen for the next experiments to limit bias due to hormonal fluctuations occurring during the female reproductive cycle.

### Overfeeding induces peripheral disorders including hyperglycemia and enhanced oxidative stress

Overweight is well known to be associated with insulin resistance and consequently with increased fasting blood glucose levels.<sup>7,55</sup> Thus, the glycemia of CTRL and DIO fish was investigated. As shown in Figure 2, DIO fish exhibited a significantly increased hyperglycemia compared with CTRL (Fig. 2A; 132% increase; *p*=0.024). High levels of glucose can lead to the formation of advanced glycation end products (AGEs).<sup>56,57</sup> AGEs are generated through the Maillard reaction occurring between reducing sugars and free amino groups of lipids, nucleic acids, or proteins.<sup>56</sup> The dot-blot analysis of the AGEs at the periphery using a piece of the zebrafish tail demonstrated a significant increased level in DIO conditions (Fig. 2B; 138% increase; *p*=0.006). Given that hyperglycemia and AGEs are well known to promote oxidative stress, quantification of the levels of the oxidative stress marker 4-HNE was monitored. 4-HNE is produced by lipid peroxidation and generates protein adducts reflecting oxidative stress. The 4-HNE levels tended to be increased at the periphery from the tail protein extracts investigated (Fig. 2C; 148% increase; *p*=0.051) in DIO fish compared with CTRL. Finally, liver steatosis was also studied performing Oil Red O staining. This pathological condition is usually associated with obesity and diabetes.<sup>11,58</sup> As shown in Figure 2D, no difference between CTRL and DIO livers was observed, while fish fed with egg yolk from chicken displayed a strong intestinal staining compared with CTRL (Fig. 2D).

Consequently, this overfeeding protocol results in hyperglycemia, enhanced peripheral AGEs without inducing a significant increase in peripheral 4-HNE levels and hepatosteatosis.

### Overfeeding has a neglected impact on BBB leakage and neuroinflammation but leads to central oxidative stress

Considering the peripheral disruptions observed in DIO conditions, the impact of overweight was next investigated on the brain. We first studied the BBB functions as this structure corresponds to a highly protective and selective interphase, separating the blood flow from the brain parenchyma. After Evans blue intraperitoneal injection, allowing us to study the permeability of the BBB, no striking differences were observed between CTRL and DIO brains (Fig. 3A), while the stab-wounded telencephalon (used as a positive control of BBB disruption) displayed a strong

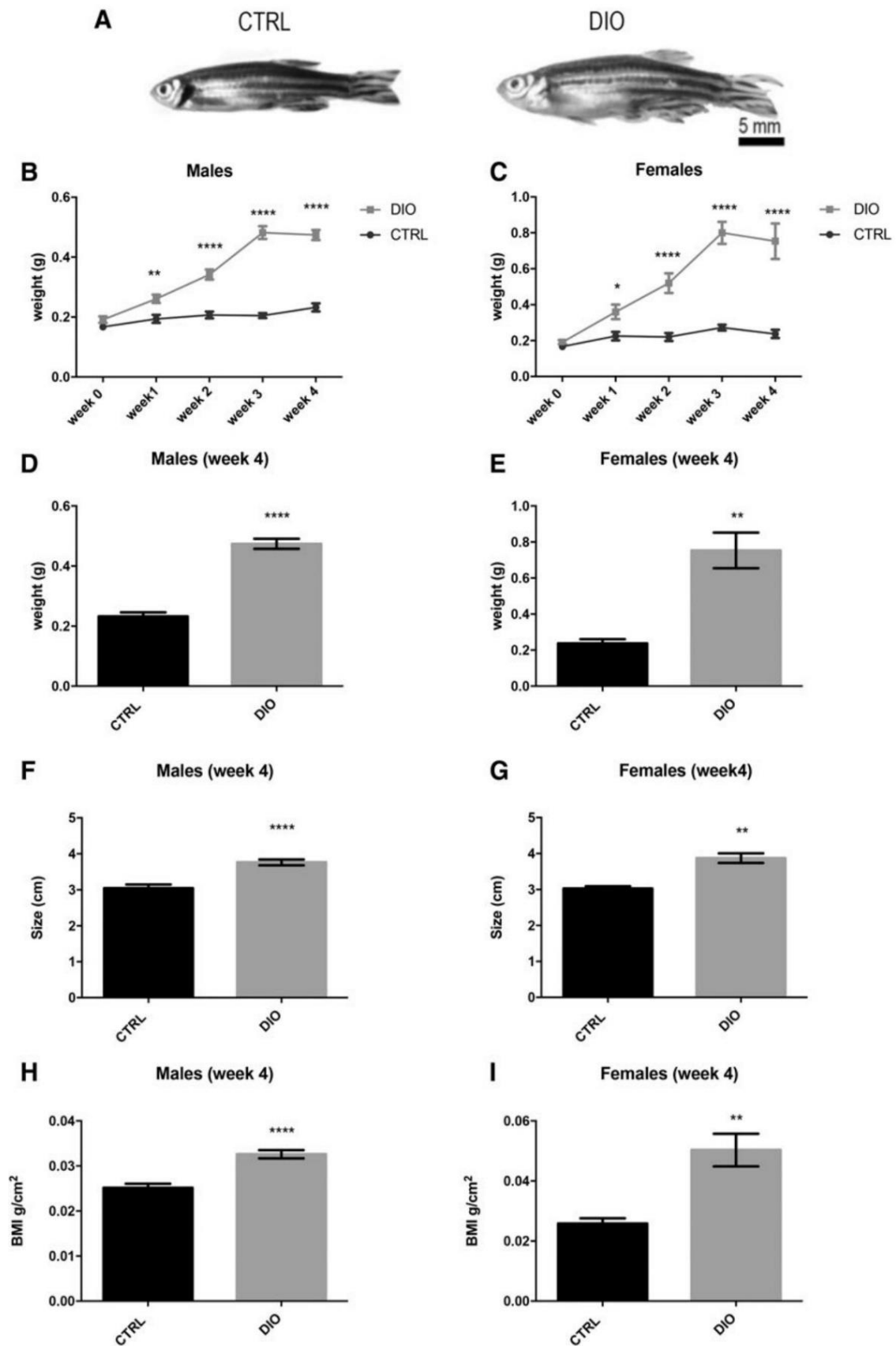


**FIG. 1.** DIO results in increased body weight, length, and BMI in both male and female zebrafish. (A) Zebrafish pictures highlighting the morphological differences at week 4 in male. (B, C) Graphs illustrating the body weight measurements during 4 weeks for both CTRL and DIO-treated zebrafish in male and female, respectively. (D, E) Body weight at week 4 in male and female, respectively. (F, G) Body length at week 4 in male and female zebrafish, respectively. (H, I) BMI (g/cm<sup>2</sup>) calculated at week 4.  $n = 8-10$  for males and  $n = 3-4$  for females. Error bars correspond to SEM. Two-way ANOVA (B, C) and Student's  $t$ -test (D-I)  $*p < 0.05$ ;  $**p < 0.01$ ;  $****p < 0.0001$ . Scale bar: 7 mm. ANOVA, analysis of variance; BMI, body mass index; CTRL, control; DIO, diet-induced obesity/overweight; SEM, standard error of the mean.

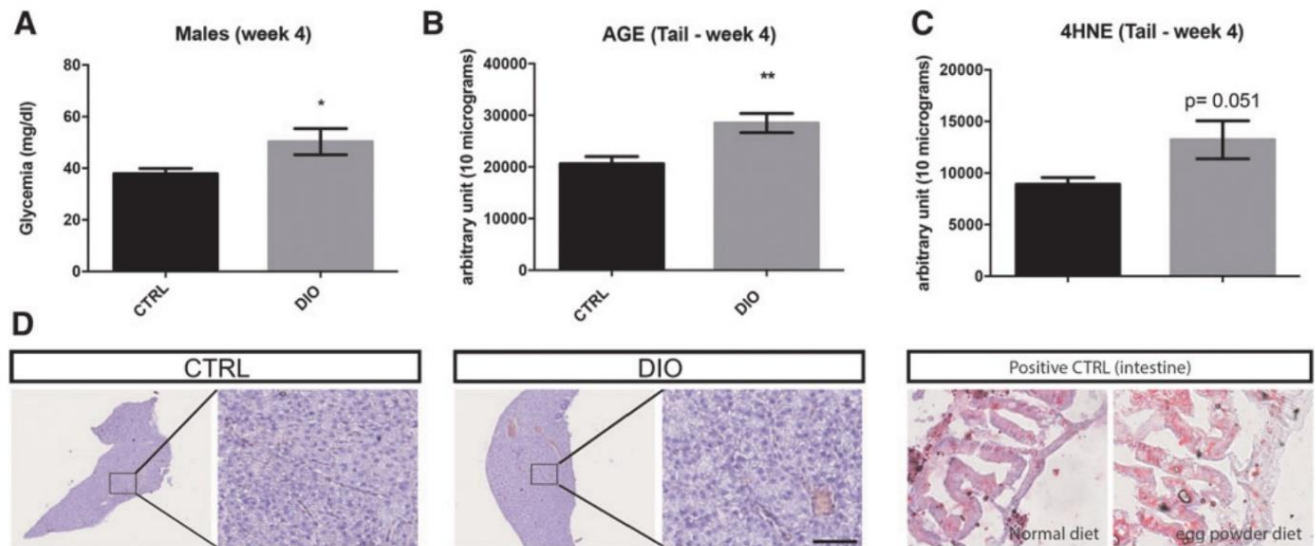


**FIG. 2.** DIO effects on hyperglycemia, AGE levels, 4-HNE levels, and liver steatosis. **(A)** Fasting blood glucose measurements at week 4 in CTRL and DIO-treated fish ( $n = 10\text{--}12$ ). **(B, C)** Graphs showing dot-blot quantification of AGE and 4-HNE levels in the tail of CTRL and DIO fish at week 4 ( $n = 6$ ). **(D)** Cryostat liver sections stained with Oil Red O in control fish showing no lipid accumulation, and consequently no liver steatosis in CTRL and DIO conditions at week 4 ( $n = 3$ ). A positive control shows a stronger Oil Red O staining in the intestine of fish overfed 1 week with egg yolk from chicken compared with a fish receiving a normal diet. Bar graph: SEM. Student's  $t$ -test:  $*p < 0.05$ .  $**p < 0.01$ . Error bars correspond to SEM. Scale bar:  $250\ \mu\text{m}$  for lower magnification pictures,  $50\ \mu\text{m}$  for higher magnification ones. 4-HNE, 4-hydroxynonenal; AGE, advanced glycation end product;  $n$ , number of fish. Color images are available online.

staining (Fig. 3A, see arrow). However, although the dye is mainly observed in the blood vessels, the careful observation of the stained brains showed a very weak hypothalamic staining in DIO compared with CTRL conditions (Fig. 3A, arrows). Consequently, the brains of DIO fish were slightly stained in the parenchyma (two brains on three studied displayed a slight blue parenchymal staining) as shown in Figure 3, indicating that this DIO model has only a very limited impact on the BBB integrity. Vibratome sections through the hypothalamus further reinforced the weak BBB leakage as revealed by the low red staining in the hypothalamic parenchyma (Fig. 3A).

The cerebral oxidative stress was also analyzed by investigating the 4-HNE levels on brain protein extracts. Dot-blot quantifications revealed a significant increase in brain 4-HNE levels in overfed fish (Fig. 3B;  $132\%$ ,  $p = 0.049$ ).

Obesity is also well known to be associated with chronic inflammation.<sup>7–9</sup> To determine the effects of overfeeding on neuroinflammation, qPCR for proinflammatory cytokine gene expression was performed in the brain of adult zebrafish (*il1 $\beta$* , *il6*, and *tnf $\alpha$* ). No change in *il1 $\beta$* , *il6*, and *tnf $\alpha$*  gene

expression was observed between CTRL and DIO fish (Fig. 3C). To better ascertain these results, the morphology of microglia was studied by L-plastin IHC. In homeostatic conditions, microglial cells exhibit a ramified morphology, while under neuroinflammatory conditions they display an amoeboid morphology demonstrating their activated and phagocytic properties. Our analysis at the level of the ventral telencephalon documented the absence of microglial activation in DIO fish (Fig. 3D).

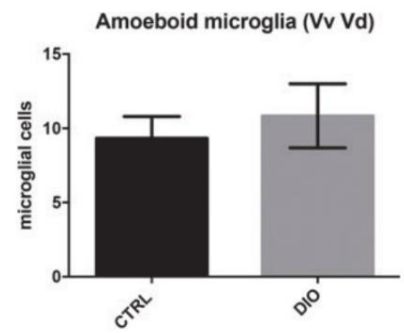
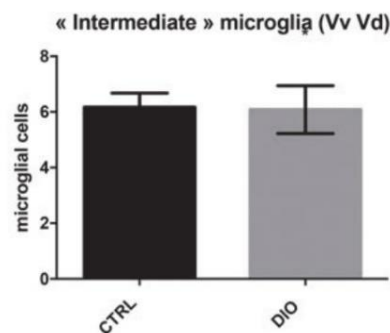
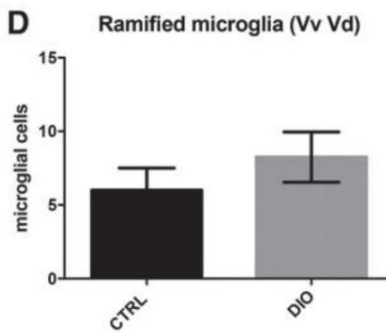
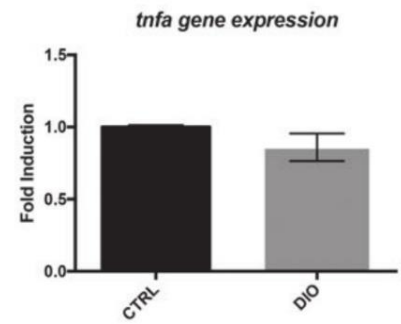
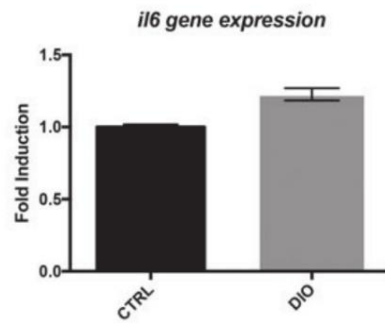
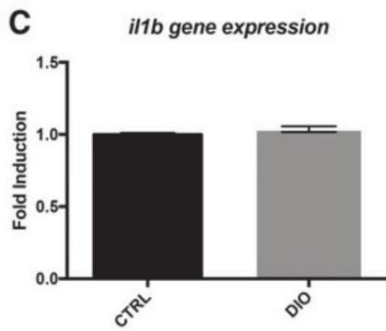
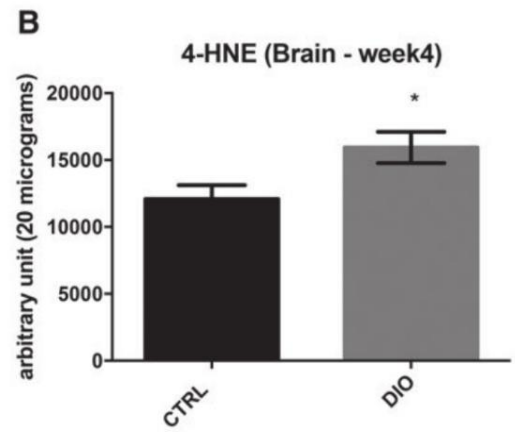
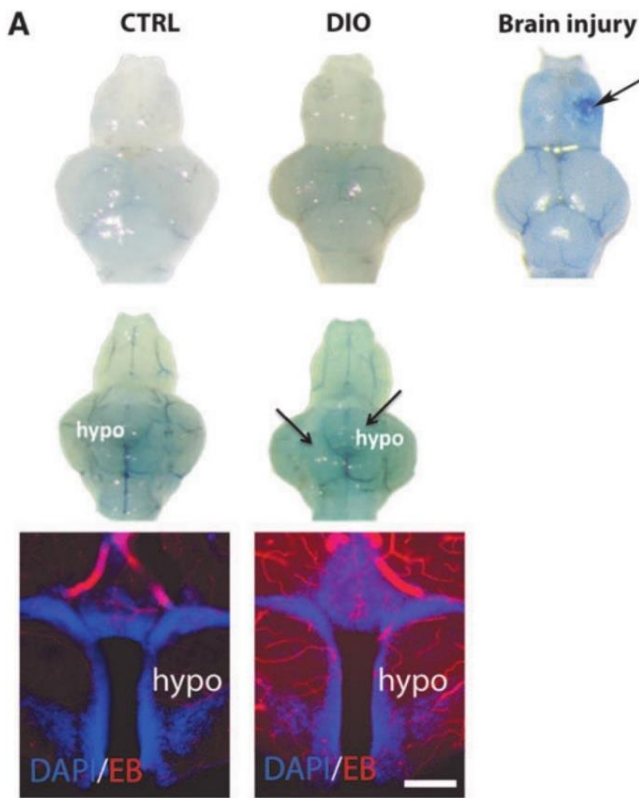
Taken together, these data showed that DIO induced a weak BBB leakage in some discrete brain regions and enhanced central oxidative stress without impacting the inflammatory status.

*DIO disrupts brain cell proliferation in adult neurogenic niches*

For investigating the impact of overfeeding on brain plasticity, we monitored the neural stem cell proliferation through IHC against the proliferative marker PCNA in different neurogenic niches across the brain (Fig. 4A–F). Interestingly,

**FIG. 3.** DIO impact on BBB leakage, cerebral oxidative stress, and neuroinflammation. **(A)** First row: dorsal view pictures of the brain from DIO model CTRL and DIO fish. Second row: ventral view pictures of the brain from DIO model CTRL and DIO fish ( $n = 3\text{--}6$  brains). Note the barely blue stained brain parenchyma of DIO-treated fish. Third column: positive control showing Evans blue extravasation in the injured telencephalon (arrows). In **(A)**, hypothalamic vibratome section showing Evans blue staining (Red) extravasation in the parenchyma. **(B)** Graph showing dot-blot quantification of 4-HNE staining in the brains of CTRL and DIO fish ( $n = 4$ ). **(C)** Proinflammatory cytokines (*il1 $\beta$* , *il6*, and *tnf $\alpha$* ) cerebral gene expression in CTRL and DIO conditions ( $n = 3$  pools of 2 brains). **(D)** Counting of ramified, “intermediate,” and amoeboid microglia in the ventral part of the telencephalon (Vv Vd region) in both CTRL and DIO fish ( $n = 6$ ). Bar graph: SEM. Student's  $t$ -test:  $*p < 0.05$ . Scale bar: 1 mm for whole brain picture and  $75\ \mu\text{m}$  for hypothalamic sections. BBB, blood–brain barrier;  $n$ , number of fish; Vd, dorsal nucleus of ventral telencephalic area; Vv, ventral nucleus of ventral telencephalic area. Color images are available online.







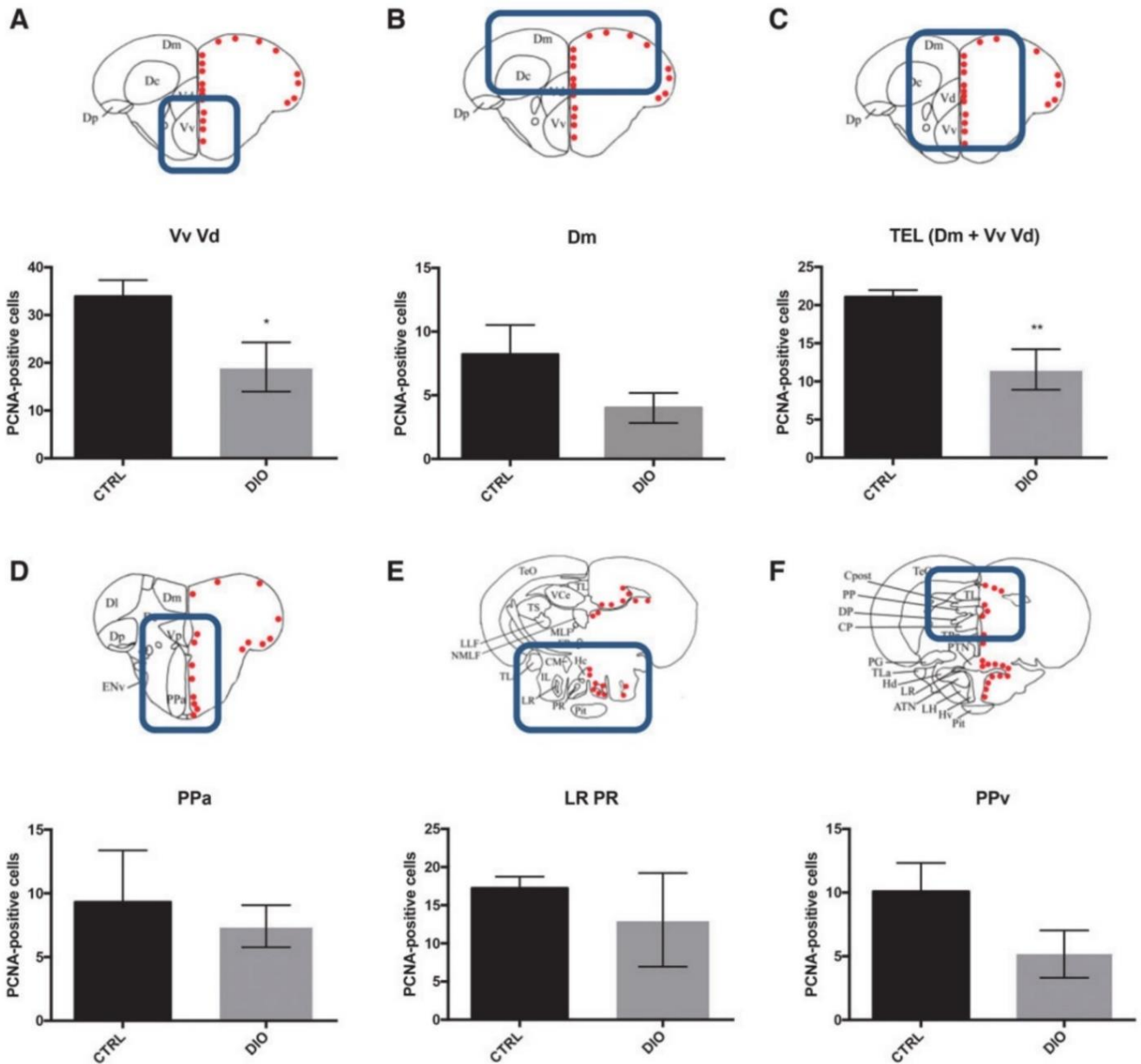


**FIG. 4.** DIO impairs neurogenesis in the forebrain of adult zebrafish. (A–F) Statistical analysis of the number of PCNA-positive cells in CTRL and DIO zebrafish. A significant decrease in proliferative activity was observed between CTRL and DIO group in the Vv-Vd and in the telencephalic region (Dm + Vv-Vd). Only a decreasing trend was observed in the Dm, PPa, PPv, and in the region surrounding the LR PR regions ( $n=6$ ).  $n$  = number of brains studied. Bar graph: SEM. Student’s  $t$ -test: \* $p < 0.05$ ; \*\* $p < 0.01$ . Scale bar =  $32 \mu\text{m}$ . The brain schemes correspond to the transversal sections of the zebrafish brain for the region studied and showing the main brain domains/nuclei according to the Zebrafish Brain Atlas from Wullmann *et al.* and were adapted from Menuet *et al.*<sup>84,85</sup> Dm, medial zone of dorsal telencephalic area; LR, lateral recess of diencephalic nucleus; PCNA, Proliferating Cell Nuclear Antigen; PPa, parvocellular preoptic nucleus, anterior part; PPv, periventricular prepectal nucleus; PR, posterior recess of diencephalic ventricle. Color images are available online.

DIO fish brains displayed a general decrease in cell proliferation at week 4. Such a decrease was observed in the telencephalon and the diencephalon as well as in the tectum. In the ventral and dorsal nuclei of the ventral telencephalon (Vv and Vd, respectively), a significant lower number of proliferative cells were observed (Fig. 4A), and a trend toward a decreased proliferation was shown in the dorsomedian telencephalon (Dm) (Fig. 4B). Overall, the telencephalic proliferation (Dm+Vv-Vd) from overfed fish was significantly

decreased (Fig. 4C). In the diencephalon, a reduced proliferation rate was noticed in the anterior part of the preoptic area (PPa) and in the caudal hypothalamus along the lateral recess and posterior recess of diencephalic ventricle (LR PR) (Fig. 4D, E); however, these trends did not reach significant levels. As well, the same was observed in the periventricular prepectal nucleus (PPv) (Fig. 4F). Consequently, it appears that DIO globally reduced adult brain cell proliferation within the main neurogenic niches from the brain.

*DIO impairs the normal zebrafish locomotor behavior*

Finally, the question of the impact of such an overfeeding protocol on zebrafish behavior was raised. A fine-tuned monitoring of the locomotion was performed by using a recently developed, automated system to record locomotor

activity (ZebraCube). A significant decrease in locomotor activity was observed in DIO fish compared with their respective controls (Fig. 5). Indeed, DIO fish were more in inactive and small activity states (Fig. 5A, D). They spent more time (Fig. 5B, E) and traveled more distance in low or no activity states (Fig. 5C, F) compared with CTRL.

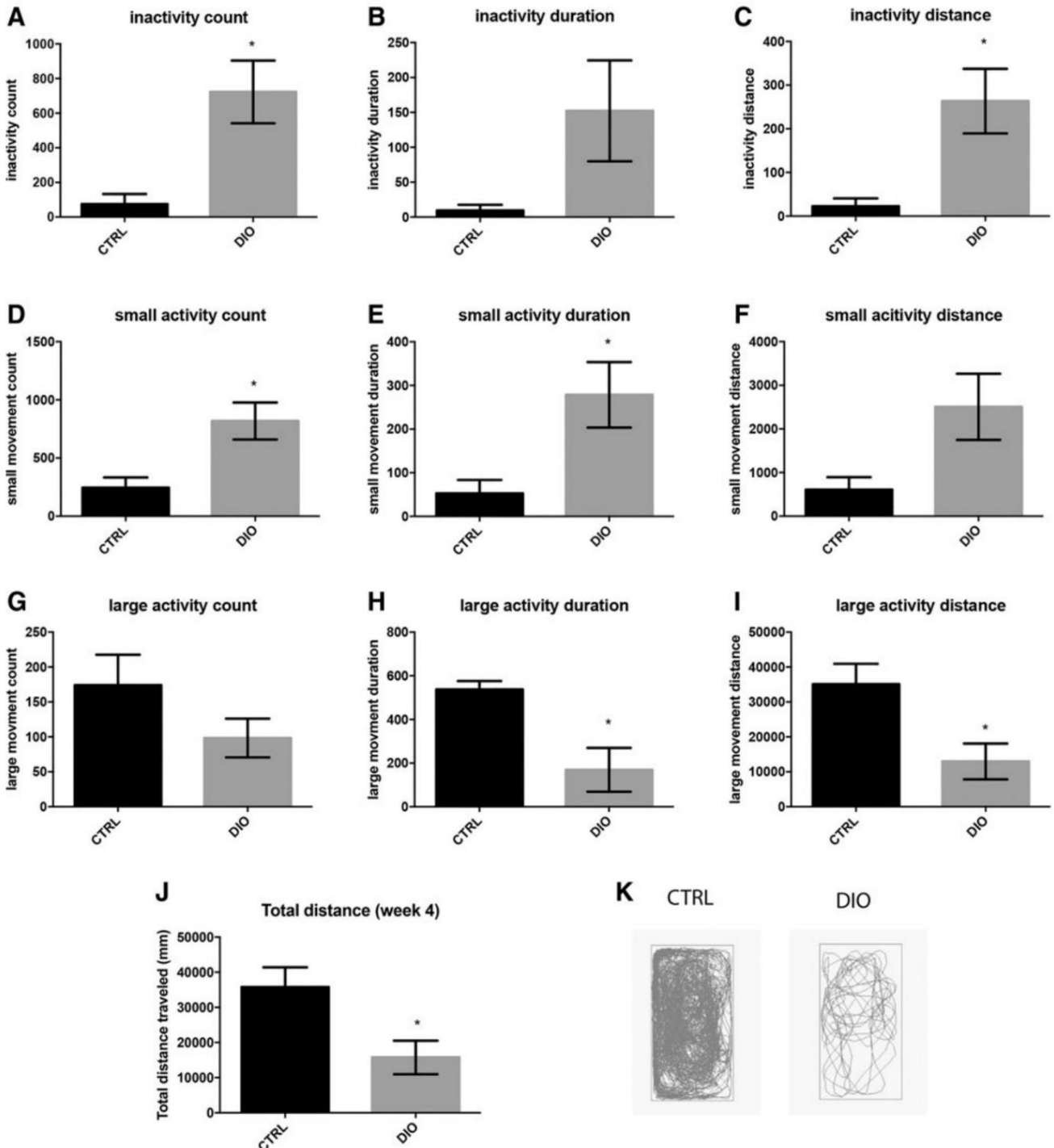


**FIG. 5.** DIO increases the occurrence of inactivity in zebrafish. (A–I) Graphs showing the number of inactivity, small and large activity events (*left column*); the duration of inactivity, small and large activity states (*middle column*) and the distance traveled in inactivity, small and large activity states (locomotion <4 mm/s) in DIO fish compared with controls. (J) Graph showing that the total distance traveled during 10 min is significantly reduced in DIO compared with CTRL fish. (K) Zebrafish path tracking in CTRL and DIO fish.  $n=4$  number of fish. Student's  $t$ -test:  $*p < 0.05$ . Error bar: SEM.

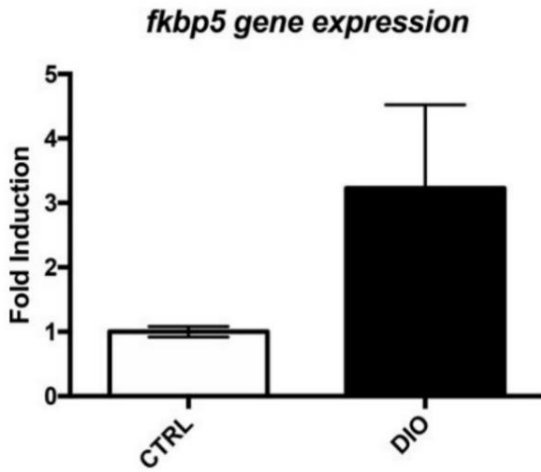


**FIG. 6.** DIO upregulates brain *fkbp5* gene expression, a marker of glucocorticoid signaling. *fkbp5* gene expression in CTRL and DIO brains.  $n = 3$  pools of 2 brains. Bar graph: SEM. Student's *t*-test.

In contrast, DIO fish displayed less events in a large activity state, spent less time, and traveled less distance in this large activity state (Fig. 5G–I). Furthermore, the total distance traveled by DIO fish during the 10 min of recording was strongly decreased compared with CTRL (Fig. 5J) as reflected by their representative paths (Fig. 5K). Such data

imply that overfeeding induces behavioral changes that could reflect central disorders such as chronic stress and/or depressive behaviors.

*Overfeeding and cerebral fkbp5 gene expression*

Stress hormone levels (glucocorticoids) could be responsible for decreased neurogenesis and altered behavior in our model as previously suggested in mammals.<sup>59–61</sup> Unfortunately, we were not able to sample sufficient plasma for measuring glucocorticoids. We consequently investigated brain *fkbp5* gene expression, a gene coding for a cochaperone of the glucocorticoid receptors and upregulated under glucocorticoid signaling.<sup>62</sup> Interestingly, *fkbp5* gene expression was consistently upregulated in our DIO model although it did not reach a significant level (Fig. 6; the respective fold inductions were 4.13 for CTRL1 vs. DIO 1; 15.66 for CTRL2 vs. DIO 2 and 8.6 for CTRL3 vs. DIO 3).

*Switching from an overfeeding diet to a normal diet partially counteracts the deleterious effects induced by overfeeding*

To determine if the deleterious effects of overfeeding were reversible, we performed a new overfeeding experiment with 4 weeks of overfeeding and 2 additional weeks of normal feeding. At the end of the 4th week of overfeeding, the DIO fish displayed higher body weight and BMI reinforcing our previous results (Fig. 7A, B). Then, the DIO fish were

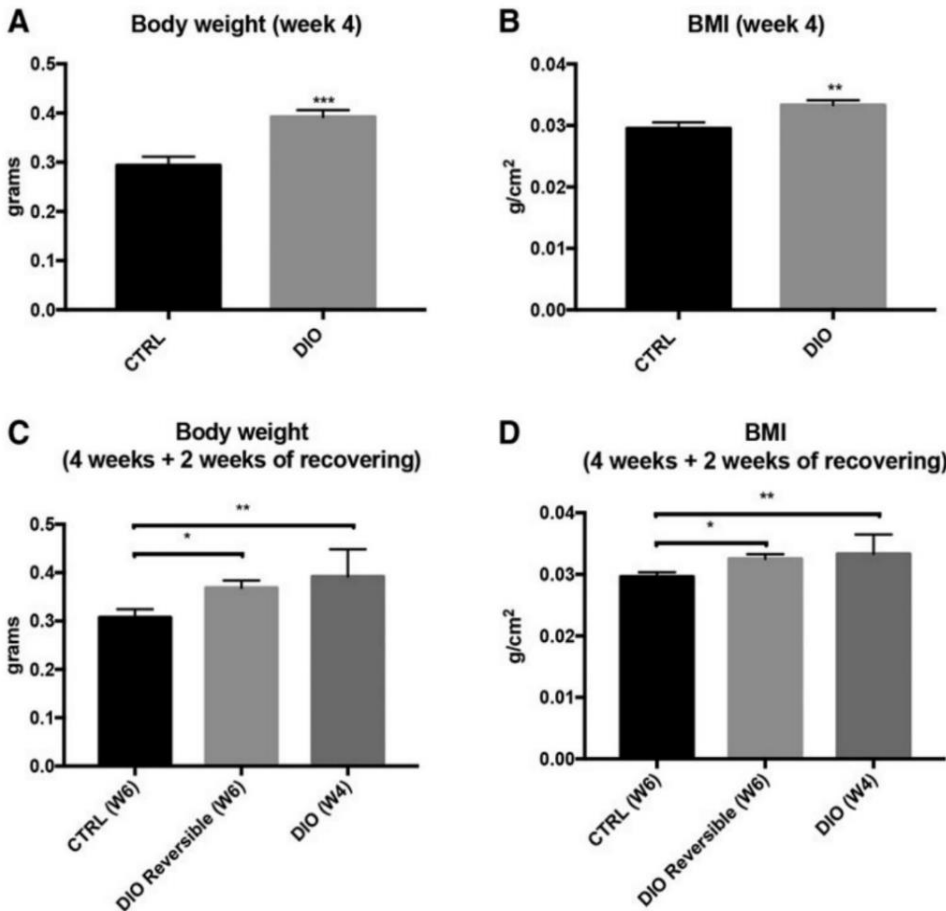


**FIG. 7.** Switch from an overfeeding diet to a normal diet partially decreased body weight and BMI of DIO fish. (A) Body weight of CTRL and DIO zebrafish after 4 weeks of overfeeding. (B) BMI (g/cm<sup>2</sup>) after 4 weeks of overfeeding. (C, D) Body weight and BMI following 2 weeks of standard diet after the 4th week of overfeeding. These measurements were done at week 6 (W6: 4 weeks of overfeeding + 2 weeks of normal diet). The DIO fish involved in this procedure were called “DIO Reversible” fish.  $n = 14–16$ . Error bars correspond to SEM. Student's *t*-test (A, B) and one-way ANOVA (C, D). \* $p < 0.05$ ; \*\* $p < 0.01$ ; \*\*\* $p < 0.001$ .

subjected to a normal diet for additional 2 weeks, and were called “DIO Reversible” fish. At the end of the 6th week, the body weight and BMI of “DIO Reversible” fish were still significantly higher than the CTRL ones. However, these differences appear weaker than for CTRL versus DIO at week 4 (Fig. 7C, D). Interestingly, in contrast to what was previously observed at the end of the overfeeding protocol (week 4, see Fig. 2A), the fasting blood glucose levels were not significantly different from CTRL and “DIO Reversible” fish at week 6 (Fig. 8A), demonstrating the beneficial effect of a 2-week normal diet feeding in regulating the glycemia of obese fish. However, “DIO Reversible” fish still maintained a significant increase in peripheral AGE levels (similar to what was shown at week 4) (Fig. 8B). As well, the 4-HNE levels were similar between CTRL and “DIO Reversible” fish at the periphery, and remain close to the significant level in the brain (Fig. 8C, D). Concerning the BBB, no striking differences were observed between CTRL and “DIO Reversible” fish (Fig. 8E, F). Of interest, the brain cell proliferation that was significantly different in the Vv Vd and TEL regions was similar after 2 weeks of normal diet feeding (Fig. 8G, H). The preoptic area (PPa) and the hypothalamus (Hv LR) also exhibited similar brain cell proliferation compared with CTRL (data not shown).

Last but not least, the behavior of “DIO Reversible” fish was similar to the CTRL ones (Fig. 9). Indeed, while in the 4-week overfeeding protocol DIO fish exhibited a reduced global activity (Fig. 5), the “DIO Reversible” fish displayed normal locomotor behavior, suggesting that the 2 weeks of normal feeding after the 4 weeks of overfeeding was sufficient to rescue the deleterious effects on locomotion.

Taken together, these data provide evidence that many physiological parameters were restored in only 2 weeks after switching from an overfeeding to a normal diet (glycemia, locomotion, and neurogenesis).

## Discussion

### *Zebrafish overfeeding efficiently induces metabolic disorders and shares features of human overweight and/or obesity*

In this study, we have developed a rapid and relevant zebrafish overnutrition model leading to the development of overweight and overweight-related dysfunctions at the peripheral and central levels, in only 4 weeks (Fig. 1). This model has the advantage to be easily set up as it uses only commercially available dry food (GEMMA 300; Planktovie) without HFD supplementation and without artemia production in contrast to other zebrafish models.<sup>29,31,32,63</sup> The development of overweight starts from the first week of treatment until the fourth one. Such an overfeeding leads to an increase in BMI at the end of the experimental procedure in DIO fish compared with CTRL in both males and females. DIO females display a significant higher body weight and BMI than DIO males. These weight gain and higher BMI in overfed fish reflect the development of an overweight state as previously observed in other DIO models in zebrafish using artemia or a mix of artemia with other types of food.<sup>29,31,32,50</sup> In our study, DIO fish also display hyperglycemia compared with CTRL. Higher levels of fasting blood glucose were previously observed in zebrafish overfed with artemia and egg powder,<sup>32</sup> or in fish overfed with a mix of artemia and dry

food,<sup>50</sup> reinforcing the data obtained in this study. Such difference in the induction of hyperglycemia between the models could be also explained by the quantity of food provided as well as frequency of the feedings during the day. In line with this increase in fasting blood glucose, we also observed higher AGE levels in peripheral tissues from DIO fish, associated with an increasing trend in peripheral oxidative stress. Such data are consistent with the literature, mentioning that overweight can lead to (1) hyperglycemia,<sup>64,65</sup> (2) the production of AGEs,<sup>66</sup> and (3) the generation of oxidative stress.<sup>67</sup>

Although liver steatosis condition is often associated with overweight/obesity as well as hyperglycemic status,<sup>11,58,68</sup> we did not observe liver steatosis in our experimental conditions. However, the observation of liver steatosis depends on the overfeeding model in zebrafish (the duration of overfeeding, type and quantity of food).<sup>29,32,50,69</sup> Our previous study using dry food and artemia for overfeeding leads to a partial and heterogeneous liver steatosis.<sup>50</sup> The only difference between this protocol and the one developed in this study is the introduction of artemia in the diet in addition to the dry food. Thus, these could favor the development of liver steatosis in contrast to the diet developed in this study due to their content in cholesterol and/or lipids. Consequently, we can hypothesize that the duration and/or the nature of the diet is not sufficient for the development of liver steatosis in our experimental conditions.

To conclude, we developed an alternative and easier model for inducing overweight, mimicking some features of the human pathology such as weight gain, high BMI, hyperglycemia, and enhanced peripheral AGE. However, this model does not lead to liver steatosis, and the peripheral levels of oxidative stress remain not significantly changed despite an increasing trend.

### *DIO promotes brain homeostasis impairments*

Overweight and/or obesity are correlated with cognitive impairments.<sup>14,17</sup> In this work, we were particularly interested in studying the effects of overfeeding on BBB integrity, central inflammation, and oxidative stress, as well as on brain plasticity focusing on neurogenesis. For this purpose, zebrafish is an interesting model, given that it displays a BBB as tetrapod, and shows an important neurogenic activity during adulthood.<sup>38,40,45,54,70</sup> In our experimental conditions, overfeeding did not strikingly impact the BBB physiology except in the hypothalamus that appears more stained (Fig. 3). This result is peculiarly interesting, given that our previous study using a mix of dry food and artemia leads to a severe BBB leakage.<sup>50</sup> It demonstrates substantial differences between the two overfeeding protocols. As well, obesity and diabetes are associated with BBB leakage,<sup>16,18</sup> and these disruptions could lead to oxidative stress and chronic neuroinflammation.

Our dot-blot analysis reveals an increase in cerebral 4-HNE levels demonstrating the enhanced oxidative stress in DIO conditions. A recent work performed in zebrafish showed the deleterious impact of a HFD on the expression of genes related to BBB physiology and oxidative stress.<sup>48</sup> Furthermore, oxidative stress is well known to promote BBB disruption.<sup>71</sup> Another interesting aspect to consider is the inflammatory status of the brain in this overfeeding condition. Although overfeeding induces some dysfunctions in brain homeostasis, our qPCR analysis for proinflammatory cytokines does not



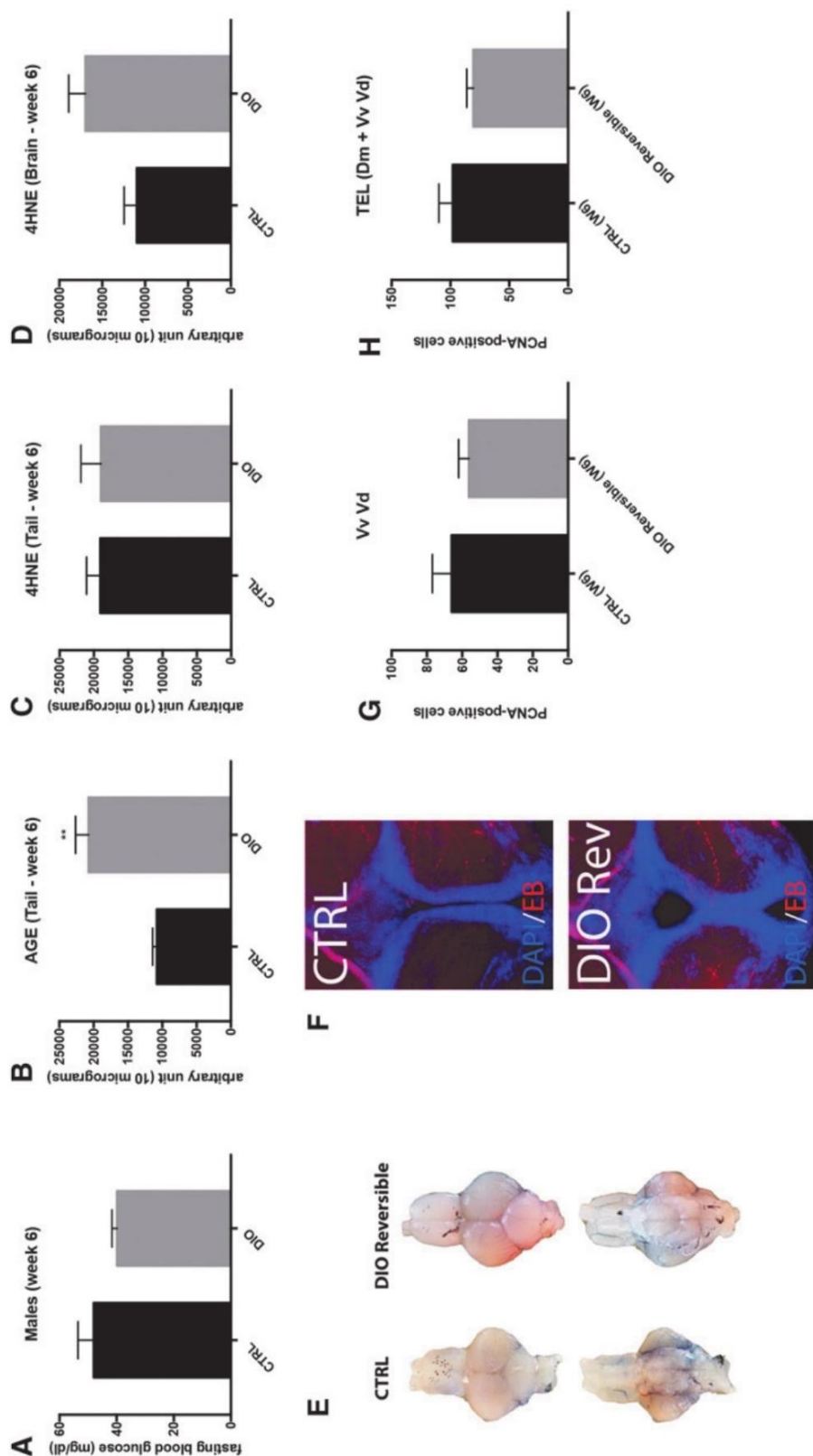


**FIG. 8.** Switch from an overfeeding diet to a standard diet partially restores normal metabolic parameters and brain homeostasis. **(A)** Fasting blood glucose measurements at week 6 in CTRL and "DIO Reversible" fish ( $n = 10$ ). **(B, C)** Graphs showing dot-blot quantification of peripheral AGE and 4-HNE levels (tail) of CTRL and "DIO Reversible" fish at week 6 ( $n = 4$ ). **(D)** Graph showing dot-blot quantification of 4-HNE levels in the brain of CTRL and "DIO Reversible" fish at week 6 ( $n = 4$ ,  $p = 0.051$ ). **(E)** Representative dorsal (first row) and ventral (second row) view pictures of CTRL and "DIO Reversible" fish brains after Evans blue intraperitoneal injection at week 6 ( $n = 3$ ). **(F)** Hypothalamic vibratome section showing no striking difference in Evans blue staining between CTRL and "DIO Reversible" fish ( $Red$ ,  $p = 0.051$ ). **(G, H)** Statistical analysis of the PCNA-positive area in CTRL and "DIO Reversible" zebrafish in the ventral telencephalon (Vv Vd) and in the telencephalic region (Dm+Vv Vd;  $n = 3$ ), showing no statistical difference in proliferation between groups. Bar graph: SEM. Student's *t*-test:  $**p < 0.01$ . *n*, number of fish. Color images are available online.

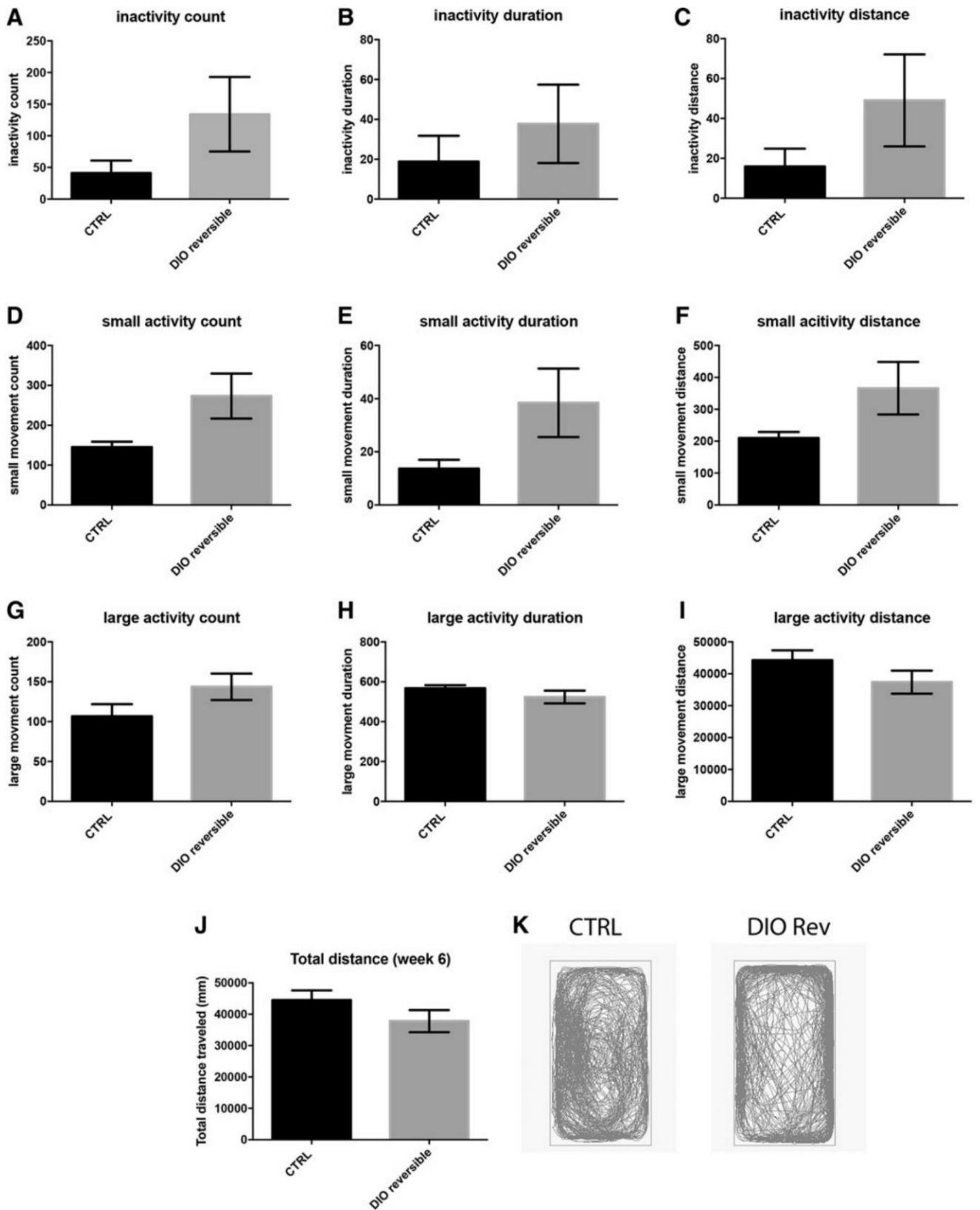


**FIG. 9.** Switch from an overfeeding diet to a standard diet partially restores normal behavioral activity in zebrafish. (**A–I**) Graphs showing the number of inactivity, small and large activity events (*left column*); the duration of inactivity, small and large activity states (*middle column*) and the distance traveled in inactivity, small and large activity states (locomotion <4 mm/s; *right column*) in “DIO Reversible” fish compared with controls. (**J**) Graph showing that the total distance traveled during 10 min is similar in DIO reversible compared with CTRL fish. (**K**) Zebrafish path tracking in CTRL and “DIO Reversible” fish.  $n=6$  number of fish. Student’s  $t$ -test. Error bar: SEM.

reveal any change between DIO and CTRL fish. These results were corroborated by the study of microglia morphology showing no differences in ramified versus amoeboid appearance in DIO and CTRL groups. This is interesting, given that obesity is known to promote neuroinflammation that could also participate in neurodegeneration with aging.<sup>18,21,72,73</sup>

Similarly, we have previously shown that overfeeding (dry food and artemia) induces neuroinflammation in contrast with the results of this study.<sup>50</sup> We could hypothesize that the absence of neuroinflammation, at least for the parameter investigated here, could take origin from (1) a weak BBB leakage; (2) an insufficient duration of the overfeeding; or from (3) the nature of the food provided, which is not different from CTRL fish, except for quantity.

#### *DIO decreases brain cell proliferation and alters locomotor activity*

Interestingly, we observed a decrease in brain cell proliferation in many neurogenic niches, including the telencephalon, the preoptic area, the hypothalamus, and some regions of the tectum, which is only significant for Vv/Vd and for Vv/Vd+Dm. Such data are consistent with the mammalian literature in which overweight/obesity results in blunted neurogenesis,<sup>20–22,24</sup> and also with a long-term overfeeding model in zebrafish leading to decreased proliferation in cerebellar neurogenic niches.<sup>74</sup> More recently, we demonstrated that overnutrition (mix of dry food and artemia) also impairs brain cell proliferation in a more efficient way.<sup>50</sup> The question of the mechanisms causing such a decreased neurogenesis in our model remains open. We could hypothesize that the BBB dysfunctions, the oxidative stress, or the hyperglycemia could be in part responsible for impaired neurogenesis. Indeed, these parameters are well known to be potent disruptors of neurogenesis.<sup>33,75–77</sup> In zebrafish, it was shown that hyperglycemia has a deleterious impact on genes involved in the BBB maintenance (*zonula occludens 1a* and *1b*), and is responsible for blunted neurogenesis under constitutive and regenerative conditions and impaired memory.<sup>33,47</sup> It would be also interesting to study the effect of this overfeeding protocol on other aspects of neurogenesis such as new born cell migration, differentiation, and survival under constitutive and regenerative conditions.

Finally, our overfeeding protocol also results in impaired locomotor behavior. Indeed, DIO fish appear to spend more time in inactivity or small activity states and less time in a large activity state. As a consequence, the total distance traveled by DIO fish is significantly decreased compared with CTRL. Such behavioral changes observed in our experimental conditions are similar to depressive and/or anxiety behaviors documented in obese mouse,<sup>78</sup> and have been also described in rodents and humans. Indeed, obese boys display reduced motor skills and daily activity,<sup>79</sup> and obese mice exhibit a decreased locomotor activity in an open-field test.<sup>22</sup>

We could hypothesize that the increase in the stress hormone levels (glucocorticoids) could be responsible for impaired neurogenesis and altered behavior. The FKBP5 protein is a cochaperone of the glucocorticoid receptors, which is upregulated under glucocorticoid signaling.<sup>62</sup> This gene was previously shown to be also upregulated in zebrafish under glucocorticoid stimulation.<sup>80–82</sup> As shown in Figure 6, *fkbp5* gene expression was consistently upregu-

lated. This result could suggest a higher glucocorticoid signaling in DIO fish than in controls, and could highlight the occurrence of chronic stress in DIO fish. However, further investigations are needed to ascertain this hypothesis.

#### *Switching from an overfeeding to a normal diet partially counteracts the effects of DIO*

Interestingly, we investigated the potential beneficial effects of switching from an overfeeding to a standard diet for 2 weeks (after the 4th week of overfeeding). We demonstrated that this switch in the food quantity provided was able to normalize glycemia even if the body weight and BMI of “DIO Reversible” fish were still higher than CTRL ones (Figs. 7 and 8). Although DIO and “DIO Reversible” fish display AGE levels higher in the periphery than CTRL, the cerebral 4-HNE levels were not significantly different in “DIO Reversible” versus CTRL, but remain close to be significant. More interestingly, “DIO Reversible” fish display normalized neurogenesis and locomotor behavior. Interestingly, almost similar results were observed in mice switching from a HFD to a standard diet.<sup>83</sup> Indeed, in this study performed in rodents, the diet switch leads to better metabolic parameters (body mass, fasting blood glucose levels, and glucose tolerance) as well as to behavioral improvements.<sup>83</sup>

Taken together, these data suggest that most deleterious effects of overfeeding are reversible in a short period of time in our experimental conditions.

#### **Conclusion**

We demonstrated, in zebrafish, that overfeeding induces detrimental effects on peripheral homeostasis (i.e., body weight, BMI, hyperglycemia, oxidative stress) and on brain homeostasis as shown by enhanced oxidative stress, impaired neurogenesis, and disturbed locomotor activity. These results are parallel with our recent findings, showing that overfeeding using artemia and dry food mainly leads to more severe dysfunctions such as a BBB leakage, the development of neuroinflammation, and a higher reduction of neurogenesis.<sup>50</sup> They highlight the importance of the type of diet used in overfeeding in the development of cerebral disruptions. It also raises the questions of the molecular and cellular mechanisms sustaining such differences. Interestingly, glucocorticoid signaling could be an interesting signaling pathway to investigate in overfed zebrafish. Furthermore, these two studies reinforce the fact that zebrafish could be an interesting model for studying the effects of overfeeding on brain homeostasis and plasticity. These overfeeding models would allow further investigations of the molecular and cellular mechanisms by which overweight could disturb brain homeostasis, particularly basal and injury-induced neurogenesis. It could be interesting to further study if such deleterious effects could be more prominently reversed by a recovery phase. Indeed, our results reinforce pre-existing evidence in mammals, showing that metabolic alterations and brain homeostasis impairments can be improved by switching simply back to a standard feeding.

Last but not least, these overfeeding models developed in zebrafish can also be used for further understanding the impact of overfeeding on some behavioral characteristics.



### Authors' Contributions

N.D. and O.M. designed the experiments. B.G., M.B., and N.D. performed the experiments. All the authors participated in the analysis of the experiments and/or in the writing of the article.

### Acknowledgments

We thank Cynthia Planesse for excellent technical support with the fish facility as well as Dr. M. Redd for providing L-plastin antibody.

### Disclosure Statement

The authors declare no competing interests.

### Funding Information

This work was supported by grants from La Réunion University and from FEDER (RE0022527-ZEBRATOX) EU-Région Réunion-French State national counterpart.

### References

- Bhupathiraju SN, Hu FB. Epidemiology of obesity and diabetes and their cardiovascular complications. *Circ Res* 2016;118:1723–1735.
- World Health Organization (WHO). 2020. Obesity and overweight. <https://www.who.int/news-room/fact-sheets/detail/obesity-and-overweight> Updated: April 1, 2020 (accessed May 8, 2021).
- Purnell JQ. Definitions, classification, and epidemiology of obesity. In: Endotext. Feingold KR, Anawalt B, Boyce A, Chrousos G, de Herder WW, Dungan K, *et al.* (eds), Endotext, South Dartmouth, MA, 2000.
- Church T, Martin CK. The obesity epidemic: a consequence of reduced energy expenditure and the uncoupling of energy intake? *Obesity* (Silver Spring) 2018;26:14–16.
- Apovian CM. Obesity: definition, comorbidities, causes, and burden. *Am J Manag Care* 2016;22:s176–s185.
- Dixon JB. The effect of obesity on health outcomes. *Mol Cell Endocrinol* 2010;316:104–108.
- Marseglia L, Manti S, D'Angelo G, *et al.* Oxidative stress in obesity: a critical component in human diseases. *Int J Mol Sci* 2014;16:378–400.
- Dludla PV, Nkambule BB, Jack B, *et al.* Inflammation and oxidative stress in an obese state and the protective effects of gallic acid. *Nutrients* 2018;11:1–29.
- Calder PC, Ahluwalia N, Brouns F, *et al.* Dietary factors and low-grade inflammation in relation to overweight and obesity. *Br J Nutr* 2011;106(Suppl 3):S5–S78.
- Knight JA. Diseases and disorders associated with excess body weight. *Ann Clin Lab Sci* 2011;41:107–121.
- Polyzos SA, Kountouras J, Mantzoros CS. Obesity and nonalcoholic fatty liver disease: from pathophysiology to therapeutics. *Metabolism* 2019;92:82–97.
- Whitmer RA, Gustafson DR, Barrett-Connor E, Haan MN, Gunderson EP, Yaffe K. Central obesity and increased risk of dementia more than three decades later. *Neurology* 2008;71:1057–1064.
- Whitmer RA, Gunderson EP, Quesenberry CP, Jr., Zhou J, Yaffe K. Body mass index in midlife and risk of Alzheimer disease and vascular dementia. *Curr Alzheimer Res* 2007;4:103–109.
- Cifre M, Palou A, Oliver P. Cognitive impairment in metabolically-obese, normal-weight rats: identification of early biomarkers in peripheral blood mononuclear cells. *Mol Neurodegener* 2018;13:14.
- Qizilbash N, Gregson J, Johnson ME, *et al.* BMI and risk of dementia in two million people over two decades: a retrospective cohort study. *Lancet Diabetes Endocrinol* 2015;3:431–436.
- Pugazhenth S, Qin L, Reddy PH. Common neurodegenerative pathways in obesity, diabetes, and Alzheimer's disease. *Biochim Biophys Acta Mol Basis Dis* 2017;1863:1037–1045.
- Nguyen JC, Killcross AS, Jenkins TA. Obesity and cognitive decline: role of inflammation and vascular changes. *Front Neurosci* 2014;8:375.
- Van Dyken P, Lacoste B. Impact of metabolic syndrome on neuroinflammation and the blood-brain barrier. *Front Neurosci* 2018;12:930.
- Roh HT, Cho SY, So WY. Obesity promotes oxidative stress and exacerbates blood-brain barrier disruption after high-intensity exercise. *J Sport Health Sci* 2017;6:225–230.
- Ogrodnik M, Zhu Y, Langhi LGP, *et al.* Obesity-induced cellular senescence drives anxiety and impairs neurogenesis. *Cell Metab* 2019;29:1061.e8–1077.e8.
- Purkayastha S, Cai D. Disruption of neurogenesis by hypothalamic inflammation in obesity or aging. *Rev Endocr Metab Disord* 2013;14:351–356.
- Bracke A, Domanska G, Bracke K, *et al.* Obesity impairs mobility and adult hippocampal neurogenesis. *J Exp Neurosci* 2019;13:1–10.
- Ramos-Rodriguez JJ, Molina-Gil S, Ortiz-Barajas O, *et al.* Central proliferation and neurogenesis is impaired in type 2 diabetes and prediabetes animal models. *PLoS One* 2014;9:e89229.
- Park HR, Park M, Choi J, Park KY, Chung HY, Lee J. A high-fat diet impairs neurogenesis: involvement of lipid peroxidation and brain-derived neurotrophic factor. *Neurosci Lett* 2010;482:235–239.
- Lutz TA, Woods SC. Overview of animal models of obesity. *Curr Protoc Pharmacol* 2012;Chapter 5:Unit 5.61.
- Barrett P, Mercer JG, Morgan PJ. Preclinical models for obesity research. *Dis Model Mech* 2016;9:1245–1255.
- Howe K, Clark MD, Torroja CF, *et al.* The zebrafish reference genome sequence and its relationship to the human genome. *Nature* 2013;496:498–503.
- Williams CH, Hong CC. Multi-step usage of in vivo models during rational drug design and discovery. *Int J Mol Sci* 2011;12:2262–2274.
- Oka T, Nishimura Y, Zang L, *et al.* Diet-induced obesity in zebrafish shares common pathophysiological pathways with mammalian obesity. *BMC Physiol* 2010;10:21.
- Montalbano G, Mania M, Guerrero MC, *et al.* Morphological differences in adipose tissue and changes in BDNF/Trkb expression in brain and gut of a diet induced obese zebrafish model. *Ann Anat* 2016;204:36–44.
- Meguro S, Hasumura T, Hase T. Body fat accumulation in zebrafish is induced by a diet rich in fat and reduced by supplementation with green tea extract. *PLoS One* 2015;10:e0120142.
- Landgraf K, Schuster S, Meusel A, *et al.* Short-term overfeeding of zebrafish with normal or high-fat diet as a model for the development of metabolically healthy versus unhealthy obesity. *BMC Physiol* 2017;17:4.
- Dorsemans AC, Soule S, Weger M, *et al.* Impaired constitutive and regenerative neurogenesis in adult hyperglycemic zebrafish. *J Comp Neurol* 2017;525:442–458.

34. Dorsemans AC, Lefebvre d'Helencourt C, Ait-Arsa I, Jestin E, Meilhac O, Diotel N. Acute and chronic models of hyperglycemia in zebrafish: a method to assess the impact of hyperglycemia on neurogenesis and the biodistribution of radiolabeled molecules. *J Vis Exp* 2017;124:1–8.
35. Capiotti KM, Antonioli R, Jr., Kist LW, Bogo MR, Bonan CD, Da Silva RS. Persistent impaired glucose metabolism in a zebrafish hyperglycemia model. *Comp Biochem Physiol B Biochem Mol Biol* 2014;171:58–65.
36. Olsen AS, Sarras MP, Jr., Intine RV. Limb regeneration is impaired in an adult zebrafish model of diabetes mellitus. *Wound Repair Regen* 2010;18:532–542.
37. Krishnan J, Rohner N. Sweet fish: fish models for the study of hyperglycemia and diabetes. *J Diabetes* 2018;11:193–203.
38. Jurisch-Yaksi N, Yaksi E, Kizil C. Radial glia in the zebrafish brain: functional, structural, and physiological comparison with the mammalian glia. *Glia* 2020;68:2451–2470.
39. Grandel H, Brand M. Comparative aspects of adult neural stem cell activity in vertebrates. *Dev Genes Evol* 2013;223:131–147.
40. Diotel N, Lubke L, Strahle U, Rastegar S. Common and distinct features of adult neurogenesis and regeneration in the telencephalon of zebrafish and mammals. *Front Neurosci* 2020;14:568930.
41. Kizil C, Kaslin J, Kroehne V, Brand M. Adult neurogenesis and brain regeneration in zebrafish. *Dev Neurobiol* 2012;72:429–461.
42. Lindsey BW, Tropepe V. A comparative framework for understanding the biological principles of adult neurogenesis. *Prog Neurobiol* 2006;80:281–307.
43. Schmidt R, Beil T, Strähle U, Rastegar S. Stab wound injury of the zebrafish adult telencephalon: a method to investigate vertebrate brain neurogenesis and regeneration. *J Vis Exp* 2014:e51753.
44. Zupanc GK. Towards brain repair: insights from teleost fish. *Semin Cell Dev Biol* 2008;20:683–690.
45. Ghaddar B, Lubke L, Couret D, Rastegar S, Diotel N. Cellular mechanisms participating in brain repair of adult zebrafish and mammals after injury. *Cells* 2021;10:1–24.
46. Dorsemans AC, Couret D, Hoarau A, et al. Diabetes, adult neurogenesis and brain remodeling: new insights from rodent and zebrafish models. *Neurogenesis (Austin)* 2017;4:e1281862.
47. Capiotti KM, De Moraes DA, Menezes FP, Kist LW, Bogo MR, Da Silva RS. Hyperglycemia induces memory impairment linked to increased acetylcholinesterase activity in zebrafish (*Danio rerio*). *Behav Brain Res* 2014;274:319–325.
48. Meguro S, Hosoi S, Hasumura T. High-fat diet impairs cognitive function of zebrafish. *Sci Rep* 2019;9:17063.
49. Cai D. Neuroinflammation and neurodegeneration in overnutrition-induced diseases. *Trends Endocrinol Metab* 2013;24:40–47.
50. Ghaddar B, Veeren B, Rondeau P, et al. Impaired brain homeostasis and neurogenesis in diet-induced overweight zebrafish: a preventive role from *A. borbonica* extract. *Sci Rep* 2020;10:14496.
51. Diotel N, Vaillant C, Gabbero C, et al. Effects of estradiol in adult neurogenesis and brain repair in zebrafish. *Horm Behav* 2013;63:193–207.
52. Ormerod BK, Lee TT, Galea LA. Estradiol initially enhances but subsequently suppresses (via adrenal steroids) granule cell proliferation in the dentate gyrus of adult female rats. *J Neurobiol* 2003;55:247–260.
53. Witt KA, Sandoval KE. Steroids and the blood-brain barrier: therapeutic implications. *Adv Pharmacol* 2014;71:361–390.
54. Diotel N, Charlier TD, Lefebvre d'Helencourt C, et al. Steroid transport, local synthesis, and signaling within the brain: roles in neurogenesis, neuroprotection, and sexual behaviors. *Front Neurosci* 2018;12:84.
55. Castro AV, Kolka CM, Kim SP, Bergman RN. Obesity, insulin resistance and comorbidities? Mechanisms of association. *Arq Bras Endocrinol Metabol* 2014;58:600–609.
56. Uribarri J, Woodruff S, Goodman S, et al. Advanced glycation end products in foods and a practical guide to their reduction in the diet. *J Am Diet Assoc* 2010;110:911.e12–916.e12.
57. Ahmed N, Thornalley PJ. Advanced glycation endproducts: what is their relevance to diabetic complications? *Diabetes Obes Metab* 2007;9:233–245.
58. Dharmalingam M, Yamasandhi PG. Nonalcoholic fatty liver disease and type 2 diabetes mellitus. *Indian J Endocrinol Metab* 2018;22:421–428.
59. Vyas S, Rodrigues AJ, Silva JM, et al. Chronic stress and glucocorticoids: from neuronal plasticity to neurodegeneration. *Neural Plast* 2016;2016:6391686.
60. Schoenfeld TJ, Gould E. Differential effects of stress and glucocorticoids on adult neurogenesis. *Curr Top Behav Neurosci* 2013;15:139–164.
61. Stranahan AM, Arumugam TV, Cutler RG, Lee K, Egan JM, Mattson MP. Diabetes impairs hippocampal function through glucocorticoid-mediated effects on new and mature neurons. *Nat Neurosci* 2008;11:309–317.
62. Binder EB. The role of FKBP5, a co-chaperone of the glucocorticoid receptor in the pathogenesis and therapy of affective and anxiety disorders. *Psychoneuroendocrinology* 2009;34(Suppl 1):S186–S195.
63. Montalbano G, Mania M, Guerrera MC, et al. Effects of a flavonoid-rich extract from *Citrus sinensis* juice on a diet-induced obese zebrafish. *Int J Mol Sci* 2019;20:5116.
64. Wellen KE, Hotamisligil GS. Inflammation, stress, and diabetes. *J Clin Invest* 2003;113:1111–1119.
65. Martyn JA, Kaneki M, Yasuhara S. Obesity-induced insulin resistance and hyperglycemia: etiologic factors and molecular mechanisms. *Anesthesiology* 2008;109:137–148.
66. Amin MN, Mosa AA, El-Shishtawy MM. Clinical study of advanced glycation end products in Egyptian diabetic obese and non-obese patients. *Int J Biomed Sci* 2011;7:191–200.
67. Manna P, Jain SK. Obesity, oxidative stress, adipose tissue dysfunction, and the associated health risks: causes and therapeutic strategies. *Metab Syndr Relat Disord* 2015;13:423–444.
68. Patche J, Girard D, Catan A, et al. Diabetes-induced hepatic oxidative stress: a new pathogenic role for glycated albumin. *Free Radic Biol Med* 2017;102:133–148.
69. Nakayama H, Shimada Y, Zang L, et al. Novel anti-obesity properties of *Palmaria mollis* in zebrafish and mouse models. *Nutrients* 2018;10:1401.
70. März M, Chapouton P, Diotel N, et al. Heterogeneity in progenitor cell subtypes in the ventricular zone of the zebrafish adult telencephalon. *Glia* 2010;58:870–888.
71. Lochhead JJ, McCaffrey G, Quigley CE, et al. Oxidative stress increases blood-brain barrier permeability and induces alterations in occludin during hypoxia-reoxygenation. *J Cereb Blood Flow Metab* 2010;30:1625–1636.

72. Spielman LJ, Little JP, Klegeris A. Inflammation and insulin/IGF-1 resistance as the possible link between obesity and neurodegeneration. *J Neuroimmunol* 2014;273: 8–21.
73. Parimisetty A, Dorsemans AC, Awada R, Ravanan P, Diotel N, Lefebvre d’Hellencourt C. Secret talk between adipose tissue and central nervous system via secreted factors-an emerging frontier in the neurodegenerative research. *J Neuroinflammation* 2016;13:67.
74. Stankiewicz AJ, McGowan EM, Yu L, Zhdanova IV. Impaired sleep, circadian rhythms and neurogenesis in diet-induced premature aging. *Int J Mol Sci* 2017;18:2243.
75. Yuan TF, Gu S, Shan C, Marchado S, Arias-Carrion O. Oxidative stress and adult neurogenesis. *Stem Cell Rev Rep* 2015;11:706–709.
76. Ho N, Sommers MS, Lucki I. Effects of diabetes on hippocampal neurogenesis: links to cognition and depression. *Neurosci Biobehav Rev* 2013;37:1346–1362.
77. Pozhilenkova EA, Lopatina OL, Komleva YK, Salmin VV, Salmina AB. Blood-brain barrier-supported neurogenesis in healthy and diseased brain. *Rev Neurosci* 2017;28:397–415.
78. Andre C, Dinel AL, Ferreira G, Laye S, Castanon N. Diet-induced obesity progressively alters cognition, anxiety-like behavior and lipopolysaccharide-induced depressive-like behavior: focus on brain indoleamine 2,3-dioxygenase activation. *Brain Behav Immun* 2014;41:10–21.
79. Arcos-Burgos M, Acosta MT, Martinez AF, Muenke M, Enriori PJ, Mastronardi CA. Neural plasticity in obesity and psychiatric disorders. *Neural Plast* 2016;2016:6053871.
80. Weger BD, Weger M, Nusser M, Brenner-Weiss G, Dickmeis T. A chemical screening system for glucocorticoid stress hormone signaling in an intact vertebrate. *ACS Chem Biol* 2012;7:1178–1183.
81. Rodriguez Viales R, Diotel N, Ferg M, *et al.* The helix-loop-helix protein id1 controls stem cell proliferation during regenerative neurogenesis in the adult zebrafish telencephalon. *Stem Cells* 2015;33:892–903.
82. Rastegar S, Parimisetty A, Cassam Sulliman N, *et al.* Expression of adiponectin receptors in the brain of adult zebrafish and mouse: links with neurogenic niches and brain repair. *J Comp Neurol* 2019;527:2317–2333.
83. Braga SP, Delanogare E, Machado AE, Prediger RD, Moreira ELG. Switching from high-fat feeding (HFD) to regular diet improves metabolic and behavioral impairments in middle-aged female mice. *Behav Brain Res* 2021; 398:112969.
84. Wullimann MF, Rupp B, Reichert H: *Neuroanatomy of the Zebrafish Brain: A Topological Atlas*. Birhäuser Verlag, Basel, Switzerland, 1996:1–144.
85. Menuet A, Pellegrini E, Brion F, *et al.* Expression and estrogen-dependent regulation of the zebrafish brain aromatase gene. *J Comp Neurol* 2005;485:304–320.

Address correspondence to:

Nicolas Diotel, PhD  
*Diabète athérombose Thérapies  
 Réunion Océan Indien (DÉTROÏ)  
 INSERM, UMR 1188  
 Université de La Réunion  
 2 rue Maxime Rivière  
 97490 Sainte-Clotilde  
 La Réunion  
 France*

E-mail: nicolas.diotel@univ-reunion.fr



## Chapter 2: Phenolic profile of herbal infusion and polyphenol-rich extract from leaves of the medicinal plant *Antirhea borbonica*: toxicity assay determination in zebrafish embryos and larvae

One of our objectives is to test the efficacy of medicinal plants from Reunion's biodiversity on our developed DIO model. *Antirhea borbonica* is one of the interesting plants we wanted to study for its known antioxidant, anti-inflammatory and suggested "anti-diabetic" properties. Thus, before testing the plant extracts on DIO model, it is crucial to characterize the main components and the toxicity of these extracts.

So far, this article aims to characterize the main polyphenolic content of *A. borbonica* and to determine *in vivo* its toxicity using zebrafish models. Two types of *A. borbonica* leaves extracts were investigated: aqueous (herbal infusion) and acetonic (polyphenol rich) extracts. Both types of *A. borbonica* exhibits high anti-oxidant capacity, phenolic content and flavonoid content as shown by the DPPH, Folin-Ciocalteu and aluminum chloride colorimetric assays, respectively. The characterization of polyphenols by mass spectrometry from *A. borbonica* acetonic extract led to the identification of and quantification of 19 main polyphenols as phenolic acids and flavonoids, namely, quercetin and its derivative and caffeic acids and its derivatives. After confirming the antioxidant capacity of *A. borbonica* due to its polyphenolic rich extract, toxicity test was performed on zebrafish embryos (0hpf - 96hpf) and larva (3dpf - 5 dpf). The Fish Embryo Acute Toxicity (FET) test, performed according to the OECD guidelines, allows the calculation of the median lethal concentration (LC<sub>50</sub>) corresponding to the concentration in which 50% mortality in the treated embryos occurs. LC<sub>50</sub> was 5 g/L for the acetonic extract and 17.6 g/L aqueous extract. As well, the non-lethal concentrations were 2.3 g/L and 7.2 g/L for acetonic and aqueous extracts, respectively. Yet, still at 2.3 g/L for both extracts some morphological malformations exist. Below 2.3 g/L the morphological defects disappear.



In summary, the acetonic and aqueous extracts of *A. borbonica* show strong anti-oxidant properties due to their high polyphenolic content with a well-defined median lethal toxicity and non-lethal toxicity concentrations. Therefore, this article achieves its goal at the level of *A. borbonica* characterization to be used for further investigations concerning the DIO model.





Article

# Phenolic Profile of Herbal Infusion and Polyphenol-Rich Extract from Leaves of the Medicinal Plant *Antirhea borbonica*: Toxicity Assay Determination in Zebrafish Embryos and Larvae

Bryan Veeren , Batoul Ghaddar, Matthieu Bringart, Shaymaa Khazaal, Marie-Paule Gonthier , Olivier Meilhac, Nicolas Diotel and Jean-Loup Bascands \*

INSERM, UMR 1188, Diabète Athérombose Thérapies Réunion Océan Indien (DéTROI), Plateforme CYROI, Université de La Réunion, 2 rue Maxime Rivière, 97490 Sainte-Clotilde, Reunion, France;

bryan.veeren@univ-reunion.fr (B.V.); batoul.ghaddar@univ-reunion.fr (B.G.);

matthieu.bringart@inserm.fr (M.B.); shaymaa.khazaal@hotmail.com (S.K.);

marie-paule.gonthier@univ-reunion.fr (M.-P.G.); olivier.meilhac@inserm.fr (O.M.);

nicolas.diotel@univ-reunion.fr (N.D.)

\* Correspondence: jean-loup.bascands@inserm.fr; Tel.: +33-0-262-93-88-07

Received: 9 September 2020; Accepted: 24 September 2020; Published: 29 September 2020



**Abstract:** *Antirhea borbonica* (*A. borbonica*) is an endemic plant from the Mascarene archipelago in the Indian Ocean commonly used in traditional medicine for its health benefits. This study aims (1) at exploring polyphenols profiles from two types of extracts—aqueous (herbal infusion) and acetonic (polyphenol rich) extracts from *A. borbonica* leaves—and (2) at evaluating their potential toxicity in vivo for the first time. We first demonstrated that, whatever type of extraction is used, both extracts displayed significant antioxidant properties and acid phenolic and flavonoid contents. By using selective liquid chromatography–tandem mass spectrometry, we performed polyphenol identification and quantification. Among the 19 identified polyphenols, we reported that the main ones were caffeic acid derivatives and quercetin-3-*O*-rutinoside. Then, we performed a Fish Embryo Acute Toxicity test to assess the toxicity of both extracts following the Organisation for Economic Cooperation and Development (OECD) guidelines. In both zebrafish embryos and larvae, the polyphenols-rich extract obtained by acetonic extraction followed by evaporation and resuspension in water exhibits a higher toxic effect with a median lethal concentration (LC<sub>50</sub>: 5.6 g/L) compared to the aqueous extract (LC<sub>50</sub>: 20.3 g/L). Our data also reveal that at non-lethal concentrations of 2.3 and 7.2 g/L for the polyphenol-rich extract and herbal infusion, respectively, morphological malformations such as spinal curvature, pericardial edema, and developmental delay may occur. In conclusion, our study strongly suggests that the evaluation of the toxicity of medicinal plants should be systematically carried out and considered when studying therapeutic effects on living organisms.

**Keywords:** *Antirhea borbonica*; medicinal plants; polyphenols; zebrafish; toxicity; LC-MS/MS

## 1. Introduction

Réunion island, a French volcanic overseas department belonging to the Mascarene Archipelago (Indian Ocean), has never been connected to any other landmasses [1] and is described as one of the 36 world biodiversity hotspots [2]. It displays a wide and rich flora with a high percentage of endemic species. Many of the indigenous and endemic plants from Reunion island have been and are still used for traditional medicine [3]. Although some studies have reported the potential therapeutic effects of these plants in combatting hypertension [4], oxidative stress, inflammation [5],

parasitosis (i.e., plasmodium), and viruses (i.e., Chikungunya, Dengue, and Zika) [6–8], their deep content characterization as well as their real efficiency *in vivo* remains largely unknown.

Since 2012, 22 medicinal plants have been registered at the French pharmacopeia [9]. Among these medicinal plants, *Antirhea borbonica* (*A. borbonica*) leaves are peculiarly interesting, as they are widely used in traditional medicine for treating, among other things, diabetes, urinary tract infection, diarrhea, hemorrhage, rheumatism, and also kidney stones [3,10]. Most of these interesting presumptive effects have been attributed to the antioxidant and anti-inflammatory properties of *A. borbonica* leaves. Based on these beneficial effects, it has been previously reported that polyphenol-rich extracts from *A. borbonica* exhibited strong antioxidant and anti-inflammatory effects, *in vitro*, on preadipocytes, cerebral endothelial cells, and red blood cells [5,11,12], as well as, *in vivo*, in a mouse stroke model [13] and a diet-induced overweight zebrafish model [14]. Importantly, these antioxidant and anti-inflammatory biological effects were associated with the capacity of polyphenols to regulate key molecular targets, such as ROS-producing and detoxifying enzymes and the redox-sensitive transcriptional factor Nrf2, and improve vasoactive markers in these *in vitro* and *in vivo* pathological models [5,11–14].

Because *A. borbonica* seems to display therapeutic effects correlated to its polyphenol content, a thorough investigation was required to determine its precise phenolic profile composition and its subsequent potential toxicity. To the best of our knowledge, although registered in French pharmacopeia and despite the various therapeutic effects suggested in a number of *in vitro* studies (see above), no developmental toxicity study has been reported for any of these 22 medicinal plants.

In the present study, we compared the precise phenolic profile of aqueous and acetic (polyphenol rich) extracts from dried leaves of *A. borbonica* by performing LC-MS/MS analysis. In a second part, we investigated the potential toxicity of several concentrations of these extracts using a zebrafish model. Zebrafish (*Danio rerio*), due to its small-size, high reproductive ability, and rapid embryogenesis and organogenesis, has become the most famous cost-effective alternative model used for large-scale and high-throughput toxicological and physiopathological studies [15,16]. The transparency of zebrafish embryos and larvae enables the real-time visualization and imaging of drug effects throughout the developmental process. This laboratory model is widely used to test compounds' toxicity. We consequently determine the median lethal concentration (LC<sub>50</sub>) in a zebrafish embryo and larvae models.

## 2. Results

### 2.1. Determination of Total Antioxidant Activity and Phenolic/Flavonoid Contents of Aqueous and Acetic Extracts

In their traditional use, *A. borbonica* leaves are used for herbal infusion. We assessed the antioxidant capacity of *A. borbonica* aqueous extract and compared it with a polyphenols-rich extract obtained by acetic solvent-assisted extraction, which is supposed to contain the maximal yield of polyphenols. To this end, an 2,2-Diphenyl-1-picrylhydrazyl (DPPH) assay was performed. As shown in Figure 1A, both extracts displayed, compared to ascorbic acid (40 g GAE/L) (94.7% ± 0.5%), an important antioxidant capacity of up to 90.7% ± 0.6% and 84.8% ± 1.2% (\* *p* < 0.05 vs. 40 g/L of acetic extract and <sup>\$\$</sup> *p* < 0.01 vs. 40 g/L (GAE) ascorbic acid) for polyphenol rich and aqueous extracts, respectively. The DPPH assay on both *A. borbonica* extracts at different concentrations of 40, 30, 22.5, 16.9, 12.7, 9.5, 7.2, and 2.3 g GAE/L is shown in Figure S1a. The antioxidant activity is reported in Table 1 as IC<sub>50</sub>, the required concentration for a 50% reduction in DPPH radicals. There was a minimum IC<sub>50</sub> value of 3.1 ± 0.3 g/L for the acetic extract, followed by the IC<sub>50</sub> value of the aqueous extract at 3.3 ± 0.3 g/L. These results confirm the important free radical-scavenging activity of both extracts compared to ascorbic acid (2.8 ± 0.1 g/L).



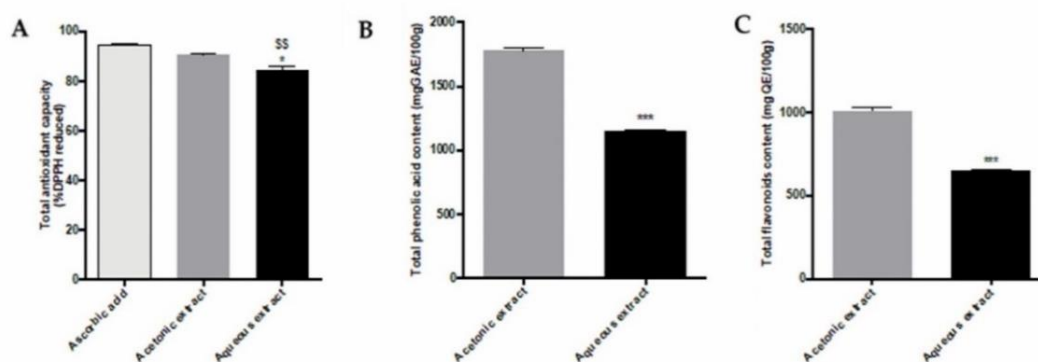


**Figure 1.** Antioxidant capacity, total phenolic acid, and flavonoid contents from *A. borbonica* extracts. (A) Total antioxidant capacity of polyphenols-rich extracts from *A. borbonica* was measured by the 2,2-Diphenyl-1-picrylhydrazyl (DPPH) assay. Ascorbic acid was used as a positive control. The results are expressed as the % of reduced DPPH. (B) Total phenolic contents of acetonic and aqueous extracts from *A. borbonica* were determined using the Folin–Ciocalteu colorimetric assay at a concentration of 40 g/L (plant dried powder). The results are expressed as the mg gallic acid equivalent (GAE)/100 g of plant dried powder. (C) Total flavonoid contents were determined using an aluminum chloride colorimetric assay. The results are expressed as the mg quercetin equivalent (QE)/100 g of plant dried powder. Data are the means  $\pm$  SDs of three independent experiments. \*  $p < 0.05$ , \*\*\*  $p < 0.001$  (vs. 40 g/L of acetonic extract), and <sup>SS</sup>  $p < 0.01$  (vs. 40 g/L (GAE) ascorbic acid).

**Table 1.** Antioxidant activities of polyphenols-rich extracts from *A. borbonica* were measured by DPPH assay. Ascorbic acid was used as a positive control. The  $IC_{50}$  values were obtained by plotting the percentage of free radical-quenching activity against the logarithm of the different concentrations, ranging from 40 to 2.3 g/L (plant dried powder) for aqueous and acetonic extracts. The results were expressed in g/L. Data are the mean  $\pm$  SD of three independent experiments.

$IC_{50}$ (g/L)		
Ascorbic Acid	Acetonic Extract	Aqueous Extract
2.8 $\pm$ 0.1	3.1 $\pm$ 0.3	3.3 $\pm$ 0.3

The total phenolic acid and flavonoid contents of acetonic and aqueous extracts were measured by the Folin–Ciocalteu and aluminum chloride colorimetric methods, respectively, for the following range of concentrations of *A. borbonica* (40, 30, 22.5, 16.9, 12.7, 9.5, 7.2, and 2.3 g/L) (Figure S1b,c). The highest phenolic content was exhibited by the acetonic extract with  $1778.9 \pm 34.1$  (\*\*\*)  $p < 0.001$  (vs. 40 g/L of acetonic extract) mg GAE/100 g dried powder, followed by the aqueous extract with  $1146.9 \pm 14.7$  mg GAE/100 g dried powder at a concentration of 40 g/L (Figure 1B). As shown in Figure 1C, the acetonic extract exhibited the highest flavonoid content with  $1005.6 \pm 19.3$  mg QE/100 g dried powder, followed by the aqueous extract with  $648.3 \pm 8$  (\*\*\*)  $p < 0.001$  (vs. 40 g/L of acetonic extract) mg QE/100 g dry powder at the concentration of 40 g/L.

## 2.2. Characterization of Polyphenols from *Antirhea borbonica* Acetonic Extract

In order to determine the composition of *A. borbonica* acetonic extract, a high-resolution accurate mass spectrometry analysis was performed using a Q-Exactive™ Plus mass spectrometer (Table 2). The identification of polyphenols was based on their exact mass, their elemental composition, and their fragmentation behavior (Figure S2), in comparison with standards and databases. The high-resolution accurate mass spectrometry analysis revealed the presence of 19 compounds, including phenolic acids and flavonoids in *A. borbonica* acetonic extracts (Table 2). Similar profiles were obtained from the *A. borbonica* aqueous extract (Table S1).

**Table 2.** Identification of 19 compounds in the *Antirhea borbonica* acetonic extract by LC-UV-HESI-MS/MS in negative mode.

Peak Number	RT (min)	Compound	Molecular Formula	Mass Error (ppm)	[M – H] <sup>–</sup>	MS/MS Fragments	mzCloud Best Match (%)
1	0.52	D-Quinic acid	C <sub>7</sub> H <sub>12</sub> O <sub>6</sub>	0.4	191.0554	111.0076	85.5
2	2.17	Protocatechuic acid	C <sub>7</sub> H <sub>6</sub> O <sub>4</sub>	0.13	153.0184	109.0283	82.7
3	2.63	3-Caffeoylquinic acid	C <sub>16</sub> H <sub>18</sub> O <sub>9</sub>	1.03	353.0877	191.0554, 179.0343, 173.0447, 135.0441	85
4	3.47	5-Caffeoylquinic acid	C <sub>16</sub> H <sub>18</sub> O <sub>9</sub>	1.03	353.0877	191.0554, 179.0343, 173.0447, 135.0441	88.3
5	3.68	Caffeic acid	C <sub>9</sub> H <sub>8</sub> O <sub>4</sub>	0.2	179.0341	135.0441	80.2
6	4.09	<i>p</i> -Coumaroyl quinic acid isomer	C <sub>16</sub> H <sub>18</sub> O <sub>8</sub>	1.3	337.0931	191.0550, 173.0446, 163.0392	84.6
7	4.18	<i>p</i> -Coumaroyl quinic acid isomer	C <sub>16</sub> H <sub>18</sub> O <sub>8</sub>	1.3	337.0931	191.0550, 173.0446, 163.0392	84.6
8	4.2	<i>o/m</i> -Coumaric acid	C <sub>9</sub> H <sub>8</sub> O <sub>3</sub>	0.2	163.0391	119.049	81.2
9	4.36	Feruloylquinic acid	C <sub>17</sub> H <sub>20</sub> O <sub>9</sub>	0.5	367.1035	191.0550, 173.0446	–
10	4.43	<i>p</i> -Coumaric acid	C <sub>9</sub> H <sub>8</sub> O <sub>3</sub>	0.1	163.0391	119.049	81.2
11	4.74	Quercetin-3- <i>O</i> -rutinoside (Rutin)	C <sub>27</sub> H <sub>30</sub> O <sub>16</sub>	1.6	609.1466	300.0274	94.8
12	4.94	Quercetin-3- <i>O</i> -galactoside	C <sub>21</sub> H <sub>20</sub> O <sub>12</sub>	1.33	463.0884	300.0274	90.9
13	5.01	Quercetin-3- <i>O</i> -glucoside	C <sub>21</sub> H <sub>20</sub> O <sub>12</sub>	1.33	463.0884	300.0274	90.9
14	5.26	Kaempferol- <i>O</i> -hexoside	C <sub>21</sub> H <sub>20</sub> O <sub>11</sub>	1.35	447.0935	284.0326	83.7
15	5.45	Kaempferol- <i>O</i> -hexoside	C <sub>21</sub> H <sub>20</sub> O <sub>11</sub>	1.35	447.0935	284.0326	83.7
16	5.82	3,5-Dicaffeoylquinic acid	C <sub>25</sub> H <sub>24</sub> O <sub>12</sub>	1.04	515.1196	353.0878, 191.0554, 179.0343, 173.0447, 135.0441	83.6
17	6.02	3,4-Dicaffeoylquinic acid	C <sub>25</sub> H <sub>24</sub> O <sub>12</sub>	1.04	515.1195	353.0878, 173.0447, 191.0554, 179.0343, 135.0441	88.1
18	6.2	4-Caffeoylquinic acid	C <sub>16</sub> H <sub>18</sub> O <sub>9</sub>	1.03	353.0877	173.0447, 191.0554, 179.0343, 173.0447, 135.0441	86.3
19	6.36	1,4/4,5-Dicaffeoylquinic acid	C <sub>25</sub> H <sub>24</sub> O <sub>12</sub>	1.04	515.1194	353.0878, 173.0447, 191.0554, 179.0343, 135.0441	89.1

Chromatographic peak 1 (0.52 min) (Figure 2A) showed a precursor ion [M – H]<sup>–</sup> at *m/z* 191.0554 with the predicted molecular formula C<sub>7</sub>H<sub>11</sub>O<sub>6</sub> (mass error 0.4 ppm), suggesting the presence of quinic acid. The MS2 spectrum (Figure S2a) indicated a base peak at *m/z* 111.0076, associated with the successive loss of two water molecules and a -CO<sub>2</sub> group from quinic acid.

Chromatographic peak 2 (2.17 min) showed a precursor ion [M – H]<sup>–</sup> at *m/z* 153.0184, with the following composition of C<sub>7</sub>H<sub>5</sub>O<sub>4</sub> (mass error 0.13 ppm) and a MS2 base peak at *m/z* 109.0283, resulting from the removal of a -CO<sub>2</sub> group (Figure S2b). Assignment to protocatechuic acid was achieved using a commercial standard.

Chromatographic peaks 3, 4, and 18 showed a precursor ion [M – H]<sup>–</sup> at *m/z* 353.0878, with the following predicted molecular formula of C<sub>16</sub>H<sub>17</sub>O<sub>9</sub> (mass error 1.03 ppm), suggesting the presence of caffeoylquinic acid isomers (CQA). Indeed, the MS2 spectra (Figure S2j,c,d) show the same fragmentation pattern, with a base peak at *m/z* 191.0554 due to the loss of caffeic acid moiety, and the main product ions at *m/z* 179.0343, corresponding to loss of quinic acid moiety; *m/z* 173.0447, corresponding to water loss from quinic acid; and *m/z* 135.0441, corresponding to loss of a -CO<sub>2</sub> group from caffeic acid. Among these three isomers, only peak 18 (6.2 min) had an MS2 base peak at *m/z* 173.0447, allowing the identification of 4-CQA, which is consistent with the 4-acylated mono-acyl CGAs [17] (Figure S2j). Peaks 3 (2.63 min) and 4 (3.47 min) (Figure 2A) can be easily distinguished by their fragmentation. These peaks had both the same MS2 base peak at *m/z* 191.0554, which is consistent with 3-CQA and 5-CQA acylation but different intensities for the MS2 ion at *m/z* 179.0343, as previously reported [18–20]. They were identified as 3-CQA and 5-CQA, respectively (Figure S2c,d).

Chromatographic peak 5 (3.68 min) had a precursor ion [M – H]<sup>–</sup> at *m/z* 179.0350, with a predicted molecular formula C<sub>9</sub>H<sub>7</sub>O<sub>4</sub> (mass error 0.2 ppm), suggesting the presence of caffeic acid. A MS2



base peak was observed at  $m/z$  135.0441, corresponding to the loss of  $-CO_2$  group from caffeic acid. Furthermore, its identity was confirmed by comparing the fragmentation spectra and retention time of a caffeic acid reference standard.

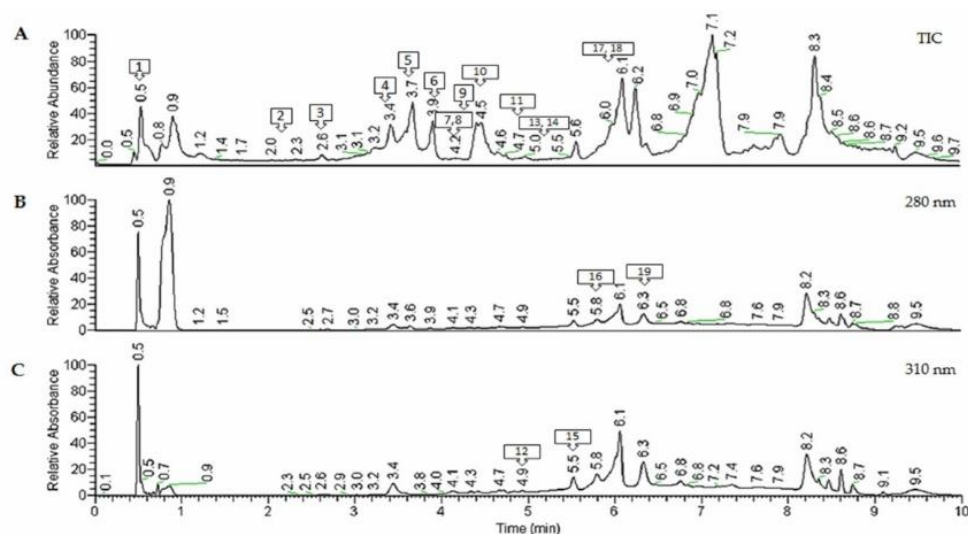


**Figure 2.** Spectra obtained for a representative *A. borbonica* acetone-evaporated extract. (A) Representative total ion chromatogram (TIC) obtained in negative mode. (B) UHPLC-UV chromatograms obtained at 280 and 310 nm (C). The different molecules are numbered according to their retention times.

Chromatographic peaks 6 (4.09 min) and 7 (4.18 min) showed a precursor ion  $[M - H]^-$  at  $m/z$  337.0931, which has the predicted molecular formula  $C_{16}H_{17}O_8$  (mass error 0.1 ppm), corresponding to *p*-coumaroylquinic acid isomers (*p*-CoQA). These two peaks had the same MS2 base peak at  $m/z$  191.0550 and secondary ions at  $m/z$  173.0446 and 163.0392, corresponding to the dehydrated forms of quinic acid and coumaric acid, respectively. Peaks 6 and 7 were identified as 3- or 5-*p*-coumaroylquinic acids [21,22] (Figure S2l,m).

Chromatographic peaks 8 (4.2 min) and 10 (4.43 min) with a precursor ion  $[M - H]^-$  at  $m/z$  163.0391, which had the predicted molecular formula  $C_{16}H_{17}O_9$  (mass error 0.2 ppm), could be coumaric acid isomers. Indeed, these two peaks had the same MS2 ion at  $m/z$  119.049, corresponding to the removal of a  $-CO_2$  group from coumaric acid. The identification was further confirmed by comparing the MS2 fragmentation behavior and the retention time of a *p*-coumaric acid reference standard. Therefore, peak 8 was identified as *m/o*-coumaric acid and peak 10 as *p*-coumaric acid (Figure S1p).

For the chromatographic peak 9 (4.36 min), a precursor ion  $[M - H]^-$  at  $m/z$  367.1035 with a predicted molecular formula  $C_{17}H_{19}O_9$  (mass error 0.5 ppm) was detected, suggesting the presence of feruloylquinic acid (FQA). The MS2 base peak at  $m/z$  191.0550, associated with quinic acid and a product ion at  $m/z$  173.0444, was often found for the 5-FQA [23] (Figure S2o).

Chromatographic peak 11 (4.74 min) shows a precursor ion  $[M - H]^-$  at  $m/z$  609.1464, with the following composition of  $C_{27}H_{29}O_{16}$  (mass error 1.6 ppm) and an MS2 base peak at  $m/z$  300.0274, resulting from the neutral loss of a disaccharide rutinose linked to quercetin. Its identification as quercetin-3-*O*-rutinoside (rutin) was confirmed by comparing the MS2 fragmentation pattern and the retention time of its commercial standard (Figure S1e).

Chromatographic peak 12 (4.94 min) and 13 (5.01 min) show a precursor ion  $[M - H]^-$  at  $m/z$  463.0884, with the following composition of  $C_{21}H_{19}O_{12}$  (mass error 1.33 ppm) and an MS2 base peak at  $m/z$  300.0274, resulting from the neutral loss of a hexose linked to quercetin. Their identification as quercetin-3-*O*-galactoside (hyperoside) (peak 12) and quercetin-3-*O*-glucoside (peak 13) (Figure S2f) was solved by comparing their MS2 fragmentation pattern and their retention time to a hyperoside commercial standard that allowed a reliable discrimination.

For the chromatographic peaks 14 (5.26 min) and 15 (6.45 min), a precursor ion  $[M - H]^-$  at  $m/z$  447.0935 with the predicted molecular formula  $C_{21}H_{19}O_{11}$  (mass error 1.35 ppm) was detected, suggesting the presence of kaempferol hexosides. The MS2 base peak at  $m/z$  284.0326 was linked to the loss of the hexoside part, which reinforced their identification (Figure S2g).

For the chromatographic peaks 16, 17, and 19, a precursor ion  $[M - H]^-$  at  $m/z$  515.1195 with a predicted molecular formula of  $C_{25}H_{23}O_{12}$  (mass error 1.04 ppm) was detected, suggesting the presence of di-caffeoylquinic acid isomers (di-CQA). The main MS2 product ions were at  $m/z$  353.0878, due to the loss of the caffeic acid moiety;  $m/z$  191.0554, corresponding to quinic acid;  $m/z$ , 179.0342 corresponding to caffeic acid;  $m/z$  173.0447, corresponding to a dehydrated quinic acid; and  $m/z$  135.0440, corresponding to a decarboxylated form of caffeic acid. Interestingly, among these four isomers, only peak 16 (5.82 min) had an MS2 base peak at  $m/z$  191.0554, allowing the identification of 3,5-diCQA (Figure S2h). The other three isomers had an MS2 base peak at  $m/z$  173.0447, which is consistent with the 4-acylated mono-acyl CGAs. In this way, the peak 17 (6.02 min) was assigned to 3,4-diCQA due to a higher intensity of the quinic acid product ion ( $m/z$  191.0554) than the remaining peaks (Figure S2i). Due to the lack of standards, peak 19 (6.36 min) was tentatively characterized as either 1,4-diCQA or 4,5-diCQA (Figure S2q) [17,18]. Of note, for most of the identified compounds we found an 80% coverage with the MS2 spectra from the mzCloud Database.

### Phenolic Acids Quantification by UHPLC-HESI-MS

The quantification by mass spectrometry highlighted a high abundance of cinnamic and benzoic acid derivatives in both extracts (Table 3, Figure S3). Most of the compounds were found in significantly higher concentrations in acetonic versus aqueous extracts: 0.002162 vs. 0.000703 mg/mL for caffeic acid, 0.007596 and 0.001437 mg/mL for dicaffeoylquinic acids isomers, and 0.004070 and 0.002415 mg/mL for protocatechuic acid. Interestingly, the concentration of caffeoylquinic acid isomers (5-CQA/3-CQA) was higher in the aqueous relative to the acetonic extracts (0.010163 vs. 0.005559 mg/mL). Indeed, the total amount of phenolic acids and flavonoids is higher in the acetonic extract than in the aqueous extract. These results highlight a notable amount of phenolic acids in both *A. borbonica* extracts.

**Table 3.** Quantification of polyphenols-rich acetonic and aqueous extracts from *A. borbonica* by HPLC-HESI-MS. The analysis was performed using a Q-Exactive™ Plus mass spectrometer at a concentration of 40 g/L. The concentrations of the different compounds were expressed as ng/mL. Data are the mean  $\pm$  SD of three independent experiments. \*  $p < 0.05$ , \*\*  $p < 0.01$  \*\*\*,  $p < 0.001$  (vs. 40 g/L of acetonic extract). CQA: caffeoylquinic acid. Di-CQA: dicaffeoylquinic acid.

Peak		Concentration in Acetonic Extract (mg/mL)	Concentration in Aqueous Extract (mg/mL)
<b>Phenolic Acids</b>			
5	Caffeic acid	0.002162 $\pm$ 0.000066	0.000703 $\pm$ 0.000039 ***
10	<i>p</i> -Coumaric acid	0.002755 $\pm$ 0.000728	0.001768 $\pm$ 0.000176 *
8	<i>m/o</i> -Coumaric acid	0.000470 $\pm$ 0.000003	0.000208 $\pm$ 0.000004
4	5-CQA	0.004718 $\pm$ 0.000279	0.008558 $\pm$ 0.000477 ***
3	3-CQA	0.000840 $\pm$ 0.000093	0.001604 $\pm$ 0.000157 ***
17	3,4-diCQA	0.004704 $\pm$ 0.000326	0.000503 $\pm$ 0.000034 ***
19	1,4/4,5-diCQA	0.000262 $\pm$ 0.000020	0.000090 $\pm$ 0.000003 **
16	3,5-diCQA	0.002629 $\pm$ 0.000161	0.000842 $\pm$ 0.000029 ***
2	Protocatechuic acid	0.004070 $\pm$ 0.000250	0.002415 $\pm$ 0.000387 ***
	Total	0.023061	0.016693
<b>Flavonols</b>			
11	Quercetin-3-O-rutinoside	0.011933 $\pm$ 0.002018	0.003977 $\pm$ 0.000473 ***
12	Quercetin-3-O-galactoside	0.001791 $\pm$ 0.000204	0.000591 $\pm$ 0.000033 ***
14/15	Kaempferol hexosides	0.000216 $\pm$ 0.000054	0.000044 $\pm$ 0.000005 **
	Total	0.013941	0.004612



Quantification by mass spectrometry confirmed the abundance of flavonol derivatives in both extracts (Table 3, Figure S3). Interestingly, we found three times more quercetin-3-*O*-rutinoside and quercetin-3-*O*-galactoside in the acetonic than in the aqueous extract, and five times more kaempferol-hexoxides in the acetonic than in the aqueous extract. These results confirmed the presence of notable amounts of flavonoids in both *A. borbonica* extracts.

### 2.3. Zebrafish Embryo and Larvae Acute Toxicity Test

#### Survival and Lethality Curves on Zebrafish Embryos

In order to investigate the toxic effect of polyphenols-rich acetonic and aqueous extracts from *A. borbonica*, a Fish Embryo Acute Toxicity (FET) test was performed according to the OECD guidelines [24]. Briefly, fertilized zebrafish eggs (0–3 hpf) were incubated with different concentrations of *A. borbonica* (acetonic or aqueous extract) until 96 hpf (developmental day 4), the extract being freshly renewed every day. Within the first day (0–24 hpf), none of the embryos survived at the highest concentrations of acetonic (16.9 g/L) and aqueous (40–22.5 g/L) extracts (Figure 3A,B) as shown by the coagulated eggs (Figure 4A, representative picture).

Obviously, the mortality rate is dose-dependent (Figure 3A–F). As shown in Figure 3C,D, the median lethal concentration (LC<sub>50</sub>) corresponding to the concentration that induced a 50% mortality was lower with the acetonic extract than with the aqueous extract ( $5 \pm 0.2$  vs.  $17.6 \pm 1.7$  g/L, respectively), demonstrating the higher toxicity of the acetonic extract. At non-lethal concentrations (2.3 and 7.2 g/L for acetonic and aqueous extracts, respectively), incubation with polyphenols-rich acetonic and aqueous extracts from *A. borbonica* leads to developmental delay and malformations (Figure 4A–D). Although a 90% hatching was measured in the E3 medium, a significant decrease of 75% and 38% in hatching was observed at 96 hpf for the acetonic (2.3 g/L) and aqueous (7.2 g/L) extracts, respectively. This percentage reached 0% at 7.2 g/L (acetonic) and 9.5 g/L (aqueous) (Figure 4B). For the hatched embryos who have been exposed to the two types of extracts, we observed  $21 \pm 3\%$  and  $15 \pm 1.6\%$  pericardial edema with 2.3 g/L of acetonic and aqueous extracts, respectively, this percentage reaching 50% with 7.2 g/L of aqueous extract (Figure 4C). Spinal curvature was observed in  $14 \pm 2\%$  and  $15 \pm 1.5\%$  of these hatched embryos exposed, respectively, to acetonic and aqueous extracts, and reached 50% at 7.2 g/L of aqueous extract of *A. borbonica* (Figure 4A). Taken together, these data demonstrate the deleterious impact of such non-lethal concentrations during zebrafish development.

The toxicity of polyphenols-rich acetonic and aqueous extracts from *A. borbonica* was also studied in zebrafish larvae from 3 to 5 dpf. Indeed, at 3 dpf the swimming larvae already displayed functional livers and kidneys, allowing them to metabolize a variety of compounds [25–27]. As a consequence, the toxicity of the respective extracts could be different in zebrafish embryos and larvae. By treating the zebrafish larvae for 2 days in a way similar to the embryos, the respective LC<sub>50</sub> values were determined for both extracts (Figure 3E,F). In embryos, the LC<sub>50</sub> is higher with the aqueous extract than with the acetonic one (20.3 g/L vs.  $5.6 \pm 0.4$  g/L). In addition, although no significant differences in LC<sub>50</sub> were observed between the embryos and larvae, the LC<sub>50</sub> is weakly higher for larvae than for embryos (20.3 g/L vs.  $17.6 \pm 1.7$  g/L, respectively). Our data strongly suggest that even at non-lethal concentrations, these extracts can lead to developmental defects.

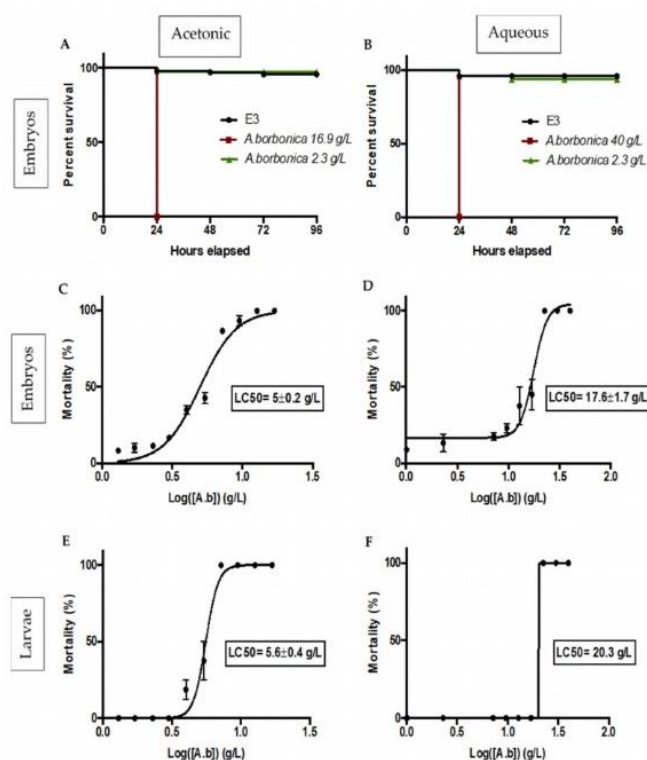


**Figure 3.** Survival curves for 96 hpf zebrafish embryos exposed with acetonic (A) or aqueous (B) extracts from *A. borbonica* at high concentrations of 16.9 g/L (acetonic) and 40 g/L (aqueous) and a low concentration of 2.3 g/L (acetonic and aqueous), and E3 was considered as control. Median lethal concentration curves (LC<sub>50</sub>) for 96 hpf zebrafish embryos and 72 hpf larvae exposed to acetonic (C,E) or aqueous (D,F) extracts at different concentrations ranging from 16.9 to 1.3 g/L (acetonic) and 40 to 2.3 g/L (aqueous) for 4 and 2 days, respectively. The LC<sub>50</sub> values were expressed in g/L. Data are the mean ± SD of three independent experiments.

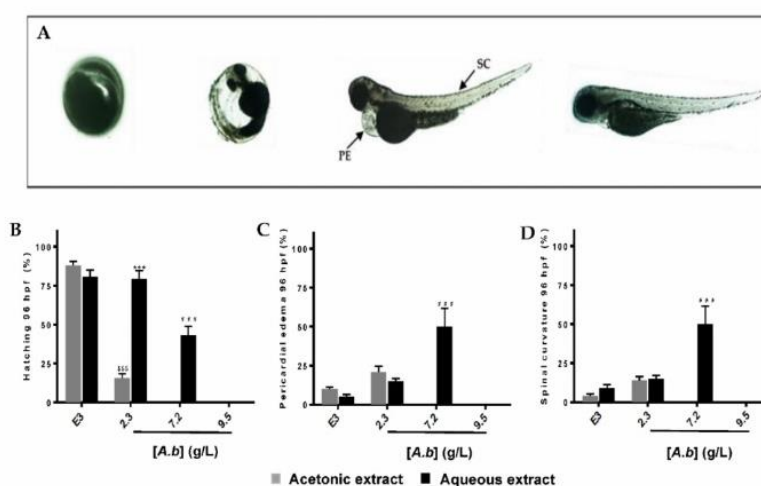


**Figure 4.** Morphological malformations and delayed development of zebrafish embryos/larvae exposed to *A. borbonica* extracts. (A) From left to right, coagulated egg (at 24 hpf), delayed hatching, spinal curvature, pericardial edema, and control embryos/larvae (96 hpf). Arrows indicate the presence of pericardial edema (PE) and spinal curvature (SC). Hatchability rates after 4 days of exposure with acetonic and aqueous extracts at 2.3, 7.2, and 9.5 g/L are represented in (B–D) represent the percentage of PE and SC, respectively. E3 medium was used as a positive control. Data are the mean ± SD of three independent experiments. \$\$\$  $p < 0.001$  (vs. E3 (acetonic)), \*\*\*  $p < 0.001$  (vs. acetonic extract), and ###  $p < 0.001$  (vs. E3 (aqueous)).



### 3. Discussion

Over the years, natural phenolic compounds have represented major preventive and/or therapeutic compounds for improving health issues. Indeed, many epidemiological studies have exhibited the beneficial effect of a polyphenol-rich diet on cancer, diabetes, obesity, and cardiovascular and neurodegenerative diseases [28–35]. Réunion island, a famous biodiversity hotspot, exhibits a wide and rich flora, with 22 medicinal plants registered to the French pharmacopeia [9]. These plants are known for their use in traditional medicine [3] and have been reported to be rich in polyphenols [36]. However, they are only poorly characterized concerning their contents, toxicities, and real in vivo preventive and/or therapeutic properties.

Among these medicinal plants, *A. borbonica*, belonging to the *Rubiaceae* family, is particularly interesting, as it widely used in traditional medicine for treating, among other things, diabetes, urinary tract infections, diarrhea, hemorrhage, rheumatism, and also kidney stones [10]. Interestingly, in an ischemia-reperfusion stroke mouse model exposed to hyperglycemia, *A. borbonica* polyphenols display neuroprotective effects, preventing the elevation of the brain pro-inflammatory cytokine (IL-6) level and exerting its antioxidant property by decreasing reactive oxygen species (ROS) [13]. More recently, a preventive protective effect of *A. borbonica* aqueous extract was evidenced in a diet-induced overweight model in zebrafish displaying oxidative stress and blood–brain barrier leakage [14].

In this work, to the best of our knowledge, we performed for the first time an in-depth characterization of the polyphenol content of *A. borbonica* aqueous and acetonic extracts, demonstrating the presence of new molecules never described before for that plant. Furthermore, although used in humans, the safety profile of *A. borbonica* is largely unknown and no toxicological studies have been carried out so far. We consequently provided data concerning the toxicity of the *A. borbonica* aqueous and acetonic extracts on relevant in vivo physiological models using zebrafish embryos and larvae.

#### 3.1. Polyphenol Content of Aqueous and Acetonic Extracts

A quantification by high-resolution mass spectrometry of the acetonic and aqueous extracts revealed the presence of polyphenol derivatives belonging to the phenolic acid and flavonoid classes known to be the most abundant in plant and plant-based foods [37,38]. From a qualitative point of view, no difference was observed between both extracts. Interestingly, although herbal infusion allows a very powerful polyphenol extraction yield, from a quantitative point of view the total amount of phenolic acids and flavonoids remains a little higher in the acetonic extract than in the aqueous extract. This result was expected, since it is well known that the polyphenol solubility depends on the solvent polarity and the kind of extraction used [39–41].

In this work, we have identified 19 main polyphenols. Among them, we observed that the major compounds of both extracts were quercetin-3-*O*-rutinoside, caffeoyl- and dicaffeoyl-quinic acids isomers, protocatechuic acid, coumaric acids isomers, and caffeic acid. These results were consistent with previous ones reported from our laboratory [5]. However, we provide a significant input to this previous work, since our MS<sup>2</sup> spectral analysis identified new compounds such as quercetin-3-*O*-rutinoside, protocatechuic acid, and coumaric acids isomers.

The identification of these new compounds could be explained by a different geographical location of *A. borbonica* leading to different environmental conditions, such as moisture, illumination, altitude, and temperature [42]. Furthermore, in these previous studies, conventional C18 reverse-phase column was used, while in the present study we used a pentafluorophenyl-phase column known to offer a greater selectivity for several compound classes such as aromatic and isomeric compounds, achieved not only by hydrophobic interactions as C18 reverse-phase but also by aromatic,  $\pi$ - $\pi$ , dipole–dipole, and ionic interactions and hydrogen bonding [43].

High phenolic acid and flavonoid contents are often associated with a high antioxidant capacity of the plant extract [44,45]. These compounds are characterized by one or several aromatic rings with at least one hydroxyl group [37]. This particular chemical structure conferred them different antioxidant activities due to their ability to directly scavenge free radicals by donating protons/electrons [46,47] or



by activating antioxidant signaling pathways [48]. Interestingly, the DPPH experiment highlighted the strong capacity of both extracts to reduce DPPH radicals due to their high content in bioactive molecules. These high antioxidant properties for the acetonic extract are consistent with a previous study [5].

### 3.2. Aqueous and Acetonic Extracts of *Antirhea borbonica* Exhibit Developmental and Toxicity at High Concentrations

Despite the beneficial effects of natural polyphenols, the safe consumption of beverages from medicinal plants remains poorly studied. Indeed, polyphenols can also display adverse effects, including carcinogenic/genotoxic ones; act as endocrine disruptors; disturb iron absorption; and also interact with drugs [49]. We consequently decided to investigate for the first time the potential toxicity of the medicinal plant *A. borbonica* using the zebrafish model. Whilst the classical approach for the assessment of drug and plant extract toxicity is time consuming, expensive, and requires in vitro and in vivo models (mainly rodents), the zebrafish embryo model emerged as a relevant tool for a first toxicological screening approach. This developmental model is widely used to assess drug toxicity [15] and appears as a relevant model, given its strong genic homology (more than 70% of human genes have an orthologue in zebrafish). As well, zebrafish display many evolutionary conserved organs and physiological processes [16] and exhibit a high fertility rate as well as transparent eggs, allowing their easily monitoring at the different stages of organogenesis [50].

In the present study, we used the Fish Embryo Acute Toxicity test (FET) designed by OECD and known to be a reference in the field [24]. At the highest doses tested (40–16.9 g/L), a 100% mortality was observed at 24 hpf for both extracts, in spite of the chorion presence, which potentially acts as a barrier. The toxicity of both plant extracts evidenced that the acetonic extract was more toxic than the aqueous extract ( $LC_{50}$ :  $5 \pm 0.2$  g/L vs.  $17.6 \pm 1.7$  g/L, respectively). Such a toxicity may be associated with the high bioactivity of the plant extracts or the presence of other phytochemical compounds, such as alkaloids and terpenes, known to be produced for defense against abiotic and probiotic stresses in plants. Previous studies have reported that alkaloids significantly contribute to the toxic effect of various plants [51–53].

Interestingly, for the highest non-lethal concentrations (2.3 g/L (acetonic), 7.2 g/L (aqueous)), we observed a delay in hatching in a concentration- and exposure time-dependent manner. A significant hatching reduction of 38% and 75% was observed at 96 hpf for the aqueous (7.2 g/L) and acetonic (2.3 g/L) extracts, respectively. Hatching normally occurs between 72 and 96 hpf. Although this remains to be investigated, we can speculate that the delayed hatching observed in our experimental conditions for the treated embryos may be induced by an impairment in the hatching process, such as the production-secretion of hatching enzymes (zhe1), cathepsin L (catL1), involved in this physiological process [54], as well as in the expression of genes (Zip10 and Znt1a) involved in zinc metabolism that are known to be essential in the development of the hatching gland [55]. In the chorion, a decrease in larvae motricity due to a delay in the muscular development or an altered larval morphology may also explain the delayed hatching.

As well, we noticed several malformations such as spinal curvature and the presence of pericardium edema. These defects are known to occur in the presence of toxic molecules, leading to kidney impairments or kidney malformations [56–58]. Further investigations are needed to identify the presence of compounds or metabolites inside the zebrafish embryos responsible for the acute toxicity of *A. borbonica* extracts.

We also aimed at identifying the potential toxicity of our extracts in larvae (from 3 to 5 dpf). At 3 dpf, zebrafish larvae exhibit functional livers and kidneys, suggesting the possible metabolism of several compounds [59,60]. Interestingly, the study of the toxicity of polyphenols-rich acetonic and aqueous extracts from *A. borbonica* in zebrafish larvae from 3 to 5 dpf revealed no significant differences in the median lethal concentrations between the larvae and embryos, with  $5 \pm 0.2$  vs.  $5.6 \pm 0.4$  g/L and  $17.6 \pm 1.7$  vs.  $20.3$  g/L for acetonic and aqueous extracts, respectively.

Medicinal plants known as “green gold” have been widely used in traditional medicine for centuries across the world. The relatively toxic effect of the medicinal plant relies on different parameters, such as the plant part used, composition, preparation method, and concentration. Among plant-based beverage preparations, the infusion is the most commonly used after decoction. Therefore, we studied the potential toxic effect of an aqueous extract from *A. borbonica* on zebrafish embryos. A median lethal concentration of  $17.6 \pm 1.7$  g/L was found. This concentration is higher than the concentration recommended by the herbalist for this method of preparation, around 1–4 g for 1 L. However, we must remain vigilant about taking this aqueous extract, which can have teratogenic effects, especially during pregnancy.

## 4. Materials and Methods

### 4.1. Reagents/Standards

Folin-Ciocalteu reagent, sodium carbonate, sodium nitrite, aluminum chloride, DPPH, caffeic acid, caffeoyquinic acid, *p*-coumaric acid, protocatechuic acid, kaempferol, hyperoside, rutin hydrate, and dimethylsulfoxide (DMSO) were purchased from Sigma Aldrich (St. Louis, MO, USA). Solvents such as acetone, acetonitrile, methanol, and water (HPLC-MS grade) were purchased from Carlo erba (Peypin, France).

### 4.2. Plant Material

*Antirhea borbonica* J.F Gmelin (*A. borbonica*) powder (leaves) was obtained from APLAMEDOM institute (Association pour les plantes aromatiques et médicinales de La Réunion) and registered under the following code, DÉTROI.002/2018, stating the date of collection and the GPS coordinates (21°05′44.9″ S, 55°39′06.6″ E), altitude: 770 m. The pharmacist and director of APLAMEDOM performed the botanical identification of *A. borbonica*. The dried (air-dried protected from direct light) leaves were reduced to powder using a laboratory grinder. The crushed leaves of *A. borbonica* were conserved at  $-20$  °C.

### 4.3. Preparation of the Plant Extracts

Acetonic extract from *A. borbonica* was obtained after dissolving 1 g of crushed leaves in 25 mL of an aqueous acetonic solution (70%, *v/v*). After incubation at 4 °C for 90 min, the mixture was centrifuged at 3500 rpm at 4 °C for 20 min and the polyphenol-rich supernatant was collected and dried using a rotary evaporator. The extract was resuspended with an identical volume of E3 medium (classical embryonic medium), filtered with a 20 µm membrane, and stored at  $-20$  °C until analysis.

Aqueous plant extract (40 g/L) was prepared by the infusion technique. Briefly, 1 g of crushed leaves was added to 25 mL of boiled E3 medium for 10 min under stirring. The resultant extract was filtered with a 20 µm membrane, aliquoted, and stored at  $-20$  °C until analysis.

For a toxicity test using fertilized eggs and larvae zebrafish, aqueous extract was prepared every day extemporaneously.

### 4.4. Measurement of the Total Antioxidant Capacity of Polyphenol-Rich Plant Extracts

The total antioxidant capacity was assessed using the 2,2-Diphenyl-1-picrylhydrazyl (DPPH) radical scavenging assay. Briefly, in a 96-well microplate, 200 µL of a 0.25 mM DPPH solution and 40 µL from different concentrations (40–2.5 g/L (GAE)) of acetone-evaporated or aqueous extracts were added and incubated at 25 °C for 30 min. Ascorbic acid solutions prepared at the same concentration range (gallic acid equivalent) were used as an antioxidant standard. The absorbance (Abs) was read at 517 nm (FLUOstar Optima, Bmg Labtech, Offenburg, Germany). The percentage of the free radical-quenching activity of DPPH was calculated from the following formula:

$$\text{Antioxidant capacity (\%)} = \left[ \frac{(\text{Abs}_{\text{control}} - \text{Abs}_{\text{sample}})}{\text{Abs}_{\text{control}}} \right] \times 100. \quad (1)$$



Inhibitory concentration ( $IC_{50}$ ) values corresponding to the concentrations reducing 50% of the initial DPPH• values were obtained by plotting the percentage of free radical-quenching activity against the logarithm of the different concentrations ranging from 16.9 to 1.4 g/L (acetic) and 40 to 2.5 g/L (aqueous). Once the concentration values were transformed, a nonlinear regression (log (inhibitor) vs. response-variable slope) was applied to obtain a sigmoid curve.

#### 4.5. Determination of Phenolic Acid Content

The total phenolic acid contents in acetone-evaporated and aqueous extracts were determined by using the Folin–Ciocalteu assay [61] with slight modifications. Briefly, in a 96-well microplate, 25  $\mu$ L of plant extract, 125  $\mu$ L of Folin–Ciocalteu's phenol reagent (Sigma Aldrich), and 100  $\mu$ L of 75 g/L sodium carbonate (Sigma) were added and incubated at 50 °C for 15 min and then at 4 °C for 3 min. The absorbance was measured at 760 nm (FLUOstar Optima, Bmg Labtech). A calibration curve between 12.5 and 300  $\mu$ M was prepared using a standard solution of gallic acid (Sigma-Aldrich, Darmstadt, Germany). The total phenolic acid contents were expressed as the mg gallic acid equivalent (GAE) per 100 g of dried plant powder.

#### 4.6. Determination of Flavonoid Content

The total flavonoid content was determined using the aluminum chloride ( $AlCl_3$ ) colorimetric assay adapted from Zhishen et al. [62]. For this measurement, 100  $\mu$ L of sample was mixed in a 96-well microplate with 6  $\mu$ L of 5% aqueous sodium nitrite ( $NaNO_2$ ) solution. After 5 min, 6  $\mu$ L of 10% aqueous  $AlCl_3$  were added and the mixture was vortexed. Then, after 1 min incubation, 40  $\mu$ L of 1 M NaOH was added. The absorbance was read at 510 nm (FLUOstar Optima, BMG Labtech). A calibration curve between 6.25 and 300  $\mu$ M was prepared using a standard solution of quercetin. The total flavonoid contents were expressed as the mg quercetin equivalent (QE) per 100 g of dried plant powder.

#### 4.7. Polyphenolic Compounds Identification and Quantification LC-UV-HESI-MS/MS

Polyphenols extracted from *A. borbonica* acetone-evaporated or aqueous extracts were identified by ultra-high-performance liquid chromatography, coupled with diode array detection and HESI-Orbitrap mass spectrometer (Q-Exacte™ Plus, Thermo Scientific, Waltham, MA, USA). Briefly, 10  $\mu$ L of the sample was injected using an UHPLC system equipped with a Thermo Fisher Ultimate 3000 series WPS-3000 RS autosampler and then separated on a PFP column (2.6  $\mu$ m, 100 mm  $\times$  2.1 mm, Phenomenex, Torrance, CA, USA). The column was eluted with a gradient mixture of 0.1% formic acid in water (A) and 0.1% formic acid in acetonitrile (B) at the flow rate of 0.450 mL/min, with 5% B at 0.00 to 0.1 min, 35% B at 0.1 to 7.1 min, 95% B at 7.2 to 7.9 min, and 5% B at 8.0 to 10 min. The column temperature was held at 30 °C and the detection wavelengths were set to 280 and 310 nm, allowing the identification of phenolic acids and flavonoids, respectively.

For the mass spectrometer conditions, a Heated Electrospray Ionization source II (HESI II) was used. Nitrogen was used as the drying gas. The mass spectrometric conditions were optimized as follows: spray voltage 2.8 kV, capillary temperature 350 °C, sheath gas flow rate 60 units, aux gas flow rate 20 units, and S lens RF level 50. Mass spectra were registered in full scan mode from  $m/z$  100 to 1500 in negative ion mode at a resolving power of 70,000 FWHM at  $m/z$  400. The automatic gain control (AGC) was set at  $1e6$ . The MS/MS spectra were obtained by applying a relative higher energy collisional dissociation (HCD) energy of 25%. The identification of the compounds of interest was based on their retention time, exact mass, elemental composition, MS fragmentation pattern, and comparisons with available standards and the advanced mass spectral database,  $m/z$  Cloud, <https://www.mzcloud.org>. Data were acquired with the XCalibur 4.1 software (Thermo Fisher Scientific Inc.) and processed with the compound discoverer 2.1 and the Skyline 20.1 software (MacCoss Lab.)  $1 \times 10^6$ .



## Preparation of Standard Solution, Calibration Curves, and Method Validation

Standard stock solutions of caffeic acid, caffeoylquinic acid, kaempferol, quercetin-3-*O*-rutinoside, quercetin-3-*O*-galactoside, protocatechuic acid, and coumaric acid were dissolved in methanol at a concentration of 1 mg/mL. A mixed stock solution containing 10 µg/mL of each polyphenol standard was prepared in methanol. The calibration standard solutions were prepared by the dilution of the mixed stock solutions in 0.1% formic acid in water to obtain the desired calibration curves ranging from 10 to 4000 ng/mL. The quality control (QC) samples were prepared at 25, 250, and 4000 ng/mL and analyzed in triplicate within each batch.

The calibration curves were built by plotting the peak area of the analytes against the corresponding analytes concentrations with linear regression using standard samples at nine concentrations. The calibration curves of each polyphenol had a correlation coefficient ( $R^2$ ) of 0.99. The method accuracy was estimated by calculating the percent deviation observed in the analysis of QC samples and expressed by relative error. The intraday precision was estimated by analyzing QC samples at three concentration levels (25, 250, 4000 ng/mL) of the seven analytes within 24 h ( $n = 8$ ). The inter-day accuracy was estimated by the repeated analysis of QC samples ( $n = 8$ ).

The variability was expressed as the relative standard deviation (RSD, %), and the accuracy was expressed as the relative error (RE, %). The limit of quantification (LOQ) was defined as the lowest analytical concentration of the calibration curve at which the measured precision, expressed as relative standard deviation (RSD), was within 20% and the accuracy, expressed as relative error (RE), was in the range of 20%.

### 4.8. Zebrafish Husbandry

Adult AB wildtype zebrafish (*Danio rerio*, AB strain) were housed in the zebrafish facility of the CYROI/DéTROU, La Réunion (A974001). They were maintained under the standard conditions of photoperiod (14 h dark/10 h light), temperature (28.5 °C), conductivity (400 µS), and pH (7.4). Zebrafish were fed daily (3 times a day) with commercially available food (Planktovie, GEMMA 300). All the animal experiments were performed in CYROI/DéTROU (UMR 1188) and conducted in accordance with the French and European Community Guidelines for the Use of Animals in Research (86/609/EEC and 2010/63/EU).

### 4.9. Developmental Toxicity Test (Zebrafish Embryos)

The day before the start of the toxicity test assay, breeding males and females (optimal ratio 2:1) were placed in the same tank but were physically separated. The next day, 1 h after light onset, fish couples were allowed to spawn for 1 h. The eggs were collected, rinsed with fish water system, randomly mixed, and quickly distributed in the different concentrations of *A. borbonica* aqueous and acetone-evaporated extracts prepared with E3 medium. The treatment was performed between 1 and 3 h post fertilization (dpf) for embryos and between 3 and 5 dpf for larvae. The quality of the spawn (>70% of fertilization) was checked for fitting with the OECD recommendations (guidelines 236: Fish Embryo Acute Toxicity (FET) Test) [24]. The fertilized eggs were selected using a stereomicroscope and dispatched in a 24-well plate as follows: in each well, five fertilized eggs were placed in 2 mL of the respective concentrations of either *A. borbonica* aqueous extract (40, 30, 22.5, 16.9, 12.7, 9.5, 7.2, and 2.3 g/L) or *A. borbonica* acetone-evaporated extract (16.9, 12.7, 9.5, 7.2, 5.4, 4, 3, 2.3, 1.7, and 1.3 g/L) diluted in E3 medium. The concentration range was chosen on the basis of traditional use, which consists of infusion of 1–4 g of dried leaves in 1 L of boiled water for 10 min. Because *A. borbonica* has been registered at the French pharmacopeia, this concentration was supposed to be non-toxic in adults. Thus, the lowest doses tested were 2.3 and 1.3 g/L for aqueous and acetone-evaporated extract, respectively.

A total of 20 eggs or 10 larvae were tested for each concentration. These experiments were repeated three times independently. The 24-well plate was incubated at 26 °C ± 1 °C. Negative

controls (E3 medium only) and positive controls (E3 medium + 25% DMSO) were also placed in the 24-well plate.

The treatment was renewed each day using a freshly prepared *A. borbonica* extracts. Zebrafish development was carefully checked by using a stereo microscope (Nikon SMZ18) at 24, 48, 72, and 96 hpf looking at four apical observations as indicators of lethality according to the OECD guidelines 236: (i) coagulation of fertilized eggs, (ii) lack of somite formation, (iii) lack of detachment of the tail-bud from the yolk sac, and (iv) lack of heartbeat. At the end of the exposure period, the acute and developmental toxicity (teratogenicity) were determined according to the OECD ruled based on a positive outcome in any of the four apical observations recorded. The percentage of mortality was determined by using the following equation:

$$(\text{Mortality } (\%)) = (\text{Number of dead embryos} / \text{Total number of embryos}) \times 100. \quad (2)$$

Lethal concentrations (LC<sub>50</sub>) corresponding to the concentration that induced a 50% mortality were obtained by plotting the percentage of cumulative mortality at 96 hpf against logarithm of the different concentrations. A nonlinear regression (log (inhibitor) vs. response-variable slope) was applied to obtain a sigmoid curve. In addition, morphological abnormalities such as spinal curvature, delay in pigmentation, delay in eye color, and delay hatching were recorded.

#### 4.10. Statistical Analyses

Data are expressed as the mean ± standard deviation (SD) from at least three independent experiments performed in triplicate. Statistical analyses and determination of IC<sub>50</sub>/LC<sub>50</sub> were performed with Graph-Pad Prism 6.3 (GraphPad Software, Inc., San Diego, CA, USA). Comparison between more than 2 groups was determined using a one-way ANOVA followed by Dunnett's test. A *p*-value < 0.05 was considered statistically significant.

## 5. Conclusions

In this study, we identified new major polyphenols such as quercetine-3-*O*-rutinoside, protocatechuic acid, and coumaric acids isomers, which have to be taken into account regarding the anti-oxidant and anti-inflammatory effect of *A. borbonica*. We report for the first time the potential embryonic and larval toxicity at high concentrations of both acetonic and aqueous extracts from the medicinal plant *A. borbonica* by using the zebrafish embryo model. The present work will be useful to supplement current data on medicinal plants registered at the French pharmacopeia and more generally can be considered as a “proof of concept study” for the further analysis of medicinal plants.

**Supplementary Materials:** The following are available online. Figure S1: Total phenolic acid, flavonoid contents and antioxidant capacity from *A. borbonica* extracts. Figure S2: Fragmentation pattern of each identified compound obtained in negative mode. Figure S3: Quantification of polyphenols-rich acetonic and aqueous extracts from *A. borbonica* by UHPLC-ESI-MS. Table S1: Identification of 20 compounds in *Antirhea borbonica* herbal infusion by LC-HESI-UV-MS/MS in negative mode.

**Author Contributions:** Conceptualization: B.V., N.D. and J.-L.B.; data curation: B.V., B.G., M.B. and S.K.; formal analysis: B.V., N.D. and J.-L.B.; funding acquisition: J.-L.B. and O.M.; investigation: B.V., B.G., M.B. and S.K.; methodology: B.V. and M.B.; resources: N.D.; writing—original draft: B.V. and J.-L.B.; writing—review and editing: B.V., M.-P.G., O.M., N.D. and J.-L.B. All the authors have read and agreed to the published version of the manuscript.

**Funding:** This research was funded by the European Regional Development Funds (FEDER RE0022527 ZEBRATOX, EU-Région Réunion-French State national counterpart), the University of La Réunion, and the Institut National de la Santé et de la Recherche Médicale. Bryan Veeren is a recipient of a fellowship from the Région Réunion.

**Conflicts of Interest:** The authors declare no conflict of interest.



## References

1. McDougall, I.; Chamalaun, F.H. Isotopic Dating and Geomagnetic Polarity Studies on Volcanic Rocks from Mauritius, Indian Ocean. *Geol. Soc. Am. Bull.* **1969**, *80*, 1419. [[CrossRef](#)]
2. Agnarsson, I.; Kuntner, M. The Generation of a Biodiversity Hotspot: Biogeography and Phylogeography of the Western Indian Ocean Islands. In *Current Topics in Phylogenetics and Phylogeography of Terrestrial and Aquatic Systems*; Anamthawat-Jnsson, K., Ed.; InTech: London, UK, 2012; ISBN 978-953-51-0217-5.
3. Lavergne, R. *Tisaneurs et Plantes Médicinales Indigènes à la Réunion*; Orphie: Livry Gargan, France, 2016; ISBN 979-10-298-0073-3.
4. Adersen, A.; Adersen, H. Plants from Réunion Island with alleged antihypertensive and diuretic effects—An experimental and ethnobotanical evaluation. *J. Ethnopharmacol.* **1997**, *58*, 189–206. [[CrossRef](#)]
5. Marimoutou, M.; Le Sage, F.; Smadja, J.; Lefebvre d’Hellencourt, C.; Gonthier, M.-P.; Robert-Da Silva, C. Antioxidant polyphenol-rich extracts from the medicinal plants *Antirhea borbonica*, *Doratoxylon apetalum* and *Gouania mauritiana* protect 3T3-L1 preadipocytes against H<sub>2</sub>O<sub>2</sub>, TNF $\alpha$  and LPS inflammatory mediators by regulating the expression of superoxide dismutase and NF- $\kappa$ B genes. *J. Inflamm. (London)* **2015**, *12*, 10. [[CrossRef](#)]
6. Fortin, H.; Vigor, C.; Lohézic-Le Dévéhat, F.; Robin, V.; Le Bossé, B.; Boustie, J.; Amoros, M. In vitro antiviral activity of thirty-six plants from La Réunion Island. *Fitoterapia* **2002**, *73*, 346–350. [[CrossRef](#)]
7. Ledoux, A.; Cao, M.; Jansen, O.; Mamede, L.; Campos, P.-E.; Payet, B.; Clerc, P.; Grondin, I.; Girard-Valenciennes, E.; Hermann, T.; et al. Antiplasmodial, anti-chikungunya virus and antioxidant activities of 64 endemic plants from the Mascarene Islands. *Int. J. Antimicrob. Agents* **2018**, *52*, 622–628. [[CrossRef](#)]
8. Haddad, J.G.; Koishi, A.C.; Gaudry, A.; Nunes Duarte Dos Santos, C.; Viranaicken, W.; Desprès, P.; El Kalamouni, C. *Doratoxylon apetalum*, an Indigenous Medicinal Plant from Mascarene Islands, Is a Potent Inhibitor of Zika and Dengue Virus Infection in Human Cells. *Int. J. Mol. Sci.* **2019**, *20*. [[CrossRef](#)]
9. Giraud-Techer, S. Plantes médicinales de La Réunion inscrites à la Pharmacopée française. *Ethnopharmacologia* **2016**, *7*–33.
10. Poullain, C.; Girard-Valenciennes, E.; Smadja, J. Plants from reunion island: Evaluation of their free radical scavenging and antioxidant activities. *J. Ethnopharmacol.* **2004**, *95*, 19–26. [[CrossRef](#)]
11. Tailé, J.; Arcambal, A.; Clerc, P.; Gauvin-Bialecki, A.; Gonthier, M.-P. Medicinal Plant Polyphenols Attenuate Oxidative Stress and Improve Inflammatory and Vasoactive Markers in Cerebral Endothelial Cells during Hyperglycemic Condition. *Antioxidants* **2020**, *9*, 573. [[CrossRef](#)]
12. Delveaux, J.; Turpin, C.; Veeren, B.; Diotel, N.; Bravo, S.B.; Begue, F.; Álvarez, E.; Meilhac, O.; Bourdon, E.; Rondeau, P. *Antirhea borbonica* Aqueous Extract Protects Albumin and Erythrocytes from Glycoxidative Damages. *Antioxidants* **2020**, *9*, 415. [[CrossRef](#)]
13. Arcambal, A.; Tailé, J.; Couret, D.; Planesse, C.; Veeren, B.; Diotel, N.; Gauvin-Bialecki, A.; Meilhac, O.; Gonthier, M.-P. Protective Effects of Antioxidant Polyphenols against Hyperglycemia-Mediated Alterations in Cerebral Endothelial Cells and a Mouse Stroke Model. *Mol. Nutr. Food Res.* **2020**, *64*, e1900779. [[CrossRef](#)]
14. Ghaddar, B.; Veeren, B.; Rondeau, P.; Bringart, M.; Lefebvre d’Hellencourt, C.; Meilhac, O.; Bascands, J.-L.; Diotel, N. Impaired brain homeostasis and neurogenesis in diet-induced overweight zebrafish: A preventive role from *A. borbonica* extract. *Sci. Rep.* **2020**, *10*, 14496. [[CrossRef](#)]
15. Horzmann, K.A.; Freeman, J.L. Making Waves: New Developments in Toxicology with the Zebrafish. *Toxicol. Sci.* **2018**, *163*, 5–12. [[CrossRef](#)]
16. Tal, T.; Yaghoobi, B.; Lein, P.J. Translational toxicology in zebrafish. *Curr. Opin. Toxicol.* **2020**, *23–24*, 56–66. [[CrossRef](#)]
17. Clifford, M.N.; Knight, S.; Kuhnert, N. Discriminating between the Six Isomers of Dicafeoylquinic Acid by LC-MSn. *J. Agric. Food Chem* **2005**, *53*, 3821–3832. [[CrossRef](#)]
18. Clifford, M.N.; Johnston, K.L.; Knight, S.; Kuhnert, N. Hierarchical Scheme for LC-MSn Identification of Chlorogenic Acids. *J. Agric. Food Chem.* **2003**, *51*, 2900–2911. [[CrossRef](#)]
19. Fang, N.; Yu, S.; Prior, R.L. LC/MS/MS characterization of phenolic constituents in dried plums. *J. Agric. Food Chem.* **2002**, *50*, 3579–3585. [[CrossRef](#)]

20. Jaiswal, R.; Patras, M.A.; Eravuchira, P.J.; Kuhnert, N. Profile and characterization of the chlorogenic acids in green Robusta coffee beans by LC-MS(n): Identification of seven new classes of compounds. *J. Agric. Food Chem.* **2010**, *58*, 8722–8737. [[CrossRef](#)]
21. Clifford, M.N.; Marks, S.; Knight, S.; Kuhnert, N. Characterization by LC-MS(n) of four new classes of p-coumaric acid-containing diacyl chlorogenic acids in green coffee beans. *J. Agric. Food Chem.* **2006**, *54*, 4095–4101. [[CrossRef](#)]
22. Wu, S.-B.; Meyer, R.S.; Whitaker, B.D.; Litt, A.; Kennelly, E.J. A new liquid chromatography–mass spectrometry-based strategy to integrate chemistry, morphology, and evolution of eggplant (*Solanum*) species. *J. Chromatogr. A* **2013**, *1314*, 154–172. [[CrossRef](#)]
23. Clifford, M.N.; Knight, S.; Surucu, B.; Kuhnert, N. Characterization by LC-MSn of Four New Classes of Chlorogenic Acids in Green Coffee Beans: Dimethoxycinnamoylquinic Acids, Diferuloylquinic Acids, Caffeoyl-dimethoxycinnamoylquinic Acids, and Feruloyl-dimethoxycinnamoylquinic Acids. *J. Agric. Food Chem.* **2006**, *54*, 1957–1969. [[CrossRef](#)]
24. OECD. *Test No. 236: Fish Embryo Acute Toxicity (FET) Test, OECD Guidelines for the Testing of Chemicals, Section 2*; OECD Publishing: Paris, France, 2013.
25. Drummond, I.A.; Majumdar, A.; Hentschel, H.; Elger, M.; Solnica-Krezel, L.; Schier, A.F.; Neuhauss, S.C.; Stemple, D.L.; Zwartkruis, F.; Rangini, Z.; et al. Early development of the zebrafish pronephros and analysis of mutations affecting pronephric function. *Development* **1998**, *125*, 4655–4667. [[PubMed](#)]
26. Goldstone, J.V.; McArthur, A.G.; Kubota, A.; Zquette, J.; Parente, T.; Jönsson, M.E.; Nelson, D.R.; Stegeman, J.J. Identification and developmental expression of the full complement of Cytochrome P450 genes in Zebrafish. *BMC Genom.* **2010**, *11*, 643. [[CrossRef](#)] [[PubMed](#)]
27. Field, H.A.; Ober, E.A.; Roeser, T.; Stainier, D.Y.R. Formation of the digestive system in zebrafish. I. Liver morphogenesis. *Dev. Biol.* **2003**, *253*, 279–290. [[CrossRef](#)]
28. Flores-Pérez, A.; Marchat, L.A.; Sánchez, L.L.; Romero-Zamora, D.; Arechaga-Ocampo, E.; Ramírez-Torres, N.; Chávez, J.D.; Carlos-Reyes, Á.; Astudillo-de la Vega, H.; Ruiz-García, E.; et al. Differential proteomic analysis reveals that EGCG inhibits HDGF and activates apoptosis to increase the sensitivity of non-small cells lung cancer to chemotherapy. *Prot. Clin. Appl.* **2016**, *10*, 172–182. [[CrossRef](#)] [[PubMed](#)]
29. Zamora-Ros, R.; Touillaud, M.; Rothwell, J.A.; Romieu, I.; Scalbert, A. Measuring exposure to the polyphenol metabolome in observational epidemiologic studies: Current tools and applications and their limits. *Am. J. Clin. Nutr.* **2014**, *100*, 11–26. [[CrossRef](#)] [[PubMed](#)]
30. Khan, N.; Mukhtar, H. Modulation of signaling pathways in prostate cancer by green tea polyphenols. *Biochem. Pharm.* **2013**, *85*, 667–672. [[CrossRef](#)]
31. Afshin, A.; Micha, R.; Khatibzadeh, S.; Mozaffarian, D. Consumption of nuts and legumes and risk of incident ischemic heart disease, stroke, and diabetes: A systematic review and meta-analysis. *Am. J. Clin. Nutr.* **2014**, *100*, 278–288. [[CrossRef](#)] [[PubMed](#)]
32. Hooper, L.; Kroon, P.A.; Rimm, E.B.; Cohn, J.S.; Harvey, I.; Le Cornu, K.A.; Ryder, J.J.; Hall, W.L.; Cassidy, A. Flavonoids, flavonoid-rich foods, and cardiovascular risk: A meta-analysis of randomized controlled trials. *Am. J. Clin. Nutr.* **2008**, *88*, 38–50. [[CrossRef](#)]
33. Rasines-Perea, Z.; Teissedre, P.-L. Grape Polyphenols' Effects in Human Cardiovascular Diseases and Diabetes. *Molecules* **2017**, *22*, 68. [[CrossRef](#)]
34. Colizzi, C. The protective effects of polyphenols on Alzheimer's disease: A systematic review. *Alzheimers Dement. (New York)* **2019**, *5*, 184–196. [[CrossRef](#)]
35. Scalbert, A.; Manach, C.; Morand, C.; Rémésy, C.; Jiménez, L. Dietary polyphenols and the prevention of diseases. *Crit. Rev. Food Sci. Nutr.* **2005**, *45*, 287–306. [[CrossRef](#)] [[PubMed](#)]
36. Le Sage, F.; Meilhac, O.; Gonthier, M.-P. Anti-inflammatory and antioxidant effects of polyphenols extracted from *Antirhea borbonica* medicinal plant on adipocytes exposed to *Porphyromonas gingivalis* and *Escherichia coli* lipopolysaccharides. *Pharm. Res.* **2017**, *119*, 303–312. [[CrossRef](#)]
37. Manach, C.; Scalbert, A.; Morand, C.; Rémésy, C.; Jiménez, L. Polyphenols: Food sources and bioavailability. *Am. J. Clin. Nutr.* **2004**, *79*, 727–747. [[CrossRef](#)] [[PubMed](#)]
38. Pérez-Jiménez, J.; Neveu, V.; Vos, F.; Scalbert, A. Systematic analysis of the content of 502 polyphenols in 452 foods and beverages: An application of the phenol-explorer database. *J. Agric. Food Chem.* **2010**, *58*, 4959–4969. [[CrossRef](#)] [[PubMed](#)]



39. Santos-Buelga, C.; Williamson, G. *Methods in Polyphenol Analysis*; Royal Society of Chemistry: Cambridge, UK, 2003; ISBN 978-0-85404-580-8.
40. Stalikas, C.D. Extraction, separation, and detection methods for phenolic acids and flavonoids. *J. Sep. Sci.* **2007**, *30*, 3268–3295. [[CrossRef](#)] [[PubMed](#)]
41. Złotek, U.; Mikulska, S.; Nagajek, M.; Świeca, M. The effect of different solvents and number of extraction steps on the polyphenol content and antioxidant capacity of basil leaves (*Ocimum basilicum* L.) extracts. *Saudi J. Biol. Sci.* **2016**, *23*, 628–633. [[CrossRef](#)]
42. Liu, W.; Yin, D.; Li, N.; Hou, X.; Wang, D.; Li, D.; Liu, J. Influence of Environmental Factors on the Active Substance Production and Antioxidant Activity in *Potentilla fruticosa* L. and Its Quality Assessment. *Sci. Rep.* **2016**, *6*, 28591. [[CrossRef](#)]
43. Regos, I.; Treutter, D. Optimization of a high-performance liquid chromatography method for the analysis of complex polyphenol mixtures and application for sainfoin extracts (*Onobrychis vicifolia*). *J. Chromatogr. A* **2010**, *1217*, 6169–6177. [[CrossRef](#)]
44. Aryal, S.; Baniya, M.K.; Danekhu, K.; Kunwar, P.; Gurung, R.; Koirala, N. Total Phenolic Content, Flavonoid Content and Antioxidant Potential of Wild Vegetables from Western Nepal. *Plants* **2019**, *8*, 96. [[CrossRef](#)]
45. Dudonné, S.; Vitrac, X.; Coutière, P.; Woillez, M.; Mérillon, J.-M. Comparative study of antioxidant properties and total phenolic content of 30 plant extracts of industrial interest using DPPH, ABTS, FRAP, SOD, and ORAC assays. *J. Agric. Food Chem.* **2009**, *57*, 1768–1774. [[CrossRef](#)]
46. Balasundram, N.; Sundram, K.; Samman, S. Phenolic compounds in plants and agri-industrial by-products: Antioxidant activity, occurrence, and potential uses. *Food Chem.* **2006**, *99*, 191–203. [[CrossRef](#)]
47. Hatia, S.; Septembre-Malaterre, A.; Le Sage, F.; Badiou-Bénéteau, A.; Baret, P.; Payet, B.; Lefebvre d'hellencourt, C.; Gonthier, M.P. Evaluation of antioxidant properties of major dietary polyphenols and their protective effect on 3T3-L1 preadipocytes and red blood cells exposed to oxidative stress. *Free Radic. Res.* **2014**, *48*, 387–401. [[CrossRef](#)]
48. Sirota, R.; Gibson, D.; Kohen, R. The timing of caffeic acid treatment with cisplatin determines sensitization or resistance of ovarian carcinoma cell lines. *Redox Biol.* **2017**, *11*, 170–175. [[CrossRef](#)]
49. Mennen, L.I.; Walker, R.; Bennetau-Pelissero, C.; Scalbert, A. Risks and safety of polyphenol consumption. *Am. J. Clin. Nutr.* **2005**, *81*, 326S–329S. [[CrossRef](#)]
50. Kimmel, C.B.; Ballard, W.W.; Kimmel, S.R.; Ullmann, B.; Schilling, T.F. Stages of embryonic development of the zebrafish. *Dev. Dyn.* **1995**, *203*, 253–310. [[CrossRef](#)]
51. Cortinovis, C.; Caloni, F. Alkaloid-Containing Plants Poisonous to Cattle and Horses in Europe. *Toxins* **2015**, *7*, 5301–5307. [[CrossRef](#)]
52. Cheeke, P.R. Toxicity and metabolism of pyrrolizidine alkaloids. *J. Anim. Sci.* **1988**, *66*, 2343–2350. [[CrossRef](#)]
53. Diaz, G.J. Toxicosis by Plant Alkaloids in Humans and Animals in Colombia. *Toxins* **2015**, *7*, 5408–5416. [[CrossRef](#)]
54. Sano, K.; Inohaya, K.; Kawaguchi, M.; Yoshizaki, N.; Iuchi, I.; Yasumasu, S. Purification and characterization of zebrafish hatching enzyme—An evolutionary aspect of the mechanism of egg envelope digestion. *FEBS J.* **2008**, *275*, 5934–5946. [[CrossRef](#)]
55. Muraina, I.A.; Maret, W.; Bury, N.R.; Hogstrand, C. Hatching gland development and hatching in zebrafish embryos: A role for zinc and its transporters Zip10 and Znt1a. *Biochem. Biophys. Res. Commun.* **2020**, *528*, 698–705. [[CrossRef](#)]
56. Hill, A.J.; Teraoka, H.; Heideman, W.; Peterson, R.E. Zebrafish as a model vertebrate for investigating chemical toxicity. *Toxicol. Sci.* **2005**, *86*, 6–19. [[CrossRef](#)] [[PubMed](#)]
57. McCampbell, K.K.; Wingert, R.A. New tides: Using zebrafish to study renal regeneration. *Transl. Res.* **2014**, *163*, 109–122. [[CrossRef](#)] [[PubMed](#)]
58. Hanke, N.; Staggs, L.; Schroder, P.; Litteral, J.; Fleig, S.; Kaufeld, J.; Pauli, C.; Haller, H.; Schiffer, M. “Zebrafishing” for novel genes relevant to the glomerular filtration barrier. *BioMed Res. Int.* **2013**, *2013*, 658270. [[CrossRef](#)]
59. Morello, J.; Derks, R.J.E.; Lopes, S.S.; Steenvoorden, E.; Monteiro, E.C.; Mayboroda, O.A.; Pereira, S.A. Zebrafish Larvae Are a Suitable Model to Investigate the Metabolic Phenotype of Drug-Induced Renal Tubular Injury. *Front. Pharm.* **2018**, *9*, 1193. [[CrossRef](#)] [[PubMed](#)]
60. Van Wijk, R.C.; Krekels, E.H.J.; Hankemeier, T.; Spaink, H.P.; van der Graaf, P.H. Systems pharmacology of hepatic metabolism in zebrafish larvae. *Drug Discov. Today Dis. Models* **2016**, *22*, 27–34. [[CrossRef](#)]



61. Singleton, V.L. Colorimetry of Total Phenolics with Phosphomolybdic-Phosphotungstic Acid Reagents. *Am. J. Enol. Vitic.* **1965**, *16*, 144–158.
62. Zhishen, J.; Mengcheng, T.; Jianming, W. The determination of flavonoid contents in mulberry and their scavenging effects on superoxide radicals. *Food Chem.* **1999**, *64*, 555–559. [[CrossRef](#)]

**Sample Availability:** Crushed leaves of *A. borbonica* available from the authors.



© 2020 by the authors. Licensee MDPI, Basel, Switzerland. This article is an open access article distributed under the terms and conditions of the Creative Commons Attribution (CC BY) license (<http://creativecommons.org/licenses/by/4.0/>).

### **Chapter 3: Impaired brain homeostasis and neurogenesis in diet-induced overweight zebrafish: a preventive role from *A. borbonica* extract.**

Despite that our previously developed DIO model (page 87), successfully reproduces some aspects of obesity and prediabetic state, and shows an impact on the central nervous system, we raised several critical points. Most DIO models in rodents developed liver steatosis, and increased substantially BBB permeability and neuro-inflammation. Thus, we decided to boost this model by introducing artemia to the overfeeding protocol to (i) increase the calorie intake, (ii) provide diversity of diet and (iii) enrichment for zebrafish. Introducing artemia to the feeding protocol was not possible due to the unavailability of this diet at the beginning of my thesis.

The first part of this article was to design the new DIO model and characterize its impact metabolic impact. The control group was fed once a day with dry food in the morning (15 mg/fish/day) and freshly hatched artemia (6 mg/fish/day) in the afternoon. The DIO group was fed six times a day with dry food (52.5 mg/fish/day) and three times with freshly hatched artemia (30 mg/fish/day) in the afternoon. At the end of the experimental procedure, this protocol appears be stronger than the previous one impacting the DIO zebrafish at different levels. As in the first DIO model, these new overfeeding model leads to a significantly increased body weight, length, BMI and glycemia. In addition, the liver from DIO fish was phenotypically bigger and more yellowish than those from CTRL, suggesting liver lipid accumulation. The Oil Red O staining of the liver confirmed our observation and showed the existence of liver steatosis in DIO zebrafish, a hall mark in DIO models and the prediabetes state.

The newly developed protocol not only led to overweight and dysregulation in lipid and glucose metabolism, but also alters strongly brain homeostasis. Indeed, DIO zebrafish displayed a leaky BBB (disrupted physiology and integrity), neuro-inflammation and cerebral oxidative stress. These modifications consequently are associated to decreased neurogenesis throughout all the brain regions and altered behavioral performance in DIO fish. Therefore, this new developed DIO model exhibits more adverse effects at the peripheral and central levels.

The second part of this article investigated the potential preventive effect of the polyphenol and antioxidant rich extract of *A. borbonica* against the DIO model established. The overnight treatment of overfed zebrafish with aqueous extract of *A. borbonica* (0.5g/L) during 4 weeks parallel to the DIO model, reduces the destructive effects observed on the DIO zebrafish. Despite that DIO fish treated with *A. borbonica* still have significantly higher body

weight and BMI compared to the CTRL, the *A. borbonica* treatment prevented from BBB disruption, cerebral oxidative stress and impaired neurogenesis in most regions of the brain.

In conclusion, this new DIO model using conventional dry food and artemia exhibits a stronger impact at the periphery and in central nervous system. In addition, it enables us to test the preventive effect of *A. borbonica* and demonstrates that the aqueous extract of this plant (0.5g/L) shows preventive effect against brain disruptions induced by the DIO. Further investigations are now needed to better characterize the therapeutic effects of this extract.



OPEN

# Impaired brain homeostasis and neurogenesis in diet-induced overweight zebrafish: a preventive role from *A. borbonica* extract

Batoul Ghaddar<sup>1</sup>, Bryan Veeren<sup>1</sup>, Philippe Rondeau<sup>1</sup>, Matthieu Bringart<sup>1</sup>, Christian Lefebvre d'Hellencourt<sup>1</sup>, Olivier Meilhac<sup>1,2</sup>, Jean-Loup Bascands<sup>1</sup> & Nicolas Diotel<sup>1✉</sup>

Overweight and obesity are worldwide health concerns leading to many physiological disorders. Recent data highlighted their deleterious effects on brain homeostasis and plasticity, but the mechanisms underlying such disruptions are still not well understood. In this study, we developed and characterized a fast and reliable diet-induced overweight (DIO) model in zebrafish, for (1) studying the effects of overfeeding on brain homeostasis and for (2) testing different preventive and/or therapeutic strategies. By overfeeding zebrafish for 4 weeks, we report the disruption of many metabolic parameters reproducing human overweight features including increased body weight, body mass index, fasting blood glucose levels and liver steatosis. Furthermore, DIO fish displayed blood–brain barrier leakage, cerebral oxidative stress, neuroinflammation and decreased neurogenesis. Finally, we investigated the preventive beneficial effects of *A. borbonica*, an endogenous plant from Reunion Island. Overnight treatment with *A. borbonica* aqueous extract during the 4 weeks of overfeeding limited some detrimental central effects of DIO. In conclusion, we established a relevant DIO model in zebrafish demonstrating that overfeeding impairs peripheral and central homeostasis. This work also highlights the preventive protective effects of *A. borbonica* aqueous extracts in DIO, and opens a way to easily screen drugs aiming at limiting overweight and associated neurological disorders.

Obesity and overweight are defined as excessive body weight characterized by body fat accumulation and could be easily estimated by calculating the body mass index (BMI)<sup>1</sup>. Both obesity and overweight are among the main health concerns worldwide. Their prevalence is increasing annually in developing and developed countries and has nearly tripled since 1980s according to the World Health Organization (2019).

Overweight and obesity are due to an imbalance between energy intake, storage, and expenditure including interactions with hereditary and environmental factors<sup>2–4</sup>. They result in numerous metabolic disorders such as dyslipidemia, non-alcoholic fatty liver, hyperglycemia, insulin resistance, and are characterized by chronic inflammation and oxidative stress<sup>5–7</sup>. These pathologies lead to many physiological disorders such as cardiovascular complications as well as the development of type 2 diabetes and contribute to increased morbidities<sup>7,8</sup>.

In addition to impair peripheral metabolism and homeostasis, overweight and obesity could have a negative impact on central nervous system (CNS) homeostasis, leading to cognitive impairments and dementia<sup>9</sup>. Such cognitive defects have been reported in many animal models such as in high fat diet (HFD)- treated rodents displaying hippocampal-dependent cognitive impairments<sup>10,11</sup>. Among factors contributing to these cognitive dysfunctions, inflammatory and oxidative stress appear as key players leading to blood–brain barrier (BBB) leakage through decreased expression of tight junction proteins in the hippocampus<sup>12</sup>. Other studies have also shown that HFD/DIO could impair brain plasticity such as neurogenesis, a process involved in memory<sup>9</sup>. Although some links between obesity and CNS disruptions have been highlighted, the mechanisms whereby it adversely disturbs brain homeostasis remain unclear.

In order to investigate the impact of metabolic disorders on the CNS, zebrafish recently emerged as an interesting model. Firstly, it is a relevant organism for studying overweight/obesity<sup>13–17</sup>, hyperglycemia<sup>18–21</sup> and

<sup>1</sup>INSERM, UMR 1188, Diabète athérombose Thérapies Réunion Océan Indien (DéTROI), Université de La Réunion, Saint-Denis de La Réunion, France. <sup>2</sup>CHU de La Réunion, Saint-Denis, France. ✉email: nicolas.diotel@univ-reunion.fr



diabetes<sup>22,23</sup>. Secondly, in contrast to mammals in which adult neurogenesis is restricted to two main regions, adult zebrafish display an important number of neurogenic niches throughout the brain<sup>24</sup>. Such neurogenic capacities are relied on the maintenance of numerous neural stem cells during adulthood, namely radial glial cells, as well as further committed progenitors allowing to easily study neurogenesis<sup>25–28</sup>.

Given the health threats due to overweight and obesity, it becomes crucial to attempt to reverse these deleterious effects by preventive and/or therapeutic strategies. Many endemic plants from Reunion Island, a biodiversity hot-spot localized in the Mascarene Archipelago, are traditionally used for their anti-inflammatory, anti-oxidant, anti-diabetic and weight-loss properties. From these plants, 22 were recently registered to the French Pharmacopeia<sup>29–32</sup>. However, scientific data demonstrating the real beneficial effects of these plants in vitro and in vivo are lacking. *Antirhea borbonica* (*A. borbonica*) could be envisioned as an interesting candidate according to its reported anti-inflammatory, anti-oxidant and anti-diabetic effects<sup>29,32,33</sup>.

In this work, we aimed at setting up a fast and reliable zebrafish model of overweight (DIO) by overfeeding fish for 4 weeks in order to investigate the impact of overfeeding on (1) peripheral metabolic parameters (i.e. body weight, body mass index, fasting blood glucose, liver steatosis) and on (2) brain homeostasis focusing on the BBB, neuroinflammation and oxidative stress as well as on neurogenesis. Finally, we aimed at investigating the possible beneficial effects of *A. borbonica* aqueous extract administration in preventing peripheral and central impairments induced by DIO.

## Results

**DIO models induces phenotypic and metabolic changes.** In order to set up a fast and reliable DIO model in zebrafish, a 4-week overfeeding treatment was performed by providing dry food and freshly hatched artemia during the day (dry food: 15 mg (CTRL) vs. 52,5 mg (DIO)/fish/day; artemia: 6 mg (CTRL) vs 30 mg (DIO)/fish/day; see Suppl Fig. 1). The effects of such a diet were subsequently investigated for body weight, body length and BMI (Body Mass Index). After the first week of diet, a significant increase in body weight was observed and was maintained until week 4 in DIO fish compared to controls (CTRL) in both male and female groups (Fig. 1A,B). DIO-treated fish were markedly bigger than CTRL at week 4, corresponding to a 144.5% and 240% increase in body weight for males and females, respectively.

In addition, at the end of the experimental procedure, the body length of male and female fish was significantly higher in DIO-treated fish (108% and 122% increase in males and females, respectively) (Fig. 1C,D). The body mass index (BMI) was significantly increased in the DIO fish compared to CTRL (125% and 162% increase in males and females, respectively), suggesting that the gain in body weight is not only due to an increase in body length (Fig. 1E,F). Blood cholesterol and triglycerides levels were also measured and no significant changes were observed between CTRL and DIO fish (data not shown). Taken together, these data indicate that a 4-week overfeeding was sufficient to markedly increase body weight and BMI. Given that egg production could lead to a bias in body weight measurements in female and that sex hormones (i.e. estrogens) are known to impact brain plasticity including neurogenesis in both mammals and fish<sup>34,35</sup>, the next experiments were performed only in males.

Numerous studies have previously shown that obesity and overweight result in metabolic disorders such as dysregulation in glucose and lipid metabolisms including the development of liver steatosis<sup>5</sup>. In the model developed in this study, fasting blood glucose was significantly increased in DIO-treated fish compared to CTRL (Fig. 2A). In addition, the liver from DIO fish was phenotypically bigger and more yellowish than those from CTRL, suggesting liver lipid accumulation (Fig. 2B). Oil Red O staining was consequently performed on liver cryo-sections to test this hypothesis. The liver of DIO fish exhibited an obvious red staining compared to controls (Fig. 2C–F), demonstrating hepatic lipid accumulation in overfed fish. Of note, the intensity of the liver red oil staining was heterogeneous among the DIO fish analyzed (Fig. 2D,F). Together, these data indicate that overfed fish exhibit dysregulations in glucose and hepatic lipid metabolism at week 4.

As a first conclusion, the phenotypic and metabolic data obtained from the DIO model strongly support that the developed protocol efficiently led to overweight and dysregulation in lipid and glucose metabolism.

**DIO induces BBB leakage, neuroinflammation and oxidative stress.** Metabolic disorders such as diabetes and obesity are known to disrupt BBB<sup>36,37</sup>, an important interface corresponding to a highly selective barrier, that separates the blood flow from the fluids in the CNS. BBB disruption induced by obesity results in the leakage of substances into the brain and can consequently disrupt central homeostasis leading to increased brain inflammation and oxidative stress<sup>37</sup>. In the present study, DIO fish displayed an increased body weight and BMI and showed metabolism dysfunctions. Consequently, the impact of overfeeding was next investigated for brain homeostasis focusing on blood–brain barrier (BBB) physiology, neuroinflammation, oxidative stress and neurogenesis. Given the impact of sex steroids on brain homeostasis and peculiarly in zebrafish neurogenesis<sup>38</sup>, we decided to perform the following investigations in males.

To investigate the impact of DIO on the BBB physiology, intraperitoneal injection of Evans Blue was performed, this dye quickly reaching the bloodstream. It results that overfeeding led to BBB leakage as revealed by the blue staining of the DIO brains (Fig. 3A; 5 brains out of 6 were blue) compared to CTRL, that mostly remained white (Fig. 3A; 5 brains out of 6 were white). The effect of overfeeding was next investigated on neuroinflammation by performing qPCR analyses. A consistent trend towards increased *il1 $\beta$* , *il6* and *tnf $\alpha$*  gene expression was observed in the brains of DIO fish compared to those of controls (Fig. 3C–E). Furthermore, the pro-inflammatory *nfkb* transcription factor was slightly but significantly up-regulated (Fig. 3B). The morphology of microglial cells was also studied as a reflect of the cerebral neuroinflammatory state. In homeostatic conditions, microglial cells displayed a ramified morphology, while under activation, they became amoeboid (rounded morphology without ramifications) and exhibit phagocytic properties. By performing L-plastin immunohistochemistry, a switch in microglia morphology was observed (Fig. 3F,G). Microglial cells from DIO-treated fish appear more roundish



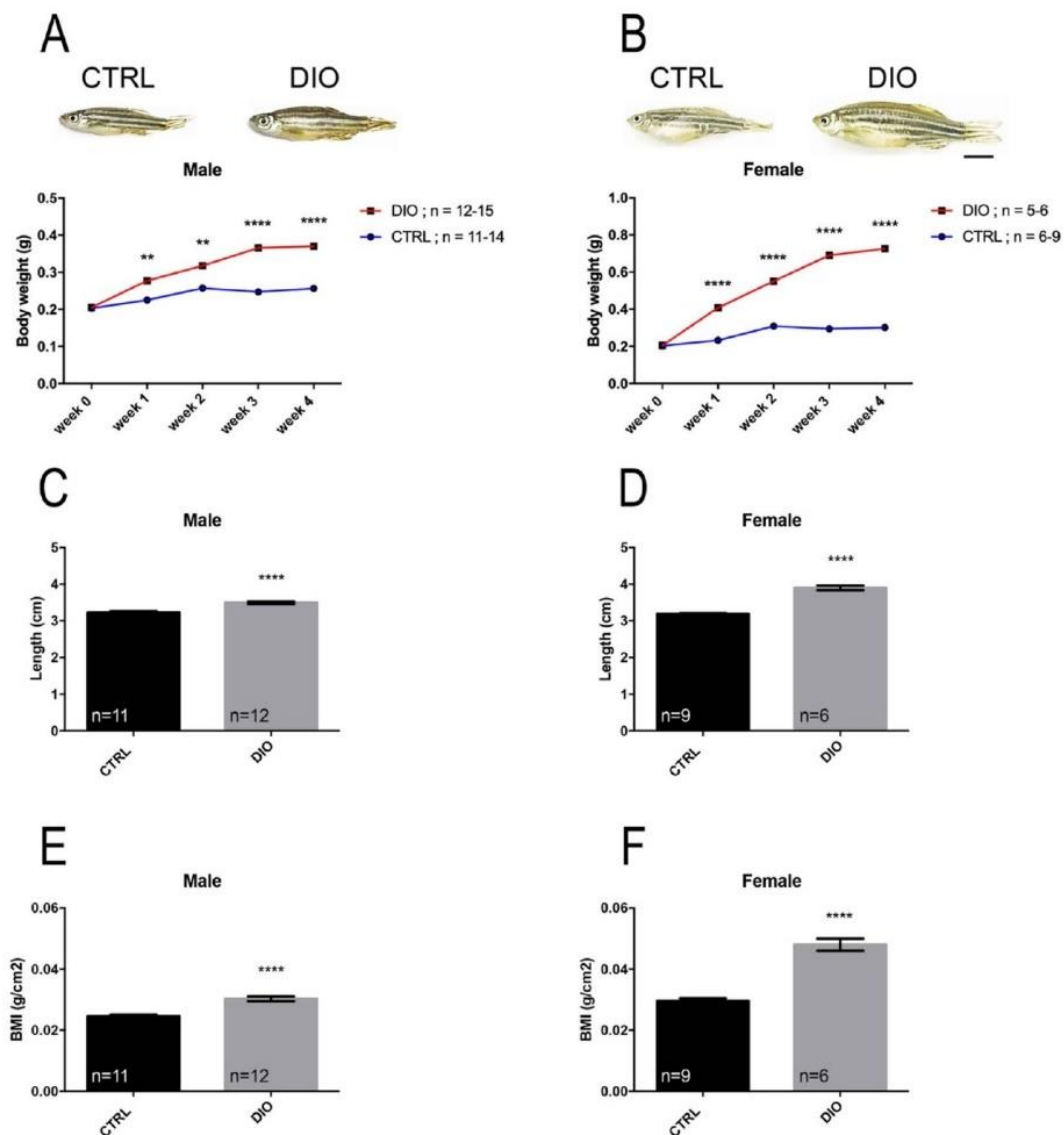


**Figure 1.** DIO results in increased body weight, length and BMI in both male and female zebrafish. (A), (B) Graphs illustrating the body weight measurements during 4 weeks for both CTRL and DIO-treated zebrafish in male and female, respectively. The zebrafish pictures highlight the morphological differences at week 4. (C), (D) Body length measurements at week 4 in male and female zebrafish, respectively. (E), (F) Body mass index (BMI; grams per square centimeter) calculated at week 4. n = number of fish. One-way ANOVA (A, B) and Student's t-test (C–F): \*\*p < 0.01; \*\*\*\*p < 0.0001. Error bars correspond to standard error of the mean (SEM). Scale bar: 7 mm.

and display stronger L-plastin staining along the neurogenic niches compared to controls (Fig. 3G). As shown in Fig. 3F, the number of ramified microglia was lower in DIO fish than in CTRL in the ventral telencephalon (Vv Vd: p-value = 0.0027) and in the anterior part of the hypothalamic region (Hv: p-value = 0.2762). In addition, the number of amoeboid microglial cells was significantly higher in DIO fish compared to controls in both regions (Fig. 3F). Taken together, these qPCR and IHC data demonstrate that DIO promotes neuroinflammation.

The dysregulations in lipid and glucose metabolisms observed in overfed fish could potentially affect redox homeostasis. The enzymatic antioxidant system associated with proteasome participates in the maintenance of this redox homeostasis. Consequently, some antioxidant enzymes activities (catalase, superoxide dismutase and peroxidase) and the chymotrypsin like activity of the proteasome were investigated in brain (Fig. 4). While there is no significant difference between DIO and control fish for SOD activity, a significant enhanced peroxidase activity was measured in brain lysates from DIO fish (+ 25%, p < 0.05 vs. CTRL) and a slight increase in catalase activity was also observed in DIO but failed to reach statistical significance (+ 24%, p = 0.09 vs. CTRL). These enhanced peroxidase and catalase activities could reflect the antioxidant response of the main detoxifying enzymes following a redox status imbalance in fish subjected to an overfeeding. In addition, a significant reduction of the chymotrypsin-like activity of the proteasome was measured in brain from DIO fish (– 48%, p < 0.001 vs. CTRL). This reduced proteasome activity may contribute to the altered redox status in overfed zebrafish

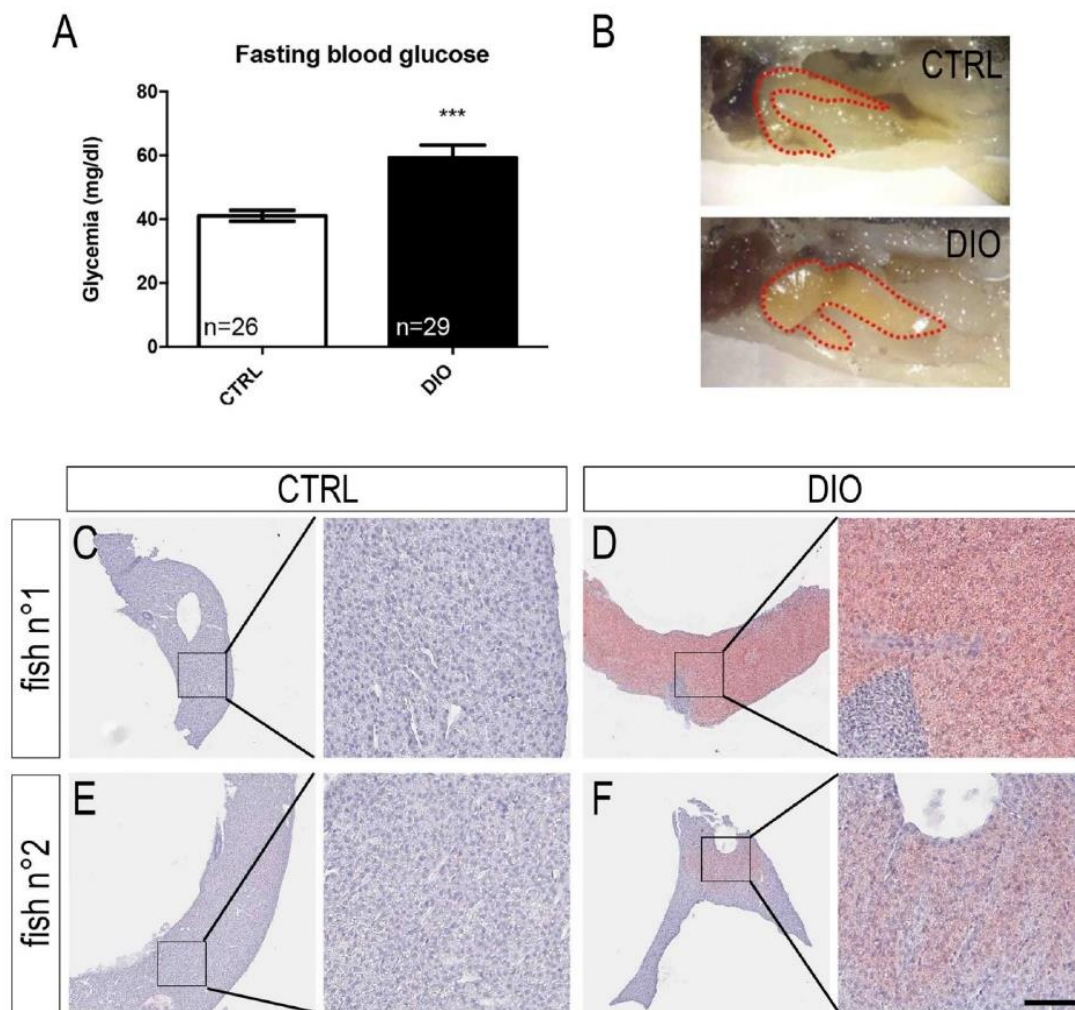


**Figure 2.** DIO leads to increased fasting blood glucose levels and to liver steatosis in zebrafish. **(A)** Fasting blood glucose measurements at week 4 in CTRL and DIO-treated fish. **(B)** Zebrafish liver pictures highlighting the increased size and yellowish color of liver in DIO-treated fish compared to CTRL. **(C), (E)** Liver sections stained with Oil Red O in two control fish showing no lipid accumulation. **(D), (F)** Liver sections stained with Oil Red O in two DIO-treated fish showing different levels of lipid accumulation (red color) and highlighting liver steatosis. Nuclei were stained with hematoxylin **(C–F)**. These pictures are representative of 3 fish studied. n = number of fish. Student's t-test: \*\*\* $p < 0.001$ . Error bars correspond to standard error of the mean (SEM). Scale bar: 1.5 mm **(A)**; 250  $\mu\text{m}$  for lower magnification pictures, 50  $\mu\text{m}$  for higher magnification ones **(C–F)**.

leading to the accumulation of oxidized protein or lipid peroxidation products. In this line, we also demonstrated that the brain of DIO fish displayed stronger levels of 4-hydroxynonenal (4-HNE), a well-established end-product marker of lipid peroxidation (Fig. 8B).

Consequently, it appears that overfeeding disrupts brain homeostasis and promotes BBB leakage, cerebral inflammation and oxidative stress.

**DIO impairs adult neurogenesis and locomotor activity.** BBB disruption and neuroinflammation are well-established to be potential disruptors of adult neurogenesis. Brain cell proliferation in neurogenic niches was consequently studied by performing immunohistochemistry against the proliferative marker PCNA (Proliferating Cell Nuclear Antigen) in key neurogenic regions including the ventral (Vv-Vd) and dorsal (Dm) telencephalon, the anterior part of the preoptic area (Ppa), the periventricular pretecal nucleus (PPv) and two caudal hypothalamic regions (Hv LR and LR PR) (Fig. 5). Overfed fish displayed a general blunted neurogenesis in all the regions studied. Although, it did not reach statistical significance, a consistent trend was observed towards lower proliferation in the dorsomedian telencephalon (Dm SY) and around the lateral (LR) and posterior (PR) recess of the hypothalamic nucleus (Fig. 5A). Furthermore, a significant decrease in proliferative cells was observed along the neurogenic niches from the ventral (Vv) and dorsal (Vd) nuclei of the ventral telencephalic area, the anterior part of the parvocellular preoptic nucleus (PPa), the periventricular pretecal nucleus (PPv), the ventral zone of the periventricular hypothalamus as well as along the lateral recess of the diencephalic nucleus (Hv LR). Importantly, such decreased brain cell proliferation was observed in independent experiments, reinforcing the fact that overfeeding strongly resulted in blunted neurogenesis.



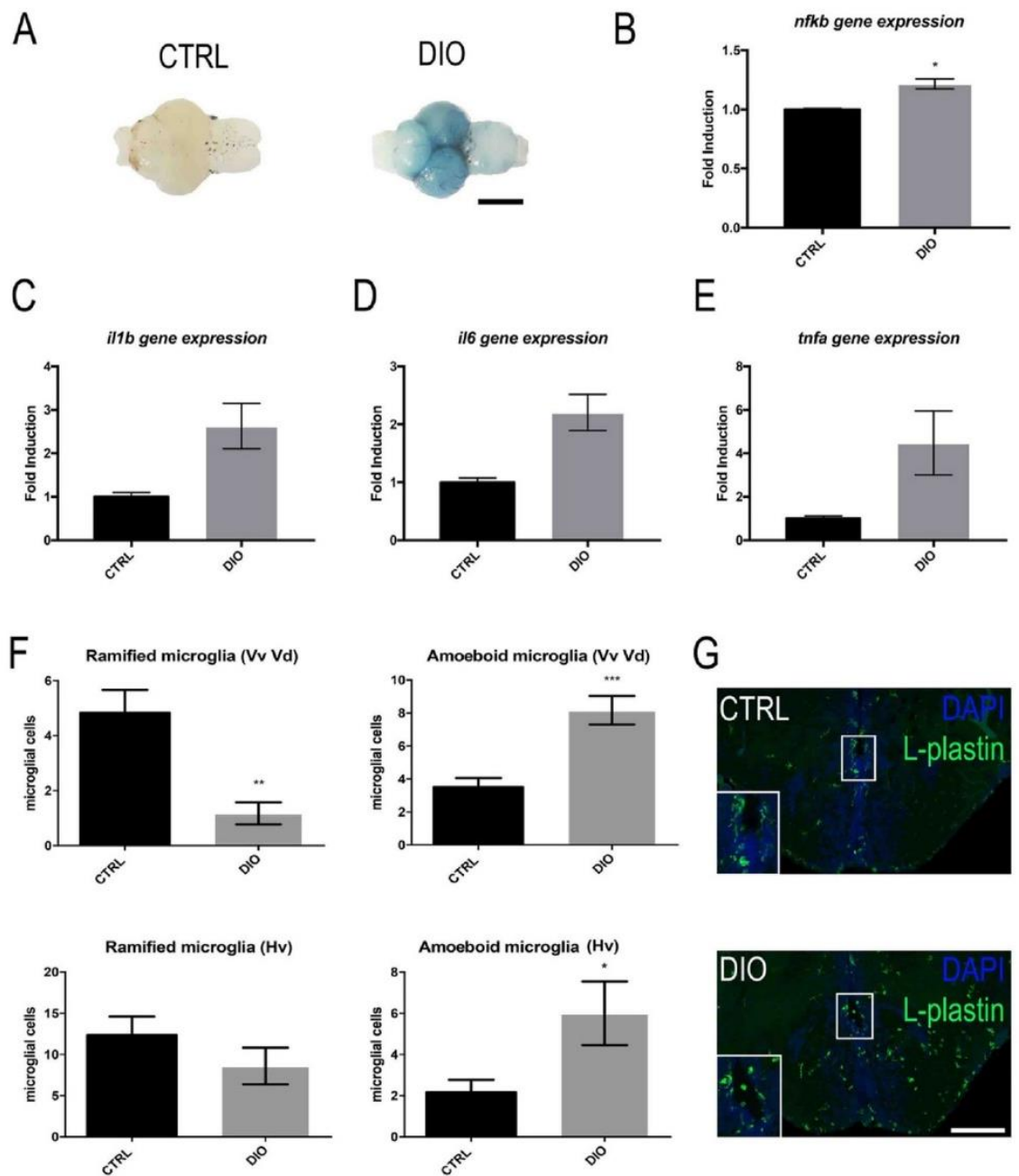


**Figure 3.** DIO increases BBB leakage and neuroinflammation. (A) Dorsal view pictures of the CTRL and DIO zebrafish brains following Evans blue staining. Note the blue staining observed in DIO-treated fish compared to controls ( $n = 6$  brains). (B–E) qPCR gene expression analysis of *nfkb* and pro-inflammatory cytokines (*il1 $\beta$* , *il6* and *tnfa*) in CTRL and DIO fish ( $n = 3$  pools of 2 brains). (F) Counting of ramified and amoeboid microglia in the ventral telencephalon (Vv Vd) and the anterior hypothalamus (Hv) regions in both CTRL and DIO-treated fish. (G) Representative L-plastin immunohistochemistry pictures showing microglia morphology in CTRL and DIO zebrafish brain in the subpallium (Vv Vd). Note the apparent increase in amoeboid-like morphology and the stronger L-plastin staining intensity in DIO fish compared to the control ones.  $n =$  number of fish. Student's t-test: \*  $p < 0.05$ ; \*\*  $p < 0.01$ ; \*\*\*  $p < 0.001$ . Error bar: standard error of the mean (SEM). Scale bar: 0.8 mm (A); 148  $\mu$ m (G).

We next addressed the potential effects of overfeeding on fish behavior and thus monitored the locomotor activity. By recording the locomotion of individual fish during a 10 min period, a significant increase in inactive state was observed in DIO fish compared to their respective controls, while the total distance traveled remained unchanged (Fig. 6). These data reveal the existence of different locomotion patterns between CTRL and DIO fish.

**A. borbonica** herbal tea treatment prevents from deleterious effects induced by DIO. Overfed zebrafish appear as an appropriate model to test the effects of some compounds on weight gain and its

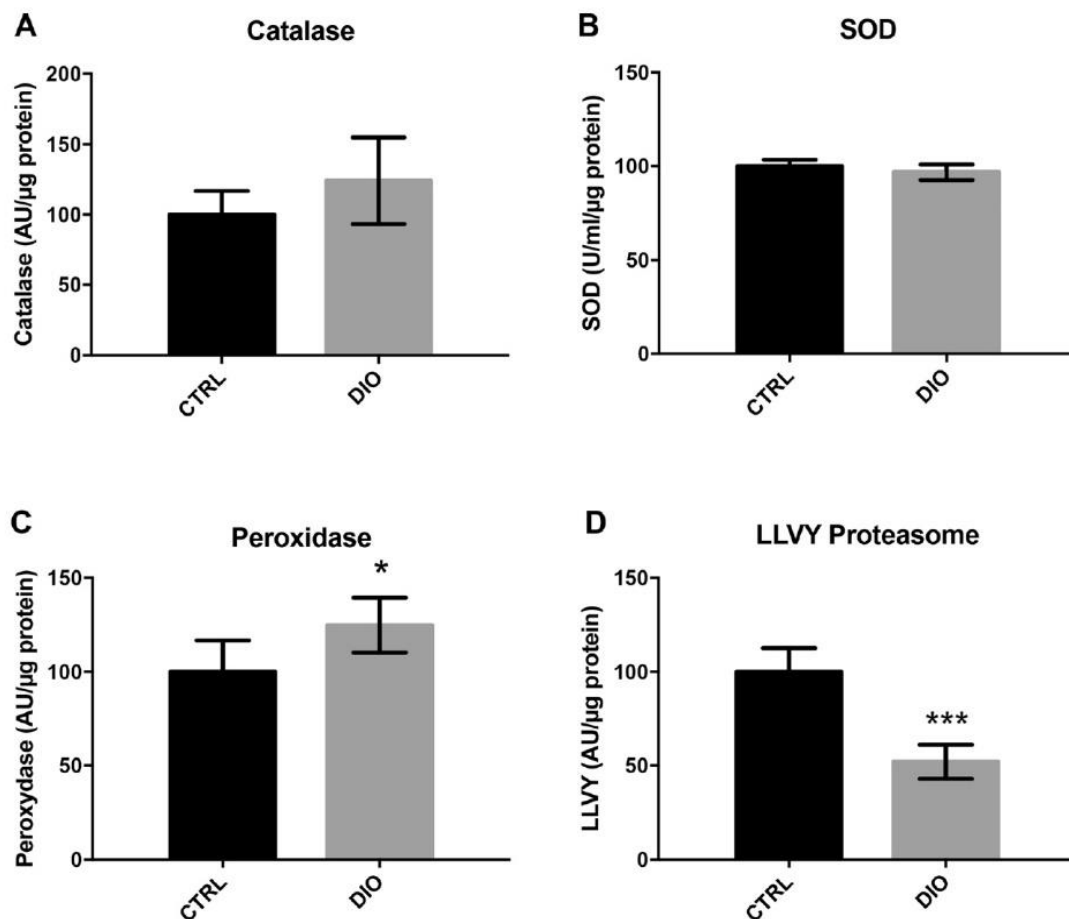


**Figure 4.** DIO disrupts antioxidant enzymes and proteasome activity in the brain of adult zebrafish. (A–D) Cerebral catalase, total superoxide dismutase (SOD), peroxidase and LLVY proteasome activities performed in lysates of adult zebrafish brain.  $n = 7$  from two independent experiments. Student's  $t$ -test: \* $p < 0.05$  \*\*\* $p < 0.001$ . Error bar: standard error of the mean (SEM).

complications<sup>15,39,40</sup>. *A. borbonica* was selected as an interesting candidate given its potential or demonstrated anti-oxidant, anti-inflammatory, and anti-diabetic according to its traditional use and to in vitro studies<sup>29,32,33</sup>.

First, the total phenolic acids content of the *A. borbonica* mother infusion (4 g/L), evaluated by using Folin-Ciocalteu assay, showed a concentration of  $17.2 \pm 0.9$  mg GAE/g of plant dry powder. By using an aluminium chloride colorimetric method, the total flavonoids content determined was of  $8.9 \pm 0.5$  mg EE/g of plant dry powder, twice less compared to phenolic acids content (Suppl. Figure 2). These results confirmed that *A. Borbonica* extract contains a substantial significant level of polyphenols and antioxidant properties as other medicinal plants as *Rosmarinus officinalis L* ( $16.67 \pm 0.40$  mg GAE/g)<sup>41</sup>. Then, a high-resolution mass spectrometry (HR-MS) analysis showed that a 4 g/L *A. Borbonica* infusion contained a variety of polyphenols including phenolic acids such as caffeic acid, caffeoylquinic acid, dicaffeoylquinic acid and some flavonoids such as Kaempferol hexoside and quercetin hexoside (Suppl. Figure 3). Caffeic acid derivatives including caffeoylquinic acid and dicaffeoylquinic acid were the most concentrated polyphenols identified in *A. Borbonica* infusion, at  $1,278 \pm 75$  ng/mL and  $531 \pm 83$  ng/mL, respectively.

Next, to study the effects of *A. Borbonica* on weight gain and its consequences, DIO fish were treated overnight (6 pm to 8 am; 5 days a week) with water containing *A. borbonica* infusion (final concentration: 0.5 g/L water) during the 4-week period. We confirmed that overfed fish without plant extract displayed a significant increase in body weight from week 1 to week 4 compared to controls (Fig. 7A). Interestingly, DIO + *A. borbonica* did not result in any significant change in body weight during the first two weeks, compared to the DIO, but significantly exhibited a decrease in body weight gain during the third and fourth week compared to the DIO fish (Fig. 7A). At week 4 (Fig. 7B) DIO and DIO + *A. borbonica* fish displayed a significant BMI increase compared to CTRL but no significant difference was observed between DIO groups. The size of DIO and DIO + *A. borbonica* fish was also significantly higher compared to controls, but not significant differences were observed between the groups (data not shown). As well, *A. Borbonica* did not exhibit striking preventive effects on lipid deposits in the liver (data not shown) and did not strikingly prevent from increased fasting blood glucose levels induced by DIO (DIO vs CTRL: +144.4%, DIO + *A. borbonica* vs CTRL: +129%;  $n = 19$ –22, data not shown).

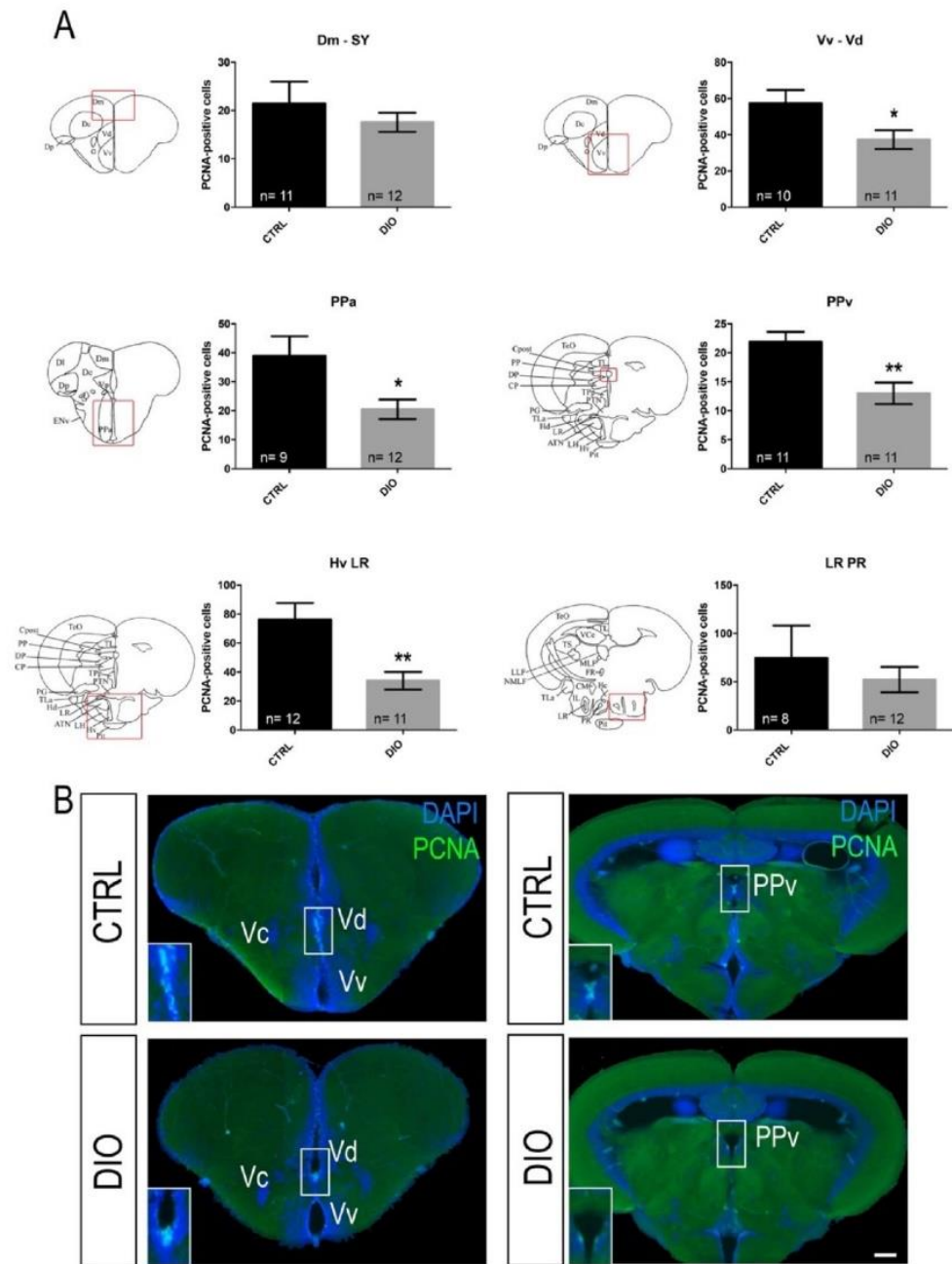


**Figure 5.** DIO impairs neurogenesis in the forebrain of adult zebrafish. **(A)** Statistical analysis of the number of proliferative cell (PCNA-positive) in CTRL and DIO-treated zebrafish. The respective brain schemes correspond to the transversal sections of the zebrafish brain for each studied region showing the main brain domains/nuclei according to the Zebrafish Brain Atlas from Wullimann et al. and were adapted from Menuet et al.<sup>84,85</sup>. A significant decrease in proliferative activity was observed between CTRL and DIO zebrafish in the Vv Vd, PPa, PPv and Hv LR neurogenic regions. **(B)** Representative digital pictures of PCNA immunohistochemistry (green) and cell nuclei counterstaining (DAPI in blue) on cryostat brain sections of CTRL (up) and DIO-treated fish (down). n = number of brains studied pooled from two independent experiments. Student's t-test: \*p < 0.05 \*\*p < 0.01. Error bar: standard error of the mean (SEM). Scale bar = 32  $\mu$ m. Vv: ventral nucleus of ventral telencephalic area; Vd: dorsal nucleus of ventral telencephalic area; Dm: medial zone of dorsal telencephalic area; PPa: parvocellular preoptic nucleus, anterior part; PPv: periventricular pretecal nucleus; Hv: ventral zone of periventricular hypothalamus; LR: lateral recess of diencephalic nucleus; PR: posterior recess of diencephalic ventricle.



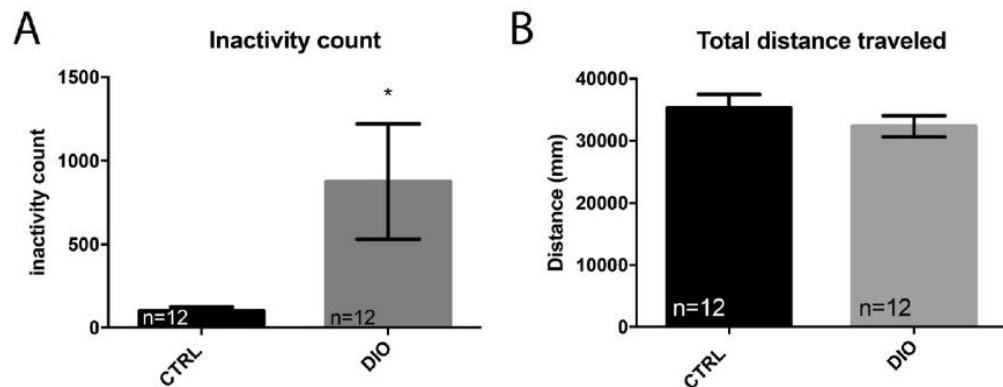


**Figure 6.** DIO increases the occurrence of inactivity in zebrafish. (A) graph showing the increased number of inactivity state (locomotion < 4 mm/sec) in DIO fish compared to controls, normalized to 100%. (B) graph showing that the total distance traveled during 10 min is similar between CTRL and DIO fish. n = 12 from 3 independent experiments. Student's t-test: \*p < 0.05. Error bar: standard error of the mean (SEM).

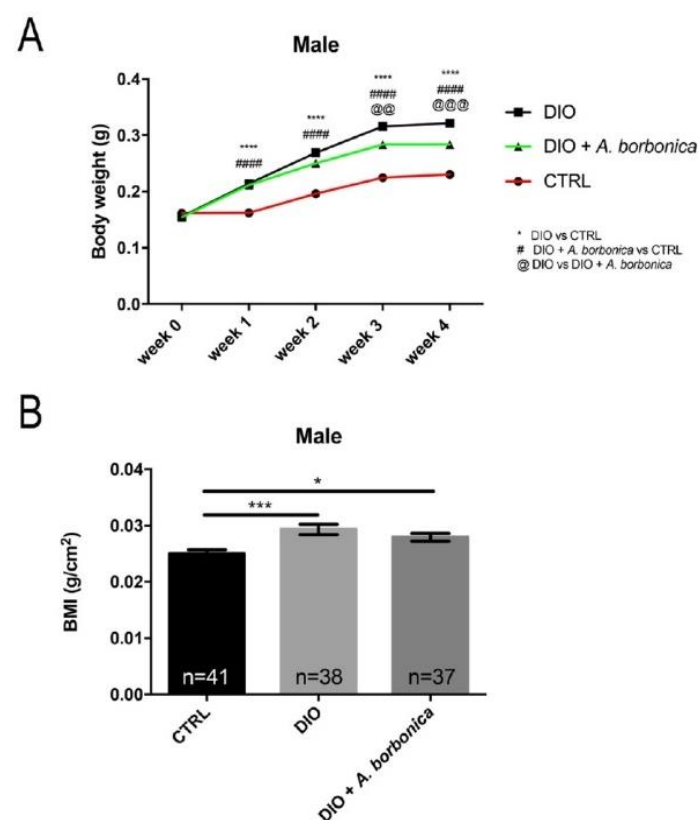


**Figure 7.** *A. borbonica* aqueous extracts slightly prevents from body weight gain and excessive BMI increase induced by DIO. (A) Line graph showing the increase in body weight of CTRL, DIO and DIO + *A. borbonica* during 4 weeks. (B) Graph showing the BMI of all groups at week 4. n = number of fish. One-way ANOVA (A) and Student's t-test (B): \*p < 0.05 \*\*\*p < 0.001. Bar graph: standard error of the mean (SEM).

***A. borbonica* aqueous extracts prevent BBB leakage and oxidative stress but has mitigated effects on neuroinflammation and neurogenesis.** Given the anti-oxidant properties of *A. borbonica* infusion, its effect on the central disruptions (BBB leakage, oxidative stress and neurogenesis) induced by DIO was investigated. We confirmed that DIO resulted in BBB leakage and we showed that *A. Borbonica* extracts limited BBB disruption (Fig. 8A). Cerebral oxidative stress was next investigated by performing dot-blot against 4-hydroxynonenal (4-HNE), a well-established marker of oxidative stress. 4-HNE levels were increased in the brain of DIO-treated fish (Fig. 8B), and remained at basal levels in DIO + *A. Borbonica* treated fish showing that *A. borbonica* prevented the increase in oxidative stress induced by DIO (Fig. 8B). However, neuroinflammation

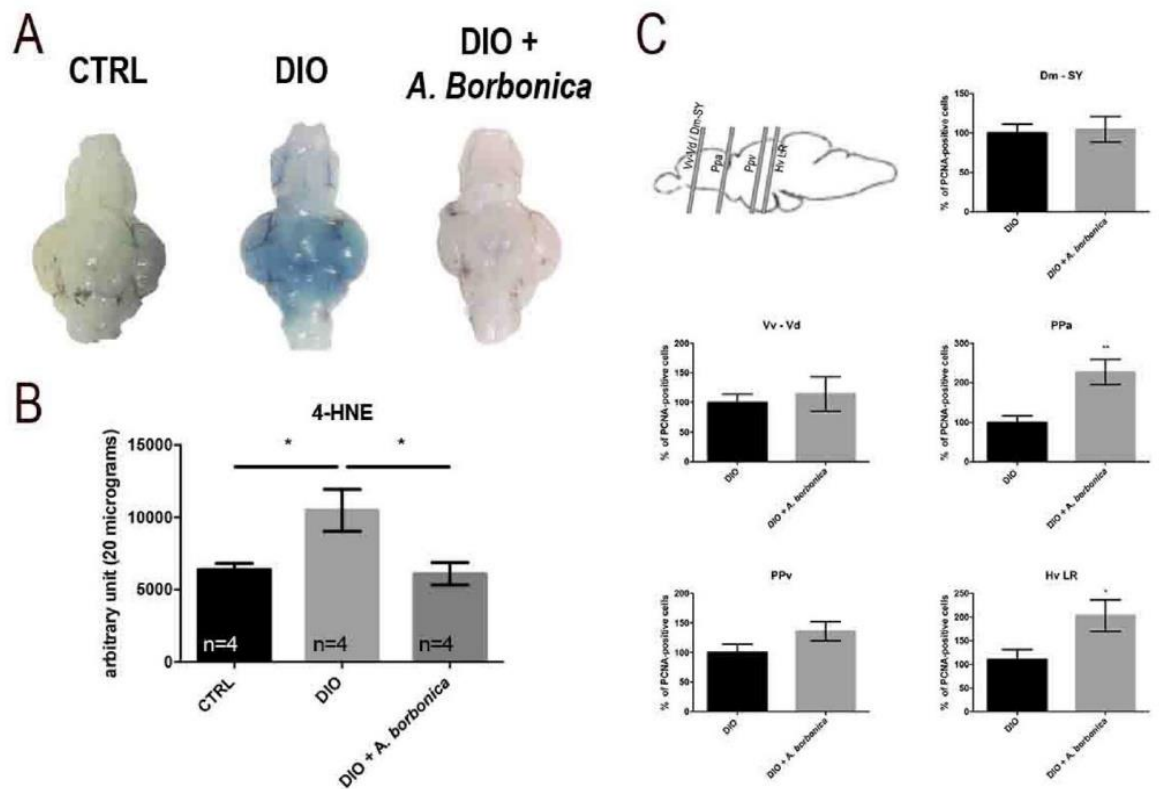


**Figure 8.** *A. borbonica* aqueous extracts treatment prevents from BBB leakage, brain oxidative stress and partially protects from the decreased neurogenesis induced by DIO. (A) Dorsal views of zebrafish brains after Evans Blue dye injection in CTRL, DIO, and DIO + *A. borbonica* treated fish. Zebrafish brains remain mostly white except for the DIO brains. (B) Dot blot quantification showing that the *A. borbonica* treatment in DIO fish prevents the cerebral increase in 4-HNE levels induced by overfeeding. n = number of brain fish studied. One-way ANOVA: \*p < 0.05. Bar graph: standard error of the mean (SEM). (C) Statistical analysis of the number of proliferative cell (PCNA-positive) in DIO and DIO + *A. borbonica* treated zebrafish normalized to 100%. The sagittal brain scheme shows the corresponding section through the Dm-SY/Vv-Vd, the PPa, the PPv and the Hv LR. A weak significant increase in proliferative activity was observed between DIO and DIO + *A. borbonica* in the preoptic area (PPa) and the hypothalamic region (Hv LR). n = 8–11 fish. Student's t-test: \*p < 0.05 \*\*p < 0.01. Bar graph: standard error of the mean (SEM).

in the brain of DIO + *A. Borbonica* appeared mitigated. Indeed, some pro-inflammatory cytokines were slightly decreased (i.e. *tnfa* fold induction is 1,36 vs. 4,47; data not shown) and microglial cells tended to be less amoeboid in the ventral telencephalon (Vv Vd) than in DIO fish, but remained activated in the hypothalamus (Hv), suggesting the persistence of a local neuroinflammatory state (data not shown).

Finally, the potential effect of *A. Borbonica* on impaired neurogenesis induced by overfeeding was also studied. It did not induce any striking change in brain cell proliferation in the neurogenic niches, except in the preoptic area and the caudal hypothalamus (Hv LR) for which proliferation was slightly up-regulated and was maintained at basal level (Fig. 8C). It suggests that *A. Borbonica* aqueous extract could partially rescue the impaired neurogenesis induced by overfeeding in a regional dependent manner.

## Discussion

We developed a reliable overfeeding zebrafish model resulting in many metabolic disorders including increased body weight, BMI and fasting blood glucose levels as well as the development of liver steatosis (Figs. 1, 2). Such increase in body weight and BMI appears more pronounced in female than male, probably in links with oogenesis and egg storage. In zebrafish, several DIO and/or HFD models have been proposed and lead to similar metabolic impairments as observed in our study, reinforcing the data obtained in this work<sup>13–17,42,43</sup>. The higher body weight and BMI observed in overfed fish should reflect the development of adipose tissue, as overfeeding protocols using artemia have been previously shown to promote subcutaneous and/or visceral adipocyte expansion in zebrafish<sup>14,15,17</sup>. In our work, we decided to use a mix of dry food and artemia in order to provide a diversity in the feeding as well as enrichment for zebrafish.

We also showed that DIO fish display heterogeneous levels of liver steatosis. This pathological process was also previously observed in fish by Nakayama et al.<sup>43</sup> in a 6-week DIO model using artemia. In contrast, Landgraf et al.<sup>42</sup> observed hepatic steatosis only in fish overfed with both artemia and egg powder, but not with artemia alone, and this even after 8 weeks of treatment. Such differences could be explained by the quantity of food



supplied to the overfed fish between these respective different protocols, and put our model as an intermediate one concerning liver steatosis.

Interestingly, overweight and obesity are known to be associated with insulin resistance and increased glycemia<sup>44</sup>. Lipid steatosis is also associated with fasting hyperglycemia and type 2 diabetes<sup>45,46</sup>. In our work, fasting blood glucose levels of DIO-treated fish were significantly higher than in controls (Fig. 2; ~40 mg/dl in CTRL vs ~60 mg/dl in DIO). Such an increase was previously obtained in fish overfed with artemia (without liver steatosis) but did not reach significant levels, while fish overfed with artemia and egg powder (with liver steatosis) exhibited a significant hyperglycemia<sup>42</sup>. Among the possible explanations for such differences, we could argue (1) for the power of the statistical analysis (26–29 fish/group in our study versus 10 for Landgraf et al.), (2) that the food quantity supplied in our study is higher than those from Landgraf's one (137% increase in feeding), and (3) last but not least, it is tempting to speculate that the degree of liver steatosis could be correlated with hyperglycemia levels in accordance with the literature<sup>47</sup>, as it is known to promote chronic inflammation and insulin-resistance.

Taken together, these data highlight that the model developed in this study is relevant to other overfeeding models in the field. In addition, our data demonstrate that overfed zebrafish share common features with overweight/obese pathologies in human<sup>1</sup>. It consequently reinforces its use for studying the deleterious impact of overweight on several physiological processes such as brain homeostasis and plasticity.

Numerous works have shown that overweight and obesity were associated with cognitive impairments and that adult neurogenesis is involved in memory<sup>11,48–50</sup>, raising the question of the effects of DIO on brain homeostasis. In this context, the integrity of the blood–brain barrier and brain plasticity (i.e. neurogenesis) are two key parameters to investigate as they are linked to cognitive impairments. In our work, we report an increased BBB leakage, neuroinflammation and oxidative stress in the brain of overweight fish compared to controls (Figs. 3, 4, 8). These results are of peculiar interest given that oxidative stress and inflammation are known to promote BBB disruption<sup>51,52</sup>. The neuroinflammatory state observed in the brain of overfed fish through the up-regulation of pro-inflammatory cytokines and *nfkB* gene expression was reinforced by the switch from ramified to amoeboid microglia (Fig. 3). In a similar way, the impact of a high-glucose/high-cholesterol diet in zebrafish was recently associated with the increase in pro-inflammatory cytokines and *cd11b* gene expression, a microglial marker<sup>53</sup>, reinforcing the results obtained in our work. As well, these results should be also paralleled with the mammalian situation for which overweight and/or high fat diets in rodents induce neuroinflammation and microglial reactivity, mainly in the hypothalamus<sup>54–56</sup>.

Interestingly, in our experimental conditions, DIO fish display an increase in cerebral oxidative stress (Figs. 4, 8; increased 4-HNE levels and higher catalase and peroxidase activity), with a reduced proteasome activity that could contribute to impair redox balance in overfed fish and could result in increased oxidized protein or lipid peroxidation product accumulation. Indeed, oxidized proteins that are not degraded by the altered proteasome system may also contribute to the enhanced reactive oxygen species generation in DIO zebrafish tissues. For instance, increased 4-HNE accumulation observed in the brain of DIO fish may induce adduct formation in proteasome subunit leading to the inhibition of proteolytic activity. Very interestingly, it has been previously shown that oxidative stress homeostasis could affect the differentiation and proliferation of progenitor cells<sup>57,58</sup>, bringing evidence that redox imbalance, and generation of 4-HNE levels in the brain, could affect the behavior of the neural progenitor/stem cells.

Indeed, we demonstrated from independent experiments that DIO fish display a consistent and significant decrease in brain cell proliferation in most neurogenic niches including the ventral telencephalon, the preoptic area, the hypothalamus and the periventricular region of the pretectal nucleus (Fig. 5). It fits with another model of high caloric consumption in zebrafish resulting in decreased cerebellar proliferation<sup>59</sup>. In addition, in mammals, genetic and/or diet models of overweight/obesity were shown to result in decreased neural stem cell proliferation and subsequently to a lower number of newborn neurons generated<sup>54,60–63</sup>. Such a decreased neurogenesis was also observed in other metabolic disorders including hyperglycemia in both rodents and fish<sup>18,64</sup>. Further investigations would be required for determining the impact of overfeeding in newborn cell migration, differentiation and survival in both constitutive and regenerative conditions in zebrafish. As well, the identification of the misregulated extrinsic and intrinsic factors responsible for blunted neurogenesis should be further investigated, considering for example the Delta-Notch signaling pathway known for controlling NSC activity. In addition, in the offspring of mice that have followed a HFD, NSC upregulates Notch receptors and its downstream effector Hes, promoting NSC quiescence and limiting neurogenesis<sup>65</sup>. Also, given the links between neurogenesis and cognitive functions<sup>50</sup>, it is important to mention that a HFD zebrafish model was shown to display impaired cognitive functions as revealed by active avoidance test and by the disturbed expression of numerous genes involved in neuronal activity, anti-oxidative stress, and BBB functions<sup>66</sup>.

Consequently, we demonstrated for the first time in a same zebrafish model that overfeeding induces many detrimental effects on brain homeostasis as shown by BBB leakage, neuroinflammation, enhanced oxidative stress and impaired neurogenesis. These results also raised the question of the chicken or the egg between the first factors (inflammation? oxidative stress?) disrupting brain homeostasis and would allow to further investigate the mechanisms by which metabolic disorders disturb neurogenic activity and behavior.

*A. borbonica* herbal tea has been traditionally used as a natural remedy for its potential anti-inflammatory, anti-oxidant and anti-diabetic properties<sup>29–33</sup>. For this reason, we decided to work on aqueous extract. The subsequent HR-MS analysis allowed us to confirm previously published data demonstrating that *A. Borbonica* extracts contain high phenolic and flavonoid contents associated with antioxidant properties<sup>29,33</sup>. HR-MS and Folin-Ciocalteu assay analyses revealed that *A. Borbonica* infusion contains major phenolic acids including caffeic acids derivatives (dicafeoylquinic acid and chlorogenic acid) and some glycosylated flavonoids (kaempferol hexosides and quercetin hexosides). In HFD mice, dicafeoylquinic acids (150 mg/kg of body weight) improve metabolic parameters (i.e. liver and adipose tissue masses, decreased inflammatory factors, better hepatic lipid



synthesis and degradation)<sup>67</sup>. A study of Jung et al.<sup>68</sup> also showed the interesting effect of quercetin by regulating genes involved in lipid metabolism. As well, intraperitoneal injection of chlorogenic acid (100 mg/kg of body weight) was shown to ameliorate HFD-induced liver steatosis, insulin resistance and adipocyte hypertrophy in mice<sup>69</sup>. In addition, caffeic acids including dicaffeoylquinic acid and chlorogenic acid have been shown to exert antioxidant properties especially in the brain<sup>70–72</sup>. Although *A. borbonica* did not prevent from liver steatosis in our experimental conditions, and did not significantly decrease fasting blood glucose levels, a decreasing trend was observed (DIO vs CTRL: +144.4% increase in fasting glycemia while DIO + *A. borbonica* vs CTRL: +129% increase in fasting glycemia). Importantly, *A. borbonica* treatment significantly limited weight gain from week 3 to week 4 compared to DIO, without modulating feeding behavior (data not shown). This result is of peculiar interest given that the BMI of DIO + *A. borbonica* fish is higher than CTRL, but this increase is less significant than the one of DIO vs. CTRL (Fig. 7), while the size of DIO and DIO + *A. borbonica* remain unchanged (data not shown: 33.46 mm for DIO vs 33.04 mm for DIO + *A. borbonica*). This result have to be paralleled with those in HFD mice for which treatment with chlorogenic acid and dicaffeoylquinic acid avoid or limited gain weight<sup>67,69</sup>. The effects observed in our study are probably less spectacular given the low concentrations of these polyphenols.

In addition, DIO + *A. Borbonica* fish are protected from BBB leakage and brain oxidative stress induced by DIO (Figs. 7, 8). These preventive effects could be attributed *A. Borbonica* anti-oxidant activity supported by its polyphenol content (phenolic acids, flavonoids and tannins) and are consistent with in vitro studies showing its anti-oxidant properties<sup>29,33</sup>. Interestingly, in almost all the neurogenic niches studied, DIO fish treated with *A. borbonica* still display blunted neurogenesis that nevertheless appeared less severe in the preoptic area and the hypothalamus. Consequently, *A. borbonica* did not fully prevent from neurogenic defects induced by DIO, showing that other mechanisms than BBB leakage and oxidative stress should be involved in such neurogenic impairments. It would be also interesting to determine the *A. borbonica* metabolites found within the brain fish in order to elucidate which compounds could be responsible for the central protective effects.

## Conclusion

To conclude, we have developed an overfeeding model in zebrafish that mimics the mammalian overweight state in the periphery and also in the central nervous system. To our knowledge, this is the first report showing the deleterious impact of DIO on brain homeostasis and especially considering the forebrain neurogenesis in zebrafish.

*A. borbonica* aqueous extract (mimicking herbal tea consumption) was shown to limit significantly weight gain in overfed zebrafish. The DIO protocol developed in this work could serve as a new physiological screening tool for identifying “anti-overweight” and “anti-obesity” drugs. It will allow the discovery of new preventive and therapeutic treatments against weight gain and associated central deleterious effects such as BBB leakage, neuroinflammation, oxidative stress and impaired neurogenesis. Although *A. borbonica* aqueous extract has only a limited effect on body weight and associated BMI, it prevents BBB leakage, cerebral oxidative stress and partly improve neurogenesis. Thus, natural compounds have a limited effect on the body weight but could prevent some central disorders induced by overfeeding.

## Material and methods

**Animals and ethics.** Three to four month-old adult wildtype male and female zebrafish (*Danio rerio*) were obtained from our zebrafish facility and were maintained under standard conditions of temperature (28.5 °C), photoperiod (14 h dark/10 h light), pH (7.4) and conductivity (400 µS). The gender of the animal was performed visually according to sexual dimorphisms (males are thinner and females have a bigger belly). All experiments were conducted in accordance with the French and European Community Guidelines for the Use of Animals in Research (86/609/EEC and 2010/63/EU) and approved by the local Ethics Committee for animal experimentation of CYROI and the French Government (APAFIS\_20191105105351\_v10).

**Diet-induced overweight/obesity (DIO) protocol.** Adult zebrafish (3–4 months) were divided into 2 or 3 groups (control and DIO or CTRL, DIO, DIO + *A. borbonica*) at the same density between each group (10 to 20 fish maximum per 3.5 L tank, according to the experiment); males and females being mixed in each tank. The control group was fed once a day with dry food in the morning (15 mg/fish/day, GEMMA 300, Planktovie) and freshly hatched artemia (6 mg/fish/day, Artemia cysts; REF: B052-P) in the afternoon. The DIO and DIO + *A. Borbonica* group was fed six times a day with dry food (52.5 mg/fish/day) and three times with freshly hatched artemia (30 mg/fish/day) in the afternoon. These treatments were performed on a four-week period (see Suppl Fig. 1).

***A. Borbonica* herbal tea treatments.** Leaves of *A. borbonica* (Bois d’osto; Saint-Joseph de La Réunion; REF: BOSJDTC171218AA) were obtained from the Cooperative des Huilles Essentielles de Bourbon (CAHEB). Leaves were crushed and stored at –20 °C. Infusions were prepared every day by mixing 1 g of crushed plants with 250 mL of boiled fish water for 10 min. After filtering, the 250 mL of *A. borbonica* infusion were added to 1,750 mL of fish water to reach a final volume of 2L and a final *A. borbonica* concentration of 0.5 g/L. The DIO fish treated with *A. borbonica* were fed as the DIO fish during the day from 8 AM to 6 PM and treated with the plants from 6 PM to 8 AM (5 days a week). During the infusion treatment, all the groups (CTRL, DIO, DIO + *A. borbonica*) were maintained out of the system.

**Body weight, body mass index (BMI) and fasting blood glucose measurements.** Fish of each group were weighted every week. They were captured using a net, quickly dried on a tissue paper, briefly weighed and immediately placed back into water. This procedure is usually done in less than 20 s. In addition, the body length of the fish was measured at the beginning (first day, during the weighing process) and at the end of the



experiment (week 4, after euthanasia—see below-) from the tip of the mouth to the end of the tail (total length). The body mass index (BMI) was calculated by dividing the body weight (g) with the square of the length (cm<sup>2</sup>).

For blood glucose measurements, fish were fasted the day before and euthanized using ice water (2–4 °C) in order to avoid blood glucose fluctuations due to tricaine use<sup>73</sup>. Fish were gently dried with a tissue and one eye was removed allowing the ocular cavity to fill with blood. The glycemia (mg/dl) was measured using a glucometer (One-Touch Ultra, LifeScan, France), as previously described<sup>19</sup>.

**Blood collection for metabolic analyses.** The fish were first euthanized with tricaine, then one eye was removed and the blood was collected using a pipet that was previously equilibrated by 1X PBS and EDTA (1 mL of 1X PBS is added in EDTA blood tube and vortexed). The blood of 5 fish was pooled (around 10 µL) in one Eppendorf with 40 µL of 1X PBS 1 × EDTA to avoid its clotting. After that, the blood samples are centrifuged and the plasma was collected frozen at – 80 °C.

**Cholesterol and triglyceride measurements.** The blood of 5 fish (around 10 µL) was collected and pooled in one tube containing 40 µL of 1X PBS EDTA. 20 µL of plasma in the tube is diluted to the half with 1X PBS EDTA. 1 µL of diluted plasma is plotted in 96 well plate and cholesterol measurements were performed using the kit of Cholesterol FS according to manufacturer's recommendation (DiaSys Diagnostic Systems—CODE CQN: KS from DiaSys). For triglyceride measurement, Triglyceride FS kit was used (DiaSys Diagnostic Systems—CODE CQN: KS from DiaSys). The absorbance at 500 nm was then measured using TECAN SUNRISE and cholesterol and triglyceride concentrations were determined.

**Tissue preparation.** At the end of the experimental period, fish were euthanized before being fixed in 4% PFA (Paraformaldehyde) dissolved in 1X Phosphate Buffer Saline (PBS).

For cryostat sections, the brain and the liver were dissected and cryopreserved by an overnight incubation in 1X PBS, containing 30% sucrose. Then, they were embedded in OCT matrix and cut using a cryostat at 12 µm thickness.

For qPCR or protein analyses, the tissues of interest were immediately dissected, snap-frozen and kept at – 80 °C.

**Immunostaining.** For immunohistochemistry experiments, cryostat sections were rehydrated twice with 1X PBS containing 0.2% Triton (PBS-T). Antigen retrieval was performed using sodium citrate (pH 6) heated at 80 °C for 15 min. Sections were washed twice in PBS-T before being blocked in PBS-T containing 2% BSA. Next, sections were incubated with the following primary antibodies: rabbit anti zebrafish L-plastin (kindly provided by Dr Michael Redd<sup>74</sup>) and/or mouse anti-PCNA (1:100; clone PC10, Dako; RRID: M0879) overnight at room temperature. The slides were then washed twice in PBS-T and incubated with DAPI (4',6'-diamidino-2-phenylindole) and secondary antibodies: donkey anti-rabbit Alexa Fluor 488 for L-plastin (1:300; REF: A21206; Life Technologies, Bethesda, MD; RRID: AB\_10049650) and goat anti-mouse Alexa Fluor 594 or 488 for PCNA (1:300; REF: A11005 for Alexa 594 and A28175 for Alexa 488; Life Technologies; RRID: AB\_141372 and AB\_2536161) for 1h30 at room temperature. Sections were rinsed and the slides were mounted with anti-fading medium (IMM Ibi; REF: 50001). Note that PCNA antibody allows the detection of proliferative cells along the neurogenic niches as previously described<sup>75</sup>, and L-Plastin antibody the detection of microglial cells, displaying ramified processes when quiescent, or amoeboid morphology when activated (phagocytic functions)<sup>76</sup>.

**Oil Red O staining.** Frozen liver sections were dried, rehydrated and rinsed with 60% isopropanol before being stained for 40 min with the freshly prepared Oil Red O (Sigma-Aldrich; REF: 00625) according to standard protocol. Nuclei counterstaining was performed by incubating the sections for 30 s with Mayer's hematoxylin. Finally, the sections were dehydrated and mounted with mounting medium (IMM Ibi; REF: 50001).

**Investigation of BBB permeability (Evans Blue dye injection).** For investigating BBB physiology, Evans Blue dye was used as a tracer to monitor BBB permeability<sup>77</sup>. Briefly, fish were anesthetized with 0.02% tricaine and intraperitoneally injected with freshly prepared 1% Evans Blue dye diluted in 1X PBS (10 µL of 1% Evans Blue for 0.1 g of zebrafish body weight). Fish were allowed to recover for 10 min before being sacrificed. Then, fish heads were fixed with 4% PFA-PBS. After, the brains were dissected and imaged.

**Protein extraction and dot blot.** Zebrafish brain were lysed with Tris HCL buffer (50 mM pH7.4 EDTA 0.01 mM) and centrifuged (10,000 rpm, 4 °C for 5 min). Supernatants were kept at – 80 °C. Protein concentration was determined according to Bradford protein assay following manufacturer's protocol. For dot blot, 20 µg of protein were plotted on a nitrocellulose membrane. Following Ponceau S (Ponceau Red) staining, membranes were blocked in blocking buffer (5% milk in 1 × PBS containing 0.02% Tween 20) and subsequently incubated for 1h30 with rabbit anti-4-hydroxynonenal (4-HNE, a marker of oxidative stress) antibodies (Abcam; REF: ab46545). Next, membranes were washed and incubated with secondary antibody coupled to HRP (1:2000) (Jackson's laboratories; Goat anti-Rabbit coupled with HRP, REF: J11035003) for 1h30, before being revealed with enhanced chemiluminescence substrates and imaged with Amersham Imager 680.

**Protein extraction for cerebral antioxidant activities.** For enzymatic activities determination, protein isolation from brains was performed as follow: between 4 to 8 mg of zebrafish brain previously collected and stored at – 80 °C were homogenized with a TissueLyser II (Qiagen) in 100 µL of Tris buffer (Tris (25 mM),



Gene	Forward primer	Reverse primer
<i>ef1α</i>	AGCAGCAGCTGAGGAGTGAT	CCGCATTTGTAGATCAGATGG
<i>Il1β</i>	GCTGGAGATCCAAACGGATA	ATACGCGGTGCTGATAAACCC
<i>tnfα</i>	GCGCTTTTCTGAATCCTACGT	GCCCAGTCTGTCTCCTTCT
<i>il6</i>	TCAACTTCTCCAGCGTGATG	TCTTTCCTCTTTTCCTCCTG
<i>nfkb</i>	CGGCCCACTGTAGTTGTG	TGCGTTTCCGTTATAAGTGTG

**Table 1.** Zebrafish qPCR primer sequences of *ef1α*, *il8*, *ilβ*, *tnfα* and *il6*.

EDTA (1 mM), pH 7.4). After centrifugation (5,000 rpm, 4 °C for 10 min), the supernatant was used for protein quantification and enzymatic assays. Total protein concentration of lysates was quantified by the bicinchoninic acid assay (BCA).

The catalase activity assay was estimated on 15–20 μg of protein lysates in 25 mM Tris–HCl (pH 7.5), using protocols previously described<sup>78,79</sup>. Blanks were measured at 240 nm just before adding 80 μL of H<sub>2</sub>O<sub>2</sub> (10 mM final) to start the reaction. Catalase activity was determined by measuring the absorbance at 240 nm and was calculated using a calibration standard curve of increasing amount of catalase between 12.5 and 125 units/mL. Catalase activity was expressed as international catalytic units per mg of proteins and then normalized in percentage versus the control condition.

Total SOD activity was determined using the cytochrome *c* reduction assay, as previously described<sup>80</sup>. In this method, superoxide radicals generated by the xanthine/xanthine oxidase system reduce cytochrome *c*, thereby leading to an increase in absorbance at 560 nm. 20 μL aliquot (about 10 μg of protein) of the lysates was combined with 170 μL reaction mixture (xanthine oxidase, xanthine (0.5 mM), cytochrome *c* (0.2 mM), KH<sub>2</sub>PO<sub>4</sub> (50 mM, pH 7.8), EDTA (2 mM) and NaCN (1 mM)). The reaction was monitored in a microplate reader (Fluostar OPTIMA, BMG Labtech France) at 560 nm for 1 min, at 25 °C. Total SOD activity was calculated using a calibration standard curve of SOD (up to 6 units/mg). Results were expressed as international catalytic units per milligram of cell proteins and then normalized in percentage versus the control condition.

Peroxidase activity of tissue lysates was assessed according to the protocol described by Everse and colleagues<sup>81</sup>. A reaction mixture was prepared with 200 μL of 50 mM citrate buffer/0.2% o-dianisidine and 20 μL of lysates (between 5 to 10 μg of protein). The reaction was initiated by adding 20 μL of 200 mM H<sub>2</sub>O<sub>2</sub>. Peroxidase activity was determined by measuring the absorbance at 450 nm at 25 °C for 3 min. Peroxidase activity was expressed as international catalytic units per mg of proteins and then normalized in percentage versus the control condition.

Chymotrypsin-like activity of the proteasome was assayed using fluorogenic peptide (Sigma-Aldrich, St Louis): Suc-Leu-Leu-Val-Tyr-7-amido-4-methylcoumarin (LLVYMCA at 25 mM), as described previously<sup>78</sup>. Analyses were carried out with 5–10 μg of protein in 25 mM potassium phosphate buffer (pH 7.5) containing LLVY-MCA, at 37 °C for a 0–30 min incubation period. The fluorescence of aminomethylcoumarin was determined at excitation/emission wavelengths of 350/440 nm using a microplate spectrofluorometer reader (Fluostar OPTIMA, BMG labtech France). Peptidase activity was measured in the absence or in the presence of 20 μM proteasome inhibitor MG132 (N-Cbz-Leu-Leu-leucinal) and the specific proteasome activity was obtained by subtracting the residual activity (not inhibited by MG132), i.e. total cellular peptidase activity and non-proteasomal peptidase activity.

**RNA extraction and reverse transcription.** Zebrafish brains were removed from the skull, pooled ( $n = 2$ ), and stored at – 80 °C prior to RNA extraction. Three pools of 2 brains from control and DIO-treated fish were grinded with TissueLyser II (Qiagen, Chatsworth, CA) and RNA extraction was performed using RNA easy Mini Kit (Qiagen) according to manufacturer's protocol. Then, 2 μg of RNA were reverse transcribed into cDNA using random hexamer primers (Invitrogen, REF: 100026484) and MMLV reverse transcriptase (Invitrogen, REF: 28025-021).

**Gene expression analysis by qPCR.** Semi-quantitative PCR experiments were performed using the Bio-rad CFX Connect Real-Time System (BR006305) using the SYBR green master-mix (Eurogentec) and specific zebrafish primers. Each PCR cycle was conducted for 15 s at 95 °C and 1 min at 60 °C. Melting curve analyses and PCR efficiency were performed to confirm correct amplification. Results were analyzed and the relative expressions of the pro-inflammatory cytokine genes (*il1β*, *il6* and *tnfα*) and *nfkb* were normalized against the housekeeping *ef1a* gene. The sequences of the primers are provided in Table 1.

**Microscopy.** Micrographs were obtained with an Eclipse 80i Nikon microscope equipped with a Hamamatsu digital camera (Life Sciences, Japan), and with a nanozoomer S60 (Hamamatsu). Pictures were adjusted for brightness and contrast in Adobe Photoshop.

**Cell counting.** For analyzing constitutive neurogenesis, proliferative activity was determined by quantification of PCNA-positive from 2 to 3 cryostat consecutive sections (12 μm thickness/section) by region of interest. Images were analyzed for detection of PCNA positive nuclei using ImageJ software (National Institutes of Health, Bethesda, MD; RRID: SCR\_003070) by adjusting parameters (threshold, binary, and watershed).



Briefly, the parameters were set up as follows for each picture: threshold 65, 255, particle size 200-infinity. Minor modifications in these parameters could be slightly adjusted according to the experiments. In addition, ImageJ automated selection of PCNA-positive nuclei was manually double-checked and adjusted if necessary, for each picture. Neuroanatomical structures were identified with DAPI counterstaining. Cell counting was performed in blind conditions by two different people and the provided graphs correspond to the mean of proliferative cells per section.

For determining the number of resting and amoeboid microglia, manual counting was performed on 2 consecutive brain cryosection (12  $\mu\text{m}$  thickness/section) for each region of interest (ventral telencephalon and anterior hypothalamus). The counting was performed on a total of 5 to 6 fish per condition, and the provided graphs correspond to the mean of proliferative cells per section.

**Behavioral analysis.** The locomotor activity of zebrafish was monitored by the ZebraCube equipment (Viewpoint). Fish were placed in tanks within the ZebraCube equipment. Locomotor activity was recorded using the viewpoint software and inactivity, small and large activity counts, distance and duration were analyzed. A total number of 12 fish (from 3 independent experiments) were subjected to behavioral analysis. Individual fish were placed in separate tanks in an equal volume of water (750 mL in each tank, corresponding to a column height of 7 cm). The tanks were placed in the ZebraCube equipment with equivalent distance between them and a separation was placed between the tanks in order to avoid visual interaction between the fish from CTRL and DIO groups. The fish were allowed to discover freely this new environment for 10 min in order to adapt to the new space without excessive amount of stress. Then, the locomotor activity was recorded for 10 min: the movement of the fish was tracked as follows: the inactivity (< 4 mm/s), small activity (4–8 mm/s) or high activity (> 8 mm/s).

**Instrumentation and LC–MS/MS Conditions.** Polyphenols extracted from *A. borbonica* infusion were identified by Ultra-high-performance liquid chromatography coupled with diode array detection and HESI-Orbitrap mass spectrometer (Q Exactive Plus, Thermo Fisher). Briefly, 10  $\mu\text{L}$  of sample was injected using an UHPLC system equipped with a Thermo Fisher Ultimate 3,000 series WPS-3000 RS autosampler and then separated on a C18 column (5  $\mu\text{m}$ , 4.6 mm  $\times$  100 mm, Thermo Fisher Scientific Inc.). The column was eluted with a gradient mixture of 0.1% formic acid in water (A) and 0.1% formic acid in acetonitrile (B) at the flow rate of 0.450 mL/min, with 5% B at 0.00 to 0.1 min, 75% B at 0.1 to 7.1 min, 95% B at 7.2 to 7.9 min and 5% B at 8.0 to 10 min. The column temperature was held at 30  $^{\circ}\text{C}$  and the detection wavelengths were set to 280 nm and 310 nm.

For the mass spectrometer conditions, a Heated Electrospray Ionization source II (HESI II) was used. Nitrogen was used as drying gas. The mass spectrometric conditions were optimized as follows: spray voltage = 2.8 kV, capillary temperature = 350  $^{\circ}\text{C}$ , sheath gas flow rate = 60 units, aux gas flow rate = 20 units and S lens RF level = 50.

Mass spectra were registered in full scan mode from  $m/z$  100 to 1,500 in negative ion mode at a resolving power of 70,000 FWHM at  $m/z$  400. The automatic gain control (AGC) was set at  $1 \times 10^6$ . The Orbitrap performance in negative ionization mode was evaluated weekly and external calibration of the mass spectrometer was performed with a LTQ ESI negative ion calibration solution (PIERCE). Identification of the compounds of interest was based on their exact mass, retention time and MS/MS analysis. Data were acquired and processed by XCalibur 4.0 software (Thermo Fisher Scientific Inc.).

**Identification and quantification of polyphenols in *Antirhea borbonica* infusion.** To determine total phenolic acids content in plant extract, Folin-Ciocalteu test was used<sup>82</sup>. Briefly, in a 96-well microplate, 25  $\mu\text{L}$  of plant extract, 125  $\mu\text{L}$  of Folin-Ciocalteu's phenol reagent (Sigma Aldrich) and 100  $\mu\text{L}$  of sodium carbonate (Sigma Aldrich) were added and incubated at 50  $^{\circ}\text{C}$  for 5 min and then at 4  $^{\circ}\text{C}$  for 5 min. The absorbance was measured at 760 nm (FLUOstar Optima, BMG Labtech). A calibration curve between 12.5 – 300  $\mu\text{M}$  was prepared using a standard solution of gallic acid (Sigma-Aldrich, Germany). Total phenol content was expressed as g gallic acid equivalent (GAE) per g plant powder.

Total flavonoids content was also measured using the aluminium chloride ( $\text{AlCl}_3$ ) colorimetric assay and adapted from Zhishen et al.<sup>83</sup>. For this measurement, 100  $\mu\text{L}$  of herbal tea extract were mixed in a 96-well microplate with 6  $\mu\text{L}$  of 5% aqueous sodium nitrite ( $\text{NaNO}_2$ ) solution. After 5 min, 6  $\mu\text{L}$  of 10% aqueous  $\text{AlCl}_3$  were added and the mixture was vortexed. Then, after 1 min incubation, 40  $\mu\text{L}$  of 1 M NaOH were added. The absorbance was read at 510 nm (FLUOstar Optima, BMG Labtech). A calibration curve between 6.25–300  $\mu\text{M}$  was prepared using a standard solution of epicatechin (Sigma-Aldrich). Total flavonoid content was expressed as g epicatechin acid equivalent (EE) per g plant powder.

The identification and the quantification analysis of caffeic acid, dicaffeoylquinic acid, caffeoylquinic acid, quercetin and kaempferol were achieved by an LC–MS/MS analysis as previously described by<sup>29</sup>, with minor modifications. For the mass spectrometry quantification, a mixed stock solution containing 10  $\mu\text{g}/\text{mL}$  of each polyphenols was prepared in methanol.

Calibration curves were constructed by plotting the peak area of the analytes *versus* the concentration of the analytes with linear regression using standard samples at eleven concentrations. The calibration curves of each polyphenols had a correlation coefficient ( $R^2$ ) of 0.99.

**Statistical analysis.** Comparisons between two groups were performed using a statistical Student's t-test. If more than two groups were analyzed, multiple testing was performed by one-way ANOVA. Error bars correspond to the standard error of the mean (SEM), and n values correspond to the number of animals or to



the number of samples for all experiments. P-values < 0.05 were considered statistically significant (\* $p < 0.05$ , \*\* $p < 0.01$ , \*\*\* $p < 0.001$ , \*\*\*\* $p < 0.0001$ ).

Received: 5 April 2020; Accepted: 6 August 2020

Published online: 02 September 2020

## References

- World Health Organisation, W. Obesity and overweight. <https://www.who.int/news-room/fact-sheets/detail/obesity-and-overweight> (2019).
- Church, T. & Martin, C. K. The obesity epidemic: a consequence of reduced energy expenditure and the uncoupling of energy intake?. *Obesity (Silver Spring)* **26**, 14–16. <https://doi.org/10.1002/oby.22072> (2018).
- Kostovski, M. *et al.* Obesity in childhood and adolescence, genetic factors. *Pril (Makedon Akad Nauk Umet Odd Med Nauki)* **38**, 121–133. <https://doi.org/10.2478/prilozi-2018-0013> (2017).
- Rolland-Cachera, M. F., Akrouf, M. & Peneau, S. Nutrient intakes in early life and risk of obesity. *Int. J. Environ. Res. Public Health* <https://doi.org/10.3390/ijerph13060564> (2016).
- Marseglia, L. *et al.* Oxidative stress in obesity: a critical component in human diseases. *Int. J. Mol. Sci.* **16**, 378–400. <https://doi.org/10.3390/ijms16010378> (2014).
- Bays, H. E. *et al.* Obesity, adiposity, and dyslipidemia: a consensus statement from the National Lipid Association. *J. Clin. Lipidol.* **7**, 304–383. <https://doi.org/10.1016/j.jacl.2013.04.001> (2013).
- Gramlich, Y. *et al.* Oxidative stress in cardiac tissue of patients undergoing coronary artery bypass graft surgery: the effects of overweight and obesity. *Oxidative Med. Cell. Longev.* **2018**, 6598326. <https://doi.org/10.1155/2018/6598326> (2018).
- Abdullah, A., Peeters, A., de Courten, M. & Stoelwinder, J. The magnitude of association between overweight and obesity and the risk of diabetes: a meta-analysis of prospective cohort studies. *Diabetes Res. Clin. Pract.* **89**, 309–319. <https://doi.org/10.1016/j.diabres.2010.04.012> (2010).
- Pugazhenth, S., Qin, L. & Reddy, P. H. Common neurodegenerative pathways in obesity, diabetes, and Alzheimer's disease. *Biochim. Biophys. Acta Mol. Basis Dis.* **1037–1045**, 2017. <https://doi.org/10.1016/j.bbadis.2016.04.017> (1863).
- Corder, Z. A. & Tamashiro, K. L. Effects of high-fat diet exposure on learning & memory. *Physiol. Behav.* **152**, 363–371. <https://doi.org/10.1016/j.physbeh.2015.06.008> (2015).
- Cifre, M., Palou, A. & Oliver, P. Cognitive impairment in metabolically-obese, normal-weight rats: identification of early biomarkers in peripheral blood mononuclear cells. *Mol. Neurodegener.* **13**, 14. <https://doi.org/10.1186/s13024-018-0246-8> (2018).
- Davidson, T. L., Tracy, A. L., Schier, L. A. & Swithers, S. E. A view of obesity as a learning and memory disorder. *J. Exp. Psychol. Anim. Learn. Cogn.* **40**, 261–279. <https://doi.org/10.1037/xan000029> (2014).
- Oka, T. *et al.* Diet-induced obesity in zebrafish shares common pathophysiological pathways with mammalian obesity. *BMC Physiol.* **10**, 21. <https://doi.org/10.1186/1472-6793-10-21> (2010).
- Zang, L., Maddison, L. A. & Chen, W. Zebrafish as a model for obesity and diabetes. *Front. Cell Dev. Biol.* **6**, 91. <https://doi.org/10.3389/fcell.2018.00091> (2018).
- Montalbano, G. *et al.* Effects of a flavonoid-rich extract from *Citrus sinensis* juice on a diet-induced obese zebrafish. *Int. J. Mol. Sci.* <https://doi.org/10.3390/ijms20205116> (2019).
- Montalbano, G. *et al.* Melatonin treatment suppresses appetite genes and improves adipose tissue plasticity in diet-induced obese zebrafish. *Endocrine* **62**, 381–393. <https://doi.org/10.1007/s12020-018-1653-x> (2018).
- Montalbano, G. *et al.* Morphological differences in adipose tissue and changes in BDNF/Trkb expression in brain and gut of a diet induced obese zebrafish model. *Ann. Anat.* **204**, 36–44. <https://doi.org/10.1016/j.aanat.2015.11.003> (2016).
- Dorsemans, A. C. *et al.* Impaired constitutive and regenerative neurogenesis in adult hyperglycemic zebrafish. *J. Comp. Neurol.* **525**, 442–458. <https://doi.org/10.1002/cne.24065> (2017).
- Dorsemans, A. C. *et al.* Acute and chronic models of hyperglycemia in zebrafish: a method to assess the impact of hyperglycemia on neurogenesis and the biodistribution of radiolabeled molecules. *J. Vis. Exp.* <https://doi.org/10.3791/55203> (2017).
- Capiotti, K. M. *et al.* Hyperglycemia induces memory impairment linked to increased acetylcholinesterase activity in zebrafish (*Danio rerio*). *Behav. Brain Res.* **274**, 319–325. <https://doi.org/10.1016/j.bbr.2014.08.033> (2014).
- Capiotti, K. M. *et al.* Persistent impaired glucose metabolism in a zebrafish hyperglycemia model. *Comp. Biochem. Physiol. B Biochem. Mol. Biol.* **171**, 58–65. <https://doi.org/10.1016/j.cbpb.2014.03.005> (2014).
- Zang, L., Shimada, Y. & Nishimura, N. Development of a novel zebrafish model for type 2 diabetes mellitus. *Sci. Rep.* **7**, 1461. <https://doi.org/10.1038/s41598-017-01432-w> (2017).
- Intine, R. V., Olsen, A. S. & Sarra, M. P. Jr. A zebrafish model of diabetes mellitus and metabolic memory. *J. Vis. Exp.* <https://doi.org/10.3791/50232> (2013).
- Lindsey, B. W. & Tropepe, V. A comparative framework for understanding the biological principles of adult neurogenesis. *Prog. Neurobiol.* **80**, 281–307. <https://doi.org/10.1016/j.pneurobio.2006.11.007> (2006).
- März, M. *et al.* Heterogeneity in progenitor cell subtypes in the ventricular zone of the zebrafish adult telencephalon. *Glia* **58**, 870–888. <https://doi.org/10.1002/glia.20971> (2010).
- Schmidt, R., Strähle, U. & Scholpp, S. Neurogenesis in zebrafish—from embryo to adult. *Neural Dev.* **8**, 3. <https://doi.org/10.1186/1749-8104-8-3> (2013).
- Pellegrini, E. *et al.* Identification of aromatase-positive radial glial cells as progenitor cells in the ventricular layer of the forebrain in zebrafish. *J. Comp. Neurol.* **501**, 150–167. <https://doi.org/10.1002/cne.21222> (2007).
- Diotel, N. *et al.* Cxcr4 and Cxcl12 expression in radial glial cells of the brain of adult zebrafish. *J. Comp. Neurol.* **518**, 4855–4876. <https://doi.org/10.1002/cne.22492> (2010).
- Marimoutou, M. *et al.* Antioxidant polyphenol-rich extracts from the medicinal plants *Antirhea borbonica*, *Doratoxylon apetalum* and *Gouania mauritiana* protect 3T3-L1 preadipocytes against H<sub>2</sub>O<sub>2</sub>, TNF $\alpha$  and LPS inflammatory mediators by regulating the expression of superoxide dismutase and NF- $\kappa$ B genes. *J. Inflamm. (Lond.)* **12**, 10. <https://doi.org/10.1186/s12950-015-0055-6> (2015).
- Ledoux, A. *et al.* Antiplasmodial, anti-chikungunya virus and antioxidant activities of 64 endemic plants from the Mascarene Islands. *Int. J. Antimicrob. Agents* **52**, 622–628. <https://doi.org/10.1016/j.ijantimicag.2018.07.017> (2018).
- Jonville, M. C. *et al.* Screening of medicinal plants from Reunion Island for antimalarial and cytotoxic activity. *J. Ethnopharmacol.* **120**, 382–386. <https://doi.org/10.1016/j.jep.2008.09.005> (2008).
- Smadja, J. & Marodon, C. Plantes médicinales de la Réunion. *Orphie G. doyen Editions*, 1–232 (2016).
- Le Sage, F., Meilhac, O. & Gonthier, M. P. Anti-inflammatory and antioxidant effects of polyphenols extracted from *Antirhea borbonica* medicinal plant on adipocytes exposed to *Porphyromonas gingivalis* and *Escherichia coli* lipopolysaccharides. *Pharmacol Res* **119**, 303–312. <https://doi.org/10.1016/j.phrs.2017.02.020> (2017).



34. Diotel, N. *et al.* Effects of estradiol in adult neurogenesis and brain repair in zebrafish. *Horm. Behav.* **63**, 193–207. <https://doi.org/10.1016/j.yhbeh.2012.04.003> (2013).
35. Veyrac, A. & Bakker, J. Postnatal and adult exposure to estradiol differentially influences adult neurogenesis in the main and accessory olfactory bulb of female mice. *FASEB J.* **25**, 1048–1057. <https://doi.org/10.1096/fj.10-172635> (2011).
36. Prasad, S., Sajja, R. K., Naik, P. & Cucullo, L. Diabetes mellitus and blood–brain barrier dysfunction: an overview. *J. Pharmacovigil.* **2**, 125. <https://doi.org/10.4172/2329-6887.1000125> (2014).
37. Van Dyken, P. & Lacoste, B. Impact of metabolic syndrome on neuroinflammation and the blood–brain barrier. *Front. Neurosci.* **12**, 930. <https://doi.org/10.3389/fnins.2018.00930> (2018).
38. Diotel, N. *et al.* Effects of estradiol in adult neurogenesis and brain repair in zebrafish. *Horm. Behav.* **63**, 193–207. <https://doi.org/10.1016/j.yhbeh.2012.04.003> (2013).
39. Kaur, N. *et al.* Cinnamon attenuates adiposity and affects the expression of metabolic genes in diet-induced obesity model of zebrafish. *Artif. Cells Nanomed. Biotechnol.* **47**, 2930–2939. <https://doi.org/10.1080/21691401.2019.1641509> (2019).
40. Meguro, S., Hasumura, T. & Hase, T. Body fat accumulation in zebrafish is induced by a diet rich in fat and reduced by supplementation with green tea extract. *PLoS ONE* **10**, e0120142. <https://doi.org/10.1371/journal.pone.0120142> (2015).
41. Afonso, M. S. *et al.* Phenolic compounds from Rosemary (*Rosmarinus officinalis* L.) attenuate oxidative stress and reduce blood cholesterol concentrations in diet-induced hypercholesterolemic rats. *Nutr. Metab. (Lond.)* **10**, 19. <https://doi.org/10.1186/1743-7075-10-19> (2013).
42. Landgraf, K. *et al.* Short-term overfeeding of zebrafish with normal or high-fat diet as a model for the development of metabolically healthy versus unhealthy obesity. *BMC Physiol.* **17**, 4. <https://doi.org/10.1186/s12899-017-0031-x> (2017).
43. Nakayama, H. *et al.* Novel anti-obesity properties of *Palmaria mollis* in zebrafish and mouse models. *Nutrients* <https://doi.org/10.3390/nu10101401> (2018).
44. Hardy, O. T., Czech, M. P. & Corvera, S. What causes the insulin resistance underlying obesity?. *Curr. Opin. Endocrinol. Diabetes Obes.* **19**, 81–87. <https://doi.org/10.1097/MED.0b013e3283514e13> (2012).
45. Expert Panel on Detection, E. & Treatment of High Blood Cholesterol in, A. Executive summary of the third report of The National Cholesterol Education Program (NCEP) expert panel on detection, evaluation, and treatment of high blood cholesterol in adults (Adult Treatment Panel III). *JAMA* **285**, 2486–2497. <https://doi.org/10.1001/jama.285.19.2486> (2001).
46. Dharmalingam, M. & Yamasandhi, P. G. Nonalcoholic fatty liver disease and type 2 diabetes mellitus. *Indian J. Endocrinol. Metab.* **22**, 421–428. [https://doi.org/10.4103/ijem.IJEM\\_585\\_17](https://doi.org/10.4103/ijem.IJEM_585_17) (2018).
47. Williams, K. H., Shackel, N. A., Gorrell, M. D., McLennan, S. V. & Twigg, S. M. Diabetes and nonalcoholic Fatty liver disease: a pathogenic duo. *Endocr. Rev.* **34**, 84–129. <https://doi.org/10.1210/er.2012-1009> (2013).
48. Parimisetty, A. *et al.* Secret talk between adipose tissue and central nervous system via secreted factors—an emerging frontier in the neurodegenerative research. *J. Neuroinflamm.* **13**, 67. <https://doi.org/10.1186/s12974-016-0530-x> (2016).
49. Nguyen, J. C., Killcross, A. S. & Jenkins, T. A. Obesity and cognitive decline: role of inflammation and vascular changes. *Front. Neurosci.* **8**, 375. <https://doi.org/10.3389/fnins.2014.00375> (2014).
50. Alam, M. J. *et al.* Adult neurogenesis conserves hippocampal memory capacity. *J. Neurosci.* **38**, 6854–6863. <https://doi.org/10.1523/JNEUROSCI.2976-17.2018> (2018).
51. Roh, H. T., Cho, S. Y. & So, W. Y. Obesity promotes oxidative stress and exacerbates blood–brain barrier disruption after high-intensity exercise. *J. Sport Health Sci.* **6**, 225–230. <https://doi.org/10.1016/j.jshs.2016.06.005> (2017).
52. Lochhead, J. J. *et al.* Oxidative stress increases blood–brain barrier permeability and induces alterations in occludin during hypoxia-reoxygenation. *J. Cereb. Blood Flow Metab.* **30**, 1625–1636. <https://doi.org/10.1038/jcbfm.2010.29> (2010).
53. Wang, J. *et al.* High-glucose/high-cholesterol diet in zebrafish evokes diabetic and affective pathogenesis: the role of peripheral and central inflammation, microglia and apoptosis. *Prog. Neuropsychopharmacol. Biol. Psychiatry* <https://doi.org/10.1016/j.pnpbp.2019.109752> (2019).
54. Purkayastha, S. & Cai, D. Disruption of neurogenesis by hypothalamic inflammation in obesity or aging. *Rev. Endocr. Metab. Disord.* **14**, 351–356. <https://doi.org/10.1007/s11154-013-9279-z> (2013).
55. Mendes, N. F., Kim, Y. B., Velloso, L. A. & Araujo, E. P. Hypothalamic microglial activation in obesity: a mini-review. *Front. Neurosci.* **12**, 846. <https://doi.org/10.3389/fnins.2018.00846> (2018).
56. Valdearcos, M. *et al.* Microglia dictate the impact of saturated fat consumption on hypothalamic inflammation and neuronal function. *Cell Rep.* **9**, 2124–2138. <https://doi.org/10.1016/j.celrep.2014.11.018> (2014).
57. Albadri, S. *et al.* Redox signaling via lipid peroxidation regulates retinal progenitor cell differentiation. *Dev. Cell.* **50**, 73e76–89e76. <https://doi.org/10.1016/j.devcel.2019.05.011> (2019).
58. Bailey, A. P. *et al.* Antioxidant role for lipid droplets in a stem cell niche of drosophila. *Cell* **163**, 340–353. <https://doi.org/10.1016/j.cell.2015.09.020> (2015).
59. Stankiewicz, A. J., McGowan, E. M., Yu, L. & Zhdanova, I. V. Impaired sleep, circadian rhythms and neurogenesis in diet-induced premature aging. *Int. J. Mol. Sci.* <https://doi.org/10.3390/ijms18112243> (2017).
60. Park, H. R. *et al.* A high-fat diet impairs neurogenesis: involvement of lipid peroxidation and brain-derived neurotrophic factor. *Neurosci. Lett.* **482**, 235–239. <https://doi.org/10.1016/j.neulet.2010.07.046> (2010).
61. Bracke, A. *et al.* Obesity impairs mobility and adult hippocampal neurogenesis. *J. Exp. Neurosci.* **13**, 1179069519883580. <https://doi.org/10.1177/1179069519883580> (2019).
62. Dorsemans, A. C. *et al.* Diabetes, adult neurogenesis and brain remodeling: new insights from rodent and zebrafish models. *Neurogenesis (Austin)* **4**, e1281862. <https://doi.org/10.1080/23262133.2017.1281862> (2017).
63. McNay, D. E., Briancon, N., Kokoeva, M. V., Maratos-Flier, E. & Flier, J. S. Remodeling of the arcuate nucleus energy-balance circuit is inhibited in obese mice. *J. Clin. Invest.* **122**, 142–152. <https://doi.org/10.1172/JCI43134> (2012).
64. Ho, N., Sommers, M. S. & Lucki, I. Effects of diabetes on hippocampal neurogenesis: links to cognition and depression. *Neurosci. Biobehav. Rev.* **37**, 1346–1362. <https://doi.org/10.1016/j.neubiorev.2013.03.010> (2013).
65. Yu, M. *et al.* Maternal high-fat diet affects Msi/Notch/Hes signaling in neural stem cells of offspring mice. *J. Nutr. Biochem.* **25**, 227–231. <https://doi.org/10.1016/j.jnutbio.2013.10.011> (2014).
66. Meguro, S., Hosoi, S. & Hasumura, T. High-fat diet impairs cognitive function of zebrafish. *Sci. Rep.* **9**, 17063. <https://doi.org/10.1038/s41598-019-53634-z> (2019).
67. Xie, M. *et al.* Effects of dicaffeoylquinic acids from ilex kudingcha on lipid metabolism and intestinal microbiota in high-fat-diet-fed mice. *J. Agric. Food Chem.* **67**, 171–183. <https://doi.org/10.1021/acs.jafc.8b05444> (2019).
68. Jung, C. H., Cho, L., Ahn, J., Jeon, T. I. & Ha, T. Y. Quercetin reduces high-fat diet-induced fat accumulation in the liver by regulating lipid metabolism genes. *Phytother. Res.* **27**, 139–143. <https://doi.org/10.1002/ptr.4687> (2013).
69. Ma, Y., Gao, M. & Liu, D. Chlorogenic acid improves high fat diet-induced hepatic steatosis and insulin resistance in mice. *Pharm. Res.* **32**, 1200–1209. <https://doi.org/10.1007/s11095-014-1526-9> (2015).
70. Khan, F. A., Maalik, A. & Murtaza, G. Inhibitory mechanism against oxidative stress of caffeic acid. *J. Food Drug Anal.* **24**, 695–702. <https://doi.org/10.1016/j.jfda.2016.05.003> (2016).
71. Liang, N. & Kitts, D. D. Role of chlorogenic acids in controlling oxidative and inflammatory stress conditions. *Nutrients* <https://doi.org/10.3390/nu8010016> (2015).
72. Heitman, E. & Ingram, D. K. Cognitive and neuroprotective effects of chlorogenic acid. *Nutr. Neurosci.* **20**, 32–39. <https://doi.org/10.1179/1476830514Y.0000000146> (2017).



73. Eames, S. C., Philipson, L. H., Prince, V. E. & Kinkel, M. D. Blood sugar measurement in zebrafish reveals dynamics of glucose homeostasis. *Zebrafish* **7**, 205–213. <https://doi.org/10.1089/zeb.2009.0640> (2010).
74. Le Guyader, D. *et al.* Origins and unconventional behavior of neutrophils in developing zebrafish. *Blood* **111**, 132–141. <https://doi.org/10.1182/blood-2007-06-095398> (2008).
75. Diotel, N., Vaillant, C., Kah, O. & Pellegrini, E. Mapping of brain lipid binding protein (Blbp) in the brain of adult zebrafish, co-expression with aromatase B and links with proliferation. *Gene Expr. Patterns* **20**, 42–54. <https://doi.org/10.1016/j.gep.2015.11.003> (2016).
76. Sieger, D. & Peri, F. Animal models for studying microglia: the first, the popular, and the new. *Glia* **61**, 3–9. <https://doi.org/10.1002/glia.22385> (2013).
77. Kaya, M. & Ahishali, B. Assessment of permeability in barrier type of endothelium in brain using tracers: Evans blue, sodium fluorescein, and horseradish peroxidase. *Methods Mol. Biol.* **763**, 369–382. [https://doi.org/10.1007/978-1-61779-191-8\\_25](https://doi.org/10.1007/978-1-61779-191-8_25) (2011).
78. Patche, J. *et al.* Diabetes-induced hepatic oxidative stress: a new pathogenic role for glycated albumin. *Free Radic. Biol. Med.* **102**, 133–148. <https://doi.org/10.1016/j.freeradbiomed.2016.11.026> (2017).
79. Boyer, F. *et al.* Enhanced oxidative stress in adipose tissue from diabetic mice, possible contribution of glycated albumin. *Biochem. Biophys. Res. Commun.* **473**, 154–160. <https://doi.org/10.1016/j.bbrc.2016.03.068> (2016).
80. Dobi, A. *et al.* Advanced glycation end-products disrupt human endothelial cells redox homeostasis: new insights into reactive oxygen species production. *Free Radic. Res.* **53**, 150–169. <https://doi.org/10.1080/10715762.2018.1529866> (2019).
81. Everse, J., Johnson, M. C. & Marini, M. A. Peroxidative activities of hemoglobin and hemoglobin derivatives. *Methods Enzymol.* **231**, 547–561. [https://doi.org/10.1016/0076-6879\(94\)31038-6](https://doi.org/10.1016/0076-6879(94)31038-6) (1994).
82. Singleton, V. & Rossi, J. Colorimetric of total phenolics with phosphomolydic–phosphotungstic acid reagents. *Am. J. Enol. Vitic.* **16**, 144–158 (1965).
83. Zhishen, J., Mengcheng, T. & Jianming, W. The determination of flavonoid contents in mulberry and their scavenging effects on superoxide radicals. *Food Chem.* **64**, 555–559 (1999).
84. Mennet, A. *et al.* Expression and estrogen-dependent regulation of the zebrafish brain aromatase gene. *J. Comp. Neurol.* **485**, 304–320. <https://doi.org/10.1002/cne.20497> (2005).
85. Wullimann, M. *et al.* (eds) *Neuroanatomy of the Zebrafish Brain: A Topological Atlas* 1–144 (Birhäuser Verlag, Basel, 1996).

## Acknowledgements

We thank CP and CT for excellent technical support with the fish facility and for advices in dot-blot, the Vegetal Biodiversity Comity from the DéTROU laboratory (especially Pr MPG and Dr CM) for discussion about plants from the French Pharmacopeia, as well as Dr M. Redd for kindly providing L-plastin antibody.

## Author contributions

ND, OM and JLB designed the experiments. BG, BV, PR, MB, ND and JLB performed the experiments. All the authors participated in the analysis of the experiments and/or in the writing of the manuscript.

## Funding

This work was supported by grants from La Réunion University (Bonus Qualité Recherche, Dispositifs incitatifs), FEDER RE0001897 (Biomarqueurs and Therapy), FEDER RE0022527 (ZEBRATOX), EU- Région Réunion-French State national counterpart as well as the BIOST Fédération.

## Competing interests

The authors declare no competing interests.


## Additional information

**Supplementary information** is available for this paper at <https://doi.org/10.1038/s41598-020-71402-2>.

**Correspondence** and requests for materials should be addressed to N.D.

**Reprints and permissions information** is available at [www.nature.com/reprints](http://www.nature.com/reprints).

**Publisher's note** Springer Nature remains neutral with regard to jurisdictional claims in published maps and institutional affiliations.

 **Open Access** This article is licensed under a Creative Commons Attribution 4.0 International License, which permits use, sharing, adaptation, distribution and reproduction in any medium or format, as long as you give appropriate credit to the original author(s) and the source, provide a link to the Creative Commons licence, and indicate if changes were made. The images or other third party material in this article are included in the article's Creative Commons licence, unless indicated otherwise in a credit line to the material. If material is not included in the article's Creative Commons licence and your intended use is not permitted by statutory regulation or exceeds the permitted use, you will need to obtain permission directly from the copyright holder. To view a copy of this licence, visit <http://creativecommons.org/licenses/by/4.0/>.

© The Author(s) 2020



## Chapter 4: Aqueous extract of *Psiloxylon mauritianum* prevents obesity and associated deleterious effects in zebrafish (ready to submit)

Taking advantage of its traditionally anti-lipidemic and recorded anti-oxidant and anti-inflammatory effects, *Psiloxylon mauritianum* (*P. mauritianum*) represents for us an interesting plant to investigate to combat the deleterious effects induced by overfeeding (DIO related alterations). This article characterizes the *P. mauritianum* main components and its toxicity in order to study its suggested beneficial properties using.

The first set of tasks of this article converges on studying of the polyphenolic composition of *P. mauritianum* and its toxicity during developmental stages. Liquid chromatography-mass spectrometry analysis shows that *P. mauritianum* is rich in polyphenols mainly phenolic acids and flavonoids (i.e.,  $58.0 \pm 7.2$  mg GAE/g). The toxicity test on zebrafish eleutheroembryos of zebrafish according to the OECD (guidelines 236) defined the median lethal concentration ( $LC_{50}=0.71$  g/L) and the maximum non-lethal concentration (MNTC= $0.556$  g/L). However, the concentration used throughout all the experiment is  $0.25$  g/L, that is shown to be safe for adults. Furthermore, the qPCR analysis of certain cardiac, liver and renal toxicity markers reveals no toxic effect at these levels. Besides, the exploration of fat accumulation in the HFD larva treated with *P. mauritianum* asserts the anti-lipidemic known trait.

In the second part of exploring the properties of *P. mauritianum*, we take advantage of our previously developed DIO model. Interestingly, preventive treatment of adult DIO fish with the aqueous extracts of *P. mauritianum* ( $0.25$  g/L) for 4 weeks avoided the increase in the body weight, BMI, glycemia and lipid accumulation in the liver compared to the non-treated DIO fish. We noticed that the zebrafish treated with the plant extract display a normal feeding behavior, but excreted more feces. Similarly, in the brain, *P. mauritianum* prevented all the negative influences resulting from DIO. The positive effect of *P. mauritianum* observed at the brain level could be a possible consequence of its anti-weight gain property. It is worth noting that this plant does not have any effect on brain homeostasis under normal feeding conditions. Interestingly, *P. mauritianum* also demonstrated a therapeutic effect on DIO fish where a one-week treatment with the plant after one week of overfeeding decreased the body weight gain and normalized fasting blood glucoses levels compared to untreated DIO fish.

Therefore, this ready to submit article characterizes for the first time the toxicity doses of *P. mauritianum* using the toxicity assay according to the OECD (guidelines 236). Also, *in*

*vivo* experiments using the aqueous extract of *P. mauritianum* on the DIO model emphasize the previously recorded anti-oxidant, anti-hypercholesterolemic and anti-hyperglycemic effects and suggest a possible effect on nutrients absorption and gut microbiota that need be further studied.





# Aqueous extract of *Psiloxylon mauritianum*, rich in gallic acid, prevents obesity and associated deleterious effects in zebrafish

Batoul Ghaddar<sup>1</sup>, Laura Gence<sup>1§</sup>, Bryan Veeren<sup>1§</sup>, Matthieu Bringart<sup>1</sup>, Jean-Loup Bascands<sup>1</sup>, Olivier Meilhac<sup>1,2</sup>, Nicolas Diotel<sup>\*1</sup>

<sup>1</sup> Université de La Réunion, INSERM, UMR 1188, Diabète athérombose Thérapies Réunion Océan Indien (DéTROI), Saint-Denis, La Réunion, France; [batoul.ghaddar@univ-reunion.fr](mailto:batoul.ghaddar@univ-reunion.fr); [laura.gence@univ-reunion.fr](mailto:laura.gence@univ-reunion.fr); [bryan.veeren@univ-reunion.fr](mailto:bryan.veeren@univ-reunion.fr); [matthieu.bringart@inserm.fr](mailto:matthieu.bringart@inserm.fr); [jean-loup.bascands@inserm.fr](mailto:jean-loup.bascands@inserm.fr); [olivier.meilhac@univ-reunion.fr](mailto:olivier.meilhac@univ-reunion.fr); [nicolas.diotel@univ-reunion.fr](mailto:nicolas.diotel@univ-reunion.fr).

<sup>2</sup> CHU de La Réunion, Saint-Denis, La Réunion, France ; [olivier.meilhac@inserm.fr](mailto:olivier.meilhac@inserm.fr)

<sup>§</sup> These authors contribute equally to the work

\* Correspondence: [nicolas.diotel@univ-reunion.fr](mailto:nicolas.diotel@univ-reunion.fr).

**Abstract:** Obesity has reached epidemic proportions and its prevalence has been tripled worldwide between 1975 and 2016, especially in overseas regions. *Psiloxylon mauritianum*, an endemic medicinal plant from Reunion Island registered in the French pharmacopeia, has recently gain interest to combat metabolic disorders because of its traditional lipid-lowering and “anti-diabetic” use. However, scientific data are lacking regarding its toxicity and its real benefits on metabolic diseases. In this study, we aim to determine the toxicity of an aqueous extract of *P. mauritianum* on zebrafish eleutheroembryos following the OECD toxicity assay (Organization for Economic Cooperation and Development, guidelines 36). After defining a non-toxic dose, we determined by LC-MS/MS that this extract is rich in gallic acid but contains also caffeoylquinic acid, kaempferol and quercetin as well as their respective derivatives. We also showed that the non-toxic dose exhibits lipid-lowering effects in a high-fat diet zebrafish larvae model. In a next step, we demonstrated its preventive effects on body weight gain, hyperglycemia and liver steatosis in a diet-induced obesity model (DIO) performed in adults. It also limited the deleterious effects of overfeeding on the central nervous system (i.e., cerebral oxidative stress, blood-brain barrier breakdown, neuro-inflammation and blunted neurogenesis). Interestingly, adult DIO fish treated with *P. mauritianum* display a normal feeding behavior but a higher feces production. This indicates that the “anti-weight” gain effect is probably due to an action of *P. mauritianum* on the intestinal lipid absorption and/or on the microbiota leading to the increase in feces production. Therefore, in our experimental conditions, the aqueous extract of *P. mauritianum* exhibited “anti-weight gain” properties, that prevented the development of obesity and its deleterious effects at the peripheral and central levels. These effects should be further investigated in preclinical models of obese/diabetic mice as well as the impact of *P. mauritianum* on gut microbiota.

**Keywords:** blood-brain barrier, neurogenesis, obesity, oxidative stress, *P. mauritianum*

**Citation:** Lastname, F.; Lastname, F.; Lastname, F. Title. *Int. J. Mol. Sci.* **2022**, *23*, x. <https://doi.org/10.3390/xxxxx>

Academic Editor: Firstname Lastname

Received: date

Accepted: date

Published: date

**Publisher’s Note:** MDPI stays neutral with regard to jurisdictional claims in published maps and institutional affiliations.



**Copyright:** © 2022 by the authors. Submitted for possible open access publication under the terms and conditions of the Creative Commons Attribution (CC BY) license (<https://creativecommons.org/licenses/by/4.0/>).

## 1. Introduction

Obesity is a global epidemic characterized by an excessive accumulation of body fat. The World Health Organization (WHO) has estimated that over 1.9 billion adults are overweight, including 650 million obese people [1]. Obesity leads to many physiological complications, impairing body homeostasis through increased chronic inflammation and oxidative stress [2-4]. Thus, obesity can affect the cardiovascular and renal functions, and

promotes among others liver steatosis and insulin resistance [5-8]. So far, obesity resides as a great risk factor for the development of type 2 diabetes and its complications [9].

In addition to these peripheral disorders, it was also shown that obesity alters brain homeostasis and leads to a variety of central nervous system (CNS) alterations [10, 11]. For instance, obesity promotes stroke, blood-brain barrier breakdown, neuro-inflammation as well as oxidative stress. It also results in cognitive impairments (memory defects and dementia) and in increased risks to develop neurodegenerative diseases [12-16]. In addition, it was recently demonstrated that obesity worsens brain plasticity by decreasing neural stem cell proliferation and impairing other neurogenic processes [17].

Until now, no real and successful pharmacological treatments have been found to limit weight gain and/or to limit the deleterious effects of obesity on the central nervous system. Medicinal plants are envisioned as a natural storehouse of beneficial compounds including alkaloids, flavonoids, tannins, essential oils and phenolic compounds [18], that could help to combat obesity or its complications. For this reason, it is important to screen the potential beneficial effects of medicinal plants to prevent the onset of obesity or obesity-induced complications. Reunion Island is a biodiversity hotspot known for its wide distribution of endemic plants. Some of them are traditionally described and used for their suggested "anti-diabetic" and/or lipid-lowering properties [19-23]. Unfortunately, scientific data are lacking to confirm such properties, although recent data from our group document some of these beneficial effects [23-29]. Recently, 27 Reunionese plants have been registered in the French pharmacopeia [19, 20]. Among these medicinal plants, *Psiloxylon mauritianum* (*P. mauritianum*; vernacular name: bois de pêche marron) is traditionally used for the treatment of diarrhea and to decrease the formation of uric acid in the body (gout pathology) [30]. Other studies have also reported the antiseptic, antispasmodic and diuretic effects of *P. mauritianum* [30]. Of interest, *P. mauritianum* is reported to exhibit "anti-cholesterol" and "anti-diabetic" effects, highlighting its potential beneficial role in metabolic diseases [30, 31]. In the literature, the presence of flavones, flavans, flavonoids, phenols, terpenes and tannins was shown in acetonic extract of *P. mauritianum* leaves [32]. Checkouri and colleagues have further characterized the polyphenolic composition and antioxidant capacity of *P. mauritianum* [23].

Recently, zebrafish has emerged as an alternative model to study metabolic disorders including diabetes and hyperglycemia as well as overweight/obesity [28, 33-39]. Considering obesity, zebrafish shares several aspects of the mammalian pathology with high adiposity, increased body mass index (BMI), non-alcoholic fatty liver, the development of insulin resistance and hyperglycemia, cardiovascular diseases, as well as brain complications [28, 35, 40-45]. In addition, zebrafish is also a widely used model to investigate brain plasticity [46-49].

Interestingly, recent data also documented the deleterious impact of metabolic disorders (herein hyperglycemia and obesity) in the brain of adult zebrafish [28, 50-54]. These metabolic disruptions induce a blunted constitutive and regenerative neurogenesis as well as cognitive impairments, in a way similar to mammals [28, 50, 52, 53, 55]. Consequently, zebrafish has emerged as an interesting and valuable model to study the impact of metabolic disorders on the central nervous system (CNS).

In this study, based on *P. mauritianum* composition and richness in antioxidants and considering the involvement of oxidative stress in obesity, we hypothesized that this medicinal plant could limit weight gain and the development of obesity complication. We first aimed to investigate the *in vivo* toxicity of the aqueous extract of *P. mauritianum* in zebrafish eleutheroembryos using the Organization for Economic Co-operation and Development (OECD) toxicity assay (guidelines 236: Fish Embryo Acute Toxicity). Next, using a model of high-fat diet (HFD) larvae, we studied the lipid-lowering effects of the aqueous extract of *P. mauritianum* at a non-toxic concentration. Finally, taking advantage of our recently developed obese zebrafish model (diet-induced obesity: DIO) [28], we investigated the effects of *P. mauritianum* on metabolic parameters (i.e. body weight, BMI, glycemia) and brain homeostasis. In this work, we demonstrated interesting preventive

properties of *P. mauritianum* on the development of obesity and its associated complications. 97  
98

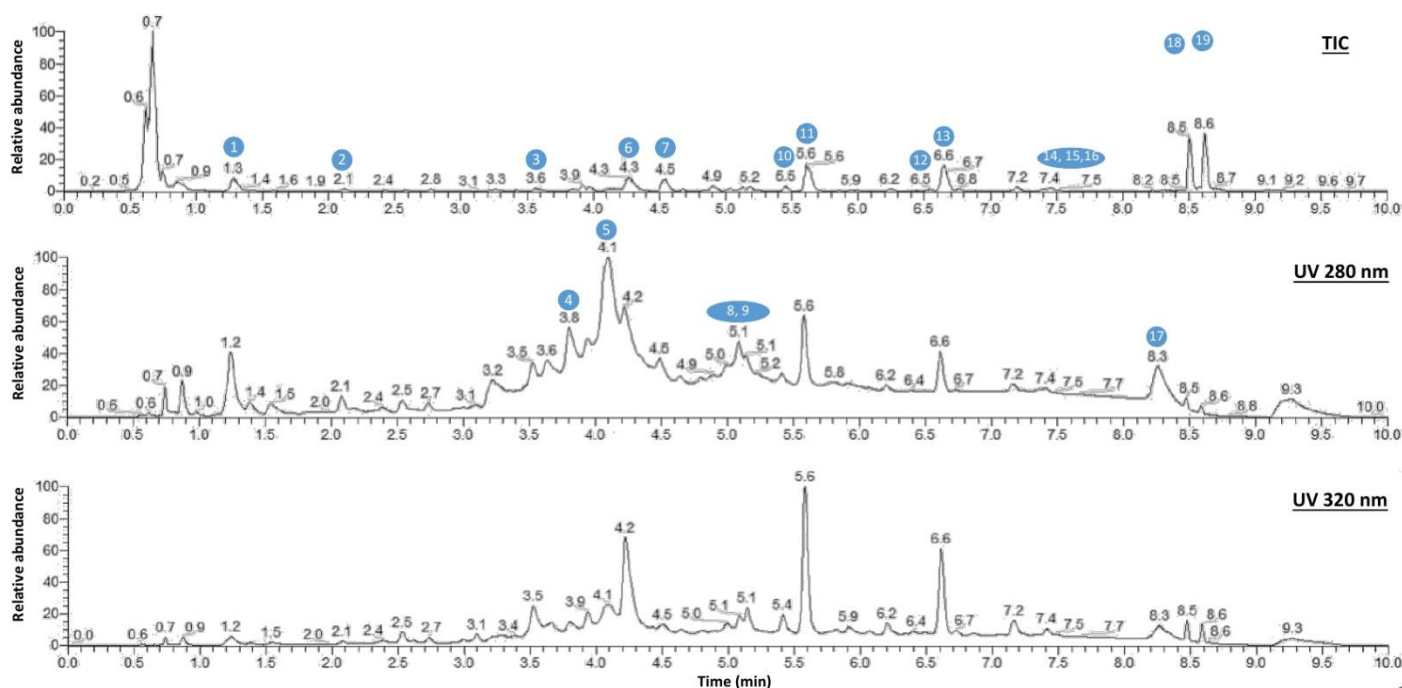
## 2. Results 100

### 2.1. Polyphenol composition of the aqueous extract of *P. mauritianum* 101

In a first step, polyphenol composition of the aqueous extract of *P. mauritianum* was 103  
determined. First, the polyphenol content was assessed by Folin-Ciocalteu method 104  
providing  $58.0 \pm 7.2$  mg GAE/g of plant dry powder. Then, the identification of com- 105  
pounds (mainly the polyphenols) from the aqueous extract of *P. mauritianum* (0.25g/L) 106  
was performed using high-resolution mass spectrometry (HR-MS). *P. mauritianum* infu- 107  
sion contained a variety of polyphenols including mainly gallic acid, caffeoylquinic acid, 108  
kaempferol derivatives, quercetin and its derivatives (Table 1). Of note, two triterpenes 109  
asiatic and corosolic acids were detected but not quantified (Table 1). 110

**Table 1:** Identification and quantification of compounds from aqueous extract of *P. mauritianum* 112  
(0.25g/L) by LC-MS/MS analysis. Spectra analysis was also performed (upper spectrum: 113  
representative total ion chromatogram (TIC) obtained in negative mode; lower spectra: HPLC-UV 114  
chromatogram obtained at 280 and 320nm). Results are expressed as mean in ng/mL. RT, retention 115  
time. Nq; not quantified. Note that numbers (in blue) shown on the different spectra corresponds to 116  
the peak numbers reported on the table. Note that some isomers were detected (ex: kaempferol 117  
hexoside) 118

Peak number	RT (min)	Compound	[M-H] <sup>-</sup>	MS/MS Fragments	Concentration in <i>P. mauritianum</i> infusion (ng/mL)
1	1.3	Gallic acid	169.0137	125.0236	172,3 ± 7,5
2	2.1	Protocatechuic acid	153.019	109.0287	5,6 ± 0,4
3	3.6	Caffeoylquinic acid	353.0886	191.0558	32,3 ± 2,1
4	3.8	Caffeic acid	179.0346	135.0445	1,6 ± 0,1
5	4.1	Caffeoylquinic acid	353.0886	191.0558	8,9 ± 1,1
6	4.3	Coumaroylquinic acid	337.0936	191.0558, 173.0452, 93.0336	nq
7	4.5	Quercetin hexoside	463.0882	300.0282	0,3 ± 0,0
8	5.1	Quercetin hexoside	463.0882	300.0282	18,2 ± 0,6
9	5.1	Quercetin-O-(acetyl-hexoside)	505.099	300.0282	2,5 ± 0,0
10	5.5	Kaempferol hexoside	447.0940	284.0332	3,7 ± 0,1
11	5.6	Kaempferol hexoside	447.0940	284.0332	32,9 ± 0,1
12	6.5	Quercetin-O-(acetyl-hexoside)	505.099	300.0282	8,3 ± 0,5
13	6.6	kaempferol-O-(acetyl-hexoside)	489.1040	284.0333, 429.0836, 447.095	20,9 ± 0,0
14	7.4	Kaempferol-O-(acetyl-rhamnoside)	473.1090	284.0333, 413.0884	3,4 ± 0,0
15	7.5	Quercetin	301.0360	151.0029, 178.9981, 121.0285	2,0 ± 0,5
16	7.6	Kaempferol-O-(acetyl-rhamnoside)	473.1090	284.0333, 413.0884	2,0 ± 0,0
17	8.3	Kaempferol	285.0411	151.0032	2,1 ± 0,0
18	8,4	Asiatic acid	487,344	-	nq
19	8,6	Corosolic acid	471,3488	-	nq





## 2.2. Toxicity of the aqueous extract of *P. mauritianum*

In order to study the toxicity of the aqueous extract of *P. mauritianum*, we first performed the well-recognized toxicity assay from the OECD guidelines 236 [56] on 3-hours post-fertilization (hpf) to 96hpf zebrafish eleutheroembryos. To this end, we incubated eleutheroembryos with a serial dilution of aqueous extract of *P. mauritianum* (1.87, 1.25, 0.83; 0.55, 0.37, 0.24 and 0.16 g/L). This treatment was renewed every day. Eleutheroembryos treated at 0.165 g/l to 0.556 g/l were alive and exhibited normal morphology according to OECD criteria, while at 0.83g/L and above, eleutheroembryos were coagulated (Fig. 1A and C). Of interest, from 0.165 g/L to 0.556 g/L, most of eleutheroembryos did not hatch as normally expected. Given that this is not a parameter of toxicity according to the OECD criteria, the LC<sub>50</sub> was estimated at 0.71 g/L.

In order to avoid any developmental toxicity, we decided to reproduce the same protocol on 3 days post fertilization (dpf) to 5dpf eleutheroembryos. From 3dpf, zebrafish morphogenesis is almost complete and eleutheroembryos have a functional liver and kidney. Similar to the first test, at highest concentrations (1.87 g/L, 1.25 g/L and 0.83 g/L), the aqueous extract led to the death of eleutheroembryos, while at lower doses, they developed normally (Fig. 1B and D). The LC<sub>50</sub> was estimated to 0.79 g/L and appeared not significantly different from the one calculated in eleutheroembryos treated from 3hpf to 96hpf (OECD assay). Consequently, the maximum non-toxic concentration (MNTC) that can be used in zebrafish eleutheroembryos was estimated at 0.556 g/L. We tested this concentration on adults and noticed immediately some behavioral abnormalities (low movement, hyperventilation) that were not observed at 0.25 g/L (data not shown). So, we decided to define 0.25 g/L as a safe dose for both eleutheroembryos and adult zebrafish, and to use this dose for further experiments.

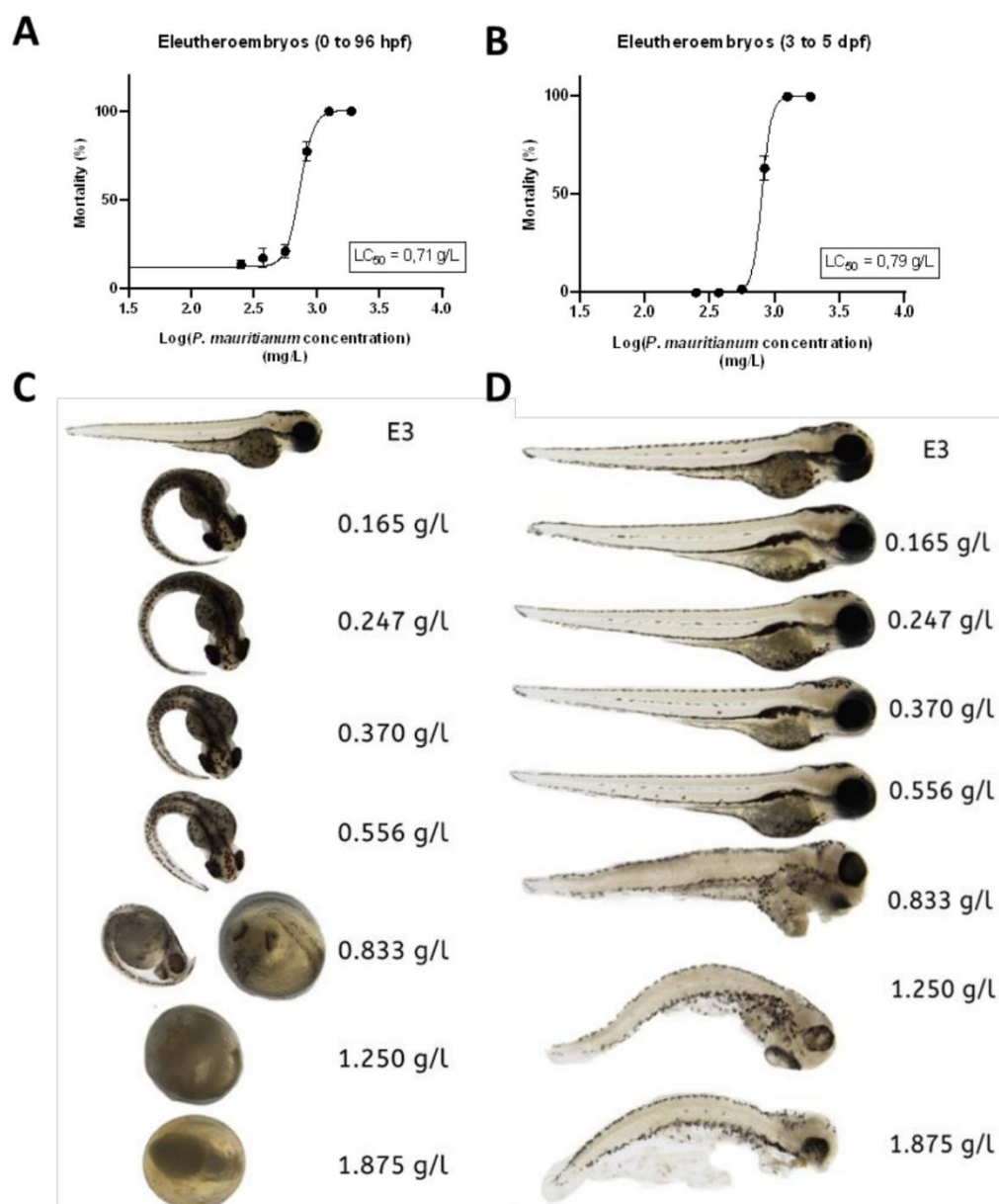


**Figure 1:** Determination of the lethal concentration  $50$  ( $LC_{50}$ ) of the aqueous extract of *P. mauritianum* on eleutheroembryos

**(A) and (B):** Survival curve showing the mortality percentages of eleutheroembryos (3hpf to 96hpf and 3dpf to 5dpf, respectively) treated with 1.87 g/L, 1.25 g/L, 0.83 g/L, 0.55 g/L, 0.37 g/L, 0.24 g/L and 0.16 g/L of the aqueous extract from *P. mauritianum*, as the function of the log *P. mauritianum* concentrations. Note that most of treated eleutheroembryos in A did not hatch. The  $LC_{50}$  were 0.71 and 0.79 g/L in A and B, respectively.

**(C) and (D):** Representative pictures of eleutheroembryos at different concentrations at the end of the experimental assay (at 96hpf for C and at 5dpf for D).

$n = 60$  eleutheroembryos for each tested concentration of three independent experiments (20 per experiment) for A and B. Data are mean  $\pm$  SD. Bar: 100  $\mu$ m.

In order to ascertain the safety of this dose, eleutheroembryos were treated from 3 to 5dpf with the aqueous extract of *P. mauritianum* (0.25g/L) and analyzed for the expression of specific genes involved in cardiac (*erg*), liver (*gclc* and *fabp10a*), and renal (*ctgf*) functions. The RT-qPCR results showed no significant change in the expression of *erg*, *ctgf* and *gclc* (Fig. 2A-C). However, *fabp10a* gene expression was significantly decreased in the

147  
148  
149  
150  
151  
152  
153  
154  
155  
156  
157  
158  
159

160  
161  
162  
163  
164

treated larvae compared to controls (Fig. 2D). This raises the question of the potential impact of the *fatty acid binding protein 10 a (fabp10a)* gene downregulation during development.

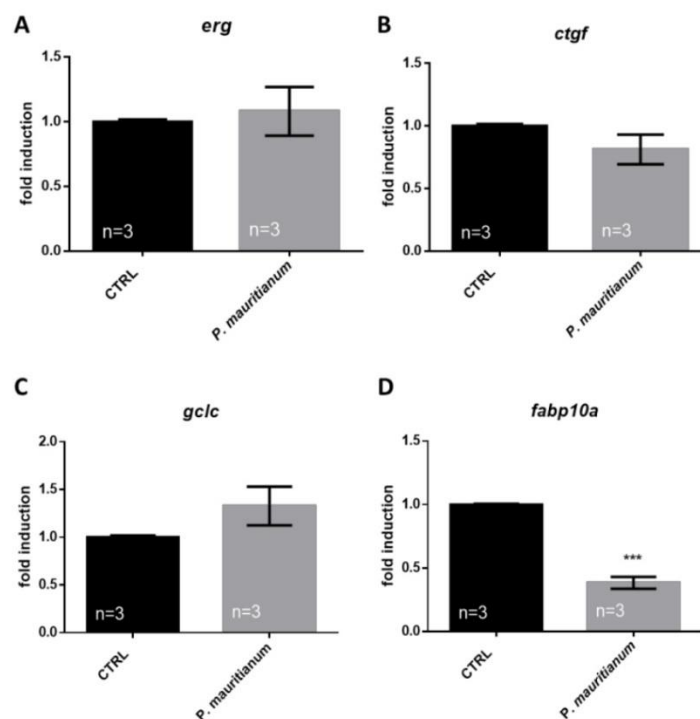


**Figure 2:** Effect of aqueous extract of *P. mauritianum* on specific markers of cardiac, renal and liver functions. (A) RT-qPCR gene expression analysis of cardiac specific gene *erg* (A), renal specific gene *ctgf* (B), and liver specific genes *gclc* and *fabp10a* (C and D), in CTRL and *P. mauritianum*-treated eleutheroembryos (3 to 5 dpf). n= 3 pools of 60 eleutheroembryos. Bar graph: standard error of the mean (SEM). Student's t-test: \*\*\* $p < 0.001$ .

### 2.3. Aqueous extract of *P. mauritianum* exhibits lipid-lowering effects in high-fat diet-fed larvae

Considering the general absence of adverse effects of the aqueous extract of *P. mauritianum* at 0.25 g/L, we decided to further explore its potential therapeutical properties. This plant is traditionally suggested to exhibit anti-lipidemic effects and so to decrease cholesterol levels. We consequently aimed to investigate these metabolic properties using a model of high-fat diet-fed larvae as previously described [57]. To this end, we separated 7dpf larvae into three group: CTRL, HFD and HFD + *P. mauritianum* (0.25 g/L). The CTRL group was fed with normal dry food (Gemma 75) and incubated in E3 medium. The HFD group was fed with 0.1% egg yolk prepared in E3 medium, and HFD + *P. mauritianum* group was fed with 0.1% egg yolk prepared in the aqueous extract of *P. mauritianum* (0.25 g/L). The medium and food were renewed every day until 11 dpf. At the end of the experimental procedure, Oil Red O staining was performed to reveal neutral triglycerides and lipid accumulation (Fig. 3). As expected, HFD larvae exhibited a stronger and wider staining than controls in the digestive tract and also in the caudal vein that were not stained in normal condition (Fig. 3A). In contrast, HFD larvae treated with *P. mauritianum* displayed a weaker staining, similar to the CTRL group (Fig. 3A). In order to further reinforce this observational result, we performed a quantification using Image J showing a significant stronger ORO staining in HFD larvae, prevented by *P. mauritianum* treatment (Fig. 3B). These experiments were repeated two times independently and led to similar results.



Consequently, the aqueous extract of *P. mauritianum* prevents lipid accumulation in the HFD fed larvae, suggesting anti-lipidemic properties.

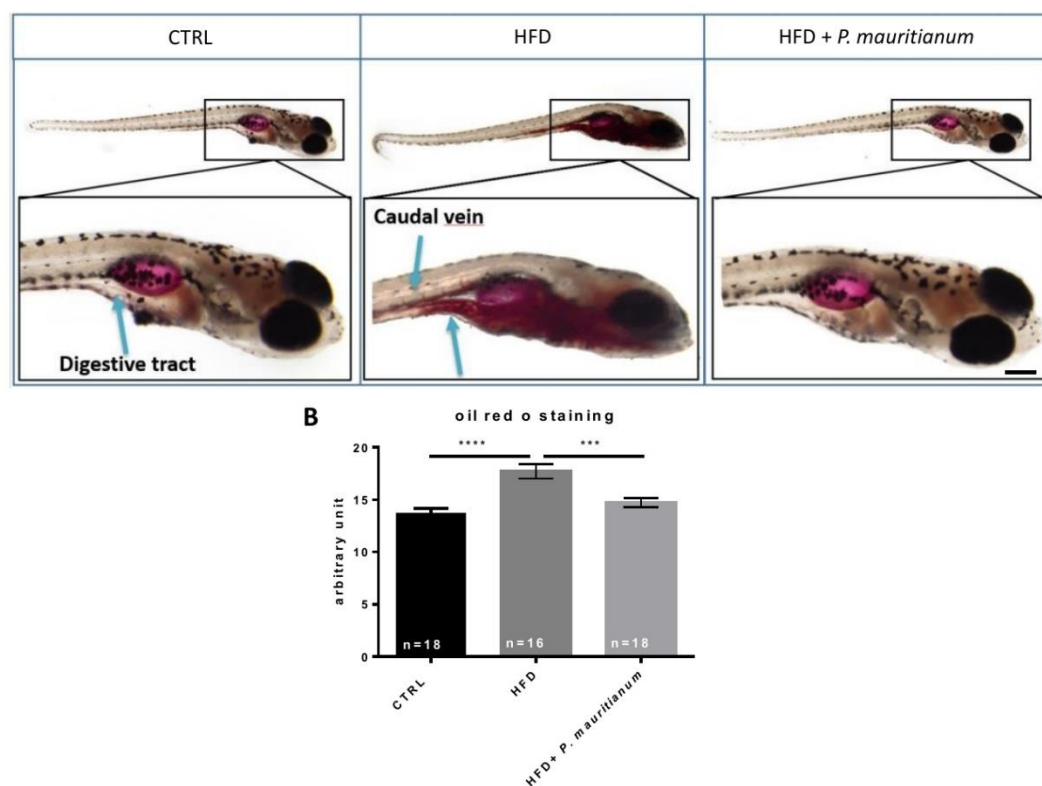


**Figure 3:** Aqueous extract of *P. mauritianum* prevents lipid accumulation in HFD larvae.

(A) Representative pictures of ORO staining in CTRL, HFD, and HFD + with *P. mauritianum* (0.25g/L).

(B) Bar graph showing Image J ORO staining quantification in CTRL, HFD, HFD + *P. mauritianum* demonstrated the efficiency of HFD treatment on lipid accumulation and the preventive effects of *P. mauritianum* on lipid accumulation.

n = 16-18 larvae from 2 independent experiments. Bar graph: standard error of the mean (SEM). One-way ANOVA (B). \*\*\* $p < 0.001$  \*\*\*\* $p < 0.0001$ . Bar: 100  $\mu\text{m}$  for low magnification and 400  $\mu\text{m}$  for high magnification larva image.

#### 2.4. Preventive effect of aqueous extract of *P. mauritianum* on overfeeding-induced weight gain in adult zebrafish

Considering the interesting properties of *P. mauritianum* in larvae, we decided to investigate its impact on a model of diet-induced obesity (DIO) previously established in adult zebrafish [28]. This model results in increased body weight, BMI and fasting blood glucose [28, 50]. From the first week of overfeeding, DIO fish gain weight compared to the CTRL fish. Interestingly, the DIO + *P. mauritianum* prevented the increase in body weight (Fig. 4A). Similar results were obtained until the 4<sup>th</sup> week (Fig. 4A and 4B). In addition, while the size of the DIO fish increased compared to CTRL ones, the DIO + *P. mauritianum* size remained similar to fish fed with normal diet (Fig. 4C). Similar results were obtained for the calculated BMI (Fig. 4D). Interestingly, the aqueous extract of *P. mauritianum* also prevented the significant increase in fasting blood glucose resulting from 4 weeks of DIO protocol (Fig. 4E). Overall, these results showed that the aqueous extract of *P. mauritianum* exhibits a protective effect on weight gain, BMI and hyperglycemia induced by DIO.



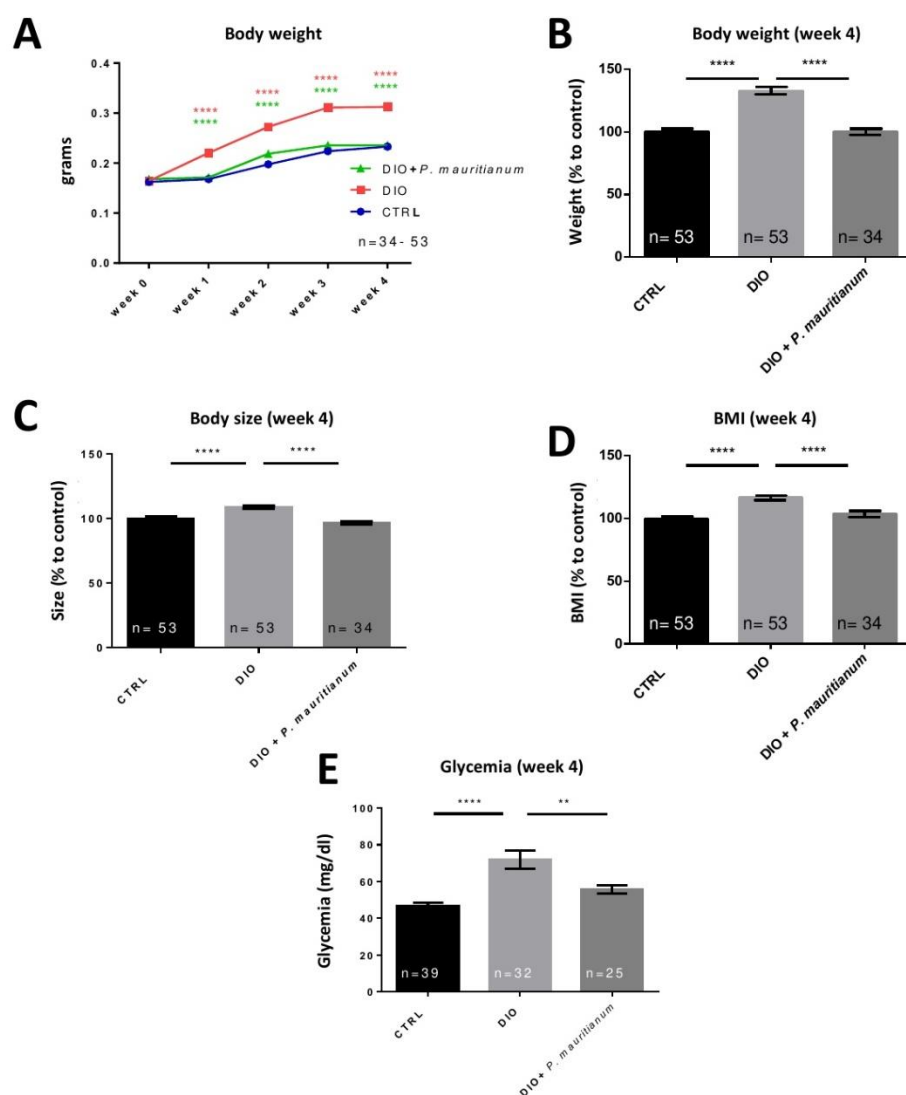


**Figure 4:** The aqueous extract of *P. mauritianum* significantly prevents body weight gain, increased BMI and hyperglycemia induced by DIO

(A) Line graph showing the increase in body weight during the experiment from week 0 to week 4 in CTRL, DIO and DIO + *P. mauritianum* (0.25 g/L) groups.

(B-E) Graphs showing the body weight (B), size (C), BMI (D) and fasting blood glucose (E) of CTRL, DIO and DIO + *P. mauritianum* at the end of the experimental procedure (week 4).

All the data result from three independent experiments providing the same results.

n = 25-53, number of fish. Bar graph: standard error of the mean (SEM). Two-way ANOVA (A); One-way ANOVA (B-E): \*\* $p < 0.01$  \*\*\*\* $p < 0.0001$ .

Liver is an important organ involved in lipid metabolism. Nonalcoholic fatty liver (NAFL) and liver steatosis are states of abnormal lipid metabolism that result in hepatic lipid accumulation and liver dysfunction. These conditions are associated with obesity and diabetes in humans as well as in many animal models such as mice and zebrafish [8, 41]. We consequently decided to study lipid accumulation by ORO staining in the liver of CTRL, DIO and DIO + *P. mauritianum*. In DIO fish, we observed abnormal lipid accumulation in the liver (Fig. 5A), while the livers of CTRL fish remained unstained. However, the ORO staining appears heterogeneous among the DIO fish, showing different individual susceptibility to liver steatosis (Fig. 5A). Interestingly, DIO fish treated with *P. mauritianum* showed only faint or undetectable ORO staining (Fig. 5A). This result was reinforced by the evaluation of the Oil Red O staining using a scoring described in the material and

227  
228  
229  
230  
231  
232  
233  
234  
235  
236  
237

238  
239  
240  
241  
242  
243  
244  
245  
246  
247  
248

methods. As shown in figure 5B, *P. mauritanum* exerts a preventive effect on lipid accumulation in the liver compared to the DIO fish.

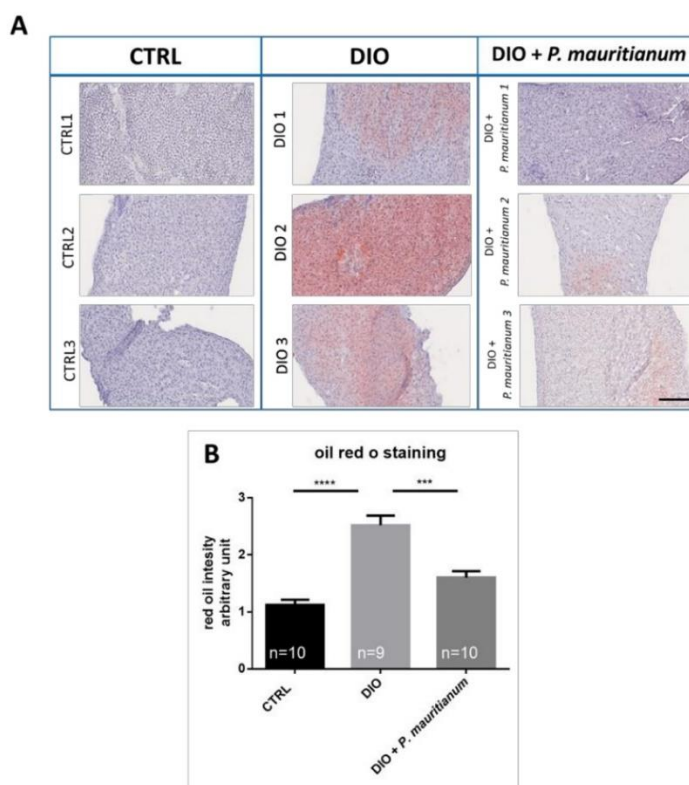


**Figure 5:** The aqueous extract of *P. mauritanum* prevents lipid accumulation in the liver of adult DIO fish

(A) Liver sections stained with Oil Red O in three representative controls (CTRL), DIO and DIO treated with *P. mauritanum* (0.25 g/L) fish, showing no lipid accumulation, heterogeneous lipid (red) accumulation and low lipid accumulation (faint red), respectively after the 4<sup>th</sup> week of feeding protocol.

(B) Red color intensity quantification on the liver sections of CTRL, DIO and DIO treated with *P. mauritanum*. Results come from two independent experiments. Score index for (B): 1: no staining, 2: medium staining, 3: high staining.

n=9-10, number of fish. Bar graph: standard error of the mean (SEM). One-way ANOVA: \*\*\* $p < 0.001$ , \*\*\*\* $p < 0.0001$ . Bar: 100  $\mu$ m.

### 2.5. *P. mauritanum* prevents brain homeostasis disruption induced by overfeeding

We then investigated whether brain homeostasis was disrupted in overfeeding conditions. Indeed, DIO is known to impair the blood-brain barrier (BBB) integrity and brain homeostasis even in fish [28, 50]. We first investigated BBB function using the Evans blue dye that is not able to cross the BBB under normal conditions. The brains of DIO fish appeared blue (with heterogeneity between animals) compared to the controls that remained white (Fig. 6A). As well, the treatment of fish with *P. mauritanum* limited the increase in brain 4-HNE levels, a marker of oxidative stress (Fig. 6B). Previously, we demonstrated that DIO induced a weak increase in neuroinflammatory state [28]. So, we decided to compare some proinflammatory markers in the brain of DIO and DIO + *P. mauritanum* fish. The RT-qPCR analysis of the whole brain shows no striking effect on *tnfa* gene expression (Fig. 6C).

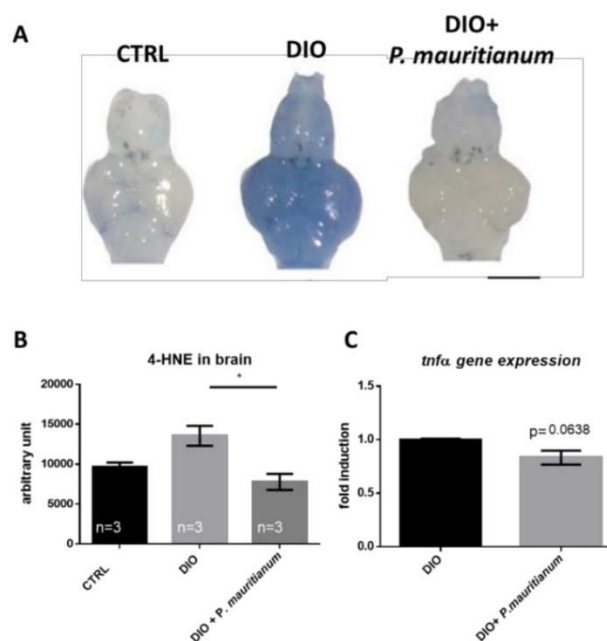


**Figure 6:** Aqueous extract of *P. mauritianum* prevents BBB leakage and brain oxidative stress

(A) Dorsal views of zebrafish brains after Evans Blue dye injection in CTRL, DIO, and DIO + *P. mauritianum* treated fish. Zebrafish brains remained mostly white except for the DIO brains. Note that in DIO, the blue staining is heterogeneous between fish.

(B) Dot blot quantification showing that the *P. mauritianum* treatment in DIO fish prevented the cerebral increase in 4-HNE levels induced by overfeeding.

(C) qPCR gene expression analysis of *tnfa* in DIO and DIO+ *P. mauritianum*.

n=5-6 number of fish brains studied for (A), n=3 pools of 2 brains for (B-C). Bar graph: standard error of the mean (SEM). Student's t-test for (B and C): \* $p < 0.05$ . Bar: 0.8 mm.

In addition, we decided to study the brain plasticity through the analysis of neurogenesis. The effects of DIO + *P. mauritianum* were analyzed in the main neurogenic niches by PCNA immunohistochemistry. In the brain of DIO fish, the number of PCNA-positive cells was generally decreased in the ventral and dorsal nuclei of the ventral telencephalon (Vv Vd), the anterior part of the preoptic area (PPa), the periventricular pretecal nucleus (PPv), the ventral zone of periventricular hypothalamus and lateral recess of the diencephalic nucleus (Hv LR), as well as along the lateral recess and posterior recesses of the diencephalic ventricle (LR PR) and the valvula cerebelli (VCe) compared to controls, as previously shown [28] (Fig. 7). In contrast, DIO fish treated with the plant extract displayed a basal neurogenesis. Indeed, in the Vv Vd, the PPa and the LR PR regions, *P. mauritianum* increased significantly the neurogenesis compared to that observed in DIO fish and the same trend was observed in the remaining regions of the brain (PPv, HvLR and VCe).



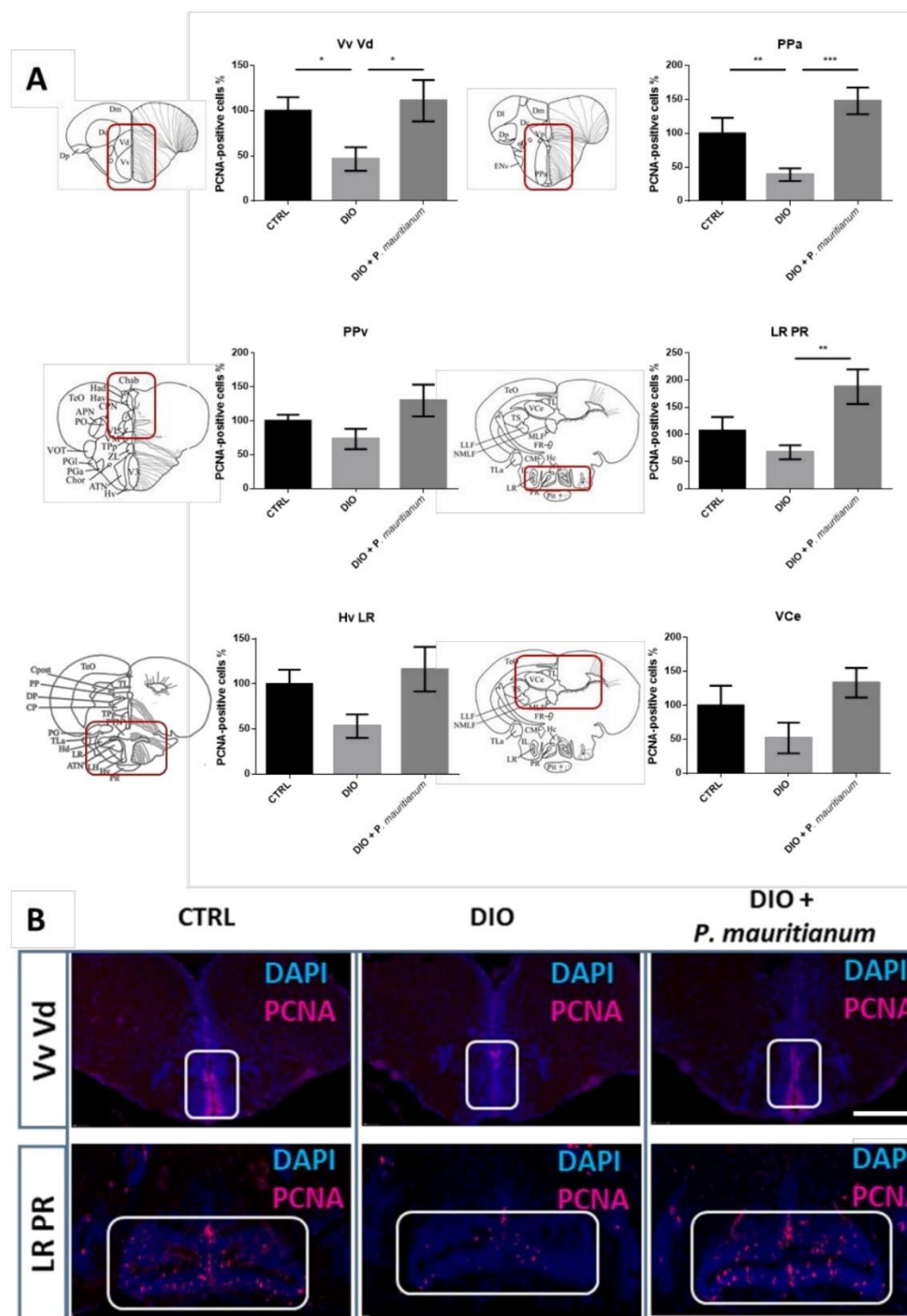


**Figure 7:** DIO reduced proliferation in the main neurogenic niches while *P. mauritianum* treatment rescued it.

(A) Statistical analysis of the number of proliferative cells (PCNA-positive) in CTRL, DIO and DIO + *P. mauritianum* treated zebrafish. The respective brain schemes correspond to the transversal sections of the zebrafish brain for each studied region showing the main brain domains/nuclei according to the Zebrafish Brain Atlas from Wullimann et al. and were adapted from Pellegrini et al. [58, 59]. DIO + *P. mauritianum* fish displayed neurogenesis similar to control in the main neurogenic niches studied.

(B) Representative pictures of PCNA immunohistochemistry (red) and cell nuclei counterstaining (DAPI in blue) on vibratome brain sections of CTRL (left) and DIO-treated fish (middle) and DIO + *P. mauritianum* treated zebrafish (right).

303  
304  
305  
306  
307  
308  
309  
310  
311  
312  
313  
314



n =5-10 number of brains studied pooled from two independent experiments. Bar graph: standard error of the mean (SEM). Student's t-test: \* $p$ <0.05; \*\* $p$ <0.01; \*\*\* $p$ <0.001. Bar = 150  $\mu$ m.

Vv: ventral nucleus of ventral telencephalic area; Vd: dorsal nucleus of ventral telencephalic area; PPa: parvocellular preoptic nucleus, anterior part; PPv: periventricular pretecal nucleus; Hv: ventral zone of periventricular hypothalamus; LR: lateral recess of diencephalic nucleus; PR: posterior recess of diencephalic ventricle; VCe: valvula cerebelli.

Taken together, the overfed fish treated with the plant extract did not show striking brain alteration at the level of the BBB, oxidative stress and neurogenesis, in contrast to untreated overfed fish. All these protective effects could be the results from the absence of metabolic disorders (weight gain, BMI, hyperglycemia).

## 2.6. Effect of *P. mauritianum* on feeding behavior and feces production

These protective effects of *P. mauritianum* suggest that DIO fish treated with *P. mauritianum* could display an altered feeding behavior. It would consequently result in no weight gain, no increase in BMI, normal fasting blood glucose and normal liver physiology. To test this hypothesis, we performed a feeding quantification by putting visible and countable feeding pellets for each group, and then compared the number of pellets eaten by each group. The DIO fish and the DIO + *P. mauritianum* fish did not display any significant change in feeding behavior (Fig. 8A), supporting our visual observations of active feeding when we fed both groups of fish 9 times a day. This indicates that fish ate the same amount of food and that the preventive effects of *P. mauritianum* was not due to reduced calorie intake. However, we noticed that the quantity of feces excreted from DIO fish treated with *P. mauritianum* was increased compared to DIO fish. After weighing the feces produced by each group during the night for 5 days, we obtained a significantly higher feces production in the DIO fish treated with *P. mauritianum* than in DIO and CTRL group (note that a student t-test comparing the feces production between CTRL and DIO group shows a significant increase in feces production in DIO) (Fig. 8B).

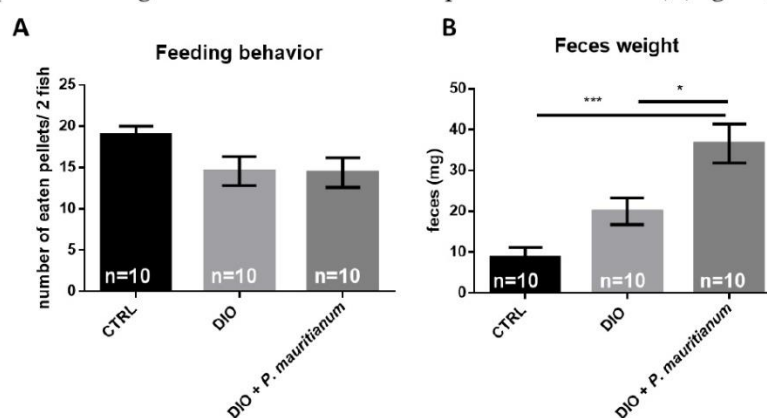


**Figure 8:** *P. mauritianum* does not impact feeding behavior and favors feces excretion

(A) Graph showing the number of pellets consumed by fish for 5 days in CTRL, DIO and DIO treated with *P. mauritianum* groups.

(B) Quantification of the feces weight excreted by the fish for 5 days in the CTRL, DIO and DIO treated with *P. mauritianum* groups.

n=10, number of zebrafish used in the experiment for 5 days (2 fish/tank/day). The feeding behavior in (A) was assessed for fish each day and in (B) the feces excretion was measured for 10 fish. Bar graph: standard error of the mean (SEM). One-way ANOVA: \* $p$ <0.05, \*\*\* $p$ <0.001.

## 2.7. Aqueous extract of *P. mauritianum* has no impact on brain homeostasis under normal chow feeding conditions

Aiming to test the effect of *P. mauritianum* on the brain, regardless its effect on preventing the increase in the body weight, we decided to normally feed zebrafish and treat them overnight for 3 days with *P. mauritianum*, in order to analyze by RT-qPCR the expression of genes involved in BBB function, inflammation, brain plasticity and brain cell proliferation. The first group (CTRL) was kept in the water while the second was treated with aqueous extract of *P. mauritianum* (0.25 g/L) overnight for 3 days. At the end of this experimental procedure, no change in body weight was observed (data not shown) and fish behaved normally. The brains were extracted and processed for gene expression analysis. We did not observe any significant change in gene expression of the inflammatory transcription factor (*nfkb*), tight junction protein (*claudin 5*), brain plasticity marker (*cyp19a1b*) and proliferative marker (*pcna* and *ccna2*) (Fig. 9). These data reinforce the hypothesis that the preventive effect of *P. mauritianum* on the brain of overfed fish was due to the prevention of body weight increase and hyperglycemia and not to the effects of *P. mauritianum* polyphenols and their metabolites on the brain.

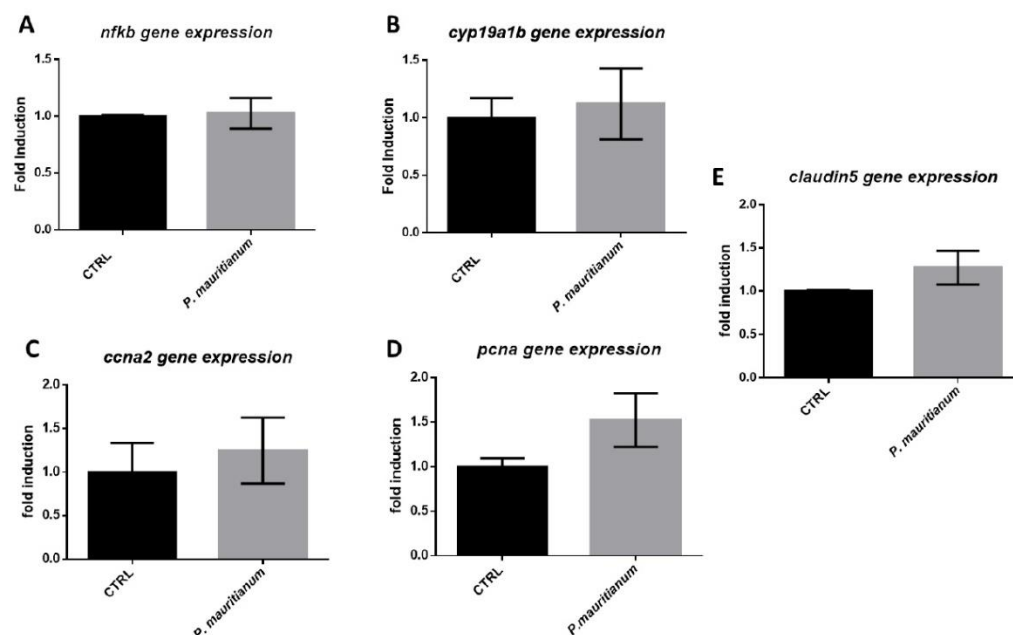


**Figure 9:** *P. mauritianum* has no effect on brain homeostasis in normal feeding conditions.

RT-qPCR gene expression analysis of nuclear factor kappa B (*nfkb*) a transcription regulator of inflammation (A), aromatase B gene (*cyp19a1b*) a brain plasticity marker (B), cyclin-a2 gene (*ccna2*) and proliferating cell nuclear antigen (*pcna*) brain, two cell proliferation markers (C and D) and claudin 5, a tight junction gene involved in the blood-brain barrier integrity (*claudin5*) (E). n=3 pools of 2 brains. Bar graph: standard error of the mean (SEM). Student's t-test.

## 2.8. Therapeutic effects of aqueous extract of *P. mauritianum* on weight gain

We next wondered whether aqueous extract of *P. mauritianum* could display a therapeutic effect. For this purpose, all fish were fed according to the DIO protocol for one week without any plant treatment. As shown in figure 10A, the body weight of DIO fish increased significantly compared to control fish. After this one week of overfeeding, a subgroup of DIO fish was treated with *P. mauritianum* for one more week still in overfeeding condition (DIO + *P. mauritianum*), while the other subgroup was just overfed (DIO). The body weight of the DIO and DIO + *P. mauritianum*-fed fish were significantly higher than



the control group. However, the weight gain of *P. mauritianum*-treated fish was less pronounced than for DIO. The fasting blood glucose measured at week 2 shows 50% higher glycemia in the DIO compared to CTRL fish and only 30% higher glycemia in DIO + *P. mauritianum* treated fish compared to CTRL (Fig. 10B). So, *P. mauritianum* limited the sharp increase in glycemia. In the brain, no significant change in cell proliferation was observed between all groups (data not shown).

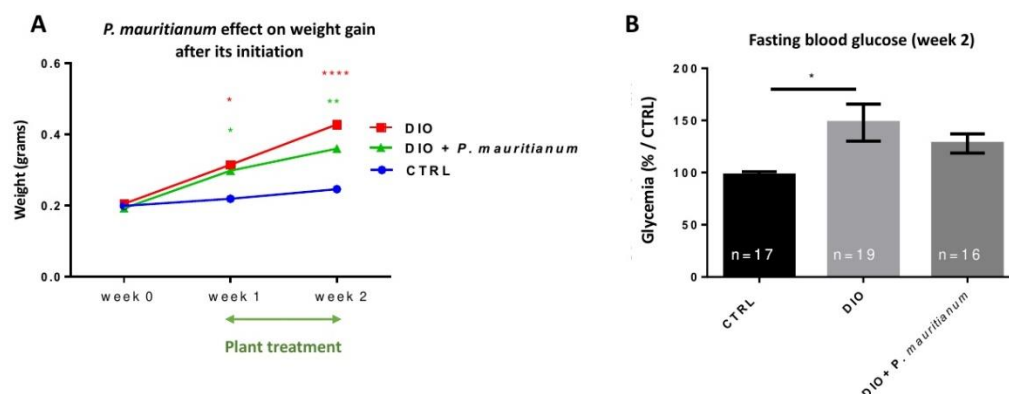


**Figure 10:** Aqueous extract of *P. mauritianum* limited the increase in the body weight and glycemia after the onset of weight gain.

(A) Line graph showing the increase in the body weight during the experiment from week 0 to week 2 in the CTRL, DIO and DIO + *P. mauritianum* groups. The green “double-arrow” represents the plant treatment from week 1 to week 2.

(B) Bar Graph showing fasting blood glucose of CTRL, DIO and DIO + *P. mauritianum* at the end of the experimental procedure (week 2).

n = 16-19, number of fish. Bar graph: standard error of the mean (SEM). Two-way ANOVA (A); One-way ANOVA (B): \* $p < 0.05$  \*\* $p < 0.01$  \*\*\*\* $p < 0.0001$ .

### 3. Discussion

*P. mauritianum* is a plant widely used for its traditional benefit in Mascarene Islands (Mauritius and Reunion Islands) considering its anti-cholesterol and “anti-diabetic” effects [30, 31]. Recent scientific experimentations on this medicinal plant have demonstrated its anti-bacterial, antiviral, anti-inflammatory and antioxidant properties [23, 24, 60, 61]. In this study, we investigated for the first time the *in vivo* toxicity of an aqueous extract of *P. mauritianum* according to the OECD guidelines using the zebrafish model. We determined a maximum non-toxic concentration of 0.25g/L on eleutheroembryos and adults and showed that this dose has interesting lipid-lowering properties in HFD larvae and anti-weight gain in overfed adult fish. This dose also prevents the deleterious impact of overfeeding on peripheral metabolic parameters (BMI, glycemia, liver steatosis) and also on the brain, probably through the absence of development of metabolic disruption in overfed fish treated with *P. mauritianum* extract. Very interestingly, our data also demonstrate that treated fish have an increase feces production, probably due to changes in gut microbiota and intestinal absorption.

#### Composition of aqueous extract of polyphenols

Performing LC-MS/MS, we observed that aqueous extract of *P. mauritianum* contained many polyphenols including mainly gallic acid, caffeoylquinic acid, kaempferol derivatives, quercetin and its derivatives. Also, two interesting triterpenoids, asiatic and corosolic acids were also in *P. mauritianum* extract. Our laboratory previously demon-

strated that other medicinal plants contained caffeic acid, caffeoylquinic acid (i.e., chlorogenic acid), dicaffeoylquinic acid and some kaempferol hexoside and quercetin hexoside as well as their respective derivatives for *A. borbonica* [25, 62], 5-caffeoylquinic acid (chlorogenic acid), quercetin glycosides and kaempferol glycosides and their respective derivatives for *H. lanceolatum* [57], and most of these compounds are also detected in other medicinal plants [23]. The particularity of *P. mauritianum* probably lies in the fact that its aqueous extract is rich in gallic acid, and contains two triterpenoids (asiatic and corosolic acids) with properties of interest regarding metabolic disorders [63, 64].

### Toxicity of the aqueous extract of *P. mauritianum*

Our toxicity assay following the guidelines of the fish acute toxicity assay from the OECD gave us similar LC<sub>50</sub> of 0.71 and 0.79 g/L for eleutheroembryos treated from 3hpf to 96hpf and 3dpf to 5dpf, respectively. The maximum non-lethal concentration determined in eleutheroembryos toxicity assays was theoretically around 0.5 g/L. However, at this concentration, eleutheroembryos (3hpf to 96hpf) did not hatch and behavioral change have been observed in adults. Considering this point, we performed our experiments at 0.25 g/L during developmental and adult stages. Indeed, this dose exhibited no apparent signs of disturbance in both eleutheroembryos and adults (i.e. normal behavior and feeding). In addition, gene expression of most genes involved in cardiac, hepatic and renal functions remained at normal level in eleutheroembryos. Nevertheless, we observed a significant decrease in *fabp10a* gene expression (fatty acid binding protein 10a or liver bile acid-binding protein) that is responsible for the intracellular binding and trafficking of long chain fatty acid to the liver and that is sometimes used as a hepatic toxicity marker [65-67]. However, some data also document its expression in the ventral endoderm during development [65], raising the question of the cells downregulating its expression following *P. mauritianum* treatment during embryogenesis. It could be interesting to further investigate the protein expression and function of this fatty acid binding protein in the clearance of lipids and their metabolism under *P. mauritianum* treatment to ascertain its non-toxic effects in developmental and adult stages. Of interest, this fatty acid binding protein is also expressed in the intestine of adult zebrafish and maybe could be involved in lipid absorption [68].

### Effects of the aqueous extract of *P. mauritianum* on metabolic parameters

The dose of 0.25 g/L limited lipid accumulation in HFD larvae (i.e., digestive tract + blood vessels and liver) and in overfed adult fish (i.e., liver). These findings support the traditional lipid-lowering effect of *P. mauritianum*. Indeed, this medicinal plant is supposed to increase cholesterol elimination from the body, and recent work also showed the decrease in oxidized-LDL uptake by the macrophages under *P. mauritianum* treatment [19, 24, 30]. Of interest, *P. mauritianum* exerts striking effects on overfed adult zebrafish (DIO protocol) by preventing weight gain, increased BMI, hyperglycemia and liver steatosis, and consequently improving almost all deleterious effects induced by overfeeding. Indeed, the body weight of DIO fish treated with the plant extract followed the same trend as the CTRL group during the 4 weeks of the experimentation. This result is not the consequence of a modification in feeding behavior as DIO + *P. mauritianum* fish ate the same amount of food as DIO fish. Also, in a therapeutic approach, we demonstrated that after 1 week of overfeeding and the establishment of weight gain, a treatment with *P. mauritianum* partly reduced weight gain and normalized glycemia. Such effect was also observed with another medicinal plant *H. lanceolatum* rich in quercetin, kaempferol and chlorogenic acid [27, 57]. So, this result raises the question of the compounds behind this effect and suggests the potential role of common polyphenols found in *H. lanceolatum* and *P. mauritianum* such as quercetin, kaempferol and their respective derivatives.



### **Aqueous extract of *P. mauritianum*: polyphenol content, lipid absorption/metabolism and microbiota**

DIO fish treated with *P. mauritianum* have a higher production of feces compared to DIO fish. It suggests that *P. mauritianum* could affect lipid absorption and gut microbiota in overfeeding condition. This is particularly interesting given that the aqueous extract of *P. mauritianum* is enriched in polyphenols, and that polyphenols modulate microbiota and nutrients absorption/metabolism [69]. According to the LC-MS/MS analysis for polyphenol identification, the aqueous extract of *P. mauritianum* is rich in gallic acid, caffeoylquinic acid, kaempferol hexoside and derivatives as well as in quercetin and derivatives, corroborating data obtained in previous work [23].

Interestingly, the kaempferols tested on high-fat diet obese mice were capable of reverting the disorders resulting from obesity including body weight, glucose intolerance and fat accumulation [70] similarly to what we observed by preventive treatment with *P. mauritianum* in DIO zebrafish. More interestingly, fecal microbiota analysis showed the capability of the kaempferol treatment to alleviates the gut dysbiosis resulting from obesity [70]. This anti-obesity effect displayed by kaempferols on the high-fat diet mouse model, and its way of action, resembles strongly the anti-obesity effect of *P. mauritianum* extract treatment in the zebrafish model of DIO. As well, several studies confirm the role of quercetin in ameliorating the dysbiosis state resulting from abdominal obesity [71], and in reducing insulin resistance in diet-induced models [72]. *In vitro* and *in vivo* studies indicate that gallic acid could positively affect gut microbiota and decrease the growth of pathogenic bacteria [73]. It was also shown that gallic acid improves glucose tolerance, lipid metabolism, adipocyte hypertrophy and inflammation in obese mice [74, 75]. Finally, Rangasamy and collaborators identified two triterpenoid molecules present in *P. mauritianum*: corosolic and asiatic acids [32], that were also identified in our LC-MS/MS analysis (table 2). Interestingly, asiatic acid was shown to limit the deleterious effects of obesity and diabetes in diabetic mice and HFD rats [63, 64].

Together, the anti-obesity effect of *P. mauritianum* extract could be exerted by a synergy of its main polyphenols acting on the gut microbiota, lipid absorption and metabolism. It will be interesting to further explore the impact of *P. mauritianum* extract on the (i) reduction of lipid intestinal transport, (ii) the reduction of plasma cholesterol, lipoproteins and triglycerides, and (iii) on their elimination. Also, the protective effect of *P. mauritianum* against the increased glycemia in overfed fish could reflect the “anti-diabetic” property of this traditional plant. This property is probably achieved through the prevention of weight gain and liver steatosis, that are both enhancers for a prediabetic state and increased glycemia [76, 77]. Further investigations are now necessary to determine the polyphenol or polyphenol cocktail behind the beneficial properties of *P. mauritianum* on weight gain in our model (gallic acid, kaempferols, corosolic and asiatic acids?)

### **Aqueous extract of *P. mauritianum* and brain homeostasis**

Under overweight and obesity conditions, brain homeostasis is impaired in both mammals and zebrafish [28, 50, 78]. We and others have previously demonstrated that DIO disrupts brain homeostasis by inducing BBB breakdown, cerebral oxidative stress and neuro-inflammation associated with impaired neurogenesis [28, 37, 38, 50, 54, 55, 79]. In our study, we confirmed this decreased brain plasticity observed in overfeeding conditions. Interestingly, overfed fish treated with *P. mauritianum* have a “normal” neurogenesis, BBB function and cerebral redox balance. The antioxidant capacity and protective effect of *P. mauritianum* extract against oxidative stress have been documented *in vitro* and are supported by bioactive polyphenols as phenolic acids and flavonoids [23]. In rat models of metabolic disorder (hypercaloric diet), gallic acid improves neurological parameters (memory, redox status) that were disrupted by the diet [80]. However, the potential ben-

eficial effects of *P. mauritianum* on CNS protection is probably due to the absence of metabolic disorders in this overfed fish model. Indeed, the treatment of normally fed zebrafish with the plant extract did not impact the expression of genes involved in BBB function, inflammation and brain cell proliferation. Consequently, the preventive effect of the plant extract on the brain could be due to its indirect effect on the prevention of obesity development and its subsequent consequences (i.e., hyperglycemia), that are factors disrupting the brain homeostasis [28, 52].

## Conclusion

We determined the non-toxic dose for aqueous extract of *P. mauritianum* (0.25 g/L) in eleutheroembryos and adult zebrafish. In drugstore and traditional medicine, 1 to 5 g of dried leaves should be infused in 1 liter of water for 10-15 min, and drunk during the day. Considering that only a small percentage of total polyphenolic compounds may be absorbed in the small intestine, and considering the metabolism of polyphenols, we can consider that the dose used in zebrafish is higher than in humans. In zebrafish, we demonstrated for the first time to our knowledge that the 0.25 g/L dose shows real lipid-lowering effects in HFD treated larvae and overfed adults. Similarly, *P. mauritianum* at 0.25 g/L displays a preventive effect against the increase in body weight, glycemia and liver steatosis following overfeeding. It also improves metabolic parameters such as weight and fasting blood glucose after the onset of body weight gain. Therefore, our data confirmed that *P. mauritianum* extract could be an interesting “lipid-lowering” and “anti-diabetic” treatment. In addition, *P. mauritianum* has also an impact on feces production. Future work should further explore its role on gut functions (lipid absorption and metabolism) and on gut microbiota. It would be consequently crucial to further investigate such properties on preclinical models of obesity and/or diabetes, such as HFD or *db/db* mice, in order to better understand the mechanisms and compounds responsible for these interesting properties of *P. mauritianum*.

## 4. Materials and Methods

### *Animals and ethics*

Three- to four-month-old adult wildtype male and female zebrafish (*Danio rerio*) were obtained from our zebrafish facility and were maintained under standard conditions of temperature (28.5 °C), photoperiod (14 h dark/10 h light), pH (7.4) and conductivity (400 µS). Zebrafish embryos were obtained from the crossing of adult animals and were maintained in Embryonic medium (E3 as prepared by [81]) at 26.5°C. All experiments were conducted in accordance with the French and European Community Guidelines for the Use of Animals in Research (86/609/EEC and 2010/63/EU) and approved by the local Ethics Committee for animal experimentation of CYROI and the French Government (APAFIS\_20191105105351\_v10 and APAFIS\_2021080209405969\_v8).

### *Eleutheroembryos toxicity assay*

The toxicity tests were performed according to the OECD test guide line 236 [56]. Newly fertilized zebrafish eggs (< 3 hours post fertilization (hpf)) were incubated until 96 hpf to different aqueous extract concentrations of *P. mauritianum* (1.87, 1.25, 0.83, 0.55, 0.37, 0.24 and 0.16 g/L), or kept in E3 embryo medium as control condition. The treatment was done on 20 embryos/concentration and renewed every day. Four apical endpoints were recorded daily as indicators of acute lethality: coagulation of the embryo, lack of somite formation, non-detachment of the tail bud from the yolk sac and lack of heartbeat.

The concentration of the aqueous extract leading to 50% of death (LC<sub>50</sub>) was calculated and the maximum non-toxic concentration (MNTC) was determined as 0.25g/L

### *Larvae overfeeding protocol*

In order to analyze the potential lipid-lowering effects of the plant extract, we selected 7 days post fertilization (dpf) larvae that were divided into 3 groups (CTRL, HFD, HFD + *P. mauritianum*; 20 per group) according to a previously established protocol [27]. CTRL group was fed with normal food (GEMMA 75), HFD group with 0.1% egg yolk diluted in E3 medium, and HFD + *P. mauritianum* with 0.1% egg yolk dissolved in the aqueous extract (0.25 g/L) prepared in E3 medium. The treatment was renewed every day with freshly prepared solution and diet. At 11 dpf, the larvae were anesthetized and fixed for Oil Red O (ORO) labelling.

### *Diet-induced overweight/obesity (DIO) protocol*

Adult zebrafish (3 to 4 months) were divided into 2 or 3 groups (CTRL and DIO or CTRL, DIO, DIO + *P. mauritianum* at 0.25g/L). Fish were distributed to each tank at the same density per group (10 to 20 fish maximum per 3.5 L tank, according to the experiment). Adult zebrafish were fed as described previously in [28]. Briefly, the control group was fed once a day with dry food in the morning (15 mg/fish/day, GEMMA 300, Planktovie) and freshly hatched artemia (6 mg/fish/day, Artemia cysts; REF: B052-P) in the afternoon. The DIO and DIO + *P. mauritianum* group were fed six times a day with dry food (52.5 mg/fish/day) and three times with freshly hatched artemia (30 mg/fish/day) in the afternoon. These treatments were performed on a two- or four-week period according to experiments (see below).

### *Plant material and preparation of the aqueous plant extract for toxicity tests and preventive/therapeutic treatments*

Leaves of *P. mauritianum* (Industrial lot: FLBPM 20180427; GPS coordinate: -20.947334, 55.548979") were obtained from the Cooperative des Huilles Essentielles de Bourbon (CAHEB). Leaves were dried, crushed and stored at -20 °C. Aqueous extracts of *P. mauritianum* were prepared every day to renew the treatments performed on eleutheroembryos, larvae and adult zebrafish, respectively.

Briefly, for toxicity assay in eleutheroembryos, infusion of 0.75 g of *P. mauritianum* was done with 50 ml of boiled E3 for 10 min under agitation. The solution was next filtered and a serial dilution was done to obtain the following concentrations 1.87, 1.25, 0.83, 0.55, 0.37, 0.24 and 0.16 g/L. A similar protocol was done for the treatment of HFD larvae at 0.25 g/L.

To prepare the plant infusion for adults, 0.5 g of crushed plants was infused with 250 mL of boiled fish water for 10 min under agitation. After filtering, 250 mL of *P. mauritianum* extract was added to 1.750 L of fish water to reach a final volume of 2L (final concentration of *P. mauritianum*: 0.25 g/L). Adult fish were treated with *P. mauritianum* from 6 PM to 8 AM (5 days a week) during the whole experimental DIO protocol. The overfeeding protocol occurs during 4 weeks for the preventive treatment. For the therapeutic treatment, fish were overfed under a DIO protocol during 1 week before being treated with *P. mauritianum* for 1 week. During these overnight *P. mauritianum* exposure, all the groups (CTRL, DIO, DIO + *P. mauritianum*) were maintained out of the fish system with a same volume of water.

### ***Body weight, body mass index (BMI) and fasting blood glucose measurements***

Every week, fish of each group were weighted. After being fished using a net and dried on a tissue paper, they were briefly weighed and immediately placed back into water. This procedure lasted around 20 seconds. In addition, the body length of the fish was measured at the beginning (first day, during the weighing process) and at the end of the experiments in order to calculate the BMI as previously described [28, 50]. Fasting blood glucose was measured using a glucometer as previously described [39, 52]

### ***Tissue preparation***

At the end of the experimentations, fish were euthanatized before being fixed in 4% PFA (Paraformaldehyde) dissolved in 1X Phosphate Buffer Saline (PBS). For cryostat sections, the liver was dissected and cryopreserved by an overnight incubation in 1X PBS, containing 30% sucrose. Then, they were embedded in OCT matrix and cut using a cryostat at 12  $\mu\text{m}$  thickness. For vibratome sections, the brain was dissected from fixed fish in 4% PFA for overnight. Brains were kept in 100% methanol at  $-20^{\circ}\text{C}$  for immunohistochemistry. For qPCR or protein analyses, the tissues of interest were immediately dissected, snap-frozen and kept at  $-80^{\circ}\text{C}$ .

### ***Oil Red O (ORO) staining***

For ORO staining in HFD larvae, after euthanasia and overnight fixation in 4% PFA at room temperature, samples were washed and dehydrated. Oil Red O (Sigma-Aldrich; REF: 00625) was dissolved in 60% isopropanol (final concentration: 0.15% Oil Red O in 60% Isopropanol). The larvae were kept in Oil Red O solution overnight at room temperature. After rehydration and washing in 1X PBS, larvae were finally imaged with a binocular microscope. The staining intensity was measured using image J.

For ORO staining on the liver of CTRL, DIO, DIO + *P. mauritianum* fish, frozen liver sections were rehydrated and rinsed with 60% isopropanol. The liver sections were stained for 40 min with the freshly prepared Oil Red O (Sigma-Aldrich; REF: 00625) according to a standard protocol. The sections were incubated for 30 s with Mayer's hematoxylin for nuclei counterstaining. Finally, the sections were dehydrated and mounted with mounting medium (IMM Ibbidi; REF: 50001). After imaging with the nanozoomer S60 (Hamamatsu) the red intensity was evaluated manually according to a standard scale by 2 independent individuals blindly. The scale score is "1" for the no red staining, "2" for medium red staining and "3" for high/intense red staining.

### ***RNA extraction and reverse transcription***

Zebrafish brains were removed from the skull, pooled ( $n=2$ ) and stored at  $-80^{\circ}\text{C}$  for the later RNA extraction. Similarly, euthanized larvae were pooled ( $n=40$ ) and stored at  $-80^{\circ}\text{C}$ . Three pools of brains or larvae were grinded with TissueLyser II (Qiagen, Chatsworth, CA) and RNA extraction was performed using RNA easy Mini Kit (Qiagen) according to manufacturer's protocol. Then, reverse transcription for 2  $\mu\text{g}$  of RNA into cDNA using random hexamer primers was performed (Invitrogen, REF: 100026484) and MMLV reverse transcriptase (Invitrogen, REF: 28025-021).

### ***Gene expression analysis by qPCR***

Semi-quantitative PCR experiments were performed using the Biorad CFX Connect Real-Time System using the SYBR green master-mix (Eurogentec) and specific zebrafish primers. Each PCR cycle was conducted for 15 s at  $95^{\circ}\text{C}$  and 1 min at  $60^{\circ}\text{C}$ . Melting curve analyses and PCR efficiency were performed to confirm correct amplification. Results



were analyzed and the relative expressions of the pro-inflammatory cytokine genes (*il8*) and the Nuclear Factor Kappa-B (*nfkb*), liver toxicity genes fatty acid binding protein 10a (*fabp10a*) and Glutamate-Cysteine Ligase Catalytic Subunit (*gclc*), the cardiac toxicity gene ether-a-go-go related gene (*erg*), kidney toxicity marker connective tissue growth factor (*ctgf*), proliferative markers (*pcna* and *ccna2*) and , tight junction protein gene (*claudin5*) and brain plasticity marker (*cyp19a1b*) were normalized against the housekeeping elongation factor 1-alpha (*ef1a*) gene. The sequences of the primers are provided in Table 2.

**Table 2.** Zebrafish qPCR primer sequences

Gene	Forward primer	Reverse primer
<i>ef1a</i>	AGCAGCAGCTGAGGAGTGAT	CCGCATTTGTAGATCAGATGG
<i>erg</i>	CAGATGCTCCGTGTGAAAGA	TGCGGTTTCAGATGAAGACAG
<i>fabp10a</i>	CCAGTGACAGAAATCCAGCA	GTTCTGCAGACCAGCTTTCC
<i>gclc</i>	AAAATGTCCGGAAGTATCG	AACGTTTCCATTTTCGTTGC
<i>tnfa</i>	GCGCTTTTCTGAATCCTACG	TGCCAGTCTGTCTCCTTCT
<i>claudin 5</i>	TCCTGGGTCTGATCCTGTG	CTCGATGAAGGCGGTGAC
<i>ccna2</i>	AAAGCAGCTAACAACAGGACAGT	GGTTTACACGCAATTATCTGTGG
<i>cyp19a1b</i>	TCGGCACGGCGTGCAACTAC	CATACCTATGCATTGCAGACC
<i>pcna</i>	GGACAGAGGAGTGGCTTTGG	CTCACAGACCAGCAACGTCG
<i>ctgf</i>	CTCCCAAGTAACCGTCGTA	TCCACCAAAACACACAAGTGG

### Immunostainings

For immunohistochemistry experiments, cryostat and vibratome sectioning were applied. For cryostat sectioning, cryostat sections were rehydrated twice with PBS containing 0.2% Triton X100 (PBS-T). Antigen retrieval was performed using sodium citrate (pH 6) heated at 80 °C for 15 min. Sections were washed twice in PBS-T before being blocked in PBS-T containing 2% BSA. Next, sections were incubated with the following primary antibodies: rabbit anti zebrafish L-plastin (kindly provided by Dr Michael Redd [82]) and/or mouse anti-PCNA (1:100; clone PC10, Dako; RRID: M0879) overnight at room temperature. The slides were then washed twice in PBS-T and incubated with DAPI (4',6'-diamidino-2-phenylindole) and secondary antibodies: donkey anti-rabbit Alexa Fluor 488 for L-plastin (1:300; REF: A21206; Life Technologies, Bethesda, MD; RRID: AB\_10049650) and goat anti-mouse Alexa Fluor 594 or 488 for PCNA (1:300; REF: A11005 for Alexa 594 and A28175 for Alexa 488; Life Technologies; RRID: AB\_141372 and AB\_2536161) for 1h30 at room temperature. Sections were rinsed and the slides were mounted with anti-fading medium (IMM Ibidi; REF: 50001).

For vibratome sectioning, brains were rehydrated, washed in 1X PBS and included in agarose to be process for vibratome sectioning (50 µm thickness). Sections were blocked in PBS-T containing 2% BSA. Next, sections were incubated with the following primary antibody: mouse anti-PCNA (1:100; clone PC10, Dako; RRID: M0879) overnight at 4°C.

The sections were then washed and incubated with DAPI (4',6'-diamidino-2-phenylindole) and secondary antibodies: goat anti-mouse Alexa Fluor 594 or 488 for PCNA (1:300; REF: A11005 for Alexa 594 and A11001 for Alexa 488; Life Technologies; RRID: AB\_AB\_2534073 and AB\_2534069) for 2h at room temperature. Sections were rinsed and the slides were mounted with Aqua-Poly/Mount (Polysciences). Note that PCNA antibody allows the detection of proliferative cells along the neurogenic niches as previously described [83].

#### ***Investigation of BBB permeability (Evans Blue dye injection)***

Evans Blue dye was used as a tracer to assess the permeability of BBB [84]. Briefly, fish were anesthetized with 0.02% tricaine and intraperitoneally injected with 1% Evans Blue dye diluted in PBS (10  $\mu$ L of 1% Evans Blue for 0.1 g of zebrafish body weight) before being put back in water. After 10 min, injected fish were sacrificed and heads were fixed with 4% PFA-PBS. Finally, the brains were dissected to be imaged.

#### ***Protein extraction and dot blot***

Zebrafish brain were lysed with TRIS HCl buffer (50 mM pH7.4 EDTA 0.01 mM) and centrifuged (10,000 rpm, 4  $^{\circ}$ C for 5 min). Supernatants were collected and frozen at  $-80^{\circ}$ C. Following manufacturer's protocol, protein concentration was determined according to Bradford protein assay. For dot blot analysis, 20  $\mu$ g of protein were plotted on a nitrocellulose membrane. Following Ponceau Red staining, membranes were blocked with blocking buffer (5% milk in PBS containing 0.02% Tween 20) and incubated for 1h30 with rabbit anti-4-hydroxynonenal (4-HNE, a marker of oxidative stress) antibodies (Abcam; REF: ab46545). Membranes were then washed and incubated with secondary antibody coupled to HRP (1:2000) (Jackson's laboratories; Goat anti-Rabbit coupled with HRP, REF: JII035003) for 1h30 in order to be revealed with enhanced chemiluminescence substrates and imaged with Amersham Imager 680.

#### ***Microscopy***

Micrographs were obtained with an Eclipse 80i Nikon microscope equipped with a Hamamatsu digital camera (Life Sciences, Japan), and with a nanozoomer S60 (Hamamatsu). Pictures were adjusted for brightness and contrast in Adobe Photoshop.

#### ***Cell counting***

The quantification of PCNA-positive specific regions from cryostat and vibratome sections (12  $\mu$ m and 50  $\mu$ m thickness/section for the cryostat and vibratome sections, respectively) allows the analysis of constitutive neurogenesis and proliferative activity. Images were analyzed for detection of PCNA positive nuclei using ImageJ software (National Institutes of Health, Bethesda, MD; RRID: SCR\_003070) after adjusting parameters (threshold, binary, and watershed). Briefly, the parameters were set up as follows for each picture: threshold 65, 255, particle size 200-infinity. Minor modifications in these parameters could be slightly adjusted according to the experiments. In addition, ImageJ automated selection of PCNA-positive nuclei was manually double-checked and adjusted, if necessary, for each picture. Neuroanatomical structures were identified with DAPI counterstaining. Cell counting was performed in blind condition by two different people and the provided graphs correspond to the mean or percentage (%) of proliferative cells per section. The counting was performed on a total of 5 to 10 fish per condition, and the provided graphs correspond to the % mean of proliferative cells per section.

### **Instrumentation and LC–MS/MS conditions**

The total polyphenol content of the aqueous extract was determined by the Folin-Ciocalteu assays as recently done by [57]. Polyphenols contained in aqueous extract of *P. mauritianum* (0.25g/L) were identified by Ultra-high-performance liquid chromatography coupled with diode array detection and HESI Orbitrap mass spectrometer (Q Exactive Plus, Thermo Fisher). Briefly, 10  $\mu$ L of sample were injected using an UHPLC system equipped with a Thermo Fisher Ultimate 3,000 series WPS-3000 RS autosampler and then separated on a PFP column (2.6 $\mu$ m, 100mm  $\times$  2.1mm, Phenomenex, Torrance, CA, USA). The column was eluted with a gradient mixture of 0.1% formic acid in water (A) and 0.1% formic acid in acetonitrile (B) at the flow rate of 450  $\mu$ L/min, with 5% B at 0.00 to 0.1 min, 75% B at 0.1 to 7.1 min, 95% B at 7.2 to 7.9 min and 5% B at 8.0 to 10 min. The column temperature was held at 30 °C and the detection wavelengths were set to 280 nm and 320 nm.

For mass spectrometer parameters, heated electrospray ionization (HESI) was set to 2.8 kV, the capillary temperature was adjusted to 350°C, the sheath gas flow rate was set to 60 units, the auxiliary gas flow rate was set to 20 units and the S-lens RF was equal to 50%. Mass spectra were registered in full scan mode from *m/z* 100 to 1,500 in negative ion mode at a resolving power of 70,000 FWHM at *m/z* 400. The automatic gain control (AGC) was set at 1e<sup>6</sup>. Identification of the compounds of interest was based on their accurate mass, retention time, pattern fragmentation and commercial standards. Data were acquired by XCalibur 4.2.47 software (Thermo Fisher Scientific Inc.) and processed by the Skyline 21.1 software (MacCoss Lab.).

### **Statistical analysis.**

Student's t-test was performed for the comparisons between two groups. If more than two groups were analyzed, multiple testing was performed by one-way ANOVA. Error bars correspond to the standard error of the mean (SEM), and n values correspond to the number of animals or to the number of samples for all experiments. Note that for p-values: \**p*<0.05; \*\**p*<0.01; \*\*\* *p*<0.001 and \*\*\*\**p*<0.0001.

**Author Contributions:** OM, JLB and ND designed the experiments. BG, BV, LG, MB, and ND performed the experiments. All the authors participated in the analysis of the experiments and/or in the writing of the manuscript. All authors have read and agreed to the published version of the manuscript.

**Funding:** This research was funded by the European Regional Development Funds RE0022527 ZEBRATOX (EU-Région Réunion-French State national counterpart).

**Institutional Review Board Statement:** In this section, you should add the Institutional Review Board Statement and approval number, if relevant to your study. You might choose to exclude this statement if the study did not require ethical approval. Please note that the Editorial Office might ask you for further information. Please add "The study was conducted in accordance with the Declaration of Helsinki, and approved by the Institutional Review Board (or Ethics Committee) of NAME OF INSTITUTE (protocol code XXX and date of approval)." for studies involving humans. OR "The animal study protocol was approved by the Institutional Review Board (or Ethics Committee) of NAME OF INSTITUTE (protocol code XXX and date of approval)." for studies involving animals. OR "Ethical review and approval were waived for this study due to REASON (please provide a detailed justification)." OR "Not applicable" for studies not involving humans or animals.

**Data Availability Statement:** The data presented in this study are available on request from the corresponding author

**Conflicts of Interest:** The authors declare no conflict of interest

## References

1. WHO, Obesity and overweight Fact sheet N°311. *World health organisation* **2021**. 809
2. Ellulu, M. S.; Patimah, I.; Khaza'ai, H.; Rahmat, A.; Abed, Y., Obesity and inflammation: the linking mechanism and the complications. *Arch Med Sci* **2017**, *13*, (4), 851-863. 810
3. Manna, P.; Jain, S. K., Obesity, Oxidative Stress, Adipose Tissue Dysfunction, and the Associated Health Risks: Causes and Therapeutic Strategies. *Metab Syndr Relat Disord* **2015**, *13*, (10), 423-44. 811
4. Kopelman, P. G., Obesity as a medical problem. *Nature* **2000**, *404*, (6778), 635-43. 812
5. Ahmed, B.; Sultana, R.; Greene, M. W., Adipose tissue and insulin resistance in obese. *Biomed Pharmacother* **2021**, *137*, 111315. 813
6. Powell-Wiley, T. M.; Poirier, P.; Burke, L. E.; Despres, J. P.; Gordon-Larsen, P.; Lavie, C. J.; Lear, S. A.; Ndumele, C. E.; Neeland, I. J.; Sanders, P.; St-Onge, M. P.; American Heart Association Council on, L.; Cardiometabolic, H.; Council on, C.; Stroke, N.; Council on Clinical, C.; Council on, E.; Prevention; Stroke, C., Obesity and Cardiovascular Disease: A Scientific Statement From the American Heart Association. *Circulation* **2021**, *143*, (21), e984-e1010. 814
7. Azhar, A.; Hassan, N.; Tapolyai, M.; Molnar, M. Z., Obesity, Chronic Kidney Disease, and Kidney Transplantation: An Evolving Relationship. *Semin Nephrol* **2021**, *41*, (2), 189-200. 815
8. Polyzos, S. A.; Kountouras, J.; Mantzoros, C. S., Obesity and nonalcoholic fatty liver disease: From pathophysiology to therapeutics. *Metabolism: clinical and experimental* **2019**, *92*, 82-97. 816
9. Barnes, A. S., The epidemic of obesity and diabetes: trends and treatments. *Tex Heart Inst J* **2011**, *38*, (2), 142-4. 817
10. Convit, A., Obesity is associated with structural and functional brain abnormalities: where do we go from here? *Psychosom Med* **2012**, *74*, (7), 673-4. 818
11. Carmo-Silva, S.; Cavadas, C., Hypothalamic Dysfunction in Obesity and Metabolic Disorders. *Adv Neurobiol* **2017**, *19*, 73-116. 819
12. Prickett, C.; Brennan, L.; Stolwyk, R., Examining the relationship between obesity and cognitive function: a systematic literature review. *Obes Res Clin Pract* **2015**, *9*, (2), 93-113. 820
13. Ouyang, S.; Hsuchou, H.; Kastin, A. J.; Wang, Y.; Yu, C.; Pan, W., Diet-induced obesity suppresses expression of many proteins at the blood-brain barrier. *J Cereb Blood Flow Metab* **2014**, *34*, (1), 43-51. 821
14. Sobesky, J. L.; Barrientos, R. M.; De May, H. S.; Thompson, B. M.; Weber, M. D.; Watkins, L. R.; Maier, S. F., High-fat diet consumption disrupts memory and primes elevations in hippocampal IL-1beta, an effect that can be prevented with dietary reversal or IL-1 receptor antagonism. *Brain Behav Immun* **2014**, *42*, 22-32. 822
15. Ogrodnik, M.; Zhu, Y.; Langhi, L. G. P.; Tchkonja, T.; Kruger, P.; Fielder, E.; Victorelli, S.; Ruswhandi, R. A.; Giorgadze, N.; Pirtskhalava, T.; Podgorni, O.; Enikolopov, G.; Johnson, K. O.; Xu, M.; Inman, C.; Palmer, A. K.; Schafer, M.; Weigl, M.; Ikeno, Y.; Burns, T. C.; Passos, J. F.; von Zglinicki, T.; Kirkland, J. L.; Jurk, D., Obesity-Induced Cellular Senescence Drives Anxiety and Impairs Neurogenesis. *Cell metabolism* **2019**, *29*, (5), 1061-1077 e8. 823
16. Mitchell, A. B.; Cole, J. W.; McArdle, P. F.; Cheng, Y. C.; Ryan, K. A.; Sparks, M. J.; Mitchell, B. D.; Kittner, S. J., Obesity increases risk of ischemic stroke in young adults. *Stroke* **2015**, *46*, (6), 1690-2. 824
17. Bonds, J. A.; Shetti, A.; Stephen, T. K. L.; Bonini, M. G.; Minshall, R. D.; Lazarov, O., Deficits in hippocampal neurogenesis in obesity-dependent and -independent type-2 diabetes mellitus mouse models. *Scientific reports* **2020**, *10*, (1), 16368. 825
18. Bahramsoltani, R.; Farzaei, M. H.; Rahimi, R., Medicinal plants and their natural components as future drugs for the treatment of burn wounds: an integrative review. *Arch Dermatol Res* **2014**, *306*, (7), 601-17. 826
19. Aplamedom, LES PLANTES MÉDICINALES DE LA RÉUNION. **2021**. 827



20. Smadja, J.; Marodon, C., Le Grand Livre des Plantes Médicinales de l'île de La Réunion: Inscrites à la Pharmacopée Française. . *Orphie Edition* **2016**. 851  
852
21. Poullain, C.; Girard-Valenciennes, E.; Smadja, J., Plants from reunion island: evaluation of their free radical scavenging and antioxidant activities. *J Ethnopharmacol* **2004**, *95*, (1), 19-26. 853  
854
22. Aplamedom, PLANTES MÉDICINALES DE LA RÉUNION INSCRITES À LA PHARMACOPÉE FRANÇAISE. *Aplamedom Reunion* **2015**. 855  
856
23. Checkouri, E.; Reignier, F.; Robert-Da Silva, C.; Meilhac, O., Evaluation of Polyphenol Content and Antioxidant Capacity of Aqueous Extracts from Eight Medicinal Plants from Reunion Island: Protection against Oxidative Stress in Red Blood Cells and Preadipocytes. *Antioxidants (Basel)* **2020**, *9*, (10). 857  
858  
859
24. Checkouri, E.; Ramin-Mangata, S.; Diotel, N.; Viranaicken, W.; Marodon, C.; Reignier, F.; Robert-Da Silva, C.; Meilhac, O., Protective Effects of Medicinal Plant Decoctions on Macrophages in the Context of Atherosclerosis. *Nutrients* **2021**, *13*, (1). 860  
861
25. Veeren, B.; Bringart, M.; Turpin, C.; Rondeau, P.; Planesse, C.; Ait-Arsa, I.; Gimie, F.; Marodon, C.; Meilhac, O.; Gonthier, M. P.; Diotel, N.; Bascands, J. L., Caffeic Acid, One of the Major Phenolic Acids of the Medicinal Plant *Antirhea borbonica*, Reduces Renal Tubulointerstitial Fibrosis. *Biomedicines* **2021**, *9*, (4). 862  
863  
864
26. Taile, J.; Patche, J.; Veeren, B.; Gonthier, M. P., Hyperglycemic Condition Causes Pro-Inflammatory and Permeability Alterations Associated with Monocyte Recruitment and Deregulated NFkappaB/PPARgamma Pathways on Cerebral Endothelial Cells: Evidence for Polyphenols Uptake and Protective Effect. *International journal of molecular sciences* **2021**, *22*, (3). 865  
866  
867  
868
27. Gence, L.; Fernezelian, D.; Bringart, M.; Veeren, B.; Christophe, A.; Brion, F.; Meilhac, O.; Bascands, J. L.; Diotel, N., *Hypericum lanceolatum* Lam. Medicinal Plant: Potential Toxicity and Therapeutic Effects Based on a Q2 Zebrafish Model. *Frontiers in Pharmacology* **2022**, *13*. 869  
870  
871
28. Ghaddar, B.; Veeren, B.; Rondeau, P.; Bringart, M.; Lefebvre d'Hellencourt, C.; Meilhac, O.; Bascands, J. L.; Diotel, N., Impaired brain homeostasis and neurogenesis in diet-induced overweight zebrafish: a preventive role from *A. borbonica* extract. *Scientific reports* **2020**, *10*, (1), 14496. 872  
873  
874
29. Arcambal, A.; Taile, J.; Couret, D.; Planesse, C.; Veeren, B.; Diotel, N.; Gauvin-Bialecki, A.; Meilhac, O.; Gonthier, M. P., Protective Effects of Antioxidant Polyphenols against Hyperglycemia-Mediated Alterations in Cerebral Endothelial Cells and a Mouse Stroke Model. *Mol Nutr Food Res* **2020**, *64*, (13), e1900779. 875  
876  
877
30. Mahomoodally, M. F.; Korumtollie, H. N.; Chady, Z. Z., *Psiloxylon mauritianum* (Bouton ex Hook.f.) Baillon (Myrtaceae): A promising traditional medicinal plant from the Mascarene Islands. *J Intercult Ethnopharmacol* **2014**, *3*, (4), 192-5. 878  
879
31. Mootoosamy, A.; Fawzi Mahomoodally, M., Ethnomedicinal application of native remedies used against diabetes and related complications in Mauritius. *J Ethnopharmacol* **2014**, *151*, (1), 413-44. 880  
881
32. Rangasamy, O.; Mahomoodally, F. M.; Gurib-Fakim, A.; Quetin-Leclercq, J., Two anti-staphylococcal triterpenoid acids isolated from *Psiloxylon mauritianum* (Bouton ex Hook.f.) Baillon, an endemic traditional medicinal plant of Mauritius. *South African Journal of Botany* **2014**, *93*, 198-203. 882  
883  
884
33. Benchoula, K.; Khatib, A.; Jaffar, A.; Ahmed, Q. U.; Sulaiman, W.; Wahab, R. A.; El-Seedi, H. R., The promise of zebrafish as a model of metabolic syndrome. *Exp Anim* **2019**, *68*, (4), 407-416. 885  
886
34. Zang, L.; Shimada, Y.; Nishimura, N., Development of a Novel Zebrafish Model for Type 2 Diabetes Mellitus. *Scientific reports* **2017**, *7*, (1), 1461. 887  
888
35. Zang, L.; Maddison, L. A.; Chen, W., Zebrafish as a Model for Obesity and Diabetes. *Front Cell Dev Biol* **2018**, *6*, 91. 889
36. Capiotti, K. M.; Antonioli, R., Jr.; Kist, L. W.; Bogo, M. R.; Bonan, C. D.; Da Silva, R. S., Persistent impaired glucose metabolism in a zebrafish hyperglycemia model. *Comp Biochem Physiol B Biochem Mol Biol* **2014**, *171*, 58-65. 890  
891

37. Montalbano, G.; Mania, M.; Guerrero, M. C.; Laura, R.; Abbate, F.; Levanti, M.; Maugeri, A.; Germana, A.; Navarra, M., Effects of a Flavonoid-Rich Extract from Citrus sinensis Juice on a Diet-Induced Obese Zebrafish. *International journal of molecular sciences* **2019**, *20*, (20). 892-894
38. Montalbano, G.; Maugeri, A.; Guerrero, M. C.; Miceli, N.; Navarra, M.; Barreca, D.; Cirimi, S.; Germana, A., A White Grape Juice Extract Reduces Fat Accumulation through the Modulation of Ghrelin and Leptin Expression in an In Vivo Model of Overfed Zebrafish. *Molecules* **2021**, *26*, (4). 895-897
39. Dorsemans, A. C.; Lefebvre d'Hellencourt, C.; Ait-Arsa, I.; Jestin, E.; Meilhac, O.; Diotel, N., Acute and Chronic Models of Hyperglycemia in Zebrafish: A Method to Assess the Impact of Hyperglycemia on Neurogenesis and the Biodistribution of Radiolabeled Molecules. *J Vis Exp* **2017**, (124). 898-900
40. O'Brien, P. D.; Hinder, L. M.; Callaghan, B. C.; Feldman, E. L., Neurological consequences of obesity. *Lancet Neurol* **2017**, *16*, (6), 465-477. 901-902
41. Milic, S.; Lulic, D.; Stimac, D., Non-alcoholic fatty liver disease and obesity: biochemical, metabolic and clinical presentations. *World J Gastroenterol* **2014**, *20*, (28), 9330-7. 903-904
42. Brockman, D. A.; Chen, X.; Gallaher, D. D., High-viscosity dietary fibers reduce adiposity and decrease hepatic steatosis in rats fed a high-fat diet. *J Nutr* **2014**, *144*, (9), 1415-22. 905-906
43. Calligaris, S. D.; Lecanda, M.; Solis, F.; Ezquer, M.; Gutierrez, J.; Brandan, E.; Leiva, A.; Sobrevia, L.; Conget, P., Mice long-term high-fat diet feeding recapitulates human cardiovascular alterations: an animal model to study the early phases of diabetic cardiomyopathy. *PLoS one* **2013**, *8*, (4), e60931. 907-909
44. Montalbano, G.; Mania, M.; Guerrero, M. C.; Abbate, F.; Laura, R.; Navarra, M.; Vega, J. A.; Ciriaco, E.; Germana, A., Morphological differences in adipose tissue and changes in BDNF/Trkb expression in brain and gut of a diet induced obese zebrafish model. *Ann Anat* **2016**, *204*, 36-44. 910-912
45. Landgraf, K.; Schuster, S.; Meusel, A.; Garten, A.; Riemer, T.; Schleinitz, D.; Kiess, W.; Korner, A., Short-term overfeeding of zebrafish with normal or high-fat diet as a model for the development of metabolically healthy versus unhealthy obesity. *BMC physiology* **2017**, *17*, (1), 4. 913-915
46. Cosacak, M. I.; Papadimitriou, C.; Kizil, C., Regeneration, Plasticity, and Induced Molecular Programs in Adult Zebrafish Brain. *Biomed Res Int* **2015**, *2015*, 769763. 916-917
47. Diotel, N.; Lubke, L.; Strahle, U.; Rastegar, S., Common and Distinct Features of Adult Neurogenesis and Regeneration in the Telencephalon of Zebrafish and Mammals. *Front Neurosci* **2020**, *14*, 568930. 918-919
48. März, M.; Schmidt, R.; Rastegar, S.; Strahle, U., Regenerative response following stab injury in the adult zebrafish telencephalon. *Dev Dyn* **2011**, *240*, (9), 2221-31. 920-921
49. Labusch, M.; Mancini, L.; Morizet, D.; Bally-Cuif, L., Conserved and Divergent Features of Adult Neurogenesis in Zebrafish. *Front Cell Dev Biol* **2020**, *8*, 525. 922-923
50. Ghaddar, B.; Bringart, M.; Lefebvre d'Hellencourt, C.; Meilhac, O.; Diotel, N., Deleterious Effects of Overfeeding on Brain Homeostasis and Plasticity in Adult Zebrafish. *Zebrafish* **2021**, *18*, (3), 190-206. 924-925
51. Dorsemans, A. C.; Couret, D.; Hoarau, A.; Meilhac, O.; Lefebvre d'Hellencourt, C.; Diotel, N., Diabetes, adult neurogenesis and brain remodeling: New insights from rodent and zebrafish models. *Neurogenesis (Austin)* **2017**, *4*, (1), e1281862. 926-927
52. Dorsemans, A. C.; Soule, S.; Weger, M.; Bourdon, E.; Lefebvre d'Hellencourt, C.; Meilhac, O.; Diotel, N., Impaired constitutive and regenerative neurogenesis in adult hyperglycemic zebrafish. *J Comp Neurol* **2017**, *525*, (3), 442-458. 928-929
53. Capiotti, K. M.; De Moraes, D. A.; Menezes, F. P.; Kist, L. W.; Bogo, M. R.; Da Silva, R. S., Hyperglycemia induces memory impairment linked to increased acetylcholinesterase activity in zebrafish (*Danio rerio*). *Behavioural brain research* **2014**, *274*, 319-25. 930-932
54. Meguro, S.; Hosoi, S.; Hasumura, T., High-fat diet impairs cognitive function of zebrafish. *Scientific reports* **2019**, *9*, (1), 17063. 933

55. Stankiewicz, A. J.; Mortazavi, F.; Kharchenko, P. V.; McGowan, E. M.; Kharchenko, V.; Zhdanova, I. V., Cell Kinetics in the Adult Neurogenic Niche and Impact of Diet-Induced Accelerated Aging. *J Neurosci* **2019**, *39*, (15), 2810-2822. 934-935
56. OECD, OECD guidelines for the testing of chemicals. Test No. 236: Fish Embryo Acute Toxicity (FET) Test. **2013**. 936
57. Gence, L.; Fernezelian, D.; Bringart, M.; Veeren, B.; Christophe, A.; Brion, F.; Meilhac, O.; Bascands, J. L.; Diotel, N., Hypericum lanceolatum Lam. Medicinal Plant: Potential Toxicity and Therapeutic Effects Based on a Zebrafish Model. *Front Pharmacol* **2022**, *13*, 832928. 937-939
58. Wullimann, M. F.; Reichert, B. R., *Neuroanatomy of the Zebrafish Brain*. 1996. 940
59. Pellegrini, E.; Mouriec, K.; Anglade, I.; Menuet, A.; Le Page, Y.; Gueguen, M. M.; Marmignon, M. H.; Brion, F.; Pakdel, F.; Kah, O., Identification of aromatase-positive radial glial cells as progenitor cells in the ventricular layer of the forebrain in zebrafish. *J Comp Neurol* **2007**, *501*, (1), 150-67. 941-943
60. Sorres, J.; Andre, A.; Elslande, E. V.; Stien, D.; Eparvier, V., Potent and Non-Cytotoxic Antibacterial Compounds Against Methicillin-Resistant Staphylococcus aureus Isolated from Psiloxylon mauritianum, A Medicinal Plant from Reunion Island. *Molecules* **2020**, *25*, (16). 944-946
61. Clain, E.; Haddad, J. G.; Koishi, A. C.; Sinigaglia, L.; Rachidi, W.; Despres, P.; Duarte Dos Santos, C. N.; Guiraud, P.; Jouvenet, N.; El Kalamouni, C., The Polyphenol-Rich Extract from Psiloxylon mauritianum, an Endemic Medicinal Plant from Reunion Island, Inhibits the Early Stages of Dengue and Zika Virus Infection. *International journal of molecular sciences* **2019**, *20*, (8). 947-950
62. Veeren, B.; Ghaddar, B.; Bringart, M.; Khazaal, S.; Gonthier, M. P.; Meilhac, O.; Diotel, N.; Bascands, J. L., Phenolic Profile of Herbal Infusion and Polyphenol-Rich Extract from Leaves of the Medicinal Plant Antirhea borbonica: Toxicity Assay Determination in Zebrafish Embryos and Larvae. *Molecules* **2020**, *25*, (19). 951-953
63. Sun, W.; Xu, G.; Guo, X.; Luo, G.; Wu, L.; Hou, Y.; Guo, X.; Zhou, J.; Xu, T.; Qin, L.; Fan, Y.; Han, L.; Matsabisa, M.; Ma, X.; Liu, T., Protective effects of asiatic acid in a spontaneous type 2 diabetic mouse model. *Mol Med Rep* **2017**, *16*, (2), 1333-1339. 954-955
64. Uddand Rao, V. V. S.; Rameshreddy, P.; Brahmanaidu, P.; Ponnusamy, P.; Balakrishnan, S.; Ramavat, R. N.; Swapna, K.; Pothani, S.; Nemani, H.; Meriga, B.; Vadivukkarasi, S.; P, R. N.; Ganapathy, S., Antiobesity efficacy of asiatic acid: down-regulation of adipogenic and inflammatory processes in high fat diet induced obese rats. *Arch Physiol Biochem* **2020**, *126*, (5), 453-462. 956-959
65. Her, G. M.; Yeh, Y. H.; Wu, J. L., 435-bp liver regulatory sequence in the liver fatty acid binding protein (L-FABP) gene is sufficient to modulate liver regional expression in transgenic zebrafish. *Dev Dyn* **2003**, *227*, (3), 347-56. 960-961
66. Wang, G.; Bonkovsky, H. L.; de Lemos, A.; Burczynski, F. J., Recent insights into the biological functions of liver fatty acid binding protein 1. *J Lipid Res* **2015**, *56*, (12), 2238-47. 962-963
67. Liu, L.; Zhu, H.; Yan, Y.; Lv, P.; Wu, W., Toxicity Evaluation and Biomarker Selection with Validated Reference Gene in Embryonic Zebrafish Exposed to Mitoxantrone. *International journal of molecular sciences* **2018**, *19*, (11). 964-965
68. Sharma, M. K.; Liu, R. Z.; Thisse, C.; Thisse, B.; Denovan-Wright, E. M.; Wright, J. M., Hierarchical subfunctionalization of fabp1a, fabp1b and fabp10 tissue-specific expression may account for retention of these duplicated genes in the zebrafish (Danio rerio) genome. *FEBS J* **2006**, *273*, (14), 3216-29. 966-968
69. Ma, J.; Zheng, Y.; Tang, W.; Yan, W.; Nie, H.; Fang, J.; Liu, G., Dietary polyphenols in lipid metabolism: A role of gut microbiome. *Anim Nutr* **2020**, *6*, (4), 404-409. 969-970
70. Bian, Y.; Lei, J.; Zhong, J.; Wang, B.; Wan, Y.; Li, J.; Liao, C.; He, Y.; Liu, Z.; Ito, K.; Zhang, B., Kaempferol reduces obesity, prevents intestinal inflammation, and modulates gut microbiota in high-fat diet mice. *J Nutr Biochem* **2022**, *99*, 108840. 971-972
71. Zhao, L.; Zhu, X.; Xia, M.; Li, J.; Guo, A. Y.; Zhu, Y.; Yang, X., Quercetin Ameliorates Gut Microbiota Dysbiosis That Drives Hypothalamic Damage and Hepatic Lipogenesis in Monosodium Glutamate-Induced Abdominal Obesity. *Front Nutr* **2021**, *8*, 671353. 973-975

72. Etxeberria, U.; Arias, N.; Boque, N.; Macarulla, M. T.; Portillo, M. P.; Martinez, J. A.; Milagro, F. I., Reshaping faecal gut microbiota composition by the intake of trans-resveratrol and quercetin in high-fat sucrose diet-fed rats. *J Nutr Biochem* **2015**, *26*, (6), 651-60. 976  
977  
978
73. Yang, K.; Zhang, L.; Liao, P.; Xiao, Z.; Zhang, F.; Sindaye, D.; Xin, Z.; Tan, C.; Deng, J.; Yin, Y.; Deng, B., Impact of Gallic Acid on Gut Health: Focus on the Gut Microbiome, Immune Response, and Mechanisms of Action. *Front Immunol* **2020**, *11*, 580208. 979  
980  
981
74. Bak, E. J.; Kim, J.; Jang, S.; Woo, G. H.; Yoon, H. G.; Yoo, Y. J.; Cha, J. H., Gallic acid improves glucose tolerance and triglyceride concentration in diet-induced obesity mice. *Scand J Clin Lab Invest* **2013**, *73*, (8), 607-14. 982  
983
75. Tanaka, M.; Sugama, A.; Sumi, K.; Shimizu, K.; Kishimoto, Y.; Kondo, K.; Iida, K., Gallic acid regulates adipocyte hypertrophy and suppresses inflammatory gene expression induced by the paracrine interaction between adipocytes and macrophages in vitro and in vivo. *Nutr Res* **2020**, *73*, 58-66. 984  
985  
986
76. Al-Goblan, A. S.; Al-Alfi, M. A.; Khan, M. Z., Mechanism linking diabetes mellitus and obesity. *Diabetes Metab Syndr Obes* **2014**, *7*, 587-91. 987  
988
77. Richard, J.; Lingvay, I., Hepatic steatosis and Type 2 diabetes: current and future treatment considerations. *Expert Rev Cardiovasc Ther* **2011**, *9*, (3), 321-8. 989  
990
78. Totten, M. S.; Pierce, D. M.; Erikson, K. M., Diet-Induced Obesity Disrupts Trace Element Homeostasis and Gene Expression in the Olfactory Bulb. *Nutrients* **2020**, *12*, (12). 991  
992
79. Stankiewicz, A. J.; McGowan, E. M.; Yu, L.; Zhdanova, I. V., Impaired Sleep, Circadian Rhythms and Neurogenesis in Diet-Induced Premature Aging. *International journal of molecular sciences* **2017**, *18*, (11). 993  
994
80. Diaz, A.; Munoz-Arenas, G.; Caporal-Hernandez, K.; Vazquez-Roque, R.; Lopez-Lopez, G.; Kozina, A.; Espinosa, B.; Flores, G.; Trevino, S.; Guevara, J., Gallic acid improves recognition memory and decreases oxidative-inflammatory damage in the rat hippocampus with metabolic syndrome. *Synapse* **2020**, *75*, (2), e22186. 995  
996  
997
81. Williams, S. Y.; Renquist, B. J., High Throughput Danio Rerio Energy Expenditure Assay. *Journal of visualized experiments : JoVE* **2016**, (107), e53297. 998  
999
82. Redd, M. J.; Kelly, G.; Dunn, G.; Way, M.; Martin, P., Imaging macrophage chemotaxis in vivo: studies of microtubule function in zebrafish wound inflammation. *Cell Motil Cytoskeleton* **2006**, *63*, (7), 415-22. 1000  
1001
83. Diotel, N.; Vaillant, C.; Kah, O.; Pellegrini, E., Mapping of brain lipid binding protein (Blbp) in the brain of adult zebrafish, co-expression with aromatase B and links with proliferation. *Gene Expr Patterns* **2016**, *20*, (1), 42-54. 1002  
1003
84. Kaya, M.; Ahishali, B., Assessment of permeability in barrier type of endothelium in brain using tracers: Evans blue, sodium fluorescein, and horseradish peroxidase. *Methods in molecular biology* **2011**, *763*, 369-82. 1004  
1005  
1006





## **Chapter 5: Zebrafish: A new promise to study the impact of metabolic disorders on the brain (submitted manuscript)**

Zebrafish is an interesting model to investigate the metabolic diseases such as obesity and diabetes. It is also widely used in the field of neurosciences to further examine brain homeostasis, brain plasticity including neurogenesis and cognitive functions (i.e., behavior). Taken together, zebrafish appears as a relevant model to explore the impact of metabolic disorders (overweight/obesity) on brain homeostasis and functions. In this review, we aim to (1) summarize the different zebrafish models of obesity and diabetes and highlight their relevance to mammalian models, (2) to explore their impact on the central nervous system, and finally (3) to highlight some interesting neurogenic signaling pathways that could be disrupted in the brain of obese/diabetic fish subsequently explaining the dis-plasticity observed.

The first part of this review, provides an overview on the diabetic and obese models of zebrafish. Several hyperglycemic models have been developed using zebrafish: acute hyperglycemia models and chronic hyperglycemia models corresponding mainly to type 1 and type 2 diabetes. Concerning obesity, the models developed in zebrafish are mostly diet-induced obesity (DIO), high-fat diet (HFD) and genetic obese models that results in a hyperglycemic state. All the above-mentioned models share common features with mammals (rodents and human) that are explained in details in this review.

The second part of this review article discusses the effect of such metabolic disorders on brain plasticity and functions. Both hyperglycemia and obesity in zebrafish were shown to disturb brain homeostasis through several mechanisms as BBB leakage, neuro-inflammation, brain oxidative stress, and impaired neurogenesis. As a consequence, fish behavior is also disturbed. These outcomes are also observed in obese and diabetic rodent models as well as in humans.

Finally, the last part of this review proposes some neurogenic mechanisms and signaling pathways to investigate to explain the disrupted brain plasticity induced by metabolic disorders. Among these mechanisms, we discuss the conserved Notch signaling that is mostly known to decrease brain neurogenesis and was reported to be increased in obesity and diabetic models. Bone morphogenetic proteins (BMPs) and the inhibitor of differentiation /DNA binding 1 (Id1) are other factors suggested to disturb the balance between NSC activity and quiescence. Finally, we highlight the potent deleterious role of glucocorticoid stress hormones in the decreased brain plasticity observed in case of obesity and diabetes.

In conclusion, zebrafish appears as an interesting and relevant model to study the impact of metabolic disorders on the central nervous system. The convenience of this model will allow researchers to better understand the mechanisms underlying the disruptions of brain homeostasis in metabolic disease conditions, with the goal of developing better therapeutics to limit these disturbances.



# Zebrafish: A new promise to study the impact of metabolic disorders on the brain

Batoul Ghaddar <sup>1</sup>, and Nicolas Diotel <sup>1,\*</sup>

<sup>1</sup> Université de La Réunion, INSERM, UMR 1188, Diabète athérombose Thérapies Réunion Océan Indien (DÉTROI), Saint-Denis de La Réunion, France; [batoul.ghaddar@univ-reunion.fr](mailto:batoul.ghaddar@univ-reunion.fr) and [nicolas.diotel@univ-reunion.fr](mailto:nicolas.diotel@univ-reunion.fr)

\* Correspondence: [nicolas.diotel@univ-reunion.fr](mailto:nicolas.diotel@univ-reunion.fr)

**Abstract:** Zebrafish has become a popular model to study many physiological and pathophysiological processes in humans. In recent years, it is rapidly emerging in the study of metabolic disorders, namely obesity and diabetes, as the regulatory mechanisms and metabolic pathways of glucose and lipid homeostasis are highly conserved between fish and mammals. Zebrafish is also widely used in the field of neurosciences to study brain plasticity and regenerative mechanisms due to the high maintenance and activity of neural stem cells during adulthood. Recently, a large body of evidences has established that metabolic disorders can alter brain homeostasis, leading to neuro-inflammation and oxidative stress, and causing decreased neurogenesis. To date, these pathological metabolic conditions are also a risk factor for the development of cognitive dysfunctions and neurodegenerative diseases. In this review, we first aimed to describe the main metabolic models established in zebrafish to demonstrate their similarities with their respective mammalian/human counterparts. Then, in a second part, we reported the impact of metabolic disorders (obesity and diabetes) on brain homeostasis with a particular focus on the blood-brain barrier, neuro-inflammation, oxidative stress, cognitive functions and brain plasticity. Finally, we proposed interesting signaling pathways and regulatory mechanisms to explore in order to better understand how metabolic disorders can negatively impact neural stem cell activity.

**Keywords:** brain plasticity, diabetes, metabolic disorders, neural stem cell, obesity, zebrafish

## 1. Introduction

Metabolic syndrome is a combination of at least three of the following metabolic disorders: abdominal obesity, hypertriglyceridemia, low serum high-density lipoprotein (HDL) levels, hyperglycemia (associated with insulin resistance), and hypertension [1]. These biochemical and physiological dysfunctions significantly increase the risk of chronic kidney disease, hepatic steatosis, cardiovascular diseases including myocardial infarction and stroke among others [2-4]. Recently, metabolic syndrome has also been suggested to be associated with cognitive and behavioral impairments [5].

Diabetes and obesity are two metabolic diseases related to the metabolic syndrome. Both diseases are closely associated with approximately 84% of people with type 2 diabetes who are also obese and/or overweight [6]. In addition, diabetes and obesity cause many deleterious effects on the body. For example, they strongly affect the renal glomerular filtration rate and increase the risk of developing chronic kidney disease [7]. They are also risk factors for the development of cardiovascular diseases affecting blood pressure, endothelial cell and cardiomyocyte functions [8, 9]. In mice, obesity promotes adipose tissue inflammation, leading to liver inflammation and promoting glucose



intolerance and insulin resistance [10]. Similarly, insulin resistance was correlated with an increased risk of hepatic steatosis in a Korean cohort, even before the onset of a diabetic state [11]. Overall, diabetes and obesity impair the cardiovascular, renal, visual, intestinal, and metabolic systems.

Obesity and diabetes have been more recently documented for their deleterious consequences on the central nervous system, especially in cognitive processes [12, 13]. Both diseases disrupt the blood-brain barrier (BBB) [14, 15] and promote neuro-inflammation and cerebral oxidative stress [16]. Obesity and diabetes have also been suggested to be involved in neuronal degeneration, being risk factors for the development of neurodegenerative diseases, including Alzheimer's disease [17]. This is likely related to increased oxidative stress through mitochondrial dysfunction and neuro-inflammation [18-20]. Strikingly, recent data have demonstrated that diabetes and obesity have a deleterious impact on brain plasticity and among others on neurogenesis.

Neurogenesis is an evolutionarily conserved process that involves the division of neural stem cells, the genesis of other committed progenitors, and finally the birth of new neurons that can migrate and differentiate within the nervous tissue [21-24]. This interesting and intriguing process occurs primarily during development, but has also been documented in the adult brain of all species studied to date, including humans [25, 26]. In mammals, adult neurogenesis occurs mainly in two regions: (1) the subventricular zone (SVZ) of the lateral ventricle and (2) the subgranular zone (SGZ) of the dentate gyrus of the hippocampus [27, 28]. Neurogenesis is tightly regulated by many different factors including hormones, oxygen supply, as well as trophic, immune and epigenetic factors [29, 30]. The microenvironment of the neurogenic niche can consequently disrupt neural stem cell activity namely under chronic and/or acute inflammation, as well as under pro-oxidant conditions [31-36].

To better understand the mechanisms underlying the deleterious effects of metabolic disorders in the brain of obese and/or diabetic individuals, several animal models have been used such as non-human primate models (i.e., chimpanzee), large animal models (i.e., dog and pig), rodent models (i.e., rat and mouse) and non-mammalian models such as nematode (*C. elegans*) and zebrafish [37]. Of course, working with large mammalian models has many drawbacks, including ethical concerns, difficult manipulations as well as high costs. For these reasons, the main models used to study neurogenesis remain rodents. However, in recent years, zebrafish have emerged as an interesting model to study the impact of metabolic disorder in the brain [38-43].

Zebrafish is indeed an attractive organism to study metabolic disorders. This small teleost fish has metabolic organs conserved with humans, including the liver, adipose tissue, pancreas and kidney [44]. As in mammals, many methods are available to measure insulin, blood glucose, lipid and cholesterol levels in this small and easily manipulated model. Finally, over 70% of the human genome have ortholog in zebrafish and many physiological processes are conserved between fish and mammals, including humans [45]. Thus, several groups have developed models of metabolic disorders to successfully mimic the human pathologies of diabetes and obesity. These include diet-induced obesity (DIO), high-fat diets (HFD), hyperglycemic/diabetic models, as well as genetic models of metabolic disturbances. Interestingly, the pathological disorders induced by hyperglycemia and/or obesity are parallel to those in humans [46-48]. In addition, zebrafish have almost unique characteristics when considering the central nervous system. The adult zebrafish brain retains a broad distribution of active neurogenic niches throughout the encephalon [22, 49-51]. This is in striking contrast to mammals, in which neurogenic niches are restricted to two main regions, the SVZ and SGZ [21, 27, 28]. Furthermore, unlike mammals, the brain of adult zebrafish is able to regenerate efficiently

after large lesions, without generating persistent glial scarring and without striking residual disabilities [21, 52-55].

Today, more and more efforts are being made to better understand how metabolic disorders can alter brain regeneration in order to find new therapeutic approaches to combat their impacts on the CNS under constitutive and regenerative conditions. In this general context, zebrafish is a promising model that offers new hope in understanding the disrupted mechanisms occurring during metabolic disorders. It also offers the possibility to discover new effective drugs to combat the deleterious effects induced by metabolic disruptions. In this review, we will discuss the main zebrafish models developed to study the effects of obesity and diabetes on CNS functions. We will then highlight, in a comparative approach, the deleterious effects of these models on brain homeostasis, focusing on BBB, constitutive and regenerative neurogenesis, as well as on cognitive functions. Finally, we will discuss potential mechanisms that could explain the deleterious effect of obesity and/or diabetes on the CNS.

## 2. Different models of metabolic disorders in adult zebrafish

A growing number of studies have used zebrafish to investigate its relevance to hyperglycemia/diabetes as well as overweight/obesity. In this first section, we will document the main models of metabolic disorders developed in zebrafish, focusing mainly on the adult stages.

### 2.1. Models of acute and chronic hyperglycemia

**Acute hyperglycemia:** An interesting model aimed to develop acute hyperglycemia in fish by intraperitoneal injection of D-glucose (2.5g/kg body weight) [40, 56]. Such an injection resulted in a rapid and transient increase in blood glucose compared to zebrafish injected with vehicle. Thus, 1.5 hours after D-glucose injection, blood glucose levels reached high values compared to control-injected fish (350-500 mg/dl glucose versus 100-150 mg/dl, respectively) [40, 56]. In mice, a similar injection can be performed to study the impact of acute hyperglycemia in stroke models [57, 58], or in cerebral blood flow and tissue oxygen saturation [59].

**Chronic hyperglycemia:** Other hyperglycemic models aim to induce chronic and persistent hyperglycemia. In mammals, chronic hyperglycemia is mainly due to an alteration of insulin production, secretion and signaling. The zebrafish pancreas is quite similar to that of mammals with the presence of endocrine islets and in particular insulin-producing pancreatic  $\beta$ -cells [60]. Two main methods have been used to establish a larger and stable diabetic state: (1) the induction of hyperglycemia by destruction of pancreatic  $\beta$ -cells (relative to type 1 diabetes), and (2) the induction of chronic hyperglycemia by dissolving D-glucose in fish water (relative to type 2 diabetes).

Type 1 diabetes could be induced in fish by pancreatectomy [61, 62] or chemical-dependent ablation [63, 64]. The former method is difficult to perform and not really used in the zebrafish community. In contrast, chemical ablation by intraperitoneal injection of drugs such as streptozotocin (STZ) and alloxan are widely developed [63, 64]. These drugs that have been widely used in mammals [65] lead to the death of pancreatic  $\beta$ -cells through the generation of oxidative stress. This results in impaired insulin production and high fasting blood glucose levels [66]. In zebrafish, several studies have demonstrated that injection of STZ and/or alloxan lead to hyperglycemia in larvae and adults [61, 64, 67-69]. For example, Olsen and colleagues showed that a serial injection of STZ to adult zebrafish leads to an increase in fasting blood glucose compared to control fish (~300 mg/dl vs. 60 mg/dl) from week 1 to 3 [67]. This treatment also induces higher levels of serum glycated

protein (over 300%) and a ~80% reduction in insulin levels [67]. Interestingly, after 3 weeks, these hyperglycemic fish develop renal and retinal defects as revealed by increased glomerular basement membrane thickness and decreased retinal layer thickness [67]. This is similar to the human situation, in which type 1 diabetic patients suffered from increased serum protein glycation levels [70, 71], increased glomerular basement membrane thickness [72] and retinal complications [73]. Interestingly, hyperglycemic zebrafish also exhibit a reduced ability to regenerate their caudal fin after transection [67]. This interesting feature parallels the wound healing defects observed in diabetic patients [74]. In other experiments using STZ, hyperglycemia has a deleterious impact on the cardiovascular system, leading to the misexpression of important cardiac proteins (P53, Ampk, and Klf2a), to the loss of cardiac myofibrils and their apoptosis, as well as to cardiac dysfunction [75]. In these hyperglycemic fish, stroke volume, cardiac output, and ejection fraction (end-diastolic volume minus end-systolic volume) are lower than in control fish [75]. In addition, the expression of glucose transporters (GLUTs) is decreased in the heart of zebrafish, indicating a decreased ability of the zebrafish myocardium to utilize glucose [75].

Overall, these type 1 diabetes models exhibit many features of diabetic pathology in mammals (including humans), such as increased fasting blood glucose, increased plasma protein glycation, retinal and renal dysfunctions, cardiovascular complications, as well as impaired regenerative processes [67, 76, 77]. However, these diabetic models using STZ and alloxan have limitations given the ability of fish to regenerate pancreatic  $\beta$  cells over time [77-79].

Models of type 2 diabetes have been developed by supplementing fish water with D-glucose using different concentrations of D-glucose (55, 111 and 133 mM) (55, 111 and 133 mM) [42, 56, 80]. However, young zebrafish (4-11 months) can acclimate better to glucose immersion than old fish (1-3 years) [81]. Although the different glucose concentrations lead to significant hyperglycemia between day 2 and day 3 of treatment, the 111mM concentration remains the frequently used among the literature [42, 56]. Immersion of zebrafish in 111mM D-glucose solution significantly increased blood glucose levels from nearly 3 mM (54 mg/dl) to 12 mM (216 mg/dl) in control and hyperglycemic fish, respectively [42]. Accordingly, our own experiments also demonstrated the significant increase in blood glucose levels after 14 days of treatment, from 60 mg/dl to 280 mg/ml [56, 82]. Interestingly, this diabetic state is dependent on D-glucose dissolved in the water as a 7-day washout after 2 weeks of D-glucose treatment is sufficient to return to normal blood glucose levels [42]. This model also leads to the induction of hyperinsulinemia and impaired glucose metabolism, as well as higher glycation of ocular proteins, altered expression levels of insulin receptors in skeletal muscle, and decreased blood glucose levels after treatment with antidiabetic drugs [42].

These general characteristics are commonly observed in diabetic mammalian models and human patients [83-85]. Type 2 diabetic rodents correspond mainly to (1) NOD mice (non-obese diabetic mice), (2) ob/ob and db/db mice with a mutation on leptin signaling (leptin and its receptor, respectively), and (3) HFD or DIO models. In all these models, insulinemia, hyperglycemia, and increased levels of serum protein glycation are observed. Overall, this work reflects the reliability of using hyperglycemic zebrafish to mimic human pathology.

**Genetic and transgenic models of hyperglycemia:** The use of genetic tools such as morpholinos, CrispR-Cas9 targeted gene ablation, transgenic and/or mutant lines also allowed to generate hyperglycemic larvae and adult fish. For example, overexpression of foxn3, a gene associated with fasting blood glucose regulation, leads to increased hepatic gluconeogenesis and fasting blood glucose in adulthood [86, 87]. In adult zebrafish, knocking out the pdx1 gene (a gene implicated in the development of type 2 diabetes) results in a reduced number of pancreatic  $\beta$ -cells, in a decreased insulin levels and

consequently hyperglycemia. It also delays body growth in fish [88]. Another transgenic model was achieved by overfeeding insulin-resistant skeletal muscle (zMIR) fish mutated on the IGF1 receptor [89]. Adult zMIR fish have normal glucose levels similar to control fish, but glucose levels increased significantly after the fish are overfed and described the transitional state between insulin resistance and the development of type 2 diabetes [89]. Many other transgenic fish have been used such as deiodinase 2 KO and aldh3a1 KO [90]. In addition to all these models, many diabetic and hyperglycemic protocols have been developed in the larva [90, 91].

## 2.2. Models of overweight and obesity in zebrafish leading to hyperglycemia

Obesity and overweight are characterized by hypertrophy and hyperplasia of adipocyte cells, resulting in increased body weight and body mass index (BMI). Zebrafish share with mammals the major metabolic organs regulating energy homeostasis (intestine, liver, pancreas, adipose tissue and muscle). Their respective functions are also evolutionarily conserved between taxa, including regulation of feeding behavior, lipid storage and insulin secretion among others [91]. Interestingly, the conserved metabolic pathways in adipocytogenesis and cholesterol metabolism between zebrafish and humans have made zebrafish an appropriate and alternative model in the field of metabolic disruptions [92]. Many zebrafish models of obesity have been developed in larvae and adults using overfeeding (diet-induced obesity - DIO) and/or high-fat diet (HFD) [38, 39, 41, 93-95] [90]. Similarly, some genetic models have also been established [90, 96-98].

**Overfeeding models:** Numerous obesity-inducing diet protocols have been conducted, with the difference between these models being either the nature of the food provided and/or the duration of the feeding. In 2010, Oka and colleagues overfed fish with artemia (a small shrimp used as a food source in aquaculture) [99]. In their overfeeding protocol, they provide 60 mg of artemia/fish/day for 8 weeks versus 5 mg for the control [99]. At the end of their experimental procedure, the DIO fish had increased body weight, BMI, triglyceride levels, and developed hepatic steatosis.

Similar studies by Husmura and Hiramitsu show increased visceral and subcutaneous adipose tissue volume in overfed fish and hepatic mitochondrial dysfunction [100, 101]. In addition, several models of overfeeding have noted increased lipid deposition in the liver of overfed fish, by Oil Red O staining which allows the labeling of neutral lipids and cholesterol esters [38, 39]. Overfed fish have also an increased phosphorylation of hepatic Akt protein, a pathway involved in the development of insulin resistance [39]. The investigations of other groups have also documented that overfeeding induces higher body weight and BMI linked to the expansion of visceral and subcutaneous adipose tissue [41, 95].

A different overfeeding protocol, applied for 8 months (DIO fish being fed twice as much as controls), results in similar disturbances: increased weight gain and steatosis of the liver (cell vacuolization) as well as an altered inflammatory response of the liver [102]. Indeed, DIO fish were unable to modulate the expression of genes involved in the inflammatory/immune system response after LPS stimulation (i.e., Toll-like receptor signaling pathway, ubiquitin-mediated proteolysis, MAPK and Jak-STAT signaling pathway, cell cycle and apoptotic genes) [102].

More recently, we established rapid and reliable models of overweight/obesity by feeding in an "ad-libitum"-like way with conventional dry food or with a mix of artemia/conventional food for a period of 4 weeks. These models also induce higher body weight, BMI, hyperglycemia, and heterogeneous liver steatosis [21, 38]. Similarly, zebrafish overfed with 120 mg of commercial dry food versus 20 mg for controls for a



period of 8 weeks exhibited higher body weight and BMI, hyperglycemia, glucose intolerance and increased insulin production [47].

Other experimentations have been proposed using HFD protocol. These diets contain high amounts of fat and can be achieved using, for example, heavy whipping cream, chicken egg yolk, corn oil and lard, ancient vegetables added (or not) to the conventional diet [39, 93, 103, 104]. These HFD fish suffer from increased body weight including increased fat mass and hypertrophy, cardiovascular disorders, hepatic steatosis and hyperglycemia.

These different metabolic disturbances described in HFD/DIO zebrafish are also found in DIO and HFD mouse models [105-108]. Overall, these overfeeding protocols performed in zebrafish shared features with human pathology: increased body weight and BMI, expansion of adipose tissue, hypertriglyceridemia, hepatic steatosis and altered expression of genes involved in lipid metabolism and inflammatory response. Hyperinsulinemia and hyperglycemia could also be observed as well as altered expression levels of adipokines (i.e., adiponectin and leptin) and advanced glycation end products [109].

In conclusion, numerous models of diabetes and overweight/obesity have been established in zebrafish and have demonstrated that many mammalian (and human) features of these pathologies are shared with zebrafish (Figure 1). Interesting reviews document the different protocols of transgenic models to establish these different states of diabetes and/or obesity in zebrafish larvae and adults [90]. In this review, Salehpour and colleagues established a scoring system for type 2 diabetes in zebrafish compared to humans. Among the non-genetic models, glucose immersion as performed by [42, 47] and the hyperglycemia obesity model have the highest score [90].

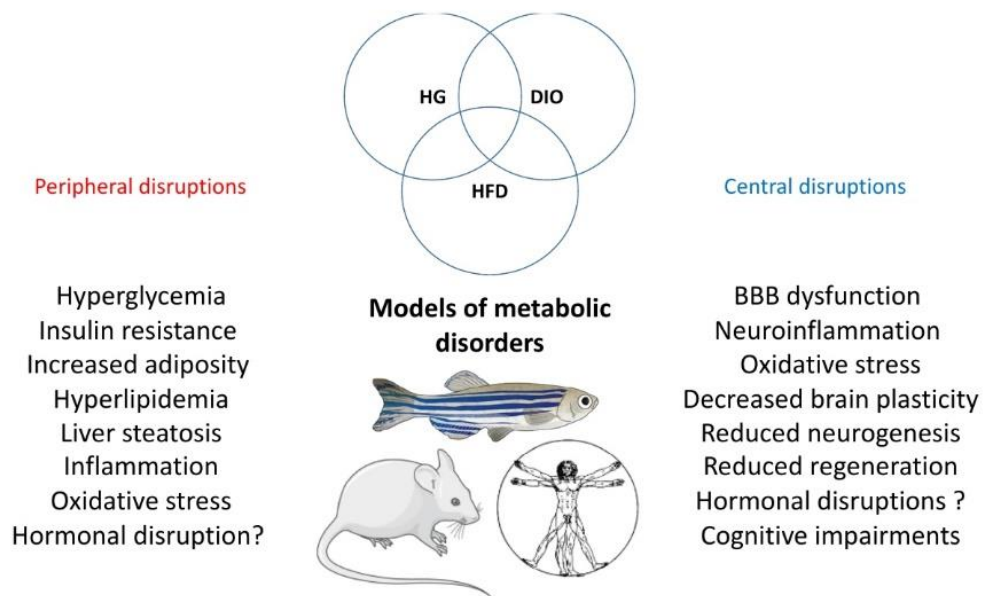


**Figure 1: General overview of the peripheral and central disruptions induced by metabolic disorder.**

The main peripheral and central disruptions are observed in the different models of metabolic disorders (hyperglycemia (HG), DIO and HFD) in fish and rodents. These pathological processes are also found in humans.

**3. The effects of metabolic disorders on brain plasticity and function: focus on zebrafish and comparative aspects**

As previously mentioned, the brain of adult zebrafish exhibits numerous neurogenic niches due to the persistence of many neural stem cells during adulthood. Zebrafish has also a strong capacity for nervous tissue regeneration [50, 52, 110, 111]. The brain of zebrafish is also protected by a blood-brain barrier (BBB) that helps in maintaining brain homeostasis as in mammals [112]. Taken together, these intrinsic characteristics highlight the use of zebrafish to explore the deleterious effects of metabolic disorders on the central nervous system.

### 3.1. Hyperglycemia and brain homeostasis in adult zebrafish

Only a few studies have examined the impact of hyperglycemia on brain homeostasis and plasticity in adult zebrafish. While acute hyperglycemia induced by intraperitoneal injection of D-glucose (2.5g/kg) resolves after 24 hours, it nonetheless resulted in the upregulation of pro-inflammatory cytokines including *il1b*, *il6*, *il8* and *tnfa* [40]. In contrast, acute hyperglycemia has no effect on the expression of genes involved in BBB establishment (i.e., *claudin5a*, *zonula occludens 1a* and *1b*). As well, it does not impact brain cell proliferation in the main neurogenic niches studied (OB/TEL, ventral and dorsal telencephalic domains, pretectum and hypothalamus) [40]. Further studies are needed to understand the impact of acute hyperglycemia on neuro-inflammation, with a focus on microglia reactivity and BBB leakage performing extravasation assay.

Chronic hyperglycemia (111 mM D-glucose for 14 days) results in more severe detrimental effects in the brain. Although it does not alter the cerebral expression of pro-inflammatory genes, probably due to compensatory mechanisms, it leads to the significant upregulation of those related to BBB integrity [40]. These results obtained in adults are to be linked with studies performed in zebrafish larvae for which chronic glucose exposure leads to defects in tectal blood vessel patterning and neurovascular coupling, altering both vascular NO production and the number of cells in the vascular wall. It also induces a change in neuronal calcium concentration and leads to the upregulation of GFAP, a marker of reactive gliosis expressed in NSCs in fish [113, 114].

The cerebral redox balance is also altered in diabetic fish as evidenced by increased levels of lipid peroxidation (TBARS analysis) and carbonylated brain proteins [115]. Similarly, the activity of the antioxidant enzyme superoxide dismutase (SOD) is reduced as well as the expression of some redox-sensitive genes (*sod1* and *2*, *gpx3a*, *nrf2*) [115]. These data were also partially corroborated in the retina of hyperglycemic fish [116] and in another hyperglycemic zebrafish model displaying modification in brain catalase activity [117].

Interestingly, chronic hyperglycemia alters neurogenesis within the major neurogenic areas of adult zebrafish (OB/TEL; ventral and dorsal telencephalic domains, pretectum and hypothalamus) [40]. It furthermore impairs the injury-induced neurogenesis process observed after a telencephalic injury [40]. This blunted regenerative capacity was also reported after caudal fin amputation in hyperglycemic fish as previously mentioned [67].

From a behavioral perspective, hyperglycemic fish exhibit anxiety-like behavior and memory impairment as shown by inhibitory avoidance test [43, 118]. These cognitive defects could originate from an alteration of the purinergic system [43]. Indeed, a significant decrease in brain ATP, ADP and AMP hydrolysis levels is observed in hyperglycemic fish, linked to down-regulation of ectonucleoside triphosphate diphosphohydrolases (*entpd2a.1*, *2a.2*, *3*, and *entpd8*) and adenosine receptors (*adora1*, *adora2aa*, *adora2ab* and *adora2b*). Interestingly, acetylcholinesterase gene expression and activity are also altered [43].

Overall, these data demonstrate that hyperglycemia in zebrafish promotes BBB alterations, neuroinflammation and oxidative stress in the central nervous system. It also leads to reactive gliosis and to impaired neurogenesis, as well as to the development of cognitive defects and depressive-like behavior. All these disrupted processes reported in zebrafish are also observed in mammals during diabetes. For example, Claudin-5 and Occludin expressions are downregulated, reflecting the increased BBB permeability observed in the brain of hyperglycemic mice [119]. Similarly, the number of microglia and reactive astrocytes in the hippocampus of hyperglycemic animals is increased demonstrating a neuro-inflammatory state [120]. Other studies have shown the upregulation of pro-inflammatory genes (i.e. TNF $\alpha$ ) associated with microglia activation in type 1 and type 2 diabetic mice [119]. The levels of antioxidant defenses and enzymes (i.e., glutathione - GSH - and glutathione peroxidase -GPX-) are decreased in the brain of diabetic rodents [121]. To date, numerous studies have found reduced hippocampal neurogenesis in diabetic rodents associated with cognitive defects and depressive behaviors [122-129].

Therefore, in both zebrafish and mammals, diabetes impacts BBB, inflammatory and redox status, brain plasticity and cognitive functions (**Figure 2**). However, data should be reinforced in zebrafish to better understand the global impact of hyperglycemia on brain homeostasis, looking at, for instance, microglia reactivity, BBB physiology as well as cell death under constitutive and brain injury conditions in hyperglycemic zebrafish.

### 3.2. Obesity and brain homeostasis in zebrafish

Like diabetes, overweight and obesity are associated with a range of physiological disorders affecting the central nervous system. Models of overfeeding developed in zebrafish share many pathophysiological disturbances with their human counterparts, as described previously.

In zebrafish, 4-week overfeeding with a mixture of artemia and dry food induces BBB disruption, as shown by Evans blue leakage [38]. In comparison, overfeeding with only dry food results in lower BBB leakage [130], suggesting that “diet quality” may impair differentially BBB dysfunction. Similarly, a HFD protocol provided for 11 weeks with a mixture of standard food and lard (80% + 20%, respectively) results in the downregulation of genes involved in blood-brain barrier functions [103]. The BBB disruption was also associated with an increase in the number of activated microglia (amoeboid) in the ventral telencephalon and hypothalamus, a general increase in the brain expression of pro-inflammatory cytokines (il1b, il6 and tnfa) and of the inflammatory transcription factor nfkb [38]. These data were corroborated in another overfed zebrafish model showing increased amoeboid and dystrophic microglia in the hypothalamus [131]. In a hybrid obesity model (high glucose/high cholesterol experimental protocol), the treated fish upregulate the cerebral expression of pro-inflammatory cytokine and apoptotic genes [132].

Interestingly, obese fish also have a disturbed brain redox balance. They exhibit higher levels of 4-HNE (4-Hydroxynonenal), a lipid peroxidation product known as a marker of oxidative stress [38]. The activities of antioxidant enzymes peroxidase and catalase in the brain are increased, suggesting the activation of the antioxidant response [38]. Meguro and colleagues also showed that HFD zebrafish exhibit disrupted expression of genes involved in antioxidant stress [103].

In general, obese fish (HFD and/or DIO) exhibit a decreased brain plasticity, as revealed by the mis-regulation of bdnf (brain derived neurotrophic factor) and psd95 (postsynaptic density protein 95) genes [95, 103]. The ptn growth factor is also significantly reduced in obese fish, while caspase 9 gene expression is upregulated, suggesting increased cell death. Interestingly, several genes involved in  $\beta$ -amyloid metabolism are also modulated



suggesting links between diet and neurodegeneration [103]. This decrease in genes involved in brain plasticity parallels the consistent reduction in cell proliferation along the neurogenic niches of obese fish, through PCNA immunohistochemistry and qPCR analysis (decreased expression of *pcna* and the progenitor marker *sox2*) [38, 130, 133, 134]. Very interestingly, Stankiewicz and colleagues showed that obese fish display a decrease in the daily amplitude of central clock gene expression associated with misalignment or decreased amplitude of daily patterns of key cell cycle regulators (ex: cyclins A and B, and p20) [134]. Clock genes are known to be involved in the regulation of stem cell activity and are expressed in the neurogenic niches in zebrafish [135, 136], raising the question of the links between circadian clock perturbations and the decreased neurogenesis observed in obese fish. Considering neurological functions, the active avoidance test and locomotion is impaired in obese fish compared to controls [38, 103, 130].

Taken together, these central disruptions are also described in obese mammals. For example, HFD rodents exhibit BBB leakage associated with decreased expression of tight junctions (claudin-5 and occludins) [137, 138]. Similarly, HFD induces hippocampal and/or hypothalamic neuroinflammation with microglia activation and increased oxidative stress, and leads to decreases synaptic density and expression of genes involved in synaptogenesis [139-142]. Numerous studies have also highlighted the effect of a HFD on neurogenesis. For example, obese mice show decreased cell proliferation in neurogenic niches namely in the hypothalamus and hippocampus associated with decreased memory and mood-related disruptive behavior [143]. Such brain alterations are strongly associated with cognitive impairments and increased anxiety [139-141, 144, 145].

Overall, these studies have demonstrated similar effects of obesity on the mammalian and fish brain, with impairment of the BBB leading to increased oxidative stress and neuro-inflammation, decreased brain plasticity including neurogenesis and altered cognitive behaviors (Figure 2). It also raises the question of the mechanisms sustaining such deleterious effects. Indeed, most zebrafish and mammalian models of obesity are hyperglycemic suggesting that this condition could be already sufficient to impair BBB function and brain homeostasis.

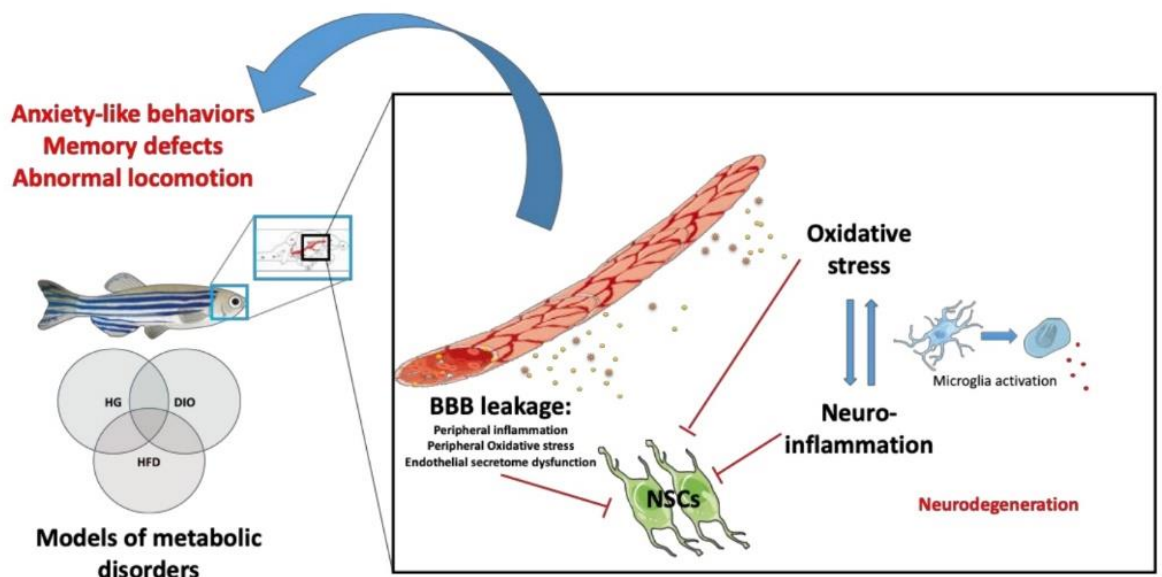


**Figure 2: Peripheral and central mechanisms impacting brain homeostasis in metabolic diseases**

In hyperglycemic (HG), DIO and HFD conditions, BBB breakdown occurs and leads to central oxidative stress and neuroinflammation, namely through the activation of microglia (switch from ramified to amoeboid state). It can result in neurodegeneration. In



addition, the metabolic disorders could lead to impaired secretion of endothelial factors that could in synergy with the disrupted peripheral and central factors impair neural stem cell (NSC) activity. The ultimate consequences of such disruptions are the development of cognitive impairments (locomotion, anxiety, memory) and neurodegenerative diseases.

#### 4. Brain dis-plasticity and metabolic disorders: molecular mechanisms to investigate

Neurogenesis is a tightly orchestrated process regulated by a combination of extrinsic and intrinsic factors [146-148]. Among them, inflammation and oxidative stress (induced during diabetes and obesity) are known to modulate the proliferation of the neural stem/progenitor cells, the differentiation, migration and survival of the new born cells. Zebrafish share many neurogenic signaling pathways and transcriptional regulations with mammals in both healthy and regenerative conditions [21, 22, 49, 53, 149-151]. However, there are not so much data highlighting the mechanisms regulating key neurogenic signaling pathways in these pathologies in both fish and mammals.

##### 4.1 Notch signaling in mammal and zebrafish neurogenesis

One of the important signaling pathways that directly affects neural stem/progenitor proliferation and differentiation is the Notch 1 pathway [22, 152-160]. This conserved signaling from drosophila to human plays a critical role in neural stem cells maintenance and neurogenesis during embryonic development and adult stages. The deregulation in Notch signaling was implicated in many neurodegenerative diseases [156]. In mice, the conditional knock-out of this gene increased the proliferation of neural stem cells, while the constitutive expression of Notch-1 increased the number of the progenitor cells [152, 161]. Similarly, the pharmacological inhibition of Notch signaling in zebrafish increases the proliferation of neural stem cells [151, 154, 157, 162].

Studies support the role of Notch signaling as a possible candidate for decreasing neurogenesis in case of metabolic disorders [163, 164]. The offspring from HFD mice suffer from decreased neuronal progenitor proliferation, differentiation and synaptic plasticity, correlated with increased expression level of the Notch-1 signaling and its effector genes, namely Hes5 [163, 164]. Furthermore, in another study, HFD mice display increased notch signaling and exhibit defects in hypothalamic neurogenesis (differentiation) [165]. In these mice, the inhibition of Notch signaling or of the inflammatory transcription factor NF- $\kappa$ B improve hypothalamic NSC differentiation. So, in HFD mice, the resulted inflammation could activate Notch signaling in neural stem cells and lead to neurogenic defects [165]

To our knowledge, in diabetic and/or obese fish, there are no clear data showing the disruption of Notch signaling. The DIO and hyperglycemic zebrafish models have increased brain inflammation associated with defective neurogenesis [38, 40, 130, 134]. Similar to mammal, Notch signaling is an important regulator of adult zebrafish neurogenesis [153, 154]. The different notch receptors are expressed in several neurogenic niches [154, 158]. However, the links between Notch signaling and the impaired neurogenesis in obese and/or hyperglycemic zebrafish is not yet investigated. Our preliminary results studying the expression of the target gene of Notch signaling in zebrafish, her4.1, do not show striking differences in the main neurogenic niches of control and obese fish (Figure 3). Such investigations can contribute widely to the understanding of Notch involvement in the neurogenic disruption in case of metabolic diseases.

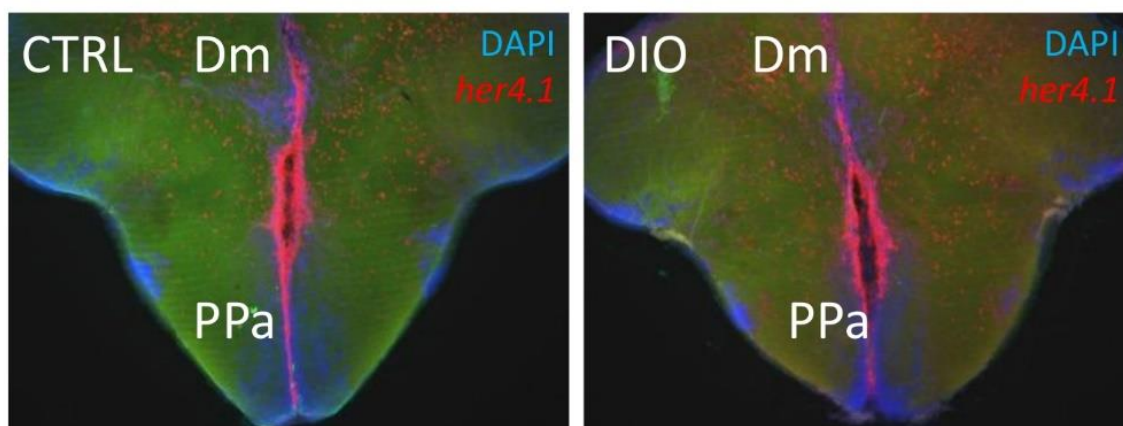


**Figure 3: *her4.1* in situ hybridization on brain section of CTRL and DIO fish**

Preliminary data on DIO fish (4 weeks) did not show striking difference in the expression of the Notch target gene, *her4.1* (red), in CTRL and DIO fish. Cell nuclei are counterstained with DAPI (blue). Dm: dorsomedian telencephalon. PPa: Anterior part of the preoptic area

In addition, it was shown that NSCs from embryo of pregnant diabetic mice exhibit altered expression of genes implied in the proliferation and cell-fate specification such as delta-like 1 (a Notch ligand), Hes1 and Hes5 (key factors for Notch/Delta signaling) [166]. Furthermore, methylglyoxal, a highly reactive glycolytic intermediate metabolite, was shown to regulate Notch signaling and subsequently neural progenitor fate [167].

Therefore, the disruption of Notch signaling in NSCs during obesity and/or diabetes may occur in zebrafish, and modulate NSC proliferation and cell fate. But these hypotheses definitively require further investigations

#### 4.2 BMP/Id1 signaling and cross-talk with Notch signaling in NSCs

Bone morphogenetic proteins (BMPs) are members of the transforming growth factor b (TGF-b) family [168], binding to transmembrane type I and type II receptors and leading to the activation Smad proteins (Smad1/5/8). Smad1/5/8 bind to Smad4 [22, 169]. This complex translocates to the nucleus and activates many target genes including *id1*, the inhibitor of differentiation /DNA binding 1[170]. In zebrafish, there are 5 helix loop helix transcriptional regulator of the Id family, and 4 members in mice [171, 172]. In both mammals and zebrafish, Id1 have overlapping and distinct functions during development and body homeostasis, controlling many cellular events such as cell quiescence, differentiation and migration of different cell types [171].

In mammals, Id1 is an important factor regulating NSC quiescence in the mouse SVZ (a neurogenic niche), with quiescent adult NSCs strongly expressing Id1 [173]. In zebrafish, Id1 is expressed only in radial glial cells (neural stem cells) and mainly in the quiescent ones [172, 174-176]. Interestingly, Id1 gain- and loss-of-function studies show that Id1 promote the quiescence of neural stem cells while its down-regulation allows the entry of the neural stem cell into the cell cycle [176]. The Id1 promoter regulation appears evolutionarily conserved and BMP signaling is important for the correct expression of Id1 in zebrafish NSC and in the regulation of their quiescent/proliferative state [175]. Id1 could promote NSC quiescence in both mouse and fish through Id1 interaction with members of the Hes/Her protein (Notch target genes) [22, 176].

Together these data show that BMP and Id1 are important regulators of neurogenic processes promoting neural stem cell quiescence in both mammals and fish [177]. With Notch, BMP/Id1 are also important actors of brain plasticity that should be studied in zebrafish during metabolic disorders. Indeed, in rodent, recent data suggest a role of BMP in the development of metabolic disorders. Indeed, reduced BMP4 signaling may promote

the development of obesity, insulin resistance, and associated disruptions [178]. Other data show a role of BMP signaling in the regulation of feeding behavior in different mice models [179, 180]. So far, BMPs play key roles in the regulation of energy balance in the brain and in adult neural plasticity [177]. It would be interesting to better understand the modulation and role of BMP/id signaling in the neurogenic niche of diabetic and/or obese model of mice and zebrafish, namely in the hypothalamus, a key neurogenic region controlling the genesis of anorexigenic and orexigenic neurons.

#### 4.3 The role of stress hormones signaling in neurogenesis

Glucocorticoids are steroid hormones secreted mainly by adrenal cortex. They are involved in several processes such as metabolism [181], immune response [182], cardiovascular functions [183] and development [184]. De novo glucocorticoid synthesis also occurs in the brain suggesting key roles of the local synthesis in neurological functions [185, 186]. In normal physiological conditions, glucocorticoids are involved in adaptive responses. However, chronic exposure to glucocorticoids was shown to be associated with chronic stress state and several metabolic disorders as obesity, insulin resistance, glucose intolerance dyslipidemia and hypertension [187]. For instance, glucocorticoid levels were shown to be upregulated in the adrenal glands in case of obesity [188-190]. Indeed, the  $11\beta$ -HSD1 enzyme that transforms cortisone into cortisol, the main active form of glucocorticoid, is increased in the adipose tissue of obese human [191, 192]. Similarly, diabetic individuals are also subjected to higher levels of glucocorticoids associated to chronic stress and depression [193, 194]. The glucocorticoid responsive gene, *fkbp5*, was also shown to be upregulated in the subcutaneous adipose tissue of type 2 diabetic patients, linked to the increase in glucose levels [195]. Also, glucocorticoid levels are associated with non-alcoholic fatty liver, a hepatic disorder found in both obesity and diabetes [196].

In the central nervous system, chronic exposure to glucocorticoids increases neuro-inflammation and hippocampal neuronal damage [197]. Several studies show that high glucocorticoid levels are associated with decreased brain plasticity. Indeed, in vitro studies performed on embryonic neural stem/progenitor cells confirm that the chronic exposure to glucocorticoids suppresses differentiation and survival of NSCs affecting several signaling pathways and decreases the expression of neuronal and synaptic markers [198]. In parallel, long term exposure leads, in vivo, to blunted hippocampal neurogenesis [199, 200], that is restored through the use of glucocorticoid receptor antagonists [201]. Together, glucocorticoids increase the loss of hippocampal neurons, reduce adult neurogenesis and compromise cognitive functions leading to an increasing risk for developing Alzheimer's disease [200, 202]. This is further corroborated by the study of diabetic mice that display higher levels of corticosteroids and have increased tau protein phosphorylation correlated to memory impairments [203]. Overall, these data support the fact that chronic exposure to glucocorticoids negatively affects brain homeostasis and plasticity, promoting behavioral change and increasing risk factor of cognitive defects and neurodegenerative disease.

In zebrafish, the inter-renal gland ensures the function of the adrenal gland found in mammals and secrete glucocorticoids [204]. As well, the brain is able to de novo steroidogenesis and glucocorticoid synthesis [205-208]. In a zebrafish model of obesity associated with hyperglycemia, the expression of the glucocorticoid responsive gene *fkbp5* was up-regulated but did not reach a significant level [130]. Unpublished data from our laboratory using a stronger model of overfeeding also demonstrated an increase in the cerebral expression of *fkbp5*. Together, these data suggest that the peripheral and/or locally produced glucocorticoids may be increased under overfeeding condition. Our preliminary data for measuring glucocorticoid levels in the brain of obese/hyperglycemic fish tend to show an increase of glucocorticoid levels. Further investigations are consequently required to understand whether glucocorticoids are indeed significantly



increased during zebrafish obesity and diabetes or not and what are their roles in brain plasticity in these pathologies in zebrafish.

Many other factors well-known to modulate and regulate neurogenesis should be also investigated such as Wnt signaling, SHH, endothelial factors, inflammation, oxidative stress and other steroids than glucocorticoids. Figure 4 provides a scheme overview of some pathway to investigate in the brain and NSCs under metabolic disease conditions.

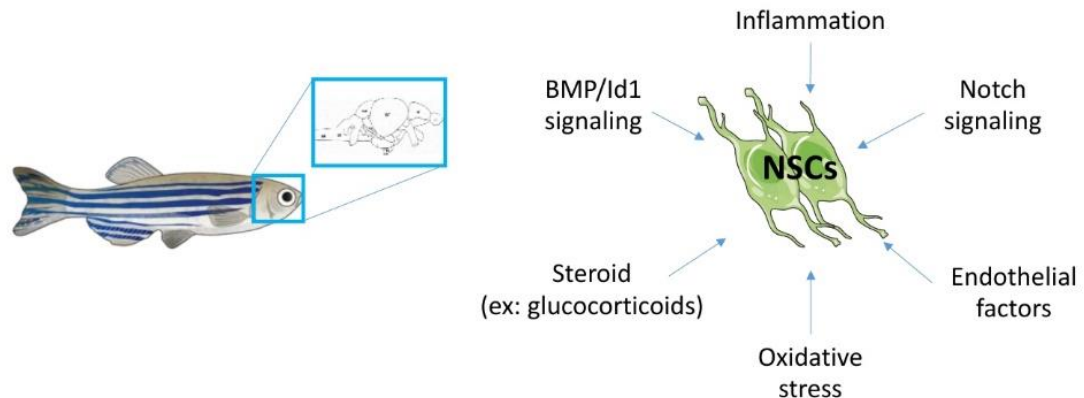


**Figure 4:** Investigate the misregulated neurogenic signaling pathway under conditions of metabolic diseases

### Conclusion

Under diabetic and obesity condition, the central nervous system is greatly affected through the disruption of the BBB and the subsequent neuro-inflammation and oxidative stress. In both mammalian and zebrafish models, metabolic disorders induce decreased brain plasticity, impaired cognitive functions and abnormal behaviors. However, the precise cellular and molecular mechanisms sustaining such impairments are not well understood. In this review, we aimed to demonstrate that zebrafish is an alternative model to study the impact of metabolic disorders on brain homeostasis and NSC activity. Several groups have developed successful metabolic models in zebrafish, mimicking overweight, obesity and hyperglycemic/diabetic states. Indeed, zebrafish under appropriate experimental procedures can show many features of human metabolic disruption: higher body weight and BMI, expansion of visceral and subcutaneous adipose tissues, liver steatosis, disturbed lipidic profiles (LDL, HDL, body cholesterol and triglycerides), insulin resistance and hyperglycemia. Furthermore, zebrafish is well-recognized as an interesting model for studying brain plasticity including homeostatic and regenerative neurogenesis [21, 22, 49, 55, 151, 158, 176, 209, 210]. Consequently, this model is appropriate to further investigate the role of metabolic disorders on adult neurogenesis. Now, further explorations of the molecular mechanisms and signaling pathways disrupted in NSCs should be done under metabolic disorder conditions.

**Author Contributions:** Writing and Review: BG and ND

**Funding:** This work was supported by the European Regional Development Funds (RE0022527) ZEBRATOX (EU-Région Réunion-French State national counterpart).

### References:

1. Saklayen, M. G., The Global Epidemic of the Metabolic Syndrome. *Curr Hypertens Rep* **2018**, *20*, (2), 12.



2. Gurgel, M. H. C.; Montenegro Junior, R. M.; Melo Ponte, C. M.; Sousa, T. C. S.; Silva, P. G. B.; de Sousa Belem, L.; Furtado, F. L. B.; de Araujo Batista, L. A.; Pereira, A. C.; Santos, R. D., Metabolic syndrome, diabetes and inadequate lifestyle in first-degree relatives of acute myocardial infarction survivors younger than 45 years old. *Lipids Health Dis* **2017**, *16*, (1), 224.
3. DeBoer, M. D.; Filipp, S. L.; Sims, M.; Musani, S. K.; Gurka, M. J., Risk of Ischemic Stroke Increases Over the Spectrum of Metabolic Syndrome Severity. *Stroke* **2020**, *51*, (8), 2548-2552.
4. Katsiki, N.; Anagnostis, P.; Kotsa, K.; Goulis, D. G.; Mikhailidis, D. P., Obesity, Metabolic Syndrome and the Risk of Microvascular Complications in Patients with Diabetes mellitus. *Curr Pharm Des* **2019**, *25*, (18), 2051-2059.
5. Bangen, K. J.; Armstrong, N. M.; Au, R.; Gross, A. L., Metabolic Syndrome and Cognitive Trajectories in the Framingham Offspring Study. *J Alzheimers Dis* **2019**, *71*, (3), 931-943.
6. Blumentals, W. A.; Hwu, P.; Kobayashi, N.; Ogura, E., Obesity in hospitalized type 2 diabetes patients: a descriptive study. *Med Sci Monit* **2013**, *19*, 359-65.
7. Ritz, E., Metabolic syndrome and kidney disease. *Blood Purif* **2008**, *26*, (1), 59-62.
8. Tune, J. D.; Goodwill, A. G.; Sassoon, D. J.; Mather, K. J., Cardiovascular consequences of metabolic syndrome. *Transl Res* **2017**, *183*, 57-70.
9. Artunc, F.; Schleicher, E.; Weigert, C.; Fritsche, A.; Stefan, N.; Haring, H. U., The impact of insulin resistance on the kidney and vasculature. *Nat Rev Nephrol* **2016**, *12*, (12), 721-737.
10. van der Heijden, R. A.; Sheedfar, F.; Morrison, M. C.; Hommelberg, P. P.; Kor, D.; Kloosterhuis, N. J.; Gruben, N.; Youssef, S. A.; de Bruin, A.; Hofker, M. H.; Kleemann, R.; Koonen, D. P.; Heeringa, P., High-fat diet induced obesity primes inflammation in adipose tissue prior to liver in C57BL/6j mice. *Aging (Albany NY)* **2015**, *7*, (4), 256-68.
11. Hazlehurst, J. M.; Woods, C.; Marjot, T.; Cobbold, J. F.; Tomlinson, J. W., Non-alcoholic fatty liver disease and diabetes. *Metabolism* **2016**, *65*, (8), 1096-108.
12. Andre, C.; Dinel, A. L.; Ferreira, G.; Laye, S.; Castanon, N., Diet-induced obesity progressively alters cognition, anxiety-like behavior and lipopolysaccharide-induced depressive-like behavior: focus on brain indoleamine 2,3-dioxygenase activation. *Brain, behavior, and immunity* **2014**, *41*, 10-21.
13. Vieira, M. N. N.; Lima-Filho, R. A. S.; De Felice, F. G., Connecting Alzheimer's disease to diabetes: Underlying mechanisms and potential therapeutic targets. *Neuropharmacology* **2018**, *136*, (Pt B), 160-171.
14. Roh, H. T.; Cho, S. Y.; So, W. Y., Obesity promotes oxidative stress and exacerbates blood-brain barrier disruption after high-intensity exercise. *J Sport Health Sci* **2017**, *6*, (2), 225-230.
15. Yoo, D. Y.; Yim, H. S.; Jung, H. Y.; Nam, S. M.; Kim, J. W.; Choi, J. H.; Seong, J. K.; Yoon, Y. S.; Kim, D. W.; Hwang, I. K., Chronic type 2 diabetes reduces the integrity of the blood-brain barrier by reducing tight junction proteins in the hippocampus. *The Journal of veterinary medical science / the Japanese Society of Veterinary Science* **2016**.
16. Pugazhenthii, S.; Qin, L.; Reddy, P. H., Common neurodegenerative pathways in obesity, diabetes, and Alzheimer's disease. *Biochim Biophys Acta Mol Basis Dis* **2017**, *1863*, (5), 1037-1045.
17. Miller, A. A.; Spencer, S. J., Obesity and neuroinflammation: a pathway to cognitive impairment. *Brain Behav Immun* **2014**, *42*, 10-21.
18. Milanski, M.; Degasperii, G.; Coope, A.; Morari, J.; Denis, R.; Cintra, D. E.; Tsukumo, D. M.; Anhe, G.; Amaral, M. E.; Takahashi, H. K.; Curi, R.; Oliveira, H. C.; Carvalheira, J. B.; Bordin, S.; Saad,

- M. J.; Velloso, L. A., Saturated fatty acids produce an inflammatory response predominantly through the activation of TLR4 signaling in hypothalamus: implications for the pathogenesis of obesity. *J Neurosci* **2009**, *29*, (2), 359-70. 643-645
19. Sarparanta, J.; Garcia-Macia, M.; Singh, R., Autophagy and Mitochondria in Obesity and Type 2 Diabetes. *Curr Diabetes Rev* **2017**, *13*, (4), 352-369. 646-647
20. Bondia-Pons, I.; Ryan, L.; Martinez, J. A., Oxidative stress and inflammation interactions in human obesity. *J Physiol Biochem* **2012**, *68*, (4), 701-11. 648-649
21. Ghaddar, B.; Lubke, L.; Couret, D.; Rastegar, S.; Diotel, N., Cellular Mechanisms Participating in Brain Repair of Adult Zebrafish and Mammals after Injury. *Cells* **2021**, *10*, (2). 650-651
22. Diotel, N.; Lubke, L.; Strahle, U.; Rastegar, S., Common and Distinct Features of Adult Neurogenesis and Regeneration in the Telencephalon of Zebrafish and Mammals. *Front Neurosci* **2020**, *14*, 568930. 652-654
23. Fares, J.; Bou Diab, Z.; Nabha, S.; Fares, Y., Neurogenesis in the adult hippocampus: history, regulation, and prospective roles. *The International journal of neuroscience* **2019**, *129*, (6), 598-611. 655-656
24. Alam, M. J.; Kitamura, T.; Saitoh, Y.; Ohkawa, N.; Kondo, T.; Inokuchi, K., Adult Neurogenesis Conserves Hippocampal Memory Capacity. *J Neurosci* **2018**, *38*, (31), 6854-6863. 657-658
25. Kempermann, G.; Gage, F. H.; Aigner, L.; Song, H.; Curtis, M. A.; Thuret, S.; Kuhn, H. G.; Jessberger, S.; Frankland, P. W.; Cameron, H. A.; Gould, E.; Hen, R.; Abrous, D. N.; Toni, N.; Schinder, A. F.; Zhao, X.; Lucassen, P. J.; Frisen, J., Human Adult Neurogenesis: Evidence and Remaining Questions. *Cell Stem Cell* **2018**, *23*, (1), 25-30. 659-662
26. Boldrini, M.; Fulmore, C. A.; Tartt, A. N.; Simeon, L. R.; Pavlova, I.; Poposka, V.; Rosoklija, G. B.; Stankov, A.; Arango, V.; Dwork, A. J.; Hen, R.; Mann, J. J., Human Hippocampal Neurogenesis Persists throughout Aging. *Cell Stem Cell* **2018**, *22*, (4), 589-599 e5. 663-665
27. Ernst, A.; Frisen, J., Adult neurogenesis in humans- common and unique traits in mammals. *PLoS Biol* **2015**, *13*, (1), e1002045. 666-667
28. Lindsey, B. W.; Tropepe, V., A comparative framework for understanding the biological principles of adult neurogenesis. *Prog Neurobiol* **2006**, *80*, (6), 281-307. 668-669
29. Kohman, R. A.; Rhodes, J. S., Neurogenesis, inflammation and behavior. *Brain Behav Immun* **2013**, *27*, (1), 22-32. 670-671
30. Yirmiya, R.; Goshen, I., Immune modulation of learning, memory, neural plasticity and neurogenesis. *Brain Behav Immun* **2011**, *25*, (2), 181-213. 672-673
31. Ryan, S. M.; Nolan, Y. M., Neuroinflammation negatively affects adult hippocampal neurogenesis and cognition: can exercise compensate? *Neurosci Biobehav Rev* **2015**, *61*, 121-131. 674-675
32. Covacu, R.; Brundin, L., Effects of Neuroinflammation on Neural Stem Cells. *Neuroscientist* **2017**, *23*, (1), 27-39. 676-677
33. Singh, S.; Mishra, A.; Tiwari, V.; Shukla, S., Enhanced neuroinflammation and oxidative stress are associated with altered hippocampal neurogenesis in 1-methyl-4-phenyl-1,2,3,6-tetrahydropyridine treated mice. *Behav Pharmacol* **2019**, *30*, (8), 689-699. 678-680
34. Borsini, A.; Zunszain, P. A.; Thuret, S.; Pariante, C. M., The role of inflammatory cytokines as key modulators of neurogenesis. *Trends Neurosci* **2015**, *38*, (3), 145-57. 681-682

35. Zonis, S.; Ljubimov, V. A.; Mahgerefteh, M.; Pechnick, R. N.; Wawrowsky, K.; Chesnokova, V., p21Cip restrains hippocampal neurogenesis and protects neuronal progenitors from apoptosis during acute systemic inflammation. *Hippocampus* **2013**, *23*, (12), 1383-94.
36. Zonis, S.; Pechnick, R. N.; Ljubimov, V. A.; Mahgerefteh, M.; Wawrowsky, K.; Michelsen, K. S.; Chesnokova, V., Chronic intestinal inflammation alters hippocampal neurogenesis. *J Neuroinflammation* **2015**, *12*, 65.
37. Kleinert, M.; Clemmensen, C.; Hofmann, S. M.; Moore, M. C.; Renner, S.; Woods, S. C.; Huypens, P.; Beckers, J.; de Angelis, M. H.; Schurmann, A.; Bakhti, M.; Klingenspor, M.; Heiman, M.; Cherrington, A. D.; Ristow, M.; Lickert, H.; Wolf, E.; Havel, P. J.; Muller, T. D.; Tschop, M. H., Animal models of obesity and diabetes mellitus. *Nat Rev Endocrinol* **2018**, *14*, (3), 140-162.
38. Ghaddar, B.; Veeren, B.; Rondeau, P.; Bringart, M.; Lefebvre d'Hellencourt, C.; Meilhac, O.; Bascands, J. L.; Diotel, N., Impaired brain homeostasis and neurogenesis in diet-induced overweight zebrafish: a preventive role from *A. borbonica* extract. *Scientific reports* **2020**, *10*, (1), 14496.
39. Landgraf, K.; Schuster, S.; Meusel, A.; Garten, A.; Riemer, T.; Schleinitz, D.; Kiess, W.; Korner, A., Short-term overfeeding of zebrafish with normal or high-fat diet as a model for the development of metabolically healthy versus unhealthy obesity. *BMC physiology* **2017**, *17*, (1), 4.
40. Dorsemans, A. C.; Soule, S.; Weger, M.; Bourdon, E.; Lefebvre d'Hellencourt, C.; Meilhac, O.; Diotel, N., Impaired constitutive and regenerative neurogenesis in adult hyperglycemic zebrafish. *J Comp Neurol* **2017**, *525*, (3), 442-458.
41. Montalbano, G.; Mania, M.; Guerrero, M. C.; Laura, R.; Abbate, F.; Levanti, M.; Maugeri, A.; Germana, A.; Navarra, M., Effects of a Flavonoid-Rich Extract from *Citrus sinensis* Juice on a Diet-Induced Obese Zebrafish. *International journal of molecular sciences* **2019**, *20*, (20).
42. Capiotti, K. M.; Antonioli, R., Jr.; Kist, L. W.; Bogo, M. R.; Bonan, C. D.; Da Silva, R. S., Persistent impaired glucose metabolism in a zebrafish hyperglycemia model. *Comp Biochem Physiol B Biochem Mol Biol* **2014**, *171*, 58-65.
43. Capiotti, K. M.; De Moraes, D. A.; Menezes, F. P.; Kist, L. W.; Bogo, M. R.; Da Silva, R. S., Hyperglycemia induces memory impairment linked to increased acetylcholinesterase activity in zebrafish (*Danio rerio*). *Behavioural brain research* **2014**, *274*, 319-25.
44. Menke, A. L.; Spitsbergen, J. M.; Wolterbeek, A. P.; Woutersen, R. A., Normal anatomy and histology of the adult zebrafish. *Toxicol Pathol* **2011**, *39*, (5), 759-75.
45. Howe, K.; Clark, M. D.; Torroja, C. F.; Torrance, J.; Berthelot, C.; Muffato, M.; Collins, J. E.; Humphray, S.; McLaren, K.; Matthews, L.; McLaren, S.; Sealy, I.; Caccamo, M.; Churcher, C.; Scott, C.; Barrett, J. C.; Koch, R.; Rauch, G. J.; White, S.; Chow, W.; Kilian, B.; Quintais, L. T.; Guerra-Assuncao, J. A.; Zhou, Y.; Gu, Y.; Yen, J.; Vogel, J. H.; Eyre, T.; Redmond, S.; Banerjee, R.; Chi, J.; Fu, B.; Langley, E.; Maguire, S. F.; Laird, G. K.; Lloyd, D.; Kenyon, E.; Donaldson, S.; Sehra, H.; Almeida-King, J.; Loveland, J.; Trevanion, S.; Jones, M.; Quail, M.; Willey, D.; Hunt, A.; Burton, J.; Sims, S.; McLay, K.; Plumb, B.; Davis, J.; Clee, C.; Oliver, K.; Clark, R.; Riddle, C.; Elliot, D.; Threadgold, G.; Harden, G.; Ware, D.; Begum, S.; Mortimore, B.; Kerry, G.; Heath, P.; Phillimore, B.; Tracey, A.; Corby, N.; Dunn, M.; Johnson, C.; Wood, J.; Clark, S.; Pelan, S.; Griffiths, G.; Smith, M.; Glithero, R.; Howden, P.; Barker, N.; Lloyd, C.; Stevens, C.; Harley, J.; Holt, K.; Panagiotidis, G.; Lovell, J.; Beasley, H.; Henderson, C.; Gordon, D.; Auger, K.; Wright, D.; Collins, J.; Raisin, C.; Dyer, L.; Leung, K.; Robertson, L.; Ambridge, K.; Leongamornlert, D.; McGuire, S.; Gilderthorp, R.; Griffiths, C.;

- Manthravadi, D.; Nichol, S.; Barker, G.; Whitehead, S.; Kay, M.; Brown, J.; Murnane, C.; Gray, E.; 725  
Humphries, M.; Sycamore, N.; Barker, D.; Saunders, D.; Wallis, J.; Babbage, A.; Hammond, S.; 726  
Mashreghi-Mohammadi, M.; Barr, L.; Martin, S.; Wray, P.; Ellington, A.; Matthews, N.; Ellwood, M.; 727  
Woodmansey, R.; Clark, G.; Cooper, J.; Tromans, A.; Grafham, D.; Skuce, C.; Pandian, R.; Andrews, 728  
R.; Harrison, E.; Kimberley, A.; Garnett, J.; Fosker, N.; Hall, R.; Garner, P.; Kelly, D.; Bird, C.; Palmer, 729  
S.; Gehring, I.; Berger, A.; Dooley, C. M.; Ersan-Urun, Z.; Eser, C.; Geiger, H.; Geisler, M.; Karotki, L.; 730  
Kirn, A.; Konantz, J.; Konantz, M.; Oberlander, M.; Rudolph-Geiger, S.; Teucke, M.; Lanz, C.; 731  
Raddatz, G.; Osoegawa, K.; Zhu, B.; Rapp, A.; Widaa, S.; Langford, C.; Yang, F.; Schuster, S. C.; 732  
Carter, N. P.; Harrow, J.; Ning, Z.; Herrero, J.; Searle, S. M.; Enright, A.; Geisler, R.; Plasterk, R. H.; 733  
Lee, C.; Westerfield, M.; de Jong, P. J.; Zon, L. I.; Postlethwait, J. H.; Nusslein-Volhard, C.; Hubbard, 734  
T. J.; Roest Crollius, H.; Rogers, J.; Stemple, D. L., The zebrafish reference genome sequence and its 735  
relationship to the human genome. *Nature* **2013**, *496*, (7446), 498-503. 736
46. Heckler, K.; Kroll, J., Zebrafish as a Model for the Study of Microvascular Complications of 737  
Diabetes and Their Mechanisms. *International journal of molecular sciences* **2017**, *18*, (9). 738
47. Zang, L.; Shimada, Y.; Nishimura, N., Development of a Novel Zebrafish Model for Type 2 739  
Diabetes Mellitus. *Scientific reports* **2017**, *7*, (1), 1461. 740
48. Wiggenhauser, L. M.; Kroll, J., Vascular Damage in Obesity and Diabetes: Highlighting Links 741  
Between Endothelial Dysfunction and Metabolic Disease in Zebrafish and Man. *Curr Vasc Pharmacol* 742  
**2019**, *17*, (5), 476-490. 743
49. Grandel, H.; Brand, M., Comparative aspects of adult neural stem cell activity in vertebrates. 744  
*Development genes and evolution* **2013**, *223*, (1-2), 131-47. 745
50. Grandel, H.; Kaslin, J.; Ganz, J.; Wenzel, I.; Brand, M., Neural stem cells and neurogenesis in 746  
the adult zebrafish brain: origin, proliferation dynamics, migration and cell fate. *Dev Biol* **2006**, *295*, 747  
(1), 263-77. 748
51. Pellegrini, E.; Mouriec, K.; Anglade, I.; Menuet, A.; Le Page, Y.; Gueguen, M. M.; Marmignon, 749  
M. H.; Brion, F.; Pakdel, F.; Kah, O., Identification of aromatase-positive radial glial cells as 750  
progenitor cells in the ventricular layer of the forebrain in zebrafish. *J Comp Neurol* **2007**, *501*, (1), 150- 751  
67. 752
52. Lucini, C.; D'Angelo, L.; Cacialli, P.; Palladino, A.; de Girolamo, P., BDNF, Brain, and 753  
Regeneration: Insights from Zebrafish. *Int J Mol Sci* **2018**, *19*, (10). 754
53. Zambusi, A.; Ninkovic, J., Regeneration of the central nervous system-principles from brain 755  
regeneration in adult zebrafish. *World J Stem Cells* **2020**, *12*, (1), 8-24. 756
54. Lupperger, V.; Buggenthin, F.; Chapouton, P.; Marr, C., Image analysis of neural stem cell 757  
division patterns in the zebrafish brain. *Cytometry A* **2018**, *93*, (3), 314-322. 758
55. Schmidt, R.; Beil, T.; Strähle, U.; Rastegar, S., Stab wound injury of the zebrafish adult 759  
telencephalon: a method to investigate vertebrate brain neurogenesis and regeneration. *J Vis Exp* 760  
**2014**, (90), e51753. 761
56. Dorsemans, A. C.; Lefebvre d'Hellencourt, C.; Ait-Arsa, I.; Jestin, E.; Meilhac, O.; Diotel, N., 762  
Acute and Chronic Models of Hyperglycemia in Zebrafish: A Method to Assess the Impact of 763  
Hyperglycemia on Neurogenesis and the Biodistribution of Radiolabeled Molecules. *J Vis Exp* **2017**, 764  
(124). 765



57. Couret, D.; Bourane, S.; Catan, A.; Nativel, B.; Planesse, C.; Dorsemans, A. C.; Ait-Arsa, I.; Cournot, M.; Rondeau, P.; Patche, J.; Tran-Dinh, A.; Lambert, G.; Diotel, N.; Meilhac, O., A hemorrhagic transformation model of mechanical stroke therapy with acute hyperglycemia in mice. *J Comp Neurol* **2018**, *526*, (6), 1006-1016. 766-769
58. Couret, D.; Planesse, C.; Patche, J.; Diotel, N.; Nativel, B.; Bourane, S.; Meilhac, O., Lack of Neuroprotective Effects of High-Density Lipoprotein Therapy in Stroke under Acute Hyperglycemic Conditions. *Molecules* **2021**, *26*, (21). 770-772
59. Abookasis, D.; Shemesh, D.; Bokobza, N.; Bloygrund, H.; Franjy-Tal, Y.; Rozenberg, K.; Rosenzweig, T., Evaluation the effect of acute hyperglycemia on cerebral tissue properties with diffuse optical imaging systems. *Proc. SPIE 11360, Neurophotonics, 113600F* **2020**. 773-775
60. Kinkel, M. D.; Eames, S. C.; Philipson, L. H.; Prince, V. E., Intraperitoneal injection into adult zebrafish. *J Vis Exp* **2010**, (42). 776-777
61. Moss, J. B.; Koustubhan, P.; Greenman, M.; Parsons, M. J.; Walter, I.; Moss, L. G., Regeneration of the pancreas in adult zebrafish. *Diabetes* **2009**, *58*, (8), 1844-51. 778-779
62. Delaspre, F.; Beer, R. L.; Rovira, M.; Huang, W.; Wang, G.; Gee, S.; Vitery Mdel, C.; Wheelan, S. J.; Parsons, M. J., Centroacinar Cells Are Progenitors That Contribute to Endocrine Pancreas Regeneration. *Diabetes* **2015**, *64*, (10), 3499-509. 780-782
63. Intine, R. V.; Olsen, A. S.; Sarras, M. P., Jr., A zebrafish model of diabetes mellitus and metabolic memory. *J Vis Exp* **2013**, (72), e50232. 783-784
64. Benchoula, K.; Khatib, A.; Quzwain, F. M. C.; Che Mohamad, C. A.; Wan Sulaiman, W. M. A.; Abdul Wahab, R.; Ahmed, Q. U.; Abdul Ghaffar, M.; Saiman, M. Z.; Alajmi, M. F.; El-Seedi, H., Optimization of Hyperglycemic Induction in Zebrafish and Evaluation of Its Blood Glucose Level and Metabolite Fingerprint Treated with Psychotria malayana Jack Leaf Extract. *Molecules* **2019**, *24*, (8). 785-789
65. Islam, M. S.; Loots du, T., Experimental rodent models of type 2 diabetes: a review. *Methods Find Exp Clin Pharmacol* **2009**, *31*, (4), 249-61. 790-791
66. Szkudelski, T., The mechanism of alloxan and streptozotocin action in B cells of the rat pancreas. *Physiol Res* **2001**, *50*, (6), 537-46. 792-793
67. Olsen, A. S.; Sarras, M. P., Jr.; Intine, R. V., Limb regeneration is impaired in an adult zebrafish model of diabetes mellitus. *Wound repair and regeneration : official publication of the Wound Healing Society [and] the European Tissue Repair Society* **2010**, *18*, (5), 532-42. 794-796
68. Nam, Y. H.; Hong, B. N.; Rodriguez, I.; Ji, M. G.; Kim, K.; Kim, U. J.; Kang, T. H., Synergistic Potentials of Coffee on Injured Pancreatic Islets and Insulin Action via KATP Channel Blocking in Zebrafish. *J Agric Food Chem* **2015**, *63*, (23), 5612-21. 797-799
69. Shin, E.; Na Hong, B.; Ho Kang, T., An optimal establishment of an acute hyperglycemia zebrafish model. **2012**, Vol.6(42), 2922-2928. 800-801
70. Neelofar, K.; Arif, Z.; Alam, K.; Ahmad, J., Hyperglycemia induced structural and functional changes in human serum albumin of diabetic patients: a physico-chemical study. *Mol Biosyst* **2016**, *12*, (8), 2481-9. 802-804
71. Steele, C.; Hagopian, W. A.; Gitelman, S.; Masharani, U.; Cavaghan, M.; Rother, K. I.; Donaldson, D.; Harlan, D. M.; Bluestone, J.; Herold, K. C., Insulin secretion in type 1 diabetes. *Diabetes* **2004**, *53*, (2), 426-33. 805-807

72. Zhang, J.; Wang, Y.; Gurung, P.; Wang, T.; Li, L.; Zhang, R.; Li, H.; Guo, R.; Han, Q.; Zhang, J.; Lei, S.; Liu, F., The relationship between the thickness of glomerular basement membrane and renal outcomes in patients with diabetic nephropathy. *Acta Diabetol* **2018**, *55*, (7), 669-679.
73. Zeng, Y.; Cao, D.; Yu, H.; Yang, D.; Zhuang, X.; Hu, Y.; Li, J.; Yang, J.; Wu, Q.; Liu, B.; Zhang, L., Early retinal neurovascular impairment in patients with diabetes without clinically detectable retinopathy. *Br J Ophthalmol* **2019**, *103*, (12), 1747-1752.
74. Patel, S.; Srivastava, S.; Singh, M. R.; Singh, D., Mechanistic insight into diabetic wounds: Pathogenesis, molecular targets and treatment strategies to pace wound healing. *Biomed Pharmacother* **2019**, *112*, 108615.
75. Wang, Q.; Luo, C.; Lu, G.; Chen, Z., Effect of adenosine monophosphate-activated protein kinase-p53-Kruppel-like factor 2a pathway in hyperglycemia-induced cardiac remodeling in adult zebrafish. *J Diabetes Investig* **2021**, *12*, (3), 320-333.
76. Olsen, A. S.; Sarras, M. P., Jr.; Leontovich, A.; Intine, R. V., Heritable transmission of diabetic metabolic memory in zebrafish correlates with DNA hypomethylation and aberrant gene expression. *Diabetes* **2012**, *61*, (2), 485-91.
77. Wang, X.; Yang, X. L.; Liu, K. C.; Sheng, W. L.; Xia, Q.; Wang, R. C.; Chen, X. Q.; Zhang, Y., Effects of streptozotocin on pancreatic islet beta-cell apoptosis and glucose metabolism in zebrafish larvae. *Fish Physiol Biochem* **2020**, *46*, (3), 1025-1038.
78. Prince, V. E.; Anderson, R. M.; Dalgin, G., Zebrafish Pancreas Development and Regeneration: Fishing for Diabetes Therapies. *Curr Top Dev Biol* **2017**, *124*, 235-276.
79. Matsuda, H., Zebrafish as a model for studying functional pancreatic beta cells development and regeneration. *Dev Growth Differ* **2018**, *60*, (6), 393-399.
80. Benchoula, K.; Khatib, A.; Jaffar, A.; Ahmed, Q. U.; Sulaiman, W.; Wahab, R. A.; El-Seedi, H. R., The promise of zebrafish as a model of metabolic syndrome. *Exp Anim* **2019**, *68*, (4), 407-416.
81. Connaughton, V. P.; Baker, C.; Fonde, L.; Gerardi, E.; Slack, C., Alternate Immersion in an External Glucose Solution Differentially Affects Blood Sugar Values in Older Versus Younger Zebrafish Adults. *Zebrafish* **2016**, *13*, (2), 87-94.
82. Gence, L.; Fernezelian, D.; Bringart, M.; Veeren, B.; Christophe, A.; Brion, F.; Meilhac, O.; Bascands, J. L.; Diotel, N., Hypericum lanceolatum Lam. Medicinal Plant: Potential Toxicity and Therapeutic Effects Based on a Q2 Zebrafish Model. *Frontiers in Pharmacology* **2022**, *13*.
83. Alsahli, M.; Gerich, J. E., Renal glucose metabolism in normal physiological conditions and in diabetes. *Diabetes Res Clin Pract* **2017**, *133*, 1-9.
84. Schwartzburd, P., Glucose-lowering Strategies in Diabetes: Pharmacological Development of New Antidiabetic Drugs. *Curr Pharm Des* **2018**, *24*, (9), 1007-1011.
85. Block, N. E.; Buse, M. G., Effects of hypercortisolemia and diabetes on skeletal muscle insulin receptor function in vitro and in vivo. *Am J Physiol* **1989**, *256*, (1 Pt 1), E39-48.
86. Karanth, S.; Chaurasia, B.; Bowman, F. M.; Tippetts, T. S.; Holland, W. L.; Summers, S. A.; Schlegel, A., FOXN3 controls liver glucose metabolism by regulating gluconeogenic substrate selection. *Physiol Rep* **2019**, *7*, (18), e14238.
87. Karanth, S.; Zinkhan, E. K.; Hill, J. T.; Yost, H. J.; Schlegel, A., FOXN3 Regulates Hepatic Glucose Utilization. *Cell Rep* **2016**, *15*, (12), 2745-55.

88. Kimmel, R. A.; Dobler, S.; Schmitner, N.; Walsen, T.; Freudenblum, J.; Meyer, D., Diabetic pdx1-mutant zebrafish show conserved responses to nutrient overload and anti-glycemic treatment. *Sci Rep* **2015**, *5*, 14241. 849-851
89. Maddison, L. A.; Joest, K. E.; Kammeyer, R. M.; Chen, W., Skeletal muscle insulin resistance in zebrafish induces alterations in beta-cell number and glucose tolerance in an age- and diet-dependent manner. *Am J Physiol Endocrinol Metab* **2015**, *308*, (8), E662-9. 852-854
90. Salehpour, A.; Rezaei, M.; Khoradmehr, A.; Tahamtani, Y.; Tamadon, A., Which Hyperglycemic Model of Zebrafish (Danio rerio) Suits My Type 2 Diabetes Mellitus Research? A Scoring System for Available Methods. *Front Cell Dev Biol* **2021**, *9*, 652061. 855-857
91. Zang, L.; Maddison, L. A.; Chen, W., Zebrafish as a Model for Obesity and Diabetes. *Front Cell Dev Biol* **2018**, *6*, 91. 858-859
92. Anderson, J. L.; Carten, J. D.; Farber, S. A., Zebrafish lipid metabolism: from mediating early patterning to the metabolism of dietary fat and cholesterol. *Methods Cell Biol* **2011**, *101*, 111-41. 860-861
93. Meguro, S.; Hasumura, T.; Hase, T., Body fat accumulation in zebrafish is induced by a diet rich in fat and reduced by supplementation with green tea extract. *PLoS One* **2015**, *10*, (3), e0120142. 862-863
94. Montalbano, G.; Mania, M.; Abbate, F.; Navarra, M.; Guerrero, M. C.; Laura, R.; Vega, J. A.; Levanti, M.; Germana, A., Melatonin treatment suppresses appetite genes and improves adipose tissue plasticity in diet-induced obese zebrafish. *Endocrine* **2018**, *62*, (2), 381-393. 864-866
95. Montalbano, G.; Mania, M.; Guerrero, M. C.; Abbate, F.; Laura, R.; Navarra, M.; Vega, J. A.; Ciriaco, E.; Germana, A., Morphological differences in adipose tissue and changes in BDNF/Trkb expression in brain and gut of a diet induced obese zebrafish model. *Ann Anat* **2016**, *204*, 36-44. 867-869
96. Ahima, R. S.; Lazar, M. A., Physiology. The health risk of obesity--better metrics imperative. *Science* **2013**, *341*, (6148), 856-8. 870-871
97. Chu, C. Y.; Chen, C. F.; Rajendran, R. S.; Shen, C. N.; Chen, T. H.; Yen, C. C.; Chuang, C. K.; Lin, D. S.; Hsiao, C. D., Overexpression of Akt1 enhances adipogenesis and leads to lipoma formation in zebrafish. *PloS one* **2012**, *7*, (5), e36474. 872-874
98. Hsu, C. C.; Lai, C. Y.; Lin, C. Y.; Yeh, K. Y.; Her, G. M., MicroRNA-27b Depletion Enhances Endotrophic and Intravascular Lipid Accumulation and Induces Adipocyte Hyperplasia in Zebrafish. *Int J Mol Sci* **2017**, *19*, (1). 875-877
99. Oka, T.; Nishimura, Y.; Zang, L.; Hirano, M.; Shimada, Y.; Wang, Z.; Umemoto, N.; Kuroyanagi, J.; Nishimura, N.; Tanaka, T., Diet-induced obesity in zebrafish shares common pathophysiological pathways with mammalian obesity. *BMC Physiol* **2010**, *10*, 21. 878-880
100. Hasumura, T.; Shimada, Y.; Kuroyanagi, J.; Nishimura, Y.; Meguro, S.; Takema, Y.; Tanaka, T., Green tea extract suppresses adiposity and affects the expression of lipid metabolism genes in diet-induced obese zebrafish. *Nutr Metab (Lond)* **2012**, *9*, (1), 73. 881-883
101. Hiramitsu, M.; Shimada, Y.; Kuroyanagi, J.; Inoue, T.; Katagiri, T.; Zang, L.; Nishimura, Y.; Nishimura, N.; Tanaka, T., Eriocitrin ameliorates diet-induced hepatic steatosis with activation of mitochondrial biogenesis. *Scientific reports* **2014**, *4*, 3708. 884-886
102. Forn-Cuni, G.; Varela, M.; Fernandez-Rodriguez, C. M.; Figueras, A.; Novoa, B., Liver immune responses to inflammatory stimuli in a diet-induced obesity model of zebrafish. *J Endocrinol* **2015**, *224*, (2), 159-70. 887-889

103. Meguro, S.; Hosoi, S.; Hasumura, T., High-fat diet impairs cognitive function of zebrafish. *Scientific reports* **2019**, *9*, (1), 17063. 890-891
104. Ye, L.; Mueller, O.; Bagwell, J.; Bagnat, M.; Liddle, R. A.; Rawls, J. F., High fat diet induces microbiota-dependent silencing of enteroendocrine cells. *Elife* **2019**, *8*. 892-893
105. Grisotto, C.; Taile, J.; Planesse, C.; Diotel, N.; Gonthier, M. P.; Meilhac, O.; Couret, D., High-Fat Diet Aggravates Cerebral Infarct, Hemorrhagic Transformation and Neuroinflammation in a Mouse Stroke Model. *International journal of molecular sciences* **2021**, *22*, (9). 894-896
106. Kothari, V.; Luo, Y.; Tornabene, T.; O'Neill, A. M.; Greene, M. W.; Geetha, T.; Babu, J. R., High fat diet induces brain insulin resistance and cognitive impairment in mice. *Biochim Biophys Acta Mol Basis Dis* **2017**, *1863*, (2), 499-508. 897-899
107. Della Vedova, M. C.; Munoz, M. D.; Santillan, L. D.; Plateo-Pignatari, M. G.; Germano, M. J.; Rinaldi Tosi, M. E.; Garcia, S.; Gomez, N. N.; Fornes, M. W.; Gomez Mejiba, S. E.; Ramirez, D. C., A Mouse Model of Diet-Induced Obesity Resembling Most Features of Human Metabolic Syndrome. *Nutr Metab Insights* **2016**, *9*, 93-102. 900-903
108. Cao, M.; Pan, Q.; Dong, H.; Yuan, X.; Li, Y.; Sun, Z.; Dong, X.; Wang, H., Adipose-derived mesenchymal stem cells improve glucose homeostasis in high-fat diet-induced obese mice. *Stem Cell Res Ther* **2015**, *6*, 208. 904-906
109. Carnovali, M.; Luzi, L.; Terruzzi, I.; Banfi, G.; Mariotti, M., Metabolic and bone effects of high-fat diet in adult zebrafish. *Endocrine* **2018**, *61*, (2), 317-326. 907-908
110. Diotel, N.; Rodriguez Viales, R.; Armant, O.; Marz, M.; Ferg, M.; Rastegar, S.; Strahle, U., Comprehensive expression map of transcription regulators in the adult zebrafish telencephalon reveals distinct neurogenic niches. *J Comp Neurol* **2015**, *523*, (8), 1202-21. 909-911
111. Kizil, C.; Kaslin, J.; Kroehne, V.; Brand, M., Adult neurogenesis and brain regeneration in zebrafish. *Dev Neurobiol* **2012**, *72*, (3), 429-61. 912-913
112. Eliceiri, B. P.; Gonzalez, A. M.; Baird, A., Zebrafish model of the blood-brain barrier: morphological and permeability studies. *Methods Mol Biol* **2011**, *686*, 371-8. 914-915
113. Chhabria, K.; Vouros, A.; Gray, C.; MacDonald, R. B.; Jiang, Z.; Wilkinson, R. N.; Plant, K.; Vasilaki, E.; Howarth, C.; Chico, T. J. A., Sodium nitroprusside prevents the detrimental effects of glucose on the neurovascular unit and behaviour in zebrafish. *Dis Model Mech* **2019**, *12*, (9). 916-918
114. Chhabria, K.; Plant, K.; Bandmann, O.; Wilkinson, R. N.; Martin, C.; Kugler, E.; Armitage, P. A.; Santoscoy, P. L.; Cunliffe, V. T.; Huisken, J.; McGown, A.; Ramesh, T.; Chico, T. J.; Howarth, C., The effect of hyperglycemia on neurovascular coupling and cerebrovascular patterning in zebrafish. *J Cereb Blood Flow Metab* **2020**, *40*, (2), 298-313. 919-922
115. Dos Santos, M. M.; de Macedo, G. T.; Prestes, A. S.; Ecker, A.; Muller, T. E.; Leitemperger, J.; Fontana, B. D.; Ardisson-Araujo, D. M. P.; Rosemberg, D. B.; Barbosa, N. V., Modulation of redox and insulin signaling underlie the anti-hyperglycemic and antioxidant effects of diphenyl diselenide in zebrafish. *Free radical biology & medicine* **2020**, *158*, 20-31. 923-926
116. Nellore, J.; Pauline P, C.; Mohanan, S. P.; Ravikumar, R.; Pillai, R. C., Vinca rosea Normalizes Oxidative Stress and Inhibits Hyperglycemia Induced Increase in VEGF in Zebrafish Retina. *Research Journal of Pharmaceutical, Biological and Chemical Sciences* **2013**, *4*, (4), 927-936. 927-929



117. Oyelaja-Akinsipo, O. B.; Dare, E. O.; Katare, D. P., Protective role of diosgenin against hyperglycaemia-mediated cerebral ischemic brain injury in zebrafish model of type II diabetes mellitus. *Heliyon* **2020**, *6*, (1), e03296.
118. Dos Santos, M. M.; de Macedo, G. T.; Prestes, A. S.; Loro, V. L.; Heidrich, G. M.; Picoloto, R. S.; Rosemberg, D. B.; Barbosa, N. V., Hyperglycemia elicits anxiety-like behaviors in zebrafish: Protective role of dietary diphenyl diselenide. *Prog Neuropsychopharmacol Biol Psychiatry* **2018**, *85*, 128-135.
119. Rom, S.; Zuluaga-Ramirez, V.; Gajghate, S.; Seliga, A.; Winfield, M.; Heldt, N. A.; Kolpakov, M. A.; Bashkirova, Y. V.; Sabri, A. K.; Persidsky, Y., Hyperglycemia-Driven Neuroinflammation Compromises BBB Leading to Memory Loss in Both Diabetes Mellitus (DM) Type 1 and Type 2 Mouse Models. *Mol Neurobiol* **2019**, *56*, (3), 1883-1896.
120. Wanrooy, B. J.; Kumar, K. P.; Wen, S. W.; Qin, C. X.; Ritchie, R. H.; Wong, C. H. Y., Distinct contributions of hyperglycemia and high-fat feeding in metabolic syndrome-induced neuroinflammation. *Journal of neuroinflammation* **2018**, *15*, (1), 293.
121. Alvarez-Nolting, R.; Arnal, E.; Barcia, J. M.; Miranda, M.; Romero, F. J., Protection by DHA of early hippocampal changes in diabetes: possible role of CREB and NF-kappaB. *Neurochem Res* **2012**, *37*, (1), 105-115.
122. Piazza, F. V.; Pinto, G. V.; Trott, G.; Marcuzzo, S.; Gomez, R.; Fernandes Mda, C., Enriched environment prevents memory deficits in type 1 diabetic rats. *Behav Brain Res* **2011**, *217*, (1), 16-20.
123. Balu, D. T.; Hodes, G. E.; Hill, T. E.; Ho, N.; Rahman, Z.; Bender, C. N.; Ring, R. H.; Dwyer, J. M.; Rosenzweig-Lipson, S.; Hughes, Z. A.; Schechter, L. E.; Lucki, I., Flow cytometric analysis of BrdU incorporation as a high-throughput method for measuring adult neurogenesis in the mouse. *J Pharmacol Toxicol Methods* **2009**, *59*, (2), 100-7.
124. Beauquis, J.; Roig, P.; Homo-Delarche, F.; De Nicola, A.; Saravia, F., Reduced hippocampal neurogenesis and number of hilar neurones in streptozotocin-induced diabetic mice: reversion by antidepressant treatment. *The European journal of neuroscience* **2006**, *23*, (6), 1539-46.
125. Ho, N.; Sommers, M. S.; Lucki, I., Effects of diabetes on hippocampal neurogenesis: links to cognition and depression. *Neurosci Biobehav Rev* **2013**, *37*, (8), 1346-62.
126. Corem, N.; Anzi, S.; Gelb, S.; Ben-Zvi, A., Leptin receptor deficiency induces early, transient and hyperglycaemia-independent blood-brain barrier dysfunction. *Scientific reports* **2019**, *9*, (1), 2884.
127. Fujihara, R.; Chiba, Y.; Nakagawa, T.; Nishi, N.; Murakami, R.; Matsumoto, K.; Kawauchi, M.; Yamamoto, T.; Ueno, M., Albumin microvascular leakage in brains with diabetes mellitus. *Microscopy research and technique* **2016**, *79*, (9), 833-7.
128. Nerurkar, P. V.; Johns, L. M.; Buesa, L. M.; Kipyakwai, G.; Volper, E.; Sato, R.; Shah, P.; Feher, D.; Williams, P. G.; Nerurkar, V. R., Momordica charantia (bitter melon) attenuates high-fat diet-associated oxidative stress and neuroinflammation. *J Neuroinflammation* **2011**, *8*, 64.
129. Muriach, M.; Flores-Bellver, M.; Romero, F. J.; Barcia, J. M., Diabetes and the brain: oxidative stress, inflammation, and autophagy. *Oxidative medicine and cellular longevity* **2014**, *2014*, 102158.
130. Ghaddar, B.; Bringart, M.; Lefebvre d'Helencourt, C.; Meilhac, O.; Diotel, N., Deleterious Effects of Overfeeding on Brain Homeostasis and Plasticity in Adult Zebrafish. *Zebrafish* **2021**, *18*, (3), 190-206.

131. Imperatore, R.; Tunisi, L.; Mavaro, I.; D'Angelo, L.; Attanasio, C.; Safari, O.; Motlagh, H. A.; De Girolamo, P.; Cristino, L.; Varricchio, E.; Paolucci, M., Immunohistochemical Analysis of Intestinal and Central Nervous System Morphology in an Obese Animal Model (Danio rerio) Treated with 3,5-T2: A Possible Farm Management Practice? *Animals (Basel)* **2020**, *10*, (7).
132. Wang, J.; Li, Y.; Lai, K.; Zhong, Q.; Demin, K. A.; Kalueff, A. V.; Song, C., High-glucose/high-cholesterol diet in zebrafish evokes diabetic and affective pathogenesis: The role of peripheral and central inflammation, microglia and apoptosis. *Prog Neuropsychopharmacol Biol Psychiatry* **2020**, *96*, 109752.
133. Luzio, A.; Figueiredo, M.; Matos, M. M.; Coimbra, A. M.; Alvaro, A. R.; Monteiro, S. M., Effects of short-term exposure to genistein and overfeeding diet on the neural and retinal progenitor competence of adult zebrafish (Danio rerio). *Neurotoxicol Teratol* **2021**, *88*, 107030.
134. Stankiewicz, A. J.; McGowan, E. M.; Yu, L.; Zhdanova, I. V., Impaired Sleep, Circadian Rhythms and Neurogenesis in Diet-Induced Premature Aging. *International journal of molecular sciences* **2017**, *18*, (11).
135. Weger, M.; Diotel, N.; Dorsemans, A. C.; Dickmeis, T.; Weger, B. D., Stem cells and the circadian clock. *Dev Biol* **2017**, *431*, (2), 111-123.
136. Weger, M.; Weger, B. D.; Diotel, N.; Rastegar, S.; Hirota, T.; Kay, S. A.; Strahle, U.; Dickmeis, T., Real-time in vivo monitoring of circadian E-box enhancer activity: a robust and sensitive zebrafish reporter line for developmental, chemical and neural biology of the circadian clock. *Dev Biol* **2013**, *380*, (2), 259-73.
137. Ogata, S.; Ito, S.; Masuda, T.; Ohtsuki, S., Changes of Blood-Brain Barrier and Brain Parenchymal Protein Expression Levels of Mice under Different Insulin-Resistance Conditions Induced by High-Fat Diet. *Pharm Res* **2019**, *36*, (10), 141.
138. Salameh, T. S.; Mortell, W. G.; Logsdon, A. F.; Butterfield, D. A.; Banks, W. A., Disruption of the hippocampal and hypothalamic blood-brain barrier in a diet-induced obese model of type II diabetes: prevention and treatment by the mitochondrial carbonic anhydrase inhibitor, topiramate. *Fluids Barriers CNS* **2019**, *16*, (1), 1.
139. Valcarcel-Ares, M. N.; Tucsek, Z.; Kiss, T.; Giles, C. B.; Tarantini, S.; Yabluchanskiy, A.; Balasubramanian, P.; Gautam, T.; Galvan, V.; Ballabh, P.; Richardson, A.; Freeman, W. M.; Wren, J. D.; Deak, F.; Ungvari, Z.; Csiszar, A., Obesity in Aging Exacerbates Neuroinflammation, Dysregulating Synaptic Function-Related Genes and Altering Eicosanoid Synthesis in the Mouse Hippocampus: Potential Role in Impaired Synaptic Plasticity and Cognitive Decline. *J Gerontol A Biol Sci Med Sci* **2019**, *74*, (3), 290-298.
140. Hersey, M.; Woodruff, J. L.; Maxwell, N.; Sadek, A. T.; Bykalo, M. K.; Bain, I.; Grillo, C. A.; Piroli, G. G.; Hashemi, P.; Reagan, L. P., High-fat diet induces neuroinflammation and reduces the serotonergic response to escitalopram in the hippocampus of obese rats. *Brain Behav Immun* **2021**.
141. Ly, M.; Raji, C. A.; Yu, G. Z.; Wang, Q.; Wang, Y.; Schindler, S. E.; An, H.; Samara, A.; Eisenstein, S. A.; Hershey, T.; Smith, G.; Klein, S.; Liu, J.; Xiong, C.; Ances, B. M.; Morris, J. C.; Benzinger, T. L. S., Obesity and White Matter Neuroinflammation Related Edema in Alzheimer's Disease Dementia Biomarker Negative Cognitively Normal Individuals. *J Alzheimers Dis* **2021**, *79*, (4), 1801-1811.

142. Nam, S. M.; Kim, J. W.; Kwon, H. J.; Yoo, D. Y.; Jung, H. Y.; Kim, D. W.; Hwang, I. K.; Seong, J. K.; Yoon, Y. S., Differential Effects of Low- and High-dose Zinc Supplementation on Synaptic Plasticity and Neurogenesis in the Hippocampus of Control and High-fat Diet-fed Mice. *Neurochem Res* **2017**, *42*, (11), 3149-3159. 1012-1015
143. Suarez, J.; Rivera, P.; Aparisi Rey, A.; Perez-Martin, M.; Arrabal, S.; Rodriguez de Fonseca, F.; Ruiz de Azua, I.; Lutz, B., Adipocyte cannabinoid CB1 receptor deficiency alleviates high fat diet-induced memory deficit, depressive-like behavior, neuroinflammation and impairment in adult neurogenesis. *Psychoneuroendocrinology* **2019**, *110*, 104418. 1016-1019
144. Wongchitrat, P.; Lansubsakul, N.; Kamsrijai, U.; Sae-Ung, K.; Mukda, S.; Govitrapong, P., Melatonin attenuates the high-fat diet and streptozotocin-induced reduction in rat hippocampal neurogenesis. *Neurochem Int* **2016**, *100*, 97-109. 1020-1022
145. Saiyasit, N.; Chunchai, T.; Prus, D.; Suparan, K.; Pittayapong, P.; Apaijai, N.; Pratchayasakul, W.; Sripetchwandee, J.; Chattipakorn, M. D. P. D. N.; Chattipakorn, S. C., Gut dysbiosis develops before metabolic disturbance and cognitive decline in high-fat diet-induced obese condition. *Nutrition* **2020**, *69*, 110576. 1023-1026
146. Hsieh, J., Orchestrating transcriptional control of adult neurogenesis. *Genes & development* **2012**, *26*, (10), 1010-21. 1027-1028
147. Beckervordersandforth, R.; Zhang, C. L.; Lie, D. C., Transcription-Factor-Dependent Control of Adult Hippocampal Neurogenesis. *Cold Spring Harbor perspectives in biology* **2015**, *7*, (10), a018879. 1029-1030
148. Faigle, R.; Song, H., Signaling mechanisms regulating adult neural stem cells and neurogenesis. *Biochim Biophys Acta* **2013**, *1830*, (2), 2435-48. 1031-1032
149. Jurisch-Yaksi, N.; Yaksi, E.; Kizil, C., Radial glia in the zebrafish brain: Functional, structural, and physiological comparison with the mammalian glia. *Glia* **2020**. 1033-1034
150. Chapouton, P.; Jagasia, R.; Bally-Cuif, L., Adult neurogenesis in non-mammalian vertebrates. *Bioessays* **2007**, *29*, (8), 745-57. 1035-1036
151. Labusch, M.; Mancini, L.; Morizet, D.; Bally-Cuif, L., Conserved and Divergent Features of Adult Neurogenesis in Zebrafish. *Front Cell Dev Biol* **2020**, *8*, 525. 1037-1038
152. Aujla, P. K.; Naratadam, G. T.; Xu, L.; Raetzman, L. T., Notch/Rbpjkappa signaling regulates progenitor maintenance and differentiation of hypothalamic arcuate neurons. *Development* **2013**, *140*, (17), 3511-21. 1039-1041
153. Chapouton, P.; Webb, K. J.; Stigloher, C.; Alunni, A.; Adolf, B.; Hesel, B.; Topp, S.; Kremmer, E.; Bally-Cuif, L., Expression of hairy/enhancer of split genes in neural progenitors and neurogenesis domains of the adult zebrafish brain. *J Comp Neurol* **2011**, *519*, (9), 1748-69. 1042-1044
154. Chapouton, P.; Skupien, P.; Hesel, B.; Coolen, M.; Moore, J. C.; Madelaine, R.; Kremmer, E.; Faus-Kessler, T.; Blader, P.; Lawson, N. D.; Bally-Cuif, L., Notch activity levels control the balance between quiescence and recruitment of adult neural stem cells. *J Neurosci* **2010**, *30*, (23), 7961-74. 1045-1047
155. Sueda, R.; Kageyama, R., Regulation of active and quiescent somatic stem cells by Notch signaling. *Development, growth & differentiation* **2020**, *62*, (1), 59-66. 1048-1049
156. Zhang, R.; Engler, A.; Taylor, V., Notch: an interactive player in neurogenesis and disease. *Cell Tissue Res* **2018**, *371*, (1), 73-89. 1050-1051
157. Alunni, A.; Bally-Cuif, L., A comparative view of regenerative neurogenesis in vertebrates. *Development* **2016**, *143*, (5), 741-53. 1052-1053

158. de Oliveira-Carlos, V.; Ganz, J.; Hans, S.; Kaslin, J.; Brand, M., Notch receptor expression in neurogenic regions of the adult zebrafish brain. *PLoS One* **2013**, *8*, (9), e73384. 1054-1055
159. Ables, J. L.; Decarolis, N. A.; Johnson, M. A.; Rivera, P. D.; Gao, Z.; Cooper, D. C.; Radtke, F.; Hsieh, J.; Eisch, A. J., Notch1 is required for maintenance of the reservoir of adult hippocampal stem cells. *J Neurosci* **2010**, *30*, (31), 10484-92. 1056-1058
160. Gaiano, N.; Nye, J. S.; Fishell, G., Radial glial identity is promoted by Notch1 signaling in the murine forebrain. *Neuron* **2000**, *26*, (2), 395-404. 1059-1060
161. Piccin, D.; Yu, F.; Morshead, C. M., Notch signaling imparts and preserves neural stem characteristics in the adult brain. *Stem Cells Dev* **2013**, *22*, (10), 1541-50. 1061-1062
162. Kishimoto, N.; Shimizu, K.; Sawamoto, K., Neuronal regeneration in a zebrafish model of adult brain injury. *Disease models & mechanisms* **2012**, *5*, (2), 200-9. 1063-1064
163. Mendes-da-Silva, C.; Lemes, S. F.; Baliani Tda, S.; Versutti, M. D.; Torsoni, M. A., Increased expression of Hes5 protein in Notch signaling pathway in the hippocampus of mice offspring of dams fed a high-fat diet during pregnancy and suckling. *Int J Dev Neurosci* **2015**, *40*, 35-42. 1065-1067
164. Yu, M.; Jiang, M.; Yang, C.; Wu, Y.; Liu, Y.; Cui, Y.; Huang, G., Maternal high-fat diet affects Msi/Notch/Hes signaling in neural stem cells of offspring mice. *J Nutr Biochem* **2014**, *25*, (2), 227-31. 1068-1069
165. Li, J.; Tang, Y.; Cai, D., IKKbeta/NF-kappaB disrupts adult hypothalamic neural stem cells to mediate a neurodegenerative mechanism of dietary obesity and pre-diabetes. *Nat Cell Biol* **2012**, *14*, (10), 999-1012. 1070-1072
166. Fu, J.; Tay, S. S.; Ling, E. A.; Dheen, S. T., High glucose alters the expression of genes involved in proliferation and cell-fate specification of embryonic neural stem cells. *Diabetologia* **2006**, *49*, (5), 1027-38. 1073-1075
167. Rodrigues, D. C.; Harvey, E. M.; Suraj, R.; Erickson, S. L.; Mohammad, L.; Ren, M.; Liu, H.; He, G.; Kaplan, D. R.; Ellis, J.; Yang, G., Methylglyoxal couples metabolic and translational control of Notch signalling in mammalian neural stem cells. *Nat Commun* **2020**, *11*, (1), 2018. 1076-1078
168. Miyazono, K.; Kamiya, Y.; Morikawa, M., Bone morphogenetic protein receptors and signal transduction. *J Biochem* **2010**, *147*, (1), 35-51. 1079-1080
169. Shi, Y.; Massague, J., Mechanisms of TGF-beta signaling from cell membrane to the nucleus. *Cell* **2003**, *113*, (6), 685-700. 1081-1082
170. Hollnagel, A.; Oehlmann, V.; Heymer, J.; Ruther, U.; Nordheim, A., Id genes are direct targets of bone morphogenetic protein induction in embryonic stem cells. *J Biol Chem* **1999**, *274*, (28), 19838-45. 1083-1085
171. Ling, F.; Kang, B.; Sun, X. H., Id proteins: small molecules, mighty regulators. *Curr Top Dev Biol* **2014**, *110*, 189-216. 1086-1087
172. Diotel, N.; Beil, T.; Strahle, U.; Rastegar, S., Differential expression of id genes and their potential regulator znf238 in zebrafish adult neural progenitor cells and neurons suggests distinct functions in adult neurogenesis. *Gene Expr Patterns* **2015**, *19*, (1-2), 1-13. 1088-1090
173. Nam, H. S.; Benezra, R., High levels of Id1 expression define B1 type adult neural stem cells. *Cell Stem Cell* **2009**, *5*, (5), 515-26. 1091-1092
174. Zhang, G.; Ferg, M.; Lubke, L.; Takamiya, M.; Beil, T.; Gourain, V.; Diotel, N.; Strahle, U.; Rastegar, S., Bone morphogenetic protein signaling regulates Id1 mediated neural stem cell 1093-1094



- quiescence in the adult zebrafish brain via a phylogenetically conserved enhancer module. *Stem Cells* **2020**. 1095  
1096
175. Zhang, G.; Ferg, M.; Lubke, L.; Takamiya, M.; Beil, T.; Gourain, V.; Diotel, N.; Strahle, U.; Rastegar, S., Bone morphogenetic protein signaling regulates Id1-mediated neural stem cell quiescence in the adult zebrafish brain via a phylogenetically conserved enhancer module. *Stem Cells* **2020**. 1097  
1098  
1099  
1100
176. Rodriguez Viales, R.; Diotel, N.; Ferg, M.; Armant, O.; Eich, J.; Alunni, A.; Marz, M.; Bally-Cuif, L.; Rastegar, S.; Strahle, U., The helix-loop-helix protein id1 controls stem cell proliferation during regenerative neurogenesis in the adult zebrafish telencephalon. *Stem Cells* **2015**, *33*, (3), 892-903. 1101  
1102  
1103  
1104
177. Jensen, G. S.; Leon-Palmer, N. E.; Townsend, K. L., Bone morphogenetic proteins (BMPs) in the central regulation of energy balance and adult neural plasticity. *Metabolism: clinical and experimental* **2021**, *123*, 154837. 1105  
1106  
1107
178. Baboota, R. K.; Bluher, M.; Smith, U., Emerging Role of Bone Morphogenetic Protein 4 in Metabolic Disorders. *Diabetes* **2021**, *70*, (2), 303-312. 1108  
1109
179. Townsend, K. L.; Suzuki, R.; Huang, T. L.; Jing, E.; Schulz, T. J.; Lee, K.; Taniguchi, C. M.; Espinoza, D. O.; McDougall, L. E.; Zhang, H.; He, T. C.; Kokkotou, E.; Tseng, Y. H., Bone morphogenetic protein 7 (BMP7) reverses obesity and regulates appetite through a central mTOR pathway. *FASEB J* **2012**, *26*, (5), 2187-96. 1110  
1111  
1112  
1113
180. Townsend, K. L.; Madden, C. J.; Blaszkiewicz, M.; McDougall, L.; Tupone, D.; Lynes, M. D.; Mishina, Y.; Yu, P.; Morrison, S. F.; Tseng, Y. H., Reestablishment of Energy Balance in a Male Mouse Model With POMC Neuron Deletion of BMPRI1A. *Endocrinology* **2017**, *158*, (12), 4233-4245. 1114  
1115  
1116
181. Vegiopoulos, A.; Herzig, S., Glucocorticoids, metabolism and metabolic diseases. *Mol Cell Endocrinol* **2007**, *275*, (1-2), 43-61. 1117  
1118
182. Cruz-Topete, D.; Cidlowski, J. A., One hormone, two actions: anti- and pro-inflammatory effects of glucocorticoids. *Neuroimmunomodulation* **2015**, *22*, (1-2), 20-32. 1119  
1120
183. Nussinovitch, U.; de Carvalho, J. F.; Pereira, R. M.; Shoenfeld, Y., Glucocorticoids and the cardiovascular system: state of the art. *Curr Pharm Des* **2010**, *16*, (32), 3574-85. 1121  
1122
184. Fowden, A. L.; Forhead, A. J., Glucocorticoids as regulatory signals during intrauterine development. *Exp Physiol* **2015**, *100*, (12), 1477-87. 1123  
1124
185. Taves, M. D.; Gomez-Sanchez, C. E.; Soma, K. K., Extra-adrenal glucocorticoids and mineralocorticoids: evidence for local synthesis, regulation, and function. *Am J Physiol Endocrinol Metab* **2011**, *301*, (1), E11-24. 1125  
1126  
1127
186. Timmermans, S.; Souffriau, J.; Libert, C., A General Introduction to Glucocorticoid Biology. *Front Immunol* **2019**, *10*, 1545. 1128  
1129
187. McEwen, B. S., Physiology and neurobiology of stress and adaptation: central role of the brain. *Physiol Rev* **2007**, *87*, (3), 873-904. 1130  
1131
188. Vierhapper, H.; Nowotny, P.; Waldhausl, W., Production rates of cortisol in obesity. *Obes Res* **2004**, *12*, (9), 1421-5. 1132  
1133
189. Stewart, P. M.; Boulton, A.; Kumar, S.; Clark, P. M.; Shackleton, C. H., Cortisol metabolism in human obesity: impaired cortisone-->cortisol conversion in subjects with central adiposity. *J Clin Endocrinol Metab* **1999**, *84*, (3), 1022-7. 1134  
1135  
1136

190. Akalestou, E.; Genser, L.; Rutter, G. A., Glucocorticoid Metabolism in Obesity and Following Weight Loss. *Frontiers in endocrinology* **2020**, *11*, 59. 1137  
1138
191. Stomby, A.; Andrew, R.; Walker, B. R.; Olsson, T., Tissue-specific dysregulation of cortisol regeneration by 11betaHSD1 in obesity: has it promised too much? *Diabetologia* **2014**, *57*, (6), 1100-10. 1139  
1140
192. Rebuffe-Scrive, M.; Bronnegard, M.; Nilsson, A.; Eldh, J.; Gustafsson, J. A.; Bjorntorp, P., Steroid hormone receptors in human adipose tissues. *J Clin Endocrinol Metab* **1990**, *71*, (5), 1215-9. 1141  
1142
193. Chiodini, I.; Adda, G.; Scillitani, A.; Coletti, F.; Morelli, V.; Di Lembo, S.; Epaminonda, P.; Masserini, B.; Beck-Peccoz, P.; Orsi, E.; Ambrosi, B.; Arosio, M., Cortisol secretion in patients with type 2 diabetes: relationship with chronic complications. *Diabetes Care* **2007**, *30*, (1), 83-8. 1143  
1144  
1145
194. Roy, M. S.; Roy, A.; Brown, S., Increased urinary-free cortisol outputs in diabetic patients. *J Diabetes Complications* **1998**, *12*, (1), 24-7. 1146  
1147
195. Sidibeh, C. O.; Pereira, M. J.; Abalo, X. M.; G, J. B.; Skrtic, S.; Lundkvist, P.; Katsogiannos, P.; Hausch, F.; Castillejo-Lopez, C.; Eriksson, J. W., FKBP5 expression in human adipose tissue: potential role in glucose and lipid metabolism, adipogenesis and type 2 diabetes. *Endocrine* **2018**, *62*, (1), 116-128. 1148  
1149  
1150  
1151
196. Woods, C. P.; Hazlehurst, J. M.; Tomlinson, J. W., Glucocorticoids and non-alcoholic fatty liver disease. *The Journal of steroid biochemistry and molecular biology* **2015**, *154*, 94-103. 1152  
1153
197. Zhang, B.; Zhang, Y.; Wu, W.; Xu, T.; Yin, Y.; Zhang, J.; Huang, D.; Li, W., Chronic glucocorticoid exposure activates BK-NLRP1 signal involving in hippocampal neuron damage. *Journal of neuroinflammation* **2017**, *14*, (1), 139. 1154  
1155  
1156
198. Odaka, H.; Numakawa, T.; Yoshimura, A.; Nakajima, S.; Adachi, N.; Ooshima, Y.; Inoue, T.; Kunugi, H., Chronic glucocorticoid exposure suppressed the differentiation and survival of embryonic neural stem/progenitor cells: Possible involvement of ERK and PI3K/Akt signaling in the neuronal differentiation. *Neurosci Res* **2016**, *113*, 28-36. 1157  
1158  
1159  
1160
199. Morais, M.; Santos, P. A.; Mateus-Pinheiro, A.; Patricio, P.; Pinto, L.; Sousa, N.; Pedroso, P.; Almeida, S.; Filipe, A.; Bessa, J. M., The effects of chronic stress on hippocampal adult neurogenesis and dendritic plasticity are reversed by selective MAO-A inhibition. *J Psychopharmacol* **2014**, *28*, (12), 1178-83. 1161  
1162  
1163  
1164
200. Vyas, S.; Rodrigues, A. J.; Silva, J. M.; Tronche, F.; Almeida, O. F.; Sousa, N.; Sotiropoulos, I., Chronic Stress and Glucocorticoids: From Neuronal Plasticity to Neurodegeneration. *Neural plasticity* **2016**, *2016*, 6391686. 1165  
1166  
1167
201. Hu, P.; Oomen, C.; van Dam, A. M.; Wester, J.; Zhou, J. N.; Joels, M.; Lucassen, P. J., A single-day treatment with mifepristone is sufficient to normalize chronic glucocorticoid induced suppression of hippocampal cell proliferation. *PloS one* **2012**, *7*, (9), e46224. 1168  
1169  
1170
202. Caruso, A.; Nicoletti, F.; Mango, D.; Saidi, A.; Orlando, R.; Scaccianoce, S., Stress as risk factor for Alzheimer's disease. *Pharmacol Res* **2018**, *132*, 130-134. 1171  
1172
203. Dey, A.; Hao, S.; Wosiski-Kuhn, M.; Stranahan, A. M., Glucocorticoid-mediated activation of GSK3beta promotes tau phosphorylation and impairs memory in type 2 diabetes. *Neurobiol Aging* **2017**, *57*, 75-83. 1173  
1174  
1175
204. Wendelaar Bonga, S. E., The stress response in fish. *Physiol Rev* **1997**, *77*, (3), 591-625. 1176
205. Weger, M.; Diotel, N.; Weger, B. D.; Beil, T.; Zaucker, A.; Eachus, H. L.; Oakes, J. A.; do Rego, J. L.; Storbeck, K. H.; Gut, P.; Strahle, U.; Rastegar, S.; Muller, F.; Krone, N., Expression and activity 1177  
1178

- profiling of the steroidogenic enzymes of glucocorticoid biosynthesis and the fdx1 co-factors in zebrafish. *J Neuroendocrinol* **2018**, *30*, (4), e12586. 1179  
1180
206. Diotel, N.; Do Rego, J. L.; Anglade, I.; Vaillant, C.; Pellegrini, E.; Vaudry, H.; Kah, O., The brain of teleost fish, a source, and a target of sexual steroids. *Front Neurosci* **2011**, *5*, 137. 1181  
1182
207. Diotel, N.; Do Rego, J. L.; Anglade, I.; Vaillant, C.; Pellegrini, E.; Gueguen, M. M.; Mironov, S.; Vaudry, H.; Kah, O., Activity and expression of steroidogenic enzymes in the brain of adult zebrafish. *Eur J Neurosci* **2011**, *34*, (1), 45-56. 1183  
1184  
1185
208. Sakamoto, H.; Ukena, K.; Tsutsui, K., Activity and localization of 3beta-hydroxysteroid dehydrogenase/ Delta5-Delta4-isomerase in the zebrafish central nervous system. *J Comp Neurol* **2001**, *439*, (3), 291-305. 1186  
1187  
1188
209. Than-Trong, E.; Kiani, B.; Dray, N.; Ortica, S.; Simons, B.; Rulands, S.; Alunni, A.; Bally-Cuif, L., Lineage hierarchies and stochasticity ensure the long-term maintenance of adult neural stem cells. *Sci Adv* **2020**, *6*, (18), eaaz5424. 1189  
1190  
1191
210. Baumgart, E. V.; Barbosa, J. S.; Bally-Cuif, L.; Gotz, M.; Ninkovic, J., Stab wound injury of the zebrafish telencephalon: a model for comparative analysis of reactive gliosis. *Glia* **2012**, *60*, (3), 343-57. 1192  
1193  
1194  
1195





# Discussion



## A. **Metabolic diseases: is there a brain microvascular complication?**

### 1. **Diabetes and obesity induce brain oxidative stress: impact on BBB function and brain homeostasis**

Oxidative stress is a primary feature of metabolic disorders and is implicated in the progression of many diseases (Tan *et al.*, 2018). Reactive oxygen species (ROS) and reactive nitrogen species (RNS) are generated by the body through oxidative metabolism and mitochondrial activities (Sies, 2017). In healthy conditions, ROS are important factors involved in multiple intracellular signaling pathways. Overproduction of ROS in a manner that exceeds antioxidant defense creates a state of oxidative stress, unbalancing redox status. There is growing evidence that excessive production of reactive oxygen species leads to destruction of proteins, DNA and lipid membranes (Wang *et al.*, 2017).

Obesity is a well-known factor in inducing systemic and brain oxidative stress (Vincent & Taylor, 2006; Manna & Jain, 2015; Mazon *et al.*, 2017). Several factors can exacerbate oxidative stress in obesity: high tissue lipid storage (mainly adipose tissue) (Beltowski *et al.*, 2000), chronic inflammation (Fernandez-Sanchez *et al.*, 2011) and diet types (Khan *et al.*, 2006), as well as the main contributor, hyperglycemia (Aronson & Rayfield, 2002). In both of our models of diet-induced obesity, we observed hyperglycemia with a concomitant increase in peripheral AGEs and oxidative stress.

Diabetes and hyperglycemia induce oxidative stress through numerous mechanisms among others increased glucose flux through the polyol pathway, activation of AGE receptors (RAGE) due to elevated AGE levels, and decreased levels of antioxidant enzymes (Brownlee, 2001; Fiorentino *et al.*, 2013). The mechanisms by which glucose metabolism induces oxidative stress are illustrated in the figure below (Fig. 41)

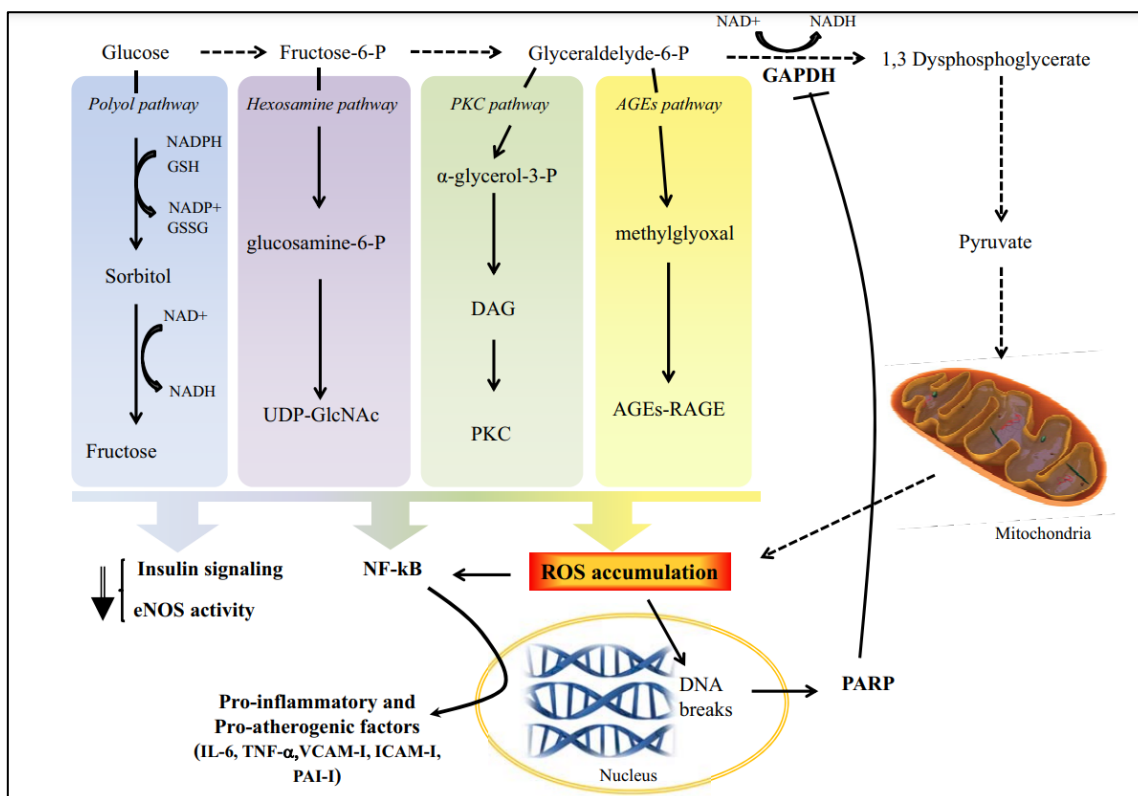


**Figure 41: The molecular pathways of hyperglycemia induced oxidative stress production.**

Hyperglycemia-induced polyol, hexosamine, protein kinase C (PKC) and advanced glycation end products (AGEs) pathways can impair insulin signaling and endothelial Nitric Oxide Synthase (eNOS) activity. It also promotes the expression of pro-inflammatory and pro-coagulant factors and induces reactive oxygen species (ROS) accumulation. Hyperglycemia also favors mitochondrial dysfunction that contributes to ROS synthesis. Oxidative stress can induce Nuclear Factor-Kappa B (NF-kB) dependent pro-inflammatory and pro-coagulant pathways and also causes DNA damage. DNA breaks can activate poly(ADP-ribose) polymerase (PARP) that inhibits glyceraldehyde-3-phosphate dehydrogenase (GAPDH), thus increasing all the glycolytic intermediates upstream of GAPDH and, therefore, the flux into polyol, hexosamine, PKC and AGEs pathways. Abbreviations: NADP: nicotinamide adenine dinucleotide phosphate, NAD: nicotinamide adenine dinucleotide, GSH: reduced glutathione, GSSG: oxidized glutathione, UDP-GlcNAc: uridine diphosphate Nacetylglucosamine, DAG: diacylglycerol, RAGE: AGEs receptor, P: phosphate, IL-6: interleukin-6, TNF-: tumor necrosis factor-, ICAM-I: intracellular adhesion Molecule-I, VCAM-I: vascular adhesion cell Molecule-I, PAI-I: plasminogen activator Inhibitor-I. From (Fiorentino *et al.*, 2013).

Oxidative stress strongly affects brain endothelial cells, which are more sensitive to oxidative stress exposure than normal endothelial cells (Banks & Rhea, 2021). The BBB is highly exposed to oxidative stress because of (i) the extensive transport of glucose to the brain, (ii) the production of high levels of nitric oxide (NO) required for vascular tone, (iii) lipid peroxidation resulting from the transport of lipids and fatty acids to the brain, and finally, (iv) the presence of a high number of mitochondria in brain endothelial cells (Banks & Rhea, 2021) (Fig. 42).



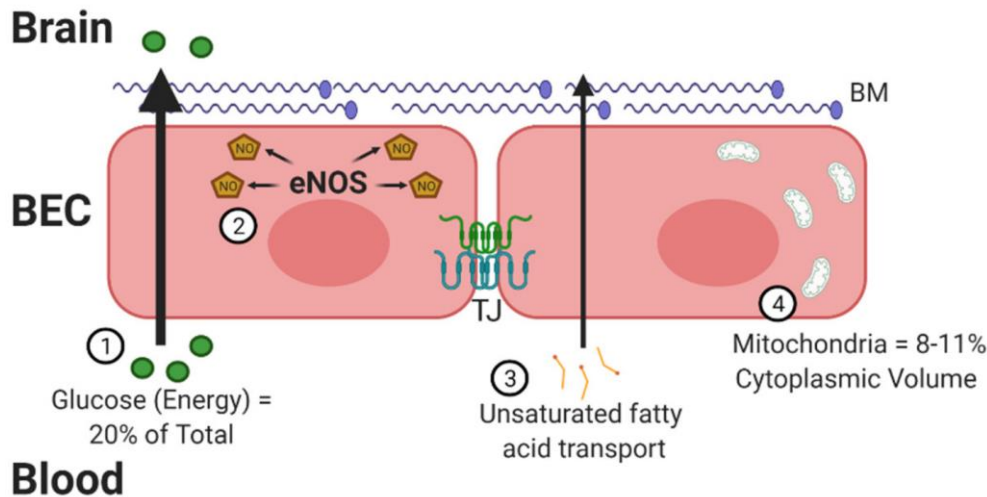


**Figure 42: The blood–brain barrier (BBB) and oxidative stress.**  
From (Banks & Rhea, 2021).

Under normal conditions, the BBB is able to fight against high oxidative stress exposure (Banks & Rhea, 2021). However, under pathophysiological conditions of high oxidative stress, BBB permeability is disrupted due to impaired tight junction protein expression, localization, and trafficking (Schreibelt *et al.*, 2007; Lochhead *et al.*, 2010), and also to activation of matrix metalloproteinases that degrade the BBB basement membrane (Gu *et al.*, 2002; Turner & Sharp, 2016). In addition, some *in vitro* experiments using human cerebral microvascular endothelial cells confirm that hyperglycemia induces BBB destruction via overproduction of ROS leading to endothelial cell apoptosis (Ryder *et al.*, 1989). Interestingly, the hyperglycemic model developed in zebrafish proved modulation of tight junction protein gene expression (Dorseman *et al.*, 2017b), but functional studies on the BBB are still lacking. Similarly, our DIO models exhibiting hyperglycemia and oxidative stress showed disturbed physiology and function of the BBB (Ghaddar *et al.*, 2020). The use of aqueous extract of *A. borbonica* extract prevents BBB disruption possibly due to its antioxidative stress property (Ghaddar *et al.*, 2020). This is probably resulting from its high content in polyphenols known to exhibit antioxidant properties.

Once the integrity of the BBB is impaired, the brain is therefore subject to infiltration of immune cells, toxins, and macromolecules from the circulation into the brain environment (Nadal *et al.*, 1995; Gingrich & Traynelis, 2000; Kadry *et al.*, 2020). In the brain, oxidative stress consequently promotes neuronal damage and affects the physiology of the nervous tissue (Mazon *et al.*, 2017). It plays an important role in the development and progression of dementia and neurodegenerative diseases (Liu & Zhang, 2012; Angelova & Abramov, 2018).

Antioxidant therapy using e.g. polyphenols (i.e., resveratrol) decreased ROS production and improved antioxidant defense such as SOD (superoxide dismutase) activity in parallel with improved cognitive decline in a rat model of induced vascular dementia, thus implicating the role of oxidative stress in brain impairment (Yadav *et al.*, 2018). In different models of HFD, increased oxidative stress was observed in the brain with reduced antioxidant defense (SOD, GPX, catalase and GSH) (Morrison *et al.*, 2010; Alzoubi *et al.*, 2018; Hajiluian *et al.*, 2018). For example, after 16 weeks of a high-fat diet, overfed rats showed increased brain oxidative stress with decreased hippocampal levels of the antioxidant enzymes glutathione peroxidase (GPx) and superoxide dismutase (SOD) (Hajiluian *et al.*, 2018). Similar results were also obtained in the hippocampus of overfed mice and resulted in cognitive decline (short- and long-term memory) compared to their control counterparts (Morrison *et al.*, 2010; Alzoubi *et al.*, 2018). Interestingly, this higher cerebral oxidative stress is related to memory impairment that is prevented by antioxidant treatment such as melatonin or resveratrol (Alzoubi *et al.*, 2018).

In the brain, neurons are highly sensible to ROS which makes oxidative stress the reason behind plenty of neurodegenerative processes (Jackson *et al.*, 1994; Dugan *et al.*, 1995). *In vitro* and *in vivo* evidences have confirmed that hyperglycemia induces neurodegeneration and neuro-inflammation through oxidative stress (Muriach *et al.*, 2014; Kumar *et al.*, 2017). Data show that ROS accumulation triggers neuro-inflammatory signaling pathways (via NF- $\kappa$ B signaling) and secretion of neurodegenerative markers (Kumar *et al.*, 2017; Richa *et al.*, 2017). Hyperglycemia-induced oxidative stress leads to neuronal degeneration through several pathological cellular pathways (Fig. 43) including mitochondrial dysfunction, ROS overproduction, over-activation of polyol pathway, and overproduction of AGEs. As a result, the neuronal macromolecules functions are altered leading to DNA mutations, protein modifications and lipid peroxidation (Mule & Singh, 2018). Therefore, neuronal degeneration is thus promoted by the induction of apoptotic or necrotic pathways and altered levels of neurotoxic A $\beta$ , a hallmark feature of Alzheimer's disease (AD) (Mule & Singh, 2018).

Several lines of evidence report the effect of oxidative stress on neurogenesis. For example, oxidative stress and resulting neuro-inflammation in mammals with T2DM have been shown to inhibit hippocampal proliferation, newborn cell migration and to promote neuronal death (Beauquis *et al.*, 2006; Wiltrout *et al.*, 2007; Jakubs *et al.*, 2008; Stranahan *et al.*, 2008). In addition, oxidative stress mediated by elevated glucose levels has been shown to impair neurogenesis by inhibiting NSC differentiation 29695191 (Chen *et al.*, 2018b). Furthermore, in the brains of hyperglycemic subjects, oxidative stress leads to mitochondrial damage and to cell

death (Merad-Boudia *et al.*, 1998), a phenomenon that has been linked to blunted neurogenesis (Cui *et al.*, 2006). These results are in agreement with our observation in DIO fish, with a decrease in neurogenesis that was restored when oxidative stress was resolved with the antioxidant extract of *A. borbonica* (Ghaddar *et al.*, 2020). Other DIO models in zebrafish also demonstrated the up-regulation of genes involved in cell death.

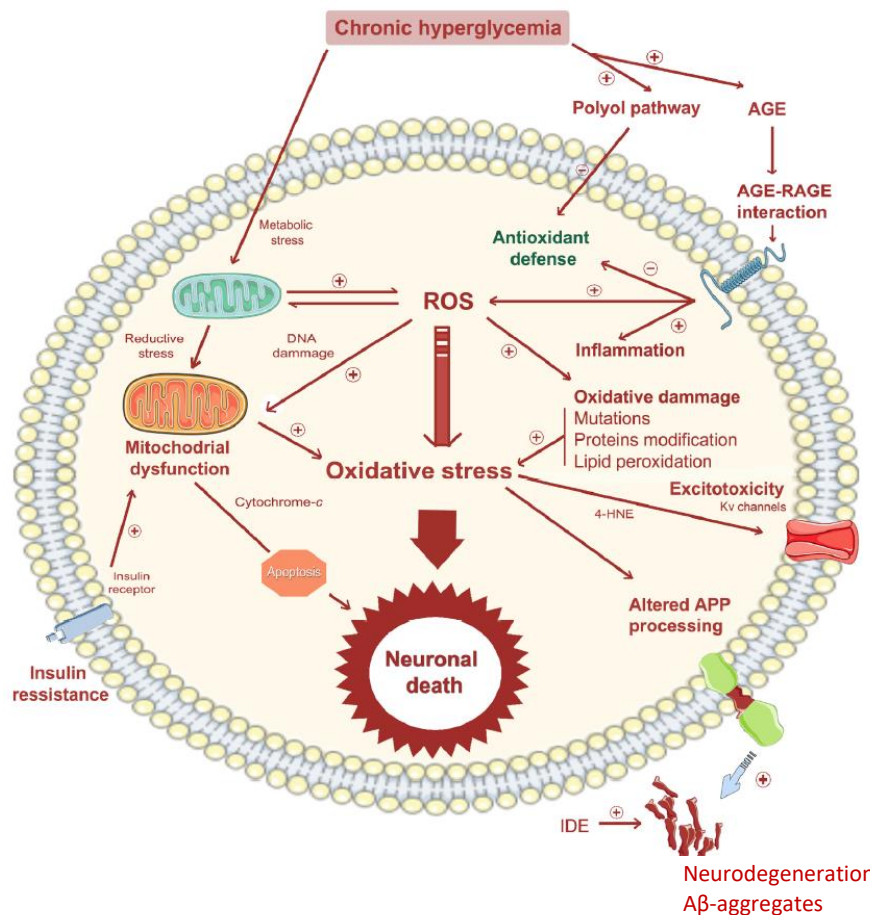


**Figure 43: pathways of neuronal degeneration as a result of hyperglycemia-induced oxidative stress.**

Chronic hyperglycemia activates the polyol pathways, increases the AGE production and leads to mitochondrial dysfunction that all increases the neuronal oxidative stress and consequently leads to neurodegeneration through apoptosis induction and the formation of Aβ aggregates.

(+) and (-) sign refers to the increase and decrease of the given pathway, respectively. From (Mule & Singh, 2018).

## 2. Diabetes and obesity induce brain inflammation: impact on BBB function and brain homeostasis

The metabolic parameters disturbed in T2DM and obese subjects such as hyperglycemia, hyperinsulinemia and increased levels of AGEs in the blood are all factors that promote chronic systemic and central inflammation (Esteve *et al.*, 2005; de Luca & Olefsky,

2008; Chang & Yang, 2016; Van Dyken & Lacoste, 2018). The most common pathway leading to inflammation is that hyperglycemia induces oxidative stress, and that oxidative stress in turn is able to activate pathways leading to inflammation (Sun *et al.*, 2014). For instance, clinical studies in human patients confirm the increase in circulating levels of inflammatory cytokines with intravenous glucose pulses, whereas no increase was observed when glucose pulses were taken with administration of the antioxidant glutathione (Sun *et al.*, 2014).

As explained previously, hyperglycemia induces BBB disruption (page 46). The disruption of the BBB lead to the activation of local immune cells, namely microglia, and thus to neuro-inflammation (Obermeier *et al.*, 2013). Neuro-inflammation is defined by the activation of brain resident immune cells (microglial cells and, to a lesser extent, astrocytes) without necessarily recruiting peripheral immune cells (Graeber *et al.*, 2011; Filiou *et al.*, 2014; Xanthos & Sandkuhler, 2014). Activation of microglia and astrocytes is involved in the pathogenesis of cognitive decline in neuro-inflammatory and neurodegenerative diseases (Fig. 44) (Hong *et al.*, 2016; Subhramanyam *et al.*, 2019). In T2DM models, disruption of BBB integrity allows leukocyte infiltration into the brain and thus induces neuronal inflammation (Van Dyken & Lacoste, 2018).

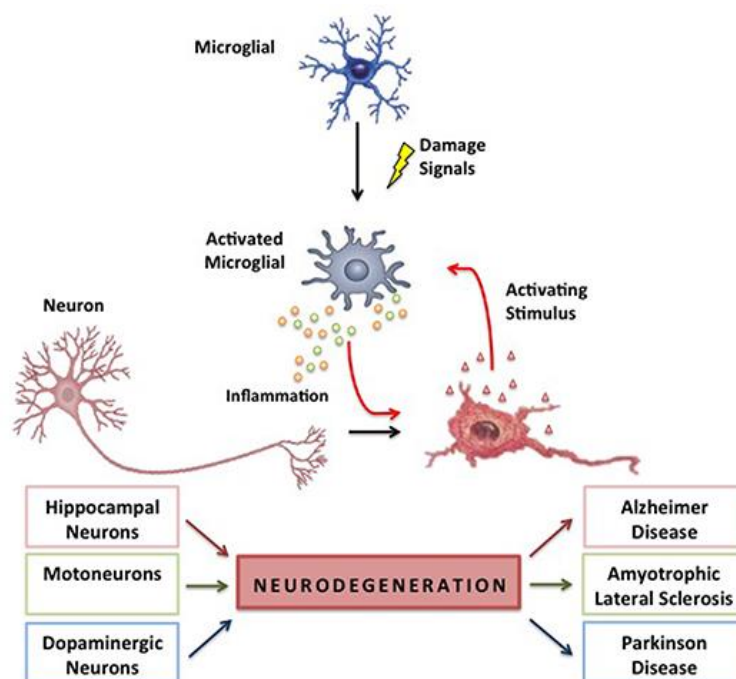


**Figure 44: Model of neuro-inflammation and neurodegeneration cycle.**

The microglial cell at rest is sensitive to different factors or signs of damage that lead to its activation. When these damage signals are maintained in time, the result is an altered response of activated microglial cells. This means that there will be a constant release of cytotoxic factors (mainly proinflammatory cytokines and ROS) that promote neuronal damage and/or lead to neurodegenerative processes. Hippocampal neurons, motor neurons, and dopaminergic neurons are susceptible to the action of overactive microglia, favoring neurodegeneration, which will trigger or will promote the development of AD, ALS and PD, respectively. In this model, once neurons



degenerate, they release substances into the extra-cellular environment that are recognized by the microglia and act as a further sign of damage, promoting a neurodegenerative cycle. From <http://dx.doi.org/10.5772/64545>.

Interestingly, the exposure of cultured human astrocytes to high concentrations of glucose increased *IL-6* and *IL-8* mRNA expression as well as the susceptibility to injury (Bahniwal *et al.*, 2017). Alteration of the BBB in genetically obese *db/db* mice has been shown to be a contributing factor to obesity-induced neuro-inflammation. Resolving BBB permeability in this model reduces neuro-inflammation (Stranahan *et al.*, 2016). As well, Rom and colleagues analyzed the genetic profiling of brain microvessels from type 2 diabetic mice with memory loss and increased BBB permeability. The data reveal upregulation of 54 genes, including genes involved in inflammation, in parallel with the activation of microglial cells revealed by analysis of brain tissue (Rom *et al.*, 2019).

There is considerable evidence that neuro-inflammation plays a role in the deterioration of neuronal and brain plasticity including neurogenesis. High-fat feeding in rodent models shows, in addition to brain neuro-inflammatory markers, increased gliosis and higher expression of neuronal injury marker (Thaler *et al.*, 2012), accompanied by decreased neuronal length, dendritic complexity (Jeon *et al.*, 2012) and altered neuronal synapse (Hao *et al.*, 2016). Regarding neurogenesis, a highly controlled process, it has been shown to be decreased after exposure to high inflammation (Song & Wang, 2011; Zunszain *et al.*, 2011; Schoenfeld & Gould, 2012). The hyperglycemic model developed in zebrafish as well as our established DIO model show decreased neurogenesis in association with elevated neuro-inflammation. In addition, high concentrations of glucose increased inflammatory cytokines production and the susceptibility of undifferentiated human neuronal cells and retinoic acid differentiated cells to damage by hydrogen peroxide and amyloid-beta protein; Together, these data suggest that hyperglycemia is a contributing factor to astrocyte-induced neuro-inflammation and neuronal injury thereby increasing the risk of AD (Bahniwal *et al.*, 2017).

Multiple lines of evidence have demonstrated that the inflammatory state (systemic or central) in animals subjected to diet-induced obesity, high-fat diet, hyperglycemia or diabetes is associated with impaired cognition and brain functions, namely, learning and memory deficits, behavioral alterations, and high anxiety (Pistell *et al.*, 2010; Lu *et al.*, 2011; Jeon *et al.*, 2012; Sivanathan *et al.*, 2015; Shi *et al.*, 2020). Some findings in humans confirm the direct relationship between systemic inflammation and cognitive decline in obese patients who have elevated plasma C-reactive protein (CRP) levels (an acute marker of inflammation) and are

prone to cognitive decline, in contrast to obese patients with normal CRP levels (Lasselin *et al.*, 2016). Rodent models of obesity and T2DM also showed cognitive dysfunction, high anxiety behavior, increased acetylcholinesterase, and reduced learning and memory capacity with a significant increase in brain inflammation (Khare *et al.*, 2017; Esmaeili *et al.*, 2020; Chen *et al.*, 2021). Interestingly, when neuro-inflammation was corrected, the cognitive impairments were resolved simultaneously, conferring a role for neuro-inflammation in exacerbating cognitive brain function (Esmaeili *et al.*, 2020).

### 3. Cognitive decline as a result of microvascular complications: what about NSCs?

Studies emphasize the contribution of hyperglycemia to the devastating effects on cognition. The observed deterioration of cognition could be directly related to neuronal activity and also to brain plasticity namely neurogenesis. Neurogenesis is known to be one of the most important mechanisms involved in brain development, learning, and memory. Alterations of neurogenic processes underlie a wide range of brain diseases (Bruel-Jungerman *et al.*, 2006; Hagihara *et al.*, 2013; Krezymon *et al.*, 2013). In adult neurogenic niches, microvessels provide a vascular scaffold for the renewal, proliferation, and differentiation of NSCs (Bjornsson *et al.*, 2015) (Fig. 45). Systematic analysis of adult neurogenic niches (SVZ and DG) in the brain of mice indicated the presence of numerous blood vessels. Obviously, NSCs interact with brain microvessels for their intrinsic metabolic needs and as an external support for their proliferative activity (Pozhilenkova *et al.*, 2017). The endothelial cells release soluble factors that stimulate the self-renewal of neural stem cells and enhance their neuron production (Shen *et al.*, 2004). Thus, this proximity between NSCs and the brain microvasculature makes them sensitive to any modification or disruption of the BBB and of the modulation of secreted factors coming from endothelial cells. Knowing that hyperglycemia leads to destruction of the BBB, it is also involved in adverse effects on neurogenesis, which are two aspects linked by a causal relationship. Thus, hyperglycemia could modulate the type and levels of endothelial factors secreted and consequently affect neurogenesis.

As previously discussed, hyperglycemia is the cause of oxidative stress and inflammation in obese or diabetic subjects. In contact with the cerebral microvascularization, NSCs are affected directly or indirectly by oxidative stress and inflammation occurring at the BBB, which is most often destroyed. The resolution of hyperglycemia and BBB permeability

with plant extracts in our DIO model was sufficient to decrease oxidative stress and inflammation (systemic and central) and maintain basal neurogenesis.

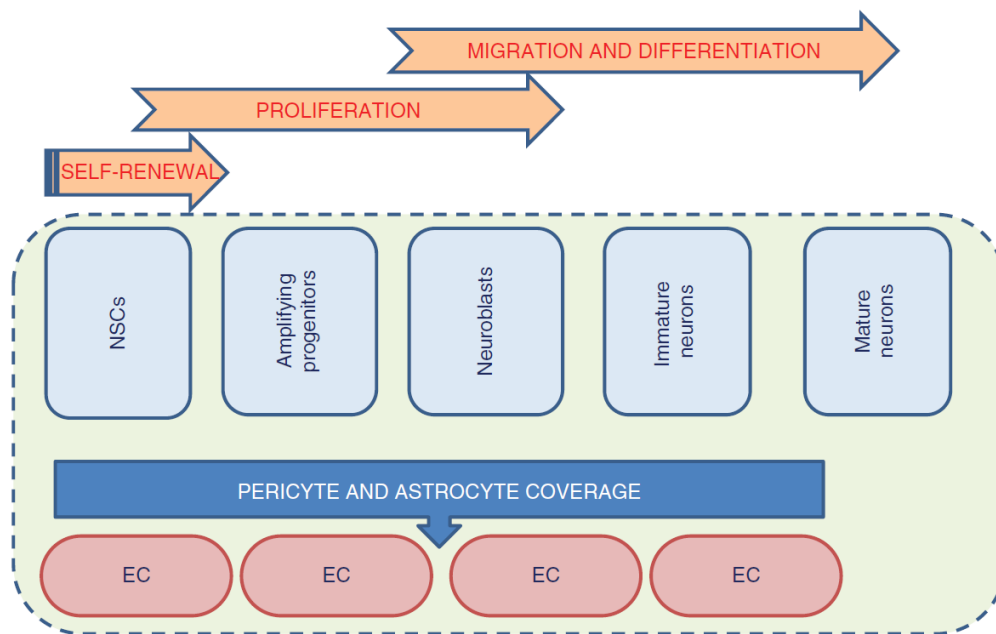


**Figure 45: Simplified diagram of the microarchitecture of a neurogenic niche in the adult brain.** Endothelial cells (ECs) covered with pericytes and astrocytes provide vascular scaffold and local microenvironment optimal for neurogenic cells self-renewal, proliferation, migration, and differentiation. From (Bjornsson *et al.*, 2015).

High BMI and hyperglycemia are well known factors for increased risk of dementia with age (Kivipelto *et al.*, 2005; Cummings *et al.*, 2022). The rapid increase in the prevalence of obesity and diabetes worldwide simultaneously increases the risk of dementia. The most common form of dementia is AD, which accounts for 70-90% of cases (Ritchie & Lovestone, 2002). Obesity and T2DM are two risk factors for the development of AD (Barnes & Yaffe, 2011). Today, the global health concern about increasing AD rates with the obesity and T2D epidemic is becoming critical, especially after predictions that the risk of AD will quadruple by 2047 in the United States (Brookmeyer *et al.*, 1998). The mechanisms by which obesity and T2DM lead to the development of AD are intertwined and share many common pathways. Alteration of the BBB in obesity and T2DM, with concomitant inflammation and oxidative stress, leads to infiltration of immune cells into the brain, which induces pathways favoring the development of AD. Microglial activation, cerebral oxidative stress, elevated insulin levels, and resulting elevated AGE levels lead, via several pathways (illustrated simply in Figure 46), to beta-amyloid accumulation, decreased synaptic plasticity, increased neurofibrillary tangles, and increased neurodegeneration (Cummings *et al.*, 2022) (Figure 46).

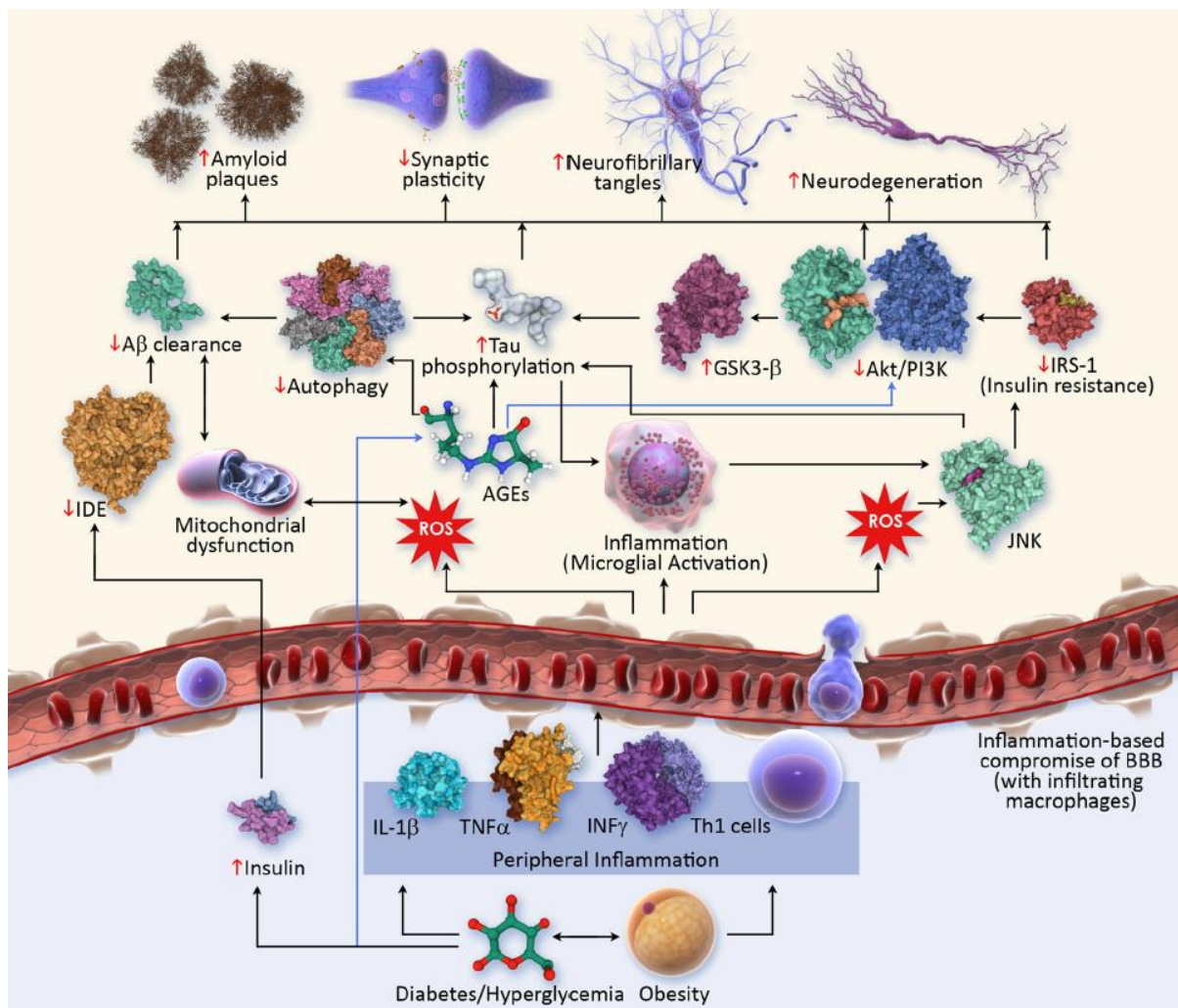


**Figure 46: Pathophysiological links between T2DM and AD.**

AD, Alzheimer's disease; AGEs, advanced glycation end products; Akt, protein kinase B; BBB, blood–brain barrier; IDE, insulin degrading enzyme; IL-1 $\beta$ , interleukin 1 B; INF $\gamma$ , interferon-gamma; IRS1, insulin receptor substrate 1; GSK3B, glycogen synthase kinase-3B; JNK, c-Jun N-terminal kinase; PI3K, phosphoinositide 3 kinase; ROS, reactive oxygen species; T2DM, type 2 diabetes mellitus; Th1, T helper cells 1; TNF- $\alpha$ , tumor necrosis factor- $\alpha$ . From (Cummings *et al.*, 2022).

In conclusion, although diabetes and obesity are considered to induce macrovascular complications in the brain, because of the increased risk of stroke, we suggest that both diseases could also result in cerebral microvascular complications. Indeed, the cerebral displasticity and namely NSC displasticity observed during obesity and/or diabetes could be considered a microvascular complication with strong neurological consequences, including neurodegeneration, cognitive decline, and increased risk of neurodegenerative diseases. Therefore, targeting the BBB could be a therapeutic option to maintain brain homeostasis under conditions of metabolic disease.



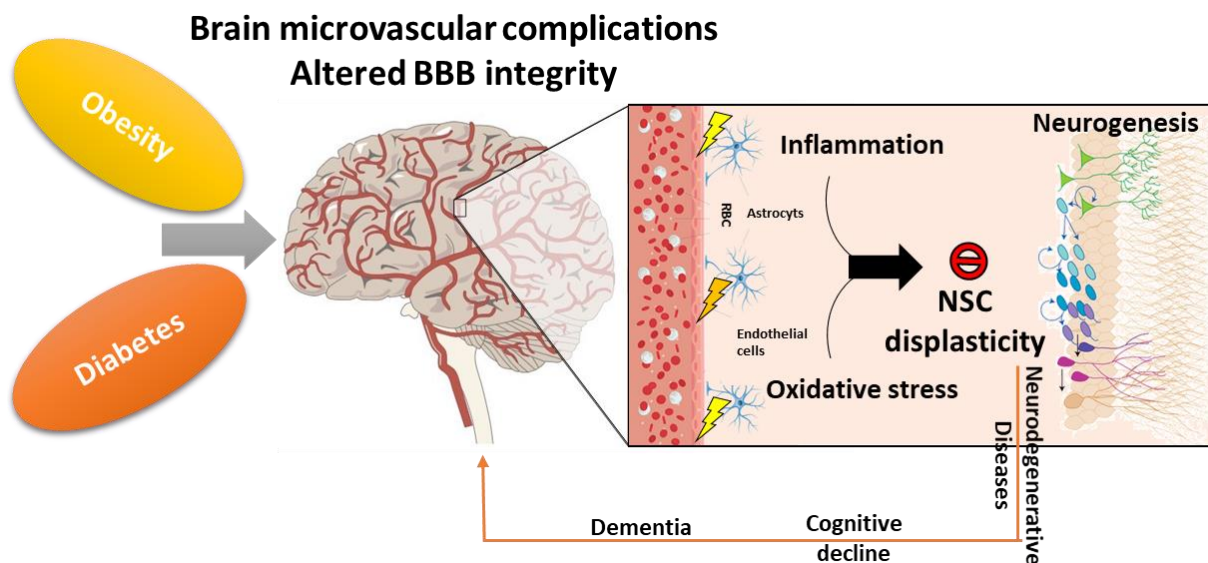


**Figure 47: Obesity and diabetes contributing to microvascular complications.**

Both obesity and diabetes lead to blood-brain barrier disruptions that are associated with neuro-inflammation and cerebral oxidative stress. Consequently, the neurogenesis and the neural stem cells are affected negatively leading to brain disruptions as neurodegenerative diseases, cognitive impairments and dementia.

### **B. Why do medicinal plants, *A. borbonica* and *P. mauritianum*, show different beneficial effects? comparison of the polyphenolic composition and the mode of action of the two aqueous extracts**

The aqueous extracts of both medicinal plants, *A. borbonica* and *P. mauritianum*, show protective effects against the effects induced by obesity, both on the body and on the brain. However, the mode of action of these plants seems to be different. For instance, *P. mauritianum* has an anti-weight gain property that is not found for *A. borbonica*. Both plants harbor a high polyphenol content according to Folin-Ciocalteu assay performed in our laboratory thanks to Dr. Laura Gence. The polyphenol content was estimated to be  $15.1 \pm 1.1$  mg GAE (Gallic Acid Equivalent)/g of dried leaves for *A. borbonica* and  $58.0 \pm 7.2$  mg GAE/g of dried leaves for *P. mauritianum*. Knowing that the concentration of our aqueous working solution was 0.5 g/L for *A. borbonica* and 0.25 g/L for *P. mauritianum*, the final total polyphenolic contents at these concentrations were around 7.55 mg GAE/L of working solution for *A. borbonica* and 14.5mg GAE/L of working solution for *P. mauritianum*. So far, the differential effects observed in our experiments could be due to different polyphenol concentration as *P. mauritianum* has twice the polyphenol content of *A. borbonica*. This could be checked by treating the DIO fish with double the concentration of the extract of *A. borbonica* to have polyphenol concentration close to that of extracts from *P. mauritianum* at 0.25 g/L and look for the effect on the body weight.

Regarding the total anti-oxidant capacity, determined by the chemical 2,2-Diphenyl-1-picrylhydrazyl (DPPH) radical scavenging assay, we observed that *P. mauritianum* ( $IC_{50}=1.1 \pm 0.2$  g/L) has a better antioxidant capacity than *A. borbonica* ( $4.5 \pm 0.3$  g/L) (Control: ascorbic acid standard  $0.08 \pm 0.01$  g/L), correlated to its higher polyphenol content. Subsequently, at their working concentration, *P. mauritianum* will be twice more antioxidant than *A. borbonica*. However, the real antioxidant activity should be determined *in vivo* as it could be different from the chemical *in vitro* DPPH assay. Therefore, the anti-weight gain effect of *P. mauritianum* could due to its higher polyphenol content and/or antioxidant activity, both being correlated.

In addition, another possibility regarding the differential effects of the two plants could lie in their polyphenolic composition. By comparing the main polyphenols of these two plants, we found that they share several ones with different amounts. These common polyphenols between *A. borbonica* and *P. mauritianum* are caffeic acid and its derivatives, protocatechuic acid, coumaroylquinic acid, quercetin and its derivatives as well as kaempferol and its derivatives. These compounds were also detected in other independent studies working on aqueous or acetonic extract (Checkouri *et al.*, 2020; Veeren *et al.*, 2020; Bonneville *et al.*, 2021). Among these common phenolic compounds, the concentrations are greatly different for some of them and close for others, according to the mass spectrometry quantifications. For example, at 1g/L of plant concentration, kaempferol and its derivatives are at quite very low quantities, 1.1 ng/ml, for *A. borbonica* while 300 ng/ml for *P. mauritianum* (0.55 ng/ml and 75 ng/ml for at working concentration 0.5 g/L of *A. borbonica* and 0.25 g/L of *P. mauritianum*, respectively). Concerning caffeic acid and its derivatives, it was found to be 300 ng/ml higher in *A. borbonica* than 200 ng/ml *P. mauritianum* (150 ng/ml and 50 ng/ml at working concentration of *A. borbonica* and *P. mauritianum*, respectively). However, for quercetin, it was quite similar for *A. borbonica* (110 ng/ml) and *P. mauritianum* (130 ng/ml) (55 ng/ml and 32.5 ng/ml at working concentrations of *A. borbonica* and *P. mauritianum*, respectively) (Veeran *et al.*, 2020; Ghaddar *et al.*, 2022).

In addition, the specific compounds of *A. borbonica* are coumaric acid and feruloylquinic acid, while the specific compounds of *P. mauritianum* are gallic acid, corosolic and asiatic acids. After the quantification of the main polyphenols in each plant, we found that caffeic acid and its derivatives, quercetin and its derivatives, and to a lesser extent protocatechuic acid, coumaroylquinic acid are the main compounds in the aqueous extract of *A. borbonica* and that gallic acid and kaempferols and to a lesser extent caffeic acid and its

derivatives, quercetin and its derivatives correspond to the main polyphenols of *P. mauritianum* (Veeran *et al.*, 2020; Ghaddar *et al.*, 2022).

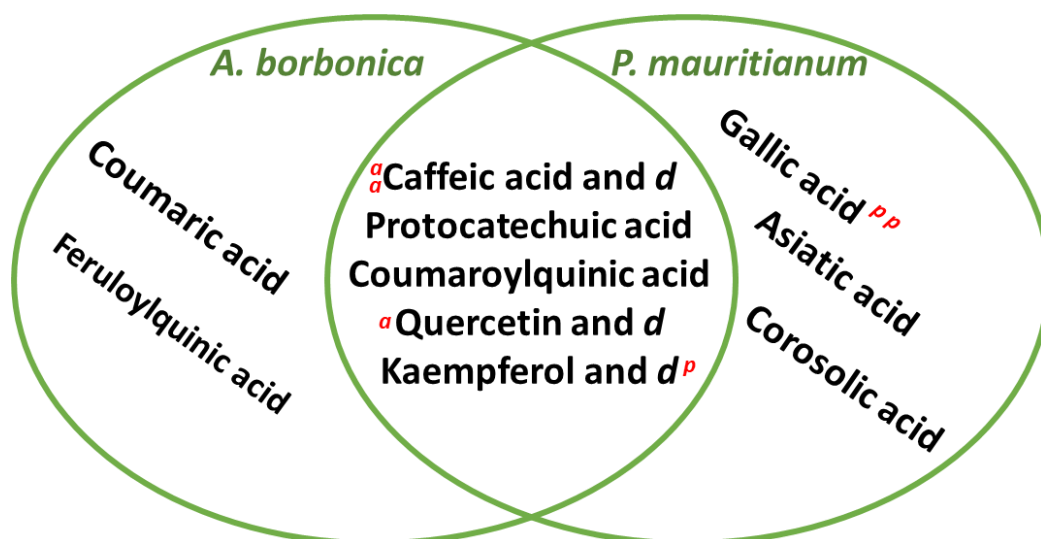


**Figure 48:** Comparison of the polyphenolic content from the aqueous extracts of *A. borbonica* and *P. mauritianum*.

The common polyphenols shared between *A. borbonica* and *P. mauritianum* are in the common area shared of each plant circle and the specific compounds are in the non-common area. The major compounds in *A. borbonica* and *P. mauritianum* are referred to by small red (a) and (p), respectively, with two letters for the highest amount. *d* means derivatives.

The potential positive effect of each plant and the designated mechanism of action could be exerted by the main polyphenolic compounds, specific compounds or the synergy of all compounds with their respective proportions (cocktail effect). *A. borbonica* shows in our experiments and in other *in vivo* and *in vitro* models antioxidant property, neuroprotective and vascular-protective effects on BBB and on cerebral endothelial cells (Arcambal *et al.*, 2020; Delveaux *et al.*, 2020; Ghaddar *et al.*, 2020; Taile *et al.*, 2020; Taile *et al.*, 2021). This antioxidant protective property could be conferred by the main compounds of *A. borbonica*, caffeic acid and its derivatives, particularly through its known antioxidant effects and the protective effect of the blood-brain barrier in the rodent model of traumatic brain injury (Gulcin, 2006; Zhao *et al.*, 2012). Knowing that the liver metabolizes caffeic acid in the body into its derivatives (caffeoylquinic acid and dicaffeoylquinic acid), it is assumed that the effect of caffeic acid is maintained through its metabolites (Piazzon *et al.*, 2012). In addition, caffeic acid has been shown to be present in cerebrospinal fluid and to cross the BBB via solute transporters, such as monocarboxylic acid transporters, existing on BBB endothelial cells (Nalecz, 2017) that actively transport caffeic acid (Grabska-Kobylecka *et al.*, 2020). Therefore,

these data could explain the specific brain antioxidant effect of *A. borbonica* extract by its main compound, caffeic acid and also its derivatives. In order to investigate the effect of caffeic acid on brain homeostasis in healthy and telencephalic injury conditions in zebrafish, we performed intraperitoneal injection (25mg/kg of body weight) for 3 consecutive days and collected the brains for further analyses. Our preliminary data demonstrated by RT-qPCR analysis and immunohistostaining that caffeic acid has no effect on neurogenesis and brain cell proliferation, inflammation, and in the expression of genes involved in brain plasticity (not shown).

Regarding *P. mauritianum*, it also shows antioxidant and BBB-protective properties, but at the same time it shows a preventive anti-weight gain effect (Ghaddar *et al.*, 2022). Besides, this plant increases feces production in the treated obese fish. Therefore, the positive effect of *P. mauritianum* is probably exerted through the anti-weight gain via gut microbiota effect and probably not directly on the brain and BBB like *A. borbonica*. However, both mechanisms could occur simultaneously. The main compounds of *P. mauritianum* (gallic acid and kaempferols) have been presented in the literature as having an anti-obesity effect by attenuating the intestinal dysbiosis resulting from obesity (Yang *et al.*, 2020; Bian *et al.*, 2022). Some data reported a potential effect of gallic acid, the main and specific component of *P. mauritianum*, on the gut microbiota. It was proved from *in vitro* and *in vivo* experimentations that gallic acid affects positively the gut microbiota by decreasing the growth of pathogenic bacteria (Yang *et al.*, 2020). Gallic acid treatment in HFD mice was shown to improve metabolic parameters as glucose intolerance and to increase thermogenesis in the adipose tissue (Paraiso *et al.*, 2019)(Fig. 49). In addition, corosolic and asiatic acids that are specific polyphenols from *P. mauritianum*, were reported to have potential beneficial effects on gut microbiota (Smith & Mackie, 2004; Ozdal *et al.*, 2016; Molino *et al.*, 2021). Interestingly, kaempferols were shown by Bian and colleagues to exhibit similar effects on HFD mice model as the effect of *P. mauritianum* aqueous extracts on the DIO treated fish. HFD mice treated with kaempferols displayed lower body weight, fat accumulation and attenuated gut dysbiosis compared to HFD non treated mice (Bian *et al.*, 2022). Knowing that kaempferols are among the phenolic content of *A. borbonica*, this could argue why *A. borbonica* aqueous extract does not have similar mode of action as *P. mauritianum* one. This is possibly due to the different quantities of kaempferols present in each plant. Thus, the dominance of certain phenolic compounds in *P. mauritianum* with a potent effect on gut microbiota, could explain the mode of action of *P. mauritianum*, especially with the observed increase in feces production of treated fish.



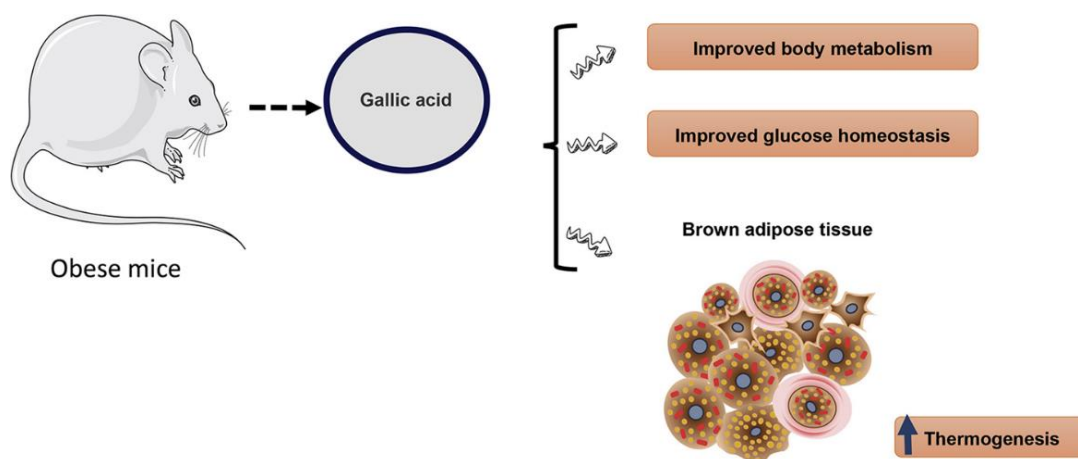


**Figure 49: Gallic acid treatment improves body metabolism parameters in HFD mice.**

The treatment with gallic acid (100 mg/Kg/body weight) for HFD fed mice improves body metabolism (body weight, HDL, total cholesterol, triglycerides), glucose intolerance and increases thermogenesis in adipose tissue. Adapted from (Paraiso *et al.*, 2019).

Thus, it seems that the distinct mode of actions of each plant are mainly influenced and due to their main phenolic compounds and concentration. In this perspective, it is interesting to discover the compound or the compound cocktail behind the specific mode of action of plants. For *A. borbonica*, caffeic acid (and its derivatives) is proposed as a candidate for specific action. This proposal could be verified by testing the effect of caffeic acid and other major compounds of *A. borbonica* on DIO fish and looking for modified parameters. Similarly, this could be done with the major components of the aqueous extract of *P. mauritianum* such gallic acid, kaempferols or its specific triterpenoids (Asiatic and corosolic acids). Furthermore, it should be kept in mind that these positive effects displayed by each plant, *A. borbonica* and *P. mauritianum*, could be the result of a combination of their phenolic contents. Taking into account the quantities, this synergy of various phenolic compounds could serve as a medicine for diabetic and obese/pre-diabetic patients.

When dealing with polyphenols, two main points should be considered, their metabolism and half-life. One of the limitations of phenolic compounds in general is the low bioavailability or their relatively low half-life (1-28h hours) (Rechner *et al.*, 2002; Manach *et al.*, 2005). Polyphenol's bioavailability and metabolism is a critical point to investigate their physiological functions and health effects (Lutz, 2014). When taken by human from plants or dietary sources, different process challenges the bioavailability of polyphenols as absorption, distribution, metabolism and elimination phases (Rein *et al.*, 2013). In human, it was reported that gallic acid is among the most well absorbed polyphenols and is followed by flavanones and quercetin and anthocyanins being among the least absorbed polyphenols (Rein *et al.*, 2013). In

addition, the relative urinary excretion 18 different studied polyphenols in human was ranging from 0.3% to 43% of the ingested dose (Manach *et al.*, 2005). This sheds the lights on the importance of analyzing the phenolic metabolites from *A. borbonica* and *P. mauritianum* extracts, their absorption and relative excretion in the zebrafish treated model.

In conclusion, *A. borbonica* and *P. mauritianum* are two promising medicinal plants that show beneficial effects on disorders induced by obesity and/or hyperglycemia, although their modes of action are probably different. Both plants showed high polyphenolic content and high antioxidant capacity. The major polyphenolic compounds in each plant were shown to alleviates metabolic disruptions resulting from obesity in a way similar to that observed by the plant extracts. This indicate that the specific mode of action of *A. borbonica* and *P. mauritianum* could be due to its polyphenolic contents, that is hypothesis to be tested.

### **C. Advanced steps beyond: From zebrafish to preclinical models**

In few years, zebrafish has demonstrated its relevance to develop and mimic human diseases, namely diabetes and obesity. Our DIO model and several other ones developed by different laboratories share common features with mammalian and human obesity (Oka *et al.*, 2010; Landgraf *et al.*, 2017; Montalbano *et al.*, 2019; Ghaddar *et al.*, 2020; Ghaddar *et al.*, 2021a). Increased BMI, hyperglycemia, liver steatosis and oxidative stress are all observed outcomes found in overweight/obese zebrafish, rodents and human. Similarly, at the level of the brain, our model and others using zebrafish shows common impairments with mammals as BBB breakdown, neuro-inflammation, increased oxidative stress and impaired neurogenesis (Ghowasi *et al.*, 2021). These data demonstrate that zebrafish could be an alternative model to study the effects of metabolic perturbations at the peripheral and central levels.

Zebrafish can be considered as a “fast” model to develop overweight/obesity considering the short time necessary to develop metabolic complications. Indeed, in solely 4 weeks, we induced body and brain alterations similarly as observed in rodent models (Wu *et al.*, 2021; de Leon-Guerrero *et al.*, 2022; Lama *et al.*, 2022). This advantage facilitates the investigation process, especially with the need to repeat independently the experiments. The conserved signaling pathways between zebrafish and mammals, particularly the ones involved in the regulation of neurogenesis such as Wnt/ $\beta$ -catenin, Notch, brain derived neutrophic factor (BDNF) (Faigle & Song, 2013; Hamada *et al.*, 2014; Cacialli *et al.*, 2016; Schultz *et al.*, 2017), allows to explore more easily their involvement in brain disruption induced by metabolic

diseases. Therefore, it is now very important to elucidate the disrupted mechanisms sustaining the decreased NSC plasticity observed during hyperglycemia and/or obesity in zebrafish. Interesting signaling pathways to study include Notch signaling, BMP/Id1 signaling, and also glucocorticoid stress hormones, as recently suggested in our submitted review (Ghaddar *et al.*, 2021b).

Despite all the previously mentioned advantages for zebrafish, this model has certain limitations. When considering therapeutic treatments and their mode of administration, it is different in zebrafish (immersion) than mammalian models (intraperitoneal/intravenous injection). In addition, due to the strong regenerative capacity in the zebrafish, the destructive outcomes on this model could be less pronounced than that in other models with less regenerative capacity. Furthermore, protein-coding regions of the zebrafish and human genome are 70 % while being higher in other models as mouse and human genomes that are 85 % identical. Thus, it is always crucial to proceed a step forward to other mammalian preclinical models.

The interesting beneficial effects we obtained with *A. borbonica* and *P. mauritianum* against obesity and its deleterious effects whether on the body or the brain are important to be confirmed in rodent preclinical models such as *db/db*, *ob/ob*, or HFD/DIO models. In addition, increased feces production in zebrafish treated with *P. mauritianum* reflects an effect on microbiota. It is essential to study this aspect in depth to find out if it affects the microbiota of mammals and humans and by what mechanisms. If such research is conducted, these medicinal plants could serve as a medical alternative with more precision on their uses and toxic doses in human subjects with obesity and/or diabetes.

As an attempt to increase polyphenols bioavailability, zebrafish could serve as a relevant model for achieving this goal. Increasing the bioavailability of the polyphenols presented in the *A. borbonica* and *P. mauritianum* extracts could be promising therapies for ameliorating metabolic conditions and brain homeostasis that are altered in obese and/or diabetic subjects. Among the well-known and safe drug delivery system are the high-density lipoproteins (HDLs) (Ma *et al.*, 2018), for which our laboratory has a strong expertise. HDLs can normally circulate for extended period (circulating half-life:12-24 hours) allowing the transport of lipids, proteins and microRNA (Vickers *et al.*, 2011; Kuai *et al.*, 2016). Using HDLs as a drug delivery system is of great interest due to the non-immunogenic property and being completely biodegradable (Ma *et al.*, 2018). Scavenger receptor B type I (SCARB1 or SR-BI), ATP-binding cassette

transporters ABCA1 and ABCG1, and the cluster of differentiation 36 (CD36) represents the main HDL receptors in mammals (Calvo *et al.*, 1998; Fidge, 1999). Besides, the HDL receptors are widely expressed in the brain including the cerebral endothelial cells, neurons and microglial cells (Ghussen & Kruger, 1989; Lein *et al.*, 2007). A successful example for HDL delivery is the HDL particles loaded with curcumin developed in our laboratory. They display a strong protective effect on ROS production, endothelial cell barrier integrity, and endoplasmic reticulum stress for endothelial cells exposed to Methylglyoxal, a highly reactive metabolite of glucose (Narra *et al.*, 2022).

Recently, we have shown by *in situ* hybridization and RNA sequencing analysis that the brain of adult zebrafish widely expresses HDL receptors: *scarb1*, *abca1a*, *abca1b*, *abcg1*, and *cd36* (Sulliman *et al.*, 2021). In addition, we showed that NSCs in zebrafish express *scarb1*. After an intra-cerebroventricular or an intraperitoneal injection of HDLs, we detected HDLs in neural stem cells or in endothelial cells respectively, demonstrating their efficient uptake (Sulliman *et al.*, 2021)(Annex 1, page: 231). In addition, after a telencephalic injury, an intraperitoneal injection of HDLs were able diffuse through the brain parenchyma and to be taken up by NSCs (Sulliman *et al.*, 2021). Therefore, these findings are of great interest and open the avenues forward for trying to load the HDL particles with a synergy of polyphenols from each plant extract and/or their main compounds in order to increase their bioavailability and their capture by NSCs and BBB. Similarly, HDL particles loaded with polyphenols from *A. borbonica* and *P. mauritianum* could be injected to obese or diabetic mice models as *ob/ob* and *db/db* in order to improve metabolic and brain parameters. However, we should consider that in order to incorporate efficiently polyphenols within HDL particles, they should show some hydrophobic properties (or should be chemically modified).

In conclusion, the zebrafish is an alternative model for the study of metabolic diseases and their impact on the central nervous system. It could be used to screen various extracts to select the most potent and study them in preclinical models.



## Conclusion

In conclusion, this current study has offered new and detailed insights into the effects of diet-induced obesity on brain homeostasis using zebrafish. Using our simple and rapid model of diet-induced obesity, we have shown that the results overlap at the periphery and brain level in zebrafish and mammals. This advantage opens perspectives to study the mechanisms behind brain perturbations, namely blood-brain barrier leakage and neurogenesis in metabolic diseases. Understanding the onset of altered brain homeostasis, starting from blood-brain barrier impairment, neuro-inflammation and oxidative stress, will help research to develop new strategies to limit brain damage in obese and prediabetic/diabetic conditions. The other part of this study focused on medicinal plants endemic to Reunion Island and on their potential preventive and/or therapeutic effect *in vivo*. The two plants, *A. borbonica* and *P. mauritianum*, have proven to be judiciously selected to combat metabolic disorders and their subsequent negative effects on the brain resulting from diet-induced obesity in our experimental conditions. The reliable DIO zebrafish model treated with the plants paves the way for the investigation of *A. borbonica* and *P. mauritianum* effects on preclinical models to confirm their positive effect against the complications resulting from obesity and prediabetes, as well as the identification of the compound or compound cocktail sustaining their beneficial effects.



# ANNEX







OPEN

# HDL biodistribution and brain receptors in zebrafish, using HDLs as vectors for targeting endothelial cells and neural progenitors

Nora Cassam Sulliman<sup>1</sup>, Batoul Ghaddar<sup>1</sup>, Laura Gence<sup>1</sup>, Jessica Patche<sup>1</sup>, Sepand Rastegar<sup>2</sup>, Olivier Meilhac<sup>1,3</sup> & Nicolas Diotel<sup>1✉</sup>

High density lipoproteins (HDLs) display pleiotropic functions such as anti-inflammatory, antioxidant, anti-protease, and anti-apoptotic properties. These effects are mediated by four main receptors: SCARB1 (SR-BI), ABCA1, ABCG1, and CD36. Recently, HDLs have emerged for their potential involvement in brain functions, considering their epidemiological links with cognition, depression, and brain plasticity. However, their role in the brain is not well understood. Given that the zebrafish is a well-recognized model for studying brain plasticity, metabolic disorders, and apolipoproteins, it could represent a good model for investigating the role of HDLs in brain homeostasis. By analyzing RNA sequencing data sets and performing *in situ* hybridization, we demonstrated the wide expression of *scarb1*, *abca1a*, *abca1b*, *abcg1*, and *cd36* in the brain of adult zebrafish. *Scarb1* gene expression was detected in neural stem cells (NSCs), suggesting a possible role of HDLs in NSC activity. Accordingly, intracerebroventricular injection of HDLs leads to their uptake by NSCs without modulating their proliferation. Next, we studied the biodistribution of HDLs in the zebrafish body. In homeostatic conditions, intraperitoneal injection of HDLs led to their accumulation in the liver, kidneys, and cerebral endothelial cells in zebrafish, similar to that observed in mice. After telencephalic injury, HDLs were diffused within the damaged parenchyma and were taken up by ventricular cells, including NSCs. However, they failed to modulate the recruitment of microglia cells at the injury site and the injury-induced proliferation of NSCs. In conclusion, our results clearly show a functional HDL uptake process involving several receptors that may impact brain homeostasis and suggest the use of HDLs as delivery vectors to target NSCs for drug delivery to boost their neurogenic activity.

High-density lipoproteins (HDLs) are complex particles composed of cholesterol (free and esterified), phospholipids, sphingolipids, triglycerides, and several proteins, including apolipoprotein A-I (ApoA-I), which is the most abundant<sup>1,2</sup>. HDLs constitute heterogeneous lipoprotein particles in terms of density (1.063–1.210 g/mL) and size (7–20 nm)<sup>3,4</sup>. Their main function is to ensure the clearance of cholesterol by promoting its reverse transport from the tissues back to the liver. However, they also exert pleiotropic functions, such as antioxidant, anti-inflammatory, anti-thrombotic, anti-proteolytic, and anti-microbial properties<sup>2,5–8</sup>. For decades, HDLs have been studied for their role in cholesterol metabolism and cardiovascular physiology. HDLs and/or ApoA-I levels being inversely correlated with the development of cardiovascular diseases, including atherosclerosis and stroke, in humans<sup>9,10</sup>.

HDLs exert their effects through four main receptors: scavenger receptor B type I (SCARB1 or SR-BI), ATP-binding cassette transporters ABCA1 and ABCG1, and the cluster of differentiation 36 (CD36)<sup>11–13</sup>. ABCA1 is a membrane protein interacting with lipid-free ApoA-I. It promotes cellular phospholipid and cholesterol efflux towards the extracellular free ApoA-I, leading to the formation of ApoA-I nanodiscs<sup>14</sup>. ABCG1 has high sequence homology with ABCA1 and interacts with mature HDL particles. It is the main transporter in charge of cholesterol and oxysterol efflux from human aortic endothelial cells, and it enhances endothelial nitric oxide synthase (eNOS) activity<sup>14</sup>. CD36, another receptor for HDLs, is a multiligand glycoprotein structurally related

<sup>1</sup>Université de La Réunion, INSERM, UMR 1188, Diabète Athéromatose Thérapies Réunion Océan Indien (DéTROI), Saint-Denis de La Réunion, France. <sup>2</sup>Institute of Biological and Chemical Systems-Biological Information Processing (IBCS-BIP), Karlsruhe Institute of Technology (KIT), Postfach 3640, 76021 Karlsruhe, Germany. <sup>3</sup>CHU de La Réunion, Saint-Denis de La Réunion, France. ✉email: nicolas.diotel@univ-reunion.fr

to SCARB1. It has a high affinity for native lipoproteins, including HDL, LDL, and VLDL, and for modified LDLs, such as oxidized and acetylated LDL<sup>13</sup>. SCARB1 (SR-BI) is a membrane glycoprotein that can recognize ApoA-I in HDL particles, as well as other apolipoproteins, that are free or in association with phospholipids. HDL particles preferentially bind to SR-BI, allowing selective uptake of cholesterol esters.

Interestingly, beyond the canonical metabolism and cardiovascular fields, plasma HDLs were more recently documented for their potential links with the central nervous system (CNS). Moreover, low HDL-cholesterol levels are correlated with neurodegenerative diseases, cognitive impairments, and depressive behaviors<sup>5,15–18</sup>. As well, many studies have pointed out the potential involvement of HDLs in neuroprotection after brain ischemia in mammals, in particular by exerting protective effects on the blood–brain barrier (BBB)<sup>19</sup>. In a rat thrombo-embolic model of stroke, intravenous injection of HDLs immediately or up to 3 h after the onset of stroke resulted in decreased infarct volume and reduced mortality<sup>19</sup>. Additionally, in both thrombo-embolic and monofilament models of focal middle cerebral artery occlusion (MCAO), HDL injection reduced hemorrhagic complications and improved the survival of rats treated with tissue plasminogen activator (tPA)<sup>20</sup>. Such neuroprotective effects were also observed in ischemic and excitotoxic lesions<sup>21</sup>. At the acute phase of stroke, HDL particles are also dysfunctional, displaying decreased anti-inflammatory and antioxidant activities, and are larger than in normal conditions<sup>22</sup>.

HDL receptors are widely expressed in the brain<sup>23,24</sup>. RNA sequencing analyses of the mouse cerebral cortex demonstrated the expression of all HDL receptors in neurons, microglial cells, astrocytes, oligodendrocytes, and endothelial cells<sup>25</sup>. Most HDL receptors appeared to be at least expressed in neurogenic regions, including the hippocampus<sup>24</sup>, and gene expression analysis in neural progenitor cultures demonstrated the enrichment of some HDL receptors in neural stem cells (NSCs), such as *Scarb1*<sup>26</sup>. Notably, the brain also appears to be an important site for the production of HDLs, with the most abundant apolipoproteins being ApoE instead of ApoA-I<sup>27</sup>. These data argue for the role of HDLs in brain plasticity and NSC activity and/or metabolism.

In recent years, zebrafish has become an emerging model for studying apolipoproteins, metabolism, and associated disorders, such as diabetes, obesity, and dyslipidemia, as well as brain plasticity<sup>28–41</sup>. Moreover, zebrafish express (1) all the main apolipoproteins sharing a high homology with human ones, (2) the major lipid transporters, and (3) the enzymes involved in lipoprotein metabolism, such as CETP, which is not expressed in rodents<sup>35,42</sup>. Cholesterol transporters *Abca1* and *Abcg1*<sup>42</sup>, as well as *Scarb1* (SR-BI) ([www.ensembl.org](http://www.ensembl.org)) and *Cd36*<sup>43</sup>, have been found in zebrafish. In addition, in contrast to mammals that have only two main cerebral neurogenic niches during adulthood and a limited capacity to repair the brain, adult zebrafish exhibit numerous neurogenic niches across their brain and an important ability for healing<sup>41,44–48</sup>. Consequently, more and more studies investigate the impact of metabolic disorders, such as hyperglycemia and obesity, on brain homeostasis and plasticity<sup>29,31,49,50</sup>. However, there are only a few studies concerning HDL receptor expression in zebrafish, in particular in the central nervous system, and no data regarding their potential involvement in brain plasticity and neurogenesis.

Due to its high homology with the human genome, zebrafish is increasingly used as an interesting model for the study of human diseases and physiological processes<sup>51</sup>. Zebrafish also exhibit strong evolutionarily conserved similarities with humans concerning metabolic diseases, lipid and lipoprotein metabolism, and neurogenic properties<sup>32,35,41,42,52,53</sup>. These intrinsic features make the zebrafish an interesting candidate to study the impact of HDLs on the central nervous system in homeostatic and injury conditions before testing their neuroprotective effects on pre-clinical models of brain injury (i.e., brain ischemia in mice). The aim of this study was to investigate the potential role of HDLs on brain plasticity and brain repair mechanisms. For that, we first analyzed RNA sequencing data sets and cloned HDL receptor genes to determine their expression and distribution by *in situ* hybridization in the brain of adult zebrafish. Next, we investigated the role of HDLs in basal neurogenesis and brain repair mechanisms following a stab wound injury of the telencephalon. For that purpose, the biodistribution of HDLs and their capacity to reach the cerebral microvasculature, as well as the nervous tissue, in constitutive and regenerative conditions were investigated. This work supports the use of zebrafish for testing the neuroprotective capacity of HDL particles used as vectors after enrichment with drugs to favor brain plasticity and repair.

## Material and methods

**Ethics and animals.** This study was conducted in accordance with the French and European Community guidelines for the use of animals in research (86/609/EEC and 2010/63/EU) and approved by the local Ethics Committee from the CYROI platform for animal experimentation (APAFIS#2018040507397248\_v3; APAFIS#20200908140689\_v5).

For zebrafish (*Danio rerio*), adult (3–6 months-old) male and female wild-type (WT), *tg(fli1:EGFP)*<sup>54</sup>, and *tg(GFAP::GFP)*<sup>55</sup> were maintained under standard conditions on a 14/10-h (h) light–dark cycle at 28.5 °C, and were fed daily with commercially available dry food (Gemma 300, Skretting). Fish were from the AB strain: WT, *tg(GFAP::GFP)*, and *tg(fli1:EGFP)*.

For mice (*Mus musculus*), C57BL/6J male (8 week-old, 25 g) mice were purchased from JANVIER LABS (Le Genest-Saint-Isle, France). They were maintained under standard conditions of light, temperature, and humidity and fed a standard diet *ad libitum*.

**Intraperitoneal injection of HDLs and HDL biodistribution in homeostatic conditions.** For studying the biodistribution of HDLs in zebrafish (WT and *fli:EGFP*) and mice (WT) in homeostatic conditions, zebrafish and mice were intraperitoneally injected with 80 mg/kg of human plasma HDLs (pHDLs), reconstituted HDL solution (CSL BEHRING, rHDLs), or 1X PBS (vehicle) for controls.

For zebrafish, animals were anesthetized with 0.02% tricaine, weighed, and subjected to intraperitoneal injection of 1X PBS (vehicle) or HDLs for reaching a final concentration of 80 mg/kg of zebrafish bodyweight.



The intraperitoneal injection of HDLs was performed using a 50  $\mu$ l Hamilton syringe equipped with a sterile needle (BD Microlance 3; 30 G  $\frac{1}{2}$ "; 0.3  $\times$  13 mm). This syringe allows the precise injection of very low volumes in zebrafish as discussed in<sup>56,57</sup>. After anesthesia, fish were briefly weighed to determine the appropriate volume of the injection. For instance, 10  $\mu$ l of HDLs at 1.6  $\mu$ g/ $\mu$ l were injected in a 0.2 g fish to reach a final concentration of 80 mg/kg. According to the weight of fish (0.2–0.3 g), the volume injected varied from 10 to 12.5  $\mu$ l. Fish were killed and fixed 1 h 30 min after injection.

For mice, intraperitoneal injections of HDLs (80 mg/kg of bodyweight) and PBS were performed, and the animals were allowed to survive 1 h 30 min post-injection.

The biodistribution study was performed in three independent experiments (n = 3 animals per condition: pHDLs, rHDLs, and vehicle) in both mice and fish.

**Stab wound of adult zebrafish telencephalon.** Zebrafish were anesthetized with 0.02% tricaine and subjected to mechanical injury of the telencephalon. Mechanical injury to the telencephalon was performed by inserting a sterile needle (BD Microlance 3; 30 G  $\frac{1}{2}$ "; 0.3  $\times$  13 mm) in the right telencephalic hemisphere, following a dorsoventral axis and guided by landmarks on the head, as previously described<sup>40,58</sup>. After this procedure, fish were put back into their respective tanks and allowed to survive for different kinetic times before being processed for gene expression analyses and/or histological analyses.

**Biodistribution of HDLs in a brain injury context.** HDL biodistribution in brain injury conditions was evaluated by intraperitoneal injection (80 mg/kg) of rHDLs either 30 min before the stab wound injury (n = 4 for rHDLs; n = 3 for PBS) or immediately after the lesion (n = 4 for rHDLs; n = 3 for PBS). In both conditions, fish were sacrificed 1 h 30 min after the injection. The results presented are from two independent experiments.

To test the effects of HDLs on microglial recruitment and injury-induced proliferation, an intraperitoneal injection (80 mg/kg) of pHDLs was performed immediately after stab wound injury of the telencephalon. Fish were then allowed to survive for 2- and 5-days post lesion (dpl) before analysis of microglia activation and ventricular proliferation, respectively. For each time point, a total number of nine fish were injected with pHDLs and ten fish with PBS; these numbers corresponded to two independent experiments.

**Intracerebroventricular injection of HDLs.** To determine the effects of HDLs on ventricular cell proliferation, intracerebroventricular injections of pHDLs or rHDLs were performed. For this purpose, fish were anesthetized with 0.02% tricaine. A hole was made in the skull at the junction between the tel- and diencephalon as previously described<sup>58</sup>. Around 2 nanoliters of pHDLs (10 mg/ml) and rHDLs (20 mg/ml) were injected into the ventricle with a glass capillary using a microinjector (Femtojet, EPPENDORF). Another group of fish was also injected with the vehicle (PBS). Fish were then allowed to recover before being killed 24 h post-injection and fixed for proliferative analysis. The total number of injected fish from two independent experiments were: n = 6 fish for PBS, n = 6 for pHDLs, and n = 4 for rHDLs.

For testing the capacity of HDL to deliver molecules of interest, a fluorescent dye (DiIc18) was incorporated into HDLs. Intracerebroventricular injections of HDLs were performed (n = 3) and fish were sacrificed 1 h 30 min post-injection and processed for confocal microscopy.

**Tissue sampling and processing.** For zebrafish, animals were euthanized using 0.02% tricaine before being decapitated. Brains and/or telencephalon were carefully removed and frozen for gene expression analysis. Alternatively, fish were fixed overnight at 4 °C in 4% paraformaldehyde (PFA) in PBS (pH 7.4) before dissection of brain, liver, and kidney tissues for immunohistochemistry (IHC) and/or in situ hybridization (ISH) analyses according to previous studies<sup>58–60</sup>.

For mice, animals were anesthetized with Isoflurane (ISOFLOR Centravet France) and killed by intracardiac puncture before intracardiac perfusion with PBS and fixation with 4% PFA. Brain, liver, and kidney tissues were subsequently processed for cryostat embedding and cutting.

**Brain RNA extraction, reverse transcription, qPCR, and RNA sequencing analyses.** Total brain and/or telencephalon RNA were extracted with the TRIzol reagent after tissue homogenization with the QIA-GEN Tissue Lyser II (90 s at 250 rpm). Two micrograms of RNA were reverse transcribed to cDNA using random hexamer primers (Life Technologies) and MMLV reverse transcriptase (INVITROGEN, REF: 28025-021) following the manufacturer's instructions.

For qPCR analysis, experiments on three pools of five telencephala were performed on an AB7500 real-time PCR system (Applied Biosystems, Foster City, CA) with SYBR green master mix (Eurogentec). Specific zebrafish primers were used (Table 1). The relative expression of the *HDL receptor* genes was normalized against the expression level of the *efla* gene.

For RNA sequencing analyses, data were reanalyzed from the work of Wong and Godwin for the whole brain (n = 4), and from the study of Rodriguez-Viales et al. and Gourain et al. for control telencephala and 5 dpl telencephala (n = 3)<sup>58,61,62</sup>.

**Cloning, probe synthesis, and in situ hybridization (ISH).** Standard PCR was performed using zebrafish brain cDNA and gene-specific primers to obtain PCR products of almost 500 bp that were subcloned into the pGEMT-Easy vector (PROMEGA, Madison, WI, USA) (Table 2). Plasmids were sequenced and linearized for the synthesis of digoxigenin (DIG) labeled antisense riboprobes using T7 or SP6 RNA polymerases.

Zebrafish	Forward	Reverse	Amplicon size
<i>abca1a</i>	AAGGAACAATCATTAAAGGAGCAA	CCACAACAGTAAACCCAAGTGA	108
<i>abca1b</i>	GCCATGGTACTTCCCTTCA	TCCTCTTCAATGGAACACAGC	111
<i>cd36</i>	TGGTCTTCTTGACATTACTTCCTG	CATCTAAGTTGGGGTTCATTCC	119
<i>scarb1</i>	GTCAGCTCCTGCAGACACG	TCTTCACTGGGGCTCAATCC	107
<i>abcg1</i>	TCTTCAGAGGGATGCCACA	CCGCAAGTGAAGTCAACACC	111
<i>ef1a</i>	AGCAGCAGCTGAGGAGTGAT	CCGCATTGTAGATCAGATGG	140

**Table 1.** qPCR primers.

ZF gene	Forward	Reverse	Amplicon size
<i>abca1a</i>	TGAAGATGGGGAATCTCCTG	GCTCTTCTCAATGCACACA	567
<i>abca1b</i>	TCCACCCAACGTCAACTACA	TGCTGATCAGGAAACTGTC	569
<i>abcg1</i>	ACGCAGTTCTGCATCCTCTT	ACAGGACCCACAAAAGTTGC	506
<i>cd36</i>	TACTTGCTGCCTGTTGATGC	ATTGCTTTTTGACGGTTTGG	543
<i>scarb1</i>	GGGGCTGTTACCATCTTCA	ACCGAACAGAGACGTTACC	515

**Table 2.** Cloning primers.

Chromogenic ISH on whole adult brains was performed as described<sup>48,59</sup>. Briefly, brains were rehydrated and washed with PTW (0.1% Tween 20, PBS buffer; pH 7.4). Tissue permeabilization was performed using proteinase K (10 µg/ml) diluted in PTW (30 min at 20 °C). Brains were subsequently post-fixed in 4% PFA and carefully washed. After a prehybridization step (3 h at 65 °C), the brains were incubated overnight with the DIG-labeled probes in hybridization buffer (pH 6) at 65 °C. The next day, they were washed, and 50 µm-thick sections were cut using a vibratome (LEICA VT1000S). Brain sections were incubated overnight at 4 °C with anti-digoxigenin-AP, Fab fragments (1:2000; ROCHE; Cat# 11093274910). Finally, the sections were stained with NBT/BCIP substrate (pH 9.5). At least five brains were investigated for each transcript studied: *scarb1* (n = 5), *abca1a* (n = 7), *abca1b* (n = 8), *abcg1* (n = 5), and *cd36* (n = 7). Three independent experiments were performed.

For *scarb1* fluorescence ISH, tyramide amplification was performed (TSA Plus Cyanine 3 System, PERKIN ELMER, Boston, MA) using DIG-POD (poly) antibody (1:1,000, ROCHE) on three brains as described in<sup>58,60</sup>.

**Immunohistochemistry.** For zebrafish brain immunostaining, vibratome sections were made. Briefly, fixed tissues were dehydrated in 100% MetOH and kept at -20 °C at least overnight. Then, samples were rehydrated, permeabilized with PTW (1X PBS containing 0.1% Tween 20), and 50 µm-thick sections were cut using a vibratome (LEICA VT 1000S). After blocking the sections for 2 h in blocking buffer (PTW containing 0.2% BSA, 1% DMSO), incubation with primary antibodies was performed overnight at 4 °C. The next day, the brain sections were washed three times with PTW before being incubated with secondary antibodies and DAPI (1 ng/ml, THERMOFISCHER) for 2 h at room temperature. Finally, sections were washed in PTW and mounted on slides with Aqua-Poly/Mount (POLYSCIENCES).

For cryostat brain, liver, and kidney sections, mice and zebrafish tissues were cryoprotected in PBS containing 30% sucrose for one night at 4 °C. The next day, the tissues were embedded in Tissue-Tek OCT, frozen at -80 °C and cut with a Leica CM 1520 cryotome at a 12 µm thickness. The slides were dried and then rehydrated twice in 1X PBS, permeabilized with PTW, and blocked for 45 min in blocking buffer. Incubation with primary antibodies was performed overnight at room temperature. The next day, slides were rinsed three times with PTW, and incubations with secondary antibodies and DAPI were performed for 1 h 30 min. Slides were washed three times in PBT and mounted with antifading medium Vectashield (H-1000, VECTOR LABORATORIES, Burlingame, CA).

The references and concentrations of the primary and secondary antibodies, as well as the DAPI nuclear counterstaining, used in this work are shown in Table 3.

Each IHC experiment was repeated in at least three independent experiments. For ApoA-I immunohistochemistry, a negative control was performed using IgG from rabbit (Negative CTRL Rabbit IgG, X0903, DAKO), diluted at the same concentration as the anti-ApoA-I antibodies. No staining was observed in these conditions in both fish and mice, reinforcing the specificity of ApoA-1 staining.

**Preparation of HDLs and HDL fluorescence labeling.** Lipoproteins were isolated from a pool of EDTA-treated plasma of healthy male and female volunteers by ultracentrifugation. Briefly, the plasma density was adjusted to  $d = 1.22$  with KBr (0.003 g/l) and overlaid with KBr saline solution ( $d = 1.063$ ). Ultracentrifugation was performed at  $100,000 \times g$  for 20 h at 10 °C. The density of the bottom fraction containing HDLs was adjusted to 1.25 with KBr and overlaid with KBr saline solution ( $d = 1.22$ ). The HDL fraction (top layer) was recovered as a single band and was desalted and concentrated by three washes with saline using a centrifugal concentrating device (cutoff 10 kDa; Vivascience, Stonehouse, UK). The protein concentration was determined by the BCA method (BCA Protein Assay Kit, Thermo Scientific Pierce).



Primary antibody			
Antibodies	Dilution	Reference	Host
ApoA-1	1:100	CALBIOCHEM 178422	Rabbit
PCNA	1:100	DAKO M0879	Mouse
L-Plastin (Lcp1)	1:8000	Gift from M. Redd <sup>63</sup>	Rabbit
Aromatase B	1:600	Gift from F. Brion <sup>27,64</sup>	Rabbit
HuC/D	1:300	INVITROGEN, A21271, Clone 16A11	Mouse
Control Ig	As for ApoA-1	DAKO, X0903	Rabbit
Secondary antibody			
Antibodies or dye	Dilution	Reference	
Goat anti-rabbit Alexa 488	1:200	THERMOFISCHER A11008	
Goat anti-rabbit Alexa 594	1:200	THERMOFISCHER A11012	
Goat anti-mouse Alexa 488	1:200	THERMOFISCHER A11001	
Goat anti-mouse Alexa 594	1:200	THERMOFISCHER A11005	
DAPI (4',6'-diamidino-2-phenylindole, dihydrochloride)	1 ng/ml	THERMOFISCHER D1306	

**Table 3.** Antibodies for immunocytochemistry.

For 1,1'-dioctadecyl-3,3',3'-tetramethylindocarbocyanine perchlorate (DiI) labeling (REF: D3911; THERMOFISCHER), which labels the phospholipid moiety, 300 µg of DiI was added to 2 mg HDL in PBS overnight at 37 °C. Labeled HDL preparations were then re-isolated by ultracentrifugation to eliminate free DiI, and then it was sterile-filtered and stored at 4 °C until further use.

**Microscopy.** Observations were carried out using a NanoZoomer S60 (HAMAMATSU) slide scanner, a Nikon eclipse 80i equipped with a Hamamatsu camera, and a confocal microscope (Confocal NIKON C2si) and its NIS elements software.

**Cell count.** For analyzing brain cell proliferation following intracerebroventricular injection of HDLs, brains were fixed and processed for PCNA immunostaining. The PCNA positive area was counted in blind conditions on three vibratome sections/fish for each condition (PBS; rHDLs, pLHDLs). Similarly, for analyzing the number of microglia and proliferative cells in the ventricular layer at 2 dpf and 5 dpf, respectively, three vibratome sections per fish were selected in the control and lesioned telencephalon.

Images were analyzed using the ImageJ software considering the area stained (along the ventricular layer for PCNA and in the brain parenchyma for L-plastin), and after adjusting the appropriate parameters (threshold, binary, and watershed). These analyses were done in blind conditions.

**Statistical analyses.** Comparisons between groups were performed using a statistical Student t test or using one-way ANOVA for multiple comparisons using PRISM v7 from GRAPHPAD software company.

**ARRIVE guidelines.** The study was carried out in compliance with ARRIVE guidelines.

## Results

**Expression of HDL receptors during zebrafish development.** Given the few numbers of studies documenting HDL receptors in zebrafish, their expression was first investigated during zebrafish development looking at the mammalian homologues of *scarb1*, *abca1*, *abcg1*, and *cd36* (Suppl. Fig. 1). Reanalyzing a recently published RNA sequencing data set from<sup>65</sup> that provided global transcriptomic profiling from the zygote stage (1-cell) to 5 days post-fertilization (dpf), we investigated the temporal gene expression of HDL receptors during embryogenesis. Briefly, *scarb1* was expressed from the zygote stage to larval day 5 with expression peaking at the blastula stage (128–1000 cells). In contrast, *abca1a* and *abca1b* were only barely detected until the blastula dome/gastrula 50%-epiboly stages. Expression of the *abca1a* gene reached a peak at 5 dpf, and *abca1b* gene expression was high until the pharyngula prim 15 stage. *abcg1* and *cd36* gene expressions were very low or undetectable until the larval protruding mouth stage, then it increased strongly to 5 dpf. These data also showed that *scarb1* displayed an important maternal contribution and that HDL receptors are dynamically expressed during zebrafish embryogenesis.

**HDL receptors are widely expressed in the brain of adult zebrafish.** Despite the presence of the BBB, it was shown and/or suggested that some of the smaller circulating HDLs can enter the brains of humans and mice<sup>66–68</sup>. These data suggest a possible role for peripheral HDLs in the central nervous system. However, the cerebral expression and distribution of HDL receptors are not known in zebrafish. We consequently reanalyzed two different RNA sequencing data sets from the whole brain (Fig. 1A) and from telencephala (Fig. 1B) published by Rodriguez Viales et al., and Wong and Godwin, respectively. *HDL receptor* genes appeared to be significantly expressed in the brains of adult zebrafish<sup>58,62</sup>. Our own qPCR experiments also demonstrated the expression of these receptors in the telencephalon with similar relative expression of *HDL receptors* as the ones

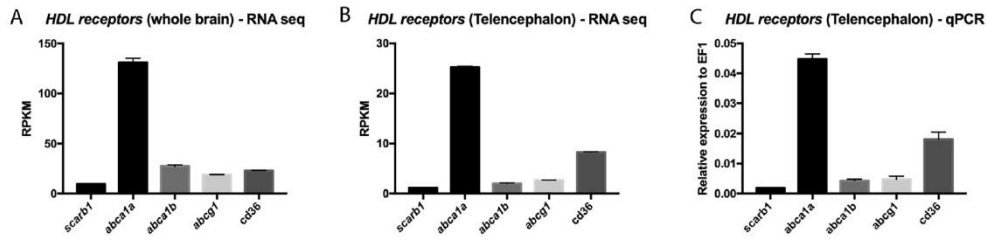


**Figure 1.** HDL receptor mRNA expression in the whole brain and in the telencephalon of adult zebrafish. RNA sequencing data showing the relative levels of expression of HDL receptors in the whole zebrafish brain (n = 4) (A) and in the zebrafish telencephalon (n = 3) (B) of adult animals (data from Rodriguez-Vialez et al. 2015; Gourain et al. 2020; Wong and Godwin 2015)<sup>58,61,62</sup>. (C) qPCR analysis from 3 pools of 5 telencephala, providing the relative gene expression of HDL receptors in the telencephalon. RPKM reads per kilobase million.

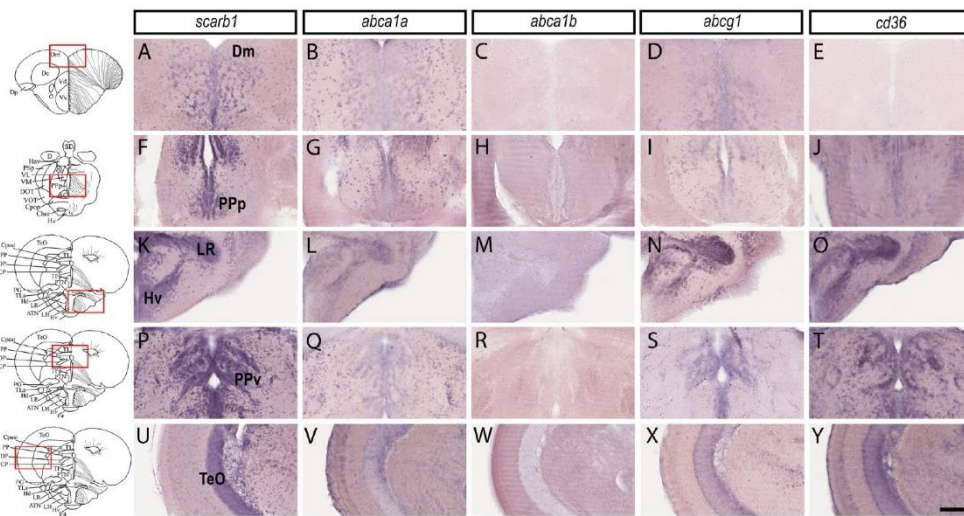


**Figure 2.** HDL receptors are expressed in the brain parenchyma and along the periventricular zones. In situ hybridization of HDL receptors in the brain of adult zebrafish. The scheme provides the localization of the transversal section performed and the red square shows the regions where the high-magnification views were made. In situ hybridization in the medial zone of telencephalic area (Dm, A–E), the posterior part of the preoptic area (PPp, F–J), the ventral zone of the periventricular hypothalamus (Hv, K–O), around the lateral recess of the diencephalic ventricle (Lr, K–O), the periventricular pretectal nucleus ventral part (PPv, P–T), and the optic tectum (TeO, U–Y). Note that most HDL receptors are expressed in the brain parenchyma where neurons are localized and in periventricular zones where NSCs are localized. Scale bar = 50  $\mu$ m.

documented by RNA sequencing (Fig. 1C). *abca1* was the most highly expressed HDL receptor in the brain and telencephalon (Fig. 1). Considering the significant expression of HDL receptors in the brain of adult zebrafish, their distribution was further investigated by in situ hybridization (ISH).

As a result, independent in situ hybridization experiments (n = 3–6) demonstrated a wide expression of *scarb1*, *abca1a*, *abcg1*, and *cd36* in the brain, while *abca1b* was almost not detected (Fig. 2). *scarb1*, *abca1a*, *abcg1*, and *cd36* were widely expressed in the whole brain from the junction between the telencephalon/olfactory bulbs to the cerebellum. In contrast, *abca1b* gene expression failed to be detected by in situ hybridization except in the cerebellum (data not shown). In summary, *scarb1*, *abca1a*, and *abcg1* displayed almost similar patterns and were detected in the dorsal (Vd), ventral (Vv), and central (Vc) nuclei of the ventral telencephalic area, as well as in the central zone (Dc) and medial zone (Dm) of the dorsal telencephalic area. In more posterior regions, these genes were expressed in the supra- (Vs) and post-commissural nucleus (Vp). In the diencephalon, all transcripts

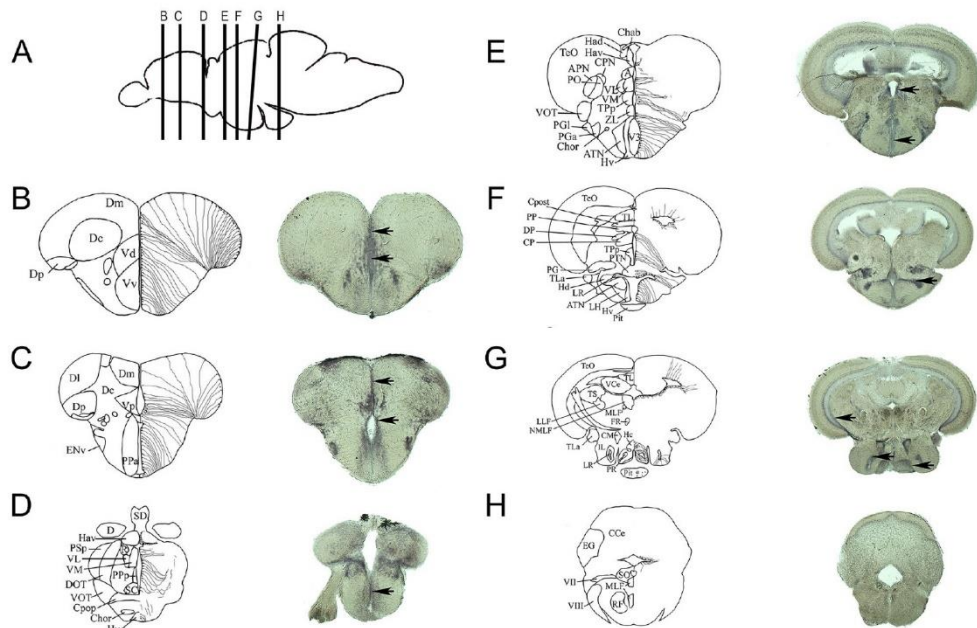


**Figure 3.** Relationship between *scarb1* expression and the distribution of radial glial cells. (A) Sagittal zebrafish brain view showing the respective transverse sections provided from B to H. (B–H) The schemes adapted from the zebrafish brain atlas and from Menuet et al.<sup>70,71</sup> illustrate the transverse brain section and the different brain regions/nuclei (left part), as well as the localization of radial glial cells (neural stem cells) along the brain ventricles (right part). In situ hybridization at the level of the telencephalon (B, C), the anterior and posterior preoptic area (C, D), the anterior, medial, and caudal hypothalamus (E–G), as well as the medulla oblongata (H) demonstrate a wide *scarb1* expression in the brain parenchyma and along the ventricular layer where radial glia reside (Black arrows). Scale bar = 50  $\mu$ m.

coding for HDL receptors (with the exception of *abca1b*) were detected in the anterior (PPa) and posterior (PPp) part of the preoptic and in the anterior (A), dorsal (DT), ventromedial (VM), and ventrolateral nuclei (VL) of the thalamus. In the rhombencephalon, *scarb1*, *abca1a*, *cd36*, and *abcg1* were reported in the posterior tubular nucleus (PTN), the torus lateralis (TLa), and in the different hypothalamic nuclei (Hv, LH, LR, PR, Hc, Hd). They were also expressed in the nucleus of the inferior lobe (IL), optic tectum (TeO), torus longitudinal (TL), torus semi-circularis (TS), and valva of the cerebellum and the cerebellum (VCe + Ce). The specificity of the staining was assessed by hybridization without a probe leading, to the absence of staining (data not shown), and with the use of a specific *id1* antisense probe as a positive control, resulting in a clear and obvious labeling along the ventricular layer as previously described (data not shown)<sup>58,59</sup>.

***Scarb1* is expressed in neurons and radial glial cells behaving as neural stem cells.** Although the expression patterns of *scarb1*, *abca1a*, *abcg1*, and *cd36* displayed a wide and overlapping distribution, some differences were noticed. In contrast to the other receptors for which expression in the ventricular zone was very weak, *scarb1* expression was markedly detected in the ventricular zone, where radial glial cells behaving as NSCs are localized (Figs. 2 and 3, black arrows). Indeed, *scarb1*-positive cells were observed along the ventricles of the Vv, Vd, and Dm (Fig. 3B,C), the posterior part of the preoptic area (Fig. 3D), and the anterior (Fig. 3E), mediobasal (Fig. 3F), and caudal (Fig. 3G) hypothalamus. In addition, some *scarb1*-positive cells from the periglomerular gray zone and lining the ventricles of the optic tectum were observed (Fig. 3E–G). Taken together, such data strongly argue for *scarb1* expression in NSCs. To ascertain this hypothesis, fluorescent *scarb1* ISH was performed, followed by Aromatase B and HuC/D immunohistochemistry, allowing us to label NSCs (radial glia) and neurons, respectively<sup>57,69</sup>. As shown in the dorsomedial telencephalon and in the regions surrounding the posterior recess of the hypothalamus, *scarb1*-positive cells corresponded to both HuC/D-positive neurons and AroB-positive neural stem cells (Fig. 4). These results were also confirmed by performing fluorescence ISH using the anti-digoxigenin antibody conjugated with horseradish peroxidase (data not shown). Taken together, these observations strongly argue for a possible role of *scarb1* and HDL signaling in the control of NSC activity.



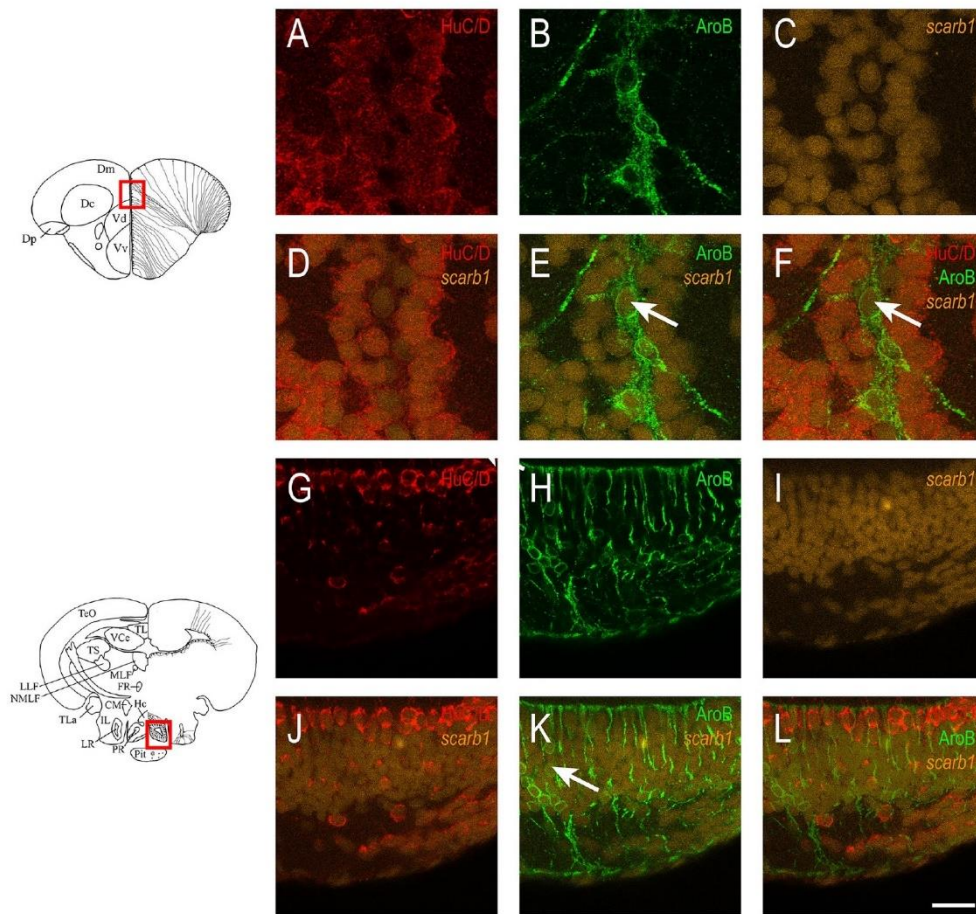


**Figure 4.** *Scarb1* is expressed in neurons and radial glial cells. Fluorescent *scarb1* in situ hybridization in the diencephalic ventricle (G–L). *Scarb1* in situ hybridization (orange) is followed by Aromatase B (green) and HuC/D (red) immunohistochemistry to label NSCs and neurons, respectively. Note that *scarb1* is expressed in both cell types. Scale bar = 50  $\mu$ m.

**Peripheral HDLs reach the brain microvasculature and the damaged brain tissue.** To investigate the capacity of HDLs to target the brain, a biodistribution analysis was performed following intraperitoneal injection in zebrafish and was compared with mice. After 1 h 30 min, the two main metabolic organs, the liver and kidneys, were investigated for human ApoA-I detection by immunohistochemistry. Positive labeling was observed in the liver and kidneys of zebrafish and mice injected with both plasma HDLs and reconstituted HDL particles (Suppl. Fig. 2, green), while no labeling was observed with the negative control IgG or in PBS-injected animals.

In the brain, HDLs were also documented to reach the cerebral blood flow and to be taken up by the cerebral endothelial cells during a stroke<sup>19</sup>. Using DilC18 HDLs, red fluorescence was observed in zebrafish and mice brain microvasculature 1 h 30 min after injection (Fig. 5). These results were confirmed by ApoA-I immunohistochemistry, showing overlapping staining with the DilC18 dye (Fig. 5). No signal was observed by incubation with control IgG or with ApoA-I immunohistochemistry in PBS-injected animals, demonstrating the specificity of the signal (Suppl. Fig. 3). Taking advantage of a *flt1*:GFP transgenic fish, in which GFP is expressed in endothelial cells, we further demonstrated by performing ApoA-I immunohistochemistry that HDLs are taken up by endothelial cells from the brain vasculature (Fig. 5M–O). We did not observe any significant staining in the



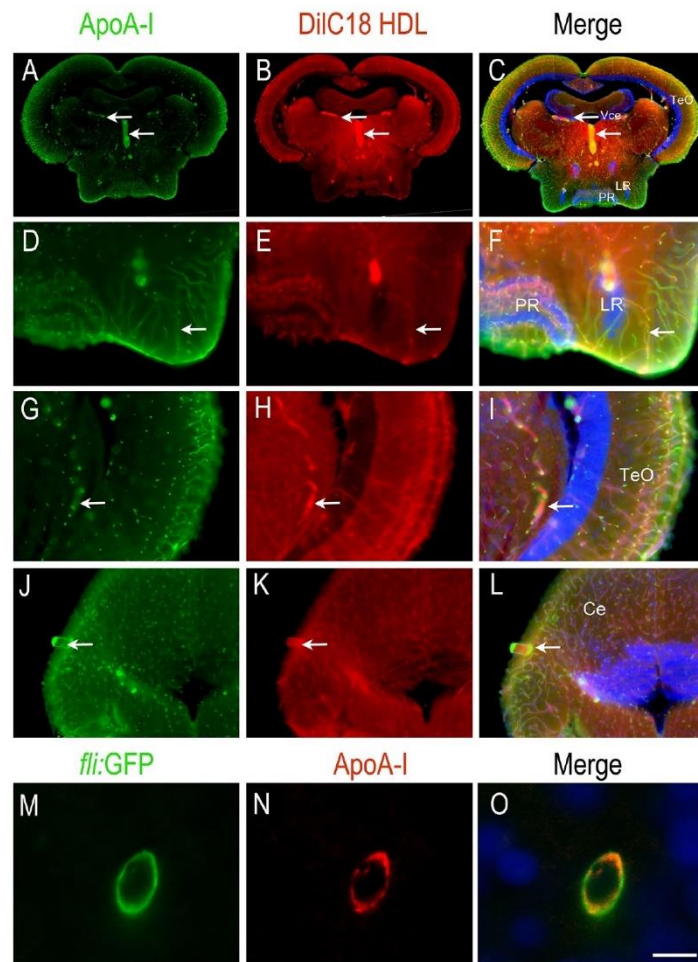


**Figure 5.** HDLs reach the brain microvasculature in zebrafish. ApoA-I immunohistochemistry (green) on zebrafish brain Sects. 1 h 30 min after intraperitoneal injection with 80 mg/kg of fluorescent HDL particles (red). Note that similar data were obtained with HDLs isolated from plasma (pHDL,  $n = 3$ ) and with reconstituted HDLs (rHDL,  $n = 7$ ). (A–L) ApoA-I staining (green) colocalizes with fluorescent HDLs (red) as clearly evidenced by the merged pictures and revealed blood vessel staining. (M–O) Confocal imaging of a transverse brain section from a Tg(fli1:EGFP) zebrafish expressing GFP in the endothelial cells from blood vessels<sup>54</sup>. Note ApoA-I staining (red) detection in endothelial cells (green). The merge pictures (C, F, I, L, O) also show cell nuclei using DAPI counterstaining (blue). Scale bar = 50  $\mu$ m.

brain parenchyma under homeostatic conditions. Such labeling of the blood vessels was also observed in mice injected with pHDLs and rHDLs (Suppl. Fig. 4).

However, after telencephalon stab wound injury, intraperitoneally injected HDLs can reach the damaged brain parenchyma as shown by DiIC18 staining and ApoA-I immunostaining in the injured hemisphere compared to the uninjured one (Fig. 6). To investigate the possible differences in the biodistribution of HDLs following a preventive or therapeutic approach, two different protocols were realized. In the first one, HDL injection occurred prior to the injury, while in the second one, it occurred 30 min after the lesion. In both conditions, fluorescent HDLs diffused within the damaged tissue and ApoA-I staining was markedly increased (Fig. 6), while no staining was observed in PBS-injected fish, showing the specificity of labeling (Fig. 6I). Notably, strong ApoA-I labelling was observed in ventricular cells, resembling NSCs (Fig. 6, arrows). By performing ApoA-I IHC on GFAP::GFP

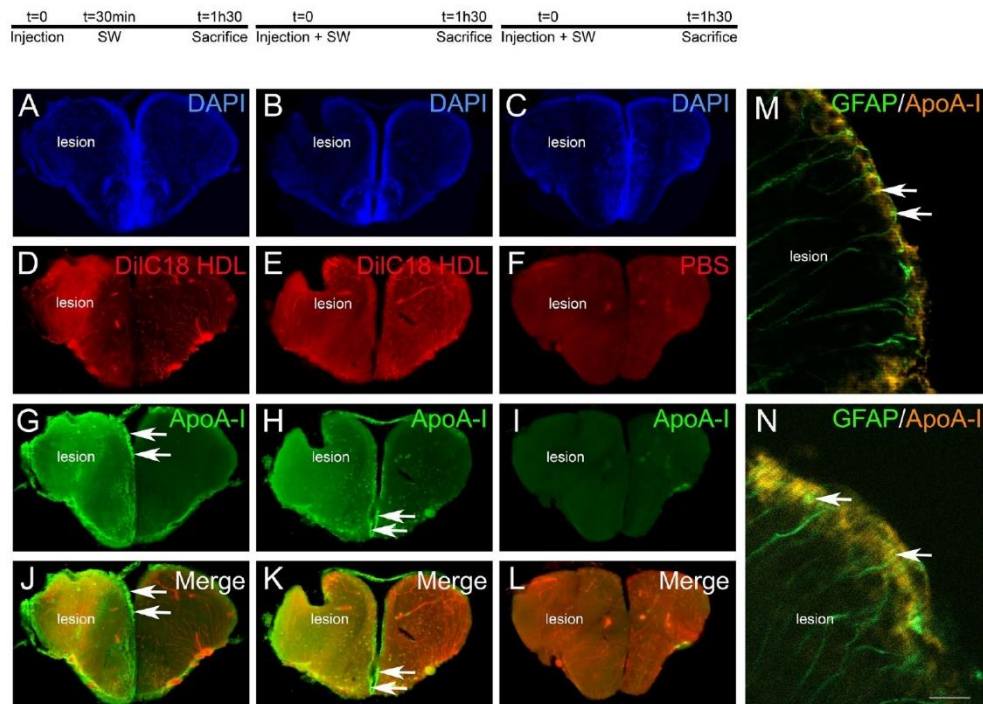


**Figure 6.** HDLs are taken up by the lesioned hemisphere after stab wound injury in zebrafish. ApoA-I immunohistochemistry (green) on injured zebrafish brain following intraperitoneal injection with 80 mg/kg of red fluorescent reconstituted HDLs (n = 8) or PBS (n = 6) as control. The design of the experiment is presented at the top of the figure. (A–L) Note that red fluorescence (HDL) and ApoA-I staining (green) are localized within the brain parenchyma of the injured hemisphere, while HDLs are clearly located in the cerebral vasculature in the contralateral (uninjured) hemisphere. The arrows indicate ApoA-I staining in ventricular cells, probably corresponding to NSCs. In PBS-injected fish (n = 3), ApoA-I immunohistochemistry did not provide any staining, demonstrating the specificity of the labeling. (M–N) ApoA-I immunohistochemistry on GFPAP::GFP transgenic fish<sup>55</sup> injected with HDLs immediately after the lesion. The arrows show GFPAP-positive NSCs co-labeled with ApoA-I. Scale bar = 200  $\mu$ m (A–H) and 20  $\mu$ m (I, J).

fish, we demonstrated the uptake of HDLs by GFPAP-positive NSCs in these conditions (Fig. 6M, N). In conclusion, in homeostatic conditions, HDLs were taken up by endothelial cells in the brain vasculature, while after brain injury, they diffused within the damaged brain hemisphere and accumulated in the ventricular layers, particularly in RGCs.

**Role of HDLs in constitutive and regenerative neurogenesis.** To study the impact of HDLs on NSC proliferation during constitutive neurogenesis, intracerebroventricular injections were performed in WT and GFPAP::GFP transgenic fish, in which GFP was expressed in NSCs<sup>55</sup>. Telencephalic proliferation was monitored 24 h post-injection as previously described<sup>58</sup>. The quality of the injection was assessed using fluorescent HDLs and/or by performing immunohistochemistry against ApoA-I on transgenic fish (Fig. 7A–C). As shown in freshly injected fish, fluorescent HDLs were observed in the telencephalic ventricular cavity (Fig. 7A). From 3 h to 1 day post-injection, ApoA-I immunohistochemistry was detected in the ventricular cavity and also in GFPAP-positive NSCs (Fig. 7B,C), while no staining was observed in PBS-injected fish (data not shown). Quantification of the PCNA-positive area in the medial telencephalic ventricular zone of PBS-, pLHDL-, and rHDL-injected fish revealed no significant difference in telencephalic brain cell proliferation (Fig. 7D,E).

After stab wound injury of the telencephalon, an increase in microglia proliferation and recruitment to the damaged site occurred 2 days post lesion (dpl)<sup>47,72</sup>. This initial step was followed by the proliferation of NSCs at 5 dpl<sup>40,47,58</sup>. Given the anti-inflammatory and neuroprotective roles of HDLs, their effects on brain repair mechanisms were thus studied. Intraperitoneal injections of pLHDLs were performed immediately after stab wound injury. First, we checked whether stab wound injury of the telencephalon resulted in increased microglia recruitment and NSC proliferation at 2 and 5 dpl, respectively (Fig. 8A,B,D,E). As shown in Fig. 8B, a significant

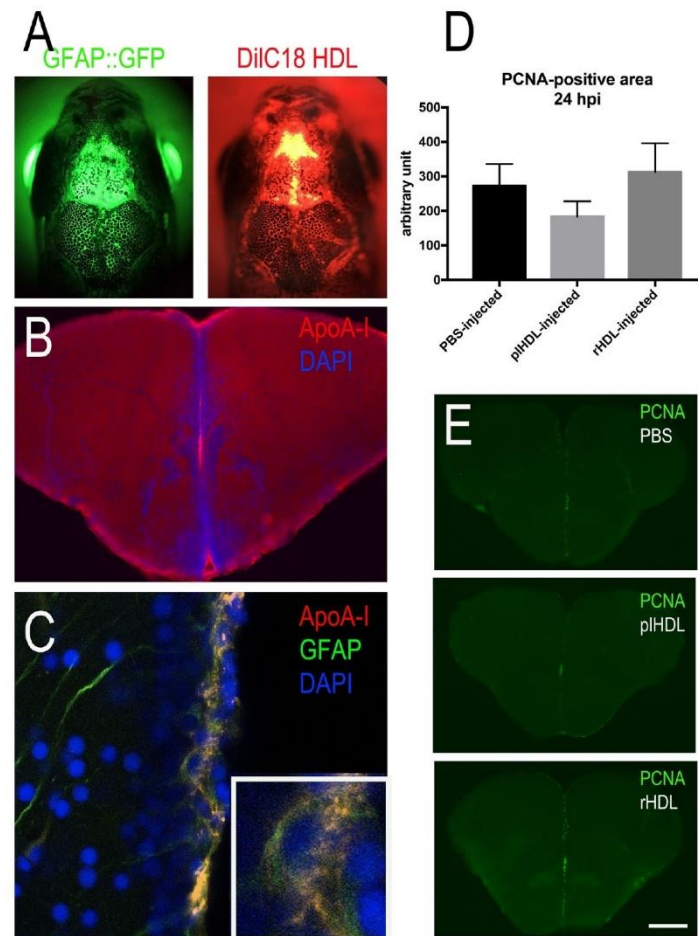


**Figure 7.** Intracerebroventricular injection of HDLs results in their uptake by neural stem cells but did not modify their proliferation. (A) Overview pictures of GFAP::GFP (green) zebrafish heads following injection with fluorescent HDLs (red). Note the diffusion of HDLs in the telencephalic ventricle. (B) ApoA-I immunohistochemistry 3 hpi showing ApoA-I detection in the ventricular cavity and the ventricular zone. (C) ApoA-I immunohistochemistry showing ApoA-I detection (yellow) in GFAP::GFP-positive radial glial cells (NSCs in green) with DAPI cell nuclear counterstaining (blue). (D) PCNA-positive area quantification following PBS, plasmatic HDL (pHDL), and reconstituted HDL (rHDL) 24 h intracerebrovascular post-injection (n = 4–6 injected fish). No significant differences were observed between the groups. (E) Representative pictures of PCNA immunostaining 24 h post-injection with PBS, plasmatic HDL (pHDL), reconstituted HDL (rHDL). Scale bar = 800  $\mu$ m (A), 150  $\mu$ m (B), 21  $\mu$ m (C), and 200  $\mu$ m (E).

increase in microglia was observed at 2 dpl in the injured hemisphere compared to the control side. Similarly, proliferation in the ventricular zone was also higher in the stab wounded hemisphere compared to the uninjured one (Fig. 8E). However, injection of pHDLs directly after the stab wound did not impact microglial recruitment at 2 dpl and injury-induced proliferation at 5 dpl (Fig. 8C,F).

Finally, the expression of *HDL receptors* was also monitored at 5 dpl, and as shown in Fig. 9, most of the HDL receptors were markedly upregulated with the exception of *scarb1*, whose expression was increased but failed to reach statistical significance, and *cd36*, for which expression remained unchanged.



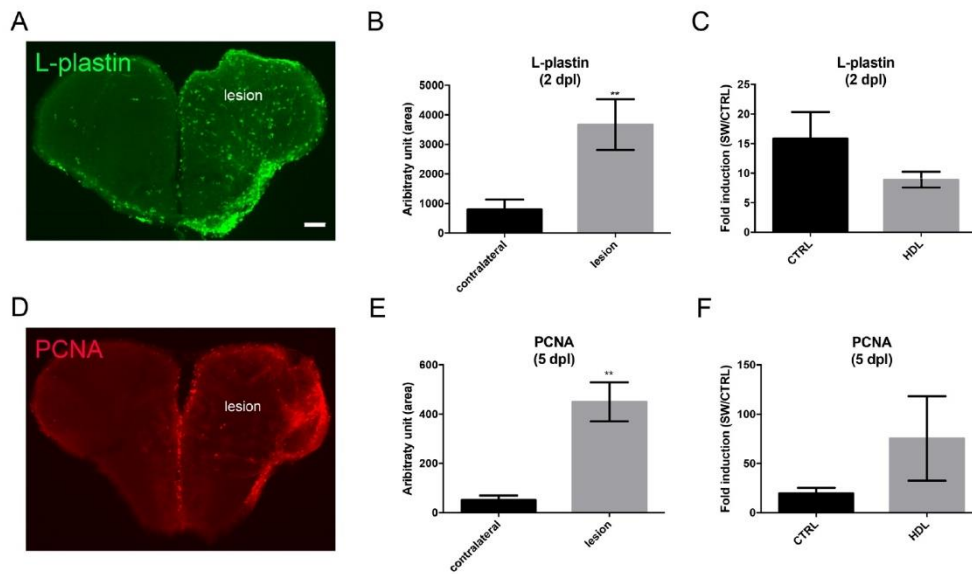


**Figure 8.** HDL injection did not impact microglia recruitment and injury-induced proliferation at the ventricular zone after telencephalic injury. Zebrafish underwent stab wound injury of the telencephalon and were injected with 80 mg/kg of plasma HDL (n = 9) or PBS as a control (n = 10) and sacrificed at 2- or 5-days post lesion (dpl). (A) I-Plastin immunohistochemistry (green) showing increased microglial recruitment in the injured telencephalon at 2 dpl. (B) Quantification of the I-Plastin-positive area in the contralateral and injured hemisphere in PBS-injected fish, demonstrating significant upregulation of microglia recruitment following brain injury at 2 dpl. (C) I-Plastin fold induction between lesioned and non-lesioned hemispheres in HDL and PBS-injected fish at 2 dpl. (D) PCNA immunohistochemistry (red) showing increased ventricular proliferation in the injured telencephalon at 5 dpl. (E) Quantification of the PCNA-positive area in the contralateral and injured hemisphere in PBS-injected fish, demonstrating a significant upregulation of proliferation following brain injury at 5 dpl. (F) PCNA fold induction between lesioned and non-lesioned hemispheres in HDL and PBS injected fish at 5 dpl. \*\*p < 0.01. Scale bar = 100  $\mu$ m.

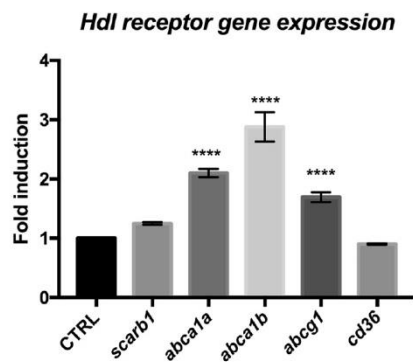


**Figure 9.** HDL receptors are upregulated at 5 days post brain injury. Reanalysis of the RNA sequencing data set from zebrafish of injured and uninjured telencephalon at 5 days post-lesions (data from<sup>58,61</sup>). \*\*\*\*p < 0.001.



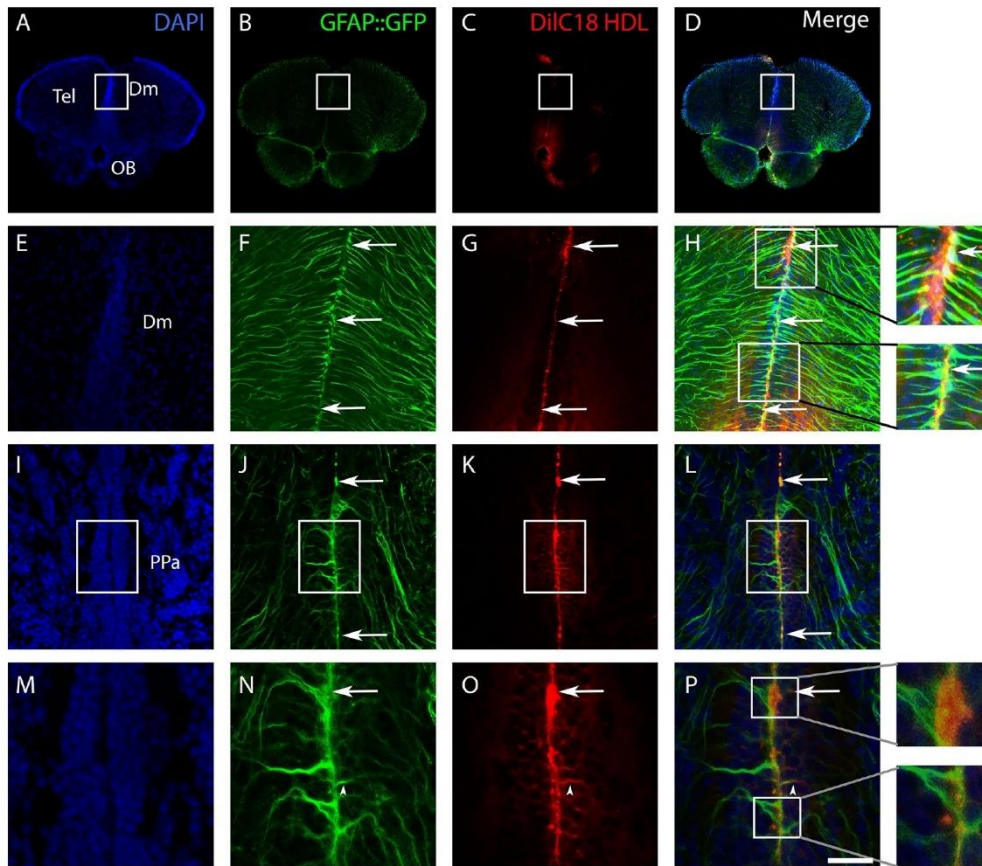


**Figure 10.** Delivery of DilC18 dye in GFAP::GFP-positive neural stem cells mediated by HDL intracerebroventricular injection. Three adult transgenic zebrafish (GFAP::GFP) were intracerebroventricularly injected with HDLs in which DilC18 dye was incorporated (fish were allowed to survive for 1 h 30 min). (A–D, I–L) Zebrafish brain sections at the junction through the olfactory bulbs (OB)/telencephalon (Tel) and through the anterior part of the preoptic area (PPa), showing DilC18 dye (red) along the ventricular layer where NSCs (green) are located. Note the uptake of the DilC18 dye (red) by NSCs (green) as shown by the yellow color in the merged pictures (see arrows). (E–H, M–P) Higher magnifications of the white boxes in (A–D, I–L), respectively. The arrows show colocalization of the dye with GFP, and arrowheads show the colocalization in neural stem cell processes. Scale bar = 700  $\mu$ m (A, B), 140  $\mu$ m (E–H), 85  $\mu$ m (I–L), and 40  $\mu$ m (M–P).

**Use of HDLs as a delivery vector to target neural stem cells.** Although HDLs did not impact NSC proliferation (Fig. 7), these results highlight the fact that they could be used to target NSCs, as ApoA-I was detected by IHC in GFAP::GFP-positive cells. To ascertain the fact that HDLs could be used as a delivery vector, a fluorescent dye (DilC18) was incorporated into HDLs, and intracerebroventricular injection was performed (Fig. 10). As clearly evidenced, the dye was detected along the ventricular layer, where NSCs are located in the anterior part of the telencephalon (Fig. 10A–H), as well as in the anterior part of the preoptic area (Fig. 10I–P). The DilC18 dye was clearly observed in the GFAP::GFP-positive NSC soma (Fig. 10, see arrows) and in some processes (Fig. 10, see arrowheads).

### Discussion

In this work, we first demonstrated that HDL receptors are widely expressed in the brain of adult zebrafish. Interestingly, *scarb1* appears to be mainly expressed in both neurons and radial glial cells that are known to be *bona fide* neural stem cells. We also showed that both HDLs isolated from human plasma and reconstituted HDL

particles (rHDLs made of human ApoA-I and phosphatidylcholines) are able to reach the brain vasculature in normal conditions and to diffuse within the injured hemisphere after mechanical injury of the telencephalon. They accumulate in the ventricular cell layer composed of radial glial cells and other neural progenitors. Additionally, we performed intracerebroventricular injection of HDLs to study their potential effects on NSC proliferation in 'homeostatic' conditions. Although intracerebroventricular injection of HDLs did not result in significant differences in telencephalic cell proliferation, it targeted NSCs and can be used as vector to modulate their proliferative activity.

**HDL receptor gene expression and links with neurogenic niches.** To our knowledge, this is the first report documenting the expression of *HDL receptors* in the brain of a teleost fish. Performing RNA sequencing analyses and in situ hybridization for HDL receptors, we reported cerebral expression of *abca1a*, *abca1b*, *abcg1*, *cd36*, and *scarb1* in adult zebrafish. Although *abca1b* was shown to be expressed by RNA sequencing and qPCR methods, we were unable to show consistent staining by in situ hybridization experiments, probably due to the lack of sensitivity of the digoxigenin-labeled probes or unexpected splicing. We showed that *abca1a*, *abca1b*, *abcg1*, *cd36*, and *scarb1* were widely expressed in the brain and displayed an overlapping distribution, in particular, in most posterior regions. Their distribution was similar to that of neurons, and they were detected in the main zebrafish neurogenic niches, such as the telencephalic, diencephalic, and rhombencephalic areas. In mammals, HDL receptors are expressed in neurons and glia (microglia, astrocytes, oligodendrocytes, and their precursors), as well as endothelial cells<sup>25</sup>. The Allen Brain Atlas also documents the expression of HDL receptors in the mouse hippocampus<sup>24</sup>, a region known to maintain substantial neurogenic activity during adulthood. The nature of the cells expressing these different receptors remains to be investigated in zebrafish.

Furthermore, we demonstrated for the first time that *scarb1* is strongly expressed along the main ventricular and periventricular layers from the most anterior part of the brain to the more dorsal ones. Performing fluorescence in situ hybridization for *scarb1* in two neurogenic regions, the dorsal telencephalon and caudal hypothalamus, we proved that some *scarb1*-positive cells were Aromatase B-positive radial glial cells, corresponding to NSCs. In the same line, *scarb1* was shown to be expressed by NSC culture<sup>26</sup>, but to our knowledge, no functional studies have tested the impact of HDLs on neurogenesis. In our work, by performing proliferation studies following intracerebroventricular injection of rHDLs and pHDLs allowed the direct action of HDLs within the brain and in particular on radial glial cells (RGCs) acting as NSCs. We observed the uptake of HDLs by RGCs, but we did not observe any impact on telencephalic brain cell proliferation. Similarly, after stab wound injury of the telencephalon, injury-induced proliferation of NSCs was similar between fish injected with HDLs and PBS. These data suggest that human HDLs did not significantly impact zebrafish brain cell proliferation. We also considered the possibility that the human ApoA-I protein may be unable to fully activate the HDL canonical signaling pathways in zebrafish as the sequence homology between human ApoA-I and zebrafish ones (*apoa1a* and *apoa1b*) is not good (less than 30% of identity and less than 50% of similarity). Nevertheless, the expression of HDL receptors in neurogenic niches, as well as their uptake by NSCs, argue for a potential role of HDLs in brain plasticity. This idea could be supported in part by the fact that knockout mice for SR-BI display decreased hippocampal synaptic plasticity during aging linked to cognitive defects in recognition and spatial memories<sup>73</sup>, supporting the idea that HDLs could be important for brain plasticity, especially when considering aging. Taken together, these data support (1) the role of HDLs in brain plasticity and NSC activity and/or metabolism and (2) the possibility to use HDLs as vector to target NSCs for drug delivery to boost their neurogenic activity.

**A role for HDLs in brain repair mechanisms?** In mammals, HDLs have been shown to display anti-inflammatory and neuroprotective effects<sup>10,19,20</sup>. To ascertain their potential role in decreasing neuroinflammation after a stab wound injury and to promote activation of NSCs in zebrafish, we quantified microglia recruitment and telencephalic ventricular cell proliferation 2 and 5-days post-injury, respectively. These time points correspond to the peak of microglia recruitment and NSC activation following stab wound injury<sup>40,47,58,72</sup>. We did not observe any impact of HDLs in these processes compared to controls, in our experimental conditions. However, the injection of HDLs prior or quickly after the injury led to the diffusion of HDLs within the brain parenchyma and to their accumulation in ventricular cells resembling NSCs. This interesting result raises the question of the use of HDLs for promoting drug delivery to NSCs to favor brain repair. HDLs are complex macromolecular lipoproteins transporting different lipids and proteins, such as sphingosine-1 phosphate or paraoxonase 1, in addition to ApoA-I, that account for their endothelial protective properties<sup>5</sup>. Different molecules may be required in zebrafish to activate HDL-dependent protective pathways. However, not much is known concerning the structure and components of HDL particles in zebrafish.

After telencephalic brain injury in zebrafish, the RNA sequencing data demonstrated an increase in *abca1*, *abcg1*, and *scarb1* gene expression in the ipsilateral hemisphere compared to the control hemisphere at 5 dpl. In mouse, it was also shown that some HDL receptors were upregulated following stroke. Moreover, *abca1* gene expression was increased in reactive astrocytes from 2 to 6 days after MCAO<sup>74</sup>, and the *cd36* and *scarb1* genes were also increased 3 days after stroke<sup>75,76</sup>. The nature of the cells upregulating HDL receptors after stab wound injury remains to be determined in fish.

Taken together, these data suggest that HDLs could be important for sustaining some NSC properties following brain damage. Furthermore, HDLs could allow the vectorization of drugs to target NSCs for improving the replacement of dead neurons following brain injury. Additionally, the upregulation of HDL receptors after brain insult argues for the key role of lipoproteins and cholesterol in brain remodeling for ensuring membrane and synaptic integrity. It also raises the question of the role of HDLs as a source of cholesterol in the central nervous system.



**HDLs as a source of cholesterol for de novo steroidogenesis.** The brains of fish, amphibians, and mammals are well-known to be a steroidogenic organ, able to synthesize its own steroids from cholesterol<sup>77–81</sup>. Radial glial cells acting as NSCs were shown to express the whole set of steroidogenic enzymes and are envisioned as true steroidogenic cells in fish<sup>79,82,83</sup>. Notably, the fact that such cells express *scarb1* and appear to take up HDL after stab wound injury reinforces the idea that HDLs could be a source of cholesterol for supporting NSC steroidogenesis. Such a cholesterol supply for ensuring steroidogenic functions was previously described in some other tissues in mammals<sup>84–86</sup>. One could argue that pHDLs were not detected in NSCs in homeostatic conditions but only in cerebral endothelial cells. However, numerous studies have shown that HDLs can cross the BBB via transcytosis in mammals<sup>87,88</sup>. Furthermore, a strong link between neurogenic niches and blood vessels was shown in both mammals and fish<sup>80,89</sup>. Furthermore, in zebrafish, it was clearly demonstrated that RGC end feet wrapped blood vessels<sup>80</sup>, arguing for potential exchanges and signaling between endothelial cells and NSCs, as shown recently with neuroblasts<sup>90</sup>. HDLs may undergo transcytosis in endothelial cells before being taken up by NSCs end feet for promoting steroidogenesis.

It is also known that the CNS increases steroidogenesis after injuries<sup>91,92</sup>. In a traumatic brain injury model in rats, the levels of several steroids were increased in the brain (i.e., pregnenolone, progesterone, and 5 $\alpha$ -dihydroprogesterone)<sup>93</sup>. Additionally, steroids such as estrogen and progesterone have been shown to display neuroprotective effects in mammals after CNS injury<sup>91,94–96</sup>. However, there is no data available concerning steroidogenesis following brain injury in zebrafish. In addition, we observed an increase in HDL receptor gene expression 5 dpl in zebrafish, suggesting an increase in HDL capture after stab wound injury. Such an increase was also observed for *abca1* following brain injury (ischemia) in mammals<sup>74</sup>. It could be hypothesized that HDL uptake by neurogenic cells may serve for steroidogenesis in a way similar to mammals.

**HDL biodistribution in zebrafish is comparable to mammals.** In mammals, it is well established that HDLs are mainly catabolized by many organs, such as the liver and kidneys<sup>12</sup>. Here, we showed that human pHDLs and rHDLs injected intraperitoneally were detected in both the liver and kidneys of adult zebrafish in a way similar to what we observed in mice (Suppl. Fig. 1). We also demonstrated that HDLs could reach the brain vasculature and accumulated in cerebral endothelial cells in both fish and mice (Fig. 5; Suppl. Fig. 2). Although in mammals the smaller circulating HDL particles can reach the brain parenchyma<sup>66,67</sup>, we were not able to detect HDL particles within the brain parenchyma in homeostatic conditions in fish. However, following brain injury, HDLs diffused into the brain parenchyma of the injured telencephalon and seemed to accumulate in the telencephalic ventricular cells known to be NSCs. These observations are particularly interesting given that after MCAO in mice, HDLs have been shown to be taken up by endothelial cells and astrocytes<sup>19</sup>. Moreover, the brain of adult zebrafish is devoid of astrocytes, and radial glial cells are suggested to support the functions of astrocytes participating, for instance, in the maintenance of the BBB<sup>53,80</sup> and supporting a part of steroidogenesis<sup>79,81,82,97</sup>. At the end of mouse embryonic development, most radial glial cells disappear and are transformed into astrocytes<sup>98</sup>, while they persist during adulthood in zebrafish and express a set of well-characterized astrocytic markers (i.e., GFAP, vimentin, nestin). Consequently, this data supports some evolutionary conserved features in the uptake of HDLs by glial cells, being mainly internalized by astrocytes in mammals and by radial glial cells in zebrafish. They also show that HDLs may preferentially target NSCs instead of neurons.

## Conclusion

In conclusion, this work demonstrates the expression of HDL receptors in the brain of adult zebrafish, their modulation after cerebral injury, and the uptake of HDLs at the injured site. It reinforces the interest of using zebrafish for better understanding the role of lipoproteins in brain plasticity. Notably, this study also suggests the use of HDLs for the vectorization of potential neuroprotective molecules, their screening, and their impact on NSC activity. Given the upregulation of HDL receptors following brain damage in both mice and zebrafish, it raises the question of a potential beneficial effect of HDL treatment in the different phases of brain repair. Despite the well-documented neuroprotective properties of HDLs in mammals, we were not able to demonstrate, in this heterologous model and in our experimental conditions, any effect of HDLs on inflammation, microglial expression, and cell proliferation in the brain of zebrafish after a stab wound injury.

Received: 9 November 2020; Accepted: 24 February 2021

Published online: 19 March 2021

## References

- Scherer, M., Bottcher, A. & Liebisch, G. Lipid profiling of lipoproteins by electrospray ionization tandem mass spectrometry. *Biochim. Biophys. Acta* **918–924**, 2011. <https://doi.org/10.1016/j.bbali.2011.06.016> (1811).
- Meilhac, O., Tanaka, S. & Couret, D. High-density lipoproteins are bug scavengers. *Biomolecules*. <https://doi.org/10.3390/biom10040598> (2020).
- Hottman, D. A., Chernick, D., Cheng, S., Wang, Z. & Li, L. HDL and cognition in neurodegenerative disorders. *Neurobiol. Dis.* **72**(Pt A), 22–36. <https://doi.org/10.1016/j.nbd.2014.07.015> (2014).
- De Miranda Teixeira, R. et al. HDL particle size and functionality comparison between patients with and without confirmed acute myocardial infarction. *Cardiol. Res. Pract.* **2019**, 3074602. <https://doi.org/10.1155/2019/3074602> (2019).
- Tran-Dinh, A. et al. HDL and endothelial protection. *Br. J. Pharmacol.* **169**, 493–511. <https://doi.org/10.1111/bph.12174> (2013).
- Barter, P. J. et al. Antiinflammatory properties of HDL. *Circ. Res.* **95**, 764–772. <https://doi.org/10.1161/01.RES.0000146094.59640.13> (2004).
- Navab, M. et al. Normal high density lipoprotein inhibits three steps in the formation of mildly oxidized low density lipoprotein: Step 1. *J. Lipid. Res.* **41**, 1481–1494 (2000).

8. Boyce, G., Button, E., Soo, S. & Wellington, C. The pleiotropic vasoprotective functions of high density lipoproteins (HDL). *J. Biomed. Res.* <https://doi.org/10.7555/JBR.31.20160103> (2017).
9. Davidson, M. H. & Toth, P. P. High-density lipoprotein metabolism: potential therapeutic targets. *Am. J. Cardiol.* **100**, n32-40. <https://doi.org/10.1016/j.amjcard.2007.08.011> (2007).
10. Meilhac, O. High-density lipoproteins in stroke. *Handb. Exp. Pharmacol.* **224**, 509–526. [https://doi.org/10.1007/978-3-319-09665-0\\_16](https://doi.org/10.1007/978-3-319-09665-0_16) (2015).
11. Fidge, N. H. High density lipoprotein receptors, binding proteins, and ligands. *J. Lipid. Res.* **40**, 187–201 (1999).
12. Zannis, V. I. *et al.* HDL biogenesis, remodeling, and catabolism. *Handb. Exp. Pharmacol.* **224**, 53–111. [https://doi.org/10.1007/978-3-319-09665-0\\_2](https://doi.org/10.1007/978-3-319-09665-0_2) (2015).
13. Calvo, D., Gomez-Coronado, D., Suarez, Y., Lasuncion, M. A. & Vega, M. A. Human CD36 is a high affinity receptor for the native lipoproteins HDL, LDL, and VLDL. *J. Lipid. Res.* **39**, 777–788 (1998).
14. Prosser, H. C., Ng, M. K. & Bursill, C. A. The role of cholesterol efflux in mechanisms of endothelial protection by HDL. *Curr. Opin. Lipidol.* **23**, 182–189. <https://doi.org/10.1097/MOL.0b013e328352c4dd> (2012).
15. Vitali, C., Wellington, C. L. & Calabresi, L. HDL and cholesterol handling in the brain. *Cardiovasc. Res.* **103**, 405–413. <https://doi.org/10.1093/cvr/cvu148> (2014).
16. Ramachandran Pillai, R. *et al.* Low serum levels of High-Density Lipoprotein cholesterol (HDL-c) as an indicator for the development of severe postpartum depressive symptoms. *PLoS ONE* **13**, e0192811. <https://doi.org/10.1371/journal.pone.0192811> (2018).
17. Yang, F. N., Stanford, M. & Jiang, X. Low cholesterol level linked to reduced semantic fluency performance and reduced gray matter volume in the medial temporal lobe. *Front. Aging Neurosci.* **12**, 57. <https://doi.org/10.3389/fnagi.2020.00057> (2020).
18. Atzmon, G. *et al.* Plasma HDL levels highly correlate with cognitive function in exceptional longevity. *J. Gerontol. A Biol. Sci. Med. Sci.* **57**, M712–715. <https://doi.org/10.1093/gerona/57.11.m712> (2002).
19. Lapergue, B. *et al.* Protective effect of high-density lipoprotein-based therapy in a model of embolic stroke. *Stroke* **41**, 1536–1542. <https://doi.org/10.1161/STROKEAHA.110.581512> (2010).
20. Lapergue, B. *et al.* High-density lipoprotein-based therapy reduces the hemorrhagic complications associated with tissue plasminogen activator treatment in experimental stroke. *Stroke* **44**, 699–707. <https://doi.org/10.1161/STROKEAHA.112.667832> (2013).
21. Paterno, R. *et al.* Reconstituted high-density lipoprotein exhibits neuroprotection in two rat models of stroke. *Cerebrovasc. Dis.* **17**, 204–211. <https://doi.org/10.1159/000075792> (2004).
22. Ortiz-Munoz, G. *et al.* Dysfunctional HDL in acute stroke. *Atherosclerosis* **253**, 75–80. <https://doi.org/10.1016/j.atherosclerosis.2016.08.035> (2016).
23. Uhlen, M. *et al.* Proteomics. Tissue-based map of the human proteome. *Science* **347**, 1260419. <https://doi.org/10.1126/science.1260419> (2015).
24. Lein, E. S. *et al.* Genome-wide atlas of gene expression in the adult mouse brain. *Nature* **445**, 168–176. <https://doi.org/10.1038/nature05453> (2007).
25. Zhang, Y. *et al.* An RNA-sequencing transcriptome and splicing database of glia, neurons, and vascular cells of the cerebral cortex. *J. Neurosci.* **34**, 11929–11947. <https://doi.org/10.1523/JNEUROSCI.1860-14.2014> (2014).
26. Karsten, S. L. *et al.* Global analysis of gene expression in neural progenitors reveals specific cell-cycle, signaling, and metabolic networks. *Dev. Biol.* **261**, 165–182. [https://doi.org/10.1016/s0012-1606\(03\)00274-4](https://doi.org/10.1016/s0012-1606(03)00274-4) (2003).
27. Mahley, R. W. Central nervous system lipoproteins: ApoE and regulation of cholesterol metabolism. *Arterioscler. Thromb. Vasc. Biol.* **36**, 1305–1315. <https://doi.org/10.1161/ATVBAHA.116.307023> (2016).
28. Krishnan, J. & Rohner, N. Sweet fish: Fish models for the study of hyperglycemia and diabetes. *J. Diabetes* <https://doi.org/10.1111/1753-0407.12860> (2018).
29. Dorsemans, A. C. *et al.* Impaired constitutive and regenerative neurogenesis in adult hyperglycemic zebrafish. *J. Comp. Neurol.* **525**, 442–458. <https://doi.org/10.1002/cne.24065> (2017).
30. Dorsemans, A. C. *et al.* Diabetes, adult neurogenesis and brain remodeling: New insights from rodent and zebrafish models. *Neurogenesis (Austin)* **4**, e1281862. <https://doi.org/10.1080/23262133.2017.1281862> (2017).
31. Capiotti, K. M. *et al.* Hyperglycemia induces memory impairment linked to increased acetylcholinesterase activity in zebrafish (*Danio rerio*). *Behav. Brain Res.* **274**, 319–325. <https://doi.org/10.1016/j.bbr.2014.08.033> (2014).
32. Zang, L., Maddison, L. A. & Chen, W. Zebrafish as a model for obesity and diabetes. *Front. Cell Dev. Biol.* **6**, 91. <https://doi.org/10.3389/fcell.2018.00091> (2018).
33. Seth, A., Stemple, D. L. & Barroso, I. The emerging use of zebrafish to model metabolic disease. *Dis. Model. Mech.* **6**, 1080–1088. <https://doi.org/10.1242/dmm.011346> (2013).
34. Schlegel, A. Zebrafish models for dyslipidemia and atherosclerosis research. *Front. Endocrinol.* **7**, 159. <https://doi.org/10.3389/fendo.2016.00159> (2016).
35. Otis, J. P. *et al.* Zebrafish as a model for apolipoprotein biology: Comprehensive expression analysis and a role for ApoA-IV in regulating food intake. *Dis. Model. Mech.* **8**, 295–309. <https://doi.org/10.1242/dmm.018754> (2015).
36. Than-Trong, E. & Bally-Cuif, L. Radial glia and neural progenitors in the adult zebrafish central nervous system. *Glia* **63**, 1406–1428. <https://doi.org/10.1002/glia.22856> (2015).
37. Pellegrini, E. *et al.* Identification of aromatase-positive radial glial cells as progenitor cells in the ventricular layer of the forebrain in zebrafish. *J. Comp. Neurol.* **501**, 150–167. <https://doi.org/10.1002/cne.21222> (2007).
38. März, M. *et al.* Heterogeneity in progenitor cell subtypes in the ventricular zone of the zebrafish adult telencephalon. *Glia* **58**, 870–888. <https://doi.org/10.1002/glia.20971> (2010).
39. Kizil, C., Kaslin, J., Kroehne, V. & Brand, M. Adult neurogenesis and brain regeneration in zebrafish. *Dev. Neurobiol.* **72**, 429–461. <https://doi.org/10.1002/dneu.20918> (2012).
40. Diotel, N. *et al.* Effects of estradiol in adult neurogenesis and brain repair in zebrafish. *Horm. Behav.* **63**, 193–207. <https://doi.org/10.1016/j.yhbeh.2012.04.003> (2013).
41. Diotel, N., Lubke, L., Strähle, U. & Rastegar, S. Common and distinct features of adult neurogenesis and regeneration in the telencephalon of zebrafish and mammals. *Front. Neurosci.* **14**, 568930. <https://doi.org/10.3389/fnins.2020.568930> (2020).
42. Fang, L., Liu, C. & Miller, Y. I. Zebrafish models of dyslipidemia: Relevance to atherosclerosis and angiogenesis. *Transl. Res.* **163**, 99–108. <https://doi.org/10.1016/j.trsl.2013.09.004> (2014).
43. Fink, I. R. *et al.* Molecular and functional characterization of the scavenger receptor CD36 in zebrafish and common carp. *Mol. Immunol.* **63**, 381–393. <https://doi.org/10.1016/j.molimm.2014.09.010> (2015).
44. Lindsey, B. W. & Tropepe, V. A comparative framework for understanding the biological principles of adult neurogenesis. *Prog. Neurobiol.* **80**, 281–307. <https://doi.org/10.1016/j.pneurobio.2006.11.007> (2006).
45. Kishimoto, N., Shimizu, K. & Sawamoto, K. Neuronal regeneration in a zebrafish model of adult brain injury. *Dis. Model. Mech.* **5**, 200–209. <https://doi.org/10.1242/dmm.007336> (2012).
46. Diotel, N. *et al.* Aromatase in the brain of teleost fish: Expression, regulation and putative functions. *Front. Neuroendocrinol.* **31**, 172–192. <https://doi.org/10.1016/j.yfrnc.2010.01.003> (2010).
47. März, M., Schmidt, R., Rastegar, S. & Strähle, U. Regenerative response following stab injury in the adult zebrafish telencephalon. *Dev. Dyn.* **240**, 2221–2231. <https://doi.org/10.1002/dvdy.22710> (2011).
48. Schmidt, R., Beil, T., Strähle, U. & Rastegar, S. Stab wound injury of the zebrafish adult telencephalon: A method to investigate vertebrate brain neurogenesis and regeneration. *J. Vis. Exp.* <https://doi.org/10.3791/51753> (2014).



49. Wang, J. *et al.* High-glucose/high-cholesterol diet in zebrafish evokes diabetic and affective pathogenesis: The role of peripheral and central inflammation, microglia and apoptosis. *Prog. Neuropsychopharmacol. Biol. Psychiatry*. <https://doi.org/10.1016/j.pnpbp.2019.109752> (2019).
50. Ghaddar, B. *et al.* Impaired brain homeostasis and neurogenesis in diet-induced overweight zebrafish: A preventive role from A. borbonica extract. *Sci. Rep.* **10**, 14496. <https://doi.org/10.1038/s41598-020-71402-2> (2020).
51. Howe, K. *et al.* The zebrafish reference genome sequence and its relationship to the human genome. *Nature* **496**, 498–503. <https://doi.org/10.1038/nature12111> (2013).
52. Zambusi, A. & Ninkovic, J. Regeneration of the central nervous system-principles from brain regeneration in adult zebrafish. *World J. Stem Cells* **12**, 8–24. <https://doi.org/10.4252/wjsc.v12.i1.8> (2020).
53. Jurisch-Yaksi, N., Yaksi, E. & Kizil, C. Radial glia in the zebrafish brain: Functional, structural, and physiological comparison with the mammalian glia. *Glia* <https://doi.org/10.1002/glia.23849> (2020).
54. Lawson, N. D. & Weinstein, B. M. In vivo imaging of embryonic vascular development using transgenic zebrafish. *Dev. Biol.* **248**, 307–318. <https://doi.org/10.1006/dbio.2002.0711> (2002).
55. Lam, C. S., Marz, M. & Strahle, U. gfap and nestin reporter lines reveal characteristics of neural progenitors in the adult zebrafish brain. *Dev. Dyn.* **238**, 475–486. <https://doi.org/10.1002/dvdy.21853> (2009).
56. Dang, M., Henderson, R. E., Garraway, L. A. & Zon, L. I. Long-term drug administration in the adult zebrafish using oral gavage for cancer preclinical studies. *Dis. Model. Mech.* **9**, 811–820. <https://doi.org/10.1242/dmm.024166> (2016).
57. Kinkel, M. D., Eames, S. C., Philipson, L. H. & Prince, V. E. Intraperitoneal injection into adult zebrafish. *J. Vis. Exp.* <https://doi.org/10.3791/2126> (2010).
58. Viales, R. R. *et al.* The helix-loop-helix protein id1 controls stem cell proliferation during regenerative neurogenesis in the adult zebrafish telencephalon. *Stem Cells* **33**, 892–903. <https://doi.org/10.1002/stem.1883> (2015).
59. Diotel, N., Beil, T., Strahle, U. & Rastegar, S. Differential expression of id genes and their potential regulator znf238 in zebrafish adult neural progenitor cells and neurons suggests distinct functions in adult neurogenesis. *Gene Expr. Patterns* **19**, 1–13. <https://doi.org/10.1016/j.gep.2015.05.004> (2015).
60. Rastegar, S. *et al.* Expression of adiponectin receptors in the brain of adult zebrafish and mouse: Links with neurogenic niches and brain repair. *J. Comp. Neurol.* **527**, 2317–2333. <https://doi.org/10.1002/cne.24669> (2019).
61. Gourain, V. *et al.* Multi-dimensional transcriptome analysis reveals modulation of cholesterol metabolism as highly integrated response to brain injury. *bioRxiv*. <https://doi.org/10.1101/2020.12.29.424680> (2020).
62. Wong, R. Y. & Godwin, J. Neurotranscriptome profiles of multiple zebrafish strains. *Genom. Data* **5**, 206–209. <https://doi.org/10.1016/j.gdata.2015.06.004> (2015).
63. Redd, M. J., Kelly, G., Dunn, G., Way, M. & Martin, P. Imaging macrophage chemotaxis in vivo: Studies of microtubule function in zebrafish wound inflammation. *Cell Motil. Cytoskeleton* **63**, 415–422. <https://doi.org/10.1002/cm.20133> (2006).
64. Menuet, A. *et al.* Expression and estrogen-dependent regulation of the zebrafish brain aromatase gene. *J. Comp. Neurol.* **485**, 304–320. <https://doi.org/10.1002/cne.20497> (2005).
65. White, R. J. *et al.* A high-resolution mRNA expression time course of embryonic development in zebrafish. *Elife*. <https://doi.org/10.7554/eLife.30860> (2017).
66. Ladu, M. J. *et al.* Lipoproteins in the central nervous system. *Ann. N. Y. Acad. Sci.* **903**, 167–175. <https://doi.org/10.1111/j.1749-6632.2000.tb06365.x> (2000).
67. Koch, S. *et al.* Characterization of four lipoprotein classes in human cerebrospinal fluid. *J. Lipid Res.* **42**, 1143–1151 (2001).
68. Stukas, S. *et al.* Intravenously injected human apolipoprotein A-I rapidly enters the central nervous system via the choroid plexus. *J. Am. Heart Assoc.* **3**, e001156. <https://doi.org/10.1161/JAHA.114.001156> (2014).
69. Tong, S. K. *et al.* A cyp19a1b-gfp (aromatase B) transgenic zebrafish line that expresses GFP in radial glial cells. *Genesis* **47**, 67–73. <https://doi.org/10.1002/dvg.20459> (2009).
70. Wullmann, M. *et al.* (eds) *Neuroanatomy of the Zebrafish Brain: A Topological Atlas* 1–144 (Birkhäuser Verlag, 1996).
71. Pellegrini, E. *et al.* Relationships between aromatase and estrogen receptors in the brain of teleost fish. *Gen. Comp. Endocrinol.* **142**, 60–66. <https://doi.org/10.1016/j.ygcen.2004.12.003> (2005).
72. Baumgart, E. V., Barbosa, J. S., Bally-Cuif, L., Gotz, M. & Ninkovic, J. Stab wound injury of the zebrafish telencephalon: A model for comparative analysis of reactive gliosis. *Glia* **60**, 343–357. <https://doi.org/10.1002/glia.22269> (2012).
73. Chang, E. H., Rigotti, A. & Huerta, P. T. Age-related influence of the HDL receptor SR-BI on synaptic plasticity and cognition. *Neurobiol. Aging* **30**, 407–419. <https://doi.org/10.1016/j.neurobiolaging.2007.07.006> (2009).
74. Morizawa, Y. M. *et al.* Reactive astrocytes function as phagocytes after brain ischemia via ABCA1-mediated pathway. *Nat. Commun.* **8**, 28. <https://doi.org/10.1038/s41467-017-00037-1> (2017).
75. Kim, E. *et al.* Daidzein augments cholesterol homeostasis via ApoE to promote functional recovery in chronic stroke. *J. Neurosci.* **35**, 15113–15126. <https://doi.org/10.1523/JNEUROSCI.2890-15.2015> (2015).
76. Kim, E. *et al.* CD36 in the periphery and brain synergizes in stroke injury in hyperlipidemia. *Ann. Neurol.* **71**, 753–764. <https://doi.org/10.1002/ana.23569> (2012).
77. Zwain, I. H. & Yen, S. S. Neurosteroidogenesis in astrocytes, oligodendrocytes, and neurons of cerebral cortex of rat brain. *Endocrinology* **140**, 3843–3852 (1999).
78. Vaudry, H. *et al.* Neurosteroid biosynthesis in the brain of amphibians. *Front. Endocrinol.* **2**, 79. <https://doi.org/10.3389/fendo.2011.00079> (2011).
79. Diotel, N. *et al.* The brain of teleost fish, a source, and a target of sexual steroids. *Front. Neurosci.* **5**, 137. <https://doi.org/10.3389/fnins.2011.00137> (2011).
80. Diotel, N. *et al.* Steroid transport, local synthesis, and signaling within the brain: Roles in neurogenesis, neuroprotection, and sexual behaviors. *Front. Neurosci.* **12**, 84. <https://doi.org/10.3389/fnins.2018.00084> (2018).
81. Weger, M. *et al.* Expression and activity profiling of the steroidogenic enzymes of glucocorticoid biosynthesis and the fdx1 co-factors in zebrafish. *J. Neuroendocrinol.* **30**, e12586. <https://doi.org/10.1111/jne.12586> (2018).
82. Pellegrini, E. *et al.* Steroid modulation of neurogenesis: Focus on radial glial cells in zebrafish. *J. Steroid. Biochem. Mol. Biol.* **160**, 27–36. <https://doi.org/10.1016/j.jsmb.2015.06.011> (2016).
83. Xing, L., Goswami, M. & Trudeau, V. L. Radial glial cell: Critical functions and new perspective as a steroid synthetic cell. *Gen. Comp. Endocrinol.* **203**, 181–185. <https://doi.org/10.1016/j.ygcen.2014.03.010> (2014).
84. Hu, J., Zhang, Z., Shen, W. J. & Azhar, S. Cellular cholesterol delivery, intracellular processing and utilization for biosynthesis of steroid hormones. *Nutr. Metab. (Lond.)* **7**, 47. <https://doi.org/10.1186/1743-7075-7-47> (2010).
85. Azhar, S. *et al.* Human granulosa cells use high density lipoprotein cholesterol for steroidogenesis. *J. Clin. Endocrinol. Metab.* **83**, 983–991. <https://doi.org/10.1210/jcem.83.3.4662> (1998).
86. Bochem, A. E. *et al.* High density lipoprotein as a source of cholesterol for adrenal steroidogenesis: A study in individuals with low plasma HDL-C. *J. Lipid Res.* **54**, 1698–1704. <https://doi.org/10.1194/jlr.P033449> (2013).
87. Fung, K. Y. *et al.* SR-BI mediated transcytosis of HDL in brain microvascular endothelial cells is independent of caveolin, clathrin, and PDZK1. *Front. Physiol.* **8**, 841. <https://doi.org/10.3389/fphys.2017.00841> (2017).
88. Balazs, Z. *et al.* Uptake and transport of high-density lipoprotein (HDL) and HDL-associated alpha-tocopherol by an in vitro blood-brain barrier model. *J. Neurochem.* **89**, 939–950. <https://doi.org/10.1111/j.1471-4159.2004.02373.x> (2004).

89. Karakatsani, A., Shah, B. & de Almodovar, C. R. Blood vessels as regulators of neural stem cell properties. *Front. Mol. Neurosci.* **12**, 85. <https://doi.org/10.3389/fnmol.2019.00085> (2019).
90. Taberner, L., Banon, A. & Alsina, B. Sensory neuroblast quiescence depends on vascular cytoneme contacts and sensory neuronal differentiation requires initiation of blood flow. *Cell Rep.* **32**, 107903. <https://doi.org/10.1016/j.celrep.2020.107903> (2020).
91. Azcoitia, I., DonCarlos, L. L., Arevalo, M. A. & Garcia-Segura, L. M. Therapeutic implications of brain steroidogenesis. *Horm. Mol. Biol. Clin. Investig.* **1**, 21–26. <https://doi.org/10.1515/HMBCL.2010.003> (2010).
92. Mirzamani, A., Spence, R. D., Naranjo, K. C., Saldanha, C. J. & Schlinger, B. A. Injury-induced regulation of steroidogenic gene expression in the cerebellum. *J. Neurotrauma* **27**, 1875–1882. <https://doi.org/10.1089/neu.2010.1330> (2010).
93. Meffre, D. *et al.* Steroid profiling in brain and plasma of male and pseudopregnant female rats after traumatic brain injury: Analysis by gas chromatography/mass spectrometry. *Endocrinology* **148**, 2505–2517. <https://doi.org/10.1210/en.2006-1678> (2007).
94. Stein, D. G., Wright, D. W. & Kellermann, A. L. Does progesterone have neuroprotective properties? *Ann. Emerg. Med.* **51**, 164–172. <https://doi.org/10.1016/j.annemergmed.2007.05.001> (2008).
95. Schreihöfer, D. A. & Ma, Y. Estrogen receptors and ischemic neuroprotection: Who, what, where, and when? *Brain Res.* **1514**, 107–122. <https://doi.org/10.1016/j.brainres.2013.02.051> (2013).
96. Schumacher, M., Sitruk-Ware, R. & De Nicola, A. F. Progesterone and progestins: Neuroprotection and myelin repair. *Curr. Opin. Pharmacol.* **8**, 740–746. <https://doi.org/10.1016/j.coph.2008.10.002> (2008).
97. Diotel, N. *et al.* Activity and expression of steroidogenic enzymes in the brain of adult zebrafish. *Eur. J. Neurosci.* **34**, 45–56. <https://doi.org/10.1111/j.1460-9568.2011.07731.x> (2011).
98. Noctor, S. C. *et al.* Dividing precursor cells of the embryonic cortical ventricular zone have morphological and molecular characteristics of radial glia. *J. Neurosci.* **22**, 3161–3173 (2002).

### Acknowledgements

We thank Cynthia Planesse for excellent technical support with the fish facility, as well as Dr M. Redd for kindly providing the L-plastin antibody and F. Brion for the Aromatase B antibody. We thank Uwe Strähle for sharing the RNA sequencing data from<sup>58</sup> and Luisa Lübke for her help in intracerebroventricular injection. We thank Christian Lefebvre d’Hellencourt for advice and discussion.

### Author contributions

N.D. and O.M. designed the experiments. All authors performed the experiments. N.C.S., B.G., L.G., S.R., O.M., and N.D. participated in the analysis of the experiments and/or in the writing of the manuscript.

### Funding

This work was supported by Grants from the University of La Réunion, European Union (EU)-Région Réunion-French State national counterpart: FEDER RE0001897 (Biomarqueurs et Thérapies) and FEDER RE0022527 (ZEBRATOX), as well as the BIOST Fédération.

### Competing interests

The authors declare no competing interests.


### Additional information

**Supplementary Information** The online version contains supplementary material available at <https://doi.org/10.1038/s41598-021-85183-9>.

**Correspondence** and requests for materials should be addressed to N.D.

**Reprints and permissions information** is available at [www.nature.com/reprints](http://www.nature.com/reprints).

**Publisher’s note** Springer Nature remains neutral with regard to jurisdictional claims in published maps and institutional affiliations.


 **Open Access** This article is licensed under a Creative Commons Attribution 4.0 International License, which permits use, sharing, adaptation, distribution and reproduction in any medium or format, as long as you give appropriate credit to the original author(s) and the source, provide a link to the Creative Commons licence, and indicate if changes were made. The images or other third party material in this article are included in the article’s Creative Commons licence, unless indicated otherwise in a credit line to the material. If material is not included in the article’s Creative Commons licence and your intended use is not permitted by statutory regulation or exceeds the permitted use, you will need to obtain permission directly from the copyright holder. To view a copy of this licence, visit <http://creativecommons.org/licenses/by/4.0/>.

© The Author(s) 2021



Review

# Cellular Mechanisms Participating in Brain Repair of Adult Zebrafish and Mammals after Injury

 Batoul Ghaddar <sup>1</sup>, Luisa Lübke <sup>2</sup>, David Couret <sup>1,3,4</sup>, Sepand Rastegar <sup>2,\*</sup>  and Nicolas Diotel <sup>1,\*</sup>

<sup>1</sup> Université de La Réunion, INSERM, UMR 1188, Diabète athérombose Thérapies Réunion Océan Indien (DÉTRO), 97400 Saint-Denis de La Réunion, France; batoul.ghaddar@univ-reunion.fr (B.G.); david.couret@chu-reunion.fr (D.C.)

<sup>2</sup> Institute of Biological and Chemical Systems-Biological Information Processing (IBCS-BIP), Karlsruhe Institute of Technology (KIT), Postfach 3640, 76021 Karlsruhe, Germany; luisa.luebke@kit.edu

<sup>3</sup> CHU de La Réunion, 97400 Saint-Denis, France

<sup>4</sup> CHU de La Réunion, 97410 Saint-Pierre, France

\* Correspondence: sepand.rastegar@kit.edu (S.R.); nicolas.diotel@univ-reunion.fr (N.D.); Tel.: +49-721-608-22886 (S.R.); +262-6-92-43-09-42 (N.D.)

**Abstract:** Adult neurogenesis is an evolutionary conserved process occurring in all vertebrates. However, striking differences are observed between the taxa, considering the number of neurogenic niches, the neural stem cell (NSC) identity, and brain plasticity under constitutive and injury-induced conditions. Zebrafish has become a popular model for the investigation of the molecular and cellular mechanisms involved in adult neurogenesis. Compared to mammals, the adult zebrafish displays a high number of neurogenic niches distributed throughout the brain. Furthermore, it exhibits a strong regenerative capacity without scar formation or any obvious disabilities. In this review, we will first discuss the similarities and differences regarding (i) the distribution of neurogenic niches in the brain of adult zebrafish and mammals (mainly mouse) and (ii) the nature of the neural stem cells within the main telencephalic niches. In the second part, we will describe the cascade of cellular events occurring after telencephalic injury in zebrafish and mouse. Our study clearly shows that most early events happening right after the brain injury are shared between zebrafish and mouse including cell death, microglia, and oligodendrocyte recruitment, as well as injury-induced neurogenesis. In mammals, one of the consequences following an injury is the formation of a glial scar that is persistent. This is not the case in zebrafish, which may be one of the main reasons that zebrafish display a higher regenerative capacity.

**Keywords:** adult neurogenesis; brain injury; neural stem cell; regeneration; stroke; zebrafish; mice



**Citation:** Ghaddar, B.; Lübke, L.; Couret, D.; Rastegar, S.; Diotel, N. Cellular Mechanisms Participating in Brain Repair of Adult Zebrafish and Mammals after Injury. *Cells* **2021**, *10*, 391. <https://doi.org/10.3390/cells10020391>

Academic Editor: Kay Sonntag

Received: 21 December 2020

Accepted: 5 February 2021

Published: 14 February 2021

**Publisher's Note:** MDPI stays neutral with regard to jurisdictional claims in published maps and institutional affiliations.



**Copyright:** © 2021 by the authors. Licensee MDPI, Basel, Switzerland. This article is an open access article distributed under the terms and conditions of the Creative Commons Attribution (CC BY) license (<https://creativecommons.org/licenses/by/4.0/>).

## 1. Introduction

Neurogenesis is an important process in which new neurons are formed from a pool of neural stem cells (NSCs). This process is initiated by the proliferation of NSCs leading then to the differentiation, migration, and the functional integration of newborn neurons into establishing and/or existing neuronal networks. Until recently, it was believed that neurogenesis only occurs during early embryonic development. However, Altman and Kaplan demonstrated in the 1960s and 1980s, respectively, that new neurons could also be produced in the brain of postnatal and adult rodents, as well as monkeys [1–3]. Since this pioneer discovery, an increasing number of works confirmed that indeed adult neurogenesis occurs in the brain of all vertebrates, including mammals [4–6]. Under physiological conditions, as well as after brain damage induced by traumatic brain injury (TBI), ischemia, or neuro-degeneration, NSCs play key roles in brain plasticity through the genesis of new neurons. Understanding the mechanisms regulating their activation and proliferation during regenerative and constitutive neurogenesis provides the chance to develop methods for combatting neurodegenerative diseases and disabilities following brain damage.

Adult neurogenesis is an important physiological process that supports brain plasticity and cognitive functions through the continuous generation of new neurons, allowed

by the sustained activity of NSCs located in discrete brain regions called neurogenic niches. The persistence of functional neurogenesis during adulthood is evolutionary conserved from invertebrates (i.e., crustaceans, insects, etc.) to vertebrates including fish, amphibians, reptiles, birds, and mammals. However, the number of neurogenic niches, the proliferation rate of neural stem/progenitor cells, the migration, and differentiation of new neurons appears to differ according to species, brain size, and lifespan [6–9]. In mammals, the two main neurogenic niches correspond to the subventricular zone of the lateral ventricles (SVZ) and the subgranular zone (SGZ) of the dentate gyrus (DG) of the hippocampus. In striking contrast, the small teleost zebrafish (*Danio rerio*) displays a high number of neurogenic niches distributed throughout its entire encephalon. In addition, while regenerative neurogenesis is imperfect in mammals, teleost fish are able to repair their telencephalon from large injuries without any striking consequences and disabilities [9]. Such outstanding regenerative capacities strongly argue for a more comprehensive study of the molecular and cellular mechanisms allowing brain regeneration in teleost fish, in order to translate some important findings to humans.

In this review, we aimed at (i) describing the proliferative areas in the brain of fish and mammals, using mouse as an example; (ii) illustrating the spatial and cellular organization of the main telencephalic neurogenic niches in a comparative approach; and (iii) highlighting the similarities and differences regarding the spatiotemporal recruitment of the different cell types involved in brain repair (microglia, oligodendrocytes and their precursors, astrocytes, and NSCs). Concerning this last point, we will document the most studied models of brain damage: telencephalic mechanical injury in zebrafish and brain ischemia in mouse. Next, we will review the similarities and differences regarding neurogenic events and molecular mechanisms occurring after brain damage in zebrafish and mouse. Finally, we will highlight the value of zebrafish as a simple model for the analysis of brain repair mechanisms.

## 2. Location of Neurogenic Niches in the Brain of Adult Zebrafish, Rodents, and Humans

In the past, pioneer works using BrdU incorporation studies and/or PcnA (Proliferating Cell Nuclear Antigen) immunohistochemistry demonstrated the existence of areas with a strong proliferative activity along the ventricular/periventricular layers in the zebrafish brain [6,10–13]. In zebrafish, these strongly proliferative areas are widespread and can be detected throughout all the brain subdivisions including the telencephalon, the diencephalon, the mesencephalon, and the metencephalon (Figure 1A–C, left column) [11,12,14–16]. In the telencephalon of adult zebrafish, the main proliferative areas are located along the ventricle in the ventral, dorsal, dorsolateral, and posterolateral domains. Prominent domains of cell proliferation were also detected in the diencephalon, in the anterior and posterior parts of the preoptic area, as well as in the anterior, mediobasal, and caudal hypothalamus. In the posterior part of the encephalon, proliferation was also reported close to the rhombencephalic ventricle (Figure 1A–C). The thalamus, the regions surrounding the habenula, the pretectal periventricular region (a subdomain close to the optic tectum) and the three subdivisions of the cerebellum including the *valvula cerebelli*, the *corpus cerebelli*, and the *lobus caudalis cerebelli* all harbor substantial proliferation as well [6,11,14,17,18]. These proliferative regions are highlighted in red in a sagittal zebrafish brain section scheme, showing the distribution of neurogenic niches across the brain (Figure 1A).

In sharp contrast with zebrafish, there are only two main proliferative regions that have been observed in the brain of adult mammals: the SVZ of the lateral ventricles and the SGZ of the DG in the hippocampus [6,19] (Figure 1E,I). In addition to these two main regions, other discrete proliferative areas have been more recently observed in the brain of adult mammals, such as in the hypothalamus [20]. However, the number of proliferative cells in these domains remains lower than in the SVZ and SGZ.



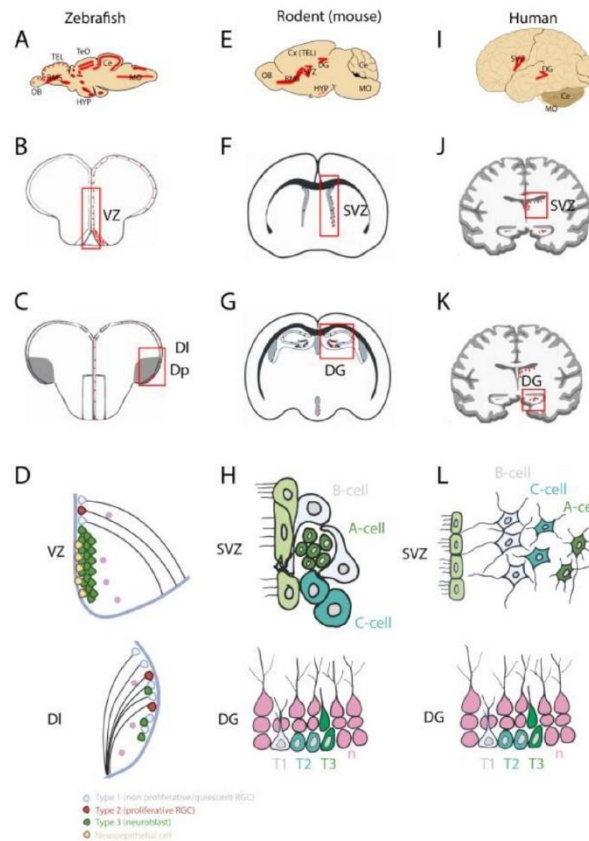


**Figure 1.** Localization and cellular organization of the main neurogenic niches in the brain of adult zebrafish, mouse, and humans. (A,E,I): sagittal sections of zebrafish (A), mouse (E) and human (I) brains with the main proliferative regions (neurogenic niches) shown in red. The mammalian brain displays only two main neurogenic niches: the subventricular zone (SVZ) of the lateral ventricles and subgranular zone of the dentate gyrus (DG) of the hippocampus. Note that the mammalian hypothalamus (HYP) also exhibits discrete neurogenesis. The zebrafish brain displays numerous niches throughout the brain. (B–K): transversal sections through the brain, marking the main neurogenic niches of the respective species shown in (A,E,I). (D–L): Cell composition of the neurogenic niches in zebrafish, mice and humans. (D): The main neurogenic niches in the subpallial ventricular zone (VZ), the dorsolateral telencephalon (DI) in zebrafish, and their respective homologues in mammals: the SVZ and the DG of the hippocampus in mouse and humans. In zebrafish, type 1 and type 2 cells are quiescent and proliferative radial glial cells (RGC), respectively (quiescent and proliferative neural stem cells (NSCs)). Type 3 cells are proliferative neuroblasts. The neuroepithelial cells are NSCs from the subpallium. (H,L): In mammals, the NSCs are shown in grey (B-cells and Type 1 -T1-), the transient amplifying cells in light green (C-Cells and Type -T2-) and the neuroblasts in dark green (A-cells and Type 3 -T3-). Note the hypocellular gap in the human SVZ compared to mice. Ce: cerebellum; Cx: cerebral cortex; DI: lateral zone of the dorsal telencephalic area; DG: dentate gyrus of the hippocampus; Dp: posterior zone of dorsal telencephalic area; HYP: hypothalamus; MO: medulla oblongata; OB: Olfactory bulbs; RGC: radial glial cell; RMS: rostral migratory stream; SVZ: subventricular zone VZ: ventricular zone; TEL: telencephalon; TeO: optic tectum.

In both zebrafish and mammals, all these proliferative areas have been shown to generate a significant number of new neurons. Consequently, the adult zebrafish exhibits a strong neurogenic capacity due to the high number of active neurogenic niches throughout its brain, while adult mammals (rodents and human) display a limited number of neurogenic niches that are mainly localized in the SVZ and SGZ (Figure 1A,E,I) [6,10,11,14,21–23].

### 3. NSCs and Neural Progenitor Cells in the Adult Zebrafish and Mammalian Telencephalon

#### 3.1. NSCs and Neural Progenitors in the Adult Zebrafish Telencephalon

In zebrafish, the main neurogenic niches that have been studied during adulthood are located in the telencephalon, the optic tectum, and the cerebellum. The telencephalon remains undoubtedly the most investigated region of the brain, because it shares many features and homologies with the mammalian telencephalon, particularly considering adult neurogenesis [9,24–26]. In the telencephalon, several studies have explored the identity and the diversity of the neural/progenitor cells sustaining the strong neurogenic activity observed in the different telencephalic subdomains of the zebrafish brain [11,15,22,24,27,28]. In their initial work, Adolf and colleagues (2006) showed through BrdU incorporation studies and Pcn immunohistochemistry that the telencephalon contains two different types of neural progenitors: (1) slow cycling ones, distributed along the ventricular surface, and (2) fast cycling ones, organized mainly in a subpallial cluster [12] (Figure 2). The slow cycling progenitors were identified as radial glial cells (RGCs). In contrast, the fast-cycling cells were described as neuroblasts (Figures 1 and 2) [11,14,15,28–31].

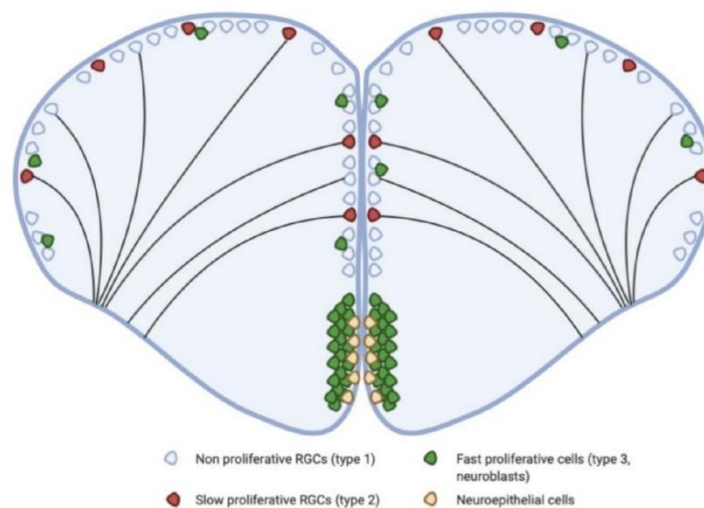


**Figure 2.** The telencephalon of adult zebrafish contains slow and fast cycling progenitors. The VZ of the dorsal telencephalon (pallium) is mainly composed of quiescent (type 1) or proliferative (type 2) RGCs corresponding to slow cycling progenitors. The ventral part of the telencephalon (subpallium) is composed of fast cycling progenitors (type 3 cells) identified as neuroblasts, grouped within a cluster and forming a rostral migratory like structure (RMS-like). Some neuroblasts are also observed scattered between RGC soma in the pallium. RGCs were identified as bona fide NSCs in the pallium and neuroepithelial cells could be NSCs in the subpallium. RGCs: radial glial cells.

In the dorsal telencephalon, type 1 and type 2 cells correspond to quiescent and proliferative RGCs, respectively [15]. These cells are morphologically defined by a small triangular or ovoid soma localized close to the ventricle and extending two cytoplasmic processes: one short process towards the ventricular surface, and one long process crossing

the brain parenchyma and reaching the pial surface. In mammals, RGCs were initially described as a scaffold for the migration of newborn neurons during embryonic neurogenesis, and were later shown to behave as NSCs [32], as in zebrafish [11,33]. At the end of the embryonic development in mammals, the majority of RGCs disappear by transforming into “conventional” astrocytes. However, RGCs persist during adulthood in the brain of adult zebrafish, maintain neurogenic properties, and support neuronal migration [9,11,34–38].

In adult zebrafish, these telencephalic RGCs were shown to perform symmetric and asymmetric division, and also, in some cases, to be able to directly convert into neurons [9,31,39]. In the pallium, lineage tracing and microscopy analyses showed that type 1 cells give rise to type 2 cells, which can give rise to type 3 cells (type 3 = neuroblasts) that are tightly inserted between RGC soma [25,31,39]. The newborn neurons will migrate radially along the long cytoplasmic RGC processes within the brain parenchyma to leave the ventricular zone [11]. At their target location they differentiate into mature neurons expressing well-characterized neuronal markers (i.e., HuC/D, Pax6a, PV) and display signs of functional integration such as synaptogenesis [11,16,31,40].

Adult RGCs in zebrafish express a set of well-identified markers (Table 1), including intermediate filaments (Gfap and Vimentin), the brain lipid binding protein (Blbp or fabp7), the calcium binding protein S100 $\beta$ , the estrogen-synthesizing enzyme (Aromatase B or Cyp19a1b), and also progenitor markers such as Nestin and Sox2 [9,11,15,28,29,37]. Recent studies also documented the expression of the inhibitor of DNA binding 1 (Id1), the chemokine receptor Cxcr4, *notch1a/b*, *notch3*, and *her4* genes in RGCs [40–45]. Most of these markers in zebrafish also label embryonic RGCs in mammals or neurogenic astrocytes during adulthood, as reviewed in [9].

**Table 1.** Main markers expressed by type 1, 2, 3a, and 3b cells in the telencephalon of adult zebrafish. The (+/–) means that these markers are expressed at lower levels in the subtype.

Type 1	Type 2	Type 3a	Type 3b
Sox2	Sox2	Sox2	Sox2
Nestin and Vimentin	Nestin and Vimentin	Nestin	Pcna
Gfap	Gfap	S100 beta (+/–)	PSA-NCAM
S100 beta	S100 beta	Blbp (+/–)	
GS (glutamine synthetase)	GS	AroB (+/–)	
Blbp	Blbp	Pcna	
AroB	AroB	PSA-NCAM	
Cxcr4	Cxcr4 (+/–)		
Id1	Id1 (+/–)		
Her 4	Her 4		
	Pcna		

Consequently, RGCs (type 1 and 2 cells) have been established as *bona fide* NSCs in the telencephalon of adult zebrafish [31,46], able to self-renew and to provide new neurons [9].

In the zebrafish telencephalon, type 3 cells correspond to fast-cycling progenitors and are considered as neuroblasts. These cells can be found tightly inserted between RGC soma in the pallium but are mainly localized within a subpallial cluster [15] (Figure 2). These progenitor cells undergo a limited amplification phase before performing symmetric neurogenic divisions [31,47]. Type 3 cells express committed progenitor markers such as *ascl1a* and PSA-NCAM (polysialylated neuronal cell adhesion molecule) in addition to progenitor markers, such as Nestin and Sox2 [15,48,49]. However, in general they do not express, or in some cases only weakly, the RGC markers. The type 3 cells can be divided into two subpopulations of neuroblasts: type 3a and type 3b (Table 1). Type 3a neuroblasts strongly express the commitment marker PSA-NCAM, but can also weakly express some of the RGC markers [15]. Type 3b neuroblasts do not express any RGC markers and are PSA-NCAM-positive [15]. Both types 3a and 3b express the Pcna proliferation marker.

The type 3 cells in the subpallial cluster will actively migrate, reaching the olfactory bulb via a rostral migratory stream-like (RMS) structure to differentiate into GABAergic



and Tyrosine Hydroxylase-positive neurons. The zebrafish RMS-like is reminiscent of the mammalian RMS [16] (Figure 1B–D).

### 3.2. NSCs and Neural Progenitors in the Telencephalon of Adult Mammals

In mammals, the *bona fide* RGCs do not persist during adulthood [32,33], in contrast to zebrafish. However, in the SVZ and SGZ of the DG, RGCs transform into cells, which display astrocytic features and some of them maintain NSC properties during adulthood [6,19].

In the rodent SVZ, astrocyte-like cells (called B cells, *bone fide* stem cells) have been shown to self-renew and generate transit-amplifying cells (C cells) that give birth to neuroblasts (A cells) (Figure 1F,H) [50,51]. These neuroblasts will then migrate in chain following the RMS to reach the olfactory bulbs like in zebrafish. They will differentiate into GABAergic, glutamatergic, and dopaminergic neurons in the periglomerular layer of the olfactory bulbs and into GABAergic interneurons in the granular cell layer of the olfactory bulbs [19]. Interestingly, in the human SVZ, post-mortem studies have revealed that GFAP-positive astrocytes are separated from the ependymal wall by a hypocellular gap (Figure 1L). Only some of these astrocytes seem to proliferate and, therefore, the adult human SVZ appears devoid of newborn neurons that migrate in chain (no RMS). Supporting this notion, only very few new neurons displaying a migratory phenotype were observed in the anterior SVZ [52]. In contrast to rodents in which the newborn neurons from the SVZ migrate towards the olfactory bulb, they appear to migrate within the adjacent striatum to become medium spiny neurons in humans [53]. Consequently, the SVZ neurogenic niche differs greatly between humans and rodents in the cellular organization of the niche and in the newborn neuron migration [52].

In the rodent SGZ of the DG, radial glial-like/astrocyte cells (type 1) can self-renew and generate type 2a and 2b progenitors, which are also able to self-renew, and finally, type 3 cells (Figure 1G–L) [50,51]. These latter will give rise to glutamatergic dentate granule neurons. Interestingly, neurogenesis in the DG has been shown to be linked to learning, environmental enrichment and social interactions [19,54]. Newborn neurons in the SGZ migrate only short distances, in contrast to the new neurons from the SVZ that migrate for longer distances through the RMS [55]. Different studies in zebrafish suggest that the dorsolateral/dorsoposterior telencephalic domains could be the homologous of the SGZ in mammals, as recently reviewed in [9]. In the human hippocampus, the SGZ neurogenic niche is very similar to the rodent one. However, from a functional point of view, post-mortem studies supported the hypothesis that hippocampal neurogenesis strongly decreases during childhood to become almost undetectable at adulthood [56]. In contrast to that, in the same year, the work of Boldrini and collaborators showed through autopsy of hippocampi from healthy humans at different ages, that many immature neurons could be detected in the DG, suggesting that healthy older individuals maintain functional neurogenesis [4]. In conclusion, the hippocampal neurogenic niche shares many similarities with the one in rodents by locally generating neurons from neural precursors close to the niche [57] (Figure 1H,L).

Taken together, these data demonstrate that zebrafish, rodents, and humans share similar features in the maintenance of adult neurogenesis with some homologies among the main telencephalic neurogenic niches, the type of NSCs, and neural progenitors as well as the type of newborn cells that are generated. Figure 1 highlights these similarities, as well as some differences between zebrafish, rodents, and humans. Interestingly, in humans, adult neurogenesis, or at least its functional relevance, is still under debate, especially when it comes to the neurogenic activity in the mammalian hippocampus [5,57–59].

## 4. Cellular Events Occurring after Telencephalic Injury in Zebrafish and Brain Damage in Mammals

Although the brain represents only 2% of the total body weight in humans, it consumes around 20% of the total body dioxygen and is highly active from a metabolic point of view using around 25% of the body's glucose [60–62]. Thus, brain damage will strongly impact brain homeostasis through a decreased supply of nutrients (i.e., glucose and dioxygen)



leading to severe outcomes. Better understanding brain plasticity could provide keys for combatting disabilities resulting from brain damage.

Teleost fish are widely used as a model for the investigation of brain plasticity due to their high constitutive neurogenesis, strong regenerative mechanisms, and striking sexual plasticity sustained by important sexual neurobehavioral changes [10,16,23,27,63–65]. Mechanical injury of the telencephalon by either inserting a small cannula through the skull or through the nasal cavity remains the most investigated model in zebrafish for studying brain regeneration [40,64–66]. Interestingly, the second injury method could lead to a damage of the olfactory bulbs, but does not alter the brain repair mechanisms substantially.

After brain injury in teleost fish and mammals, death of damaged cells occurs, followed by the recruitment and/or proliferation of microglia and peripheral immune cells, oligodendrocytes/OPCs, astrocytes (only in mammals), endothelial cells, and NSCs. As part of the immune response, microglia can be activated and leukocytes can invade the injury site, both of which can release factors required for the activation and proliferation of NSCs, consequently leading to injury-induced neurogenesis. However, compared to zebrafish, mammals have a reduced ability to regenerate their brain and to fully recover sensory and motor functions. Understanding the cellular and molecular events occurring during brain regeneration is a challenging field of research but nevertheless important for the fight against disabilities resulting from brain damage. In the following sections, we will discuss the cascade of cellular events occurring after brain damage in zebrafish and rodents.

Importantly, even if the injury models developed in zebrafish are closer to traumatic brain injury (TBI) models in mammals, we decided to mainly focus on stroke models in rodents because (i) the literature on stroke is much more abundant than TBI (PubMed research: “stroke rodent” → 31.199 articles versus “traumatic brain injury rodent” → 7.903, the 28 of January, 2021); (ii) TBI and stroke lead to almost similar cellular events and disorders such as gliosis, cognitive, neurological and psychological disorders [67]; (iii) TBI is a risk factor for stroke [68]. Furthermore, TBI and stroke share common molecular and cellular events including, among others, increased blood-brain barrier permeability, pro-inflammatory cytokine release, metabolic stress, glial reactivity, neuronal degeneration, axon damage, infarct formation, glial scar formation, nervous tissue atrophy and functional deficits [69]. Both pathologies also result in same recovery processed without striking differences in cognitive performance, suggesting similar regenerative outcomes [67]. The similar processes occurring in stroke and TBI are highlighted in Table 2. Last, but not least, it is difficult to have a realistic view of the cellular events occurring during brain damage due to the diversity of the TBI and stroke protocols. An integrative work has been realized showing cell death, astrocyte, oligodendrocyte and endothelium cell behavior from 3h post stroke to 1 week after a 30 min brain ischemia in mice [70]. This integrative work allows an easier comparison between brain repair mechanisms in fish and rodent and highlights the similarities and differences of brain reactivity following damage. For these reasons, we will mainly develop the comparison between stab wound injury of the telencephalon in fish and stroke in rodents, also discussing the respective cellular events occurring in the mammalian TBI model.

#### 4.1. Cell Death after Zebrafish and Mammalian Telencephalic Damage

In zebrafish, very soon after mechanical injury of the telencephalon (from 4 h post lesion (hpl) to 6 hpl), numerous TUNEL-positive cells (Terminal deoxynucleotidyl transferase dUTP nick end labeling) are detected in both brain parenchyma and periventricular zone, while almost no cell death is observed in the contralateral control hemisphere [40,71]. The TUNEL-positive cells exhibit features of necrotic and apoptotic cells. In their work, Kroehne et al. showed that cell death could still be observed at 1 day post lesion (dpl) in both parenchymal and periventricular regions but returned to control levels at 3 dpl [40]. In contrast, Kyritsis et al. (2012) only observed a decreased number of TUNEL-positive cells at 3 dpl in the injured hemisphere when compared to the uninjured control hemisphere.

In addition, the injury induced a strong edema, which represented 40% of the volume of the injured telencephalic hemisphere at 1 dpl [40]. At 7 dpl, this edema was strongly reduced to only 5% of the total volume of the injured hemisphere. Remarkably, 1 month after the injury, the lesioned hemisphere was almost completely restored regarding tissue morphology and histology. Moreover, no morphological differences could be observed anymore after 1 year [40]. An overview of cell death kinetics occurring after brain damage is shown in Figure 3.

**Table 2.** Similarities of processes occurring in stroke and traumatic brain injury (TBI) in mammals. +: present; -: absent (adapted in part from the work of [69]).

	Stroke	TBI
Blood-brain barrier permeability	+	+
Metabolic stress/Ionic perturbation/Cytokine	+	+
Membrane damage/Contusion/Primary axotomy	–	+
Glial swelling/Blood flow	+	+
reduction/Inflammation/Secondary axotomy	+	+
Cell death and Wallerian degeneration	+	+
Infarct formation	+	+
Nervous tissue atrophy	+	+
Cognitive and sensorimotor deficits	+	+
Reactive gliosis (microglia, astrocyte, oligodendrocytes)	+	+
Glial scar	+	+

In rodents, after brain ischemia, cell death progressively occurs within the first hours, as presented in zebrafish, but will persist for several days. This was shown through different methods using standard coloration, Fluoro-Jade C probes, and triphenyl tetrazolium chloride staining [72–75]. Additionally, numerous TUNEL-positive cells are detected after 1h, peaking at 24 h and can be still detected after 28 days in stroke models in rodents [76]. In rat, subjected to a 90 min ischemia by the Middle Cerebral Artery Occlusion (MCAO) method, the number of TUNEL-positive cells peaks at 48 h post-ischemia and returns to basal levels only 6 days post-stroke [77]. Several studies have shown that the processes/mechanisms promoting cell death are irreversibly initiated between 3 and 12 h post injury [78,79]. An overview of cell death kinetics occurring after stroke in mouse is shown in Figure 3. Considering TBI in mice, primary cell death occurs after injury followed by a second wave of neuronal cell death resulting from both biochemical and physiological disruptions, induced by the insult in a way similar to stroke [80,81].

Consequently, after brain damage, it seems that cell death is very severe and persists for several weeks in mammals including a secondary wave of neurodegeneration [82,83]. This differs greatly from the situation documented in zebrafish for which cell death is solved between 1 and 3 dpl. This important process of cell death occurring in mammals could trigger a chronic neuroinflammatory state that could be inhibitory for regenerative mechanisms.

#### 4.2. Microglia Recruitment and Function in Response to Zebrafish and Mammalian Telencephalic Damage

Microglia are the resident immune cells of the central nervous system. In contrast to the other phagocytotic cells in mammals, microglia display strong interactions with neurons, astrocytes, and oligodendrocytes leading to a prominent role of microglia in neuronal development and plasticity [84,85]. As initially documented in mammals, the most striking characteristic of microglia is their high degree of plasticity, which enables them to switch from a resting state (quiescent) to a phagocytotic state (ameboid) in response to injury [86–88], a phenomenon also observed in zebrafish after telencephalic injury (Figure 4). After their activation, microglia cells start to secrete chemokines and attract leukocytes to the injury site. This process is then followed by phagocytosis where activated immune cells (including leukocytes) start to remove dying neurons, which helps to control inflam-

mation and aids in tissue repair and functional recovery [89]. Activated microglia can release pro-inflammatory cytokines, including interleukins (IL-1 $\beta$  and IL-6) and the tumor necrosis factor (TNF- $\alpha$ ) [90,91], as well as anti-inflammatory factors, such as TGF- $\beta$  and the cytokines IL-4 and IL-10 [92–94], which are important for the different steps of brain repair.

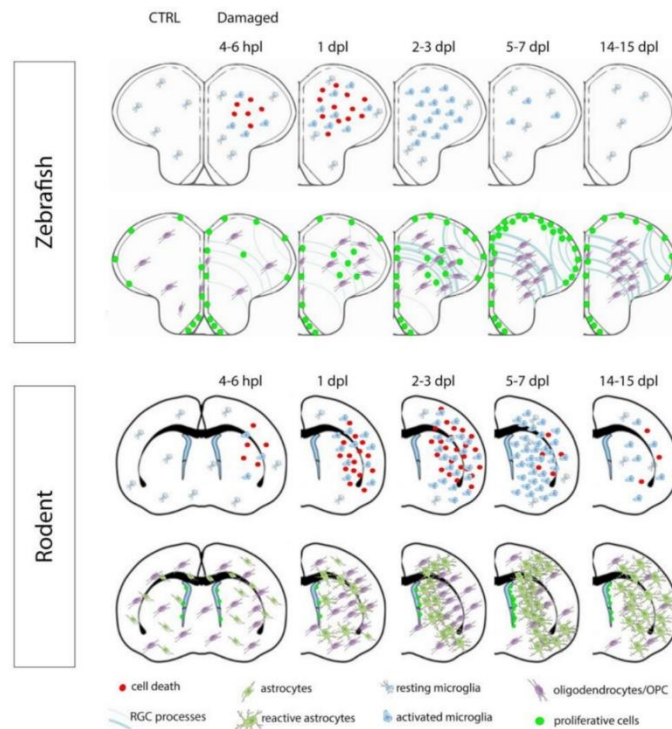


**Figure 3.** Cellular events occurring after telencephalic injury in zebrafish and stroke in mouse. After brain damage, numerous cells, mainly neurons, die. This process is followed by the activation and recruitment of microglial and other immune cells (leukocytes) in parallel to OPCs. Then an astrogliosis process occurs in mice, while RGCs become reactive and proliferative in zebrafish. Proliferation in the neurogenic niches peak at day 7 after damage in both models. Note that the cellular response on the contralateral side is not shown for zebrafish and rodent. In zebrafish and rodent, the first row shows cell death, microglial recruitment, and activation. In zebrafish, the second-row highlights the hypertrophy of RGC processes, the neurogenic injury-induced proliferation as well oligodendrocytes/OPCs response. In rodents, the second row shows astrogliosis, neurogenic proliferation along the SVZ and oligodendrocytes/OPCs response. Note that in zebrafish oligodendrocytes/OPCs accumulate close to the lesion site without increasing their number; dpl: day(s) post lesion, hpl: hour(s) post lesion.

In zebrafish, two microglial populations have been documented, differing in morphology, distribution, and functions [95]. The main population corresponds to phagocytotic microglia (ccl34b.1-positive) and is widely distributed, highly mobile, and phagocytic. The less represented microglia population (ccl34b.1-negative) is ramified and exhibits only low mobility and phagocytic properties [95]. As part of the inflammatory response, microglia appear to be among the first cells being recruited and activated following brain injury [61,66,91].



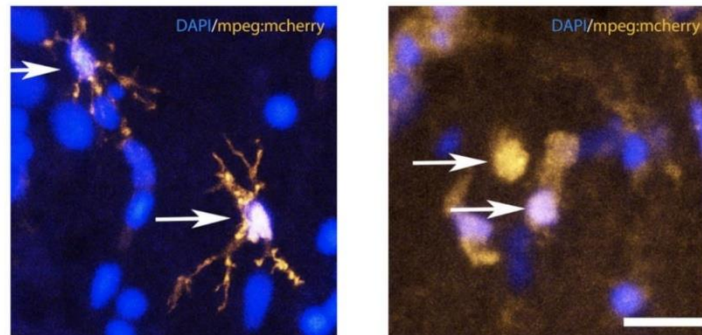


**Figure 4.** Resting and activated microglia under injured and uninjured (control) conditions in the telencephalon of zebrafish. Confocal microscopy showing quiescent (resting) microglia (left panel) and amoeboid (activated) microglia (right panel) in the adult zebrafish telencephalon. There is an obvious change in the shape of the microglia between injured and uninjured tissue, illustrated by the *mpeg:mcherry* transgenic fish line, which labels microglia in the central nervous system. Arrows show the resting morphology of microglia cells (left panel) the amoeboid shape of activated microglia at 1 dpl (right panel). Bar: 18  $\mu$ m.

In zebrafish, performing L-plastin immunohistochemistry to label both microglia and leukocytes, an increasing number of L-plastin-positive cells can be observed from 6 hpl in the injured telencephalon, peaking at 24 hpl and decreasing slightly from 3 dpl to 5 dpl [71]. Accordingly, proliferative and non-proliferative microglial cells (ApoE-GFP or L-plastin positive) are shown to be largely increased at 3 and 4 dpl in the lesioned hemisphere compared to the unlesioned ones [40,66]. Taken together, these data demonstrate that in order to aid with brain recovery, microglial and potential peripheral immune cells are quickly recruited after brain injury, starting at 6 hpl before returning back to basal levels at 7 dpl. The general recruitment of microglia/immune cells after stab wound injury of the zebrafish telencephalon is shown in Figure 3. Recently, it was confirmed in zebrafish that microglia recruitment peaks at 1 dpl before it declines, remaining still significantly up-regulated at 4 dpl [96]. As in mammals, pro-inflammatory molecules (i.e., interleukins Il-1 $\beta$ , Il-6, Il-8, and TNF- $\alpha$ ) secreted in part, by microglia have an impact on NSC plasticity, regeneration and neuronal repair, namely in injury-induced neurogenesis in zebrafish [71,96]. Although the exact contribution of microglia in brain repair mechanisms is still poorly understood in zebrafish, new data recently highlight it [96]. Indeed, the inhibition of microglia activation during zebrafish brain injury leads to a decreased expression of TNF- $\alpha$  and phospho-stat3/ $\beta$ -catenin signaling, which results in a lower proliferation of neural progenitor/stem cells and a lower number of newborn neurons without affecting differentiation [96]. These new data decipher the key roles of microglia in brain repair mechanisms. The phagocytotic activity of microglia and probably of other immune cells fortify the beneficial impact of inflammation on regeneration after telencephalic injury in the teleost fish. However, the precise function of these factors during zebrafish brain regeneration needs to be further investigated.

Similar to zebrafish, microglial cells in healthy brains of mammals remain stable and only a few of them are proliferating [97,98]. They are also among the first cells responding to brain injury/ischemia: they actively migrate to the injured site, switch from resting to amoeboid states, and proliferate [99,100]. In mammals, microglial cells display a huge diversity of phenotype and reactivity allowing them different plasticity and functions. Indeed, microglia show different regional density (being more dense in the telencephalon and in myelinated regions), can be differently activated following injury (even in regions for which no neuronal death occurs) and can display morphological change with age [101]. As for macrophages, microglia can exhibit M1 (pro-inflammatory) or M2 (anti-inflammatory)



phenotypes, the M2 phenotype being more associated with resolution of inflammation and regenerative processes, namely in stroke models [101–103]. In order to add complexity, it is also strongly suggested that microglial cells harbor different subtypes (at least 6) in the brain of mammals endowed with peculiar genomic, spatial, morphological, and functional specializations [104–106].

As nicely reviewed by Lourbopoulos and Benakis, within the first 24 h post stroke (hps), activated microglia are detected in both infarct and peri-infarct regions [107,108]. Between 2 and 7 days after stroke, microglia are further activated within the ischemic core [107,109]. Then, in the two following weeks, the number of microglia decreases in the peri-infarct and core regions. Interestingly, a substantial number of peripheral immune cells (neutrophils and macrophages) also invade the infarct and peri-infarct regions from day 1 post-stroke, due to the leakage of the blood–brain barrier and to chemoattractant factors. Their number is increased between day 3 and day 7 post-stroke but remains quite significant 7–14 days after ischemia [108]. Together, resident and peripheral immune cells play key roles in the removal of dead cell debris and potentially participate in limiting the damage to the surrounding nervous tissue. Of interest, microglia and macrophages will also accumulate around the damaged area, in a region where the glial scar will develop. Interestingly, it also appears that the sensitivity of microglial cells to brain ischemia is dependent on the regions [100]. The recruitment of microglia, during and after brain ischemia, is highlighted in Figure 3, and can be compared with zebrafish. Similar to stroke, TBI also induces microglia activation from 1 to 3 days post-injury, that can persist until 28 days after the trauma [110–113]. Other studies support these data with a significant increase in microglial cells 2 and 14 days post-TBI, as well as a microglia shape that remains different at 60 days post-TBI compared to their control phenotype [114].

Interestingly, microglia have also been shown to be part of the neurogenic niches and to produce positive and negative effects on neurogenesis according to their activation state and panels of secreted molecules. Thus, ischemia and cell death could initiate IGF-1 and TGF- $\beta$  expression and subsequently promote neurogenesis [101]. Very interestingly, new data strongly suggest that the resident microglial population does not inhibit endogenous brain regeneration processes in mouse following TBI, but rather cannot support these processes [115]. A pro-regenerative phenotype can also be induced in mammals through IL-6 trans-signaling [115], demonstrating that inflammatory signals are important contributors to brain repair mechanisms as in regenerative organisms like zebrafish.

Consequently, compared to zebrafish, microglial recruitment and activation is prolonged in mammals, which is possibly linked to the persistent cell death occurring within the damaged hemisphere. Such a persistent cell death, as well as microglia/peripheral immune cells recruitment could induce chronic disruption of brain homeostasis, impairing consequent brain repair mechanisms.

#### 4.3. Oligodendrocyte/Oligodendrocyte Progenitor Cell Recruitment after Zebrafish and Mammalian Telencephalic Damage

Oligodendrocytes are among the most important cells within the central nervous system as they participate in the development and maintenance of the myelin sheath. In mammals, mature oligodendrocytes lose their proliferative capacity and newly generated oligodendrocytes derived from non-myelinated oligodendrocyte precursor cells (OPCs) [116].

To investigate the recruitment of oligodendrocytes and OPCs in the zebrafish brain, März et al., (2011) used an *olig2:EGFP* transgenic line. They observed an increased number of OPCs and mature oligodendrocytes at 1 dpl (in 50% of the studied brains). This accumulation of OPCs is more prominent between 2 dpl and 14 dpl and is detected in almost all the studied brains (94%). Interestingly, at 35 dpl, the *olig2:EGFP* clusters are almost not observed anymore in the injured hemisphere (März et al., 2011). Surprisingly, in contrast to mammals, there is no increase in the proliferation rate of *olig2*-positive cells in the injured hemisphere, compared to the uninjured hemisphere (März et al., 2011, Baumgart et al., 2012). However, recent data suggest a higher number of proliferating parenchymal and ventricular *olig2*-positive cells at 4 dpl [117]. This study also suggests

that olig2-positive RGCs from the medial telencephalic ventricular zone can generate new oligodendrocytes following brain injury [117]. Consequently, the proliferation of the olig2-positive cells appears to be moderate after stab wound injury of the zebrafish telencephalon. In summary, immune cells (microglia and peripheral cells) and oligodendrocytes/OPCs are among the first cells recruited and activated after stab wound injury in zebrafish. At 2 dpl, around 50% of the proliferative cells within the damaged brain parenchyma could be identified as endothelial cells, olig2-GFP positive cells, and microglial-like/immune cells [40]. The general recruitment of olig2-positive cells after injury is shown in Figure 3.

In mammals, oligodendrocytes are sensitive to cerebral ischemia and TBI [118–121], and their death, as well as the loss of the myelin sheath strongly impairs neuronal function. After brain ischemia, lineage tracing showed that OPCs are generated from NSCs located in the SVZ, and provide new oligodendrocytes [120,122,123]. Thus, a significant increase in OPCs is observed, giving rise to mature myelinating oligodendrocytes in the peri-infarct gray and white matter where sprouting axons are located [120,124–126]. This oligodendrogenesis has been shown to improve brain repair processes and neurological scores [120]. After brain ischemia, OPCs also seem to be involved in post-stroke angiogenesis [127], a process linked to neurogenesis [128]. Indeed, OPCs in the cerebral cortex shift from a parenchymal to a perivascular subtype. The recruitment of oligodendrocytes/OPCs during and after brain ischemia is highlighted in Figure 3. In the TBI model, mature oligodendrocytes undergo apoptosis occurring from 2 days to 2 weeks after the insult. In parallel, olig2-positive cell proliferation is observed starting at 48 h and can persist until 21 days after the injury [121,129]. These data show that OPCs respond to brain injury in a way similar to what was shown for stroke. Such a proliferation may lead to the genesis of new oligodendrocytes contributing to remyelination.

Consequently, the situation is very different in mammals compared to zebrafish, as the number of OPCs is significantly increased, and they actively proliferate providing numerous new oligodendrocytes. In zebrafish, the proliferation rate of olig2-positive cells remains low and their number is unchanged during the regenerative process, although olig2 clusters are observed in close vicinity to the lesion [66]. Therefore, oligodendrogenesis appears to be vastly different between zebrafish and rodents. The role of olig2-positive cells at the lesion site remains largely unknown in zebrafish, but could be linked with regenerative neurogenesis, axonogenesis, and synaptogenesis.

#### *4.4. Injury-Induced Proliferation and Neurogenesis after Telencephalic Damage in Zebrafish and Mammals*

After zebrafish telencephalic lesion, brain cell proliferation occurs with different kinetics within the brain parenchyma and in neurogenic niches [65]. Simultaneous to the recruitment of immune cells and the accumulation of OPCs, starting between 1 and 2 dpl, a higher number of Pcn-positive cells can be detected in the injured hemisphere. After 48 hpl, this proliferation is especially observed along the ventricular layer where RGCs reside. This number peaks between 5 and 8 dpl and slowly decreases until 15 dpl to reach the normal proliferation rate at 35 dpl [10,64–66,130,131]. Double immunohistochemistry against proliferation and RGC markers, as well as the use of transgenic fish, have shown that the reactive proliferative cells localized along the ventricle correspond to RGCs expressing S100 $\beta$ , Blnp, Gfap, and also Vimentin [40,64–66]. This injury-induced proliferation of RGCs has been shown to produce newborn neurons (HuC/D-, parvalbumin-positive), which persist for more than 2 to 3 months after brain injury [40,64]. They also exhibit the MAP2(a+b) dendritic marker, the synaptic vesicle marker SV2 and the synaptic marker metabotropic glutamate receptor 2 (mGlu2), proving their functional maturation [40]. Consequently, after telencephalic injury, RGCs switch from a quiescent to a proliferative state and generate newborn neurons to replace neurons, which have been lost due to the damage. Interestingly, compared to constitutive neurogenesis, a shift in the mode of division of NSCs has been observed by Barbosa and colleagues during regenerative neurogenesis [46], which could lead to a depletion of NSC.



An important aspect to consider in injury-induced NSC proliferation is the influence of the pro-inflammatory cytokines transiently upregulated after telencephalic injury and shown to be necessary for NSC activation [71]. Furthermore, the transcription factor Gata3 is required for reactive proliferation of RGCs and the subsequent regenerative neurogenesis [131]. Interestingly, the Gata3 transcription factor is mainly expressed by RGCs but is also detected in L-plastin positive microglia [131], pointing again to an important role of the inflammatory response (leukotriene/gata 3 [131]). In the same line of evidence, the new data obtained demonstrate the role of microglia activation and TNF- $\alpha$  in regenerative neurogenesis in zebrafish [96].

Considering injury-induced neurogenesis in mammals, newborn neurons are produced from the SVZ and migrate within the injured striatum and cortex of rodents after stroke. During their migration, they will progressively differentiate and express neuronal markers (i.e., DCX (doublecortin), PSA-NCAM, Hu, and NeuN) [132–134]. Interestingly, these newborn neurons do not reach the olfactory bulbs through the RMS, as during constitutive neurogenesis, but reach the damaged areas due to attractive factors [134,135]. These new neurons are highly detectable between 14 and 28 days after stroke [134]. Consequently, after stroke, NSCs from the SVZ give rise to neuroblasts that migrate towards the damaged regions (striatum and cortex), where they differentiate into mature neurons [135]. New migrating neuroblasts can still be observed 1 year after stroke [136]. In addition, after stroke, hippocampal neurogenesis is also detected, but remains imperfect [137]. In rodents, TBI models also display injury-induced neurogenesis [138–140]. Thus, TBI has been shown to promote the reactivation of quiescent NSCs that actively divide producing new neural progenitors (Wang et al., 2016). The newly generated neuroblasts will migrate in chain to the lesioned areas (Chang et al., 2016). As reviewed by Chang et al. (2016), the different models of TBI seem to globally lead to increased NSC proliferation, migration, and differentiation, but a wide heterogeneity in the TBI responses is observed probably due to the differences between the severity, location, timing, and types of injury.

The similarities and differences regarding cell activation and cell recruitment after brain injuries in mammals and zebrafish are highlighted in Table 3.

**Table 3.** Comparison of events after brain damage in zebrafish and mammals. +++: strong; +: present; +/-: weak; -: absent.

	Zebrafish	Mammals
Glia reactivity/hypertrophy	+	+
Microglia recruitment	+	+
Microglia proliferation	+	+
Oligodendrocytes recruitment	+	+
Oligodendrocytes proliferation	+/-	+
Astrocyte/RGC recruitment	– (RGC)	+ (astrocyte)
Astrocyte/RGC proliferation	+ (RGC)	+ (astrocyte)
GFAP/vimentin up-regulation	+	+
Glial scar formation	–	+
Glial scar persistence	–	+
Regenerative capacities	+++	+/-

#### 4.5. Reactive Astrogliosis after Brain Injury

After any type of brain damage in mammals (i.e., stroke, TBI, neurotoxic drug exposure, neurodegenerative disease), astrocytes surrounding the damaged region will react and undergo important morphological and/or functional changes, such as hypertrophy, overexpression of some genes or astrocytic markers, such as GFAP and Nestin, which will progressively modify their function [78,141–144]. Although all the astrocytes surrounding the damaged area react, they do not constitute a homogenous population; at least two different types of reactive astrocytes have been described. The astrocytes in close vicinity to the lesioned site will start to proliferate and migrate surrounding the injured territory. These astrocytes are of peculiar importance for the establishment of the well-known glial

scar (mainly composed of extracellular matrix and numerous processes from astrocytes). The astrocytes that are further away from the lesion site will also react but will stay resident and maintain their connection to the neighboring cells.

Under stroke conditions, proliferation of astrocytes starts in the first days and remains restricted to an area 200 micrometers around the infarcted site [145,146]. Interestingly, the inhibition of astrocyte proliferation increases the size of the injury and worsens neurological scores, correlated with a higher neutrophil infiltration and impaired blood–brain barrier regeneration, as shown for TBI [147–149]. New astrocytes are also generated from NSCs that could migrate from the SVZ a few days after stroke onset, and could survive until several weeks after the stroke [150].

Reactive astrocytes become hypertrophic with thicker and bushier/ramified processes; they also upregulate many astrocytic markers, such as GFAP [151]. GFAP upregulation after brain ischemia will be weak at 24h post-injury but will increase rapidly during the first week [152,153], while the number of GFAP-positive astrocytes increases within the first two weeks [154,155]. Vimentin and Nestin, two other intermediate filaments are also upregulated after ischemia and their expression levels correlate with those of GFAP [152,156]. Interestingly, a single knock-out of GFAP or Vimentin has no real impact on reactive gliosis and glial scar formation while a double knockout (KO) severely impacts reactive gliosis, as shown by a decrease in astrocyte hypertrophy and in glial scar formation. Under stroke conditions, the double KO of these intermediate filaments increases the size of the infarct and leads to more acute neurological outcomes [157,158]. Similarly, in TBI models, astrogliosis also occurs through structural and functional changes including hypertrophy and overexpression of intermediate filaments (Nestin, Vimentin, and GFAP) [159,160]. Astrocytes appear as key cell in the development of the glial scar that is essential in the establishment of a physical and chemical barrier that isolates the damaged area and contains the spread of inflammatory cells. Inhibiting or promoting astrogliosis (and so glial scar) did not have striking curative effects [159]. However, the selective stimulation of beneficial astrocyte-derived molecules could represent an interesting therapeutic way to promote blood–brain barrier repair, neurogenesis, and synaptic plasticity [159].

Remarkably, as there are almost no astrocytic cell-like structures in the brain of adult zebrafish, no astrogliosis occurs following injury in zebrafish. Nevertheless, RGCs that express markers of mammalian astrocytes such as *Gfap*, *Nestin*, or *Vimentin*, also up-regulate these markers after telencephalic damage endowed with RGC process hypertrophy [64]. In addition, RGCs also proliferate as previously discussed. This feature constitutes a major difference between zebrafish and mammals and may have strong implications in the regenerative processes particularly concerning the glia scar process.

#### *4.6. Glial Scar: A Paradigm for Understanding the Difference between Zebrafish and Mammalian Regeneration?*

After brain damage in mammals, reactive gliosis takes place involving microglia, oligodendrocyte, and astrocyte cells. Activation of astrocytes will lead to the formation of the glial scar. The glial scar is supposed to protect the central nervous system and to participate in the healing process by forming a physical and chemical barrier that isolates the damaged area and contains the spread of inflammatory cells [161]. Thus, inhibiting the glia scar formation during brain injury has been shown to worsen damage [157,158]. During the glial scar formation, reactive astrocytes secrete many extracellular matrix components such as laminin, fibronectin, tenascin C, and proteoglycans [141,162]. In addition to representing a physical barrier, these extracellular matrix molecules can also lead to growth cone collapse, axonal guidance inhibition, as well as neural progenitor migration defects through activation of RhoA/ROCK signaling [163]. In zebrafish, as no astrocyte-like structures were observed in the telencephalon, RGCs are suggested to sustain many astrocytic features and functions, such as typical marker expression, steroidogenesis, blood–brain barrier establishment, and neurogenic properties [26,164]. Although, no astrogliosis is observed in zebrafish after telencephalic injury, reactive RGC gliosis occurs, as shown by the up-regulation of *Gfap* and *Vimentin*, as well as the hypertrophy of RGC glial processes [40].



The upregulation of RGC markers (Vimentin, Gfap, Blbp, and S100 $\beta$ ) and the hypertrophy of RGC processes is observed quickly after brain damage and can remain visible up to 1 month after injury. In addition, numerous studies also demonstrate an increase in RGC number following brain injury in the telencephalon [37,41,60,61,125]. Interestingly, collagen acid-fuchsin-orange G staining confirms the transient accumulation of collagen at 14 dpl at the injury site [40]. However, this fibrotic scar formation, including reactive glial cell accumulation, hypertrophy of glial processes, persistence of inflammatory cells and ectopic extracellular matrix deposition are not detected later or just occasionally in a small number of brains in zebrafish. Remarkably, the work from Baumgart and colleagues reports that RGC hypertrophy and reactivity is observed for large lesions but not for small ones. Therefore, RGC reactivity could be linked to the severity of the damage [64], as astrogliosis in mammals. Furthermore, discrete lesions will only allow the proliferation of RGCs, while larger lesions could potentially initiate the additional migration of some RGCs within the brain parenchyma. However, such migration should remain quite discrete, as the analysis of stab wounded brain sections did not demonstrate any migration processes in the past.

Consequently, it appears that RGC reactivity mimics, in part, astrogliosis with respect to the mammalian situation through (1) increased expression of glial markers; (2) increased proliferation and hypertrophy; (3) potential migration of RGCs in some cases; and (4) the increased extracellular matrix deposition. However, unlike in mammals, there is no evidence for permanent scar formation in the zebrafish brain as there is no persistent extracellular matrix deposition. An overview of proliferation and RGC reactivity occurring during brain lesion is shown in Figure 3.

#### 4.7. Brain Damage: What about Humans?

When it comes to the close investigation of the consequences of brain damage, for example due to stroke or TBI, unfortunately in humans, studies are highly limited due to the incapacity of collecting post mortem tissue after the onset of damage. However, it was shown that apoptosis occurs quickly in the human brain after ischemia with cell death being delayed for several days [165,166]. Similar to the situation in rodents, microglia are recruited and proliferate at the periphery of the damaged area in post-mortem human brain tissue of stroke patients [167], and peripheral immune cells are attracted as well [168,169]. Furthermore, in the peri-infarct region after ischemic stroke in humans, the development of a glial scar can be observed [170], as well as injury-induced neurogenesis [135,171].

## 5. Conclusions

Brain ischemia, traumatic brain injuries, and neurodegenerative diseases are of major concerns worldwide and constitute main health issues. These brain damages can lead to severe disabilities, including cognitive, sensorimotor, and even personality dysfunctions. Unfortunately, the brain plasticity and regenerative capacities of mammals are strongly limited. The blunted regeneration observed in mammals is largely attributed to inflammatory processes inducing the formation of a glial scar. For these reasons, the study of highly regenerative species is important for cross-comparison and for a better understanding of the molecular and cellular mechanisms that enable these organisms to efficiently regenerate without displaying disabilities [172]. Several hypotheses have been advanced in order to explain the strong plasticity of zebrafish. Among them, zebrafish appear to respond to brain damage by turning on genes, such as *gata3* and *interleukin-4* receptor that are not activated in rodent models [173–176]. Additionally, changes in regeneration-responsive enhancers of mammals might be another reason for less regenerative capacities in mammals, when compared to zebrafish. This was recently suggested for the *inhibin beta A* gene [177]. Furthermore, they display an immune response allowing an enhanced regeneration [96,178]. Last, but not least, zebrafish are still growing during their entire lifespan, and their brain seems to retain some embryonic features that could explain, in part, their strong regenerative capacities [10].

One first interesting aspect to be considered is that neural stem/progenitor cells react similarly by increasing their proliferation after brain injuries in zebrafish and mammals. In both taxa, proliferation of neural stem/progenitor cells peaks at around 7 days post injury. However, the vast majority of freshly generated newborn neurons after injury in mammals fails to reach the damaged site due to the formation of the glial scar. This scar gliosis provides an extracellular environment that does not allow the integration of newborn cells and is a potential inhibitor of neurogenesis (i.e., chondroitin sulfate proteoglycans and myelin components) [179]. As a result, new neurons are unable to cross the glial scar, will degenerate and can therefore not compensate the functions lost during the massive neuronal death induced by brain ischemia or injury. In contrast, although brain lesion in zebrafish strongly induces the proliferation of NSCs, as in mammals, it will not lead to the formation of a strong and persistent glial scar. This will consequently allow the migration of new neurons to the injured site and lead to their functional integration and to the recovery of impaired functions. These data comfort the general idea that the glial scar has a negative impact on newborn neuron integration in the brain of mammals. Data suggest that considering the glial scar as good or bad for CNS recovery is not as simple as suggested [180,181]. In spinal cord injury, the initial glial scar formation is thought to limit the spread of inflammation, but secondly impairs spinal cord regeneration [182]. However, the temporal targeted and moderated modulation of the glial scar formation could represent an interesting way to promote brain recovery, such as the case for the spinal cord.

Another interesting aspect is that the overall reactivity of the brain, following brain damage in mammals and zebrafish, is quite similar. It involves the death of parenchymal and periventricular cells (neurons and glia) that will lead to the recruitment and the activation of glial cells. However, cell death and microglia reactivity will persist longer in the brain of mammals than in zebrafish. These processes may lead to a chronic neuroinflammation that does not exist in the brain of fish, promoting an inflammatory microglia state and avoiding neuronal replacement. In contrast, the positive role of microglia in zebrafish telencephalic regeneration has been recently highlighted [96,172]. Importantly, in contrast to mammalian microglia cells, for which recent transcriptomic analysis have shown a relative homogeneity during adulthood, zebrafish microglia can be separated into two subpopulations (ccl34b positive and negative) displaying different phenotypes and functions [95]. Wu et al. raised the question of the functional specialization of microglial in fish linked to multiple rounds of genomic duplication [183]. Moreover, during zebrafish brain regeneration, microglia display a M2 (anti-inflammatory) phenotype that is known to favor tissue repair in mammals [90]. Interestingly, modulation of the microglia phenotype in mice was shown to promote newborn neuron survival and cognitive function in a TBI model [115]. Consequently, the modulation of microglia activation and functions could be a major element for improving brain recovery.

Of note, another important event to consider when discussing brain recovery is angiogenesis. In addition to serving as an important scaffold for neuroblast migration, blood vessels can secrete important factors (i.e., prostacyclin) promoting axonal growth and subsequent recovery [179]. Actually, it is more and more admitted that improving angiogenesis could favor neurogenesis and brain recovery [128]. Thus, neurogenesis cannot be considered anymore as the only way to improve functional recovery from stroke or brain damage, but should be examined in connection with angiogenesis, as it seems that angiogenesis and neurogenesis are coupled [184].

Finally, from an evolutionary point of view, a remaining question is whether the mammalian brain lost its regenerative capacities or if it inhibits the regenerative capacities. Another possibility is that the teleost fish have developed such capabilities independently of mammals. One of the main differences between these taxa remains that, in zebrafish, NSCs retain a part of their embryonic features allowing their high reactivity and plasticity and continuing growth of the brain during adulthood [10]. Last, but not least, a comprehensive understanding of the mechanisms by which the glial scar is transiently generated



and resolved in zebrafish could open a way for promoting brain regeneration in mammals and avoiding the consequences of brain damage. In addition, it could also be argued that mammals lost the ability to drive the expression of key genes involved in the regenerative process, due to a major regulatory change in their expression following injury [177]. Interestingly, studies on invertebrates such as drosophila also demonstrate common strategies in neurogenesis and brain repair with mammals and highlight the role of blood vessels in these mechanisms [185,186]. Thus, the study of different taxa is of great interest in order to better understand neurogenesis and brain repair through evolutionary conserved processes.

In summary, it seems that proposing multifactorial therapeutic approaches targeting cell death, microglia, OPCs, astrocytes, and NSCs could be more efficient for improving regeneration than targeting only one mechanism.

**Author Contributions:** Conceptualization, N.D. and S.R.; methodology, N.D. and S.R.; validation, all authors; formal analysis, all authors; investigation, all authors; resources, all authors; data curation, N.D. and S.R.; writing—original draft preparation, all authors; writing—review and editing, all authors.; visualization, all authors; supervision, N.D. and S.R.; project administration, N.D. and S.R.; funding acquisition, N.D. and S.R. All authors have read and agreed to the published version of the manuscript.

**Funding:** The research in the lab of Nicolas Diotel is supported by grants from FEDER RE0022527 (ZEBRATOX) and EU-Région Réunion-French State national counterpart. Sepand Rastegar is supported by the Helmholtz Association BioInterfaces in Technology and Medicine Program and the Deutsche Forschungsgemeinschaft training group (GRK2039).

**Institutional Review Board Statement:** Not applicable.

**Informed Consent Statement:** Not applicable.

**Data Availability Statement:** Not applicable.

**Conflicts of Interest:** The authors declare that the research was conducted in the absence of any commercial or financial relationships that could be construed as a potential conflict of interest.

## References

- Altman, J. Autoradiographic and histological studies of postnatal neurogenesis. IV. Cell proliferation and migration in the anterior forebrain, with special reference to persisting neurogenesis in the olfactory bulb. *J. Comp. Neurol.* **1969**, *137*, 433–457. [[CrossRef](#)] [[PubMed](#)]
- Altman, J.; Das, G.D. Autoradiographic and histological evidence of postnatal hippocampal neurogenesis in rats. *J. Comp. Neurol.* **1965**, *124*, 319–335. [[CrossRef](#)] [[PubMed](#)]
- Kaplan, M.S. Formation and turnover of neurons in young and senescent animals: An electronmicroscopic and morphometric analysis. *Ann. N. Y. Acad. Sci.* **1985**, *457*, 173–192. [[CrossRef](#)] [[PubMed](#)]
- Boldrini, M.; Fulmore, C.A.; Tartt, A.N.; Simeon, L.R.; Pavlova, I.; Poposka, V.; Rosoklija, G.B.; Stankov, A.; Arango, V.; Dwork, A.J.; et al. Human Hippocampal Neurogenesis Persists throughout Aging. *Cell Stem. Cell* **2018**, *22*, 589–599. [[CrossRef](#)]
- Eriksson, P.S.; Perfilieva, E.; Bjork-Eriksson, T.; Alborn, A.M.; Nordborg, C.; Peterson, D.A.; Gage, F.H. Neurogenesis in the adult human hippocampus. *Nat. Med.* **1998**, *4*, 1313–1317. [[CrossRef](#)]
- Lindsey, B.W.; Tropepe, V. A comparative framework for understanding the biological principles of adult neurogenesis. *Prog. Neurobiol.* **2006**, *80*, 281–307. [[CrossRef](#)]
- Brus, M.; Keller, M.; Levy, F. Temporal features of adult neurogenesis: Differences and similarities across mammalian species. *Front. Neurosci.* **2013**, *7*, 135. [[CrossRef](#)]
- Than-Trong, E.; Ortica-Gatti, S.; Mella, S.; Nepal, C.; Alunni, A.; Bally-Cuif, L. Neural stem cell quiescence and stemness are molecularly distinct outputs of the Notch3 signalling cascade in the vertebrate adult brain. *Development* **2018**, *145*. [[CrossRef](#)]
- Diotel, N.; Lubke, L.; Strahle, U.; Rastegar, S. Common and Distinct Features of Adult Neurogenesis and Regeneration in the Telencephalon of Zebrafish and Mammals. *Front. Neurosci.* **2020**, *14*, 568930. [[CrossRef](#)]
- Diotel, N.; Le Page, Y.; Mouriec, K.; Tong, S.K.; Pellegrini, E.; Vaillant, C.; Anglade, I.; Brion, F.; Pakdel, F.; Chung, B.C.; et al. Aromatase in the brain of teleost fish: Expression, regulation and putative functions. *Front. Neuroendocrinol.* **2010**, *31*, 172–192. [[CrossRef](#)]
- Pellegrini, E.; Mouriec, K.; Anglade, I.; Menuet, A.; Le Page, Y.; Gueguen, M.M.; Marmignon, M.H.; Brion, F.; Pakdel, F.; Kah, O. Identification of aromatase-positive radial glial cells as progenitor cells in the ventricular layer of the forebrain in zebrafish. *J. Comp. Neurol.* **2007**, *501*, 150–167. [[CrossRef](#)] [[PubMed](#)]

12. Adolf, B.; Chapouton, P.; Lam, C.S.; Topp, S.; Tannhauser, B.; Strahle, U.; Gotz, M.; Bally-Cuif, L. Conserved and acquired features of adult neurogenesis in the zebrafish telencephalon. *Dev. Biol.* **2006**, *295*, 278–293. [[CrossRef](#)]
13. Abrous, D.N.; Koehl, M.; Le Moal, M. Adult neurogenesis: From precursors to network and physiology. *Physiol. Rev.* **2005**, *85*, 523–569. [[CrossRef](#)]
14. Zupanc, G.K.; Hinsch, K.; Gage, F.H. Proliferation, migration, neuronal differentiation, and long-term survival of new cells in the adult zebrafish brain. *J. Comp. Neurol.* **2005**, *488*, 290–319. [[CrossRef](#)] [[PubMed](#)]
15. März, M.; Chapouton, P.; Diotel, N.; Vaillant, C.; Hesl, B.; Takamiya, M.; Lam, C.S.; Kah, O.; Bally-Cuif, L.; Strahle, U. Heterogeneity in progenitor cell subtypes in the ventricular zone of the zebrafish adult telencephalon. *Glia* **2010**, *58*, 870–888. [[CrossRef](#)]
16. Grandel, H.; Kaslin, J.; Ganz, J.; Wenzel, I.; Brand, M. Neural stem cells and neurogenesis in the adult zebrafish brain: Origin, proliferation dynamics, migration and cell fate. *Dev. Biol.* **2006**, *295*, 263–277. [[CrossRef](#)] [[PubMed](#)]
17. Ito, Y.; Tanaka, H.; Okamoto, H.; Ohshima, T. Characterization of neural stem cells and their progeny in the adult zebrafish optic tectum. *Dev. Biol.* **2010**, *342*, 26–38. [[CrossRef](#)]
18. Kaslin, J.; Ganz, J.; Geffarth, M.; Grandel, H.; Hans, S.; Brand, M. Stem cells in the adult zebrafish cerebellum: Initiation and maintenance of a novel stem cell niche. *J. Neurosci.* **2009**, *29*, 6142–6153. [[CrossRef](#)]
19. Grandel, H.; Brand, M. Comparative aspects of adult neural stem cell activity in vertebrates. *Dev. Genes Evol.* **2013**, *223*, 131–147. [[CrossRef](#)]
20. Yoo, S.; Blackshaw, S. Regulation and function of neurogenesis in the adult mammalian hypothalamus. *Prog. Neurobiol.* **2018**, *170*, 53–66. [[CrossRef](#)]
21. Zupanc, G.K.; Zupanc, M.M. Birth and migration of neurons in the central posterior/prepacemaker nucleus during adulthood in weakly electric knifefish (*Eigenmannia* sp.). *Proc. Natl. Acad. Sci. USA* **1992**, *89*, 9539–9543. [[CrossRef](#)] [[PubMed](#)]
22. Zupanc, G.K. Adult neurogenesis and neuronal regeneration in the brain of teleost fish. *J. Physiol. Paris* **2008**, *102*, 357–373. [[CrossRef](#)]
23. Schmidt, R.; Strähle, U.; Scholpp, S. Neurogenesis in zebrafish - from embryo to adult. *Neural. Dev.* **2013**, *8*, 3. [[CrossRef](#)] [[PubMed](#)]
24. Kizil, C.; Kaslin, J.; Kroehne, V.; Brand, M. Adult neurogenesis and brain regeneration in zebrafish. *Dev. Neurobiol.* **2012**, *72*, 429–461. [[CrossRef](#)]
25. Than-Trong, E.; Kiani, B.; Dray, N.; Ortica, S.; Simons, B.; Rulands, S.; Alunni, A.; Bally-Cuif, L. Lineage hierarchies and stochasticity ensure the long-term maintenance of adult neural stem cells. *Sci. Adv.* **2020**, *6*, eaaz5424. [[CrossRef](#)] [[PubMed](#)]
26. Jurisch-Yaksi, N.; Yaksi, E.; Kizil, C. Radial glia in the zebrafish brain: Functional, structural, and physiological comparison with the mammalian glia. *Glia* **2020**. [[CrossRef](#)]
27. Schmidt, R.; Beil, T.; Strähle, U.; Rastegar, S. Stab wound injury of the zebrafish adult telencephalon: A method to investigate vertebrate brain neurogenesis and regeneration. *J. Vis. Exp.* **2014**, e51753. [[CrossRef](#)]
28. Lindsey, B.W.; Darabie, A.; Tropepe, V. The cellular composition of neurogenic periventricular zones in the adult zebrafish forebrain. *J. Comp. Neurol.* **2012**, *520*, 2275–2316. [[CrossRef](#)]
29. Diotel, N.; Vaillant, C.; Kah, O.; Pellegrini, E. Mapping of brain lipid binding protein (Blbp) in the brain of adult zebrafish, co-expression with aromatase B and links with proliferation. *Gene Expr. Patterns* **2016**, *20*, 42–54. [[CrossRef](#)]
30. Zupanc, G.K.; Clint, S.C. Potential role of radial glia in adult neurogenesis of teleost fish. *Glia* **2003**, *43*, 77–86. [[CrossRef](#)]
31. Rothenaigner, I.; Krecsmarik, M.; Hayes, J.A.; Bahn, B.; Lepier, A.; Fortin, G.; Gotz, M.; Jagasia, R.; Bally-Cuif, L. Clonal analysis by distinct viral vectors identifies bona fide neural stem cells in the adult zebrafish telencephalon and characterizes their division properties and fate. *Development* **2011**, *138*, 1459–1469. [[CrossRef](#)]
32. Noctor, S.C.; Flint, A.C.; Weissman, T.A.; Dammerman, R.S.; Kriegstein, A.R. Neurons derived from radial glial cells establish radial units in neocortex. *Nature* **2001**, *409*, 714–720. [[CrossRef](#)] [[PubMed](#)]
33. Noctor, S.C.; Martinez-Cerdeno, V.; Kriegstein, A.R. Distinct behaviors of neural stem and progenitor cells underlie cortical neurogenesis. *J. Comp. Neurol.* **2008**, *508*, 28–44. [[CrossRef](#)]
34. Pinto, L.; Gotz, M. Radial glial cell heterogeneity—The source of diverse progeny in the CNS. *Prog. Neurobiol.* **2007**, *83*, 2–23. [[CrossRef](#)]
35. Noctor, S.C.; Flint, A.C.; Weissman, T.A.; Wong, W.S.; Clinton, B.K.; Kriegstein, A.R. Dividing precursor cells of the embryonic cortical ventricular zone have morphological and molecular characteristics of radial glia. *J. Neurosci.* **2002**, *22*, 3161–3173. [[CrossRef](#)]
36. Merkle, F.T.; Tramontin, A.D.; Garcia-Verdugo, J.M.; Alvarez-Buylla, A. Radial glia give rise to adult neural stem cells in the subventricular zone. *Proc. Natl. Acad. Sci. USA* **2004**, *101*, 17528–17532. [[CrossRef](#)]
37. Than-Trong, E.; Bally-Cuif, L. Radial glia and neural progenitors in the adult zebrafish central nervous system. *Glia* **2015**, *63*, 1406–1428. [[CrossRef](#)] [[PubMed](#)]
38. Lam, C.S.; März, M.; Strahle, U. gfap and nestin reporter lines reveal characteristics of neural progenitors in the adult zebrafish brain. *Dev. Dyn.* **2009**, *238*, 475–486. [[CrossRef](#)] [[PubMed](#)]
39. Lange, C.; Rost, F.; Machate, A.; Reinhardt, S.; Lesche, M.; Weber, A.; Kuscha, V.; Dahl, A.; Rulands, S.; Brand, M. Single cell sequencing of radial glia progeny reveals the diversity of newborn neurons in the adult zebrafish brain. *Development* **2020**, *147*. [[CrossRef](#)] [[PubMed](#)]



40. Kroehne, V.; Freudenreich, D.; Hans, S.; Kaslin, J.; Brand, M. Regeneration of the adult zebrafish brain from neurogenic radial glia-type progenitors. *Development* **2011**, *138*, 4831–4841. [[CrossRef](#)]
41. Diotel, N.; Beil, T.; Strahle, U.; Rastegar, S. Differential expression of id genes and their potential regulator znf238 in zebrafish adult neural progenitor cells and neurons suggests distinct functions in adult neurogenesis. *Gene Expr. Patterns* **2015**, *19*, 1–13. [[CrossRef](#)] [[PubMed](#)]
42. Rodriguez Viales, R.; Diotel, N.; Ferg, M.; Armant, O.; Eich, J.; Alunni, A.; Marz, M.; Bally-Cuif, L.; Rastegar, S.; Strahle, U. The helix-loop-helix protein id1 controls stem cell proliferation during regenerative neurogenesis in the adult zebrafish telencephalon. *Stem Cells* **2015**, *33*, 892–903. [[CrossRef](#)]
43. Diotel, N.; Vaillant, C.; Gueguen, M.M.; Mironov, S.; Anglade, I.; Servili, A.; Pellegrini, E.; Kah, O. Cxcr4 and Cxcl12 expression in radial glial cells of the brain of adult zebrafish. *J. Comp. Neurol.* **2010**, *518*, 4855–4876. [[CrossRef](#)] [[PubMed](#)]
44. Zhang, G.; Ferg, M.; Lubke, L.; Takamiya, M.; Beil, T.; Gourain, V.; Diotel, N.; Strahle, U.; Rastegar, S. Bone morphogenetic protein signaling regulates Id1 mediated neural stem cell quiescence in the adult zebrafish brain via a phylogenetically conserved enhancer module. *Stem Cells* **2020**. [[CrossRef](#)]
45. Chapouton, P.; Webb, K.J.; Stigloher, C.; Alunni, A.; Adolf, B.; Hesel, B.; Topp, S.; Kremmer, E.; Bally-Cuif, L. Expression of hairy/enhancer of split genes in neural progenitors and neurogenesis domains of the adult zebrafish brain. *J. Comp. Neurol.* **2011**, *519*, 1748–1769. [[CrossRef](#)] [[PubMed](#)]
46. Barbosa, J.S.; Sanchez-Gonzalez, R.; Di Giaimo, R.; Baumgart, E.V.; Theis, F.J.; Gotz, M.; Ninkovic, J. Neurodevelopment. Live imaging of adult neural stem cell behavior in the intact and injured zebrafish brain. *Science* **2015**, *348*, 789–793. [[CrossRef](#)]
47. Kishimoto, N.; Alfaro-Cervello, C.; Shimizu, K.; Asakawa, K.; Urasaki, A.; Nonaka, S.; Kawakami, K.; Garcia-Verdugo, J.M.; Sawamoto, K. Migration of neuronal precursors from the telencephalic ventricular zone into the olfactory bulb in adult zebrafish. *J. Comp. Neurol.* **2011**, *519*, 3549–3565. [[CrossRef](#)]
48. Chapouton, P.; Skupien, P.; Hesel, B.; Coolen, M.; Moore, J.C.; Madelaine, R.; Kremmer, E.; Faus-Kessler, T.; Blader, P.; Lawson, N.D.; et al. Notch activity levels control the balance between quiescence and recruitment of adult neural stem cells. *J. Neurosci.* **2010**, *30*, 7961–7974. [[CrossRef](#)]
49. Diotel, N.; Rodriguez Viales, R.; Armant, O.; Marz, M.; Ferg, M.; Rastegar, S.; Strahle, U. Comprehensive expression map of transcription regulators in the adult zebrafish telencephalon reveals distinct neurogenic niches. *J. Comp. Neurol.* **2015**, *523*, 1202–1221. [[CrossRef](#)] [[PubMed](#)]
50. Ming, G.L.; Song, H. Adult neurogenesis in the mammalian central nervous system. *Annu. Rev. Neurosci.* **2005**, *28*, 223–250. [[CrossRef](#)]
51. Obernier, K.; Alvarez-Buylla, A. Neural stem cells: Origin, heterogeneity and regulation in the adult mammalian brain. *Development* **2019**, *146*. [[CrossRef](#)]
52. Quiñones-Hinojosa, A.; Sanai, N.; Soriano-Navarro, M.; Gonzalez-Perez, O.; Mirzadeh, Z.; Gil-Perotin, S.; Romero-Rodriguez, R.; Berger, M.S.; Garcia-Verdugo, J.M.; Alvarez-Buylla, A. Cellular composition and cytoarchitecture of the adult human subventricular zone: A niche of neural stem cells. *J. Comp. Neurol.* **2006**, *494*, 415–434. [[CrossRef](#)]
53. Ernst, A.; Alkass, K.; Bernard, S.; Salehpour, M.; Perl, S.; Tisdale, J.; Possnert, G.; Druid, H.; Frisen, J. Neurogenesis in the striatum of the adult human brain. *Cell* **2014**, *156*, 1072–1083. [[CrossRef](#)]
54. Kempermann, G. Seven principles in the regulation of adult neurogenesis. *Eur. J. Neurosci.* **2011**, *33*, 1018–1024. [[CrossRef](#)]
55. Gould, E. How widespread is adult neurogenesis in mammals? *Nat. Rev. Neurosci.* **2007**, *8*, 481–488. [[CrossRef](#)]
56. Sorrells, S.F.; Paredes, M.F.; Cebrian-Silla, A.; Sandoval, K.; Qi, D.; Kelley, K.W.; James, D.; Mayer, S.; Chang, J.; Auguste, K.I.; et al. Human hippocampal neurogenesis drops sharply in children to undetectable levels in adults. *Nature* **2018**, *555*, 377–381. [[CrossRef](#)]
57. Spalding, K.L.; Bergmann, O.; Alkass, K.; Bernard, S.; Salehpour, M.; Huttner, H.B.; Bostrom, E.; Westerlund, I.; Vial, C.; Buchholz, B.A.; et al. Dynamics of hippocampal neurogenesis in adult humans. *Cell* **2013**, *153*, 1219–1227. [[CrossRef](#)] [[PubMed](#)]
58. Dennis, C.V.; Suh, L.S.; Rodriguez, M.L.; Kril, J.J.; Sutherland, G.T. Human adult neurogenesis across the ages: An immunohistochemical study. *Neuropathol. Appl. Neurobiol.* **2016**, *42*, 621–638. [[CrossRef](#)] [[PubMed](#)]
59. Kempermann, G.; Gage, F.H.; Aigner, L.; Song, H.; Curtis, M.A.; Thuret, S.; Kuhn, H.G.; Jessberger, S.; Frankland, P.W.; Cameron, H.A.; et al. Human Adult Neurogenesis: Evidence and Remaining Questions. *Cell Stem Cell* **2018**, *23*, 25–30. [[CrossRef](#)] [[PubMed](#)]
60. Magistretti, P.J.; Pellerin, L. Cellular mechanisms of brain energy metabolism. Relevance to functional brain imaging and to neurodegenerative disorders. *Ann. N. Y. Acad. Sci.* **1996**, *777*, 380–387. [[CrossRef](#)] [[PubMed](#)]
61. Quastel, J.H.; Wheatley, A.H. Oxidations by the brain. *Biochem. J.* **1932**, *26*, 725–744. [[CrossRef](#)]
62. Belanger, M.; Allaman, I.; Magistretti, P.J. Brain energy metabolism: Focus on astrocyte-neuron metabolic cooperation. *Cell Metab.* **2011**, *14*, 724–738. [[CrossRef](#)] [[PubMed](#)]
63. Becker, C.G.; Becker, T. Adult zebrafish as a model for successful central nervous system regeneration. *Restor. Neurol. Neurosci.* **2008**, *26*, 71–80.
64. Baumgart, E.V.; Barbosa, J.S.; Bally-Cuif, L.; Gotz, M.; Ninkovic, J. Stab wound injury of the zebrafish telencephalon: A model for comparative analysis of reactive gliosis. *Glia* **2012**, *60*, 343–357. [[CrossRef](#)]
65. Diotel, N.; Vaillant, C.; Gabbero, C.; Mironov, S.; Fostier, A.; Gueguen, M.M.; Anglade, I.; Kah, O.; Pellegrini, E. Effects of estradiol in adult neurogenesis and brain repair in zebrafish. *Horm. Behav.* **2013**, *63*, 193–207. [[CrossRef](#)] [[PubMed](#)]

66. März, M.; Schmidt, R.; Rastegar, S.; Strahle, U. Regenerative response following stab injury in the adult zebrafish telencephalon. *Dev. Dyn.* **2011**, *240*, 2221–2231. [\[CrossRef\]](#)
67. Castor, N.; El Massioui, F. Traumatic brain injury and stroke: Does recovery differ? *Brain. Inj.* **2018**, *32*, 1803–1810. [\[CrossRef\]](#) [\[PubMed\]](#)
68. Albrecht, J.S.; Liu, X.; Smith, G.S.; Baumgarten, M.; Rattinger, G.B.; Gambert, S.R.; Langenberg, P.; Zuckerman, I.H. Stroke incidence following traumatic brain injury in older adults. *J. Head Trauma Rehabil.* **2015**, *30*, E62–E67. [\[CrossRef\]](#)
69. Bramlett, H.M.; Dietrich, W.D. Pathophysiology of cerebral ischemia and brain trauma: Similarities and differences. *J. Cereb. Blood Flow Metab.* **2004**, *24*, 133–150. [\[CrossRef\]](#) [\[PubMed\]](#)
70. Buscemi, L.; Price, M.; Bezzi, P.; Hirt, L. Spatio-temporal overview of neuroinflammation in an experimental mouse stroke model. *Sci. Rep.* **2019**, *9*, 507. [\[CrossRef\]](#) [\[PubMed\]](#)
71. Kyritsis, N.; Kizil, C.; Zocher, S.; Kroehne, V.; Kaslin, J.; Freudenreich, D.; Iltzsche, A.; Brand, M. Acute inflammation initiates the regenerative response in the adult zebrafish brain. *Science* **2012**, *338*, 1353–1356. [\[CrossRef\]](#)
72. Zille, M.; Farr, T.D.; Przesdzing, I.; Muller, J.; Sommer, C.; Dirnagl, U.; Wunder, A. Visualizing cell death in experimental focal cerebral ischemia: Promises, problems, and perspectives. *J. Cereb. Blood Flow Metab.* **2012**, *32*, 213–231. [\[CrossRef\]](#) [\[PubMed\]](#)
73. Chen, B.; Friedman, B.; Cheng, Q.; Tsai, P.; Schim, E.; Kleinfeld, D.; Lyden, P.D. Severe blood-brain barrier disruption and surrounding tissue injury. *Stroke* **2009**, *40*, e666–e674. [\[CrossRef\]](#) [\[PubMed\]](#)
74. Liszczak, T.M.; Hedley-Whyte, E.T.; Adams, J.F.; Han, D.H.; Kolluri, V.S.; Vacanti, F.X.; Heros, R.C.; Zervas, N.T. Limitations of tetrazolium salts in delineating infarcted brain. *Acta Neuropathol.* **1984**, *65*, 150–157. [\[CrossRef\]](#) [\[PubMed\]](#)
75. Popp, A.; Jaenisch, N.; Witte, O.W.; Frahm, C. Identification of ischemic regions in a rat model of stroke. *PLoS ONE* **2009**, *4*, e4764. [\[CrossRef\]](#)
76. Zhang, C.; Chopp, M.; Cui, Y.; Wang, L.; Zhang, R.; Zhang, L.; Lu, M.; Szalad, A.; Doppler, E.; Hitzl, M.; et al. Cerebrolysin enhances neurogenesis in the ischemic brain and improves functional outcome after stroke. *J. Neurosci. Res.* **2010**, *88*, 3275–3281. [\[CrossRef\]](#) [\[PubMed\]](#)
77. Luo, Y.; Kuo, C.C.; Shen, H.; Chou, J.; Greig, N.H.; Hoffer, B.J.; Wang, Y. Delayed treatment with a p53 inhibitor enhances recovery in stroke brain. *Ann. Neurol.* **2009**, *65*, 520–530. [\[CrossRef\]](#) [\[PubMed\]](#)
78. Sims, N.R.; Yew, W.P. Reactive astrogliosis in stroke: Contributions of astrocytes to recovery of neurological function. *Neurochem. Int.* **2017**, *107*, 88–103. [\[CrossRef\]](#)
79. Moskowitz, M.A.; Lo, E.H.; Iadecola, C. The science of stroke: Mechanisms in search of treatments. *Neuron* **2010**, *67*, 181–198. [\[CrossRef\]](#)
80. Stoica, B.A.; Faden, A.I. Cell death mechanisms and modulation in traumatic brain injury. *Neurother. J. Am. Soc. Exp. Neurother.* **2010**, *7*, 3–12. [\[CrossRef\]](#)
81. Yang, Y.; Wang, H.; Li, L.; Li, X.; Wang, Q.; Ding, H.; Wang, X.; Ye, Z.; Wu, L.; Zhang, X.; et al. Sinomenine Provides Neuroprotection in Model of Traumatic Brain Injury via the Nrf2-ARE Pathway. *Front Neurosci.* **2016**, *10*, 580. [\[CrossRef\]](#)
82. Zhang, J.; Zhang, Y.; Xing, S.; Liang, Z.; Zeng, J. Secondary neurodegeneration in remote regions after focal cerebral infarction: A new target for stroke management? *Stroke* **2012**, *43*, 1700–1705. [\[CrossRef\]](#)
83. Sayed, M.A.; Eldahshan, W.; Abdelbary, M.; Pillai, B.; Althomali, W.; Johnson, M.H.; Arbab, A.S.; Ergul, A.; Fagan, S.C. Stroke promotes the development of brain atrophy and delayed cell death in hypertensive rats. *Sci. Rep.* **2020**, *10*, 20233. [\[CrossRef\]](#)
84. Frost, J.L.; Schafer, D.P. Microglia: Architects of the Developing Nervous System. *Trends Cell Biol.* **2016**, *26*, 587–597. [\[CrossRef\]](#)
85. Hong, S.; Stevens, B. Microglia: Phagocytosing to Clear, Sculpt, and Eliminate. *Dev. Cell* **2016**, *38*, 126–128. [\[CrossRef\]](#) [\[PubMed\]](#)
86. Davalos, D.; Grutzendler, J.; Yang, G.; Kim, J.V.; Zuo, Y.; Jung, S.; Littman, D.R.; Dustin, M.L.; Gan, W.B. ATP mediates rapid microglial response to local brain injury in vivo. *Nat. Neurosci.* **2005**, *8*, 752–758. [\[CrossRef\]](#) [\[PubMed\]](#)
87. Morrison, H.W.; Filosa, J.A. A quantitative spatiotemporal analysis of microglia morphology during ischemic stroke and reperfusion. *J. Neuroinflamm.* **2013**, *10*, 4. [\[CrossRef\]](#)
88. Nimmerjahn, A.; Kirchhoff, F.; Helmchen, F. Resting microglial cells are highly dynamic surveillants of brain parenchyma in vivo. *Science* **2005**, *308*, 1314–1318. [\[CrossRef\]](#)
89. Harry, G.J.; Kraft, A.D. Microglia in the developing brain: A potential target with lifetime effects. *Neurotoxicology* **2012**, *33*, 191–206. [\[CrossRef\]](#) [\[PubMed\]](#)
90. Ransohoff, R.M. How neuroinflammation contributes to neurodegeneration. *Science* **2016**, *353*, 777–783. [\[CrossRef\]](#)
91. Kanazawa, M.; Ninomiya, I.; Hatakeyama, M.; Takahashi, T.; Shimohata, T. Microglia and Monocytes/Macrophages Polarization Reveal Novel Therapeutic Mechanism against Stroke. *Int. J. Mol. Sci.* **2017**, *18*, 2135. [\[CrossRef\]](#) [\[PubMed\]](#)
92. Xiong, X.Y.; Liu, L.; Yang, Q.W. Functions and mechanisms of microglia/macrophages in neuroinflammation and neurogenesis after stroke. *Prog. Neurobiol.* **2016**, *142*, 23–44. [\[CrossRef\]](#)
93. Ma, Y.; Wang, J.; Wang, Y.; Yang, G.Y. The biphasic function of microglia in ischemic stroke. *Prog. Neurobiol.* **2017**, *157*, 247–272. [\[CrossRef\]](#)
94. Chu, H.X.; Broughton, B.R.; Kim, H.A.; Lee, S.; Drummond, G.R.; Sobey, C.G. Evidence That Ly6C(hi) Monocytes are Protective in Acute Ischemic Stroke by Promoting M2 Macrophage Polarization. *Stroke* **2015**, *46*, 1929–1937. [\[CrossRef\]](#)
95. Wu, S.; Nguyen, L.T.M.; Pan, H.; Hassan, S.; Dai, Y.; Xu, J.; Wen, Z. Two phenotypically and functionally distinct microglial populations in adult zebrafish. *Sci. Adv.* **2020**, *6*. [\[CrossRef\]](#)



96. Kanagaraj, P.; Chen, J.Y.; Skaggs, K.; Qadeer, Y.; Conner, M.; Cutler, N.; Richmond, J.; Kommidi, V.; Poles, A.; Affrunti, D.; et al. Microglia Stimulate Zebrafish Brain Repair Via a Specific Inflammatory Cascade. *BioRxiv* **2020**, *79*, 268–280. [\[CrossRef\]](#)
97. Askew, K.; Li, K.; Olmos-Alonso, A.; Garcia-Moreno, F.; Liang, Y.; Richardson, P.; Tipton, T.; Chapman, M.A.; Riecken, K.; Beccari, S.; et al. Coupled Proliferation and Apoptosis Maintain the Rapid Turnover of Microglia in the Adult Brain. *Cell Rep.* **2017**, *18*, 391–405. [\[CrossRef\]](#) [\[PubMed\]](#)
98. Boareto, M.; Iber, D.; Taylor, V. Differential interactions between Notch and ID factors control neurogenesis by modulating Hes factor autoregulation. *Development* **2017**, *144*, 3465–3474. [\[CrossRef\]](#)
99. Xing, C.; Arai, K.; Lo, E.H.; Hommel, M. Pathophysiologic cascades in ischemic stroke. *Int. J. Stroke* **2012**, *7*, 378–385. [\[CrossRef\]](#)
100. Zhang, S. Microglial activation after ischaemic stroke. *Stroke Vasc. Neurol.* **2019**, *4*, 71–74. [\[CrossRef\]](#)
101. Olah, M.; Biber, K.; Vinet, J.; Boddeke, H.W. Microglia phenotype diversity. *CNS Neurol. Disord. Drug Targets* **2011**, *10*, 108–118. [\[CrossRef\]](#) [\[PubMed\]](#)
102. Orihuela, R.; McPherson, C.A.; Harry, G.J. Microglial M1/M2 polarization and metabolic states. *Br. J. Pharmacol.* **2015**. [\[CrossRef\]](#) [\[PubMed\]](#)
103. Michell-Robinson, M.A.; Touil, H.; Healy, L.M.; Owen, D.R.; Durafourt, B.A.; Bar-Or, A.; Antel, J.P.; Moore, C.S. Roles of microglia in brain development, tissue maintenance and repair. *Brain* **2015**, *138*, 1138–1159. [\[CrossRef\]](#)
104. Stratoulas, V.; Venero, J.L.; Tremblay, M.E.; Joseph, B. Microglial subtypes: Diversity within the microglial community. *EMBO J.* **2019**, *38*, e101997. [\[CrossRef\]](#) [\[PubMed\]](#)
105. Dubbelaar, M.L.; Kracht, L.; Eggen, B.J.L.; Boddeke, E. The Kaleidoscope of Microglial Phenotypes. *Front. Immunol.* **2018**, *9*, 1753. [\[CrossRef\]](#)
106. Hammond, T.R.; Dufort, C.; Dissing-Olesen, L.; Giera, S.; Young, A.; Wysoker, A.; Walker, A.J.; Gergits, F.; Segel, M.; Nemes, J.; et al. Single-Cell RNA Sequencing of Microglia throughout the Mouse Lifespan and in the Injured Brain Reveals Complex Cell-State Changes. *Immunity* **2019**, *50*, 253–271. [\[CrossRef\]](#)
107. Loubopoulos, A.; Erturk, A.; Hellal, F. Microglia in action: How aging and injury can change the brain's guardians. *Front. Cell. Neurosci.* **2015**, *9*, 54. [\[CrossRef\]](#)
108. Benakis, C.; Garcia-Bonilla, L.; Iadecola, C.; Anrather, J. The role of microglia and myeloid immune cells in acute cerebral ischemia. *Front. Cell. Neurosci.* **2014**, *8*, 461. [\[CrossRef\]](#)
109. Chen, J.; Zhang, M.; Zhang, X.; Fan, L.; Liu, P.; Yu, L.; Cao, X.; Qiu, S.; Xu, Y. EZH2 inhibitor DZNep modulates microglial activation and protects against ischaemic brain injury after experimental stroke. *Eur. J. Pharmacol.* **2019**, *857*, 172452. [\[CrossRef\]](#)
110. Donat, C.K.; Scott, G.; Gentleman, S.M.; Sastre, M. Microglial Activation in Traumatic Brain Injury. *Front. Aging Neurosci.* **2017**, *9*, 208. [\[CrossRef\]](#)
111. Patel, A.R.; Ritzel, R.; McCullough, L.D.; Liu, F. Microglia and ischemic stroke: A double-edged sword. *Int. J. Physiol. Pathophysiol. Pharmacol.* **2013**, *5*, 73–90.
112. Perego, C.; Fumagalli, S.; De Simoni, M.G. Temporal pattern of expression and colocalization of microglia/macrophage phenotype markers following brain ischemic injury in mice. *J. Neuroinflamm.* **2011**, *8*, 174. [\[CrossRef\]](#) [\[PubMed\]](#)
113. Bye, N.; Habgood, M.D.; Callaway, J.K.; Malakooti, N.; Potter, A.; Kossmann, T.; Morganti-Kossmann, M.C. Transient neuroprotection by minocycline following traumatic brain injury is associated with attenuated microglial activation but no changes in cell apoptosis or neutrophil infiltration. *Exp. Neurol.* **2007**, *204*, 220–233. [\[CrossRef\]](#) [\[PubMed\]](#)
114. Izzy, S.; Liu, Q.; Fang, Z.; Lule, S.; Wu, L.; Chung, J.Y.; Sarro-Schwartz, A.; Brown-Whalen, A.; Perner, C.; Hickman, S.E.; et al. Time-Dependent Changes in Microglia Transcriptional Networks Following Traumatic Brain Injury. *Front. Cell Neurosci.* **2019**, *13*, 307. [\[CrossRef\]](#)
115. Willis, E.F.; MacDonald, K.P.A.; Nguyen, Q.H.; Garrido, A.L.; Gillespie, E.R.; Harley, S.B.R.; Bartlett, P.F.; Schroder, W.A.; Yates, A.G.; Anthony, D.C.; et al. Repopulating Microglia Promote Brain Repair in an IL-6-Dependent Manner. *Cell* **2020**, *180*, 833–846.e16. [\[CrossRef\]](#) [\[PubMed\]](#)
116. Gensert, J.M.; Goldman, J.E. Endogenous progenitors remyelinate demyelinated axons in the adult CNS. *Neuron* **1997**, *19*, 197–203. [\[CrossRef\]](#)
117. Kim, H.K.; Lee, D.W.; Kim, E.; Jeong, I.; Kim, S.; Kim, B.J.; Park, H.C. Notch Signaling Controls Oligodendrocyte Regeneration in the Injured Telencephalon of Adult Zebrafish. *Exp. Neurobiol.* **2020**, *29*, 417–424. [\[CrossRef\]](#) [\[PubMed\]](#)
118. Pantoni, L.; Garcia, J.H.; Gutierrez, J.A. Cerebral white matter is highly vulnerable to ischemia. *Stroke* **1996**, *27*, 1641–1646. [\[CrossRef\]](#)
119. Dewar, D.; Underhill, S.M.; Goldberg, M.P. Oligodendrocytes and ischemic brain injury. *J. Cereb. Blood Flow Metab.* **2003**, *23*, 263–274. [\[CrossRef\]](#)
120. Zhang, R.; Chopp, M.; Zhang, Z.G. Oligodendrogenesis after cerebral ischemia. *Front. Cell. Neurosci.* **2013**, *7*, 201. [\[CrossRef\]](#)
121. Dent, K.A.; Christie, K.J.; Bye, N.; Basrai, H.S.; Turbic, A.; Habgood, M.; Cate, H.S.; Turnley, A.M. Oligodendrocyte birth and death following traumatic brain injury in adult mice. *PLoS ONE* **2015**, *10*, e0121541. [\[CrossRef\]](#)
122. Zawadzka, M.; Rivers, L.E.; Fancy, S.P.; Zhao, C.; Tripathi, R.; Jamen, F.; Young, K.; Goncharevich, A.; Pohl, H.; Rizzi, M.; et al. CNS-resident glial progenitor/stem cells produce Schwann cells as well as oligodendrocytes during repair of CNS demyelination. *Cell Stem Cell* **2010**, *6*, 578–590. [\[CrossRef\]](#)

123. Rafalski, V.A.; Ho, P.P.; Brett, J.O.; Ucar, D.; Dugas, J.C.; Pollina, E.A.; Chow, L.M.; Ibrahim, A.; Baker, S.J.; Barres, B.A.; et al. Expansion of oligodendrocyte progenitor cells following SIRT1 inactivation in the adult brain. *Nat. Cell Biol.* **2013**, *15*, 614–624. [[CrossRef](#)] [[PubMed](#)]
124. Gregersen, R.; Christensen, T.; Lehrmann, E.; Diemer, N.H.; Finsen, B. Focal cerebral ischemia induces increased myelin basic protein and growth-associated protein-43 gene transcription in peri-infarct areas in the rat brain. *Exp. Brain Res.* **2001**, *138*, 384–392. [[CrossRef](#)]
125. Ueno, T.; Ito, J.; Hoshikawa, S.; Ohori, Y.; Fujiwara, S.; Yamamoto, S.; Ohtsuka, T.; Kageyama, R.; Akai, M.; Nakamura, K.; et al. The identification of transcriptional targets of Ascl1 in oligodendrocyte development. *Glia* **2012**, *60*, 1495–1505. [[CrossRef](#)] [[PubMed](#)]
126. Ueno, Y.; Chopp, M.; Zhang, L.; Buller, B.; Liu, Z.; Lehman, N.L.; Liu, X.S.; Zhang, Y.; Roberts, C.; Zhang, Z.G. Axonal outgrowth and dendritic plasticity in the cortical peri-infarct area after experimental stroke. *Stroke* **2012**, *43*, 2221–2228. [[CrossRef](#)] [[PubMed](#)]
127. Kishida, N.; Maki, T.; Takagi, Y.; Yasuda, K.; Kinoshita, H.; Ayaki, T.; Noro, T.; Kinoshita, Y.; Ono, Y.; Kataoka, H.; et al. Role of Perivascular Oligodendrocyte Precursor Cells in Angiogenesis After Brain Ischemia. *J. Am. Heart Assoc.* **2019**, *8*, e011824. [[CrossRef](#)]
128. Xiong, Y.; Mahmood, A.; Chopp, M. Angiogenesis, neurogenesis and brain recovery of function following injury. *Curr. Opin. Investig. Drugs* **2010**, *11*, 298–308.
129. Flygt, J.; Clausen, F.; Marklund, N. Diffuse traumatic brain injury in the mouse induces a transient proliferation of oligodendrocyte progenitor cells in injured white matter tracts. *Restor. Neurol. Neurosci.* **2017**, *35*, 251–263. [[CrossRef](#)]
130. Kishimoto, N.; Shimizu, K.; Sawamoto, K. Neuronal regeneration in a zebrafish model of adult brain injury. *Dis. Models. Mech.* **2012**, *5*, 200–209. [[CrossRef](#)] [[PubMed](#)]
131. Kizil, C.; Kyritsis, N.; Dudczig, S.; Kroehne, V.; Freudenreich, D.; Kaslin, J.; Brand, M. Regenerative neurogenesis from neural progenitor cells requires injury-induced expression of Gata3. *Dev. Cell* **2012**, *23*, 1230–1237. [[CrossRef](#)]
132. Arvidsson, A.; Collin, T.; Kirik, D.; Kokaia, Z.; Lindvall, O. Neuronal replacement from endogenous precursors in the adult brain after stroke. *Nat. Med.* **2002**, *8*, 963–970. [[CrossRef](#)] [[PubMed](#)]
133. Parent, J.M.; Vexler, Z.S.; Gong, C.; Derugin, N.; Ferriero, D.M. Rat forebrain neurogenesis and striatal neuron replacement after focal stroke. *Ann. Neurol.* **2002**, *52*, 802–813. [[CrossRef](#)]
134. Yamashita, T.; Ninomiya, M.; Hernandez Acosta, P.; Garcia-Verdugo, J.M.; Sunabori, T.; Sakaguchi, M.; Adachi, K.; Kojima, T.; Hirota, Y.; Kawase, T.; et al. Subventricular zone-derived neuroblasts migrate and differentiate into mature neurons in the post-stroke adult striatum. *J. Neurosci.* **2006**, *26*, 6627–6636. [[CrossRef](#)] [[PubMed](#)]
135. Lindvall, O.; Kokaia, Z. Neurogenesis following Stroke Affecting the Adult Brain. *Cold Spring Harbor Perspect. Biol.* **2015**, *7*. [[CrossRef](#)] [[PubMed](#)]
136. Osman, A.M.; Porritt, M.J.; Nilsson, M.; Kuhn, H.G. Long-term stimulation of neural progenitor cell migration after cortical ischemia in mice. *Stroke* **2011**, *42*, 3559–3565. [[CrossRef](#)] [[PubMed](#)]
137. Woitke, F.; Ceanga, M.; Rudolph, M.; Niv, F.; Witte, O.W.; Redecker, C.; Kunze, A.; Keiner, S. Adult hippocampal neurogenesis poststroke: More new granule cells but aberrant morphology and impaired spatial memory. *PLoS ONE* **2017**, *12*, e0183463. [[CrossRef](#)]
138. Ngwenya, L.B.; Danzer, S.C. Impact of Traumatic Brain Injury on Neurogenesis. *Front. Neurosci.* **2018**, *12*, 1014. [[CrossRef](#)]
139. Dash, P.K.; Mach, S.A.; Moore, A.N. Enhanced neurogenesis in the rodent hippocampus following traumatic brain injury. *J. Neurosci. Res.* **2001**, *63*, 313–319. [[CrossRef](#)]
140. Chirumamilla, S.; Sun, D.; Bullock, M.R.; Colello, R.J. Traumatic brain injury induced cell proliferation in the adult mammalian central nervous system. *J. Neurotrauma* **2002**, *19*, 693–703. [[CrossRef](#)]
141. Sofroniew, M.V. Molecular dissection of reactive astrogliosis and glial scar formation. *Trends. Neurosci.* **2009**, *32*, 638–647. [[CrossRef](#)] [[PubMed](#)]
142. Sofroniew, M.V. Reactive astrocytes in neural repair and protection. *Neuroscientist* **2005**, *11*, 400–407. [[CrossRef](#)]
143. Pekny, M.; Nilsson, M. Astrocyte activation and reactive gliosis. *Glia* **2005**, *50*, 427–434. [[CrossRef](#)]
144. Liu, Z.; Chopp, M. Astrocytes, therapeutic targets for neuroprotection and neurorestoration in ischemic stroke. *Prog. Neurobiol.* **2016**, *144*, 103–120. [[CrossRef](#)] [[PubMed](#)]
145. Barreto, G.E.; Sun, X.; Xu, L.; Giffard, R.G. Astrocyte proliferation following stroke in the mouse depends on distance from the infarct. *PLoS ONE* **2011**, *6*, e27881. [[CrossRef](#)] [[PubMed](#)]
146. Shimada, I.S.; Borders, A.; Aronshtam, A.; Spees, J.L. Proliferating reactive astrocytes are regulated by Notch-1 in the peri-infarct area after stroke. *Stroke* **2011**, *42*, 3231–3237. [[CrossRef](#)]
147. Burda, J.E.; Bernstein, A.M.; Sofroniew, M.V. Astrocyte roles in traumatic brain injury. *Exp. Neurol.* **2016**, *275 Pt 3*, 305–315. [[CrossRef](#)]
148. Sofroniew, M.V. Astrocyte barriers to neurotoxic inflammation. *Nat. Rev. Neurosci.* **2015**, *16*, 249–263. [[CrossRef](#)]
149. Myer, D.J.; Gurkoff, G.G.; Lee, S.M.; Hovda, D.A.; Sofroniew, M.V. Essential protective roles of reactive astrocytes in traumatic brain injury. *Brain* **2006**, *129*, 2761–2772. [[CrossRef](#)]
150. Faiz, M.; Sachewsky, N.; Gascon, S.; Bang, K.W.; Morshead, C.M.; Nagy, A. Adult Neural Stem Cells from the Subventricular Zone Give Rise to Reactive Astrocytes in the Cortex after Stroke. *Cell Stem Cell* **2015**, *17*, 624–634. [[CrossRef](#)]



151. Wilhelmsson, U.; Bushong, E.A.; Price, D.L.; Smarr, B.L.; Phung, V.; Terada, M.; Ellisman, M.H.; Pekny, M. Redefining the concept of reactive astrocytes as cells that remain within their unique domains upon reaction to injury. *Proc. Natl. Acad. Sci. USA* **2006**, *103*, 17513–17518. [[CrossRef](#)]
152. Zamanian, J.L.; Xu, L.; Foo, L.C.; Nouri, N.; Zhou, L.; Giffard, R.G.; Barres, B.A. Genomic analysis of reactive astrogliosis. *J. Neurosci.* **2012**, *32*, 6391–6410. [[CrossRef](#)]
153. Al Ahmad, A.; Taboada, C.B.; Gassmann, M.; Ogunshola, O.O. Astrocytes and pericytes differentially modulate blood-brain barrier characteristics during development and hypoxic insult. *J. Cereb. Blood Flow. Metab.* **2011**, *31*, 693–705. [[CrossRef](#)]
154. Ding, S. Dynamic reactive astrocytes after focal ischemia. *Neural Regen. Res.* **2014**, *9*, 2048–2052. [[CrossRef](#)]
155. Li, H.; Zhang, N.; Lin, H.Y.; Yu, Y.; Cai, Q.Y.; Ma, L.; Ding, S. Histological, cellular and behavioral assessments of stroke outcomes after photothrombosis-induced ischemia in adult mice. *BMC Neurosci.* **2014**, *15*, 58. [[CrossRef](#)] [[PubMed](#)]
156. Schroeter, M.; Schiene, K.; Kraemer, M.; Hagemann, G.; Weigel, H.; Eysel, U.T.; Witte, O.W.; Stoll, G. Astroglial responses in photochemically induced focal ischemia of the rat cortex. *Exp. Brain Res.* **1995**, *106*, 1–6. [[CrossRef](#)]
157. De Pablo, Y.; Nilsson, M.; Pekna, M.; Pekny, M. Intermediate filaments are important for astrocyte response to oxidative stress induced by oxygen-glucose deprivation and reperfusion. *Histochem. Cell Biol.* **2013**, *140*, 81–91. [[CrossRef](#)] [[PubMed](#)]
158. Li, L.; Lundkvist, A.; Andersson, D.; Wilhelmsson, U.; Nagai, N.; Pardo, A.C.; Nodin, C.; Stahlberg, A.; Aprico, K.; Larsson, K.; et al. Protective role of reactive astrocytes in brain ischemia. *J. Cereb. Blood Flow Metab.* **2008**, *28*, 468–481. [[CrossRef](#)]
159. Zhou, Y.; Shao, A.; Yao, Y.; Tu, S.; Deng, Y.; Zhang, J. Dual roles of astrocytes in plasticity and reconstruction after traumatic brain injury. *Cell Commun. Signal.* **2020**, *18*, 62. [[CrossRef](#)] [[PubMed](#)]
160. Ben-Gigi, L.; Sweetat, S.; Besser, E.; Fellig, Y.; Wiederhold, T.; Polakiewicz, R.D.; Behar, O. Astrogliosis Induced by Brain Injury Is Regulated by Sema4B Phosphorylation. *eNeuro* **2015**, *2*. [[CrossRef](#)] [[PubMed](#)]
161. Rolls, A.; Shechter, R.; Schwartz, M. The bright side of the glial scar in CNS repair. *Nat. Rev. Neurosci.* **2009**, *10*, 235–241. [[CrossRef](#)]
162. Buffo, A.; Rolando, C.; Ceruti, S. Astrocytes in the damaged brain: Molecular and cellular insights into their reactive response and healing potential. *Biochem. Pharmacol.* **2010**, *79*, 77–89. [[CrossRef](#)] [[PubMed](#)]
163. Galindo, L.T.; Mundim, M.; Pinto, A.S.; Chiarantin, G.M.D.; Almeida, M.E.S.; Lamers, M.L.; Horwitz, A.R.; Santos, M.F.; Porcionatto, M. Chondroitin Sulfate Impairs Neural Stem Cell Migration Through ROCK Activation. *Mol. Neurobiol.* **2018**, *55*, 3185–3195. [[CrossRef](#)]
164. Diotel, N.; Charlier, T.D.; Lefebvre d'Helencourt, C.; Couret, D.; Trudeau, V.L.; Nicolau, J.C.; Meilhac, O.; Kah, O.; Pellegrini, E. Steroid Transport, Local Synthesis, and Signaling within the Brain: Roles in Neurogenesis, Neuroprotection, and Sexual Behaviors. *Front. Neurosci.* **2018**, *12*, 84. [[CrossRef](#)]
165. Radak, D.; Katsiki, N.; Resanovic, I.; Jovanovic, A.; Sudar-Milovanovic, E.; Zafirovic, S.; Mousad, S.A.; Isenovic, E.R. Apoptosis and Acute Brain Ischemia in Ischemic Stroke. *Curr. Vasc. Pharmacol.* **2017**, *15*, 115–122. [[CrossRef](#)]
166. Sairanen, T.; Karjalainen-Lindsberg, M.L.; Paetau, A.; Ijas, P.; Lindsberg, P.J. Apoptosis dominant in the periinfarct area of human ischaemic stroke—A possible target of antiapoptotic treatments. *Brain* **2006**, *129*, 189–199. [[CrossRef](#)]
167. Otxoa-de-Amezaga, A.; Miro-Mur, F.; Pedragosa, J.; Gallizioli, M.; Justicia, C.; Gaja-Capdevila, N.; Ruiz-Jaen, F.; Salas-Perdomo, A.; Bosch, A.; Calvo, M.; et al. Microglial cell loss after ischemic stroke favors brain neutrophil accumulation. *Acta Neuropathol.* **2019**, *137*, 321–341. [[CrossRef](#)] [[PubMed](#)]
168. Perez-de-Puig, I.; Miro-Mur, F.; Ferrer-Ferrer, M.; Gelpi, E.; Pedragosa, J.; Justicia, C.; Urra, X.; Chamorro, A.; Planas, A.M. Neutrophil recruitment to the brain in mouse and human ischemic stroke. *Acta Neuropathol.* **2015**, *129*, 239–257. [[CrossRef](#)] [[PubMed](#)]
169. Rosell, A.; Cuadrado, E.; Ortega-Aznar, A.; Hernandez-Guillamon, M.; Lo, E.H.; Montaner, J. MMP-9-positive neutrophil infiltration is associated to blood-brain barrier breakdown and basal lamina type IV collagen degradation during hemorrhagic transformation after human ischemic stroke. *Stroke* **2008**, *39*, 1121–1126. [[CrossRef](#)]
170. Huang, L.; Wu, Z.B.; Zhuge, Q.; Zheng, W.; Shao, B.; Wang, B.; Sun, F.; Jin, K. Glial scar formation occurs in the human brain after ischemic stroke. *Int. J. Med. Sci.* **2014**, *11*, 344–348. [[CrossRef](#)] [[PubMed](#)]
171. Jin, K.; Wang, X.; Xie, L.; Mao, X.O.; Zhu, W.; Wang, Y.; Shen, J.; Mao, Y.; Banwait, S.; Greenberg, D.A. Evidence for stroke-induced neurogenesis in the human brain. *Proc. Natl. Acad. Sci. USA* **2006**, *103*, 13198–13202. [[CrossRef](#)] [[PubMed](#)]
172. Zambusi, A.; Ninkovic, J. Regeneration of the central nervous system—principles from brain regeneration in adult zebrafish. *World J. Stem Cells* **2020**, *12*, 8–24. [[CrossRef](#)] [[PubMed](#)]
173. Mashkaryan, V.; Siddiqui, T.; Popova, S.; Cosacak, M.I.; Bhattarai, P.; Brandt, K.; Govindarajan, N.; Petzold, A.; Reinhardt, S.; Dahl, A.; et al. Type 1 Interleukin-4 Signaling Obliterates Mouse Astroglia in vivo but Not in vitro. *Front. Cell Dev. Biol.* **2020**, *8*, 114. [[CrossRef](#)]
174. Celikkaya, H.; Cosacak, M.I.; Papadimitriou, C.; Popova, S.; Bhattarai, P.; Biswas, S.N.; Siddiqui, T.; Wistorf, S.; Nevado-Alcalde, I.; Naumann, L.; et al. GATA3 Promotes the Neural Progenitor State but Not Neurogenesis in 3D Traumatic Injury Model of Primary Human Cortical Astrocytes. *Front. Cell. Neurosci.* **2019**, *13*, 23. [[CrossRef](#)]
175. Chang, E.H.; Adorjan, I.; Mundim, M.V.; Sun, B.; Dizon, M.L.; Szele, F.G. Traumatic Brain Injury Activation of the Adult Subventricular Zone Neurogenic Niche. *Front. Neurosci.* **2016**, *10*, 332. [[CrossRef](#)] [[PubMed](#)]
176. Yoshiya, K.; Tanaka, H.; Kasai, K.; Irisawa, T.; Shiozaki, T.; Sugimoto, H. Profile of gene expression in the subventricular zone after traumatic brain injury. *J. Neurotrauma* **2003**, *20*, 1147–1162. [[CrossRef](#)]

177. Wang, W.; Hu, C.K.; Zeng, A.; Alegre, D.; Hu, D.; Gotting, K.; Ortega Granillo, A.; Wang, Y.; Robb, S.; Schnittker, R.; et al. Changes in regeneration-responsive enhancers shape regenerative capacities in vertebrates. *Science* **2020**, *369*. [[CrossRef](#)]
178. Marques, I.J.; Lupi, E.; Mercader, N. Model systems for regeneration: Zebrafish. *Development* **2019**, *146*. [[CrossRef](#)] [[PubMed](#)]
179. Muramatsu, R.; Takahashi, C.; Miyake, S.; Fujimura, H.; Mochizuki, H.; Yamashita, T. Angiogenesis induced by CNS inflammation promotes neuronal remodeling through vessel-derived prostacyclin. *Nat. Med.* **2012**, *18*, 1658–1664. [[CrossRef](#)]
180. Bradbury, E.J.; Burnside, E.R. Moving beyond the glial scar for spinal cord repair. *Nat. Commun.* **2019**, *10*, 3879. [[CrossRef](#)]
181. Tang, B.L. The astrocyte scar—Not so inhibitory after all? *Neural Regen. Res.* **2016**, *11*, 1054–1055. [[CrossRef](#)]
182. Yang, T.; Dai, Y.; Chen, G.; Cui, S. Dissecting the Dual Role of the Glial Scar and Scar-Forming Astrocytes in Spinal Cord Injury. *Front. Cell. Neurosci.* **2020**, *14*, 78. [[CrossRef](#)] [[PubMed](#)]
183. Steinke, D.; Hoegg, S.; Brinkmann, H.; Meyer, A. Three rounds (1R/2R/3R) of genome duplications and the evolution of the glycolytic pathway in vertebrates. *BMC Biol.* **2006**, *4*, 16. [[CrossRef](#)]
184. Ruan, L.; Wang, B.; ZhuGe, Q.; Jin, K. Coupling of neurogenesis and angiogenesis after ischemic stroke. *Brain Res.* **2015**, *1623*, 166–173. [[CrossRef](#)]
185. Simoes, A.R.; Rhiner, C. A Cold-Blooded View on Adult Neurogenesis. *Front. Neurosci.* **2017**, *11*, 327. [[CrossRef](#)]
186. Sullivan, J.M.; Benton, J.L.; Sandeman, D.C.; Beltz, B.S. Adult neurogenesis: A common strategy across diverse species. *J. Comp. Neurol.* **2007**, *500*, 574–584. [[CrossRef](#)]







## References

- Boles, A., Kandimalla, R. & Reddy, P.H. (2017) Dynamics of diabetes and obesity: Epidemiological perspective. *Biochim Biophys Acta Mol Basis Dis*, **1863**, 1026-1036.
- Abbott, N.J. (2000) Inflammatory mediators and modulation of blood-brain barrier permeability. *Cell Mol Neurobiol*, **20**, 131-147.
- Abbott, N.J. (2004) Evidence for bulk flow of brain interstitial fluid: significance for physiology and pathology. *Neurochem Int*, **45**, 545-552.
- Abbott, N.J. (2005) Dynamics of CNS barriers: evolution, differentiation, and modulation. *Cell Mol Neurobiol*, **25**, 5-23.
- Abbott, N.J. & Romero, I.A. (1996) Transporting therapeutics across the blood-brain barrier. *Mol Med Today*, **2**, 106-113.
- Ables, J.L., Decarolis, N.A., Johnson, M.A., Rivera, P.D., Gao, Z., Cooper, D.C., Radtke, F., Hsieh, J. & Eisch, A.J. (2010) Notch1 is required for maintenance of the reservoir of adult hippocampal stem cells. *J Neurosci*, **30**, 10484-10492.
- Adamson, K.I., Sheridan, E. & Grierson, A.J. (2018) Use of zebrafish models to investigate rare human disease. *J Med Genet*, **55**, 641-649.
- Adolf, B., Chapouton, P., Lam, C.S., Topp, S., Tannhauser, B., Strahle, U., Gotz, M. & Bally-Cuif, L. (2006) Conserved and acquired features of adult neurogenesis in the zebrafish telencephalon. *Developmental biology*, **295**, 278-293.
- Ahn, S.I. & Kim, Y. (2021) Human Blood-Brain Barrier on a Chip: Featuring Unique Multicellular Cooperation in Pathophysiology. *Trends Biotechnol*, **39**, 749-752.
- Ahvazi, M., Khalighi-Sigaroodi, F., Charkhchiyan, M.M., Mojab, F., Mozaffarian, V.A. & Zakeri, H. (2012) Introduction of medicinal plants species with the most traditional usage in alamut region. *Iran J Pharm Res*, **11**, 185-194.
- Akbari, E.M., Chatterjee, D., Levy, F. & Fleming, A.S. (2007) Experience-dependent cell survival in the maternal rat brain. *Behav Neurosci*, **121**, 1001-1011.
- Akter, K., Lanza, E.A., Martin, S.A., Myronyuk, N., Rua, M. & Raffa, R.B. (2011) Diabetes mellitus and Alzheimer's disease: shared pathology and treatment? *Br J Clin Pharmacol*, **71**, 365-376.
- Akter, M., Kaneko, N. & Sawamoto, K. (2021) Neurogenesis and neuronal migration in the postnatal ventricular-subventricular zone: Similarities and dissimilarities between rodents and primates. *Neurosci Res*, **167**, 64-69.

- Alpert, M.A., Omran, J., Mehra, A. & Ardhanari, S. (2014) Impact of obesity and weight loss on cardiac performance and morphology in adults. *Prog Cardiovasc Dis*, **56**, 391-400.
- Altman, J. (1969) Autoradiographic and histological studies of postnatal neurogenesis. IV. Cell proliferation and migration in the anterior forebrain, with special reference to persisting neurogenesis in the olfactory bulb. *The Journal of comparative neurology*, **137**, 433-457.
- Altman, J. & Das, G.D. (1965) Autoradiographic and histological evidence of postnatal hippocampal neurogenesis in rats. *The Journal of comparative neurology*, **124**, 319-335.
- Alzoubi, K.H., Mayyas, F.A., Mahafzah, R. & Khabour, O.F. (2018) Melatonin prevents memory impairment induced by high-fat diet: Role of oxidative stress. *Behav Brain Res*, **336**, 93-98.
- Andreu, L., Nuncio-Jauregui, N., Carbonell-Barrachina, A.A., Legua, P. & Hernandez, F. (2018) Antioxidant properties and chemical characterization of Spanish *Opuntia ficus-indica* Mill. cladodes and fruits. *J Sci Food Agric*, **98**, 1566-1573.
- Angelova, P.R. & Abramov, A.Y. (2018) Role of mitochondrial ROS in the brain: from physiology to neurodegeneration. *FEBS Lett*, **592**, 692-702.
- Anjum, I., Fayyaz, M., Wajid, A., Sohail, W. & Ali, A. (2018) Does Obesity Increase the Risk of Dementia: A Literature Review. *Cureus*, **10**, e2660.
- Arcambal, A., Taile, J., Couret, D., Planesse, C., Veeren, B., Diotel, N., Gauvin-Bialecki, A., Meilhac, O. & Gonthier, M.P. (2020) Protective Effects of Antioxidant Polyphenols against Hyperglycemia-Mediated Alterations in Cerebral Endothelial Cells and a Mouse Stroke Model. *Molecular nutrition & food research*, **64**, e1900779.
- Argenton, F., Zecchin, E. & Bortolussi, M. (1999) Early appearance of pancreatic hormone-expressing cells in the zebrafish embryo. *Mech Dev*, **87**, 217-221.
- Aronson, D. & Rayfield, E.J. (2002) How hyperglycemia promotes atherosclerosis: molecular mechanisms. *Cardiovasc Diabetol*, **1**, 1.
- Arunachalam, M., Raja, M., Vijayakumar, C., Malaiammal, P. & Mayden, R.L. (2013) Natural history of zebrafish (*Danio rerio*) in India. *Zebrafish*, **10**, 1-14.
- Astley, S. & Finglas, P. (2016. ) Reference Module in Food Science. Elsevier; Amsterdam, The Netherlands. *Nutrition and Health*.
- Bacigaluppi, M., Pluchino, S., Peruzzotti-Jametti, L., Kilic, E., Kilic, U., Salani, G., Brambilla, E., West, M.J., Comi, G., Martino, G. & Hermann, D.M. (2009) Delayed post-ischaemic neuroprotection

- following systemic neural stem cell transplantation involves multiple mechanisms. *Brain*, **132**, 2239-2251.
- Badawi, A., Klip, A., Haddad, P., Cole, D.E., Bailo, B.G., El-Sohehy, A. & Karmali, M. (2010) Type 2 diabetes mellitus and inflammation: Prospects for biomarkers of risk and nutritional intervention. *Diabetes Metab Syndr Obes*, **3**, 173-186.
- Bahniwal, M., Little, J.P. & Klegeris, A. (2017) High Glucose Enhances Neurotoxicity and Inflammatory Cytokine Secretion by Stimulated Human Astrocytes. *Curr Alzheimer Res*, **14**, 731-741.
- Banks, W.A. & Rhea, E.M. (2021) The Blood-Brain Barrier, Oxidative Stress, and Insulin Resistance. *Antioxidants*, **10**.
- Barnes, D.E. & Yaffe, K. (2011) The projected effect of risk factor reduction on Alzheimer's disease prevalence. *Lancet Neurol*, **10**, 819-828.
- Bartel, P., Van Laar, V. & Burton, E. (2020) Behavioral and Neural Genetics of Zebrafish *Behavioral and Neural Genetics of Zebrafish*, pp. 377-412.
- Batiz, L.F., Castro, M.A., Burgos, P.V., Velasquez, Z.D., Munoz, R.I., Lafourcade, C.A., Troncoso-Escudero, P. & Wyneken, U. (2015) Exosomes as Novel Regulators of Adult Neurogenic Niches. *Front Cell Neurosci*, **9**, 501.
- Bauer, B., Hartz, A.M., Fricker, G. & Miller, D.S. (2005) Modulation of p-glycoprotein transport function at the blood-brain barrier. *Exp Biol Med (Maywood)*, **230**, 118-127.
- Baumgart, E.V., Barbosa, J.S., Bally-Cuif, L., Gotz, M. & Ninkovic, J. (2012) Stab wound injury of the zebrafish telencephalon: a model for comparative analysis of reactive gliosis. *Glia*, **60**, 343-357.
- Baynes, J.W. & Thorpe, S.R. (1999) Role of oxidative stress in diabetic complications: a new perspective on an old paradigm. *Diabetes*, **48**, 1-9.
- Beard, R.S., Jr., Haines, R.J., Wu, K.Y., Reynolds, J.J., Davis, S.M., Elliott, J.E., Malinin, N.L., Chatterjee, V., Cha, B.J., Wu, M.H. & Yuan, S.Y. (2014) Non-muscle Mlck is required for beta-catenin- and FoxO1-dependent downregulation of Cldn5 in IL-1beta-mediated barrier dysfunction in brain endothelial cells. *J Cell Sci*, **127**, 1840-1853.
- Beauquis, J., Roig, P., Homo-Delarche, F., De Nicola, A. & Saravia, F. (2006) Reduced hippocampal neurogenesis and number of hilar neurones in streptozotocin-induced diabetic mice: reversion by antidepressant treatment. *The European journal of neuroscience*, **23**, 1539-1546.
- Beauquis, J., Saravia, F., Coulaud, J., Roig, P., Dardenne, M., Homo-Delarche, F. & De Nicola, A. (2008) Prominently decreased hippocampal neurogenesis in a spontaneous model of type 1 diabetes, the nonobese diabetic mouse. *Exp Neurol*, **210**, 359-367.

- Becker, C.G. & Becker, T. (2008) Adult zebrafish as a model for successful central nervous system regeneration. *Restor Neurol Neurosci*, **26**, 71-80.
- Begley, D.J. & Brightman, M.W. (2003) Structural and functional aspects of the blood-brain barrier. *Prog Drug Res*, **61**, 39-78.
- Behazin, N., Jones, S.B., Cohen, R.I. & Loring, S.H. (2010) Respiratory restriction and elevated pleural and esophageal pressures in morbid obesity. *J Appl Physiol (1985)*, **108**, 212-218.
- Beltowski, J., Wojcicka, G., Gorny, D. & Marciniak, A. (2000) The effect of dietary-induced obesity on lipid peroxidation, antioxidant enzymes and total plasma antioxidant capacity. *J Physiol Pharmacol*, **51**, 883-896.
- Benchoula, K., Khatib, A., Jaffar, A., Ahmed, Q.U., Sulaiman, W., Wahab, R.A. & El-Seedi, H.R. (2019a) The promise of zebrafish as a model of metabolic syndrome. *Exp Anim*, **68**, 407-416.
- Benchoula, K., Khatib, A., Quzwain, F.M.C., Che Mohamad, C.A., Wan Sulaiman, W.M.A., Abdul Wahab, R., Ahmed, Q.U., Abdul Ghaffar, M., Saiman, M.Z., Alajmi, M.F. & El-Seedi, H. (2019b) Optimization of Hyperglycemic Induction in Zebrafish and Evaluation of Its Blood Glucose Level and Metabolite Fingerprint Treated with Psychotria malayana Jack Leaf Extract. *Molecules*, **24**.
- Bernhoft, A. (2010) A brief review on bioactive compounds in plants. . *Bioact. Compd. Plants-Benefits Risks Man Anim.*, **50:11–17**.
- Bernier, P.J., Bedard, A., Vinet, J., Levesque, M. & Parent, A. (2002) Newly generated neurons in the amygdala and adjoining cortex of adult primates. *Proc Natl Acad Sci U S A*, **99**, 11464-11469.
- Berzin, T.M., Zipser, B.D., Rafii, M.S., Kuo-Leblanc, V., Yancopoulos, G.D., Glass, D.J., Fallon, J.R. & Stopa, E.G. (2000) Agrin and microvascular damage in Alzheimer's disease. *Neurobiol Aging*, **21**, 349-355.
- Beyer, A.M., Guo, D.F. & Rahmouni, K. (2013) Prolonged treatment with angiotensin 1-7 improves endothelial function in diet-induced obesity. *J Hypertens*, **31**, 730-738.
- Bhaskaran, K., Douglas, I., Forbes, H., dos-Santos-Silva, I., Leon, D.A. & Smeeth, L. (2014) Body-mass index and risk of 22 specific cancers: a population-based cohort study of 5.24 million UK adults. *Lancet*, **384**, 755-765.
- Bhupathiraju, S.N. & Hu, F.B. (2016) Epidemiology of Obesity and Diabetes and Their Cardiovascular Complications. *Circulation research*, **118**, 1723-1735.



- Bian, Y., Lei, J., Zhong, J., Wang, B., Wan, Y., Li, J., Liao, C., He, Y., Liu, Z., Ito, K. & Zhang, B. (2022) Kaempferol reduces obesity, prevents intestinal inflammation, and modulates gut microbiota in high-fat diet mice. *J Nutr Biochem*, **99**, 108840.
- Biemar, F., Argenton, F., Schmidtke, R., Epperlein, S., Peers, B. & Driever, W. (2001) Pancreas development in zebrafish: early dispersed appearance of endocrine hormone expressing cells and their convergence to form the definitive islet. *Developmental biology*, **230**, 189-203.
- Biesalski, H.K., Dragsted, L.O., Elmadfa, I., Grossklaus, R., Muller, M., Schrenk, D., Walter, P. & Weber, P. (2009) Bioactive compounds: definition and assessment of activity. *Nutrition*, **25**, 1202-1205.
- Biessels, G.J., Staekenborg, S., Brunner, E., Brayne, C. & Scheltens, P. (2006) Risk of dementia in diabetes mellitus: a systematic review. *Lancet Neurol*, **5**, 64-74.
- Bjornsson, C.S., Apostolopoulou, M., Tian, Y. & Temple, S. (2015) It takes a village: constructing the neurogenic niche. *Dev Cell*, **32**, 435-446.
- Bluher, M. (2020) Metabolically Healthy Obesity. *Endocr Rev*, **41**.
- Blumenthal, M. (1998) The Complete German Commission E Monographs, . *Special Expert Committee of the German Federal Institute for Drugs and Medical Devices*.
- Boillot, A., Zoungas, S., Mitchell, P., Klein, R., Klein, B., Ikram, M.K., Klaver, C., Wang, J.J., Gopinath, B., Tai, E.S., Neubauer, A.S., Hercberg, S., Brazionis, L., Saw, S.M., Wong, T.Y., Czernichow, S. & Group, M.-E.S. (2013) Obesity and the microvasculature: a systematic review and meta-analysis. *PLoS one*, **8**, e52708.
- Boitard, C., Etchamendy, N., Sauvant, J., Aubert, A., Tronel, S., Marighetto, A., Laye, S. & Ferreira, G. (2012) Juvenile, but not adult exposure to high-fat diet impairs relational memory and hippocampal neurogenesis in mice. *Hippocampus*, **22**, 2095-2100.
- Boldrini, M., Fulmore, C.A., Tartt, A.N., Simeon, L.R., Pavlova, I., Poposka, V., Rosoklija, G.B., Stankov, A., Arango, V., Dwork, A.J., Hen, R. & Mann, J.J. (2018) Human Hippocampal Neurogenesis Persists throughout Aging. *Cell Stem Cell*, **22**, 589-599 e585.
- Bonds, J.A., Shetti, A., Stephen, T.K.L., Bonini, M.G., Minshall, R.D. & Lazarov, O. (2020) Deficits in hippocampal neurogenesis in obesity-dependent and -independent type-2 diabetes mellitus mouse models. *Scientific reports*, **10**, 16368.
- Bonneville, J., Rondeau, P., Veeren, B., Faccini, J., Gonthier, M.P., Meilhac, O. & Vindis, C. (2021) Antioxidant and Cytoprotective Properties of Polyphenol-Rich Extracts from *Antirhea borbonica* and *Doratoxylon apetalum* against Atherogenic Lipids in Human Endothelial Cells. *Antioxidants*, **11**.

- Bottcher, H. (1965) *Miracle drugs*. Zagreb: Zora pp. 23–139.
- Boulton, A.J., Malik, R.A., Arezzo, J.C. & Sosenko, J.M. (2004) Diabetic somatic neuropathies. *Diabetes Care*, **27**, 1458-1486.
- Bracke, A., Domanska, G., Bracke, K., Harzsch, S., van den Brandt, J., Broker, B. & von Bohlen Und Halbach, O. (2019) Obesity Impairs Mobility and Adult Hippocampal Neurogenesis. *J Exp Neurosci*, **13**, 1179069519883580.
- Brings, S., Fleming, T., Freichel, M., Muckenthaler, M.U., Herzig, S. & Nawroth, P.P. (2017) Dicarboxyls and Advanced Glycation End-Products in the Development of Diabetic Complications and Targets for Intervention. *International journal of molecular sciences*, **18**.
- Brook, E., Mamo, J., Wong, R., Al-Salami, H., Falasca, M., Lam, V. & Takechi, R. (2019) Blood-brain barrier disturbances in diabetes-associated dementia: Therapeutic potential for cannabinoids. *Pharmacol Res*, **141**, 291-297.
- Brookmeyer, R., Gray, S. & Kawas, C. (1998) Projections of Alzheimer's disease in the United States and the public health impact of delaying disease onset. *Am J Public Health*, **88**, 1337-1342.
- Brownlee, M. (2001) Biochemistry and molecular cell biology of diabetic complications. *Nature*, **414**, 813-820.
- Bruel-Jungerman, E., Davis, S., Rampon, C. & Laroche, S. (2006) Long-term potentiation enhances neurogenesis in the adult dentate gyrus. *J Neurosci*, **26**, 5888-5893.
- Brummelte, S. & Galea, L.A. (2010) Chronic high corticosterone reduces neurogenesis in the dentate gyrus of adult male and female rats. *Neuroscience*, **168**, 680-690.
- Buranova, D.D. (2015) The value of Avicenna's heritage in development of modern integrative medicine in Uzbekistan. *Integr Med Res*, **4**, 220-224.
- Burgos-Moron, E., Abad-Jimenez, Z., Maranon, A.M., Iannantuoni, F., Escribano-Lopez, I., Lopez-Domenech, S., Salom, C., Jover, A., Mora, V., Roldan, I., Sola, E., Rocha, M. & Victor, V.M. (2019) Relationship Between Oxidative Stress, ER Stress, and Inflammation in Type 2 Diabetes: The Battle Continues. *J Clin Med*, **8**.
- Busquet, F., Strecker, R., Rawlings, J.M., Belanger, S.E., Braunbeck, T., Carr, G.J., Cenijn, P., Fochtman, P., Gourmelon, A., Hubler, N., Kleensang, A., Knobel, M., Kussatz, C., Legler, J., Lillicrap, A., Martinez-Jeronimo, F., Polleichtner, C., Rzodeczko, H., Salinas, E., Schneider, K.E., Scholz, S., van den Brandhof, E.J., van der Ven, L.T., Walter-Rohde, S., Weigt, S., Witters, H. & Halder, M. (2014) OECD validation study to assess intra- and inter-laboratory reproducibility of the zebrafish embryo toxicity test for acute aquatic toxicity testing. *Regul Toxicol Pharmacol*, **69**, 496-511.

- Cacialli, P., Gueguen, M.M., Coumailleau, P., D'Angelo, L., Kah, O., Lucini, C. & Pellegrini, E. (2016) BDNF Expression in Larval and Adult Zebrafish Brain: Distribution and Cell Identification. *PloS one*, **11**, e0158057.
- Calvo-Ochoa, E., Byrd-Jacobs, C.A. & Fuss, S.H. (2021) Diving into the streams and waves of constitutive and regenerative olfactory neurogenesis: insights from zebrafish. *Cell Tissue Res*, **383**, 227-253.
- Calvo, D., Gomez-Coronado, D., Suarez, Y., Lasuncion, M.A. & Vega, M.A. (1998) Human CD36 is a high affinity receptor for the native lipoproteins HDL, LDL, and VLDL. *J Lipid Res*, **39**, 777-788.
- Camara, J.S., Albuquerque, B.R., Aguiar, J., Correa, R.C.G., Goncalves, J.L., Granato, D., Pereira, J.A.M., Barros, L. & Ferreira, I. (2020) Food Bioactive Compounds and Emerging Techniques for Their Extraction: Polyphenols as a Case Study. *Foods*, **10**.
- Capiotti, K.M., Antonioli, R., Jr., Kist, L.W., Bogo, M.R., Bonan, C.D. & Da Silva, R.S. (2014a) Persistent impaired glucose metabolism in a zebrafish hyperglycemia model. *Comp Biochem Physiol B Biochem Mol Biol*, **171**, 58-65.
- Capiotti, K.M., De Moraes, D.A., Menezes, F.P., Kist, L.W., Bogo, M.R. & Da Silva, R.S. (2014b) Hyperglycemia induces memory impairment linked to increased acetylcholinesterase activity in zebrafish (*Danio rerio*). *Behavioural brain research*, **274**, 319-325.
- Castro, D.S., Martynoga, B., Parras, C., Ramesh, V., Pacary, E., Johnston, C., Drechsel, D., Lebel-Potter, M., Garcia, L.G., Hunt, C., Dolle, D., Bithell, A., Ettwiller, L., Buckley, N. & Guillemot, F. (2011) A novel function of the proneural factor *Ascl1* in progenitor proliferation identified by genome-wide characterization of its targets. *Genes Dev*, **25**, 930-945.
- Centers for Disease, C. & Prevention (2004) Prevalence of overweight and obesity among adults with diagnosed diabetes--United States, 1988-1994 and 1999-2002. *MMWR Morb Mortal Wkly Rep*, **53**, 1066-1068.
- Chahardehi, A.M., Arsad, H. & Lim, V. (2020) Zebrafish as a Successful Animal Model for Screening Toxicity of Medicinal Plants. *Plants (Basel)*, **9**.
- Chang, S.C. & Yang, W.V. (2016) Hyperglycemia, tumorigenesis, and chronic inflammation. *Crit Rev Oncol Hematol*, **108**, 146-153.
- Chapouton, P., Skupien, P., Hesl, B., Coolen, M., Moore, J.C., Madelaine, R., Kremmer, E., Faus-Kessler, T., Blader, P., Lawson, N.D. & Bally-Cuif, L. (2010) Notch activity levels control the balance between quiescence and recruitment of adult neural stem cells. *J Neurosci*, **30**, 7961-7974.
- Chavez, M.N., Aedo, G., Fierro, F.A., Allende, M.L. & Egana, J.T. (2016) Zebrafish as an Emerging Model Organism to Study Angiogenesis in Development and Regeneration. *Front Physiol*, **7**, 56.

- Checkouri, E., Reignier, F., Robert-Da Silva, C. & Meilhac, O. (2020) Evaluation of Polyphenol Content and Antioxidant Capacity of Aqueous Extracts from Eight Medicinal Plants from Reunion Island: Protection against Oxidative Stress in Red Blood Cells and Preadipocytes. *Antioxidants*, **9**.
- Chen, Q., Wang, Q., Zhu, J., Xiao, Q. & Zhang, L. (2018a) Reactive oxygen species: key regulators in vascular health and diseases. *Br J Pharmacol*, **175**, 1279-1292.
- Chen, R., Ovbiagele, B. & Feng, W. (2016) Diabetes and Stroke: Epidemiology, Pathophysiology, Pharmaceuticals and Outcomes. *Am J Med Sci*, **351**, 380-386.
- Chen, X., Famurewa, A.C., Tang, J., Olatunde, O.O. & Olatunji, O.J. (2021) Hyperoside attenuates neuroinflammation, cognitive impairment and oxidative stress via suppressing TNF-alpha/NF-kappaB/caspase-3 signaling in type 2 diabetes rats. *Nutr Neurosci*, 1-11.
- Chen, X., Shen, W.B., Yang, P., Dong, D., Sun, W. & Yang, P. (2018b) High Glucose Inhibits Neural Stem Cell Differentiation Through Oxidative Stress and Endoplasmic Reticulum Stress. *Stem Cells Dev*, **27**, 745-755.
- Chu, C.Y., Chen, C.F., Rajendran, R.S., Shen, C.N., Chen, T.H., Yen, C.C., Chuang, C.K., Lin, D.S. & Hsiao, C.D. (2012) Overexpression of Akt1 enhances adipogenesis and leads to lipoma formation in zebrafish. *PLoS one*, **7**, e36474.
- Chuang, Y.F., An, Y., Bilgel, M., Wong, D.F., Troncoso, J.C., O'Brien, R.J., Breitner, J.C., Ferruci, L., Resnick, S.M. & Thambisetty, M. (2016) Midlife adiposity predicts earlier onset of Alzheimer's dementia, neuropathology and presymptomatic cerebral amyloid accumulation. *Mol Psychiatry*, **21**, 910-915.
- Clain, E., Haddad, J.G., Koishi, A.C., Sinigaglia, L., Rachidi, W., Despres, P., Duarte Dos Santos, C.N., Guiraud, P., Jouvenet, N. & El Kalamouni, C. (2019) The Polyphenol-Rich Extract from *Psiloxylon mauritianum*, an Endemic Medicinal Plant from Reunion Island, Inhibits the Early Stages of Dengue and Zika Virus Infection. *International journal of molecular sciences*, **20**.
- clés, C. (2019) Le diabète et les personnes diabétiques à La Réunion.
- cnr-sante (2011) <http://www.cnr-sante.fr/2011/03/les-accidents-vasculaires-cerebraux-avc-augmentation/>.
- Collaborators, G.B.D.O. & Afshin, A. & Forouzanfar, M.H. & Reitsma, M.B. & Sur, P. & Estep, K. & Lee, A. & Marczak, L. & Mokdad, A.H. & Moradi-Lakeh, M. & Naghavi, M. & Salama, J.S. & Vos, T. & Abate, K.H. & Abbafati, C. & Ahmed, M.B. & Al-Aly, Z. & Alkerwi, A. & Al-Raddadi, R. & Amare, A.T. & Amberbir, A. & Amegah, A.K. & Amini, E. & Amrock, S.M. & Anjana, R.M. & Arnlov, J. & Asayesh, H. & Banerjee, A. & Barac, A. & Baye, E. & Bennett, D.A. & Beyene, A.S. & Biadgilign, S. & Biryukov, S. & Bjertness, E. & Boneya, D.J. & Campos-Nonato, I. & Carrero, J.J. & Cecilio, P. & Cercy, K. & Ciobanu, L.G. & Cornaby, L. & Damtew, S.A. & Dandona, L. & Dandona, R. & Dharmaratne, S.D. & Duncan, B.B. & Eshrati, B. & Esteghamati, A. & Feigin, V.L. & Fernandes,



J.C. & Furst, T. & Gebrehiwot, T.T. & Gold, A. & Gona, P.N. & Goto, A. & Habtewold, T.D. & Hadush, K.T. & Hafezi-Nejad, N. & Hay, S.I. & Horino, M. & Islami, F. & Kamal, R. & Kasaeian, A. & Katikireddi, S.V. & Kengne, A.P. & Kesavachandran, C.N. & Khader, Y.S. & Khang, Y.H. & Khubchandani, J. & Kim, D. & Kim, Y.J. & Kinfu, Y. & Kosen, S. & Ku, T. & Defo, B.K. & Kumar, G.A. & Larson, H.J. & Leinsalu, M. & Liang, X. & Lim, S.S. & Liu, P. & Lopez, A.D. & Lozano, R. & Majeed, A. & Malekzadeh, R. & Malta, D.C. & Mazidi, M. & McAlinden, C. & McGarvey, S.T. & Mengistu, D.T. & Mensah, G.A. & Mensink, G.B.M. & Mezgebe, H.B. & Mirrakhimov, E.M. & Mueller, U.O. & Noubiap, J.J. & Obermeyer, C.M. & Ogbo, F.A. & Owolabi, M.O. & Patton, G.C. & Pourmalek, F. & Qorbani, M. & Rafay, A. & Rai, R.K. & Ranabhat, C.L. & Reinig, N. & Safiri, S. & Salomon, J.A. & Sanabria, J.R. & Santos, I.S. & Sartorius, B. & Sawhney, M. & Schmidhuber, J. & Schutte, A.E. & Schmidt, M.I. & Sepanlou, S.G. & Shamsizadeh, M. & Sheikhbahaei, S. & Shin, M.J. & Shiri, R. & Shiue, I. & Roba, H.S. & Silva, D.A.S. & Silverberg, J.I. & Singh, J.A. & Stranges, S. & Swaminathan, S. & Tabares-Seisdedos, R. & Tadese, F. & Tedla, B.A. & Tegegne, B.S. & Terkawi, A.S. & Thakur, J.S. & Tonelli, M. & Topor-Madry, R. & Tyrovolas, S. & Ukwaja, K.N. & Uthman, O.A. & Vaezghasemi, M. & Vasankari, T. & Vlassov, V.V. & Vollset, S.E. & Weiderpass, E. & Werdecker, A. & Wesana, J. & Westerman, R. & Yano, Y. & Yonemoto, N. & Yonga, G. & Zaidi, Z. & Zenebe, Z.M. & Zipkin, B. & Murray, C.J.L. (2017) Health Effects of Overweight and Obesity in 195 Countries over 25 Years. *N Engl J Med*, **377**, 13-27.

Colucci-D'Amato, L., Bonavita, V. & di Porzio, U. (2006) The end of the central dogma of neurobiology: stem cells and neurogenesis in adult CNS. *Neurol Sci*, **27**, 266-270.

Correale, J. & Villa, A. (2009) Cellular elements of the blood-brain barrier. *Neurochem Res*, **34**, 2067-2077.

Cosme, P., Rodriguez, A.B., Espino, J. & Garrido, M. (2020) Plant Phenolics: Bioavailability as a Key Determinant of Their Potential Health-Promoting Applications. *Antioxidants*, **9**.

Coustan, D.R. (2013) Gestational diabetes mellitus. *Clin Chem*, **59**, 1310-1321.

Cuartero, M.I., de la Parra, J., Perez-Ruiz, A., Bravo-Ferrer, I., Duran-Laforet, V., Garcia-Culebras, A., Garcia-Segura, J.M., Dhaliwal, J., Frankland, P.W., Lizasoain, I. & Moro, M.A. (2019) Abolition of aberrant neurogenesis ameliorates cognitive impairment after stroke in mice. *J Clin Invest*, **129**, 1536-1550.

Cui, X., Zuo, P., Zhang, Q., Li, X., Hu, Y., Long, J., Packer, L. & Liu, J. (2006) Chronic systemic D-galactose exposure induces memory loss, neurodegeneration, and oxidative damage in mice: protective effects of R-alpha-lipoic acid. *J Neurosci Res*, **84**, 647-654.

Cukierman-Yaffe, T., Gerstein, H.C., Williamson, J.D., Lazar, R.M., Lovato, L., Miller, M.E., Coker, L.H., Murray, A., Sullivan, M.D., Marcovina, S.M., Launer, L.J. & Action to Control Cardiovascular Risk in Diabetes-Memory in Diabetes, I. (2009) Relationship between baseline glycemic control and cognitive function in individuals with type 2 diabetes and other cardiovascular risk factors: the action to control cardiovascular risk in diabetes-memory in diabetes (ACCORD-MIND) trial. *Diabetes Care*, **32**, 221-226.

- Cummings, J., Ortiz, A., Castellino, J. & Kinney, J. (2022) Diabetes: Risk factor and translational therapeutic implications for Alzheimer's disease. *The European journal of neuroscience*.
- Curhan, G.C., Willett, W.C., Rimm, E.B., Speizer, F.E. & Stampfer, M.J. (1998) Body size and risk of kidney stones. *J Am Soc Nephrol*, **9**, 1645-1652.
- Dalton, M., Cameron, A.J., Zimmet, P.Z., Shaw, J.E., Jolley, D., Dunstan, D.W., Welborn, T.A. & AusDiab Steering, C. (2003) Waist circumference, waist-hip ratio and body mass index and their correlation with cardiovascular disease risk factors in Australian adults. *J Intern Med*, **254**, 555-563.
- Dayer, A.G., Cleaver, K.M., Abouantoun, T. & Cameron, H.A. (2005) New GABAergic interneurons in the adult neocortex and striatum are generated from different precursors. *J Cell Biol*, **168**, 415-427.
- de Leon-Guerrero, S.D., Salazar-Leon, J., Meza-Sosa, K.F., Valle-Garcia, D., Aguilar-Leon, D., Pedraza-Alva, G. & Perez-Martinez, L. (2022) An enriched environment reestablishes metabolic homeostasis by reducing obesity-induced inflammation. *Dis Model Mech*.
- de Luca, C. & Olefsky, J.M. (2008) Inflammation and insulin resistance. *FEBS Lett*, **582**, 97-105.
- de Oliveira-Carlos, V., Ganz, J., Hans, S., Kaslin, J. & Brand, M. (2013) Notch receptor expression in neurogenic regions of the adult zebrafish brain. *PLoS one*, **8**, e73384.
- de Souza Anselmo, C., Sardela, V.F., de Sousa, V.P. & Pereira, H.M.G. (2018) Zebrafish (*Danio rerio*): A valuable tool for predicting the metabolism of xenobiotics in humans? *Comp Biochem Physiol C Toxicol Pharmacol*, **212**, 34-46.
- Dekkers, I.A., Jansen, P.R. & Lamb, H.J. (2019) Obesity, Brain Volume, and White Matter Microstructure at MRI: A Cross-sectional UK Biobank Study. *Radiology*, **291**, 763-771.
- Delarue, J. & Magnan, C. (2007) Free fatty acids and insulin resistance. *Curr Opin Clin Nutr Metab Care*, **10**, 142-148.
- Delveaux, J., Turpin, C., Veeren, B., Diotel, N., Bravo, S.B., Begue, F., Alvarez, E., Meilhac, O., Bourdon, E. & Rondeau, P. (2020) Antirhea borbonica Aqueous Extract Protects Albumin and Erythrocytes from Glycoxidative Damages. *Antioxidants*, **9**.
- Dervendzi, V. (1992) Contemporary treatment with medicinal plants. . *Skopje: Tabernakul*, pp. 5–43.
- Detrich, H.W., 3rd, Westerfield, M. & Zon, L.I. (1999) Overview of the Zebrafish system. *Methods Cell Biol*, **59**, 3-10.

- Di Meo, F., Valentino, A., Petillo, O., Peluso, G., Filosa, S. & Crispi, S. (2020) Bioactive Polyphenols and Neuromodulation: Molecular Mechanisms in Neurodegeneration. *International journal of molecular sciences*, **21**.
- Diotel, N., Lubke, L., Strahle, U. & Rastegar, S. (2020) Common and Distinct Features of Adult Neurogenesis and Regeneration in the Telencephalon of Zebrafish and Mammals. *Front Neurosci*, **14**, 568930.
- Diotel, N., Vaillant, C., Gabbero, C., Mironov, S., Fostier, A., Gueguen, M.M., Anglade, I., Kah, O. & Pellegrini, E. (2013) Effects of estradiol in adult neurogenesis and brain repair in zebrafish. *Hormones and behavior*, **63**, 193-207.
- Djalalinia, S., Qorbani, M., Peykari, N. & Kelishadi, R. (2015) Health impacts of Obesity. *Pak J Med Sci*, **31**, 239-242.
- Doane, M.G. (1984) Turnover and drainage of tears. *Ann Ophthalmol*, **16**, 111-114.
- Dorseman, A.C., Lefebvre d'Hellencourt, C., Ait-Arsa, I., Jestin, E., Meilhac, O. & Diotel, N. (2017a) Acute and Chronic Models of Hyperglycemia in Zebrafish: A Method to Assess the Impact of Hyperglycemia on Neurogenesis and the Biodistribution of Radiolabeled Molecules. *Journal of visualized experiments : JoVE*.
- Dorseman, A.C., Soule, S., Weger, M., Bourdon, E., Lefebvre d'Hellencourt, C., Meilhac, O. & Diotel, N. (2017b) Impaired constitutive and regenerative neurogenesis in adult hyperglycemic zebrafish. *J Comp Neurol*, **525**, 442-458.
- Drudge, J.H., Lyons, E.T., Wyant, Z.N. & Tolliver, S.C. (1975) Occurrence of second and third instars of *Gasterophilus intestinalis* and *Gasterophilus nasalis* in stomachs of horses in Kentucky. *Am J Vet Res*, **36**, 1585-1588.
- Duckworth, W.C., Bennett, R.G. & Hamel, F.G. (1998) Insulin degradation: progress and potential. *Endocr Rev*, **19**, 608-624.
- Dugan, L.L., Sensi, S.L., Canzoniero, L.M., Handran, S.D., Rothman, S.M., Lin, T.S., Goldberg, M.P. & Choi, D.W. (1995) Mitochondrial production of reactive oxygen species in cortical neurons following exposure to N-methyl-D-aspartate. *J Neurosci*, **15**, 6377-6388.
- Durazzo, A., Lucarini, M., Souto, E.B., Cicala, C., Caiazza, E., Izzo, A.A., Novellino, E. & Santini, A. (2019) Polyphenols: A concise overview on the chemistry, occurrence, and human health. *Phytother Res*, **33**, 2221-2243.
- Dzotam, J.K., Simo, I.K., Bitchagno, G., Celik, I., Sandjo, L.P., Tane, P. & Kuete, V. (2018) In vitro antibacterial and antibiotic modifying activity of crude extract, fractions and 3',4',7-trihydroxyflavone from *Myristica fragrans* Houtt against MDR Gram-negative enteric bacteria. *BMC Complement Altern Med*, **18**, 15.

- Eames, S.C., Philipson, L.H., Prince, V.E. & Kinkel, M.D. (2010) Blood sugar measurement in zebrafish reveals dynamics of glucose homeostasis. *Zebrafish*, **7**, 205-213.
- Elagizi, A., Kachur, S., Lavie, C.J., Carbone, S., Pandey, A., Ortega, F.B. & Milani, R.V. (2018) An Overview and Update on Obesity and the Obesity Paradox in Cardiovascular Diseases. *Prog Cardiovasc Dis*, **61**, 142-150.
- Eliceiri, B.P., Gonzalez, A.M. & Baird, A. (2011) Zebrafish model of the blood-brain barrier: morphological and permeability studies. *Methods Mol Biol*, **686**, 371-378.
- Elo, B., Villano, C.M., Govorko, D. & White, L.A. (2007) Larval zebrafish as a model for glucose metabolism: expression of phosphoenolpyruvate carboxykinase as a marker for exposure to anti-diabetic compounds. *J Mol Endocrinol*, **38**, 433-440.
- Engeszer, R.E., Patterson, L.B., Rao, A.A. & Parichy, D.M. (2007) Zebrafish in the wild: a review of natural history and new notes from the field. *Zebrafish*, **4**, 21-40.
- Eriksson, P.S., Perfilieva, E., Bjork-Eriksson, T., Alborn, A.M., Nordborg, C., Peterson, D.A. & Gage, F.H. (1998) Neurogenesis in the adult human hippocampus. *Nat Med*, **4**, 1313-1317.
- Esmaeili, M.H., Enayati, M., Khabbaz Abkenar, F., Ebrahimian, F. & Salari, A.A. (2020) Glibenclamide mitigates cognitive impairment and hippocampal neuroinflammation in rats with type 2 diabetes and sporadic Alzheimer-like disease. *Behav Brain Res*, **379**, 112359.
- Esteve, E., Ricart, W. & Fernandez-Real, J.M. (2005) Dyslipidemia and inflammation: an evolutionary conserved mechanism. *Clin Nutr*, **24**, 16-31.
- Fabbrini, E., Sullivan, S. & Klein, S. (2010) Obesity and nonalcoholic fatty liver disease: biochemical, metabolic, and clinical implications. *Hepatology*, **51**, 679-689.
- Faigle, R. & Song, H. (2013) Signaling mechanisms regulating adult neural stem cells and neurogenesis. *Biochimica et biophysica acta*, **1830**, 2435-2448.
- Farzaei, M.H., Bayrami, Z., Farzaei, F., Aneva, I., Das, S.K., Patra, J.K., Das, G. & Abdollahi, M. (2020) Poisoning by Medical Plants. *Arch Iran Med*, **23**, 117-127.
- Faselis, C., Katsimardou, A., Imprialos, K., Deligkaris, P., Kallistratos, M. & Dimitriadis, K. (2020) Microvascular Complications of Type 2 Diabetes Mellitus. *Curr Vasc Pharmacol*, **18**, 117-124.
- Fernandez-Sanchez, A., Madrigal-Santillan, E., Bautista, M., Esquivel-Soto, J., Morales-Gonzalez, A., Esquivel-Chirino, C., Durante-Montiel, I., Sanchez-Rivera, G., Valadez-Vega, C. & Morales-Gonzalez, J.A. (2011) Inflammation, oxidative stress, and obesity. *International journal of molecular sciences*, **12**, 3117-3132.



- Fidge, N.H. (1999) High density lipoprotein receptors, binding proteins, and ligands. *J Lipid Res*, **40**, 187-201.
- Filiou, M.D., Arefin, A.S., Moscato, P. & Graeber, M.B. (2014) 'Neuroinflammation' differs categorically from inflammation: transcriptomes of Alzheimer's disease, Parkinson's disease, schizophrenia and inflammatory diseases compared. *Neurogenetics*, **15**, 201-212.
- Fiorentino, T.V., Prioletta, A., Zuo, P. & Folli, F. (2013) Hyperglycemia-induced oxidative stress and its role in diabetes mellitus related cardiovascular diseases. *Curr Pharm Des*, **19**, 5695-5703.
- Fischer, A. & Gessler, M. (2007) Delta-Notch--and then? Protein interactions and proposed modes of repression by Hes and Hey bHLH factors. *Nucleic Acids Res*, **35**, 4583-4596.
- Fleming, A., Diekmann, H. & Goldsmith, P. (2013) Functional characterisation of the maturation of the blood-brain barrier in larval zebrafish. *PLoS one*, **8**, e77548.
- Flynn, E.J., 3rd, Trent, C.M. & Rawls, J.F. (2009) Ontogeny and nutritional control of adipogenesis in zebrafish (*Danio rerio*). *J Lipid Res*, **50**, 1641-1652.
- Folsom, A.R., Rasmussen, M.L., Chambless, L.E., Howard, G., Cooper, L.S., Schmidt, M.I. & Heiss, G. (1999) Prospective associations of fasting insulin, body fat distribution, and diabetes with risk of ischemic stroke. The Atherosclerosis Risk in Communities (ARIC) Study Investigators. *Diabetes Care*, **22**, 1077-1083.
- Forney, L.A., Lenard, N.R., Stewart, L.K. & Henagan, T.M. (2018) Dietary Quercetin Attenuates Adipose Tissue Expansion and Inflammation and Alters Adipocyte Morphology in a Tissue-Specific Manner. *International journal of molecular sciences*, **19**.
- Fortuno, A., Rodriguez, A., Gomez-Ambrosi, J., Fruhbeck, G. & Diez, J. (2003) Adipose tissue as an endocrine organ: role of leptin and adiponectin in the pathogenesis of cardiovascular diseases. *J Physiol Biochem*, **59**, 51-60.
- Foster, M.C., Hwang, S.J., Larson, M.G., Lichtman, J.H., Parikh, N.I., Vasan, R.S., Levy, D. & Fox, C.S. (2008) Overweight, obesity, and the development of stage 3 CKD: the Framingham Heart Study. *Am J Kidney Dis*, **52**, 39-48.
- Franco, S.J. & Muller, U. (2013) Shaping our minds: stem and progenitor cell diversity in the mammalian neocortex. *Neuron*, **77**, 19-34.
- Fuentealba, L.C., Rompani, S.B., Parraguez, J.I., Obernier, K., Romero, R., Cepko, C.L. & Alvarez-Buylla, A. (2015) Embryonic Origin of Postnatal Neural Stem Cells. *Cell*, **161**, 1644-1655.

- Furutachi, S., Miya, H., Watanabe, T., Kawai, H., Yamasaki, N., Harada, Y., Imayoshi, I., Nelson, M., Nakayama, K.I., Hirabayashi, Y. & Gotoh, Y. (2015) Slowly dividing neural progenitors are an embryonic origin of adult neural stem cells. *Nat Neurosci*, **18**, 657-665.
- Gage, F.H. (2000) Mammalian neural stem cells. *Science*, **287**, 1433-1438.
- Gaillard, P.J., de Boer, A.B. & Breimer, D.D. (2003) Pharmacological investigations on lipopolysaccharide-induced permeability changes in the blood-brain barrier in vitro. *Microvasc Res*, **65**, 24-31.
- Gama Sosa, M.A., De Gasperi, R. & Elder, G.A. (2012) Modeling human neurodegenerative diseases in transgenic systems. *Hum Genet*, **131**, 535-563.
- Gammill, L.S. & Bronner-Fraser, M. (2003) Neural crest specification: migrating into genomics. *Nat Rev Neurosci*, **4**, 795-805.
- Garcia, G.R., Noyes, P.D. & Tanguay, R.L. (2016) Advancements in zebrafish applications for 21st century toxicology. *Pharmacol Ther*, **161**, 11-21.
- Geethalakshmi, R., Sundaramurthi, J.C. & Sarada, D.V.L. (2018) Antibacterial activity of flavonoid isolated from *Trianthema decandra* against *Pseudomonas aeruginosa* and molecular docking study of FabZ. *Microb Pathog*, **121**, 87-92.
- Gerhard, G.S., Kauffman, E.J., Wang, X., Stewart, R., Moore, J.L., Kasales, C.J., Demidenko, E. & Cheng, K.C. (2002) Life spans and senescent phenotypes in two strains of Zebrafish (*Danio rerio*). *Exp Gerontol*, **37**, 1055-1068.
- Ghaddar, B., Bringart, M., Lefebvre d'Hellencourt, C., Meilhac, O. & Diotel, N. (2021a) Deleterious Effects of Overfeeding on Brain Homeostasis and Plasticity in Adult Zebrafish. *Zebrafish*, **18**, 190-206.
- Ghaddar, B., Gence, L., Veeren, B., Bringart, M., Bascands, J.L., Meilhac, O. & Diotel, N. (2022) Aqueous extract of *Psilocybe mauritianum* prevents obesity and associated deleterious effects in zebrafish. *IJMS*, **23**, 27.
- Ghaddar, B., Lubke, L., Couret, D., Rastegar, S. & Diotel, N. (2021b) Cellular Mechanisms Participating in Brain Repair of Adult Zebrafish and Mammals after Injury. *Cells*, **10**.
- Ghaddar, B., Veeren, B., Rondeau, P., Bringart, M., Lefebvre d'Hellencourt, C., Meilhac, O., Bascands, J.L. & Diotel, N. (2020) Impaired brain homeostasis and neurogenesis in diet-induced overweight zebrafish: a preventive role from *A. borbonica* extract. *Scientific reports*, **10**, 14496.

- Ghowzi, M., Qalekhani, F., Farzaei, M.H., Mahmudii, F., Yousofvand, N. & Joshi, T. (2021) Inflammation, oxidative stress, insulin resistance, and hypertension as mediators for adverse effects of obesity on the brain: A review. *Biomedicine (Taipei)*, **11**, 13-22.
- Ghribi, O., Golovko, M.Y., Larsen, B., Schrag, M. & Murphy, E.J. (2006) Deposition of iron and beta-amyloid plaques is associated with cortical cellular damage in rabbits fed with long-term cholesterol-enriched diets. *J Neurochem*, **99**, 438-449.
- Ghussen, F. & Kruger, I. (1989) Technical aspects of isolation extremity perfusion: experimental studies and clinical experience. *J Invest Surg*, **2**, 487-496.
- Giachino, C., Basak, O., Lugert, S., Knuckles, P., Obernier, K., Fiorelli, R., Frank, S., Raineteau, O., Alvarez-Buylla, A. & Taylor, V. (2014) Molecular diversity subdivides the adult forebrain neural stem cell population. *Stem cells*, **32**, 70-84.
- Gingrich, M.B. & Traynelis, S.F. (2000) Serine proteases and brain damage - is there a link? *Trends Neurosci*, **23**, 399-407.
- Giraud-Techer, S., Amédé, J., Girard-Valenciennes, E., Thomas, H., Brillant, S., Grondin, I., Marodon, C. & Smadja, J. (2016) Plantes médicinales de La Réunion inscrites à la Pharmacopée française. *Ethnopharmacologia*, **56**, 7–33.
- Goessling, W. & Sadler, K.C. (2015) Zebrafish: an important tool for liver disease research. *Gastroenterology*, **149**, 1361-1377.
- Goldstone, J.V., McArthur, A.G., Kubota, A., Zanette, J., Parente, T., Jonsson, M.E., Nelson, D.R. & Stegeman, J.J. (2010) Identification and developmental expression of the full complement of Cytochrome P450 genes in Zebrafish. *BMC Genomics*, **11**, 643.
- Gotz, M. & Huttner, W.B. (2005) The cell biology of neurogenesis. *Nat Rev Mol Cell Biol*, **6**, 777-788.
- Gould, E., Reeves, A.J., Graziano, M.S. & Gross, C.G. (1999) Neurogenesis in the neocortex of adult primates. *Science*, **286**, 548-552.
- Grabska-Kobylecka, I., Kaczmarek-Bak, J., Figlus, M., Prymont-Przyminska, A., Zwolinska, A., Sarniak, A., Wlodarczyk, A., Glabinski, A. & Nowak, D. (2020) The Presence of Caffeic Acid in Cerebrospinal Fluid: Evidence That Dietary Polyphenols Can Cross the Blood-Brain Barrier in Humans. *Nutrients*, **12**.
- Graeber, M.B., Li, W. & Rodriguez, M.L. (2011) Role of microglia in CNS inflammation. *FEBS Lett*, **585**, 3798-3805.
- Grandel, H. & Brand, M. (2013) Comparative aspects of adult neural stem cell activity in vertebrates. *Dev Genes Evol*, **223**, 131-147.

- Grandel, H., Kaslin, J., Ganz, J., Wenzel, I. & Brand, M. (2006) Neural stem cells and neurogenesis in the adult zebrafish brain: origin, proliferation dynamics, migration and cell fate. *Dev Biol*, **295**, 263-277.
- Gray, D.S. & Fujioka, K. (1991) Use of relative weight and Body Mass Index for the determination of adiposity. *Journal of clinical epidemiology*, **44**, 545-550.
- Gu, Z., Kaul, M., Yan, B., Kridel, S.J., Cui, J., Strongin, A., Smith, J.W., Liddington, R.C. & Lipton, S.A. (2002) S-nitrosylation of matrix metalloproteinases: signaling pathway to neuronal cell death. *Science*, **297**, 1186-1190.
- Gulcin, I. (2006) Antioxidant activity of caffeic acid (3,4-dihydroxycinnamic acid). *Toxicology*, **217**, 213-220.
- Guo, J., Yu, C., Li, H., Liu, F., Feng, R., Wang, H., Meng, Y., Li, Z., Ju, G. & Wang, J. (2010) Impaired neural stem/progenitor cell proliferation in streptozotocin-induced and spontaneous diabetic mice. *Neurosci Res*, **68**, 329-336.
- Gurib-Fakim, A. & Brendler, T.S. (2004) Medicinal and aromatic plants of Indian Ocean islands: Madagascar, Comoros, Seychelles and Mascarenes; . *Medpharm Scientific Publications; Germany*, 400–401.
- Gustafson, D.R., Karlsson, C., Skoog, I., Rosengren, L., Lissner, L. & Blennow, K. (2007) Mid-life adiposity factors relate to blood-brain barrier integrity in late life. *J Intern Med*, **262**, 643-650.
- Hagihara, H., Takao, K., Walton, N.M., Matsumoto, M. & Miyakawa, T. (2013) Immature dentate gyrus: an endophenotype of neuropsychiatric disorders. *Neural Plast*, **2013**, 318596.
- Hajiluan, G., Abbasalizad Farhangi, M., Nameni, G., Shahabi, P. & Megari-Abbasi, M. (2018) Oxidative stress-induced cognitive impairment in obesity can be reversed by vitamin D administration in rats. *Nutr Neurosci*, **21**, 744-752.
- Haley, M.J. & Lawrence, C.B. (2016) Obesity and stroke: Can we translate from rodents to patients? *J Cereb Blood Flow Metab*, **36**, 2007-2021.
- Hamada, H., Watanabe, M., Lau, H.E., Nishida, T., Hasegawa, T., Parichy, D.M. & Kondo, S. (2014) Involvement of Delta/Notch signaling in zebrafish adult pigment stripe patterning. *Development*, **141**, 318-324.
- Hanson, A.J., Bayer, J.L., Baker, L.D., Cholerton, B., VanFossen, B., Trittschuh, E., Rissman, R.A., Donohue, M.C., Moghadam, S.H., Plymate, S.R. & Craft, S. (2015) Differential Effects of Meal Challenges on Cognition, Metabolism, and Biomarkers for Apolipoprotein E varepsilon4 Carriers and Adults with Mild Cognitive Impairment. *J Alzheimers Dis*, **48**, 205-218.



- Hao, S., Dey, A., Yu, X. & Stranahan, A.M. (2016) Dietary obesity reversibly induces synaptic stripping by microglia and impairs hippocampal plasticity. *Brain Behav Immun*, **51**, 230-239.
- Harreiter, J. & Roden, M. (2019) [Diabetes mellitus-Definition, classification, diagnosis, screening and prevention (Update 2019)]. *Wiener klinische Wochenschrift*, **131**, 6-15.
- Hartfuss, E., Galli, R., Heins, N. & Gotz, M. (2001) Characterization of CNS precursor subtypes and radial glia. *Developmental biology*, **229**, 15-30.
- Hasumura, T., Shimada, Y., Kuroyanagi, J., Nishimura, Y., Meguro, S., Takema, Y. & Tanaka, T. (2012) Green tea extract suppresses adiposity and affects the expression of lipid metabolism genes in diet-induced obese zebrafish. *Nutr Metab (Lond)*, **9**, 73.
- Hawkins, B.T. & Davis, T.P. (2005) The blood-brain barrier/neurovascular unit in health and disease. *Pharmacol Rev*, **57**, 173-185.
- Hawkins, B.T., Lundeen, T.F., Norwood, K.M., Brooks, H.L. & Egleton, R.D. (2007) Increased blood-brain barrier permeability and altered tight junctions in experimental diabetes in the rat: contribution of hyperglycaemia and matrix metalloproteinases. *Diabetologia*, **50**, 202-211.
- Henning, R.J. (2018) Type-2 diabetes mellitus and cardiovascular disease. *Future Cardiol*, **14**, 491-509.
- Hicks, C.W. & Selvin, E. (2019) Epidemiology of Peripheral Neuropathy and Lower Extremity Disease in Diabetes. *Curr Diab Rep*, **19**, 86.
- Hierro-Bujalance, C., Del Marco, A., Jose Ramos-Rodriguez, J., Infante-Garcia, C., Bella Gomez-Santos, S., Herrera, M. & Garcia-Alloza, M. (2020) Cell proliferation and neurogenesis alterations in Alzheimer's disease and diabetes mellitus mixed murine models. *J Neurochem*, **154**, 673-692.
- Hiramitsu, M., Shimada, Y., Kuroyanagi, J., Inoue, T., Katagiri, T., Zang, L., Nishimura, Y., Nishimura, N. & Tanaka, T. (2014) Eriocitrin ameliorates diet-induced hepatic steatosis with activation of mitochondrial biogenesis. *Scientific reports*, **4**, 3708.
- Ho, A.J., Raji, C.A., Becker, J.T., Lopez, O.L., Kuller, L.H., Hua, X., Lee, S., Hibar, D., Dinov, I.D., Stein, J.L., Jack, C.R., Jr., Weiner, M.W., Toga, A.W., Thompson, P.M., Cardiovascular Health, S. & Adni (2010) Obesity is linked with lower brain volume in 700 AD and MCI patients. *Neurobiol Aging*, **31**, 1326-1339.
- Ho, N., Sommers, M.S. & Lucki, I. (2013) Effects of diabetes on hippocampal neurogenesis: links to cognition and depression. *Neurosci Biobehav Rev*, **37**, 1346-1362.

- Hollands, C., Tobin, M.K., Hsu, M., Musaraca, K., Yu, T.S., Mishra, R., Kernie, S.G. & Lazarov, O. (2017) Depletion of adult neurogenesis exacerbates cognitive deficits in Alzheimer's disease by compromising hippocampal inhibition. *Mol Neurodegener*, **12**, 64.
- Hommelberg, P.P., Plat, J., Langen, R.C., Schols, A.M. & Mensink, R.P. (2009) Fatty acid-induced NF-kappaB activation and insulin resistance in skeletal muscle are chain length dependent. *Am J Physiol Endocrinol Metab*, **296**, E114-120.
- Hong, H., Kim, B.S. & Im, H.I. (2016) Pathophysiological Role of Neuroinflammation in Neurodegenerative Diseases and Psychiatric Disorders. *Int Neurol J*, **20**, S2-7.
- Horgusluoglu, E., Nudelman, K., Nho, K. & Saykin, A.J. (2017) Adult neurogenesis and neurodegenerative diseases: A systems biology perspective. *Am J Med Genet B Neuropsychiatr Genet*, **174**, 93-112.
- Howe, K. & Clark, M.D. & Torroja, C.F. & Torrance, J. & Berthelot, C. & Muffato, M. & Collins, J.E. & Humphray, S. & McLaren, K. & Matthews, L. & McLaren, S. & Sealy, I. & Caccamo, M. & Churcher, C. & Scott, C. & Barrett, J.C. & Koch, R. & Rauch, G.J. & White, S. & Chow, W. & Kilian, B. & Quintais, L.T. & Guerra-Assuncao, J.A. & Zhou, Y. & Gu, Y. & Yen, J. & Vogel, J.H. & Eyre, T. & Redmond, S. & Banerjee, R. & Chi, J. & Fu, B. & Langley, E. & Maguire, S.F. & Laird, G.K. & Lloyd, D. & Kenyon, E. & Donaldson, S. & Sehra, H. & Almeida-King, J. & Loveland, J. & Trevanion, S. & Jones, M. & Quail, M. & Willey, D. & Hunt, A. & Burton, J. & Sims, S. & McLay, K. & Plumb, B. & Davis, J. & Clee, C. & Oliver, K. & Clark, R. & Riddle, C. & Elliot, D. & Threadgold, G. & Harden, G. & Ware, D. & Begum, S. & Mortimore, B. & Kerry, G. & Heath, P. & Phillimore, B. & Tracey, A. & Corby, N. & Dunn, M. & Johnson, C. & Wood, J. & Clark, S. & Pelan, S. & Griffiths, G. & Smith, M. & Glithero, R. & Howden, P. & Barker, N. & Lloyd, C. & Stevens, C. & Harley, J. & Holt, K. & Panagiotidis, G. & Lovell, J. & Beasley, H. & Henderson, C. & Gordon, D. & Auger, K. & Wright, D. & Collins, J. & Raisen, C. & Dyer, L. & Leung, K. & Robertson, L. & Ambridge, K. & Leongamornlert, D. & McGuire, S. & Gilderthorp, R. & Griffiths, C. & Manthavadi, D. & Nichol, S. & Barker, G. & Whitehead, S. & Kay, M. & Brown, J. & Murnane, C. & Gray, E. & Humphries, M. & Sycamore, N. & Barker, D. & Saunders, D. & Wallis, J. & Babbage, A. & Hammond, S. & Mashreghi-Mohammadi, M. & Barr, L. & Martin, S. & Wray, P. & Ellington, A. & Matthews, N. & Ellwood, M. & Woodmansey, R. & Clark, G. & Cooper, J. & Tromans, A. & Grafham, D. & Skuce, C. & Pandian, R. & Andrews, R. & Harrison, E. & Kimberley, A. & Garnett, J. & Fosker, N. & Hall, R. & Garner, P. & Kelly, D. & Bird, C. & Palmer, S. & Gehring, I. & Berger, A. & Dooley, C.M. & Ersan-Urun, Z. & Eser, C. & Geiger, H. & Geisler, M. & Karotki, L. & Kirn, A. & Konantz, J. & Konantz, M. & Oberlander, M. & Rudolph-Geiger, S. & Teucke, M. & Lanz, C. & Raddatz, G. & Osoegawa, K. & Zhu, B. & Rapp, A. & Widaa, S. & Langford, C. & Yang, F. & Schuster, S.C. & Carter, N.P. & Harrow, J. & Ning, Z. & Herrero, J. & Searle, S.M. & Enright, A. & Geisler, R. & Plasterk, R.H. & Lee, C. & Westerfield, M. & de Jong, P.J. & Zon, L.I. & Postlethwait, J.H. & Nusslein-Volhard, C. & Hubbard, T.J. & Roest Crolius, H. & Rogers, J. & Stemple, D.L. (2013) The zebrafish reference genome sequence and its relationship to the human genome. *Nature*, **496**, 498-503.
- Huang, H. & Wu, Q. (2010) Cloning and comparative analyses of the zebrafish Ugt repertoire reveal its evolutionary diversity. *PLoS one*, **5**, e9144.

- Huber, J.D., Egleton, R.D. & Davis, T.P. (2001) Molecular physiology and pathophysiology of tight junctions in the blood-brain barrier. *Trends Neurosci*, **24**, 719-725.
- Hwang, I.K., Kim, I.Y., Kim, D.W., Yoo, K.Y., Kim, Y.N., Yi, S.S., Won, M.H., Lee, I.S., Yoon, Y.S. & Seong, J.K. (2008) Strain-specific differences in cell proliferation and differentiation in the dentate gyrus of C57BL/6N and C3H/HeN mice fed a high fat diet. *Brain Res*, **1241**, 1-6.
- Hwang, K.L. & Goessling, W. (2016) Baiting for Cancer: Using the Zebrafish as a Model in Liver and Pancreatic Cancer. *Adv Exp Med Biol*, **916**, 391-410.
- Intine, R.V., Olsen, A.S. & Sarras, M.P., Jr. (2013) A zebrafish model of diabetes mellitus and metabolic memory. *Journal of visualized experiments : JoVE*, e50232.
- Ishii, H., Jirousek, M.R., Koya, D., Takagi, C., Xia, P., Clermont, A., Bursell, S.E., Kern, T.S., Ballas, L.M., Heath, W.F., Stramm, L.E., Feener, E.P. & King, G.L. (1996) Amelioration of vascular dysfunctions in diabetic rats by an oral PKC beta inhibitor. *Science*, **272**, 728-731.
- Islam, M.S. & Loots du, T. (2009) Experimental rodent models of type 2 diabetes: a review. *Methods Find Exp Clin Pharmacol*, **31**, 249-261.
- Jackson, G.R., Werrbach-Perez, K., Pan, Z., Sampath, D. & Perez-Polo, J.R. (1994) Neurotrophin regulation of energy homeostasis in the central nervous system. *Dev Neurosci*, **16**, 285-290.
- Jais, A. & Bruning, J.C. (2017) Hypothalamic inflammation in obesity and metabolic disease. *J Clin Invest*, **127**, 24-32.
- Jakubs, K., Bonde, S., Iosif, R.E., Ekdahl, C.T., Kokaia, Z., Kokaia, M. & Lindvall, O. (2008) Inflammation regulates functional integration of neurons born in adult brain. *J Neurosci*, **28**, 12477-12488.
- Jeon, B.T., Jeong, E.A., Shin, H.J., Lee, Y., Lee, D.H., Kim, H.J., Kang, S.S., Cho, G.J., Choi, W.S. & Roh, G.S. (2012) Resveratrol attenuates obesity-associated peripheral and central inflammation and improves memory deficit in mice fed a high-fat diet. *Diabetes*, **61**, 1444-1454.
- Jeong, J.Y., Kwon, H.B., Ahn, J.C., Kang, D., Kwon, S.H., Park, J.A. & Kim, K.W. (2008) Functional and developmental analysis of the blood-brain barrier in zebrafish. *Brain Res Bull*, **75**, 619-628.
- Jonville, M.C., Kodja, H., Humeau, L., Fournel, J., De Mol, P., Cao, M., Angenot, L. & Frederich, M. (2008) Screening of medicinal plants from Reunion Island for antimalarial and cytotoxic activity. *J Ethnopharmacol*, **120**, 382-386.
- Jorgensen, C. & Wang, Z. (2020) Hormonal Regulation of Mammalian Adult Neurogenesis: A Multifaceted Mechanism. *Biomolecules*, **10**.

- Jorgensen, H., Nakayama, H., Raaschou, H.O. & Olsen, T.S. (1994) Stroke in patients with diabetes. The Copenhagen Stroke Study. *Stroke*, **25**, 1977-1984.
- Jung, U.J. & Choi, M.S. (2014) Obesity and its metabolic complications: the role of adipokines and the relationship between obesity, inflammation, insulin resistance, dyslipidemia and nonalcoholic fatty liver disease. *International journal of molecular sciences*, **15**, 6184-6223.
- Jurczyk, A., Roy, N., Bajwa, R., Gut, P., Lipson, K., Yang, C., Covassin, L., Racki, W.J., Rossini, A.A., Phillips, N., Stainier, D.Y., Greiner, D.L., Brehm, M.A., Bortell, R. & dilorio, P. (2011) Dynamic glucoregulation and mammalian-like responses to metabolic and developmental disruption in zebrafish. *Gen Comp Endocrinol*, **170**, 334-345.
- Jurisch-Yaksi, N., Yaksi, E. & Kizil, C. (2020) Radial glia in the zebrafish brain: Functional, structural, and physiological comparison with the mammalian glia. *Glia*, **68**, 2451-2470.
- Kadry, H., Noorani, B. & Cucullo, L. (2020) A blood-brain barrier overview on structure, function, impairment, and biomarkers of integrity. *Fluids Barriers CNS*, **17**, 69.
- Kamal, A., Biessels, G.J., Urban, I.J. & Gispen, W.H. (1999) Hippocampal synaptic plasticity in streptozotocin-diabetic rats: impairment of long-term potentiation and facilitation of long-term depression. *Neuroscience*, **90**, 737-745.
- Kang, S., Shin, H. & Kim, S. (2012) Immature Citrus sunki Peel Extract Exhibits Antiobesity Effects by  $\beta$ -Oxidation and Lipolysis in High-Fat Diet-Induced Obese Mice.
- Kanoski, S.E., Zhang, Y., Zheng, W. & Davidson, T.L. (2010) The effects of a high-energy diet on hippocampal function and blood-brain barrier integrity in the rat. *J Alzheimers Dis*, **21**, 207-219.
- Kaplan, M.S. (1985) Formation and turnover of neurons in young and senescent animals: an electronmicroscopic and morphometric analysis. *Ann N Y Acad Sci*, **457**, 173-192.
- Kari, G., Rodeck, U. & Dicker, A.P. (2007) Zebrafish: an emerging model system for human disease and drug discovery. *Clin Pharmacol Ther*, **82**, 70-80.
- Kaslin, J., Ganz, J. & Brand, M. (2008) Proliferation, neurogenesis and regeneration in the non-mammalian vertebrate brain. *Philos Trans R Soc Lond B Biol Sci*, **363**, 101-122.
- Kaur, R., Kaur, M. & Singh, J. (2018) Endothelial dysfunction and platelet hyperactivity in type 2 diabetes mellitus: molecular insights and therapeutic strategies. *Cardiovasc Diabetol*, **17**, 121.
- Kawai, H., Kawaguchi, D., Kuebrich, B.D., Kitamoto, T., Yamaguchi, M., Gotoh, Y. & Furutachi, S. (2017) Area-Specific Regulation of Quiescent Neural Stem Cells by Notch3 in the Adult Mouse Subependymal Zone. *J Neurosci*, **37**, 11867-11880.



- Khan, N.I., Naz, L. & Yasmeen, G. (2006) Obesity: an independent risk factor for systemic oxidative stress. *Pak J Pharm Sci*, **19**, 62-65.
- Khare, P., Datusalia, A.K. & Sharma, S.S. (2017) Parthenolide, an NF-kappaB Inhibitor Ameliorates Diabetes-Induced Behavioural Deficit, Neurotransmitter Imbalance and Neuroinflammation in Type 2 Diabetes Rat Model. *Neuromolecular Med*, **19**, 101-112.
- Kim, G.S., Park, H.J., Woo, J.H., Kim, M.K., Koh, P.O., Min, W., Ko, Y.G., Kim, C.H., Won, C.K. & Cho, J.H. (2012) Citrus aurantium flavonoids inhibit adipogenesis through the Akt signaling pathway in 3T3-L1 cells. *BMC Complement Altern Med*, **12**, 31.
- Kim, H.S., Quon, M.J. & Kim, J.A. (2014) New insights into the mechanisms of polyphenols beyond antioxidant properties; lessons from the green tea polyphenol, epigallocatechin 3-gallate. *Redox Biol*, **2**, 187-195.
- Kimmel, R.A., Dobler, S., Schmitner, N., Walsen, T., Freudenblum, J. & Meyer, D. (2015) Diabetic pdx1-mutant zebrafish show conserved responses to nutrient overload and anti-glycemic treatment. *Scientific reports*, **5**, 14241.
- Kinkel, M.D. & Prince, V.E. (2009) On the diabetic menu: zebrafish as a model for pancreas development and function. *Bioessays*, **31**, 139-152.
- Kishimoto, N., Shimizu, K. & Sawamoto, K. (2012) Neuronal regeneration in a zebrafish model of adult brain injury. *Dis Model Mech*, **5**, 200-209.
- Kissela, B.M., Khoury, J., Kleindorfer, D., Woo, D., Schneider, A., Alwell, K., Miller, R., Ewing, I., Moomaw, C.J., Szaflarski, J.P., Gebel, J., Shukla, R. & Broderick, J.P. (2005) Epidemiology of ischemic stroke in patients with diabetes: the greater Cincinnati/Northern Kentucky Stroke Study. *Diabetes Care*, **28**, 355-359.
- Kivipelto, M., Ngandu, T., Fratiglioni, L., Viitanen, M., Kareholt, I., Winblad, B., Helkala, E.L., Tuomilehto, J., Soininen, H. & Nissinen, A. (2005) Obesity and vascular risk factors at midlife and the risk of dementia and Alzheimer disease. *Arch Neurol*, **62**, 1556-1560.
- Kizil, C., Kyritsis, N., Dudczig, S., Kroehne, V., Freudenreich, D., Kaslin, J. & Brand, M. (2012) Regenerative neurogenesis from neural progenitor cells requires injury-induced expression of Gata3. *Dev Cell*, **23**, 1230-1237.
- Kobessho, H., Oishi, K., Hamaguchi, H. & Kanda, F. (2008) Elevation of cerebrospinal fluid protein in patients with diabetes mellitus is associated with duration of diabetes. *Eur Neurol*, **60**, 132-136.
- Kokoeva, M.V., Yin, H. & Flier, J.S. (2005) Neurogenesis in the hypothalamus of adult mice: potential role in energy balance. *Science*, **310**, 679-683.

- Kopf, D. & Frolich, L. (2009) Risk of incident Alzheimer's disease in diabetic patients: a systematic review of prospective trials. *J Alzheimers Dis*, **16**, 677-685.
- Kozakova, M., Palombo, C., Morizzo, C., Hojlund, K., Hatunic, M., Balkau, B., Nilsson, P.M. & Ferrannini, E. (2015) Obesity and carotid artery remodeling. *Nutr Diabetes*, **5**, e177.
- Kozol, R.A., Abrams, A.J., James, D.M., Buglo, E., Yan, Q. & Dallman, J.E. (2016) Function Over Form: Modeling Groups of Inherited Neurological Conditions in Zebrafish. *Front Mol Neurosci*, **9**, 55.
- Krezymon, A., Richetin, K., Halley, H., Roybon, L., Lassalle, J.M., Frances, B., Verret, L. & Rampon, C. (2013) Modifications of hippocampal circuits and early disruption of adult neurogenesis in the tg2576 mouse model of Alzheimer's disease. *PLoS one*, **8**, e76497.
- Kroehne, V., Freudenreich, D., Hans, S., Kaslin, J. & Brand, M. (2011) Regeneration of the adult zebrafish brain from neurogenic radial glia-type progenitors. *Development*, **138**, 4831-4841.
- Kroner, Z. (2009) The relationship between Alzheimer's disease and diabetes: Type 3 diabetes? *Altern Med Rev*, **14**, 373-379.
- Kuai, R., Li, D., Chen, Y.E., Moon, J.J. & Schwendeman, A. (2016) High-Density Lipoproteins: Nature's Multifunctional Nanoparticles. *ACS Nano*, **10**, 3015-3041.
- Kumar, P., Raman, T., Swain, M.M., Mishra, R. & Pal, A. (2017) Hyperglycemia-Induced Oxidative-Nitrosative Stress Induces Inflammation and Neurodegeneration via Augmented Tuberous Sclerosis Complex-2 (TSC-2) Activation in Neuronal Cells. *Mol Neurobiol*, **54**, 238-254.
- Kumar Singh, S. & Patra, A. (2018) Evaluation of phenolic composition, antioxidant, anti-inflammatory and anticancer activities of *Polygonatum verticillatum* (L.). *J Integr Med*, **16**, 273-282.
- Kyritsis, N., Kizil, C., Zocher, S., Kroehne, V., Kaslin, J., Freudenreich, D., Iltzche, A. & Brand, M. (2012) Acute inflammation initiates the regenerative response in the adult zebrafish brain. *Science*, **338**, 1353-1356.
- Lagace, D.C., Whitman, M.C., Noonan, M.A., Ables, J.L., DeCarolis, N.A., Arguello, A.A., Donovan, M.H., Fischer, S.J., Farnbauch, L.A., Beech, R.D., DiLeone, R.J., Greer, C.A., Mandyam, C.D. & Eisch, A.J. (2007) Dynamic contribution of nestin-expressing stem cells to adult neurogenesis. *J Neurosci*, **27**, 12623-12629.
- Lama, A., Pirozzi, C., Severi, I., Morgese, M.G., Senzacqua, M., Annunziata, C., Comella, F., Del Piano, F., Schiavone, S., Petrosino, S., Mollica, M.P., Diano, S., Trabace, L., Calignano, A., Giordano, A., Mattace Raso, G. & Meli, R. (2022) Palmitoylethanolamide dampens neuroinflammation and anxiety-like behavior in obese mice. *Brain Behav Immun*, **102**, 110-123.

- Landgraf, K., Schuster, S., Meusel, A., Garten, A., Riemer, T., Schleinitz, D., Kiess, W. & Korner, A. (2017) Short-term overfeeding of zebrafish with normal or high-fat diet as a model for the development of metabolically healthy versus unhealthy obesity. *BMC Physiol*, **17**, 4.
- Lang, B.T., Yan, Y., Dempsey, R.J. & Vemuganti, R. (2009) Impaired neurogenesis in adult type-2 diabetic rats. *Brain Res*, **1258**, 25-33.
- Lasselin, J., Magne, E., Beau, C., Aubert, A., Dexpert, S., Carrez, J., Laye, S., Forestier, D., Ledaguenel, P. & Capuron, L. (2016) Low-grade inflammation is a major contributor of impaired attentional set shifting in obese subjects. *Brain Behav Immun*, **58**, 63-68.
- Lavergne, R. (1989) Plantes médicinales indigènes: Tisanerie et tisaneurs de la Réunion *II-Sciences et Techniques du Languedoc*; . Université Montpellier Montpellier, France: .
- Lawrence, T. (2009) The nuclear factor NF-kappaB pathway in inflammation. *Cold Spring Harb Perspect Biol*, **1**, a001651.
- Lazutkin, A., Podgorny, O. & Enikolopov, G. (2019) Modes of division and differentiation of neural stem cells. *Behav Brain Res*, **374**, 112118.
- Le Sage, F., Meilhac, O. & Gonthier, M.P. (2017) Anti-inflammatory and antioxidant effects of polyphenols extracted from *Antirhea borbonica* medicinal plant on adipocytes exposed to *Porphyromonas gingivalis* and *Escherichia coli* lipopolysaccharides. *Pharmacol Res*, **119**, 303-312.
- Lebovitz, H.E. (2001) Insulin resistance: definition and consequences. *Exp Clin Endocrinol Diabetes*, **109 Suppl 2**, S135-148.
- Ledoux, A., Cao, M., Jansen, O., Mamede, L., Campos, P.E., Payet, B., Clerc, P., Grondin, I., Girard-Valenciennes, E., Hermann, T., Litaudon, M., Vanderheydt, C., Delang, L., Neyts, J., Leyssen, P., Frederich, M. & Smadja, J. (2018) Antiplasmodial, anti-chikungunya virus and antioxidant activities of 64 endemic plants from the Mascarene Islands. *Int J Antimicrob Agents*, **52**, 622-628.
- Lee, H.J., Choi, E.K., Lee, S.H., Kim, Y.J., Han, K.D. & Oh, S. (2018) Risk of ischemic stroke in metabolically healthy obesity: A nationwide population-based study. *PloS one*, **13**, e0195210.
- Lee, M., Oh, M.S., Jung, S., Lee, J.H., Kim, C.H., Jang, M.U., Kim, Y.E., Bae, H.J., Park, J., Kang, Y., Lee, B.C., Lim, J.S. & Yu, K.H. (2021) Differential effects of body mass index on domain-specific cognitive outcomes after stroke. *Scientific reports*, **11**, 14168.
- Lehner, C., Gehwolf, R., Tempfer, H., Krizbai, I., Hennig, B., Bauer, H.C. & Bauer, H. (2011) Oxidative stress and blood-brain barrier dysfunction under particular consideration of matrix metalloproteinases. *Antioxid Redox Signal*, **15**, 1305-1323.

- Leisherer, A., Stoemmer, K., Muendlein, A., Saely, C.H., Kinz, E., Brandtner, E.M., Fraunberger, P. & Drexel, H. (2016) Quercetin Impacts Expression of Metabolism- and Obesity-Associated Genes in SGBS Adipocytes. *Nutrients*, **8**.
- Lein, E.S. & Hawrylycz, M.J. & Ao, N. & Ayres, M. & Bensinger, A. & Bernard, A. & Boe, A.F. & Boguski, M.S. & Brockway, K.S. & Byrnes, E.J. & Chen, L. & Chen, L. & Chen, T.M. & Chin, M.C. & Chong, J. & Crook, B.E. & Czaplinska, A. & Dang, C.N. & Datta, S. & Dee, N.R. & Desaki, A.L. & Desta, T. & Diep, E. & Dolbeare, T.A. & Donelan, M.J. & Dong, H.W. & Dougherty, J.G. & Duncan, B.J. & Ebbert, A.J. & Eichele, G. & Estin, L.K. & Faber, C. & Facer, B.A. & Fields, R. & Fischer, S.R. & Fliss, T.P. & Frensley, C. & Gates, S.N. & Glattfelder, K.J. & Halverson, K.R. & Hart, M.R. & Hohmann, J.G. & Howell, M.P. & Jeung, D.P. & Johnson, R.A. & Karr, P.T. & Kawal, R. & Kidney, J.M. & Knapik, R.H. & Kuan, C.L. & Lake, J.H. & Laramee, A.R. & Larsen, K.D. & Lau, C. & Lemon, T.A. & Liang, A.J. & Liu, Y. & Luong, L.T. & Michaels, J. & Morgan, J.J. & Morgan, R.J. & Mortrud, M.T. & Mosqueda, N.F. & Ng, L.L. & Ng, R. & Orta, G.J. & Overly, C.C. & Pak, T.H. & Parry, S.E. & Pathak, S.D. & Pearson, O.C. & Puchalski, R.B. & Riley, Z.L. & Rockett, H.R. & Rowland, S.A. & Royall, J.J. & Ruiz, M.J. & Sarno, N.R. & Schaffnit, K. & Shapovalova, N.V. & Sivisay, T. & Slaughterbeck, C.R. & Smith, S.C. & Smith, K.A. & Smith, B.I. & Sodt, A.J. & Stewart, N.N. & Stumpf, K.R. & Sunkin, S.M. & Sutram, M. & Tam, A. & Teemer, C.D. & Thaller, C. & Thompson, C.L. & Varnam, L.R. & Visel, A. & Whitlock, R.M. & Wohnoutka, P.E. & Wolkey, C.K. & Wong, V.Y. & Wood, M. & Yaylaoglu, M.B. & Young, R.C. & Youngstrom, B.L. & Yuan, X.F. & Zhang, B. & Zwingman, T.A. & Jones, A.R. (2007) Genome-wide atlas of gene expression in the adult mouse brain. *Nature*, **445**, 168-176.
- Leto, D. & Saltiel, A.R. (2012) Regulation of glucose transport by insulin: traffic control of GLUT4. *Nat Rev Mol Cell Biol*, **13**, 383-396.
- Lewis, J. (2003) Autoinhibition with transcriptional delay: a simple mechanism for the zebrafish somitogenesis oscillator. *Curr Biol*, **13**, 1398-1408.
- Li, J., Tang, Y. & Cai, D. (2012) IKKbeta/NF-kappaB disrupts adult hypothalamic neural stem cells to mediate a neurodegenerative mechanism of dietary obesity and pre-diabetes. *Nat Cell Biol*, **14**, 999-1012.
- Li, W., Risacher, S.L., Huang, E., Saykin, A.J. & Alzheimer's Disease Neuroimaging, I. (2016) Type 2 diabetes mellitus is associated with brain atrophy and hypometabolism in the ADNI cohort. *Neurology*, **87**, 595-600.
- Li, X., Shi, Z., Zhu, Y., Shen, T., Wang, H., Shui, G., Loo, J.J., Fang, Z., Chen, M., Wang, X., Peng, Z., Song, Y., Wang, Z., Du, X. & Liu, G. (2020) Cyanidin-3-O-glucoside improves non-alcoholic fatty liver disease by promoting PINK1-mediated mitophagy in mice. *Br J Pharmacol*, **177**, 3591-3607.
- Liebner, S., Fischmann, A., Rascher, G., Duffner, F., Grote, E.H., Kalbacher, H. & Wolburg, H. (2000) Claudin-1 and claudin-5 expression and tight junction morphology are altered in blood vessels of human glioblastoma multiforme. *Acta Neuropathol*, **100**, 323-331.



- Lieschke, G.J. & Currie, P.D. (2007) Animal models of human disease: zebrafish swim into view. *Nat Rev Genet*, **8**, 353-367.
- Lindqvist, A., Mohapel, P., Bouter, B., Frielingsdorf, H., Pizzo, D., Brundin, P. & Erlanson-Albertsson, C. (2006) High-fat diet impairs hippocampal neurogenesis in male rats. *Eur J Neurol*, **13**, 1385-1388.
- Lindsey, B.W., Darabie, A. & Tropepe, V. (2012) The cellular composition of neurogenic periventricular zones in the adult zebrafish forebrain. *The Journal of comparative neurology*, **520**, 2275-2316.
- Lindsey, B.W. & Tropepe, V. (2006) A comparative framework for understanding the biological principles of adult neurogenesis. *Prog Neurobiol*, **80**, 281-307.
- Lithner, F., Asplund, K., Eriksson, S., Hagg, E., Strand, T. & Wester, P.O. (1988) Clinical characteristics in diabetic stroke patients. *Diabete Metab*, **14**, 15-19.
- Liu, H. & Zhang, J. (2012) Cerebral hypoperfusion and cognitive impairment: the pathogenic role of vascular oxidative stress. *Int J Neurosci*, **122**, 494-499.
- Liu, S. & Leach, S.D. (2011) Zebrafish models for cancer. *Annu Rev Pathol*, **6**, 71-93.
- Lo, E.H., Dalkara, T. & Moskowitz, M.A. (2003) Mechanisms, challenges and opportunities in stroke. *Nat Rev Neurosci*, **4**, 399-415.
- Lochhead, J.J., McCaffrey, G., Quigley, C.E., Finch, J., DeMarco, K.M., Nametz, N. & Davis, T.P. (2010) Oxidative stress increases blood-brain barrier permeability and induces alterations in occludin during hypoxia-reoxygenation. *J Cereb Blood Flow Metab*, **30**, 1625-1636.
- Louissaint, A., Jr., Rao, S., Leventhal, C. & Goldman, S.A. (2002) Coordinated interaction of neurogenesis and angiogenesis in the adult songbird brain. *Neuron*, **34**, 945-960.
- Lu, J., Wu, D.M., Zheng, Y.L., Hu, B., Cheng, W., Zhang, Z.F. & Shan, Q. (2011) Ursolic acid improves high fat diet-induced cognitive impairments by blocking endoplasmic reticulum stress and I $\kappa$ B kinase beta/nuclear factor-kappaB-mediated inflammatory pathways in mice. *Brain Behav Immun*, **25**, 1658-1667.
- Lu, Y., Hajifathalian, K., Ezzati, M., Woodward, M., Rimm, E.B. & Danaei, G. (2014) Metabolic mediators of the effects of body-mass index, overweight, and obesity on coronary heart disease and stroke: a pooled analysis of 97 prospective cohorts with 1.8 million participants. *Lancet*, **383**, 970-983.
- Lui, J.H., Hansen, D.V. & Kriegstein, A.R. (2011) Development and evolution of the human neocortex. *Cell*, **146**, 18-36.

- Lutz, M. (2014) Bioavailability of bioactive compounds in foods. *Nutr. Humana*, **15**, 217–226.
- Ma, X., Song, Q. & Gao, X. (2018) Reconstituted high-density lipoproteins: novel biomimetic nanocarriers for drug delivery. *Acta Pharm Sin B*, **8**, 51-63.
- MacRae, C.A. & Peterson, R.T. (2015) Zebrafish as tools for drug discovery. *Nat Rev Drug Discov*, **14**, 721-731.
- Maddison, L.A. & Chen, W. (2017) Modeling Pancreatic Endocrine Cell Adaptation and Diabetes in the Zebrafish. *Front Endocrinol (Lausanne)*, **8**, 9.
- Maddison, L.A., Joest, K.E., Kammeyer, R.M. & Chen, W. (2015) Skeletal muscle insulin resistance in zebrafish induces alterations in beta-cell number and glucose tolerance in an age- and diet-dependent manner. *Am J Physiol Endocrinol Metab*, **308**, E662-669.
- Maggi, R., Zasso, J. & Conti, L. (2014) Neurodevelopmental origin and adult neurogenesis of the neuroendocrine hypothalamus. *Front Cell Neurosci*, **8**, 440.
- Mahomoodally, M.F., Korumtollee, H.N. & Chady, Z.Z. (2014) Psiloxylon mauritianum (Bouton ex Hook.f.) Baillon (Myrtaceae): A promising traditional medicinal plant from the Mascarene Islands. *J Intercult Ethnopharmacol*, **3**, 192-195.
- Malatesta, P., Hartfuss, E. & Gotz, M. (2000) Isolation of radial glial cells by fluorescent-activated cell sorting reveals a neuronal lineage. *Development*, **127**, 5253-5263.
- Manach, C., Williamson, G., Morand, C., Scalbert, A. & Remesy, C. (2005) Bioavailability and bioefficacy of polyphenols in humans. I. Review of 97 bioavailability studies. *Am J Clin Nutr*, **81**, 230S-242S.
- Manna, P. & Jain, S.K. (2015) Obesity, Oxidative Stress, Adipose Tissue Dysfunction, and the Associated Health Risks: Causes and Therapeutic Strategies. *Metab Syndr Relat Disord*, **13**, 423-444.
- Marchesini, G., Moscatiello, S., Di Domizio, S. & Forlani, G. (2008) Obesity-associated liver disease. *J Clin Endocrinol Metab*, **93**, S74-80.
- Marimoutou, M., Le Sage, F., Smadja, J., Lefebvre d'Hellencourt, C., Gonthier, M.P. & Robert-Da Silva, C. (2015) Antioxidant polyphenol-rich extracts from the medicinal plants *Antirhea borbonica*, *Doratoxylon apetalum* and *Gouania mauritiana* protect 3T3-L1 preadipocytes against H<sub>2</sub>O<sub>2</sub>, TNF $\alpha$  and LPS inflammatory mediators by regulating the expression of superoxide dismutase and NF-kappaB genes. *J Inflamm (Lond)*, **12**, 10.
- Marques, A., Peralta, M., Naia, A., Loureiro, N. & de Matos, M.G. (2018) Prevalence of adult overweight and obesity in 20 European countries, 2014. *Eur J Public Health*, **28**, 295-300.

- Marques, I.J., Lupi, E. & Mercader, N. (2019) Model systems for regeneration: zebrafish. *Development*, **146**.
- März, M., Chapouton, P., Diotel, N., Vaillant, C., Hesl, B., Takamiya, M., Lam, C.S., Kah, O., Bally-Cuif, L. & Strahle, U. (2010) Heterogeneity in progenitor cell subtypes in the ventricular zone of the zebrafish adult telencephalon. *Glia*, **58**, 870-888.
- Marz, M., Schmidt, R., Rastegar, S. & Strahle, U. (2011) Regenerative response following stab injury in the adult zebrafish telencephalon. *Dev Dyn*, **240**, 2221-2231.
- Mateus-Pinheiro, A., Pinto, L., Bessa, J.M., Morais, M., Alves, N.D., Monteiro, S., Patricio, P., Almeida, O.F. & Sousa, N. (2013) Sustained remission from depressive-like behavior depends on hippocampal neurogenesis. *Transl Psychiatry*, **3**, e210.
- Mazon, J.N., de Mello, A.H., Ferreira, G.K. & Rezin, G.T. (2017) The impact of obesity on neurodegenerative diseases. *Life Sci*, **182**, 22-28.
- McCluskey, B.M. & Postlethwait, J.H. (2015) Phylogeny of zebrafish, a "model species," within Danio, a "model genus". *Mol Biol Evol*, **32**, 635-652.
- McCrimmon, R.J., Ryan, C.M. & Frier, B.M. (2012) Diabetes and cognitive dysfunction. *Lancet*, **379**, 2291-2299.
- Meguro, S. & Hasumura, T. (2018) Fish Oil Suppresses Body Fat Accumulation in Zebrafish. *Zebrafish*, **15**, 27-32.
- Meguro, S., Hasumura, T. & Hase, T. (2015) Body fat accumulation in zebrafish is induced by a diet rich in fat and reduced by supplementation with green tea extract. *PLoS one*, **10**, e0120142.
- Meng, X.H., Chen, B. & Zhang, J.P. (2017) Intracellular Insulin and Impaired Autophagy in a Zebrafish model and a Cell Model of Type 2 diabetes. *Int J Biol Sci*, **13**, 985-995.
- Mentella, M.C., Scaldaferrri, F., Ricci, C., Gasbarrini, A. & Miggiano, G.A.D. (2019) Cancer and Mediterranean Diet: A Review. *Nutrients*, **11**.
- Merad-Boudia, M., Nicole, A., Santiard-Baron, D., Saille, C. & Ceballos-Picot, I. (1998) Mitochondrial impairment as an early event in the process of apoptosis induced by glutathione depletion in neuronal cells: relevance to Parkinson's disease. *Biochem Pharmacol*, **56**, 645-655.
- Milanski, M., Degasperi, G., Coope, A., Morari, J., Denis, R., Cintra, D.E., Tsukumo, D.M., Anhe, G., Amaral, M.E., Takahashi, H.K., Curi, R., Oliveira, H.C., Carvalheira, J.B., Bordin, S., Saad, M.J. & Velloso, L.A. (2009) Saturated fatty acids produce an inflammatory response predominantly

- through the activation of TLR4 signaling in hypothalamus: implications for the pathogenesis of obesity. *J Neurosci*, **29**, 359-370.
- Minagar, A. & Alexander, J.S. (2003) Blood-brain barrier disruption in multiple sclerosis. *Mult Scler*, **9**, 540-549.
- Ming, G.L. & Song, H. (2005) Adult neurogenesis in the mammalian central nervous system. *Annu Rev Neurosci*, **28**, 223-250.
- Ming, G.L. & Song, H. (2011) Adult neurogenesis in the mammalian brain: significant answers and significant questions. *Neuron*, **70**, 687-702.
- Mira, H. & Lie, D.C. (2017) Regulation of Adult Neurogenesis 2.0 - Beyond Signaling Pathways and Transcriptional Regulators. *Brain Plast*, **3**, 1-3.
- Mishra, A., Sharma, A.K., Kumar, S., Saxena, A.K. & Pandey, A.K. (2013) Bauhinia variegata leaf extracts exhibit considerable antibacterial, antioxidant, and anticancer activities. *Biomed Res Int*, **2013**, 915436.
- Mittendorfer, B., Magkos, F., Fabbrini, E., Mohammed, B.S. & Klein, S. (2009) Relationship between body fat mass and free fatty acid kinetics in men and women. *Obesity (Silver Spring)*, **17**, 1872-1877.
- Molino, S., Lerma-Aguilera, A., Jimenez-Hernandez, N., Gosalbes, M.J., Rufian-Henares, J.A. & Francino, M.P. (2021) Enrichment of Food With Tannin Extracts Promotes Healthy Changes in the Human Gut Microbiota. *Front Microbiol*, **12**, 625782.
- Montalbano, G., Mania, M., Guerrera, M.C., Abbate, F., Laura, R., Navarra, M., Vega, J.A., Ciriaco, E. & Germana, A. (2016) Morphological differences in adipose tissue and changes in BDNF/Trkb expression in brain and gut of a diet induced obese zebrafish model. *Ann Anat*, **204**, 36-44.
- Montalbano, G., Mania, M., Guerrera, M.C., Laura, R., Abbate, F., Levanti, M., Maugeri, A., Germana, A. & Navarra, M. (2019) Effects of a Flavonoid-Rich Extract from Citrus sinensis Juice on a Diet-Induced Obese Zebrafish. *International journal of molecular sciences*, **20**.
- Montalbano, G., Maugeri, A., Guerrera, M.C., Miceli, N., Navarra, M., Barreca, D., Cirmi, S. & Germana, A. (2021a) A White Grape Juice Extract Reduces Fat Accumulation through the Modulation of Ghrelin and Leptin Expression in an In Vivo Model of Overfed Zebrafish. *Molecules*, **26**.
- Montalbano, G., Mhalhel, K., Briglia, M., Levanti, M., Abbate, F., Guerrera, M.C., D'Alessandro, E., Laura, R. & Germana, A. (2021b) Zebrafish and Flavonoids: Adjuvants against Obesity. *Molecules*, **26**.



- Mootoosamy, A. & Fawzi Mahomoodally, M. (2014) Ethnomedicinal application of native remedies used against diabetes and related complications in Mauritius. *J Ethnopharmacol*, **151**, 413-444.
- Morrison, C.D., Pistell, P.J., Ingram, D.K., Johnson, W.D., Liu, Y., Fernandez-Kim, S.O., White, C.L., Purpera, M.N., Uranga, R.M., Bruce-Keller, A.J. & Keller, J.N. (2010) High fat diet increases hippocampal oxidative stress and cognitive impairment in aged mice: implications for decreased Nrf2 signaling. *J Neurochem*, **114**, 1581-1589.
- Moss, J.B., Koustubhan, P., Greenman, M., Parsons, M.J., Walter, I. & Moss, L.G. (2009) Regeneration of the pancreas in adult zebrafish. *Diabetes*, **58**, 1844-1851.
- Mule, N.K. & Singh, J.N. (2018) Diabetes Mellitus to Neurodegenerative Disorders: Is Oxidative Stress Fueling the Flame? *CNS Neurol Disord Drug Targets*, **17**, 644-653.
- Muriach, M., Flores-Bellver, M., Romero, F.J. & Barcia, J.M. (2014) Diabetes and the brain: oxidative stress, inflammation, and autophagy. *Oxid Med Cell Longev*, **2014**, 102158.
- Murray, F., Smith, D.W. & Hutson, P.H. (2008) Chronic low dose corticosterone exposure decreased hippocampal cell proliferation, volume and induced anxiety and depression like behaviours in mice. *Eur J Pharmacol*, **583**, 115-127.
- Nadal, A., Fuentes, E., Pastor, J. & McNaughton, P.A. (1995) Plasma albumin is a potent trigger of calcium signals and DNA synthesis in astrocytes. *Proc Natl Acad Sci U S A*, **92**, 1426-1430.
- Nalecz, K.A. (2017) Solute Carriers in the Blood-Brain Barrier: Safety in Abundance. *Neurochem Res*, **42**, 795-809.
- Nam, Y.H., Hong, B.N., Rodriguez, I., Ji, M.G., Kim, K., Kim, U.J. & Kang, T.H. (2015) Synergistic Potentials of Coffee on Injured Pancreatic Islets and Insulin Action via KATP Channel Blocking in Zebrafish. *J Agric Food Chem*, **63**, 5612-5621.
- Narra, S.S., Rosanaly, S., Rondeau, P., Patche, J., Veeren, B., Gonthier, M.P., Viranaicken, W., Diotel, N., Ravanan, P., Hellencourt, C.L. & Meilhac, O. (2022) ApoA-I Nanoparticles as Curcumin Carriers for Cerebral Endothelial Cells: Improved Cytoprotective Effects against Methylglyoxal. *Pharmaceuticals (Basel)*, **15**.
- Nehus, E. (2018) Obesity and chronic kidney disease. *Curr Opin Pediatr*, **30**, 241-246.
- Newman, D.J. & Cragg, G.M. (2007) Natural products as sources of new drugs over the last 25 years. *J Nat Prod*, **70**, 461-477.
- Newman, D.J., Cragg, G.M. & Snader, K.M. (2003) Natural products as sources of new drugs over the period 1981-2002. *J Nat Prod*, **66**, 1022-1037.

- Ninkovic, J., Mori, T. & Gotz, M. (2007) Distinct modes of neuron addition in adult mouse neurogenesis. *J Neurosci*, **27**, 10906-10911.
- Nishio, S., Gibert, Y., Berekelya, L., Bernard, L., Brunet, F., Guillot, E., Le Bail, J.C., Sanchez, J.A., Galzin, A.M., Triqueneaux, G. & Laudet, V. (2012) Fasting induces CART down-regulation in the zebrafish nervous system in a cannabinoid receptor 1-dependent manner. *Mol Endocrinol*, **26**, 1316-1326.
- Noctor, S.C., Flint, A.C., Weissman, T.A., Wong, W.S., Clinton, B.K. & Kriegstein, A.R. (2002) Dividing precursor cells of the embryonic cortical ventricular zone have morphological and molecular characteristics of radial glia. *J Neurosci*, **22**, 3161-3173.
- Noyes, P.D., Haggard, D.E., Gonnerman, G.D. & Tanguay, R.L. (2015) Advanced morphological - behavioral test platform reveals neurodevelopmental defects in embryonic zebrafish exposed to comprehensive suite of halogenated and organophosphate flame retardants. *Toxicol Sci*, **145**, 177-195.
- Nuzzo, D., Picone, P., Giardina, C., Scordino, M., Mudo, G., Pagliaro, M., Scurria, A., Meneguzzo, F., Ilharco, L.M., Fidalgo, A., Alduina, R., Presentato, A., Ciriminna, R. & Di Liberto, V. (2021) New Neuroprotective Effect of Lemon IntegroPectin on Neuronal Cellular Model. *Antioxidants*, **10**.
- Nwaozuzu, O.M., Sellers, L.A. & Barrand, M.A. (2003) Signalling pathways influencing basal and H<sub>2</sub>O<sub>2</sub>-induced P-glycoprotein expression in endothelial cells derived from the blood-brain barrier. *J Neurochem*, **87**, 1043-1051.
- Obermeier, B., Daneman, R. & Ransohoff, R.M. (2013) Development, maintenance and disruption of the blood-brain barrier. *Nat Med*, **19**, 1584-1596.
- Obernier, K. & Alvarez-Buylla, A. (2019) Neural stem cells: origin, heterogeneity and regulation in the adult mammalian brain. *Development*, **146**.
- OECD (2013) OECD guidelines for the testing of chemicals. Test No. 236: Fish Embryo Acute Toxicity (FET) Test.
- Ohara, T., Doi, Y., Ninomiya, T., Hirakawa, Y., Hata, J., Iwaki, T., Kanba, S. & Kiyohara, Y. (2011) Glucose tolerance status and risk of dementia in the community: the Hisayama study. *Neurology*, **77**, 1126-1134.
- Ohtsuka, T., Ishibashi, M., Gradwohl, G., Nakanishi, S., Guillemot, F. & Kageyama, R. (1999) Hes1 and Hes5 as notch effectors in mammalian neuronal differentiation. *EMBO J*, **18**, 2196-2207.
- Oka, T., Nishimura, Y., Zang, L., Hirano, M., Shimada, Y., Wang, Z., Umemoto, N., Kuroyanagi, J., Nishimura, N. & Tanaka, T. (2010) Diet-induced obesity in zebrafish shares common pathophysiological pathways with mammalian obesity. *BMC Physiol*, **10**, 21.

- Olsen, A.S., Sarras, M.P., Jr., Leontovich, A. & Intine, R.V. (2012) Heritable transmission of diabetic metabolic memory in zebrafish correlates with DNA hypomethylation and aberrant gene expression. *Diabetes*, **61**, 485-491.
- Ott, A., Stolk, R.P., van Harskamp, F., Pols, H.A., Hofman, A. & Breteler, M.M. (1999) Diabetes mellitus and the risk of dementia: The Rotterdam Study. *Neurology*, **53**, 1937-1942.
- Ouyang, S., Hsueh, H., Kastin, A.J., Wang, Y., Yu, C. & Pan, W. (2014) Diet-induced obesity suppresses expression of many proteins at the blood-brain barrier. *J Cereb Blood Flow Metab*, **34**, 43-51.
- Oyama, T., Miyasita, Y., Watanabe, H. & Shirai, K. (2006) The role of polyol pathway in high glucose-induced endothelial cell damages. *Diabetes Res Clin Pract*, **73**, 227-234.
- Ozawa, Y., Kurihara, T., Sasaki, M., Ban, N., Yuki, K., Kubota, S. & Tsubota, K. (2011) Neural degeneration in the retina of the streptozotocin-induced type 1 diabetes model. *Exp Diabetes Res*, **2011**, 108328.
- Ozdamar, T., Sela, D.A., Xiao, J., Boyacioglu, D., Chen, F. & Capanoglu, E. (2016) The Reciprocal Interactions between Polyphenols and Gut Microbiota and Effects on Bioaccessibility. *Nutrients*, **8**, 78.
- Padilla, S., Corum, D., Padnos, B., Hunter, D.L., Beam, A., Houck, K.A., Sipes, N., Kleinstreuer, N., Knudsen, T., Dix, D.J. & Reif, D.M. (2012) Zebrafish developmental screening of the ToxCast Phase I chemical library. *Reprod Toxicol*, **33**, 174-187.
- Palmer, T.D., Willhoite, A.R. & Gage, F.H. (2000) Vascular niche for adult hippocampal neurogenesis. *The Journal of comparative neurology*, **425**, 479-494.
- Papa, G., Degano, C., Iurato, M.P., Licciardello, C., Maiorana, R. & Finocchiaro, C. (2013) Macrovascular complication phenotypes in type 2 diabetic patients. *Cardiovasc Diabetol*, **12**, 20.
- Papadopoulos, M.C., Saadoun, S., Davies, D.C. & Bell, B.A. (2001) Emerging molecular mechanisms of brain tumour oedema. *Br J Neurosurg*, **15**, 101-108.
- Paraiso, A.F., Sousa, J.N., Andrade, J.M.O., Mangabeira, E.S., Lelis, D.F., de Paula, A.M.B., Martins, A., Lima, W.J.N., Guimaraes, A.L.S., Melo, G.A., Schwarz, M. & Santos, S.H.S. (2019) Oral gallic acid improves metabolic profile by modulating SIRT1 expression in obese mice brown adipose tissue: A molecular and bioinformatic approach. *Life Sci*, **237**, 116914.
- Paridaen, J.T. & Huttner, W.B. (2014) Neurogenesis during development of the vertebrate central nervous system. *EMBO Rep*, **15**, 351-364.
- Pellegrini, E., Mouriec, K., Anglade, I., Menuet, A., Le Page, Y., Gueguen, M.M., Marmignon, M.H., Brion, F., Pakdel, F. & Kah, O. (2007) Identification of aromatase-positive radial glial cells as

- progenitor cells in the ventricular layer of the forebrain in zebrafish. *The Journal of comparative neurology*, **501**, 150-167.
- Pereira-Caixeta, A.R., Guarnieri, L.O., Medeiros, D.C., Mendes, E., Ladeira, L.C.D., Pereira, M.T., Moraes, M.F.D. & Pereira, G.S. (2018) Inhibiting constitutive neurogenesis compromises long-term social recognition memory. *Neurobiol Learn Mem*, **155**, 92-103.
- Pereira, A.C., Huddleston, D.E., Brickman, A.M., Sosunov, A.A., Hen, R., McKhann, G.M., Sloan, R., Gage, F.H., Brown, T.R. & Small, S.A. (2007) An in vivo correlate of exercise-induced neurogenesis in the adult dentate gyrus. *Proc Natl Acad Sci U S A*, **104**, 5638-5643.
- Petrovska, B.B. (2012) Historical review of medicinal plants' usage. *Pharmacogn Rev*, **6**, 1-5.
- Piazzon, A., Vrhovsek, U., Masuero, D., Mattivi, F., Mandoj, F. & Nardini, M. (2012) Antioxidant activity of phenolic acids and their metabolites: synthesis and antioxidant properties of the sulfate derivatives of ferulic and caffeic acids and of the acyl glucuronide of ferulic acid. *J Agric Food Chem*, **60**, 12312-12323.
- Picone, P., Di Carlo, M. & Nuzzo, D. (2020) Obesity and Alzheimer's disease: Molecular bases. *The European journal of neuroscience*, **52**, 3944-3950.
- Pintana, H., Lietzau, G., Augestad, I.L., Chiazza, F., Nystrom, T., Patrone, C. & Darsalia, V. (2019) Obesity-induced type 2 diabetes impairs neurological recovery after stroke in correlation with decreased neurogenesis and persistent atrophy of parvalbumin-positive interneurons. *Clinical science*, **133**, 1367-1386.
- Pistell, P.J., Morrison, C.D., Gupta, S., Knight, A.G., Keller, J.N., Ingram, D.K. & Bruce-Keller, A.J. (2010) Cognitive impairment following high fat diet consumption is associated with brain inflammation. *J Neuroimmunol*, **219**, 25-32.
- Planas, J.V., Capilla, E. & Gutierrez, J. (2000) Molecular identification of a glucose transporter from fish muscle. *FEBS Lett*, **481**, 266-270.
- Pozhilenkova, E.A., Lopatina, O.L., Komleva, Y.K., Salmin, V.V. & Salmina, A.B. (2017) Blood-brain barrier-supported neurogenesis in healthy and diseased brain. *Rev Neurosci*, **28**, 397-415.
- Pugazhenthii, S., Qin, L. & Reddy, P.H. (2017) Common neurodegenerative pathways in obesity, diabetes, and Alzheimer's disease. *Biochim Biophys Acta Mol Basis Dis*, **1863**, 1037-1045.
- Qiao, J., Lawson, C.M., Rentrup, K.F.G., Kulkarni, P. & Ferris, C.F. (2020) Evaluating blood-brain barrier permeability in a rat model of type 2 diabetes. *J Transl Med*, **18**, 256.
- Quinonez-Silvero, C., Hubner, K. & Herzog, W. (2020) Development of the brain vasculature and the blood-brain barrier in zebrafish. *Developmental biology*, **457**, 181-190.



- Rakic, P. (1972) Mode of cell migration to the superficial layers of fetal monkey neocortex. *The Journal of comparative neurology*, **145**, 61-83.
- Rakic, P. (2009) Evolution of the neocortex: a perspective from developmental biology. *Nat Rev Neurosci*, **10**, 724-735.
- Ramon-Arbues, E., Martinez-Abadia, B., Gracia-Tabuenca, T., Yuste-Gran, C., Pellicer-Garcia, B., Juarez-Vela, R., Guerrero-Portillo, S. & Saez-Guinoa, M. (2019) [Prevalence of overweight/obesity and its association with diabetes, hypertension, dyslipidemia and metabolic syndrome: a cross-sectional study of a sample of workers in Aragon, Spain]. *Nutr Hosp*, **36**, 51-59.
- Ran, G., Ying, L., Li, L., Yan, Q., Yi, W., Ying, C., Wu, H. & Ye, X. (2017) Resveratrol ameliorates diet-induced dysregulation of lipid metabolism in zebrafish (*Danio rerio*). *PloS one*, **12**, e0180865.
- Rasool, M., Malik, A., Waquar, S., Zaheer, A., Asif, M., Iqbal, Z., Gauthaman, K., Kamal, M.A. & Pushparaj, P.N. (2021) Cellular and Molecular Mechanisms of Dementia: Decoding the Causal link of Diabetes Mellitus in Alzheimer's Disease. *CNS Neurol Disord Drug Targets*, **20**, 602-612.
- Ray, S.K. & Mukherjee, S. (2021) Evolving Interplay Between Dietary Polyphenols and Gut Microbiota- An Emerging Importance in Healthcare. *Front Nutr*, **8**, 634944.
- Rechner, A.R., Kuhnle, G., Hu, H., Roedig-Penman, A., van den Braak, M.H., Moore, K.P. & Rice-Evans, C.A. (2002) The metabolism of dietary polyphenols and the relevance to circulating levels of conjugated metabolites. *Free Radic Res*, **36**, 1229-1241.
- Redondo, M.J., Hagopian, W.A., Oram, R., Steck, A.K., Vehik, K., Weedon, M., Balasubramanyam, A. & Dabelea, D. (2020) The clinical consequences of heterogeneity within and between different diabetes types. *Diabetologia*, **63**, 2040-2048.
- Rein, M.J., Renouf, M., Cruz-Hernandez, C., Actis-Goretta, L., Thakkar, S.K. & da Silva Pinto, M. (2013) Bioavailability of bioactive food compounds: a challenging journey to bioefficacy. *Br J Clin Pharmacol*, **75**, 588-602.
- Rhea, E.M. & Banks, W.A. (2019) Role of the Blood-Brain Barrier in Central Nervous System Insulin Resistance. *Frontiers in neuroscience*, **13**, 521.
- Richa, R., Yadawa, A.K. & Chaturvedi, C.M. (2017) Hyperglycemia and high nitric oxide level induced oxidative stress in the brain and molecular alteration in the neurons and glial cells of laboratory mouse, *Mus musculus*. *Neurochem Int*, **104**, 64-79.
- Richter, L.H.J., Herrmann, J., Andreas, A., Park, Y.M., Wagmann, L., Flockerzi, V., Muller, R. & Meyer, M.R. (2019) Tools for studying the metabolism of new psychoactive substances for toxicological screening purposes - A comparative study using pooled human liver S9, HepaRG cells, and zebrafish larvae. *Toxicol Lett*, **305**, 73-80.

- Risau, W. & Wolburg, H. (1990) Development of the blood-brain barrier. *Trends Neurosci*, **13**, 174-178.
- Ritchie, K. & Lovestone, S. (2002) The dementias. *Lancet*, **360**, 1759-1766.
- Rivière, M. (2007) Medicinal Plants from Reunion Island, the friends and false friend, Saint Denis. *Azalées*
- Roh, H.T., Cho, S.Y. & So, W.Y. (2017) Obesity promotes oxidative stress and exacerbates blood-brain barrier disruption after high-intensity exercise. *J Sport Health Sci*, **6**, 225-230.
- Rojczyk-Golebiewska, E., Palasz, A. & Wiaderkiewicz, R. (2014) Hypothalamic subependymal niche: a novel site of the adult neurogenesis. *Cell Mol Neurobiol*, **34**, 631-642.
- Rom, S., Zuluaga-Ramirez, V., Gajghate, S., Seliga, A., Winfield, M., Heldt, N.A., Kolpakov, M.A., Bashkirova, Y.V., Sabri, A.K. & Persidsky, Y. (2019) Hyperglycemia-Driven Neuroinflammation Compromises BBB Leading to Memory Loss in Both Diabetes Mellitus (DM) Type 1 and Type 2 Mouse Models. *Mol Neurobiol*, **56**, 1883-1896.
- Rorsman, P. & Braun, M. (2013) Regulation of insulin secretion in human pancreatic islets. *Annu Rev Physiol*, **75**, 155-179.
- Ruhl, C.E. & Everhart, J.E. (2003) Determinants of the association of overweight with elevated serum alanine aminotransferase activity in the United States. *Gastroenterology*, **124**, 71-79.
- Ryder, K., Lanahan, A., Perez-Albuerne, E. & Nathans, D. (1989) jun-D: a third member of the jun gene family. *Proc Natl Acad Sci U S A*, **86**, 1500-1503.
- Sahara, S. & O'Leary, D.D. (2009) Fgf10 regulates transition period of cortical stem cell differentiation to radial glia controlling generation of neurons and basal progenitors. *Neuron*, **63**, 48-62.
- Salehpour, A., Rezaei, M., Khoradmehr, A., Tahamtani, Y. & Tamadon, A. (2021) Which Hyperglycemic Model of Zebrafish (*Danio rerio*) Suits My Type 2 Diabetes Mellitus Research? A Scoring System for Available Methods. *Front Cell Dev Biol*, **9**, 652061.
- Saltiel, A.R. & Olefsky, J.M. (2017) Inflammatory mechanisms linking obesity and metabolic disease. *J Clin Invest*, **127**, 1-4.
- Sanai, N., Nguyen, T., Ihrie, R.A., Mirzadeh, Z., Tsai, H.H., Wong, M., Gupta, N., Berger, M.S., Huang, E., Garcia-Verdugo, J.M., Rowitch, D.H. & Alvarez-Buylla, A. (2011) Corridors of migrating neurons in the human brain and their decline during infancy. *Nature*, **478**, 382-386.

- Saravia, F., Revsin, Y., Lux-Lantos, V., Beauquis, J., Homo-Delarche, F. & De Nicola, A.F. (2004) Oestradiol restores cell proliferation in dentate gyrus and subventricular zone of streptozotocin-diabetic mice. *Journal of neuroendocrinology*, **16**, 704-710.
- Sasidharan, S., Chen, Y., Saravanan, D., Sundram, K.M. & Yoga Latha, L. (2011) Extraction, isolation and characterization of bioactive compounds from plants' extracts. *Afr J Tradit Complement Altern Med*, **8**, 1-10.
- Scalbert, A. & Williamson, G. (2000) Dietary intake and bioavailability of polyphenols. *J Nutr*, **130**, 2073S-2085S.
- Schlegel, A. & Stainier, D.Y. (2007) Lessons from "lower" organisms: what worms, flies, and zebrafish can teach us about human energy metabolism. *PLoS Genet*, **3**, e199.
- Schmidt, R., Beil, T., Strahle, U. & Rastegar, S. (2014) Stab wound injury of the zebrafish adult telencephalon: a method to investigate vertebrate brain neurogenesis and regeneration. *Journal of visualized experiments : JoVE*, e51753.
- Schoenfeld, T.J. & Gould, E. (2012) Stress, stress hormones, and adult neurogenesis. *Exp Neurol*, **233**, 12-21.
- Schreibelt, G., Kooij, G., Reijerkerk, A., van Doorn, R., Gringhuis, S.I., van der Pol, S., Weksler, B.B., Romero, I.A., Couraud, P.O., Piontek, J., Blasig, I.E., Dijkstra, C.D., Ronken, E. & de Vries, H.E. (2007) Reactive oxygen species alter brain endothelial tight junction dynamics via RhoA, PI3 kinase, and PKB signaling. *FASEB J*, **21**, 3666-3676.
- Schuermann, A., Helker, C.S. & Herzog, W. (2014) Angiogenesis in zebrafish. *Semin Cell Dev Biol*, **31**, 106-114.
- Schultz, L.E., Solin, S.L., Wierson, W.A., Lovan, J.M., Syrkin-Nikolau, J., Lincow, D.E., Severin, A.J., Sakaguchi, D.S. & McGrail, M. (2017) Vascular Endothelial Growth Factor A and Leptin Expression Associated with Ectopic Proliferation and Retinal Dysplasia in Zebrafish Optic Pathway Tumors. *Zebrafish*, **14**, 343-356.
- Schwaninger, M., Sallmann, S., Petersen, N., Schneider, A., Prinz, S., Libermann, T.A. & Spranger, M. (1999) Bradykinin induces interleukin-6 expression in astrocytes through activation of nuclear factor-kappaB. *J Neurochem*, **73**, 1461-1466.
- Sears, B. & Perry, M. (2015) The role of fatty acids in insulin resistance. *Lipids Health Dis*, **14**, 121.
- Sehnert, A.J., Huq, A., Weinstein, B.M., Walker, C., Fishman, M. & Stainier, D.Y. (2002) Cardiac troponin T is essential in sarcomere assembly and cardiac contractility. *Nat Genet*, **31**, 106-110.

- Seo, M.J., Choi, H.S., Jeon, H.J., Woo, M.S. & Lee, B.Y. (2014) Baicalein inhibits lipid accumulation by regulating early adipogenesis and m-TOR signaling. *Food Chem Toxicol*, **67**, 57-64.
- Seth, A., Stemple, D.L. & Barroso, I. (2013) The emerging use of zebrafish to model metabolic disease. *Dis Model Mech*, **6**, 1080-1088.
- Sethi, S. (2020).
- Sheikh, M.H., Errede, M., d'Amati, A., Khan, N.Q., Fanti, S., Loiola, R.A., McArthur, S., Purvis, G.S.D., O'Riordan, C.E., Ferorelli, D., Dell'Erba, A., Kieswich, J., Reutelingsperger, C., Maiorano, E., Yaqoob, M., Thiernemann, C., Baragetti, A., Catapano, A.L., Norata, G.D., Marelli-Berg, F., Virgintino, D. & Solito, E. (2022) Impact of metabolic disorders on the structural, functional, and immunological integrity of the blood-brain barrier: Therapeutic avenues. *FASEB J*, **36**, e22107.
- Shen, Q., Goderie, S.K., Jin, L., Karanth, N., Sun, Y., Abramova, N., Vincent, P., Pumiglia, K. & Temple, S. (2004) Endothelial cells stimulate self-renewal and expand neurogenesis of neural stem cells. *Science*, **304**, 1338-1340.
- Shen, Q., Wang, Y., Kokovay, E., Lin, G., Chuang, S.M., Goderie, S.K., Roysam, B. & Temple, S. (2008) Adult SVZ stem cells lie in a vascular niche: a quantitative analysis of niche cell-cell interactions. *Cell Stem Cell*, **3**, 289-300.
- Shepherd, M., Shields, B., Hammersley, S., Hudson, M., McDonald, T.J., Colclough, K., Oram, R.A., Knight, B., Hyde, C., Cox, J., Mallam, K., Moudiotis, C., Smith, R., Fraser, B., Robertson, S., Greene, S., Ellard, S., Pearson, E.R., Hattersley, A.T. & Team, U. (2016) Systematic Population Screening, Using Biomarkers and Genetic Testing, Identifies 2.5% of the U.K. Pediatric Diabetes Population With Monogenic Diabetes. *Diabetes Care*, **39**, 1879-1888.
- Shi, H., Wang, Q., Zheng, M., Hao, S., Lum, J.S., Chen, X., Huang, X.F., Yu, Y. & Zheng, K. (2020) Supplement of microbiota-accessible carbohydrates prevents neuroinflammation and cognitive decline by improving the gut microbiota-brain axis in diet-induced obese mice. *Journal of neuroinflammation*, **17**, 77.
- Shields, B.M., Shepherd, M., Hudson, M., McDonald, T.J., Colclough, K., Peters, J., Knight, B., Hyde, C., Ellard, S., Pearson, E.R., Hattersley, A.T. & team, U.s. (2017) Population-Based Assessment of a Biomarker-Based Screening Pathway to Aid Diagnosis of Monogenic Diabetes in Young-Onset Patients. *Diabetes Care*, **40**, 1017-1025.
- Shimizu, Y. & Kawasaki, T. (2021) Differential Regenerative Capacity of the Optic Tectum of Adult Medaka and Zebrafish. *Front Cell Dev Biol*, **9**, 686755.
- Sies, H. (2017) Hydrogen peroxide as a central redox signaling molecule in physiological oxidative stress: Oxidative eustress. *Redox Biol*, **11**, 613-619.



- Singh, V.P., Bali, A., Singh, N. & Jaggi, A.S. (2014) Advanced glycation end products and diabetic complications. *Korean J Physiol Pharmacol*, **18**, 1-14.
- Sivanathan, S., Thavartnam, K., Arif, S., Elegino, T. & McGowan, P.O. (2015) Chronic high fat feeding increases anxiety-like behaviour and reduces transcript abundance of glucocorticoid signalling genes in the hippocampus of female rats. *Behav Brain Res*, **286**, 265-270.
- Smadja, J. & Marodon, C. (2016) Le Grand Livre des Plantes Médicinales de l'île de La Réunion: Inscrites à la Pharmacopée Française. . *Orphie Edition*.
- Smith, A.H. & Mackie, R.I. (2004) Effect of condensed tannins on bacterial diversity and metabolic activity in the rat gastrointestinal tract. *Appl Environ Microbiol*, **70**, 1104-1115.
- Sofi, F., Cesari, F., Abbate, R., Gensini, G.F. & Casini, A. (2008) Adherence to Mediterranean diet and health status: meta-analysis. *BMJ*, **337**, a1344.
- Song, C. & Wang, H. (2011) Cytokines mediated inflammation and decreased neurogenesis in animal models of depression. *Prog Neuropsychopharmacol Biol Psychiatry*, **35**, 760-768.
- Song, Y. & Cone, R.D. (2007) Creation of a genetic model of obesity in a teleost. *FASEB J*, **21**, 2042-2049.
- Sorres, J., Andre, A., Elslande, E.V., Stien, D. & Eparvier, V. (2020) Potent and Non-Cytotoxic Antibacterial Compounds Against Methicillin-Resistant Staphylococcus aureus Isolated from Psiloxylon mauritianum, A Medicinal Plant from Reunion Island. *Molecules*, **25**.
- Spalding, K.L., Bergmann, O., Alkass, K., Bernard, S., Salehpour, M., Huttner, H.B., Bostrom, E., Westerlund, I., Vial, C., Buchholz, B.A., Possnert, G., Mash, D.C., Druid, H. & Frisen, J. (2013) Dynamics of hippocampal neurogenesis in adult humans. *Cell*, **153**, 1219-1227.
- Spence, R., Gerlach, G., Lawrence, C. & Smith, C. (2008) The behaviour and ecology of the zebrafish, Danio rerio. *Biol Rev Camb Philos Soc*, **83**, 13-34.
- Squillaro, T., Schettino, C., Sampaolo, S., Galderisi, U., Di Iorio, G., Giordano, A. & Melone, M.A.B. (2018) Adult-onset brain tumors and neurodegeneration: Are polyphenols protective? *J Cell Physiol*, **233**, 3955-3967.
- Stadler, J.T. & Marsche, G. (2020) Obesity-Related Changes in High-Density Lipoprotein Metabolism and Function. *International journal of molecular sciences*, **21**.
- Stapleton, P.A., James, M.E., Goodwill, A.G. & Frisbee, J.C. (2008) Obesity and vascular dysfunction. *Pathophysiology*, **15**, 79-89.
- Stappert, L., Klaus, F. & Brustle, O. (2018) MicroRNAs Engage in Complex Circuits Regulating Adult Neurogenesis. *Frontiers in neuroscience*, **12**, 707.

- Starr, J.M., Wardlaw, J., Ferguson, K., MacLulich, A., Deary, I.J. & Marshall, I. (2003) Increased blood-brain barrier permeability in type II diabetes demonstrated by gadolinium magnetic resonance imaging. *J Neurol Neurosurg Psychiatry*, **74**, 70-76.
- Stefan, N. (2020) Causes, consequences, and treatment of metabolically unhealthy fat distribution. *Lancet Diabetes Endocrinol*, **8**, 616-627.
- Stegenga, M.E., van der Crabben, S.N., Levi, M., de Vos, A.F., Tanck, M.W., Sauerwein, H.P. & van der Poll, T. (2006) Hyperglycemia stimulates coagulation, whereas hyperinsulinemia impairs fibrinolysis in healthy humans. *Diabetes*, **55**, 1807-1812.
- Stranahan, A.M., Arumugam, T.V., Cutler, R.G., Lee, K., Egan, J.M. & Mattson, M.P. (2008) Diabetes impairs hippocampal function through glucocorticoid-mediated effects on new and mature neurons. *Nat Neurosci*, **11**, 309-317.
- Stranahan, A.M., Hao, S., Dey, A., Yu, X. & Baban, B. (2016) Blood-brain barrier breakdown promotes macrophage infiltration and cognitive impairment in leptin receptor-deficient mice. *J Cereb Blood Flow Metab*, **36**, 2108-2121.
- Strasberg, D., Rouget, M., Richardson, D.M., Baret, S., Dupont, J. & Cowling, R.M. (2005) An Assessment of Habitat Diversity and Transformation on La Réunion Island (Mascarene Islands, Indian Ocean) as a Basis for Identifying Broad-scale Conservation Priorities. *Biodivers. Conserv.*, **14**, 3015– 3032.
- Streisinger, G., Singer, F., Walker, C., Knauber, D. & Dower, N. (1986) Segregation analyses and gene-centromere distances in zebrafish. *Genetics*, **112**, 311-319.
- Subhramanyam, C.S., Wang, C., Hu, Q. & Dheen, S.T. (2019) Microglia-mediated neuroinflammation in neurodegenerative diseases. *Semin Cell Dev Biol*, **94**, 112-120.
- Sulliman, N.C., Ghaddar, B., Gence, L., Patche, J., Rastegar, S., Meilhac, O. & Diotel, N. (2021) HDL biodistribution and brain receptors in zebrafish, using HDLs as vectors for targeting endothelial cells and neural progenitors. *Scientific reports*, **11**, 6439.
- Sun, Q., Li, J. & Gao, F. (2014) New insights into insulin: The anti-inflammatory effect and its clinical relevance. *World J Diabetes*, **5**, 89-96.
- Sweeney, M.D., Ayyadurai, S. & Zlokovic, B.V. (2016) Pericytes of the neurovascular unit: key functions and signaling pathways. *Nat Neurosci*, **19**, 771-783.
- Taile, J., Arcambal, A., Clerc, P., Gauvin-Bialecki, A. & Gonthier, M.P. (2020) Medicinal Plant Polyphenols Attenuate Oxidative Stress and Improve Inflammatory and Vasoactive Markers in Cerebral Endothelial Cells during Hyperglycemic Condition. *Antioxidants*, **9**.

- Taile, J., Patche, J., Veeren, B. & Gonthier, M.P. (2021) Hyperglycemic Condition Causes Pro-Inflammatory and Permeability Alterations Associated with Monocyte Recruitment and Deregulated NFkappaB/PPARgamma Pathways on Cerebral Endothelial Cells: Evidence for Polyphenols Uptake and Protective Effect. *International journal of molecular sciences*, **22**.
- Takechi, R., Lam, V., Brook, E., Giles, C., Fimognari, N., Mooranian, A., Al-Salami, H., Coulson, S.H., Nesbit, M. & Mamo, J.C.L. (2017) Blood-Brain Barrier Dysfunction Precedes Cognitive Decline and Neurodegeneration in Diabetic Insulin Resistant Mouse Model: An Implication for Causal Link. *Front Aging Neurosci*, **9**, 399.
- Tan, B.L., Norhaizan, M.E. & Liew, W.P. (2018) Nutrients and Oxidative Stress: Friend or Foe? *Oxid Med Cell Longev*, **2018**, 9719584.
- Tangvarasittichai, S. (2015) Oxidative stress, insulin resistance, dyslipidemia and type 2 diabetes mellitus. *World J Diabetes*, **6**, 456-480.
- Tavazoie, M., Van der Veken, L., Silva-Vargas, V., Louissaint, M., Colonna, L., Zaidi, B., Garcia-Verdugo, J.M. & Doetsch, F. (2008) A specialized vascular niche for adult neural stem cells. *Cell Stem Cell*, **3**, 279-288.
- Thaler, J.P., Yi, C.X., Schur, E.A., Guyenet, S.J., Hwang, B.H., Dietrich, M.O., Zhao, X., Sarruf, D.A., Izgur, V., Maravilla, K.R., Nguyen, H.T., Fischer, J.D., Matsen, M.E., Wisse, B.E., Morton, G.J., Horvath, T.L., Baskin, D.G., Tschop, M.H. & Schwartz, M.W. (2012) Obesity is associated with hypothalamic injury in rodents and humans. *J Clin Invest*, **122**, 153-162.
- Than-Trong, E. & Bally-Cuif, L. (2015) Radial glia and neural progenitors in the adult zebrafish central nervous system. *Glia*, **63**, 1406-1428.
- Thibault, S.M.P. (2019) Un Réunionnais sur dix déclare être en mauvaise santé  
Enquête Santé à La Réunion en 2019.
- Torres-Villarreal, D., Camacho, A., Castro, H., Ortiz-Lopez, R. & de la Garza, A.L. (2019) Anti-obesity effects of kaempferol by inhibiting adipogenesis and increasing lipolysis in 3T3-L1 cells. *J Physiol Biochem*, **75**, 83-88.
- Tran, N.D., Correale, J., Schreiber, S.S. & Fisher, M. (1999) Transforming growth factor-beta mediates astrocyte-specific regulation of brain endothelial anticoagulant factors. *Stroke*, **30**, 1671-1678.
- Tresserra-Rimbau, A., Lamuela-Raventos, R.M. & Moreno, J.J. (2018) Polyphenols, food and pharma. Current knowledge and directions for future research. *Biochem Pharmacol*, **156**, 186-195.
- Truong, L., Reif, D.M., St Mary, L., Geier, M.C., Truong, H.D. & Tanguay, R.L. (2014) Multidimensional in vivo hazard assessment using zebrafish. *Toxicol Sci*, **137**, 212-233.

- Tsai, P.J., Huang, W.C., Hsieh, M.C., Sung, P.J., Kuo, Y.H. & Wu, W.H. (2015) Flavones Isolated from *Scutellariae radix* Suppress Propionibacterium Acnes-Induced Cytokine Production In Vitro and In Vivo. *Molecules*, **21**, E15.
- Tsao, R. (2010) Chemistry and biochemistry of dietary polyphenols. *Nutrients*, **2**, 1231-1246.
- Tucakov, J. (1964) Pharmacognosy. . *Beograd: Institute for text book issuing in SR. Srbije* pp. 11–30.
- Tucsek, Z., Toth, P., Sosnowska, D., Gautam, T., Mitschelen, M., Koller, A., Szalai, G., Sonntag, W.E., Ungvari, Z. & Csiszar, A. (2014) Obesity in aging exacerbates blood-brain barrier disruption, neuroinflammation, and oxidative stress in the mouse hippocampus: effects on expression of genes involved in beta-amyloid generation and Alzheimer's disease. *J Gerontol A Biol Sci Med Sci*, **69**, 1212-1226.
- Tungmunnithum, D., Thongboonyou, A., Pholboon, A. & Yangsabai, A. (2018) Flavonoids and Other Phenolic Compounds from Medicinal Plants for Pharmaceutical and Medical Aspects: An Overview. *Medicines (Basel)*, **5**.
- Turner, R.J. & Sharp, F.R. (2016) Implications of MMP9 for Blood Brain Barrier Disruption and Hemorrhagic Transformation Following Ischemic Stroke. *Front Cell Neurosci*, **10**, 56.
- UKPDS (1998) Intensive blood-glucose control with sulphonylureas or insulin compared with conventional treatment and risk of complications in patients with type 2 diabetes (UKPDS 33). UK Prospective Diabetes Study (UKPDS) Group. *Lancet*, **352**, 837-853.
- Umeno, A., Horie, M., Murotomi, K., Nakajima, Y. & Yoshida, Y. (2016) Antioxidative and Antidiabetic Effects of Natural Polyphenols and Isoflavones. *Molecules*, **21**.
- Vaag, A. & Lund, S.S. (2007) Non-obese patients with type 2 diabetes and prediabetic subjects: distinct phenotypes requiring special diabetes treatment and (or) prevention? *Appl Physiol Nutr Metab*, **32**, 912-920.
- Vainik, U., Baker, T.E., Dadar, M., Zeighami, Y., Michaud, A., Zhang, Y., Garcia Alanis, J.C., Mistic, B., Collins, D.L. & Dagher, A. (2018) Neurobehavioral correlates of obesity are largely heritable. *Proc Natl Acad Sci U S A*, **115**, 9312-9317.
- Valko, M., Izakovic, M., Mazur, M., Rhodes, C.J. & Telser, J. (2004) Role of oxygen radicals in DNA damage and cancer incidence. *Mol Cell Biochem*, **266**, 37-56.
- Van der Borght, K., Kobor-Nyakas, D.E., Klauke, K., Eggen, B.J., Nyakas, C., Van der Zee, E.A. & Meerlo, P. (2009) Physical exercise leads to rapid adaptations in hippocampal vasculature: temporal dynamics and relationship to cell proliferation and neurogenesis. *Hippocampus*, **19**, 928-936.



- Van Dyken, P. & Lacoste, B. (2018) Impact of Metabolic Syndrome on Neuroinflammation and the Blood-Brain Barrier. *Front Neurosci*, **12**, 930.
- van Tetering, G. & Vooijs, M. (2011) Proteolytic cleavage of Notch: "HIT and RUN". *Curr Mol Med*, **11**, 255-269.
- Vargas, R. & Vasquez, I.C. (2017) Effects of overfeeding and high-fat diet on cardiosomatic parameters and cardiac structures in young and adult zebrafish. *Fish Physiol Biochem*, **43**, 1761-1773.
- Veeren, B., Bringart, M., Turpin, C., Rondeau, P., Planesse, C., Ait-Arsa, I., Gimie, F., Marodon, C., Meilhac, O., Gonthier, M.P., Diotel, N. & Bascands, J.L. (2021) Caffeic Acid, One of the Major Phenolic Acids of the Medicinal Plant *Antirhea borbonica*, Reduces Renal Tubulointerstitial Fibrosis. *Biomedicines*, **9**.
- Veeren, B., Ghaddar, B., Bringart, M., Khazaal, S., Gonthier, M.P., Meilhac, O., Diotel, N. & Bascands, J.L. (2020) Phenolic Profile of Herbal Infusion and Polyphenol-Rich Extract from Leaves of the Medicinal Plant *Antirhea borbonica*: Toxicity Assay Determination in Zebrafish Embryos and Larvae. *Molecules*, **25**.
- Velasco-Santamaria, Y.M., Korsgaard, B., Madsen, S.S. & Bjerregaard, P. (2011) Bezafibrate, a lipid-lowering pharmaceutical, as a potential endocrine disruptor in male zebrafish (*Danio rerio*). *Aquat Toxicol*, **105**, 107-118.
- Veldhuis, W.B., Floris, S., van der Meide, P.H., Vos, I.M., de Vries, H.E., Dijkstra, C.D., Bar, P.R. & Nicolay, K. (2003) Interferon-beta prevents cytokine-induced neutrophil infiltration and attenuates blood-brain barrier disruption. *J Cereb Blood Flow Metab*, **23**, 1060-1069.
- Vickers, K.C., Palmisano, B.T., Shoucri, B.M., Shamburek, R.D. & Remaley, A.T. (2011) MicroRNAs are transported in plasma and delivered to recipient cells by high-density lipoproteins. *Nat Cell Biol*, **13**, 423-433.
- Viigimaa, M., Sachinidis, A., Toumpourleka, M., Koutsampasopoulos, K., Alliksoo, S. & Titma, T. (2020) Macrovascular Complications of Type 2 Diabetes Mellitus. *Curr Vasc Pharmacol*, **18**, 110-116.
- Vincent, H.K. & Taylor, A.G. (2006) Biomarkers and potential mechanisms of obesity-induced oxidant stress in humans. *Int J Obes (Lond)*, **30**, 400-418.
- Vishwanath, W. (2010) "*Danio rerio*". IUCN Red List of Threatened Species.
- Wahl, S. & Drong, A. & Lehne, B. & Loh, M. & Scott, W.R. & Kunze, S. & Tsai, P.C. & Ried, J.S. & Zhang, W. & Yang, Y. & Tan, S. & Fiorito, G. & Franke, L. & Guarrera, S. & Kasela, S. & Kriebel, J. & Richmond, R.C. & Adamo, M. & Afzal, U. & Ala-Korpela, M. & Albeti, B. & Ammerpohl, O. & Apperley, J.F. & Beekman, M. & Bertazzi, P.A. & Black, S.L. & Blancher, C. & Bonder, M.J. & Brosch, M. & Carstensen-Kirberg, M. & de Craen, A.J. & de Lusignan, S. & Dehghan, A. & Elkalaawy, M. & Fischer, K. & Franco, O.H. & Gaunt, T.R. & Hampe, J. & Hashemi, M. & Isaacs,

- A. & Jenkinson, A. & Jha, S. & Kato, N. & Krogh, V. & Laffan, M. & Meisinger, C. & Meitinger, T. & Mok, Z.Y. & Motta, V. & Ng, H.K. & Nikolakopoulou, Z. & Nteliopoulos, G. & Panico, S. & Pervjakova, N. & Prokisch, H. & Rathmann, W. & Roden, M. & Rota, F. & Rozario, M.A. & Sandling, J.K. & Schafmayer, C. & Schramm, K. & Siebert, R. & Slagboom, P.E. & Soininen, P. & Stolk, L. & Strauch, K. & Tai, E.S. & Tarantini, L. & Thorand, B. & Tigchelaar, E.F. & Tumino, R. & Uitterlinden, A.G. & van Duijn, C. & van Meurs, J.B. & Vineis, P. & Wickremasinghe, A.R. & Wijmenga, C. & Yang, T.P. & Yuan, W. & Zhernakova, A. & Batterham, R.L. & Smith, G.D. & Deloukas, P. & Heijmans, B.T. & Herder, C. & Hofman, A. & Lindgren, C.M. & Milani, L. & van der Harst, P. & Peters, A. & Illig, T. & Relton, C.L. & Waldenberger, M. & Jarvelin, M.R. & Bollati, V. & Soong, R. & Spector, T.D. & Scott, J. & McCarthy, M.I. & Elliott, P. & Bell, J.T. & Matullo, G. & Gieger, C. & Kooner, J.S. & Grallert, H. & Chambers, J.C. (2017) Epigenome-wide association study of body mass index, and the adverse outcomes of adiposity. *Nature*, **541**, 81-86.
- Walker, C. & Streisinger, G. (1983) Induction of Mutations by gamma-Rays in Pregonial Germ Cells of Zebrafish Embryos. *Genetics*, **103**, 125-136.
- Walker, J.M., Dixit, S., Saulsberry, A.C., May, J.M. & Harrison, F.E. (2017) Reversal of high fat diet-induced obesity improves glucose tolerance, inflammatory response, beta-amyloid accumulation and cognitive decline in the APP/PSEN1 mouse model of Alzheimer's disease. *Neurobiol Dis*, **100**, 87-98.
- Wang, J., Cao, X., Ferchaud, V., Qi, Y., Jiang, H., Tang, F., Yue, Y. & Chin, K.L. (2016a) Variations in chemical fingerprints and major flavonoid contents from the leaves of thirty-one accessions of *Hibiscus sabdariffa* L. *Biomed Chromatogr*, **30**, 880-887.
- Wang, L., Chen, X., Du, Z., Li, G., Chen, M., Chen, X., Liang, G. & Chen, T. (2017) Curcumin suppresses gastric tumor cell growth via ROS-mediated DNA polymerase gamma depletion disrupting cellular bioenergetics. *J Exp Clin Cancer Res*, **36**, 47.
- Wang, L., Tian, X., Wei, W., Chen, G. & Wu, Z. (2016b) Fingerprint analysis and quality consistency evaluation of flavonoid compounds for fermented Guava leaf by combining high-performance liquid chromatography time-of-flight electrospray ionization mass spectrometry and chemometric methods. *J Sep Sci*, **39**, 3906-3916.
- Watson, K.C. & Kerr, E.J. (1985) Specificity of antibodies for T sites and F sites of streptolysin O. *J Med Microbiol*, **19**, 1-7.
- Whitlock, G., Lewington, S., Sherliker, P., Clarke, R., Emberson, J., Halsey, J., Qizilbash, N., Collins, R. & Peto, R. (2009) Body-mass index and cause-specific mortality in 900 000 adults: collaborative analyses of 57 prospective studies. *Lancet*, **373**, 1083-1096.
- WHO (2016a) *World health organisation*.
- WHO (2016b) diabetes data and statistics. *World Health Organization*.

- WHO (2016c) Fact sheets diabetes. *World Health Organization*.
- WHO (2016d) Health topics, diabetes. *World Health Organization*.
- WHO (2016e) Mean fasting blood glucose *World Health Organization*.
- WHO (2021) Obesity and overweight Fact sheet N°311. *World health organisation*.
- Wiat, C. (2006) Ethnopharmacology of medicinal plants. . *New Jersey: Humana Press* pp. 1–50.
- Williams, C.H. & Hong, C.C. (2011) Multi-step usage of in vivo models during rational drug design and discovery. *International journal of molecular sciences*, **12**, 2262-2274.
- Wiltrout, C., Lang, B., Yan, Y., Dempsey, R.J. & Vemuganti, R. (2007) Repairing brain after stroke: a review on post-ischemic neurogenesis. *Neurochem Int*, **50**, 1028-1041.
- Winner, B., Kohl, Z. & Gage, F.H. (2011) Neurodegenerative disease and adult neurogenesis. *The European journal of neuroscience*, **33**, 1139-1151.
- Winocur, G., Wojtowicz, J.M., Sekeres, M., Snyder, J.S. & Wang, S. (2006) Inhibition of neurogenesis interferes with hippocampus-dependent memory function. *Hippocampus*, **16**, 296-304.
- Wolburg, H. & Lippoldt, A. (2002) Tight junctions of the blood-brain barrier: development, composition and regulation. *Vascul Pharmacol*, **38**, 323-337.
- Wu, J., Zhu, Y., Zhou, L., Lu, Y., Feng, T., Dai, M., Liu, J., Xu, W., Cheng, W., Sun, F., Liu, H., Pan, W. & Yang, X. (2021) Parasite-Derived Excretory-Secretory Products Alleviate Gut Microbiota Dysbiosis and Improve Cognitive Impairment Induced by a High-Fat Diet. *Front Immunol*, **12**, 710513.
- Wu, T., Grootaert, C., Pitart, J., Vidovic, N.K., Kamiloglu, S., Possemiers, S., Glibetic, M., Smagghe, G., Raes, K., Van de Wiele, T. & Van Camp, J. (2018) Aronia (*Aronia melanocarpa*) Polyphenols Modulate the Microbial Community in a Simulator of the Human Intestinal Microbial Ecosystem (SHIME) and Decrease Secretion of Proinflammatory Markers in a Caco-2/endothelial Cell Coculture Model. *Molecular nutrition & food research*, **62**, e1800607.
- Xanthos, D.N. & Sandkuhler, J. (2014) Neurogenic neuroinflammation: inflammatory CNS reactions in response to neuronal activity. *Nat Rev Neurosci*, **15**, 43-53.
- Xie, J., Farage, E., Sugimoto, M. & Anand-Apte, B. (2010) A novel transgenic zebrafish model for blood-brain and blood-retinal barrier development. *BMC Dev Biol*, **10**, 76.

- Xu, W.L., Atti, A.R., Gatz, M., Pedersen, N.L., Johansson, B. & Fratiglioni, L. (2011) Midlife overweight and obesity increase late-life dementia risk: a population-based twin study. *Neurology*, **76**, 1568-1574.
- Xu, Z., Zeng, W., Sun, J., Chen, W., Zhang, R., Yang, Z., Yao, Z., Wang, L., Song, L., Chen, Y., Zhang, Y., Wang, C., Gong, L., Wu, B., Wang, T., Zheng, J. & Gao, F. (2017) The quantification of blood-brain barrier disruption using dynamic contrast-enhanced magnetic resonance imaging in aging rhesus monkeys with spontaneous type 2 diabetes mellitus. *Neuroimage*, **158**, 480-487.
- Yadav, A., Sunkaria, A., Singhal, N. & Sandhir, R. (2018) Resveratrol loaded solid lipid nanoparticles attenuate mitochondrial oxidative stress in vascular dementia by activating Nrf2/HO-1 pathway. *Neurochem Int*, **112**, 239-254.
- Yan, B., Chen, Z.S., Hu, Y. & Yong, Q. (2021) Insight in the Recent Application of Polyphenols From Biomass. *Front Bioeng Biotechnol*, **9**, 753898.
- Yang, K., Zhang, L., Liao, P., Xiao, Z., Zhang, F., Sindaye, D., Xin, Z., Tan, C., Deng, J., Yin, Y. & Deng, B. (2020) Impact of Gallic Acid on Gut Health: Focus on the Gut Microbiome, Immune Response, and Mechanisms of Action. *Front Immunol*, **11**, 580208.
- Yasuda, S., Burgess, M., Yasuda, T., Liu, M.Y., Bhuiyan, S., Williams, F.E., Kurogi, K., Sakakibara, Y., Suiko, M. & Liu, M.C. (2009) A novel hydroxysteroid-sulfating cytosolic sulfotransferase, SULT3 ST3, from zebrafish: identification, characterization, and ontogenic study. *Drug Metab Lett*, **3**, 217-227.
- Yau, J.W., Rogers, S.L., Kawasaki, R., Lamoureux, E.L., Kowalski, J.W., Bek, T., Chen, S.J., Dekker, J.M., Fletcher, A., Grauslund, J., Haffner, S., Hamman, R.F., Ikram, M.K., Kayama, T., Klein, B.E., Klein, R., Krishnaiah, S., Mayurasakorn, K., O'Hare, J.P., Orchard, T.J., Porta, M., Rema, M., Roy, M.S., Sharma, T., Shaw, J., Taylor, H., Tielsch, J.M., Varma, R., Wang, J.J., Wang, N., West, S., Xu, L., Yasuda, M., Zhang, X., Mitchell, P., Wong, T.Y. & Meta-Analysis for Eye Disease Study, G. (2012) Global prevalence and major risk factors of diabetic retinopathy. *Diabetes Care*, **35**, 556-564.
- Yeddes, N., Cherif, J.K., Guyot, S., Sotin, H. & Ayadi, M.T. (2013) Comparative Study of Antioxidant Power, Polyphenols, Flavonoids and Betacyanins of the Peel and Pulp of Three Tunisian *Opuntia* Forms. *Antioxidants*, **2**, 37-51.
- Yee, N.S., Kazi, A.A. & Yee, R.K. (2013) Translating discovery in zebrafish pancreatic development to human pancreatic cancer: biomarkers, targets, pathogenesis, and therapeutics. *Zebrafish*, **10**, 132-146.
- Yeo, S.Y., Kim, M., Kim, H.S., Huh, T.L. & Chitnis, A.B. (2007) Fluorescent protein expression driven by her4 regulatory elements reveals the spatiotemporal pattern of Notch signaling in the nervous system of zebrafish embryos. *Developmental biology*, **301**, 555-567.
- Yi, S.S., Hwang, I.K., Yoo, K.Y., Park, O.K., Yu, J., Yan, B., Kim, I.Y., Kim, Y.N., Pai, T., Song, W., Lee, I.S., Won, M.H., Seong, J.K. & Yoon, Y.S. (2009) Effects of treadmill exercise on cell proliferation



- and differentiation in the subgranular zone of the dentate gyrus in a rat model of type II diabetes. *Neurochem Res*, **34**, 1039-1046.
- Yin, L., Maddison, L.A., Li, M., Kara, N., LaFave, M.C., Varshney, G.K., Burgess, S.M., Patton, J.G. & Chen, W. (2015) Multiplex Conditional Mutagenesis Using Transgenic Expression of Cas9 and sgRNAs. *Genetics*, **200**, 431-441.
- Zahoor, M., Shafiq, S., Ullah, H., Sadiq, A. & Ullah, F. (2018) Isolation of quercetin and mandelic acid from *Aesculus indica* fruit and their biological activities. *BMC Biochem*, **19**, 5.
- Zang, L., Maddison, L.A. & Chen, W. (2018) Zebrafish as a Model for Obesity and Diabetes. *Front Cell Dev Biol*, **6**, 91.
- Zang, L., Shimada, Y. & Nishimura, N. (2017) Development of a Novel Zebrafish Model for Type 2 Diabetes Mellitus. *Scientific reports*, **7**, 1461.
- Zang, L., Shimada, Y., Nishimura, Y., Tanaka, T. & Nishimura, N. (2013) A novel, reliable method for repeated blood collection from aquarium fish. *Zebrafish*, **10**, 425-432.
- Zang, L., Shimada, Y., Nishimura, Y., Tanaka, T. & Nishimura, N. (2015) Repeated Blood Collection for Blood Tests in Adult Zebrafish. *Journal of visualized experiments : JoVE*, e53272.
- Zenaro, E., Piacentino, G. & Constantin, G. (2017) The blood-brain barrier in Alzheimer's disease. *Neurobiol Dis*, **107**, 41-56.
- Zhang, C., Willett, C. & Fremgen, T. (2003) Zebrafish: an animal model for toxicological studies. *Curr Protoc Toxicol*, **Chapter 1**, Unit1 7.
- Zhang, H., Lai, Q., Li, Y., Liu, Y. & Yang, M. (2017) Learning and memory improvement and neuroprotection of *Gardenia jasminoides* (Fructus gardenia) extract on ischemic brain injury rats. *J Ethnopharmacol*, **196**, 225-235.
- Zhang, S.Q. (1990) [Tongue temperature of healthy persons and patients with yin deficiency by using thermal video]. *Zhong Xi Yi Jie He Za Zhi*, **10**, 732-733, 709.
- Zhang, W.J., Tan, Y.F., Yue, J.T., Vranic, M. & Wojtowicz, J.M. (2008) Impairment of hippocampal neurogenesis in streptozotocin-treated diabetic rats. *Acta Neurol Scand*, **117**, 205-210.
- Zhao, J., Pati, S., Redell, J.B., Zhang, M., Moore, A.N. & Dash, P.K. (2012) Caffeic Acid phenethyl ester protects blood-brain barrier integrity and reduces contusion volume in rodent models of traumatic brain injury. *J Neurotrauma*, **29**, 1209-1218.

- Zhao, Q., Zhang, F., Yu, Z., Guo, S., Liu, N., Jiang, Y., Lo, E.H., Xu, Y. & Wang, X. (2019) HDAC3 inhibition prevents blood-brain barrier permeability through Nrf2 activation in type 2 diabetes male mice. *Journal of neuroinflammation*, **16**, 103.
- Zheng, L., Yu, P., Zhang, Y., Wang, P., Yan, W., Guo, B., Huang, C. & Jiang, Q. (2021) Evaluating the bio-application of biomacromolecule of lignin-carbohydrate complexes (LCC) from wheat straw in bone metabolism via ROS scavenging. *Int J Biol Macromol*, **176**, 13-25.
- Zheng, X., Liu, L., Dai, W., Wang, K., Chen, X., Zhao, L., Huang, Z. & Hou, J. (2016) [Establishment of a diet-induced obesity model in zebrafish larvae]. *Nan Fang Yi Ke Da Xue Xue Bao*, **36**, 20-25.
- Zhou, H., Lu, W., Shi, Y., Bai, F., Chang, J., Yuan, Y., Teng, G. & Zhang, Z. (2010) Impairments in cognition and resting-state connectivity of the hippocampus in elderly subjects with type 2 diabetes. *Neurosci Lett*, **473**, 5-10.
- Zhou, H., Urso, C.J. & Jadeja, V. (2020) Saturated Fatty Acids in Obesity-Associated Inflammation. *J Inflamm Res*, **13**, 1-14.
- Zlokovic, B.V. (2005) Neurovascular mechanisms of Alzheimer's neurodegeneration. *Trends Neurosci*, **28**, 202-208.
- Zlokovic, B.V. (2008) The blood-brain barrier in health and chronic neurodegenerative disorders. *Neuron*, **57**, 178-201.
- Zunszain, P.A., Anacker, C., Cattaneo, A., Carvalho, L.A. & Pariante, C.M. (2011) Glucocorticoids, cytokines and brain abnormalities in depression. *Prog Neuropsychopharmacol Biol Psychiatry*, **35**, 722-729.
- Zupanc, G.K. (2008) Adult neurogenesis and neuronal regeneration in the brain of teleost fish. *J Physiol Paris*, **102**, 357-373.

## Résumé

L'obésité est une épidémie mondiale qui entraîne de nombreux problèmes de santé et constitue un facteur de risque pour le développement du diabète de type 2. A la Réunion, ces maladies sont largement répandues dans la population. L'obésité et le diabète ont en commun plusieurs perturbations métaboliques et sont impliqués dans la perte de l'homéostasie et de la plasticité cérébrales, contribuant au développement de troubles cognitifs. Les mécanismes à l'origine de ces altérations au niveau central ne sont pas bien compris. En outre, aucune thérapie n'a encore été établie pour prévenir les perturbations du cerveau dans ces pathologies.

L'objectif de cette thèse est d'étudier l'impact de l'obésité/du diabète sur l'homéostasie et la plasticité du cerveau, puis de contrecarrer ces effets délétères à l'aide d'extraits de plantes médicinales réunionnaises. Pour ce faire, nous avons mis en place un protocole d'obésité induite par un régime alimentaire (DIO) chez le poisson zèbre (*Danio rerio*). Ce dernier apparaît comme un modèle pertinent pour mimer les perturbations métaboliques associées à l'obésité et au diabète, mais aussi pour étudier l'homéostasie et la plasticité cérébrale (ex : barrière hémato-encéphalique (BHE) et neurogenèse).

Notre modèle DIO, établi par une surnutrition de poissons adultes pendant 4 semaines, a entraîné des troubles métaboliques et une perte d'homéostasie du système nerveux central (SNC). En effet, les poissons DIO présentaient une augmentation du poids corporel, et de l'indice de masse corporelle (IMC), une hyperglycémie, une stéatose hépatique et un déséquilibre de la balance redox. Dans le SNC, nous avons observé une augmentation de la perméabilité de la BHE, une neuro-inflammation, un stress oxydatif et une diminution de la neurogenèse. De plus, un changement de comportement locomoteur a été observé chez les poissons obèses.

Dans une autre étape, nous avons étudié les possibles propriétés bénéfiques de deux plantes réunionnaises inscrites à la pharmacopée française : *Antirhea borbonica* (*A. borbonica*) et *Psiloxylon mauritianum* (*P. mauritianum*). Ces deux plantes sont traditionnellement utilisées pour leurs effets positifs sur les perturbations métaboliques : effets « anti-diabétiques » pour *A. borbonica* et « anti-cholestérolémiques » pour *P. mauritianum*. Cependant, les données scientifiques soutenant ces propriétés font cruellement défaut.

Tout d'abord, l'analyse chimique de l'extrait aqueux d'*A. borbonica* et de *P. mauritianum* a révélé une abondance en polyphénols corrélée à leurs propriétés antioxydantes. L'analyse par chromatographie en phase liquide avec spectrométrie de masse en tandem (LC-MS/MS) nous a permis de déterminer la nature des composés polyphénoliques de chaque extrait. Ensuite, nous avons réalisé des tests de toxicité selon la ligne directrice 36 de l'OCDE (Organisation de coopération et de développement économiques) (OCDE, 2013). Ceci nous a permis de définir une concentration maximale non toxique pour chaque extrait.

Le traitement avec l'extrait aqueux d'*A. borbonica* pendant les 4 semaines du protocole de surnutrition (DIO) a démontré des propriétés préventives contre les effets délétères de la suralimentation sur le SNC. En effet, *A. borbonica* a préservé la fonctionnalité de la BHE, a empêché l'augmentation du stress oxydatif cérébral et de la neuro-inflammation, mais a également normalisé la neurogenèse dans certaines régions.

De même, l'extrait aqueux de *P. mauritianum* a été testé sur des poissons adultes surnutris (DIO) et sur des larves traitées par un régime riche en graisse (HFD). Le traitement avec *P. mauritianum* a empêché l'accumulation de lipides chez les larves HFD. De plus, il a évité l'augmentation du poids corporel, de l'IMC, de la glycémie et le développement d'une stéatose hépatique chez les poissons DIO. De plus, *P. mauritianum* a montré un effet protecteur sur le SNC, probablement grâce à ses propriétés anti-obésogène de poids. Nous émettons l'hypothèse que *P. mauritianum* pourrait affecter de manière importante l'absorption et le métabolisme des lipides, probablement en modulant le microbiote intestinal.

En conclusion, au cours de cette thèse, nous avons développé un modèle de surnutrition (DIO) simple et rapide induisant des perturbations périphériques et centrales similaires à celles rencontrées chez les mammifères. Pour la première fois, nous avons étudié la toxicité d'un extrait aqueux des deux plantes médicinales *A. borbonica* et *P. mauritianum*. Nous avons confirmé leurs effets bénéfiques à des concentrations non toxiques sur différents paramètres métaboliques et sur le cerveau en utilisant un modèle de poisson zèbre présentant des caractéristiques d'obésité et de prédiabète. Ensemble, ces données mettent en valeur l'utilisation du poisson zèbre pour mimer des maladies métaboliques et pour cribler des propriétés d'intérêts d'extraits de plantes médicinales.

**Mots-clés :** obésité barrière hémato-encéphalique, diabète, inflammation, neurogenèse, stress oxydatif, système nerveux central,

## Abstract

Obesity is a worldwide epidemic leading to many health concerns and is a risk factor for the development of type 2 diabetes. In Reunion Island, obesity and diabetes are widely spread among the population. Both diseases share several metabolic disorders and have been recently implicated in deteriorating brain health, contributing to cognitive impairments. The mechanisms behind the onset of altered brain homeostasis are not well understood. Besides, no therapy has yet been established to prevent brain disruptions.

The aim of this thesis is to study the impact of obesity/prediabetes on brain homeostasis and cerebral plasticity, and then to alleviate these deleterious effects using medicinal plants from Reunion Island. To this end, we set up a diet-induced obesity (DIO) protocol in zebrafish (*Danio rerio*). Zebrafish recently emerges as a relevant model to mimic metabolic diseases (obesity and diabetes), and to investigate brain homeostasis and plasticity (i.e., blood-brain barrier (BBB) and neurogenesis).

Our DIO model, established by overfeeding adult zebrafish for 4 weeks, resulted in metabolic disorders and loss of central nervous system (CNS) homeostasis. Indeed, DIO fish displayed increased body weight and body mass index (BMI), hyperglycemia, liver steatosis and disturbed redox balance. In the central nervous system, overfeeding led to BBB leakage, neuro-inflammation, cerebral oxidative stress and decreased neurogenesis. As well, a change in the locomotor behavior was observed in obese fish.

In a next step, we tested the potential beneficial properties of two Reunionese plants registered in the French pharmacopeia: *Antirhea borbonica* (*A. borbonica*) and *Psiloxylon mauritianum* (*P. mauritianum*). Both plants were traditionally used for their positive effects on metabolic disruptions as “anti-diabetic” effects for *A. borbonica* and “anti-lipidemic” for *P. mauritianum*. However, the scientific data supporting these properties are lacking.

First, the chemical analysis of aqueous extract of *A. borbonica* and *P. mauritianum* revealed their abundance in polyphenols, correlated to their antioxidant properties. LC-MS/MS analysis was used to determine the nature of the polyphenolic compounds in each extract. Next, we performed toxicity assays using OECD guidelines 36 (Organization for Economic Co-operation and Development) (OECD, 2013) and defined a maximum non-toxic concentration for each extract.

The overnight treatment with aqueous extract of *A. borbonica* (0.5g/L) during the DIO protocol demonstrated its preventive properties against the deleterious effects on the CNS induced by overfeeding. Indeed, *A. borbonica* preserved the BBB function, prevented the increase in cerebral oxidative stress, neuro-inflammation and normalized neurogenesis.

Similarly, the aqueous extract of *P. mauritianum* (0.25 g/L) was tested on adult DIO zebrafish and in high-fat diet (HFD) treated larvae. The treatment avoided lipid accumulation in HFD larvae. It also prevented body weight increase, BMI, hyperglycemia and liver steatosis in adult DIO zebrafish. Furthermore, brain homeostasis seems to be preserved probably through *P. mauritianum* anti-weight gain properties. We suggested that *P. mauritianum* could significantly affect lipid absorption and metabolism possibly through the modulation of gut microbiota.

In conclusion, during this thesis, we have developed a simple and rapid overfeeding (DIO) model inducing peripheral and CNS disruptions similar to those encountered in mammals. For the first time, we studied the toxicity of aqueous extract of the two medicinal plants *A. borbonica* and *P. mauritianum*. We confirmed their beneficial effects on different metabolic parameters and on the brain using zebrafish model of obesity and prediabetes. Together, these data highlight the use of zebrafish to mimic metabolic diseases and to screen the beneficial properties of medicinal plants extracts.

**Key words:** blood-brain barrier, central nervous system, diabetes, inflammation, neurogenesis, obesity, oxidative stress.